

INFORMATION TO USERS

This manuscript has been reproduced from the microfilm master. UMI films the text directly from the original or copy submitted. Thus, some thesis and dissertation copies are in typewriter face, while others may be from any type of computer printer.

The quality of this reproduction is dependent upon the quality of the copy submitted. Broken or indistinct print, colored or poor quality illustrations and photographs, print bleedthrough, substandard margins, and improper alignment can adversely affect reproduction.

In the unlikely event that the author did not send UMI a complete manuscript and there are missing pages, these will be noted. Also, if unauthorized copyright material had to be removed, a note will indicate the deletion.

Oversize materials (e.g., maps, drawings, charts) are reproduced by sectioning the original, beginning at the upper left-hand corner and continuing from left to right in equal sections with small overlaps. Each original is also photographed in one exposure and is included in reduced form at the back of the book.

Photographs included in the original manuscript have been reproduced xerographically in this copy. Higher quality 6" x 9" black and white photographic prints are available for any photographs or illustrations appearing in this copy for an additional charge. Contact UMI directly to order.



Bell & Howell Information and Learning
300 North Zeeb Road, Ann Arbor, MI 48106-1346 USA
800-521-0600

THE UNIVERSITY OF ALBERTA

TREATMENT OF PULP MILL MEMBRANE CONCENTRATES
BY FREEZE-THAW

by

RODERICK M. FACEY ©

A THESIS

SUBMITTED TO THE FACULTY OF GRADUATE STUDIES AND
RESEARCH IN PARTIAL FULFILMENT OF THE REQUIREMENTS FOR
THE DEGREE OF DOCTOR OF PHILOSOPHY

IN

ENVIRONMENTAL ENGINEERING

DEPARTMENT OF CIVIL & ENVIRONMENTAL ENGINEERING

EDMONTON, ALBERTA

SPRING 1999



National Library
of Canada

Acquisitions and
Bibliographic Services

395 Wellington Street
Ottawa ON K1A 0N4
Canada

Bibliothèque nationale
du Canada

Acquisitions et
services bibliographiques

395, rue Wellington
Ottawa ON K1A 0N4
Canada

Your file Votre référence

Our file Notre référence

The author has granted a non-exclusive licence allowing the National Library of Canada to reproduce, loan, distribute or sell copies of this thesis in microform, paper or electronic formats.

The author retains ownership of the copyright in this thesis. Neither the thesis nor substantial extracts from it may be printed or otherwise reproduced without the author's permission.

L'auteur a accordé une licence non exclusive permettant à la Bibliothèque nationale du Canada de reproduire, prêter, distribuer ou vendre des copies de cette thèse sous la forme de microfiche/film, de reproduction sur papier ou sur format électronique.

L'auteur conserve la propriété du droit d'auteur qui protège cette thèse. Ni la thèse ni des extraits substantiels de celle-ci ne doivent être imprimés ou autrement reproduits sans son autorisation.

0-612-39525-1

Canada

UNIVERSITY OF ALBERTA
LIBRARY RELEASE FORM

NAME OF AUTHOR: RODERICK MICHAEL FACEY
TITLE OF THESIS: TREATMENT OF PULP MILL MEMBRANE
CONCENTRATES BY FREEZE-THAW
DEGREE: DOCTOR OF PHILOSOPHY
YEAR THIS DEGREE WAS GRANTED: 1999

Permission is hereby granted to the University of Alberta Library to reproduce single copies of this thesis and to lend or sell such copies for private, scholarly, or scientific research purposes only.

The author reserves all other publication and other rights in association with the copyright in the thesis, and except as herein before provided, neither the thesis nor any substantial portion thereof may be printed or otherwise reproduced in any material form whatever without the author's prior written permission.

(Signed) 

PERMANENT ADDRESS:

23-3811-85 Street
Edmonton, Alberta, T6K 4C7

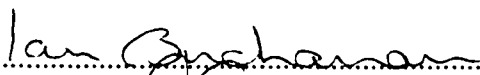
Dated April 16, 1999

THE UNIVERSITY OF ALBERTA
FACULTY OF GRADUATE STUDIES AND RESEARCH


The undersigned certify that they have read, and recommend to the Faculty of Graduate Studies and Research, for acceptance, a thesis entitled TREATMENT OF PULP MILL MEMEBRANE CONCENTRATES BY FREEZE-THAW submitted by RODERICK M. FACEY in partial fulfillment of the requirements for the degree of DOCTOR OF PHILOSOPHY in ENVIRONMENTAL ENGINEERING.

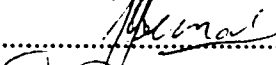
.....Dr. D.W. Smith

Supervisor

.....Dr. I.D. Buchanan

.....Dr. D.C. Sego

.....Dr. S.J. Stanley

.....Dr. L. Leonard

.....Dr. J. Martel

External Examiner

Date.....12 April 1999.....

ABSTRACT

Freeze-thaw was studied as a waste treatment method for the concentration and volume reduction of contaminated liquids of high strength kraft pulp mill effluents and waste concentrates produced from the use of membrane technology. Unidirectional freezing experiments were conducted to simulate natural freezing in which the independent variables: freezing rate, liquid depth, storage time, storage temperature, freeze layering, concentration, thawing rate and method of thawing were examined with respect to their relative significance. Method of thawing followed by freezing rate, rate of thawing, and storage temperature were identified as the most important independent variables that contribute significantly to treatment performance. Freeze-thaw was effective in concentrating and separating the constituent matter of high and moderate strength effluents originating from the alkaline extraction stage to produce a relatively clear supernatant in the upper liquid fraction. Identified was a new field of application for freeze-thaw as a waste treatment process for the management of high strength liquid wastes amenable to mechanical coagulation by freezing.

Scanning electron microscopy of frozen effluent samples showed its constituents were concentrated during freezing into thin layers of concentrated material with the thickness and morphology of this material dependent on the freezing conditions. At an initial freezing temperature of -2°C , approaching the effluent's minimum freezing point, the concentrated material produced consisted of thick, porous wafer-like structures arranged into "honey comb or box" like patterns. At higher rates of freezing (initial freezing temperatures -15°C and -25°C) the

concentrated material produced consisted of very thin, wafer-like structures. These wafer-like structures were arranged in sheet like patterns with the spacing between the zones of concentrated material being in part, determined by the freezing rate. Initial freezing temperature was found to play an important role in defining the morphology and characteristics of the concentrated material produced during freezing.

The concentrated material produced during freezing was very fragile and susceptible to break-up during thawing. The method by which the frozen effluent was thawed proved crucial in the successful operation of the process. Thawing of the frozen effluent from predominantly the bottom up allowed for the release of the concentrated material from its ice matrix enabling it to settle and be carried downward with the melt water. The degree by which the melt water assisted settlement of the concentrated material was dependent on the rate of thawing. High thawing rates was conducive to establishing a near downward vertical flow pattern which assisted to rapidly remove and concentrate the material, limiting its contact time with the bulk solution during which diffusion could occur. Constituent removal rates of as high as 80 % were achieved in the top 70 % liquid portion of different effluent types under conditions of slow freezing and rapid thawing from the bottom up.

Over time the concentrated material was observed to diffuse back into solution to indicate it was not a floc per say but a mixture of dissolved and stable colloids together with precipitated and flocculated matter, all dehydrated. Equations were derived to predict the final color concentration in the top 70 % liquid fraction of the treated effluent and to

estimate the drain time following treatment to obtain a desired treated effluent quality. These equations were verified using experimental data.

ACKNOWLEDGEMENTS

I would like to thank the members of my advisory committee (Dr. Daniel Smith, Dr. Steve Stanley, Dr. Ian Buchanan, and Dr. Dave Sego) for providing many helpful suggestions during the course of my research. More importantly I would like to especially thank Dr. Daniel W. Smith for his advice, encouragement and patience during my years as a graduate student.

I would like to extend my great appreciation and thanks to the numerous people who assisted me throughout the course of my research. In particular I would like to thank Maria Demeter, Nick Chernuka, and Carla Schumacher for their assistance in the conduct of the laboratory work. I am indebted to their help and cooperation. Also I would like to thank the Geotechnical Group of the Department for the use of their facilities and to Christine Hereygers for her helpful assistance.

I would also like to acknowledge the support of Weyerhaeuser Canada Ltd., Grande Prairie Operations for their encouragement, support and in making the pilot membrane treatment system available for test sample production. In particular the encouragement of Mr. Steve Cooper and later Ms. Rhianna Johnson was appreciated.

Finally, I would like to thank my wife and daughter, Maria Augusta and Carolina, for their patience and understanding.

Financial support for much of this research was initially provided by Weyerhaeuser Canada Ltd. through a research contract with Dr. Daniel W. Smith followed by a research grant from the Natural Sciences and

Engineering Research Council of Canada (NSERC) to Dr. Smith. The balance of the support was provided through the Sustainable Forest Management Network of Centres of Excellence, Minimal Impact Technologies theme through a grant to Dr. Daniel W. Smith.

TABLE OF CONTENTS

Chapter	Page
1.0 Introduction.....	1
1.1 Background.....	2
1.1.1 Statement of the Problem.....	2
1.1.2 Hypothesis Development.....	3
1.1.3 Research Development.....	6
1.2 Research Objectives.....	7
1.2.1 Primary Objectives.....	8
1.2.2 Secondary Objectives.....	8
2.0 Literature Review.....	9
2.1 Pulping Processes.....	9
2.1.1 Alkaline Extraction Stage Effluent Composition.....	10
2.2 Freeze-Thaw for Treatment of Membrane Concentrates.....	11
2.2.1 Freeze Concentration and Separation.....	11
2.2.1.1 Freezing of Pure Water.....	12
2.2.1.2 Freezing of Solutions.....	12
2.2.1.3 Freezing of Colloidal Aqueous Solutions.....	14
2.2.1.4 Freezing of Suspensions.....	16
2.2.1.5 Freezing of Sludges.....	16
2.2.2 Influencing Variables.....	19
2.2.2.1 Freezing Rate.....	19
2.2.2.2 Impurity Size, Shape, and Nature.....	20
2.2.2.3 Impurity Concentration.....	22

2.2.2.4 Presence of Air.....	23
2.2.2.5 Effect of Stirring.....	24
2.2.2.6 Rate and Method of Thawing.....	24
2.2.2.7 Method of Freezing.....	25
2.2.2.8 Inorganic Electrolytes.....	25
2.2.2.9 Liquid Depth.....	26
2.2.2.10 Time Frozen (Curing Time).....	26
2.2.3 Mathematical Models.....	27
3.0 Materials and Methods.....	29
3.1 Summary of Experimental Tests.....	29
3.2 Experimental Waters.....	29
3.2.1 Alkaline Extraction Stage Effluent.....	29
3.2.2 Alkaline Extraction Stage Membrane Concentrate.....	32
3.2.3 Alkaline Extraction Stage Concentrate Size Fractions.....	32
3.3 Experimental Water Preservation.....	32
3.3.1 Alkaline Extraction Stage Effluent.....	34
3.3.2 Alkaline Extraction Stage Membrane Concentrate....	34
3.4 Experimental Water Characterization.....	41
3.4.1 Alkaline Extraction Stage Membrane Concentrate.....	41
3.4.2 Alkaline Extraction Stage Effluent.....	48
3.5 Analytical and Investigative Methods.....	48
3.5.1 Wet Chemistry Analyses.....	48

3.5.1.1 Alkalinity Species.....	48
3.5.1.2 Chemical Oxygen Demand.....	48
3.5.1.3 Color.....	50
3.5.1.4 pH.....	50
3.5.1.5 Metals.....	50
3.5.1.6 Total Dissolved Solids.....	50
3.5.1.7 Total Suspended Solids.....	51
3.5.1.8 Turbidity.....	51
3.5.1.9 Volatile Suspended Solids.....	51
3.5.2 Scanning Electron Microscopy.....	51
3.5.2.1 Specimen Preparation.....	53
3.5.2.1.1 Ice Specimens.....	53
3.5.2.1.2 Filter Paper Specimens.....	63
3.5.3 Freezing Point Determination.....	63
3.5.3.1 Experimental Samples.....	63
3.5.3.2 Cryomatic Cryoscope Instrument.....	66
3.5.4 X-ray Photoelectron Spectroscopy.....	69
3.5.5 Size Fractionation by Ultrafiltration.....	69
3.6 Experimental Apparatus.....	70
3.6.1 Unidirectional Freezing Apparatus.....	70
3.6.2 Experimental Apparatus for Stability Tests and Sample Thawing.....	74
3.7 Experimental Procedures and Protocols.....	74
3.7.1 Sample Collection.....	74
3.7.1.1 Frozen Samples.....	74

3.7.1.2 Liquid Samples.....	76
3.7.2 Methods of Thawing.....	77
3.7.3 Melt Water Flow Pattern Dye Studies.....	78
3.7.4 Cycled Freeze-Thaw Experiments.....	79
3.8 Experimental Design.....	79
3.8.1 Selection of Measurement.....	79
3.8.1.1 Alkaline Extraction Stage Effluent.....	79
3.8.1.2 Alkaline Extraction Stage Membrane Concentrate.....	83
3.8.2 Factorial Design.....	88
3.9 Isotherm Data.....	91
3.9.1 Freezing Isotherm Data.....	91
3.9.1.1 Alkaline Extraction Stage Effluent.....	92
3.9.1.1.1 Initial Freezing Temperature -2 °C.	92
3.9.1.1.2 Initial Freezing Temperature -15 °C	92
3.9.1.1.3 Initial Freezing Temperature -25 °C	95
3.9.1.2 Alkaline Extraction Stage Membrane Concentrate.....	95
3.9.1.2.1 Initial Freezing Temperature -2 °C.	95
3.9.1.2.2 Initial Freezing Temperature -15 °C	95
3.9.1.2.3 Initial Freezing Temperature -25 °C	95
3.9.2 Thawing Isotherm Data.....	100
3.9.2.1 Alkaline Extraction Stage Effluent.....	100
3.9.2.2 Alkaline Extraction Stage Membrane Concentrate.....	103
4.0 Unidirectional Freeze-Thaw Studies.....	106

4.1 Procedures.....	106
4.2 Results and Discussion.....	106
4.2.1 Constituent Concentration and Removal by Freeze-Thaw.....	106
4.2.2 Process Variables and Relative Significance.....	113
4.2.2.1 Rate of Thawing.....	113
4.2.2.2 Storage Temperature and Storage Time.....	123
4.2.2.3 Liquid Depth.....	137
4.2.2.3.1 Alkaline Extraction Stage Membrane Concentrate.....	137
4.2.2.3.1.1 Initial Freezing Temperature -2 °C.....	143
4.2.2.3.1.2 Initial Freezing Temperature -15 °C.....	148
4.2.2.3.1.3 Initial Freezing Temperature -25 °C.....	153
4.2.2.3.2 Alkaline Extraction Stage Effluent...	156
4.2.2.3.2.1 Initial Freezing Temperature -2 °C.....	158
4.2.2.3.2.2 Initial Freezing Temperature -15 °C.....	161
4.2.2.3.2.3 Initial Freezing Temperature -25 °C.....	161
4.2.2.4 Freeze Concentration.....	165
4.2.2.4.1 Alkaline Extraction Stage Membrane Concentrate.....	167
4.2.2.4.2 Alkaline Extraction Stage Effluent.....	167
4.2.2.5 Cycled Freeze-thaw.....	171
4.2.2.5.1 Initial Freezing Temperature -2 °C..	175

4.2.2.5.2 Initial Freezing Temperature -15 °C	175
5.0 Scanning Electron Microscopy Studies.....	179
5.1 Procedure.....	179
5.1.1 Ice Specimen Collection.....	179
5.1.2 Method of Measurement.....	180
5.2 Cross Sectional Morphology of Frozen Concentrated Material.....	180
5.2.1 Alkaline Extraction Stage Membrane Concentrate....	181
5.2.1.1 Initial Freezing Temperature: -2 °C.....	181
5.2.1.1.1 Top Sample Location Results.....	183
5.2.1.1.2 Bottom Sample Location Results....	186
5.2.1.2 Initial Freezing Temperature: -15 °C.....	192
5.2.1.2.1 Top Sample Location Results.....	196
5.2.1.2.2 Bottom Sample Location Results....	199
5.2.1.3 Initial Freezing Temperature: -25 °C.....	204
5.2.1.3.1 Top Sample Location Results.....	204
5.2.1.3.2 Bottom Sample Location Results....	209
5.2.1.4 Initial Freezing Temperature Versus the Thickness of the Concentrated Material.	214
5.2.2 Alkaline Extraction Stage Effluent.....	218
5.2.2.1 Initial Freezing Temperature: -2 °C.....	218
5.2.2.1.1 Top Sample Location Results.....	220
5.2.2.2 Initial Freezing Temperature: -15 °C.....	224
5.2.2.2.1 Sample Location Results.....	224
5.2.2.3 Initial Freezing Temperature: -25 °C.....	229
5.2.2.3.1 Sample Location Results.....	229

5.2.2.4 Initial Freezing Temperature Versus the Thickness of the Concentrated Material.	233
5.3 Morphology of the Concentrated Material Following Thawing.....	233
5.3.1 Procedure.....	236
5.3.2 Results and Discussion.....	236
5.4 Changes in Concentrated Material Physical Properties With Respect to Concentration.....	249
5.4.1 Procedure.....	249
5.4.2 Results and Discussion.....	250
5.4.2.1 Initial Freezing Temperature: -2 °C...	250
5.4.2.2 Initial Freezing Temperature: -15 °C.	254
5.5 Morphology of the Concentrated Material for Membrane Concentrate Size Fractionated.....	277
5.5.1 Procedure.....	277
5.5.2 Results and Discussion.....	278
6.0 Postulated Mechanisms of Removal by Freeze-Thaw.....	290
6.1 Conceptual Model that Explains Effluent Freezing at the Initial Freezing Temperature -2 °C.....	294
6.2 Conceptual Model that Explains Effluent Freezing at the Initial Freezing Temperatures -15 °C and -25 °C.....	296
7.0 Concentrated Material Stability Studies.....	298
7.1 Procedure.....	298
7.2 Results and Discussion.....	298
7.2.1 Alkaline Extraction Stage Membrane Concentrate....	299
7.2.1.1 Control.....	306
7.2.1.2 Initial Freezing Temperature: -2 °C.....	306
7.2.1.3 Initial Freezing Temperature: -15 °C.....	311

7.2.2 Alkaline Extraction Stage Effluent.....	315
7.2.2.1 Control.....	317
7.2.2.2 Initial Freezing Temperature: -2 °C.....	317
7.2.2.3 Initial Freezing Temperature: -15 °C.....	322
8.0 Freeze Layering Studies.....	328
8.1 Procedure.....	328
8.2 Results and Discussion.....	328
8.2.1 Alkaline Extraction Stage Membrane Concentrate...	330
8.2.1.1 Initial Freezing Temperature: -2 °C.....	330
8.2.1.2 Initial Freezing Temperature: -15 °C.....	332
8.2.1.3 Initial Freezing Temperature: -25 °C.....	332
8.2.2 Alkaline Extraction Stage Effluent.....	335
8.2.2.1 Initial Freezing Temperature: -2 °C.....	335
8.2.2.2 Initial Freezing Temperature: -15 °C.....	337
8.2.2.3 Initial Freezing Temperature: -25 °C.....	337
9.0 Empirical Model Development.....	340
9.1 Factorial Design.....	340
9.2 Boundary Selection and Limitations.....	340
9.3 Analysis of Variance for Multiple Linear Regression	
Analysis for Each Experimental Water Type.....	344
9.3.1 Alkaline Extraction Stage Membrane Concentrate...	344
9.3.2 Alkaline Extraction Stage Effluent.....	346
9.4 Multiple Linear Regression Modeling.....	348
9.4.1 Alkaline Extraction Stage Membrane Concentrate...	348
9.4.2 Alkaline Extraction Stage Effluent.....	358

9.5 Model Testing.....	382
9.5.1 Alkaline Extraction Stage Membrane Concentrate...	382
9.5.2 Alkaline Extraction Stage Effluent.....	383
10.0 Overall Summary and Conclusions.....	386
11.0 Conceptual Engineering Design.....	396
12.0 Recommendations and Future Work.....	401
13.0 References.....	403
 APPENDIX A: Analysis Of Variance And Duncan Multiple Range Test Results - Unidirectional Freeze-Thaw Studies, Membrane Concentrate And Eop Effluent.....	408
 APPENDIX B: Analysis Of Variance And Duncan Multiple Range Test Results - Scanning Electron Microscopy Studies, Membrane Concentrate And Eop Effluent.....	423
 APPENDIX C: Stepwise Regression Analysis Stability Results - Membrane Concentrate.....	429
 APPENDIX D: Stepwise Regression Analysis Stability Results - Eop Effluent.....	432
 APPENDIX E: Stepwise Regression Analysis Results - Membrane Concentrate.....	435
 APPENDIX F: Stepwise Regression Analysis Results - Eop Effluent.....	441
 APPENDIX G: Composite Results - Membrane Concentrate.....	446
 APPENDIX H: Composite Results - Eop Effluent.....	456

LIST OF TABLES

Table	Description	Page
3.1	Summary of Experimental Tests.....	30
3.2	Experimental Water Types.....	31
3.3	Ultrafiltration Pilot Plant Design Specifications.....	35
3.4	Chemical Composition of the Alkaline Extraction Stage Effluent.....	47
3.5	Chemical Composition of the Alkaline Extraction Stage Membrane Concentrate.....	49
3.6	JSM-6301F Scanning Electron Microscope Specifications.....	52
3.7	Summary of Statistical Data Comparing the Sample Means of Calculated and Measured Color in the Top 70 % Liquid Volume Using the Paired t-test.....	84
3.8	Summary of Statistical Data Comparing the Sample Means of Calculated and Measured Color in the Top 70 % Liquid Volume Using the Paired t-test.....	89
3.9	2 ⁴ Factorial Design Matrix for the Alkaline Extraction Stage Membrane Concentrate.....	90
3.10	2 ⁴ Factorial Design Matrix for the Alkaline Extraction Stage Effluent.....	90
3.11	Fixed Variables Applied in Each Factorial Design.....	90
3.12	Thawing Times for Eop Effluent Thawed Predominantly From the Bottom Up Between the Temperature Range 4 °C to 24 °C.....	101
3.13	Thawing Times for Eop Effluent Thawed Predominantly From the Bottom Up at a Temperature of 24 °C for a Liquid Depth of 250 mm.....	102
3.14	Thawing Times for Membrane Concentrate Thawed Predominantly From the Bottom Up Between the Temperature Range 4 °C to 24 °C.....	104

3.15	Thawing Times for Membrane Concentrate Thawed Predominantly From the Bottom Up at a Temperature of 24 °C for a Liquid Depth of 250 mm.....	105
4.1	Tests of Hypotheses for the Different Storage Temperatures -2 °C and -15 °C for Membrane Concentrate Frozen at the Initial Freezing Temperature -2 °C (Thawed Bottom Up at 24 °C).....	129
4.2	Tests of Hypotheses for the Different Storage Temperatures -2 °C and -15 °C for Membrane Concentrate Frozen at the Initial Freezing Temperature -15 °C (Thawed Bottom Up at 24 °C).....	130
4.3	Tests of Hypotheses for the Different Storage Temperatures -2 °C and -15 °C for Membrane Concentrate Frozen at the Initial Freezing Temperature -2 °C (Thawed Bottom Up at 4 °C).....	131
4.4	Tests of Hypotheses for the Different Storage Temperatures -2 °C and -15 °C for Membrane Concentrate Frozen at the Initial Freezing Temperature -15 °C (Thawed Bottom Up at 4 °C).....	132
4.5	Tests of Hypotheses for the Different Storage Temperatures -2 °C and -15 °C for Eop Effluent Frozen at the Initial Freezing Temperature -2 °C (Thawed Bottom Up at 24 °C).....	138
4.6	Tests of Hypotheses for the Different Storage Temperatures -2 °C and -15 °C for Eop Effluent Frozen at the Initial Freezing Temperature -15 °C (Thawed Bottom Up at 24 °C).....	139
4.7	Tests of Hypotheses for the Different Storage Temperatures -2 °C and -15 °C for Eop Effluent Frozen at the Initial Freezing Temperature -2 °C (Thawed Bottom Up at 4 °C).....	140
4.8	Tests of Hypotheses for the Different Storage Temperatures -2 °C and -15 °C for Eop Effluent Frozen at the Initial Freezing Temperature -15 °C (Thawed Bottom Up at 4 °C).....	141
5.1	Data Representing the Average Thickness of the Concentrated Material Produced in the Top Sample Portion of the Ice Column for Membrane Concentrate Frozen at the Initial Freezing Temperature -2 °C, Sample Set #1.....	187

5.2	Data Representing the Average Thickness of the Concentrated Material Produced in the Top Sample Portion of the Ice Column for Membrane Concentrate Frozen at the Initial Freezing Temperature -2 °C, Sample Set #2.....	187
5.3	Data Representing the Average Thickness of the Concentrated Material Produced in the Top Sample Portion of the Ice Column for Membrane Concentrate Frozen at the Initial Freezing Temperature -2 °C, Sample Set #3.....	188
5.4	Summary of Statistical Data for Sample Sets 1, 2, and 3 (Initial Freezing Temperature -2 °C, Top Sample).....	188
5.5	Tests of Hypotheses for Sample Sets 1, 2, and 3 (Initial Freezing Temperature -2 °C, Top Sample).....	188
5.6	Summary of Statistical Data for Sample Sets 1, 2, and 3 (Initial Freezing Temperature -2 °C, Bottom Sample).....	191
5.7	Tests of Hypotheses for Sample Sets 1, 2, and 3 (Initial Freezing Temperature -2 °C, Bottom Sample).....	193
5.8	Tests of Hypotheses Concerning the Difference in Means Between the Top and Bottom Sample Locations (Initial Freezing Temperature -2 °C).....	193
5.9	Summary of Statistical Data Concerning the Distances Between the Concentrated Material as Observed in the Top and Bottom Ice Column for Membrane Concentrate Frozen at the Initial Freezing Temperature -15 °C.....	198
5.10	Summary of Statistical Data for Sample Sets 1, 2, and 3 (Initial Freezing Temperature -15 °C, Top Sample).....	198
5.11	Tests of Hypotheses for Sample Sets 1, 2, and 3 (Initial Freezing Temperature -15 °C, Top Sample).....	200
5.12	Summary of Statistical Data for Sample Sets 1, 2, and 3 (Initial Freezing Temperature -15 °C, Bottom Sample).....	203
5.13	Tests of Hypotheses Concerning the Difference in Means for Sample Sets 1, 2, and 3 (Initial Freezing Temperature -15 °C, Bottom Sample).....	205

5.14	Tests of Hypotheses Concerning the Difference in Means Between the Top and Bottom Sample Locations (Initial Freezing Temperature -15 °C).....	205
5.15	Summary of Statistical Data for Sample Sets 1, 2, and 3 (Initial Freezing Temperature -25 °C, Top Sample).....	210
5.16	Tests of Hypotheses Concerning the Difference in Means of Sample Sets 1, 2, and 3 (Initial Freezing Temperature -25 °C, Top Sample).....	213
5.17	Summary of Statistical Data for Sample Sets 1, 2, and 3 (Initial Freezing Temperature -25 °C, Bottom Sample).....	215
5.18	Tests of Hypotheses Concerning the Difference in Means of Sample Sets 1, 2, and 3 (Initial Freezing Temperature -25 °C, Bottom Sample).....	215
5.19	Tests of Hypotheses Concerning the Difference in Means Between the Top and Bottom Sample Locations (Initial Freezing Temperature -25 °C).....	215
5.20	Summary of Statistical Data Concerning the Cross Sectional Dimensions of the "Honey Comb" Pattern.....	221
5.21	Summary of Statistical Data for Sample Sets 1, 2, and 3 (Initial Freezing Temperature -2 °C, Top Sample).....	222
5.22	Tests of Hypotheses Concerning the Difference in Means Between Sample Sets 1, 2, and 3 (Initial Freezing Temperature -2 °C, Top Sample).....	222
5.23	Data Representing the Average Thickness of the Concentrated Material Produced in the Top Sample Portion of the Ice Column for Eop Effluent Frozen at the Initial Freezing Temperature 15 °C, Sample Set #1.....	226
5.24	Data Representing the Average Thickness of the Concentrated Material Produced in the Top Sample Portion of the Ice Column for Eop Effluent Frozen at the Initial Freezing Temperature 15 °C, Sample Set #2.....	226
5.25	Data Representing the Average Thickness of the Concentrated Material Produced in the Top Sample Portion of the Ice Column for Eop Effluent Frozen at the Initial Freezing Temperature 15 °C, Sample Set #3.....	227

5.26	Summary of Statistical Data for Sample Sets 1, 2, and 3 (Initial Freezing Temperature -15 °C, Top Sample).....	227
5.27	Tests of Hypotheses Concerning the Difference in Means Between Sample Sets 1, 2, and 3 (Initial Freezing Temperature -15 °C, Top Sample).....	227
5.28	Summary of Statistical Data for Sample Sets 1, 2, and 3 (Initial Freezing Temperature -25 °C, Top Sample).....	232
5.29	Tests of Hypotheses Concerning the Difference in Means Between Sample Sets 1, 2, and 3 (Initial Freezing Temperature -25 °C, Top Sample).....	232
5.30	Summary of Statistical Data for Sample Sets 1, 2, and 3 Combined (Initial freezing Temperature -25 °C, Top Sample).....	252
5.32	Summary of Data Showing the Measure of Dispersion of the Concentrated Material Thickness for Membrane Concentrate Diluted by 66 % and Frozen at the Initial Freezing Temperature -2 °C.....	264
5.33	Summary of Statistical Data Concerning the Concentrated Material Thickness for Different Dilutions of Membrane Concentrate Frozen at the Initial Freezing Temperature -2 °C....	275
5.34	Freezing Point Measurements for the Diluted Membrane Concentrate Solutions.....	275
5.35	Average Percent Color Removals in the Top 70 % Liquid Fraction for Various Dilutions of Membrane Concentrate Frozen Unidirectionally (Initial Freezing Temperature -2 °C and Thawed bottom up at 24 °C).....	279
5.36	Chemical Composition of the Membrane Concentrate and its Low and High Molecular Weight Fractions.....	279
7.1	Best Multiple Linear Regression Model as Determined by Stepwise Regression Representing the Desired Drain Time to Begin Collection of the Treated Effluent for Membrane Concentrate Treated by Freeze-Thaw.....	302
7.2	Change in Treated Effluent Color Concentration with Respect to Time for Membrane Concentrate Left to Stand Undisturbed Following Freeze-Thaw (Initial Freezing Temperature -2 °C, Thaw Bottom-up at 24 °C).....	314

7.3	Change in Treated Effluent Color Concentration with Respect to Time for Membrane Concentrate Left to Stand Undisturbed Following Freeze-Thaw (Initial Freezing Temperature -15 °C, Thaw Bottom-up at 24 °C).....	314
7.4	Best Multiple Linear Regression Model as Determined by Stepwise Regression Representing the Desired Drain Time to Begin Collection of the Treated Effluent for Eop Effluent Treated by Freeze-Thaw.....	316
7.5	Change in Treated Effluent Color Concentration with Respect to Time for Eop Effluent Left to Stand Undisturbed Following Freeze-Thaw (Initial Freezing Temperature -2 °C, Thaw Bottom-up at 24 °C).....	327
7.6	Change in Treated Effluent Color Concentration with Respect to Time for Eop Effluent Left to Stand Undisturbed Following Freeze-Thaw (Initial Freezing Temperature -15 °C, Thaw Bottom-up at 24 °C).....	327
9.1	Analysis of Variance Table for Membrane Concentrate Frozen and Thawed Under Different Freeze-Thaw Conditions.....	345
9.2	Analysis of Variance Table for Eop Effluent Frozen and Thawed Under Different Freeze-Thaw Conditions.....	347
9.3	Multiple Linear Regression Model for Prediction of the Color Concentration in the Top 70 % Liquid Fraction of Membrane Concentrate Treated by Freeze-Thaw.....	349
9.4	Best Multiple Linear Regression Model as Determined by Stepwise Regression for Prediction of the Color Concentration in the Top 70 % Liquid Fraction of Membrane Concentrate Treated by Freeze-Thaw.....	359
9.5	Multiple Linear Regression Model for Prediction of the Color Concentration in the Top 70 % Liquid Fraction of Eop Effluent Treated by Freeze-Thaw.....	367
9.6	Best Multiple Linear Regression Model as Determined by Stepwise Regression for Prediction of the Color Concentration in the Top 70 % Liquid Fraction of Eop Effluent Treated by Freeze-Thaw.....	375
9.7	Prediction of New Observations Using the Best Regression Model Developed From the Membrane Concentrate.....	384

9.8	Prediction of New Observations Using the Best Regression Model Developed From the Eop Data.....	385
-----	--	-----

LIST OF FIGURES

Figure	Description	Page
3.1	New Logic International V-Sep Ultrafiltration Pilot Plant.....	33
3.2	Change in Chemical Oxygen Demand with respect to Storage Time for the Alkaline Extraction Stage Effluent.....	36
3.3	Change in Color with respect to Storage Time for the Alkaline Extraction Stage Effluent.....	37
3.4	Change in pH with respect to Storage Time for the Alkaline Extraction Stage Effluent.....	38
3.5	Change in Total Alkalinity with respect to Storage Time for the Alkaline Extraction Stage Effluent.....	39
3.6	Change in Total Dissolved Solids with respect to Storage Time for the Alkaline Extraction Stage Effluent.....	40
3.7	Change in Chemical Oxygen Demand with respect to Storage Time for the Alkaline Extraction Stage Membrane Concentrate.....	42
3.8	Change in Color with respect to Storage Time for the Alkaline Extraction Stage Membrane Concentrate.....	43
3.9	Change in pH with respect to Storage Time for the Alkaline Extraction Stage Membrane Concentrate.....	44
3.10	Change in Total Alkalinity with respect to Storage Time for the Alkaline Extraction Stage Membrane Concentrate.....	45
3.11	Change in Total Dissolved Solids with respect to Storage Time for the Alkaline Extraction Stage Membrane Concentrate.....	46
3.12	High Magnification Electron Microscope Image of a Fractured Concentrated Material Edge Prior to Sublimation for Membrane Concentrate Frozen at the Initial Freezing Temperature -2 °C (Photo #1).....	55

3.13	High Magnification Electron Microscope Image of a Fractured Concentrated Material Edge Prior to Sublimation for Membrane Concentrate Frozen at the Initial Freezing Temperature -2 °C (Photo #2).....	56
3.14	Extreme High Magnification Electron Microscope Image of a Fractured Concentrated Material Edge Showing its Pore Morphology for Membrane Concentrate Frozen at the Initial Freezing Temperature -2 °C.....	58
3.15	Electron Microscope Photograph of a Fractured Ice Specimen Surface Produced by Freezing Distilled Water at the Initial Freezing Temperature -15 °C.....	59
3.16	High Magnification Electron Microscope Image Showing the Surface Morphology of Frozen Distilled Water.....	60
3.17	Electron Microscope Photograph of a Fractured Ice Specimen Surface Produced by Instantaneously Freezing Membrane Concentrate in Liquid Nitrogen.....	61
3.18	High Magnification Electron Microscope Image of a Fractured Concentrated Material Edge Produced by Instantaneously Freezing Membrane Concentrate in Liquid Nitrogen.....	62
3.19	Electron Microscope Photograph of a Clean Membrane Filter Paper Surface.....	64
3.20	High Magnification Electron Microscope Image of a Clean Filter Paper Surface Showing its Pore Morphology.....	65
3.21	Plot of Freezing Point With Respect to Different Concentration Strengths of Membrane Concentrate	67
3.22	Plot of Freezing Point With Respect to Different Concentration Strengths of Eop Effluent.....	68
3.23	Unidirectional Freezing Apparatus.....	71
3.24	Plot Showing the Comparison of the Freezing Curves for Each Experimental Apparatus Representing the Freezing of City of Edmonton Drinking Water at the Initial Freezing Temperature -15 °C.....	73
3.25	Experimental Thawing and Stability Apparatus.....	75

3.26	Plot Correlating Color to Chemical Oxygen Demand for Eop Effluent Treated by Freeze-Thaw Under Different Freezing and Thawing Conditions.....	80
3.27	Plot Correlating Color to Total Alkalinity for Eop Effluent Treated by Freeze-Thaw Under Different Freezing and Thawing Conditions.....	81
3.28	Plot Correlating Color to Total Dissolved Solids for Eop Effluent Treated by Freeze-Thaw Under Different Freezing and Thawing Conditions.....	82
3.29	Plot Correlating Color to Chemical Oxygen Demand for Membrane Concentrate Treated by Freeze-Thaw Under Different Freezing and Thawing Conditions.....	85
3.30	Plot Correlating Color to Total Alkalinity for Membrane Concentrate Treated by Freeze-Thaw Under Different Freezing and Thawing Conditions.....	86
3.31	Plot Correlating Color to Total Dissolved Solids for Membrane Concentrate Treated by Freeze-Thaw Under Different Freezing and Thawing Conditions.....	87
3.32	Freezing Curve Representative of Freezing Eop Effluent at the Initial Freezing Temperature -2 °C.....	93
3.33	Freezing Curve Representative of Freezing Eop Effluent at the Initial Freezing Temperature -15 °C.....	94
3.34	Freezing Curve Representative of Freezing Eop Effluent at the Initial Freezing Temperature -25 °C.....	96
3.35	Freezing Curve Representative of Freezing Membrane Concentrate at the Initial Freezing Temperature -2 °C.....	97
3.36	Freezing Curve Representative of Freezing Membrane Concentrate at the Initial Freezing Temperature -15 °C.....	98
3.37	Freezing Curve Representative of Freezing Membrane Concentrate at the Initial Freezing Temperature -25 °C.....	99
4.1	Plot of Average Percent Color Removal in the Top 70 % Liquid Volume with Respect to Initial Freezing Temperature for Membrane Concentrate Thawed Top Down and Bottom Up at 24 °C Immediately After Being Frozen.....	102

4.2	Plot of Average Percent Color Removal in the Top 70 % Liquid Volume with Respect to Initial Freezing Temperature for Eop Effluent Thawed Top Down and Bottom Up at 24 °C Immediately After Being Frozen.....	108
4.3	Plot of Average Percent Color Removal in the Top 70 % Liquid Volume with Respect to Material Thickness (Top Sample Specimens) for Membrane Concentrate Thawed Top Down and Bottom Up at 24 °C Immediately After Being Frozen.....	111
4.4	Plot of Average Percent Color Removal in the Top 70 % Liquid Volume with Respect to Material Thickness (Top Sample Specimens) for Eop Effluent Thawed Top Down and Bottom Up at 24 °C Immediately After Being Frozen.....	112
4.5	Plot of Average Percent Color Removal in the Top 70 % Liquid Volume with Respect to Thawing Temperature for Membrane Concentrate Thawed Top Down and Bottom Up for Different Initial Freezing Temperatures.....	114
4.6	Plot of Average Percent Color Removal in the Top 70 % Liquid Volume with Respect to Thawing Temperature for Eop Effluent Thawed Top Down and Bottom Up for Different Initial Freezing Temperatures.....	115
4.7	Plot of Average Percent Color Removal in the Top 70 % Liquid Volume with Respect to Initial Freezing Temperature for Membrane Concentrate Thawed Top Down and Bottom Up at 24 °C.....	116
4.8	Plot of Average Percent Color Removal in the Top 70 % Liquid Volume with Respect to Initial Freezing Temperature for Eop Effluent Thawed Top Down and Bottom Up at 24 °C.....	118
4.9	Melt Water Flow Pattern As Observed in Dye Studies in Melting Ice From the Bottom Up at 24 °C.....	119
4.10	Melt Water Flow Pattern As Observed in Dye Studies in Melting Ice From the Bottom Up at 4 °C.....	120
4.11	Melt Water Flow Pattern As Observed in Dye Studies in Melting Ice From the Top Down at 24 °C.....	122

4.12	Plot of Percent Color Removal with Respect to Storage Time and Storage Temperature for Membrane Concentrate Frozen at the Initial Freezing Temperature -2 °C (Thawed Bottom Up at 24 °C).....	124
4.13	Plot of Percent Color Removal with Respect to Storage Time and Storage Temperature for Membrane Concentrate Frozen at the Initial Freezing Temperature -15 °C (Thawed Bottom Up at 24 °C).....	125
4.14	Plot of Percent Color Removal with Respect to Storage Time and Storage Temperature for Membrane Concentrate Frozen at the Initial Freezing Temperature -2 °C (Thawed Bottom Up at 4 °C).....	126
4.15	Plot of Percent Color Removal with Respect to Storage Time and Storage Temperature for Membrane Concentrate Frozen at the Initial Freezing Temperature -15 °C (Thawed Bottom Up at 4 °C).....	127
4.16	Plot of Percent Color Removal with Respect to Storage Time and Storage Temperature for Eop Effluent Frozen at the Initial Freezing Temperature -2 °C (Thawed Bottom Up at 24 °C).....	133
4.17	Plot of Percent Color Removal with Respect to Storage Time and Storage Temperature for Eop Effluent Frozen at the Initial Freezing Temperature -15 °C (Thawed Bottom Up at 24 °C).....	134
4.18	Plot of Percent Color Removal with Respect to Storage Time and Storage Temperature for Eop Effluent Frozen at the Initial Freezing Temperature -2 °C (Thawed Bottom Up at 4 °C).....	135
4.19	Plot of Percent Color Removal with Respect to Storage Time and Storage Temperature for Eop Effluent Frozen at the Initial Freezing Temperature -15 °C (Thawed Bottom Up at 4 °C).....	136
4.20	Color Distribution with Respect to Depth for Frozen Membrane Concentrate and for Concentrate Thawed Top Down and Bottom Up at a Thawing Temperature of 24 °C (Initial Freezing Temperature of -2 °C).....	144

4.21	Color Distribution with Respect to Depth for Membrane Concentrate Frozen to Different Temperatures and Thawed Bottom Up at a Thawing Temperature of 24 °C (Initial Freezing Temperature of -2 °C).....	146
4.22	Comparison of Color Distributions with Respect to Depth for Membrane Concentrate of Different Liquid Depths Frozen at the Initial Freezing Temperature -2 °C and Thawed Bottom Up at a Temperature of 24 °C.....	147
4.23	Color Distribution with Respect to Depth for Frozen Membrane Concentrate and for Concentrate Thawed Top Down and Bottom Up at a Thawing Temperature of 24 °C (Initial Freezing Temperature of -15 °C).....	149
4.24	Color Distribution with Respect to Depth for Membrane Concentrate Frozen to Different Temperatures and Thawed Bottom Up at a Thawing Temperature of 24 °C (Initial Freezing Temperature of -15 °C).....	151
4.25	Color Distribution with Respect to Depth for Completely and Partially Frozen Membrane Concentrate Thawed Bottom Up at a Thawing Temperature of 24 °C (Initial Freezing Temperature of -15 °C).....	152
4.26	Comparison of Color Distributions with Respect to Depth for Membrane Concentrate of Different Liquid Depths Frozen at the Initial Freezing Temperature -15 °C and Thawed Bottom Up at a Temperature of 24 °C.....	154
4.27	Color Distribution with Respect to Depth for Frozen Membrane Concentrate and for Concentrate Thawed Top Down and Bottom Up at a Thawing Temperature of 24 °C (Initial Freezing Temperature of -25 °C).....	155
4.28	Comparison of Color Distributions with Respect to Depth for Membrane Concentrate of Different Liquid Depths Frozen at the Initial Freezing Temperature -25 °C and Thawed Bottom Up at a Temperature of 24 °C.....	157
4.29	Color Distribution with Respect to Depth for Frozen Eop Effluent and for Effluent Thawed Top Down and Bottom Up at a Thawing Temperature of 24 °C (Initial Freezing Temperature of -2 °C).....	159

4.30	Comparison of Color Distributions with Respect to Depth for Eop Effluent of Different Liquid Depths Frozen at the Initial Freezing Temperature -2 °C and Thawed Bottom Up at a Temperature of 24 °C.....	160
4.31	Color Distribution with Respect to Depth for Frozen Eop Effluent and for Effluent Thawed Top Down and Bottom Up at a Thawing Temperature of 24 °C (Initial Freezing Temperature of -15 °C).....	162
4.32	Comparison of Color Distributions with Respect to Depth for Eop Effluent of Different Liquid Depths Frozen at the Initial Freezing Temperature -15 °C and Thawed Bottom Up at a Temperature of 24 °C.....	163
4.33	Color Distribution with Respect to Depth for Frozen Eop Effluent and for Effluent Thawed Top Down and Bottom Up at a Thawing Temperature of 24 °C (Initial Freezing Temperature of -25 °C).....	164
4.34	Comparison of Color Distributions with Respect to Depth for Eop Effluent of Different Liquid Depths Frozen at the Initial Freezing Temperature -25 °C and Thawed Bottom Up at a Temperature of 24 °C.....	166
4.35	Plot of Average Percent Color Removal in the Top 70 % Liquid Volume with Respect to Thawing Temperature for Frozen and Thawed Membrane Concentrate Frozen at the Initial Freezing Temperature -2 °C.....	168
4.36	Plot of Average Percent Color Removal in the Top 70 % Liquid Volume with Respect to Thawing Temperature for Frozen and Thawed Membrane Concentrate Frozen at the Initial Freezing Temperature -15 °C.....	167
4.37	Plot of Average Percent Color Removal in the Top 70 % Liquid Volume with Respect to Thawing Temperature for Frozen and Thawed Membrane Concentrate Frozen at the Initial Freezing Temperature -25 °C.....	170
4.38	Plot of Average Percent Color Removal in the Top 70 % Liquid Volume with Respect to Thawing Temperature for Frozen and Thawed Eop Effluent Frozen at the Initial Freezing Temperature -2 °C.....	172

4.39	Plot of Average Percent Color Removal in the Top 70 % Liquid Volume with Respect to Thawing Temperature for Frozen and Thawed Eop Effluent Frozen at the Initial Freezing Temperature -15 °C.....	173
4.40	Plot of Average Percent Color Removal in the Top 70 % Liquid Volume with Respect to Thawing Temperature for Frozen and Thawed Eop Effluent Frozen at the Initial Freezing Temperature -25 °C.....	174
4.41	Plot of Average Percent Color Removal in Various Liquid Fractions with Respect to the Number of Freeze-thaw Cycles for Membrane Concentrate Frozen at the Initial Freezing Temperature -2 °C.....	176
4.42	Plot of Average Percent Color Removal in Various Liquid Fractions with Respect to the Number of Freeze-thaw Cycles for Membrane Concentrate Frozen at the Initial Freezing Temperature -15 °C.....	178
5.1	High Magnification Electron Microscope Image of the Concentrated Material Prior to Sublimation for Membrane Concentrate Frozen at the Initial Freezing Temperature -2 °C....	182
5.2	Electron Microscope Photograph of the Concentrated Material Contained Within the Ice Matrix for an Ice Specimen Collected from the Top Ice Column Portion for Membrane Concentrate Frozen at the Initial Freezing Temperature -2 °C.....	184
5.3	Electron Microscope Photograph of the Concentrated Material Contained Within the Ice Matrix for an Ice Specimen Collected from the Bottom Ice Column Portion for Membrane Concentrate Frozen at the Initial Freezing Temperature -2 °C....	185
5.4	Collection of High Magnification Electron Microscope Images of Fractured Concentrated Material Edges Produced by Freezing Membrane Concentrate at the Initial Freezing Temperature -2 °C (Top Sample Portion).....	189
5.5	Data Representing the Average Thickness of the Concentrated Material Produced in the Bottom Sample Portion of the Ice Column for Membrane Concentrate Frozen at the Initial Freezing Temperature -2 °C, Sample Set #1.....	190

5.6	Data Representing the Average Thickness of the Concentrated Material Produced in the Bottom Sample Portion of the Ice Column for Membrane Concentrate Frozen at the Initial Freezing Temperature -2 °C, Sample Set #2.....	190
5.7	Data Representing the Average Thickness of the Concentrated Material Produced in the Bottom Sample Portion of the Ice Column for Membrane Concentrate Frozen at the Initial Freezing Temperature -2 °C, Sample Set #3.....	191
5.8	Collection of High Magnification Electron Microscope Images of Fractured Concentrated Material Edges Produced by Freezing Membrane Concentrate at the Initial Freezing Temperature -2 °C (Bottom Sample Portion).....	194
5.9	Collection of Electron Microscope Photographs of Concentrated Material Contained Within the Ice Matrix for Ice Specimens Collected from the Top and Bottom Ice Column Portions for Membrane Concentrate Frozen at the Initial Freezing Temperature -15 °C.....	195
5.10	Data Representing the Average Thickness of the Concentrated Material Produced in the Top Sample Portion of the Ice Column for Membrane Concentrate Frozen at the Initial Freezing Temperature -15 °C, Sample Set #1.....	197
5.11	Data Representing the Average Thickness of the Concentrated Material Produced in the Top Sample Portion of the Ice Column for Membrane Concentrate Frozen at the Initial Freezing Temperature -15 °C, Sample Set #2.....	197
5.12	Data Representing the Average Thickness of the Concentrated Material Produced in the Top Sample Portion of the Ice Column for Membrane Concentrate Frozen at the Initial Freezing Temperature -15 °C, Sample Set #3.....	200
5.13	Collection of High Magnification Electron Microscope Images of Fractured Concentrated Material Edges Produced by Freezing Membrane Concentrate at the Initial Freezing Temperature -15 °C (Top Sample Portion).....	201
5.14	Data Representing the Average Thickness of the Concentrated Material Produced in the Bottom Sample Portion of the Ice Column for Membrane Concentrate Frozen at the Initial Freezing Temperature -15 °C, Sample Set #1.....	202

5.15	Data Representing the Average Thickness of the Concentrated Material Structures Produced in the Bottom Sample Portion of the Ice Column for Membrane Concentrate Frozen at the Initial Freezing Temperature -15 °C, Sample Set #2.....	202
5.16	Data Representing the Average Thickness of the Concentrated Material Produced in the Bottom Sample Portion of the Ice Column for Membrane Concentrate Frozen at the Initial Freezing Temperature -15 °C, Sample Set #3.....	203
5.17	Collection of High Magnification Electron Microscope Images of Fractured Concentrated Material Edges Produced by Freezing Membrane Concentrate at the Initial Freezing Temperature -15 °C (Bottom Sample Portion).....	206
5.18	Electron Microscope Photograph of Concentrated Material Contained Within the Ice Matrix for Ice Specimens Collected from the Top and Bottom Ice Column Portions for Membrane Concentrate Frozen at the Initial Freezing Temperature -25 °C.....	207
5.19	Data Representing the Average Thickness of the Concentrated Material Produced in the Top Sample Portion of the Ice Column for Membrane Concentrate Frozen at the Initial Freezing Temperature -25 °C, Sample Set #1.....	208
5.20	Data Representing the Average Thickness of the Concentrated Material Produced in the Top Sample Portion of the Ice Column for Membrane Concentrate Frozen at the Initial Freezing Temperature -25 °C, Sample Set #2.....	208
5.21	Data Representing the Average Thickness of the Concentrated Material Produced in the Top Sample Portion of the Ice Column for Membrane Concentrate Frozen at the Initial Freezing Temperature -25 °C, Sample Set #3.....	210
5.22	Collection of High Magnification Electron Microscope Images of Fractured Concentrated Material Edges Produced by Freezing Membrane Concentrate at the Initial Freezing Temperature -25 °C (Top Sample Portion).....	211

5.23	Data Representing the Average Thickness of the Concentrated Material Produced in the Bottom Sample Portion of the Ice Column for Membrane Concentrate Frozen at the Initial Freezing Temperature -25 °C, Sample Set #1.....	212
5.24	Data Representing the Average Thickness of the Concentrated Material Produced in the Bottom Sample Portion of the Ice Column for Membrane Concentrate Frozen at the Initial Freezing Temperature -25 °C, Sample Set #2.....	212
5.25	Data Representing the Average Thickness of the Concentrated Material Produced in the Bottom Sample Portion of the Ice Column for Membrane Concentrate Frozen at the Initial Freezing Temperature -25 °C, Sample Set #3.....	213
5.26	Collection of High Magnification Electron Microscope Images of Fractured Concentrated Material Edges Produced by Freezing Membrane Concentrate at the Initial Freezing Temperature -25 °C (Bottom Sample Portion).....	216
5.27	Plot of Concentrated Material Thickness with Respect to Initial Freezing Temperature for Alkaline Extraction Stage Membrane Concentrate.....	217
5.28	Electron Microscope Photograph of Concentrated Material Contained Within the Ice Matrix for an Ice Specimen Collected from the Top Ice Column Portion for Eop Effluent Frozen at the Initial Freezing Temperature -2 °C.....	219
5.29	Data Representing the Average Thickness of the Concentrated Material Produced in the Top Sample Portion of the Ice Column for Eop Effluent Frozen at the Initial Freezing Temperature -2 °C, Sample Set #1.....	221
5.30	Data Representing the Average Thickness of the Concentrated Material Produced in the Top Sample Portion of the Ice Column for Eop Effluent Frozen at the Initial Freezing Temperature -2 °C, Sample Set #2.....	221
5.31	Data Representing the Average Thickness of the Concentrated Material Produced in the Top Sample Portion of the Ice Column for Eop Effluent Frozen at the Initial Freezing Temperature -2 °C, Sample Set #3.....	222

5.32	Collection of High Magnification Electron Microscope Images of Fractured Concentrated Material Edges Produced by Freezing Eop Effluent at the Initial Freezing Temperature -2 °C (Top Sample Portion).....	223
5.33	Electron Microscope Photograph of Concentrated Material Contained Within the Ice Matrix for an Ice Specimen Collected from the Top Ice Column Portion for Eop Effluent Frozen at the Initial Freezing Temperature -15 °C.....	225
5.34	Collection of High Magnification Electron Microscope Images of Fractured Concentrated Material Edges Produced by Freezing Eop Effluent at the Initial Freezing Temperature -15 °C (Top Sample Portion).....	228
5.35	Electron Microscope Photograph of Concentrated Material Contained Within the Ice Matrix for an Ice Specimen Collected from the Top Ice Column Portion for Eop Effluent Frozen at the Initial Freezing Temperature -25 °C.....	230
5.36	Data Representing the Average Thickness of the Concentrated Material Produced in the Top Sample Portion of the Ice Column for Eop Effluent Frozen at the Initial Freezing Temperature -25 °C, Sample Set #1.....	231
5.37	Data Representing the Average Thickness of the Concentrated Material Produced in the Top Sample Portion of the Ice Column for Eop Effluent Frozen at the Initial Freezing Temperature -25 °C, Sample Set #2.....	231
5.38	Data Representing the Average Thickness of the Concentrated Material Produced in the Top Sample Portion of the Ice Column for Eop Effluent Frozen at the Initial Freezing Temperature -25 °C, Sample Set #3.....	232
5.39	Collection of High Magnification Electron Microscope Images of Fractured Concentrated Material Edges Produced by Freezing Eop Effluent at the Initial Freezing Temperature -25 °C (Top Sample Portion).....	234
5.40	Plot of Average Concentrated Material Thickness with Respect to Initial Freezing Temperature for Eop Effluent.....	235

5.41	Electron Microscope Photograph Showing the Morphology of the Concentrated Material Retained of the Filter Paper After Thawing Membrane Concentrate Frozen at the Initial Freezing Temperature -15 °C.....	238
5.42	High Magnification Electron Microscope Image Showing the Morphology of the Concentrated Material Retained on the Filter Paper After Thawing Membrane Concentrate Frozen at the Initial Freezing Temperature -15 °C.....	239
5.43	High Magnification Electron Microscope Image Showing the Morphology of the Concentrated Material Retained on the Filter Paper After Thawing Membrane Concentrate Frozen at the Initial Freezing Temperature -15 °C (Extreme Close-up)...	240
5.44	High Magnification Electron Microscope Image Showing the Morphology of Concentrated Material Retained on the Filter Paper After Thawing Membrane Concentrate Frozen at the Initial Freezing Temperature -15 °C (Extreme Close-up)...	241
5.45	X-ray Defraction Results of Precipitate Found Associated with the Concentrated Material Found on Filter Paper Samples After the Thawing of Membrane Concentrate.....	242
5.46	Electron Microscope Photograph of a Filter Paper Surface to Which Untreated Membrane Concentrate was Applied.....	243
5.47	Electron Microscope Photograph of a Clean Filter Paper Sample - Control.....	244
5.48	Electron Microscope Photograph of Filter Paper Showing the Morphology of the Concentrated Material Retained on the Filter Paper After Thawing Membrane Concentrate Frozen at the Initial Freezing Temperature -2 °C.....	245
5.49	High Magnification Electron Microscope Image Showing the Morphology of the Concentrated Material Retained on the Filter Paper After Thawing Membrane Concentrate Frozen at the Initial Freezing Temperature -2 °C.....	246
5.50	High Magnification Electron Microscope Image Showing the Morphology of the Concentrated Material Retained After Thawing Membrane Concentrate Frozen at the Initial Freezing Temperature -2 °C (Extreme Close-up).....	247

5.51	Plot of Suspended Solids Concentration with Respect to Different Freeze-thaw Conditions for Membrane Concentrate...	248
5.52	Frequency Histogram Showing the Measure of Dispersion of the Concentrated Material Thickness for Membrane Concentrate Frozen at the Initial Freezing Temperature -2 °C....	251
5.53	Frequency Histogram Showing the Measure of Dispersion of the Concentrated Material Thickness for Membrane Concentrate Diluted by 50 % and Frozen at the Initial Freezing Temperature -2 °C.....	251
5.54	Plot of Average Concentrated Material Thickness Versus Percent Dilution for Different Concentration Strengths of Membrane Concentrate Frozen at the Initial Freezing Temperature -2 °C.....	253
5.55	High Magnification Electron Microscope Image of a Fractured Concentrated Material Edge Produced by Freezing Membrane Concentrate at the Initial Freezing Temperature -2 °C.....	255
5.56	High Magnification Electron Microscope Image of a Fractured Concentrated Material Edge Produced by Freezing Membrane Concentrate Diluted to 50 % at the Initial Freezing Temperature -2 °C.....	256
5.57	High Magnification Electron Microscope Image of a Fractured Concentrated Material Edge Produced by Freezing Membrane Concentrate Diluted to 66 % at the Initial Freezing Temperature -2 °C.....	257
5.58	High Magnification Electron Microscope Image of a Fractured Concentrated Material Edge Produced by Freezing Membrane Concentrate Diluted to 75 % at the Initial Freezing Temperature -2 °C.....	258
5.59	Electron Microscope Photograph of Concentrated Material Contained Within the Ice Matrix for an Ice Specimen Collected from the Top Ice Column Portion Produced by Freezing Membrane Concentrate Diluted to 50 % at the Initial Freezing Temperature -2 °C.....	259
5.60	Electron Microscope Photograph of Concentrated Material Contained Within the Ice Matrix for an Ice Specimen Collected from the Top Column Portion Produced by Freezing Membrane Concentrate Diluted to 75 % at the Initial Freezing Temperature -2 °C.....	260

5.61	Frequency Histogram Showing the Measure of Dispersion of the Concentrated Material Thickness for Membrane Concentrate Frozen at the Initial Freezing Temperature -15 °C..	262
5.62	Frequency Histogram Showing the Measure of Dispersion of the Concentrated Material Thickness for Membrane Concentrate Diluted by 50 % and Frozen at the Initial Freezing Temperature -15 °C.....	262
5.63	Frequency Histogram Showing the Measure of Dispersion of the Concentrated Material Thickness for Membrane Concentrate Diluted by 66 % and Frozen at the Initial Freezing Temperature -15 °C.....	263
5.64	Frequency Histogram Showing the Measure of Dispersion of the Concentrated Material Thickness for Membrane Concentrate Diluted by 75 % and Frozen at the Initial Freezing Temperature -15 °C.....	263
5.65	Plot of Percent Dilution Versus Average Concentrate Material Thickness (Initial Freezing Temperature -15, Top Sample).....	264
5.66	High Magnification Electron Microscope Image of a Fractured Concentrated Material Edge Produced by Freezing Membrane Concentrate at the Initial Freezing Temperature -15 °C.....	265
5.67	High Magnification Electron Microscope Image of a Fractured Concentrated Material Edge Produced by Freezing Membrane Concentrate Diluted to 50 % at the Initial Freezing Temperature -15 °C.....	266
5.68	High Magnification Electron Microscope Image of a Fractured Concentrated Material Edge Produced by Freezing Membrane Concentrate Diluted to 66 % at the Initial Freezing Temperature -15 °C.....	267
5.69	High Magnification Electron Microscope Image of a Fractured Concentrated Material Edge Produced by Freezing Membrane Concentrate Diluted to 75 % at the Initial Freezing Temperature -15 °C.....	268
5.70	High Magnification Electron Microscope Image of a Fractured Concentrated Material Edge Produced by Freezing Membrane Concentrate Diluted to 80 % at the Initial Freezing Temperature -15 °C.....	269

5.71	Electron Microscope Photograph of Fractured Ice Specimen Surface Produced by Freezing Membrane Concentrate Diluted to 50 % at the Initial Freezing Temperature -15 °C.....	271
5.72	Electron Microscope Photograph of Fractured Ice Specimen Surface Produced by Freezing Membrane Concentrate Diluted to 66 % at the Initial Freezing Temperature -15 °C.....	272
5.73	Electron Microscope Photograph of Fractured Ice Specimen Surface Produced by Freezing Membrane Concentrate Diluted to 75 % at the Initial Freezing Temperature -15 °C.....	273
5.74	Electron Microscope Photograph of Fractured Ice Specimen Surface Produced by Freezing Membrane Concentrate Diluted to 80 % at the Initial Freezing Temperature -15 °C.....	274
5.75	Electron Microscope Photograph of the Concentrated Material Structure Observed for the Above 5000 MW Fraction for Membrane Concentrate Frozen at the Initial Freezing Temperature -15 °C (Top Sample Portion).....	280
5.76	High Magnification Electron Microscope Image of the Concentrated Material Representative of the Above 5000 MW Fraction.....	281
5.77	Electron Microscope Photograph of the Concentrated Material Structure Observed for the Below 5000 MW Fraction for Membrane Concentrate Frozen at the Initial Freezing Temperature -15 °C (Top Sample Portion).....	282
5.78	High Magnification Electron Microscope Image of the Concentrated Material Representative of the Below 5000 MW Fraction.....	283
5.79	Electron Microscope Photograph of the Concentrated Material Structure Observed for the Above 5000 MW Fraction for Membrane Concentrate Frozen at the Initial Freezing Temperature -15 °C (Bottom Sample Portion).....	284
5.80	Electron Microscope Photograph of the Concentrated Material Structure Observed for the Below 5000 MW Fraction for Membrane Concentrate Frozen at the Initial Freezing Temperature -15 °C (Bottom Sample Portion).....	286
5.81	High Magnification Electron Microscope Image of the Concentrated Material Surface Morphology Representative of the Above 5000 MW Fraction (Bottom Sample Portion).....	287

5.82	High Magnification Electron Microscope Image of the Concentrated Material Surface Morphology Representative of the Below 5000 MW Fraction.....	288
5.83	High Magnification Electron Microscope Image of the Concentrated Material Surface Morphology Representative of the Membrane Concentrate (Bottom Sample Portion).....	289
6.1	Conceptual Model for High Strength Pulp Mill Effluent Freezing	291
6.2	Steps Describing the Development of the Concentrated Material Observed at the Initial Freezing Temperature -2 °C.....	295
6.3	Steps Describing the Development of the Concentrated Material Observed at the Initial Freezing Temperatures -15 °C and -25 °C.....	297
7.1	Plot of Residuals Against Estimated Time for Concentrate Stability Produced From Freeze-Thaw of Membrane Concentrate.....	303
7.2	Plot of Residuals Against Color Concentration Ratio for Concentrate Stability Produced From Freeze-Thaw of Membrane Concentrate.....	304
7.3	Plot of Residuals Against Initial Freezing Temperature for Concentrate Stability Produced From Freeze-Thaw of Membrane Concentrate.....	305
7.4	Change in Color Concentration in the Top, Middle, and Bottom Sample Portions of the Control Sample Over Time.....	307
7.5	Plot of Change in Color Concentration in the Top and Middle Sample Portions with Respect to Time for Membrane Concentrate Frozen at the Initial Freezing Temperature -2 °C, Thawed Bottom Up at 24 °C and Then Left to Stand Undisturbed at 24 °C.....	309
7.6	Plot of Change in Color Concentration in the Bottom Sample Portions with Respect to Time for Membrane Concentrate Frozen at the Initial Freezing Temperature -2 °C, Thawed Bottom Up at 24 °C and Then Left to Stand Undisturbed at 24 °C.....	310

7.7	Plot of Change in Color Concentration in the Top and Middle Sample Portions with Respect to Time for Membrane Concentrate Frozen at the Initial Freezing Temperature -15 °C, Thawed Bottom Up at 24 °C and Then Left to Stand Undisturbed at 24 °C.....	312
7.8	Plot of Change in Color Concentration in the Bottom Sample Portions with Respect to Time for Membrane Concentrate Frozen at the Initial Freezing Temperature -15 °C, Thawed Bottom Up at 24 °C and Then Left to Stand Undisturbed at 24 °C.....	313
7.9	Plot of Residuals Against Color Concentration Ratio for Concentrate Stability Produced From Freeze-Thaw of Eop Effluent.....	318
7.10	Plot of Residuals Against Initial Freezing Temperature for Concentrate Stability Produced From Freeze-Thaw of Eop Effluent.....	319
7.11	Plot of Residuals Against Estimated Time for Concentrate Stability Produced From Freeze-Thaw of Eop Effluent.....	320
7.12	Change in Color Concentration in the Top, Middle, and Bottom Sample Portions of the Control Sample Over Time.....	321
7.13	Plot of Change in Color Concentration in the Top and Middle Sample Portions with Respect to Time for Eop Effluent Frozen at the Initial Freezing Temperature -2 °C, Thawed Bottom Up at 24 °C and Then Left to Stand Undisturbed at 24 °C.....	323
7.14	Plot of Change in Color Concentration in the Bottom Sample Portions with Respect to Time for Eop Effluent Frozen at the Initial Freezing Temperature -2 °C, Thawed Bottom Up at 24 °C and Then Left to Stand Undisturbed at 24 °C.....	324
7.15	Plot of Change in Color Concentration in the Top and Middle Sample Portions with Respect to Time for Eop Effluent Frozen at the Initial Freezing Temperature -15 °C, Thawed Bottom Up at 24 °C and Then Left to Stand Undisturbed at 24 °C.....	325

7.16	Plot of Change in Color Concentration in the Bottom Sample Portions with Respect to Time for Eop Effluent Frozen at the Initial Freezing Temperature -15 °C, Thawed Bottom Up at 24 °C and Then Left to Stand Undisturbed at 24 °C.....	326
8.1	Plot Showing the Comparison Between Color Distributions for Membrane Concentrate Frozen in Single and Multiple Layers for Different Liquid Depths at the Initial Freezing Temperature -2 °C.....	331
8.2	Plot Showing the Comparison Between Color Distributions for Membrane Concentrate Frozen in Single and Multiple Layers for Different Liquid Depths at the Initial Freezing Temperature -15 °C.....	333
8.3	Plot Showing the Comparison Between Color Distributions for Membrane Concentrate Frozen in Single and Multiple Layers for Different Liquid Depths at the Initial Freezing Temperature -25 °C.....	334
8.4	Plot Showing the Comparison Between Color Distributions for Eop Effluent Frozen in Single and Multiple Layers for Different Liquid Depths at the Initial Freezing Temperature -2 °C.....	336
8.5	Plot Showing the Comparison Between Color Distributions for Eop Effluent Frozen in Single and Multiple Layers for Different Liquid Depths at the Initial Freezing Temperature -15 °C.....	338
8.6	Plot Showing the Comparison Between Color Distributions for Eop Effluent Frozen in Single and Multiple Layers for Different Liquid Depths at the Initial Freezing Temperature -25 °C.....	339
9.1	Normal Plot of Effects for the Regression Model Developed for the Membrane Concentrate.....	351
9.2	Plot of Residuals Against Estimated Color.....	352
9.3	Plot of Residuals Against Initial Freezing Temperature.....	353
9.4	Plot of Residuals Against Thawing Temperature.....	354
9.5	Plot of Residuals Against Storage Temperature.....	355
9.6	Plot of Residuals Against Storage Time.....	356

9.7	Normal Plot of Effects for the Revised Regression Model Developed for the Membrane Concentrate.....	360
9.8	Plot of Residuals Against Estimated Color for the Revised Model (Membrane Concentrate).....	361
9.9	Plot of Residuals Against the Independent Variable Storage Time for the Revised Model (Membrane Concentrate).....	362
9.10	Plot of Residuals Against the Independent Variable Thawing Temperature for the Revised Model (Membrane Concentrate)..<	363
9.11	Plot of Residuals Against the Independent Variable Storage Temperature for the Revised Model (Membrane Concentrate)..<	364
9.12	Plot of Residuals Against the Independent Variable Initial Freezing Temperature for the Revised Model (Membrane Concentrate).....	365
9.13	Normal Plot of Effects for the Regression Model Developed for the Eop Effluent.....	368
9.14	Plot of Residuals Against Estimated Color.....	369
9.15	Plot of Residuals Against Initial Freezing Temperature.....	370
9.16	Plot of Residuals Against Thawing Temperature.....	371
9.17	Plot of Residuals Against Storage Temperature.....	372
9.18	Plot of Residuals Against Storage Time.....	373
9.19	Normal Plot of Effects for the Revised Regression Model Developed for the Eop Effluent.....	376
9.20	Plot of Residuals Against Estimated Color for the Revised Model (Eop Effluent).....	377
9.21	Plot of Residuals Against the Independent Variable Storage Time for the Revised Model (Eop Effluent).....	378
9.22	Plot of Residuals Against the Independent Variable Thawing Temperature for the Revised Model (Eop Effluent).....	379
9.23	Plot of Residuals Against the Independent Variable Storage Temperature for the Revised Model (Eop Effluent).....	380

9.24	Plot of Residuals Against the Independent Variable Initial Freezing Temperature for the Revised Model (Eop Effluent).....	381
------	---	-----

GLOSSARY OF ABBREVIATIONS AND SYMBOLS

COD	chemical oxygen demand, mg/L
C₀	initial color concentration, CU
C_t	color concentration in the top 70 % liquid volume at time t, CU
C(x,t)	solute concentration as function of time and position relative to the crystal interface, mg/L
D	diffusion coefficient, cm²/sec
E_{op}	alkaline extraction stage effluent
G	crystal growth, cm/sec
ICP	inductively coupled plasma
k	solid-liquid partition coefficient
k₁	thermal conductivity of ice, J/(mm²)(sec)
K	constant, m⁴/sec
L	latent heat of freezing, J/g
P	probability
ΔT	freezing temperature of ice less the air temperature, °C
ø	total exposure time, sec
£	density of ice (91.7 g/mm²)
R	particle radius, m
s	sample variance
SEM	scanning electron microscopy
S_i	storage time, days
S_T	storage temperature, °C
TDS	total dissolved solids, mg/L

TSS	total suspended solids, mg/L
T	calculated t-Test value
t^*	steady state time characterization term, sec
t	ice sheet thickness, mm
t_D	time to drain supernatant after thawing, hrs
T_F	initial freezing temperature, °C
T_T	thawing temperature, °C
μ	sample mean
VSS	volatile suspended solids, mg/L
V	critical velocity, m/s
x	distance, m
∂	texture parameter
T_F	Initial Freezing Temperature, °C
T_T	Thawing Temperature, °C

1.0 INTRODUCTION

Color causing pollutants found present in the wastewaters of kraft pulp mills originate almost exclusively from the bleaching process. Although the pulp industry has markedly improved the quality of its effluents from the application of new technologies, they are still faced with the technical and economical challenges to reduce further the discharge of materials to the environment. To meet future effluent regulatory requirements, the industry has been evaluating innovative water management schemes involving both internal and end of pipe effluent treatment technologies. Significant research efforts are currently being directed towards the development and integration of zero liquid effluent technologies into mill treatment processes. Unproven at this time, the industry has been hesitant in adopting these new technologies partly because of the economic uncertainties surrounding them. As an alternative some facilities have opted to evaluate specialized treatment methods for only the high strength process streams, namely the bleachery effluents. Among the most promising is the application of membrane technology for treatment of the alkaline extraction stage effluent. The application of a physical separation process to concentrate the contaminants results in the production of smaller volumes of high concentration liquid wastes which in regards to their disposal offers several key advantages. The most obvious is affordability. Its reduced volume will likely make it easier and cheaper to treat and dispose of, which may ultimately make zero liquid effluent technologies more economically accessible.

Membrane technology is a physical separation process designed to split a given waste stream into two components, producing a permeate and a concentrate. The concentrate, containing a majority of the contaminants, is still in need of treatment and disposal. The disposal of membrane concentrates in a simple, cost effective manner has not been adequately addressed in the context of pulp mill operations. Of the possible solutions available, on-site incineration is preferred. However, on-site disposal by incineration of concentrates for large pulp mills would likely not be economical because of the large volumes of contaminated liquid. Under these circumstances the use of additional technologies or a more elaborate water management scheme would be prudent with the goal to further reduce the liquid volume of contaminated waste in need of treatment and disposal.

1.1 BACKGROUND

1.1.1 STATEMENT OF THE PROBLEM

The application of membrane technology does not eliminate the problem of waste disposal and therefore consideration of the disposal method for contaminated liquids is necessary. Its purpose is to reduce the volume of contaminated liquids to quantities that are more manageable and can be effectively disposed of on-site. For membrane technology to be adopted and used by the pulp industry it will have to be designed in the context of pulp mill operations whereby small volumes of membrane concentrates can be economically disposed of on-site. In the case of large pulp mills this may require designing the concentration process to consist of membrane technology and other cost effective treatment processes to

ensure small manageable volumes of contaminated liquids are produced. Among the possible complementary technologies available, a simple, cost effective method for treatment of membrane concentrates to further reduce the volumes of contaminated liquids involves using a freeze-thaw operation.

Natural freeze-thaw is well documented as a cost effective treatment method for conditioning and dewatering sludges. Little literature exists about the use of freeze-thaw as a method for concentrating for volume reduction liquid waste streams consisting primarily of complex dissolved and colloidal organics. Waste streams of this chemical composition that are treated by freezing methods are done so typically using freeze concentration.

Preliminary test results using mechanical freeze-thaw showed that liquid waste streams that are comprised of dissolved and colloidal organic material are amenable to mechanical coagulation, where freezing to concentrate and mechanically flocculate the organics sufficiently produces a settleable concentrated mass that can be effectively removed upon rapid thawing. So promising were the results that freeze-thaw conducted naturally was investigated as a simple, cost effective solution for treatment of high strength kraft pulp mill bleachery effluents.

1.1.2 HYPOTHESIS DEVELOPMENT

Initial laboratory work lead to the development of the research hypothesis that liquid waste streams comprised of complex dissolved/colloidal organics are amenable to mechanical flocculation and separation brought about by freeze-thaw. Membrane concentrates derived

from the alkaline extraction stage effluent with oxygen and hydrogen peroxide reinforcement (Eop) are complex organic aqueous liquids. Their treatment by freeze-thaw is believed to be primarily dependent on the transformations that occurs to the concentrate's colloidal and dissolved organic and inorganic constituents during freezing. Postulated is that during freezing the constituents are concentrated and mechanically flocculated into thin wafer-like structures to produce settleable masses that can be separated from the bulk solution under ideal thawing conditions. Separation efficiency is believed to be, in part, dependent on the freezing and thawing conditions, as well as on the degree of compression related flocculation that occurs during their time frozen. Based on initial studies, the concentrated mass produced during the freezing of membrane concentrates is very fragile and susceptible to break-up during thawing. Removal of this fragile concentrated material from the bulk solution is believed to be controlled predominantly by the rate at which this material is initially thawed to separate it from its ice matrix. Other factors of importance include particle interlocking resulting from mechanical compression, and the degree of disturbance to the concentrated mass during thawing. Optimum treatment conditions believed necessary to achieve high separation efficiencies involves slow freezing rates coupled with long storage times at cold temperatures followed with minimal disturbance to the concentrated material upon thawing. The mechanism responsible for and the resultant morphology of the concentrated material from the growth of ice crystals during solidification during slow freezing is believed to be critical in producing a concentrated material that is readably separated from the ice matrix during thawing. Long frozen periods at low temperatures are necessary to freeze as much as possible of the free

available water to mechanically compress the concentrated material into tightly, compact zones reducing the material's fragile nature and susceptibility to break-up during thawing. Finally, minimal disruption to the structural integrity of the concentrated material during thawing by the melt water flow is critical in achieving high separation efficiencies. The chemical composition of the Eop effluents is also believed to be important from the point of view that it must be amenable to mechanical coagulation. That is there occurs a physical transformation to the constituents which is in part, retained after thawing that will permit their removal. Equally important is the concentration present in the waste stream must be of sufficient strength to produce sufficient amounts of concentrated material that can be readily separated from the ice matrix during thawing.

Although there exists a substantial amount of literature on freeze separation of organic and inorganic aqueous systems, lacking is information on the morphological changes that occurs to the effluent's constituents during freezing and how these transformations directly relate to separation efficiency. This absence of information formed the basis of the second research hypothesis. Postulated is separation by freeze-thaw of aqueous liquids that are organic in nature are dependent not only on those parameters that enhance freeze separation, but also on those parameters that enhance thaw separation. Both groups of parameters are believed to be equally important in achieving high separation efficiencies.

1.1.3 RESEARCH DEVELOPMENT

Several specialized treatment options were investigated as part of this research study for treatment of Eop membrane concentrates. Initial tests were conducted to investigate ozonation and coagulation (cationic polymers only), separately and in combination. As part of the coagulation studies metal based coagulants were not considered because of the operational problems the resultant sludge would pose to the mill's incinerator contemplated for disposal of the waste constituents. This is in lue of the fact that alum and lime have been demonstrated as effective coagulants in removal of nearly all of the color from waste streams of this nature. Results from using ozonation and a cationic polymer were unfavourable. Little or no improvement in color reduction was measured in the alkaline extraction stage membrane concentrate treated separately with ozonation. Ozone dosages as high as 300 mg/L were trialed with the reported changes in color being below the detection limit. Likewise extremely high cationic polymer dosages, in excess of 1,500 mg/L, were required to obtain marginal reductions of less than 10 % in color by coagulation alone. Ozonation was also trialed in combination with coagulation, whereby concentrate samples were preozonated followed by coagulation and flocculation. Results from these tests were also unfavourable. Observed was low to moderate dosages of ozone (< 100 mg/L) and polymer (< 150 mg/L) produced no or little reduction (< 5 %) in color. Based on these results it became apparent that the use of cationic polymers to treat pulp mill membrane concentrates would not be economical and therefore technologies of this nature were not further investigated.

Freeze concentration was initially studied for concentration and separation of the constituents of membrane concentrates. The experimental technique employed was the method developed by Baker (1967). This technique consisted of mixing the membrane concentrate in a round bottom Pyrex flask submerged in a temperature controlled ice/salt bath. The problems observed, which are common for this method of freezing, related to the difficulty of separating the ice crystal from the solute. Small additions of a highly charged, high molecular weight polyamine (< 100 mg/L) to the membrane concentrate was reported to improved separation. However, at coagulant dosages above 100 mg/L the separation efficiency was observed to deteriorate regardless of having vigorously mixed the sample. Flash freezing was problematic, greatly reducing solute separation and recovery.

1.2 RESEARCH OBJECTIVES

The research study was developed to evaluate the natural freeze-thaw process as a simple, cost effective method for treatment of high strength kraft pulp mill effluents. The method is applicable for kraft pulp mills located in cold regions only. As part of this investigation, the study focused on the fundamentals of the process and the mechanisms responsible for concentration and removal of the effluent's dissolved/colloidal organic and inorganic constituents from its bulk solution during freeze-thaw. Specifically, the following objectives were defined as relevant to achieving the above goals:

1.2.1 PRIMARY OBJECTIVES

- 1) Evaluate freeze-thaw as a waste treatment process for alkaline extraction stage effluents and its membrane concentrates,
- 2) Characterize the frozen and thawed physical state properties of the concentrated material produced during freezing under different freeze-thaw conditions,
- 3) Postulate the mechanism(s) of removal for the concentrated material by freeze-thaw,
- 4) Identify those process variables that significantly affect treatment performance and whether they are controllable or non-controllable,
- 5) Determine the relative stability of the concentrated material removed by freeze-thaw under different freezing and thawing conditions; and
- 6) Develop empirical mathematical models that will predict treatment performance by freeze-thaw for treatment of Eop effluents and its concentrates.

1.2.2 SECONDARY OBJECTIVES

- 1) Discuss conceptual engineering design for the application of natural freeze-thaw for treatment of high strength kraft pulp mill effluents.

2.0 LITERATURE REVIEW

This chapter reviews the theory of freeze-thaw and the mechanisms responsible for concentration and separation with respect to different waste types. Research objectives that address freeze separation of organic-inorganic aqueous systems by freeze-thaw will be presented and discussed.

2.1 PULPING PROCESSES

The objective of a pulping operation is to separate the wood fibers by dissolving the lignin. The methods used vary depending on the type of wood and end quality requirements of the pulp. One of the most commonly used pulping methods is the kraft process. The kraft pulping process is of special interest, simply because it accounts for approximately 90 percent of U.S. woodpulp production. The process involves cooking woodchips, under pressure, in a solution of sodium sulfide and caustic soda. These chemicals dissolve most of the lignin to produce a woodpulp consisting primarily of cellulose fibers. Lignin is an amorphous substance that is partly aromatic in nature and contains methoxyl, aliphatic, and phenolic hydroxyl groups plus minor amounts of various aromatic acids in ester-like combination. The pulp then passes through a series of washing stages to remove and recover most of the dark cooking chemicals referred to as the black liquor. When kraft pulp is used to produce fine papers or white board grades it must be bleached. Bleaching involves a series of chemical treatments and extractions varying in number and sequence of steps, employing chlorine, caustic soda, hyochlorites, chlorine dioxide, and oxygen and hydrogen peroxide. The bleaching extracts released consist of both acidic and alkaline waste streams, with the

alkaline extraction stage effluent accounting for about 75 % of the color released from the bleach plant. The bleachery process is the principle contributor in the total amount of color released from both pulping and bleaching with the percentage between 80 to 90 % of the total color.

2.1.1 ALKALINE EXTRACTION STAGE EFFLUENT COMPOSITION

The color constituents of the alkaline extraction stage effluent consists of oxidized lignin fragments commonly referred to as "color bodies" (Bonsor et al., 1988; Cook et al., 1973). Color bodies consist of partially degraded lignin fragments and brown-colored materials which are complex mixtures of acidic polymers ranging in molecular weight from less than 300 to as high as 30,000. Also associated with this waste can be other colorless compounds with molecular weights ranging up to about 150,000. Color causing bodies with molecular weights around 5,600 are responsible for the largest portion of the color reading. The original lignin material, through oxidation and chlorination, loses most of its methoxyl and phenolic hydroxyl groups, gaining a high carbonyl and carboxyl content (Katuscak et al. 1971; Smith et al., 1976; Kovacs et al. 1986). Color bodies are aromatic in nature, possessing a negative charge and existing primarily as soluble sodium salts in aqueous solutions. The acidic groups (carboxyl and enolic) of the color bodies dissociate in water and form anionic sites to impel them into the colloidal or soluble state. For alkaline extraction stage effluents the acidic groups are more dissociated because of the high pH. As a result the system is more stable and the color intensity increased.

Color bodies are not easily biodegradable. In fact, color intensity has been found to increase during biological treatment.

2.2 FREEZE-THAW FOR TREATMENT OF MEMBRANE CONCENTRATES

Freeze-thaw is a method that is typically used to dewater and condition sludges. Well documented are the effects of freezing and thawing on the dewaterability of water and wastewater sludges. Poorly understood are the mechanisms by which freeze-thaw alters the dewaterability of high solids suspensions. Numerous attempts to commercialize the beneficial effect of natural freeze-thaw have not been largely successful (Vesilind and Martel, 1991). Unfortunately, natural freezing is perceived as unreliable or technically unfeasible for all but in the coldest climates. The systems that have been successful are those related to the treatment of sludges which depend largely on natural freezing and thawing in open or covered beds. The near-universal limited success in the commercialization of natural freeze-thaw has resulted in it being neglected over alternative technologies or methods such as freeze crystallization or freeze concentration as methods for treatment of industrial wastewaters. Consequently, the application of freeze-thaw as proposed in this study for the near natural treatment of high strength waste streams represents a new field of application for this technology.

2.2.1 FREEZE CONCENTRATION AND SEPARATION

The fundamental phenomenon of the interaction between a solute or suspended particle and the ice-water interface during freezing are described extensively below.

2.2.1.1 FREEZING OF PURE WATER

When water freezes, it changes its chemical structure, expands, and forms ice crystals. Unique among materials, water expands immediately before freezing, with its maximum density being $+3.96^{\circ}\text{C}$. Chalmers (1959) studied the freezing of water and stated that for each temperature there is a critical radius of curvature at which the ice and water are in equilibrium. The temperature is precisely zero degrees Celsius only when the surface of the ice is essentially flat. On corners that juts outward there are more loosely bound surface molecules per unit volume of ice, and the melting process tends to predominate. Conversely, at corners that extend inward the surface-to-volume relationship is reversed, and freezing is in the ascendant. It follows that the temperature is lower for a small sphere of ice than for a larger sphere.

2.2.1.2 FREEZING OF SOLUTIONS

Chalmers (1959) described ice formation as ice crystals growing from the addition of water molecules to its structure, in a manner similar to the construction of a brick wall. The structure of the ice crystal was found to have great regularity and symmetry. When a growing ice crystal comes in contact with impurities, it rejects them in favor of water molecules. Because of its highly organized structure ice crystals cannot accommodate other atoms or molecules without very severe local strain. To understand the theory of ice formation, it is useful to consider what is known of the distribution of an ideal solute ahead of a growing crystal interface. Smith et al. (1955) developed transport equations to describe the unidirectional crystal growth at rate G (cm/s) of a planar crystal interface into a solution

of an initial solute concentration C_0 . The dependent solute concentration, $C(x,t)$, as function of its time and position relative to the crystal interface is given below in equation (2.1).

$$\begin{aligned} C(x,t)/C_0 = & 1 + ((1-k)/2k) - (Gx/D)\text{erfc}1/2(1/Dt)^{-1/2}(x-Gt) \\ & -1/2\text{erfc}1/2(1/Dt)^{-1/2}(x+Gt) + ((2k-1)/2k) - (1-k)(G/D) \\ & (x+kGt)\text{erfc}1/2(1/Dt)^{-1/2}(x+(2k-1)Gt) \end{aligned} \quad (2.1)$$

D is the diffusion coefficient of the solute; k is the solid-liquid partition coefficient. The initial time over which the system reaches steady state configuration is characterized by t^* in equation (2.2).

$$t^* = D/(kG^2) \quad (2.2)$$

At steady state growth conditions, the concentration profile of the solute ahead of the interface is given in equation (2.3).

$$C(\partial,x)/C_0 = 1 + ((1-k)/k) - ((G/D)x) \quad (2.3)$$

The distance over which the concentration gradient exists is characterized by the texture parameter ∂ defined in equation (2.4) in terms of the diffusion coefficient D and the crystal growth rate, G .

$$\partial = D/G \quad (2.4)$$

Mullins & Sekerka (1964) found the existence of a solute concentration gradient ahead of a crystal interface causes the planar interface to become unstable. The planar interface breaks down into an array of cellular projections. The nature the organics and inorganics and their resultant ratio was postulated by Baker (1967) as affecting organic inclusion by ice

formation. At high solute concentration, low temperature gradients and rapid growth rates, the instability leads to the development of a cell structure at the interface whose dimensions have been calculated from a theoretical point of view by Bolling & Tiller (1961). Sekerka et al. (1968) studied the formation of ice crystals in sodium chloride solutions and found, at growth rates of 2.8×10^{-3} mm/sec in tap water and at much lower growth rates in concentrated NaCl, the interface between the crystal and liquid was unstable. The instability caused the ice to grow in the form of thin planes separated by regions of concentrated brine, that extended over long distances into the solidified ice. Unlike sludges or suspensions, if the water contains only dissolved impurities, the ice front advances in an orderly fashion. The hypertonic solution at the advancing surface of the growing ice crystal slows down the freezing part of the liquid-solid molecular exchange by decreasing the availability of water molecules. The result is a lowering of the temperature at which the freezing and melting processes balance; a depression of the freezing point (Halde, 1979).

22.1.3 FREEZING OF COLLOIDAL AQUEOUS SOLUTIONS

In contrast to solute solutions such as brine, colloidal aqueous solutions are complex fluids containing a wide spectrum of solutes, low and high molecular weight organics, short chain polymers, oils and suspended gel particles. Compounds found in colloidal aqueous solutions aside from the electrolyte concentration contribute only minimally to the constitutional undercooling of the solution during freezing. It is the electrolyte concentration that strongly influences the freezing process. The fundamental phenomenon of the interaction between a colloidal particle and an ice-water interface during freezing was described in detail by

Ezekwo et al. (1980). At the ice-liquid interface, the water will diffuse from the liquid. Since the center of mass of the crystallizing system is not changing as the crystal grows by diffusion, all of the other noncrystallizing solutes must be moving away by a diffusive process in the opposite direction. Based on the work by English & Dole (1950) the diffusive mobility of the low molecular weight species in the colloidal solution, particularly at moderate solids contents, will not be substantially different from their values in free solution. However, as the colloidal solutes become dehydrated at the ice interface their mobility may be reduced due to the approach of a vitreous transition. Freezing can affect many colloidal solutions in an irreversible manner to flocculate and enhance the sedimentation of the colloidal suspensions (Farrell et al., 1970; Stanczyk et al., 1971; Hadzeriga, 1972; Murphy, 1973).

Documented in the literature are many investigations of ice crystal growth at isothermal or near isothermal conditions (Harrison & Tiller, 1963; Oleneva, 1973). However, natural freezing processes would occur under nonisothermal conditions. Ezekwo et al. (1979) used a modified directional solidification procedure in freezing colloidal aqueous solutions. Under steady state growth in a temperature gradient, nucleation of new crystals were inhibited and the continuous growth of ice crystals over large distances occurs. Ezekwo et al. (1979) was the first to examine the redispersal of the colloidal component of a sludge during thawing. Previous work in sludge dewatering paid little attention to these fundamental aspects of freeze flocculation.

2.2.1.4 FREEZING OF SUSPENSIONS

At sufficiently small ice growth velocities, particles of nearly all materials are rejected by a moving solid-liquid interface. In the case of suspensions, Hoekstra and Miller (1967) envisioned ice as extracting water molecules from a thin layer of surface water on the surface of particles as first postulated by Taber (1930) with the water at the particle surface constantly being replenished as the ice crystals grow. Continuous rejection requires both a force preventing incorporation and a constant addition of fresh matrix material to the region behind the particle. Uhlmann et al. (1964) in the freezing of suspensions found this applies equally well whether the particle be Brownian or non-Brownian in size. The authors showed that within a certain range of crystal growth rates, an exclusion at the crystal-melt interface due to surface energy effects can cause particulate matter to be convectively carried ahead of the growth front as it advances. Cisse & Bolling (1971a) in their consideration of inert particles in front of a growing interface, found particles are acted upon by forces of gravity and viscous drag to promote contact. For particles that are in contact with an interface at more than one point, the share of the force developed at each point will be less than the total force. The suggested effect is less distortion to the particle surface and easier diffusion at each point of contact. As well, an increase in contact area at a constant particle size causes increased migration (Halde, 1980).

2.2.1.5 FREEZING OF SLUDGES

Vesilind and Martel (1991) developed a conceptual model to describe sludge freezing. Sludge, unlike colloidal aqueous solutions, is

visualized as consisting of particles aggregated into flocs that act hydrodynamically as single particles. These flocs can be in suspension or they may form a solids matrix whereby individual flocs cannot be identified and the sludge mass forms a continuum. Water exists in sludge in several readily identifiable forms, although various classifications have been used and the measurements can vary. Water that is not associated with sludge solids is defined as free water. Free water surrounds the sludge flocs and does not move with the solids. Water that is trapped within the floc structure or is held by capillary forces between the particles is defined as interstitial water. If the floc particles are broken-up, the interstitial water becomes free water. Water that is associated with the individual particles and can be released only by thermochemical destruction of the particles is defined as surface water. Water that is chemically bound to the particles and can be released only by thermochemical destruction of the particles is defined as bound water. Based on visual experimental evidence Vesilind and Martel (1991) observed that when sludge with high suspended solids concentrations freezes unidirectionally, irregular ice needles are projected into the water. The ice needles seek available free water molecules for growth by projecting down into the sludge, bypassing the sludge solids. As the ice needles thrust into the sludge they push aside the solids, seeking more free water molecules for continued growth. As ice growth continues, some sludge solids cannot be pushed in front of the ice and are trapped within the frozen mass. In time, the ice crystals dehydrate captured sludge flocs, pushing the particles into more compact aggregates. Finally, if the temperature is low enough, the surface water also becomes frozen, further compacting the individual particles into tight, large solids.

Vesilind and Martel's conceptual model suggests that once the free water surrounding the flocs has frozen, the water molecules inside the flocs are extracted and used to build the crystalline structures, forcing the particles into more tightly compacted solids. For this model freezing temperature should affect the movement and aggregation of solids. If the temperature is sufficiently low, the surface water surrounding the particles eventually freezes and is incorporated into the ice crystals. This forces the particles together to the point that they come under the influence of surface attractive forces, causing them to aggregate into larger particles. Thus freeze-thaw conditioned sludges have a significantly larger particle size distribution and better dewaterability.

Logsdon and Edgerley (1971) schematically illustrated solids entrapment in sludge freezing. The authors characterized the resistance of water flow through the accumulated solids pushed by an interface and the concentration of electrolyte above the freezing isotherm. Under conditions of high resistance the cake buildup and sludge dewatering during freezing decrease the flowing ability of the water. The result is the repeated trapping of sludge solids in layers and that this is referred to as rhythmic banding. Organic polyelectrolytes used in normal sewage sludge dewatering have been found to reduce the resistance to flow in the accumulated cake and can be used to improve migration of solids of thick sludges.

The effect of high dissolved solute concentrations in sludges, is the more concentrated solute concentration near the ice-water interface causes a depression in the freezing point of the liquid. This causes the temperature to fall below the freezing point in the rest of the solution, and

a subsequent breakdown of the constitutional supercooling causing freezing at some distance from the ice-water interface, trapping the layer high in solute.

Sludge dewatering has been found to be dependent on freezing temperature, time frozen, initial moisture content, freezing rate, solution strength, zeta potential and chemical composition. The degree of influence of each parameter is discussed below.

2.2.2 INFLUENCING VARIABLES

2.2.2.1 FREEZING RATE

Freezing rate and its effect on particle distribution of sludges has been widely studied (Vesilind & Martel, 1991; Knock & Trahern, 1988; Logsdon & Edgerley, 1971; Cheng et al., 1970; Clements et al., 1950). A common conclusion that can be made from the above work is sludge dewatering greatly improves when allowed to freeze slowly. Vesilind & Martel (1991) conceptualized that sludge must be frozen slowly for long periods of time to promote the growth of ice crystals that will exclude the solid particles and promote particle aggregation. Research by Knock & Trahern (1989) supported this view by finding that rapid rates of freezing (characterized by freeze contact times < 45 minutes) caused significant fine particle production, possibly due to floc rupture.

Freezing rate and its effect on the constituents of solutes comprised of dissolved and colloidal organics is a topic that has not been widely examined. As an objective of this study, freezing rate was examined for its

effect on solute concentration and recovery as well as on the changes to the constituents of solute during freezing.

2.2.2.2 IMPURITY SIZE, SHAPE AND NATURE

Particle migration during freezing is in part dependent on the type, size, and shape of the particle and the area in contact with the interface. Halde (1980) studied the separation of different sizes of impurities by freezing suspensions or solutions containing calcium carbonate, kaolin clay, glucose, and NaCl. To his surprise, coarser particles like calcium carbonate (where 75 % of the mass of the calcium carbonate consisted of particles larger than 5×10^{-6} m and smaller than 15×10^{-6} m) were more easily separated than fine clay particles. As well the solution of glucose was easier to concentrate than dissolved NaCl. The author attributed this finding to the fact that glucose was a larger molecule and more easily pushed and concentrated by the interface. Corte (1962) showed an important factor in particle migration was its shape and contact area. Particles with large contact areas were easier to displace. Similarly, Cisse and Bolling (1971) reported that those particles which had a greater number of points in contact with the interface were more easily rejected. Several investigators have developed theoretical explanations for how the ice front rejects particles. Uhlmann et al. (1964) reported that each particle has a critical velocity below which the particle will be rejected by the ice front depending on its size and shape. Particles smaller than 100 Angstroms were found to have critical velocities independent of particle size. Where as particles larger than 100 Angstroms were found to have critical velocities that were shape dependent. Particles with irregularities were found to have higher critical velocities in a given matrix than

smooth particles of the same size. For rough particles the interaction with the interface takes place over several irregularities. Their effect was to make easier liquid transport, both in and to the region of contact. For smooth particles, a $1/R_0^2$ size dependence of the critical velocity was suggested where R_0 is the particle diameter. Shape dependence that arises for rough particles results from the viscous drag term, and becomes effective only for fairly large particles. In the range of particle sizes greater than $100\ \mu\text{m}$, this dependence was suggested to be proportional to $1/R_0$ assuming the average irregularity size to be independent of R_0 . Cisse and Bolling (1971) proposed a mathematical model where the critical velocity of the ice front is related to the size of the particles as (equation 2.5):

$$V = KR^{-3} \quad (2.5)$$

where V is the critical velocity above which particles of radius R will be trapped in the ice. K is a constant that takes into account the physical and chemical nature of the water and solid particles.

The theory of particle migration developed by Uhlmann et al. (1964) is based on the assumption that a very short range repulsion exists between the particle and the solid. This repulsion occurs when the particle-solid interfacial free energy is greater than the sum of the particle-liquid and liquid-solid interfacial free energies. The particle is pushed along ahead of the advancing interface and becomes incorporated into the solid if liquid cannot diffuse rapidly to the growing solid behind the particle. Reasonable agreement was obtained between calculated and experimental observed critical velocities. However, the estimated particle critical velocities were calculated assuming bulk diffusion coefficients that

did not consider modification of the water structure at the interface by the solute. Uhlmann et al. found the critical freezing velocity of inorganic slurries to be about 5×10^{-6} m/sec. In the case of solutes, smaller liquid particles (1 to 2 μm in size) had lower critical velocities. For example, particles of xylene and orthoterphenyl were trapped at growth rates of about 13 $\mu\text{m}/\text{sec}$. The higher viscosity of orthoterphenyl over xylene indicated that the process was not limited by rate of deformation of liquid particles at the interface. Baker (1967) postulated that colloidal and soluble organics, exhibiting ionization potential or molecular structural variations amenable to interface modification may influence the diffusion coefficient. However, in laboratory tests reported by the author, ionized and nonionized organics separated with equal efficiency. No evidence of limiting interfacial concentration posing a diffusion barrier was evident.

Workman and Reynolds (1950) showed the nature and location of organic substitute groups affect freeze concentration separation. Postulated was that these variables produce variations in surface dipole orientation and organic inclusion on ice formation. The authors showed that the surface orientation of ionized and nondissociated organics was likely not a factor in solute rejection if inorganic solutes are not present. Parungo and Lodge (1965) confirmed in vapor-phase studies the postulate that the organic substitute is a factor in freeze concentration.

2.2.2.3 IMPURITY CONCENTRATION

Halde (1980) studied the effect of impurity concentration. Reported by Halde was the purification of water improved with lower suspended solids concentrations. It was found that water containing only small

amounts of calcium carbonate was much more easier to purify than suspensions with higher initial concentrations. Conversely, solutes such as dissolved glucose and NaCl were more difficult to concentrate than suspended solids. The NaCl solution proved most sensitive to variations in the initial concentration than the purification of a glucose solution. Baker (1967) found that the separation of an organic solute improved as dilution is increased in the absence of an inorganic solute.

2.2.2.4 PRESENCE OF AIR

Corte (1962) reported the presence of air bubbles has a dramatic effect on particle trapping. Halde (1980) described the formation of "ice worms" in freezing in the presence of air. In his description air as a solute is rejected by freezing water. Air molecules accumulate in front of an advancing interface until its concentration is high enough for bubbles to nucleate. Once a bubble has formed, it grows because gases diffuses into it. For an interface moving forward, the bubble cannot grow laterally and grows to form a cylindrical bubble referred to as an "ice worm". Ice worm formation is dependent on the rate of freezing. Fast freezing suppresses the formation of ice worms because of insufficient gas diffusion into the bubbles. The result is the ice will contain large numbers of small bubbles. Conversely, very slow freezing permits the rejection of gas to diffuse away from the interface and neither ice worms or bubbles appear. Kuo et al. (1973) reported the effect of air bubbles on particle trapping. Found was that particles settle into the depressions formed around ice bubbles and when these bubbles occasionally break free there occurs a rapid freezing and local trapping of particles at the former site of the bubble.

2.2.2.5 EFFECT OF STIRRING

Halde (1980) found progressive stirring improved purification of water by freezing. Considerable purification was observed in waters containing suspended calcium carbonate, suspended graphite, dissolved glucose or sodium chloride if the liquid phase was stirred vigorously at a rate of 2000 rpm to avoid accretion of a layer of impurities at the interface. The general tendency of the data was more intense stirring rendered a higher degree of purification. The importance of stirring in impurity separation increased at the higher rates of freezing. Larger particles or molecules were more easily separated by stirred freezing than smaller impurities.

In freeze-thaw sludge conditioning, agitation before and after freeze-thaw can change particle sizes to be of practical significance in dewatering, however the final result was dependent on the type of sludge (Vesilind et al., 1991). Vesilind et al. (1991) suggested that an optimum floc size exists, and agitation prior to freezing may aid in attaining this size.

2.2.2.6 RATE AND METHOD OF THAWING

Rate of thawing is not typically reported as an important parameter in freeze separation. In studies conducted to examine sludge freezing, thawing time was found to be unimportant (Penman & Van Es, 1973; Tilsworth et al., 1972; Logsdon & Edgerley, 1971). Thawing rate was investigated as part of this study for its influence on constituent separation during thawing.

2.2.2.7 METHOD OF FREEZING

Mechanical freeze-thaw has been extensively studied for the conditioning of sludges (Benn & Doe, 1969; Farrel, 1971; Randall et al., 1975; Martel et al., 1998). The different mechanical freeze-thaw devices studied included bulk freezers, freeze crystallizers, and layer freezers. Martel et al. (1998) concluded the best way to freeze sludges was in thin layers. Freezing in layers avoided the structural failure problems associated with bulk freezers. However, aside from these structural problems bulk freezers designed to completely freeze the sludge worked very well. Knocke and Trahern (1989) found bulk freezing consistently improved the dewaterability of chemical and biological sludges and was a superior method to freeze crystallization. Separation of the ice crystal/solid particle interfaces was a problem common to freeze crystallization or freeze concentration. Freeze crystallization was also found in some instances to decrease sludge dewaterability.

2.2.2.8 INORGANIC ELECTROLYTES

The effect of inorganic electrolytes on the freezing process has been intensively studied. Workman and Reynolds (1950) first elucidated the phenomena of charge separation and electrical potential that was later critically reviewed by Gross (1965). Baker (1967, 1969) studied the effect of inorganic salts on organic separation by freeze concentration and found in their absence, mixing was not important in organic solute recovery. Mixtures of organics which included phenols, substituted phenols, volatile fatty acids and aceophenone were recovered without selectivity by freeze concentration in the absence of inorganics. Under these conditions,

organic dissociation, molecular size, weight, nature and the location and number of substituted groups were reported to have no effect on recovery. The recovery of organic solutes was found to be complete, regardless of the initial sample volume, until a critical range of residual unfrozen liquid volume remained. Barduhn et al. (1963) postulated that salts presence in wastewaters promote organic separation by a salting-out effect. This was supported in a subsequent report by Powell and Barduhn (1965) who clarified and repeated the postulation that only the high molecular weight organic materials would be salted-out. The removal of highly soluble organic compounds of low molecular weight, such as simple alcohols and acids, was not affected. In laboratory tests the solubility of ABS decreased at low temperatures and that sodium chloride addition further reduced markedly the solubility. However, in actual freezing tests of ABS wastewater only approximately 10 % of the total organic was forced out of solution at a 20 % salt concentration at a temperature of -20 °C.

2.2.2.9 LIQUID DEPTH

Liquid depth affects freezing and curing time (Parker et al., 1998). Empirical models exist that will calculate the freezing and thawing depth. The most notable are those models developed by Stefan, Berggren, and Neumann (Mouton, 1969). Little literature exists regarding the effect of liquid depth on thawed removal efficiency for waste streams other than sludges.

2.2.2.10 TIME FROZEN (CURING TIME)

Time frozen has been identified as an important factor affecting sludge dewatering (Vesilind & Martel, 1991; Logsdon & Edgerley, 1971).

The above authors showed storage time, allowing the "difficult" to freeze water to become part of the ice crystal and the particles to attach themselves to each other, markedly improved dewaterability. Freezing the "difficult" to freeze water is also dependent on storage temperature. Vesilind and Martel (1991) showed the filterability of sludges improved with the colder the final storage temperature.

2.2.3 MATHAMETICAL MODELS

The empirical models that have been developed are for the design and operation of sludge freeze-thaw beds where the primary focus was to determine the total quantity of sludge that could be frozen over a particular time period under different ambient conditions. An example of which was presented by Farrell et al. (1970) and Barnes (1928). These authors developed the following non-dimensional homogeneous empirical equation to determine the rate of thickening of an ice sheet on quiet water already at its freezing point (equation 2.6):

$$(t + t^2)/2 = (k_1 \Delta T \theta) / L \epsilon \quad (2.6)$$

where:

t = thickness of ice sheet (mm);

k_1 = thermal conductivity of ice (2.38 J/mm²*sec);

ΔT = freezing temperature of ice less the air temperature (°C);

θ = total exposure time (sec);

L = latent heat of freezing (335 J/g); and

ϵ = density of ice (91.70 g/mm²)

Used primarily as an operational tool in sludge freezing to select and monitor the appropriate liquid depth, the model provides no information about the end product quality or results that can be expected. This type of model provides information only about whether or not the freezing process will be successful and if the operational parameters selected by the operator are appropriate for the weather conditions.

The focus of this study was to develop empirical relationships that can be used as operational tools in the application of freeze-thaw in the treatment of high strength pulp mill effluents comprised primarily of dissolved and colloidal organic matter. The purpose of the model is to predict treatment performance based on the freezing and thawing conditions.

3.0 MATERIALS AND METHODS

3.1 SUMMARY OF EXPERIMENTAL TESTS

Table 3.1 is summary of the experimental tests conducted as part of this research. Described in this table are the parameter set points and purpose of each test.

3.2 EXPERIMENTAL WATERS

Unidirectional freeze-thaw experiments were conducted using as experimental waters bleachery effluents collected from the alkaline extraction stage of a kraft pulp mill operation. Summarized in Table 3.2 are the different types of experimental waters studied. Following collection, alkaline extraction stage effluent was processed using ultrafiltration technology to produce a high strength alkaline extraction stage membrane concentrate comprised primarily of the high molecular weight compounds (> 8000 MWCO).

3.2.1 ALKALINE EXTRACTION STAGE EFFLUENT

Bleachery effluent from the alkaline extraction stage with oxygen and hydrogen peroxide reinforcement was obtained from the Weyerhaeuser Canada Ltd. kraft pulp mill located in Grande Prairie, Alberta. Following sampling, the effluent was transferred into a single 170 litre capacity plastic container and placed a cold store room at a temperature of 4°C . The container was sampled weekly and the effluent chemically tested to monitor sample degradation.

Table 3.1 Summary of Experimental Tests

Parameter or Type of Analysis	Experimental Set Points	Purpose
Scanning Electron Microscopy Studies	*frozen and thawed liquid samples	*characterization of the frozen and thawed physical state morphology of the concentrated material produced under different freeze-thaw conditions
Size Fractionation Studies	*membrane concentrate: raw, above 5000, below 5000	*characterization of the frozen physical state cross sectional and surface morphology for different size fractions
Development of Freezing Curves	*initial freezing temperatures -2 °C, -15 °C, and -25 °C	*calibration of freezing apparatus, and comparison of duplicate runs
Parameter Selection	*correlate color with respect to COD, total alkalinity, and TDS	*parameter selection to evaluate treatment performance and possible inclusion into the model
Liquid Depth	*liquid depth range: 150 mm and 250mm	*evaluate liquid depth for its relative significance
Layer Freezing	*multiple layers (125 mm) versus single 250 m layers	*evaluate operational suitability
Selective Sampling	*collection of frozen and liquid samples at 25 mm intervals with respect to depth at each run condition	*compare constituent distributions for frozen and thawed liquid samples and identify mechanisms responsible for concentration and removal of concentrated material
Storage Temperature	*storage temperatures: -2 °C and -15 °C	*evaluate storage temperature for its relative significance with respect to treatment performance
Storage Time	*storage time: 0, 30, 60, and 90 days	*evaluate storage time for its relative significance with respect to treatment performance
Initial Freezing Temperature	*freezing temperatures: -2 °C, -15 °C, and -25 °C	*evaluate changes in concentrated material morphology, and its relative significance with respect to treatment performance
Method of Thawing	*thaw top down (ice does not float) versus thaw bottom up (ice floats)	*evaluate the importance of melt water flow in the concentration and settlement of concentrated material produced during freezing, and identify mechanisms of removal
Thawing Rate	*thawing temperatures: 4 °C, 15 °C, and 24 °C	*evaluate the importance of melt water flow in the concentration and settlement of concentrated material produced during freezing
Concentration	*percent dilutions: raw, 50 %, 66 %, 75 %, and 80 %.	*establish concentration limits suitable for treatment, and identify changes in the frozen physical state morphology of the concentrated material
Concentrated Material Stability Studies	*optimum experimental freeze-thaw conditions	*evaluate concentrated material stability, develop operational model, and identify the nature of the concentrated material

Table 3.2 Experimental Water Types

Experimental Water Type	Effluent Description	Concentration Strength
1	alkaline extraction stage effluent membrane concentrate	color concentration ratio was approximately 3.6 times higher with respect to the raw
2	alkaline extraction stage effluent	raw bleachery effluent

3.2.2 ALKALINE EXTRACTION STAGE MEMBRANE CONCENTRATE

Alkaline extraction stage membrane concentrate was obtained from the Weyerhaeuser Canada Ltd. kraft pulp mill using a New Logic International V-Sep ultrafiltration pilot plant demonstration unit (Figure 3.1). Table 3.3 is a summary of the membrane pilot plant design specifications. The pilot plant was configured to operate as a batch process. Approximately 150 liters of membrane concentrate was produced.

The membrane concentrate was stored in a single 170 litre capacity plastic container in a cold storeroom at a temperature of 4 °C. The container was sampled weekly and the effluent chemically tested to monitor sample degradation.

3.2.3 ALKALINE EXTRACTION STAGE CONCENTRATE SIZE FRACTIONS

A Minitan Acrylic Ultrafiltration System by Millipore Direct was used to size fractionate the alkaline extraction stage membrane concentrate into three size fractions. The different molecular weight size fractions were < 1000, > 1000 and < 5000, and > 5000.

3.3 EXPERIMENTAL WATER PRESEVRATION

The experimental waters were stored separately in 170 litre capacity plastic containers in a dark, cold storeroom at 4 °C. Prior to sample collection, the contents of the plastic containers were thoroughly mixed to allow collection of representative samples. The effluents were sampled weekly throughout the storage period to monitor sample degradation. The storage time for the alkaline extraction stage membrane concentrate was

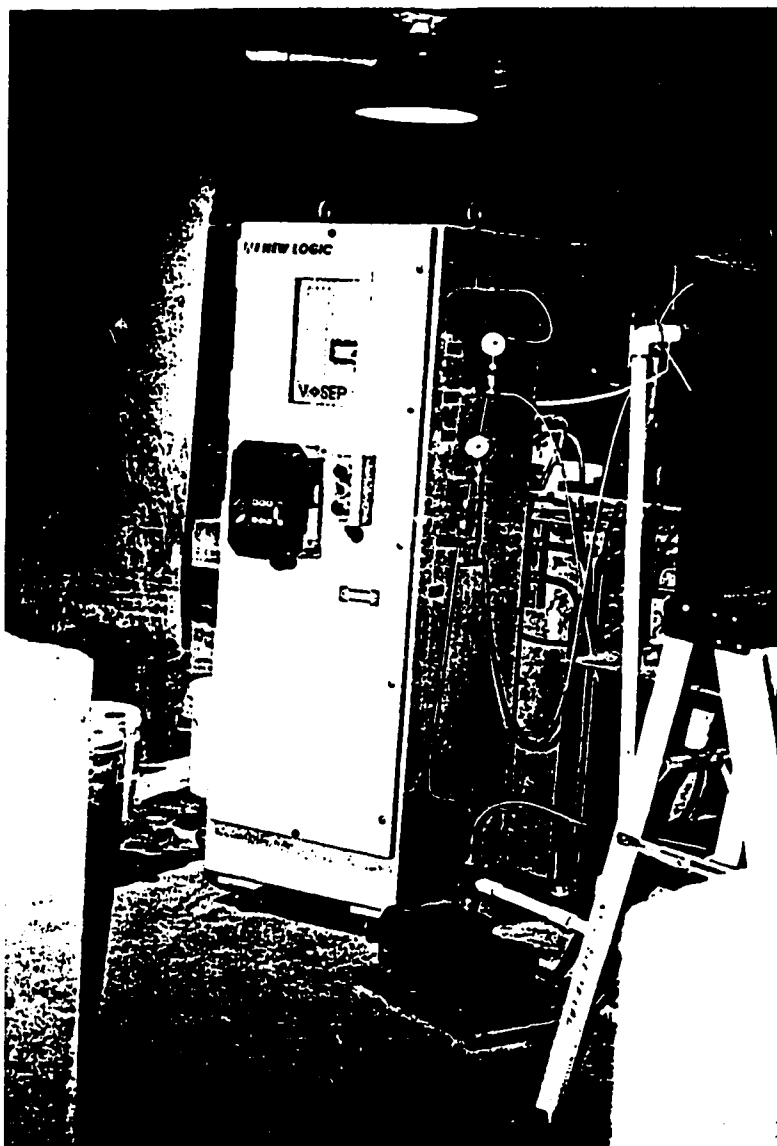


Figure 3.1 New Logic International V-Sep Ultrafiltration Pilot Plant

approximately 8 months over which samples portions were collected for experimental testing. Similarly, the storage time for the alkaline extraction stage effluent was approximately 4 months. The experimental water types were experimented with independently of each other with respect to time to minimize the time period taken to complete the factorial design.

3.3.1 ALKALINE EXTRACTION STAGE EFFLUENT

Plotted in Figures 3.2 to 3.6 are the chemical changes that occurred to the alkaline extraction stage effluent over the course of its storage period with respect to COD, color, pH, total alkalinity, and TDS. The overall change in chemical quality for the period of storage for each parameter is summarized below:

<u>Parameter</u>	<u>Maximum Unit Change</u>
COD	60.0 mg/L
Color	200 CU
pH	0.10
Total Alkalinity	40 mg/L as CaCO ₃
TDS	350 mg/L

3.3.2 ALKALINE EXTRACTION STAGE MEMBRANE CONCENTRATE

Plotted in Figures 3.7 to 3.11 are the chemical changes that occurred to the alkaline extraction stage membrane concentrate over the course of its storage period with respect to COD, color, pH, total alkalinity, and TDS. Because of the requirement to substantially dilute the sample in the analysis for various parameters, measurements obtained for COD, color and TDS were reported to within three significant figures. The overall

Table 3.3 Ultrafiltration Pilot Plant Design Specifications

Parameter	Specifications
Manufacturer	New Logic International Inc.
Model Type	V-Sep
Special Feature	Vibratory Shear
Vibrating Frequency	60 Hz
Filtration Type	Ultrafiltration
Membrane Type	NTR 7410
Molecular Weight Cutoff	8000 MWCO
NaCl Rejection Capability	10 %
Permeate Production Rate	2.2 mL/sec (average)
System Operating Pressure	0 to 2,069 kPa
pH Operating Range	1 to 13

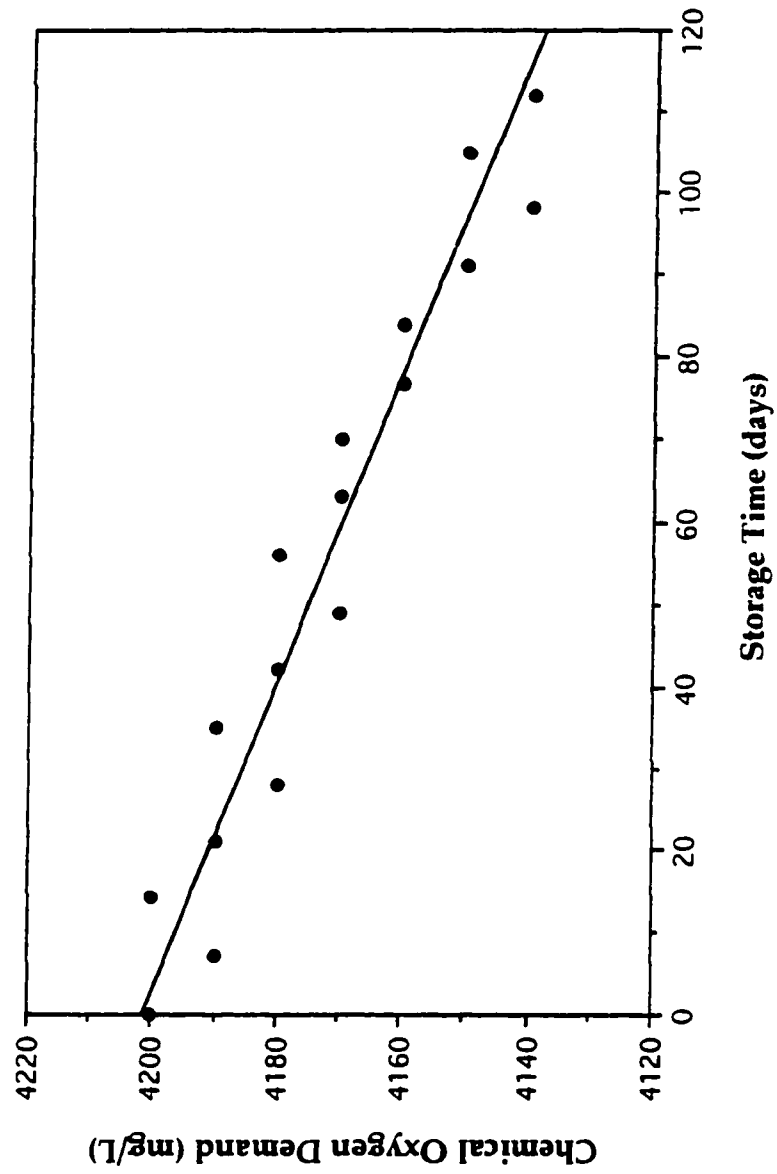


Figure 3.2 Change in Chemical Oxygen Demand with Respect to Storage Time for the Alkaline Extraction Stage Effluent

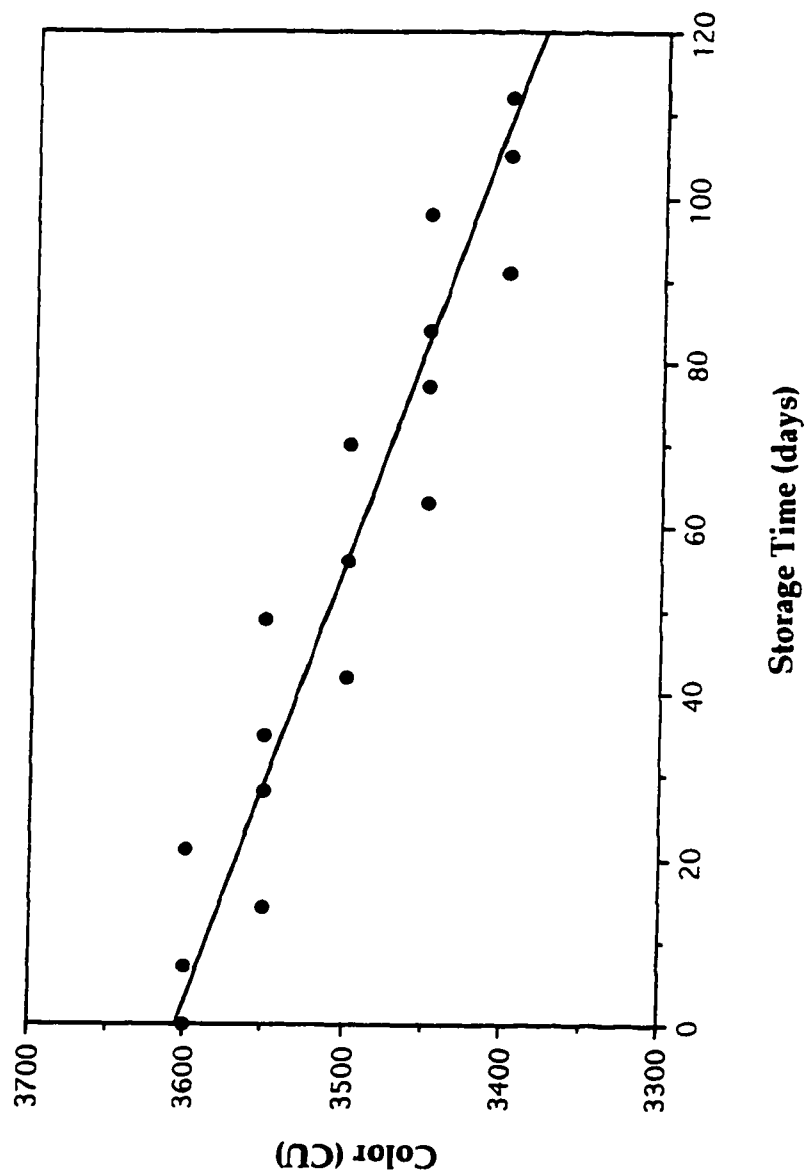


Figure 3.3 Change in Color with Respect to Storage Time for the Alkaline Extraction Stage Effluent

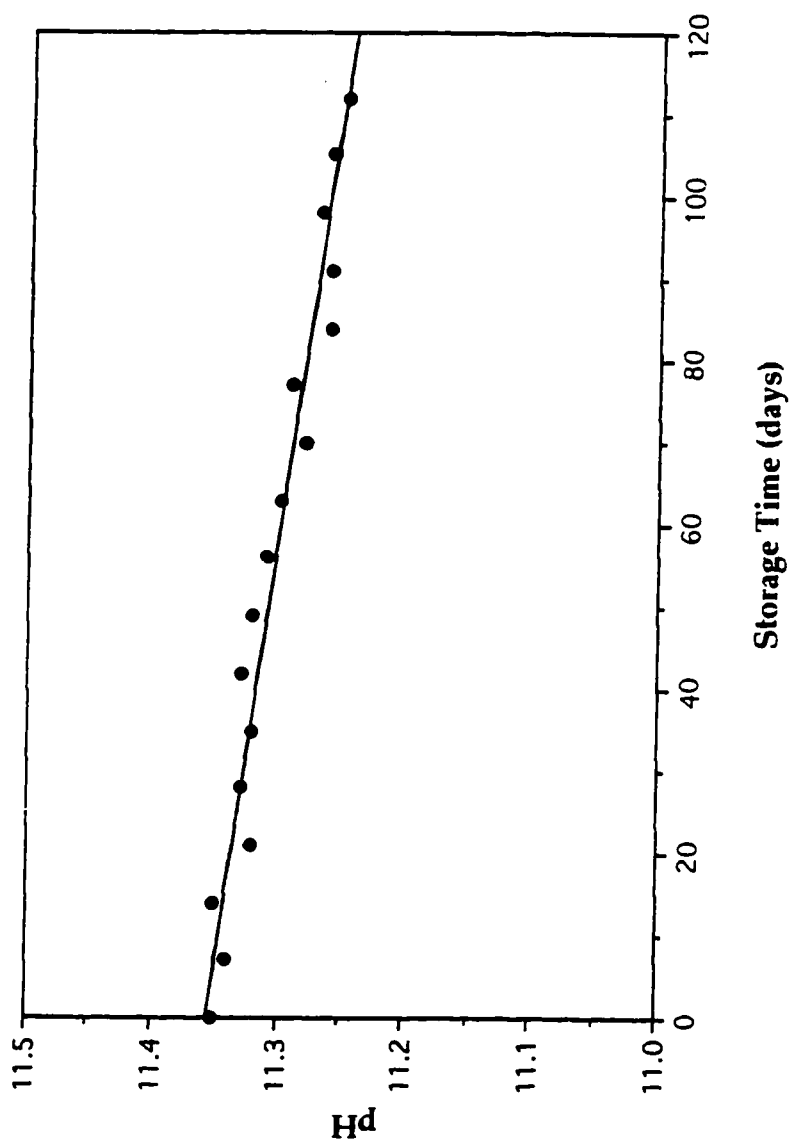


Figure 3.4 Change in pH with Respect to Storage Time for the Alkaline Extraction Stage Effluent

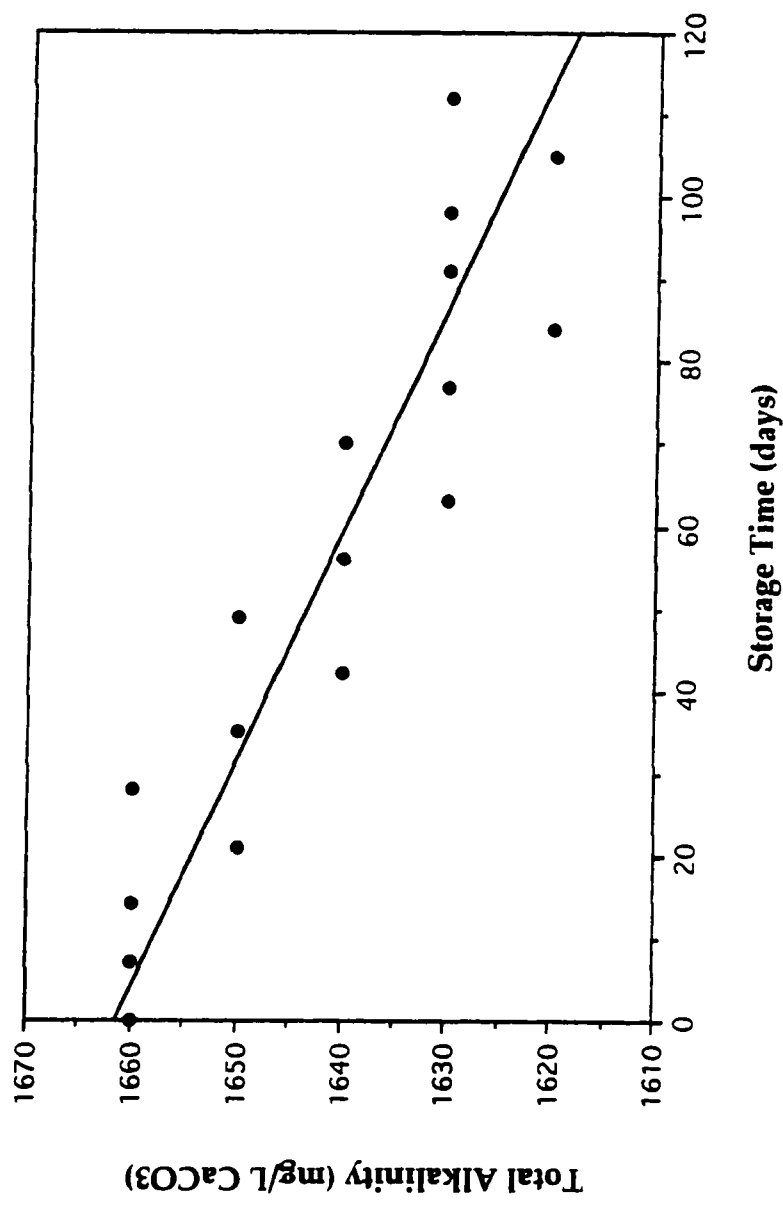


Figure 3.5 Change in Total Alkalinity with Respect to Storage Time for the Alkaline Extraction Stage Effluent

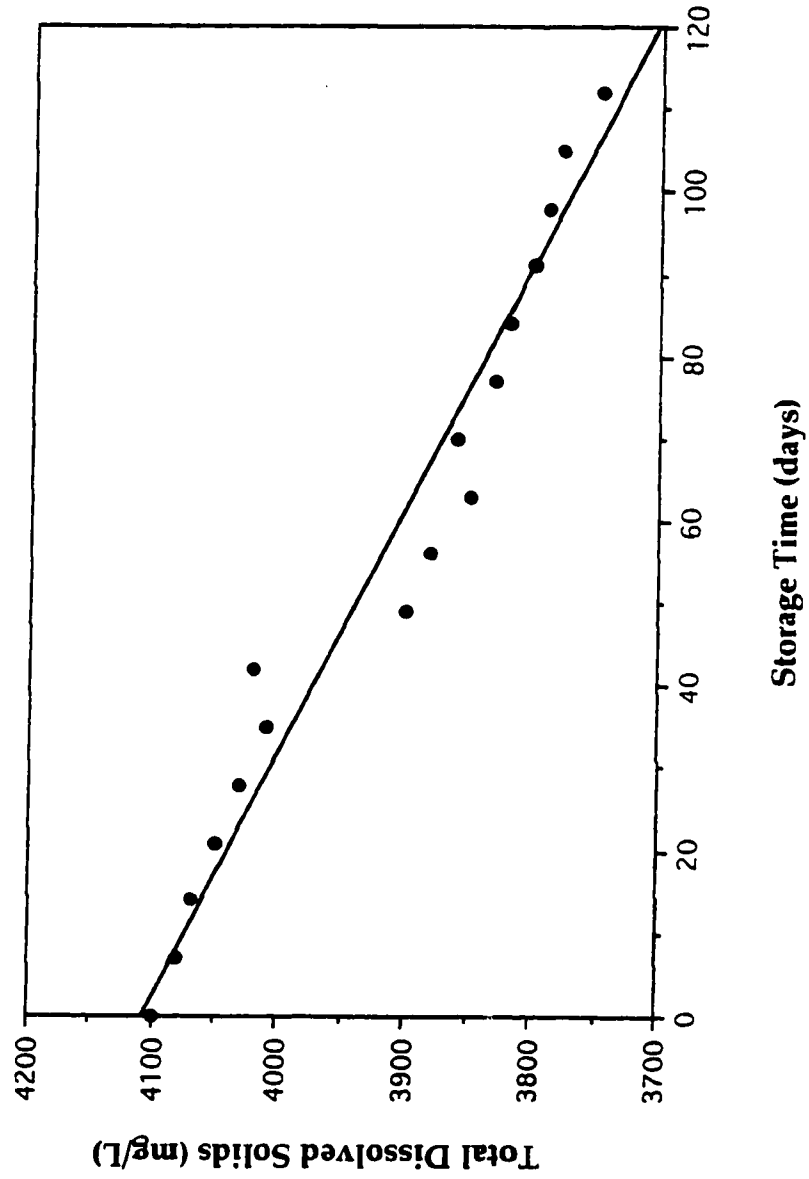


Figure 3.6 Change in Total Dissolved Solids with Respect to Storage Time for the Alkaline Extraction Stage Effluent

change in chemical quality for the period of storage for each parameter is summarized below:

<u>Parameter</u>	<u>Maximum Unit Change</u>
COD	400 mg/L
Color	300 CU
pH	0.24
Total Alkalinity	60 mg/L as CaCO ₃
TDS	300 mg/L

3.4 EXPERIMENTAL WATER CHEMICAL COMPOSITION

Presented are the chemical compositions for each experimental water type as used in the factorial design.

3.4.1 ALKALINE EXTRACTION STAGE EFFLUENT

Summarized in Table 3.4 is the chemical composition of the alkaline extraction stage effluent as used in the factorial experiment. The alkaline extraction stage effluent was routinely sampled weekly, with raw samples also collected at the beginning of each series of freeze-thaw experiments. The standard deviation and range for the average values given below are representative of the analytical error and sample degradation that occurred over the course of the experiments. The alkaline extraction stage effluent was characterized as being alkaline, highly buffered, low in suspended solids, and high in dissolved solids, of which a moderate percentage were dissolved or colloidal organics. The primary inorganic elements were sodium, calcium, magnesium, and potassium.

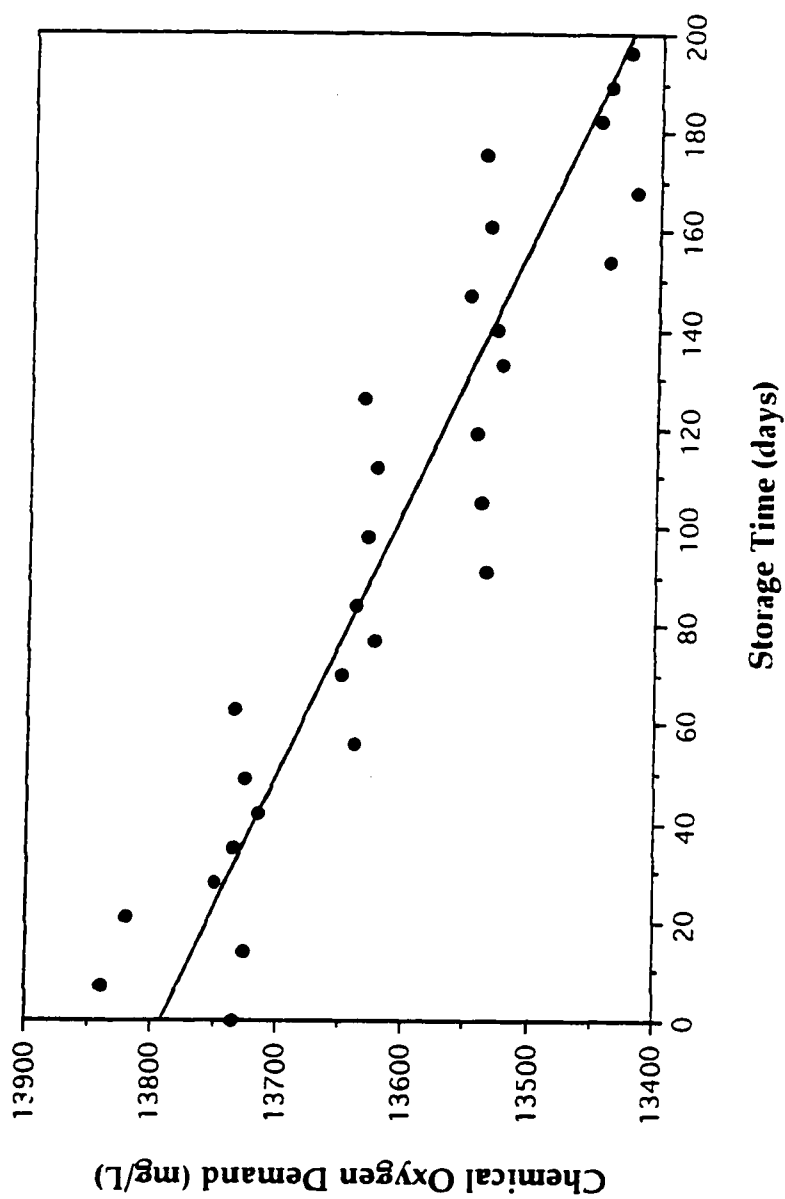


Figure 3.7 Change in Chemical Oxygen Demand with Respect to Storage Time for the Alkaline Extraction Stage Membrane Concentrate

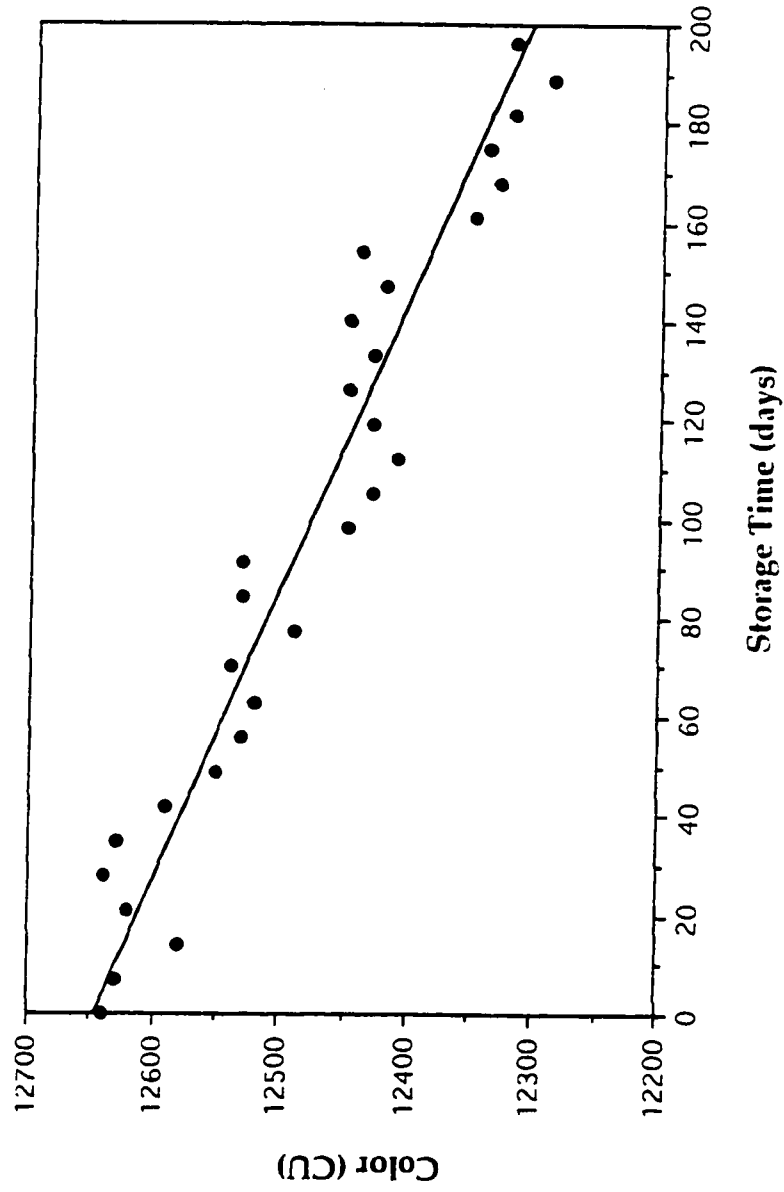


Figure 3.8 Change in Color with Respect to Storage Time for the Alkaline Extraction Stage Membrane Concentrate

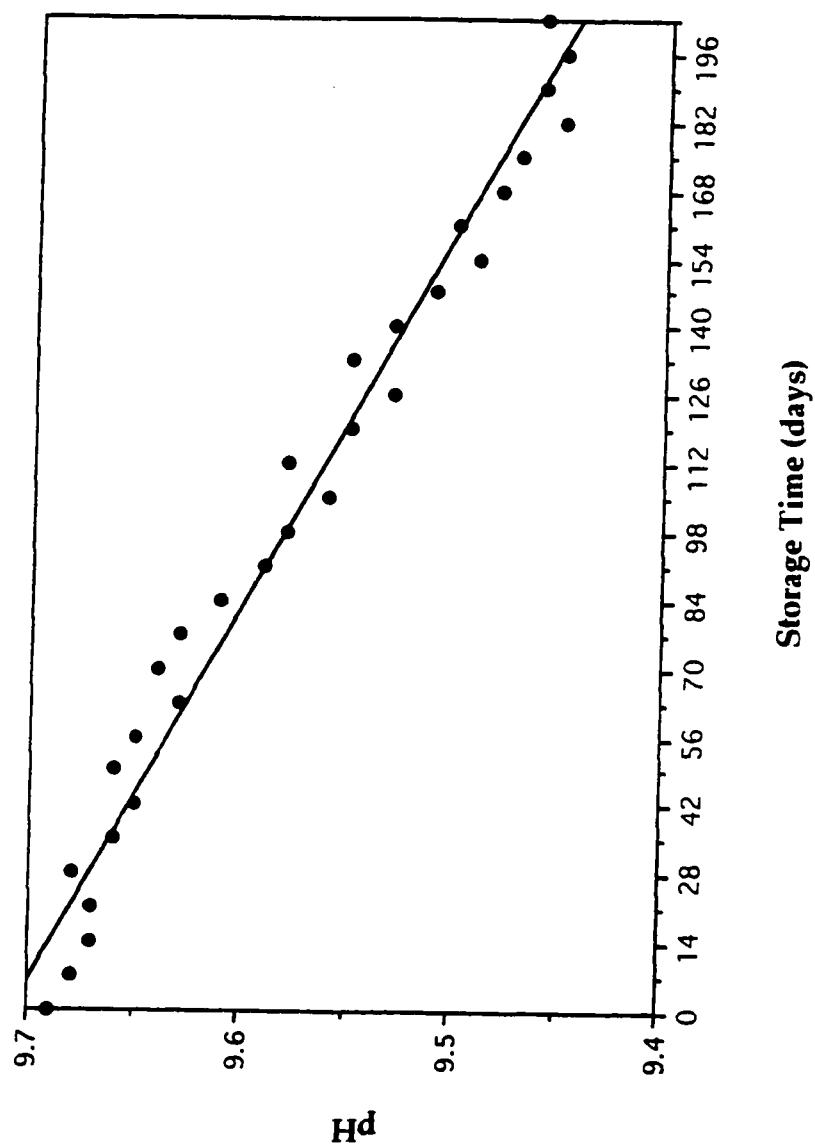


Figure 3.9 Change in pH with Respect to Storage Time for the Alkaline Extraction Stage Membrane Concentrate

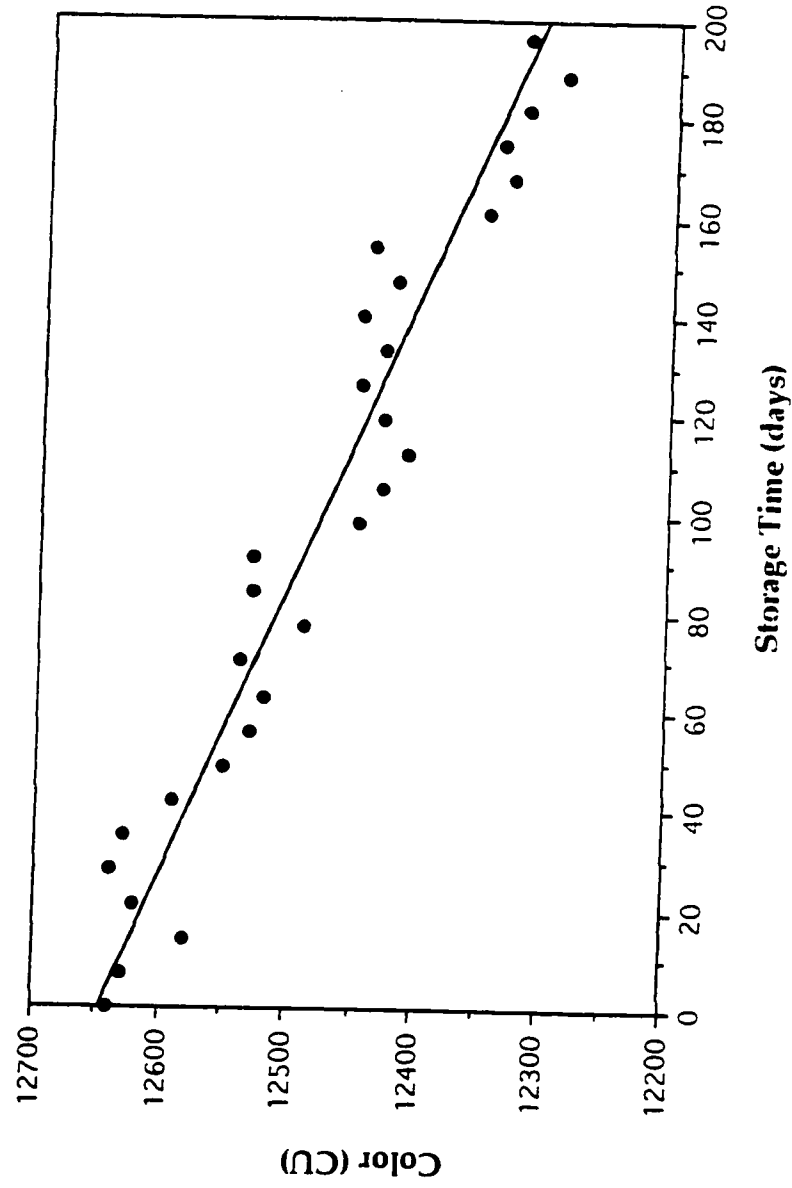


Figure 3.10 Change in Total Alkalinity with Respect to Storage Time for the Alkaline Extraction Stage Membrane Concentrate

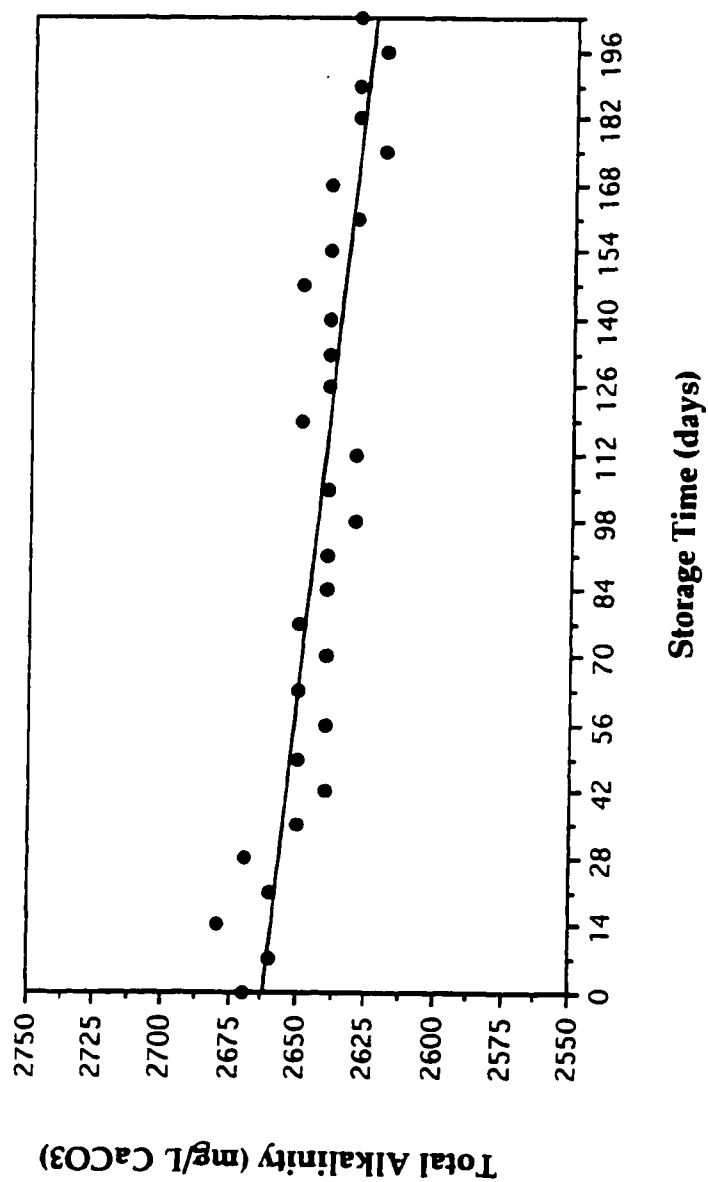


Figure 3.11 Change in Total Dissolved Solids with Respect to Storage Time for the Alkaline Extraction Stage Membrane Concentrate

Table 3.4 Chemical Composition of the Alkaline Extraction Stage Effluent

Chemical Parameter	Average Value*	Standard Deviation**	Range
Carbonate Concentration (mg/L)	1,400	± 35	1,350 to 1,430
Bicarbonate Concentration (mg/L)	235	± 25	215 to 275
Chemical Oxygen Demand (mg/L)	4,160	± 25	4,140 to 4,200
Color (CU)	3,440	± 59	3,500 to 3,360
pH	11.30	± 0.05	11.25 to 11.35
Total Alkalinity (mg/L CaCO ₃)	1,640	± 15	1,620 to 1,660
Total Dissolved Solids (mg/L)	3,930	± 115	3,790 to 4,070
Total Suspended Solids (mg/L)	12	± 0.0	12
Turbidity (NTU)	7.5	± 0.5	6.9 to 8.1
Volatile Suspended Solids (mg/L)	12	± 0.0	12
***Metals (total) (mg/L)			
Aluminum	<0.5	N/A	N/A
Barium	0.13		
Beryllium	<0.01		
Cadmium	<0.1		
Calcium	19		
Chromium	<0.1		
Cobalt	<0.1		
Copper	<0.1		
Iron	<0.1		
Lead	<0.5		
Magnesium	4.1		
Manganese	0.25		
Molybdenum	<0.5		
Nickel	<0.5		
Phosphorous	<0.5		
Potassium	7.0		
Silver	<0.1		
Sodium	1,315		
Strontium	<0.1		
Thallium	<0.1		
Tin	<0.5		
Titanium	<0.1		
Vanadium	<0.1		
Zinc	<0.1		

* average value derived from a sample set of 10 collected during sample storage, ** ± 1 standard deviation, *** single values

3.4.2 ALKALINE EXTRACTION STAGE MEMBRANE CONCENTRATE

Summarized in Table 3.5 is the chemical composition of the alkaline extraction stage membrane concentrate as used to conduct the factorial experiment. The alkaline extraction stage membrane concentrate was routinely sampled weekly, with raw samples also collected at the beginning of each series of freeze-thaw experiments. The alkaline extraction stage membrane concentrate was characterized as being slightly alkaline, highly buffered, low in suspended solids, and high in dissolved solids, of which a high percentage were high molecular weight dissolved or colloidal organics. The primary inorganic elements were sodium, calcium, magnesium, and potassium.

3.5 ANALYTICAL AND INVESTIGATIVE METHODS

3.5.1 WET CHEMISTRY ANALYSES

3.5.1.1 ALKALINITY SPECIES

Alkalinity was determined in accordance with section 2320 B of Standard Methods (AWWA-AHPA-WPCF, 1989). All determinations were conducted in duplicate.

3.5.1.2 CHEMICAL OXYGEN DEMAND

Chemical oxygen demand (COD) was determined by the open reflux method as described in section 5220 B of Standard Methods (AWWA-AHPA-WPCF, 1989). All determinations were conducted in duplicate.

Table 3.5 Chemical Composition of the Alkaline Extraction Stage
Membrane Concentrate

Chemical Parameter	Average Value*	Standard Deviation**	Range
Carbonate Concentration (mg/L)	748	± 10	740 to 760
Bicarbonate Concentration (mg/L)	1,810	± 54	1,780 to 1,890
Chemical Oxygen Demand (mg/L)	13,500	± 100	13,600 to 13,400
Color (CU)	12,500	± 87	12,600 to 12,400
pH	9.65	± 0.05	9.67 to 9.60
Total Alkalinity (mg/L CaCO ₃)	2,650	± 25	2,620 to 2,690
Total Dissolved Solids (mg/L)	13,000	± 79	12,800 to 13,100
Total Suspended Solids (mg/L)	32	± 0.0	32
Turbidity (NTU)	3.7	± 0.3	3.5 to 4.4
Volatile Suspended Solids (mg/L)	24	± 0.0	24
***Metals (total) (mg/L)			
Aluminum	0.53	N/A	N/A
Barium	0.74		
Beryllium	<0.01		
Cadmium	<0.1		
Calcium	79		
Chromium	<0.1		
Cobalt	<0.1		
Copper	<0.1		
Iron	0.64		
Lead	<0.5		
Magnesium	23		
Manganese	1.9		
Molybdenum	<0.5		
Nickel	<0.5		
Phosphorous	0.8		
Potassium	13		
Silver	<0.1		
Sodium	2,180		
Strontium	0.37		
Thallium	<1.0		
Tin	<0.5		
Titanium	<0.1		
Vanadium	<0.1		
Zinc	0.27		

* average derived from a sample set of 10 collected during sample storage,

** ± 1 standard deviation, *** single values

3.5.1.3 COLOR

Color was determined in accordance with Standard H.5P of the Physical and Chemical Standards Committee, Technical Section of the Canadian Pulp and Paper Association. The spectrophotometer used was the Pharmacia Biotech Ultrospec 3000 UV/visible spectrophotometer. All determinations were conducted in duplicate. The test was found to have an accuracy +/- 50 color units for samples diluted by a maximum factor of 100 times.

3.5.1.4 pH

pH was determined in accordance with section 4500 H⁺ of Standard Methods (AWWA-AHPA-WPCF, 1989). The instrument used was the Fisher Scientific Accumet pH meter 25. The meter had a relative accuracy of +/- 0.01 pH units.

3.5.1.5 METALS

Metal analysis was by Inductively Coupled Plasma (ICP) according to the test method EPA 6010. Core Laboratories, Calgary, Alberta was contracted to perform all metal analysis.

3.5.1.6 TOTAL DISSOLVED SOLIDS

Total dissolved solids (TDS) were determined according to section 2540 C of Standard Methods (AWWA-AHPA-WPCF, 1989). All determinations were conducted in duplicate.

3.5.1.7 TOTAL SUSPENDED SOLIDS

Total suspended solids (TSS) were determined according to section 2540 D of Standard Methods (AWWA-AHPA-WPCF, 1989). All determinations were conducted in duplicate.

3.5.1.8 TURBIDITY

Turbidity was determined by the Nephelometric method according to section 2130 B of Standard Methods (AWWA-AHPA-WPCF, 1989). The instrument used was the HACH 2100A turbidimeter. All determinations were conducted in duplicate.

3.5.1.9 VOLATILE SUSPENDED SOLIDS

Volatile suspended solids (VSS) were determined according to section 2540 E of Standard Methods (AWWA-AHPA-WPCF, 1989). All determinations were conducted in duplicate.

3.5.2 SCANNING ELECTRON MICROSCOPY

The JOEL JSM-6301F Scanning Electron Microscope complete with the cryo option was used to examine ice and filter paper specimens. The electron gun was a cold-cathode field emission type designed for ultra-high resolution scanning electron microscopy (SEM) with a modern digital image processing system. Summarized in Table 3.6 are instrument's specifications.

Table 3.6 JSM-6301F Scanning Electron Microscope Specifications

Feature	Performance
Magnification Zoom Fixed	10 X to 500,000 X Any magnification
Secondary Electron Image Resolution at 30 KV at 1 KV	1.5 nm guaranteed 5 nm guaranteed
Backscattered Electron Image Resolution (at 30 KV)	3.0 nm attainable
Probe Current	10 ⁻¹² to 10 ⁻¹⁰ A
Electron Gun	Cold-cathode field emission
Accelerating Voltage	0.5 to 30 KV, 0.1 KV steps
Emitter	<310> tungsten tip
Alignment	Mechanical and electromagnetic deflection

3.5.2.1 SPECIMEN PREPARATION

3.5.2.1.1 ICE SPECIMENS

As part of this research, an experimental protocol was developed for visual examination of the physical properties of the concentrated material contained within the ice matrix. Initial attempts to expose the physical properties of the concentrated material without first preparing the sample so that it would not begin to melt during mounting were unsuccessful. In the absence of sample preparation, it was found that ice specimens could not be mounted on the sample exchange holder and placed directly into the specimen stage without superficial melting of the ice surface which was sufficient to obscure the morphology of the concentrated material. The successful method involved supercooling the sample by submerging and fracturing the ice specimen within liquid nitrogen to produce a clean unexposed surface. To avoid exposure of the sample to condensation, the specimen transfer stage was first purged with nitrogen and the ice sample withdrawn directly from the liquid nitrogen under a vacuum. Sublimation to expose the concentrated material was conducted in the cold stage at a temperature of -40°C . A image resolution of 1.5 KV was used initially to monitor sublimation. Following the appearance of wafer-like structures, the ice sample was cooled to -180°C for 10 minutes before removal for coating. After cooling the specimen was removed under a vacuum using the specimen transfer stage and transferred into the cryo chamber where the sample was gold coated. The sample was double sputter coated with gold for a total thickness of 100 Angstroms. Coating was conducted at a temperature of -180°C . It was important to ensure adequate time was provided to allow the sample to sufficiently cool before

coating to prevent sublimation during and after coating. Insufficient sample cooling resulted in the peeling of the gold coating. Following coating, the specimen was returned to the specimen chamber of the scanning electron microscope and examined using an image resolution of 5 KV.

Supercooling the ice samples by submergence into liquid nitrogen prior to mounting were not believed to have affected the physical appearance of the concentrated material. This conclusion was based on sample photos taken during and after sublimation. Shown in Figures 3.12 and 3.13 are high resolution electron microscope images of uncoated ice sample surfaces taken during their early stage of sublimation. From examination of these photographs it can be seen that there are no visible fractures within the zones of concentrated material and that the pores were completely frozen. Freezing of this water within the porous material of the wafer was believed to have occurred during the freezing step of the treatment method and not as a result of being rapidly supercooled. For example, had the water within the pore structures not been frozen within the zone of highly concentrated material prior to supercooling, the 9 % rapid volume expansion from freezing of the free available water should have fractured the ice matrix along the plane of the wafer for its depth. This would have been particularly true since ice specimens were mounted in such a manner that they were unconstrained. The appearance of fractures along the highly concentrated zones of material were not evident in any of the ice specimens examined by SEM to support this conclusion. In addition, close examination of the pore structure showed the pores

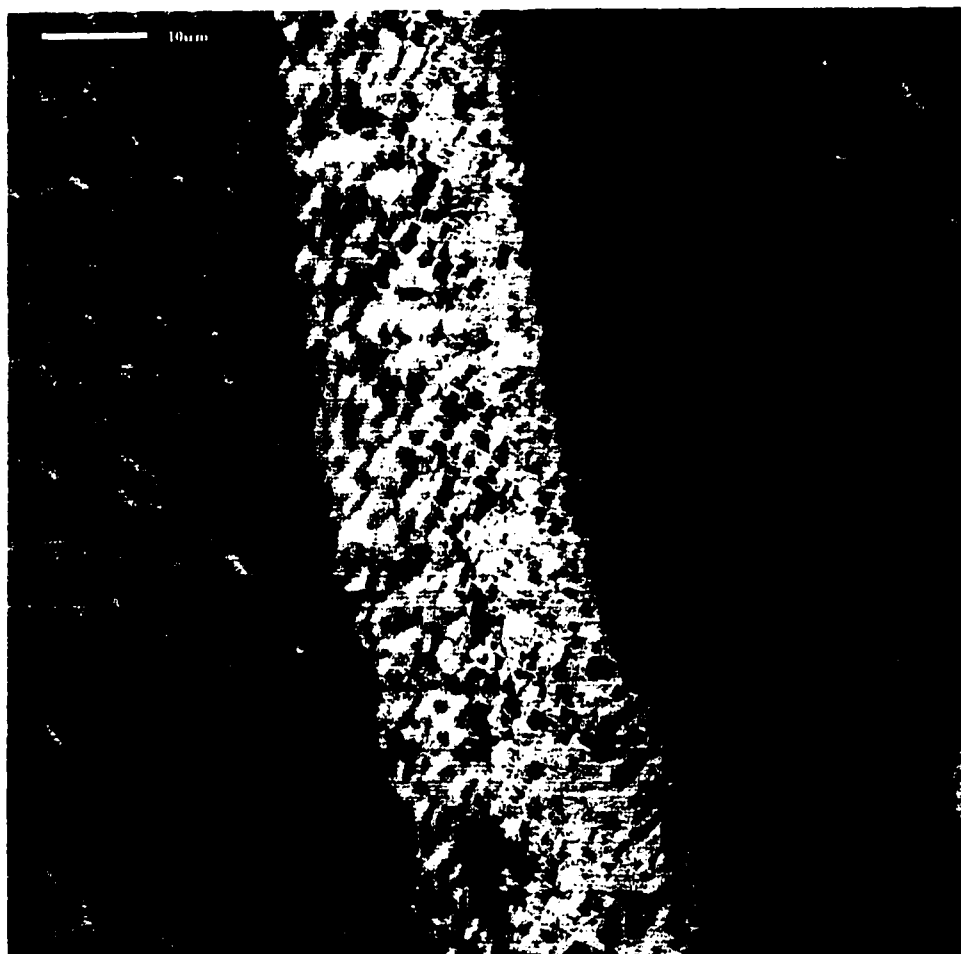


Figure 3.12 High Magnification Electron Microscope Image of a Fractured Concentrated Material Edge Prior to Sublimination for Membrane Concentrate Frozen at the Initial Freezing Temperature -2 degrees Celsius (Photo #1)

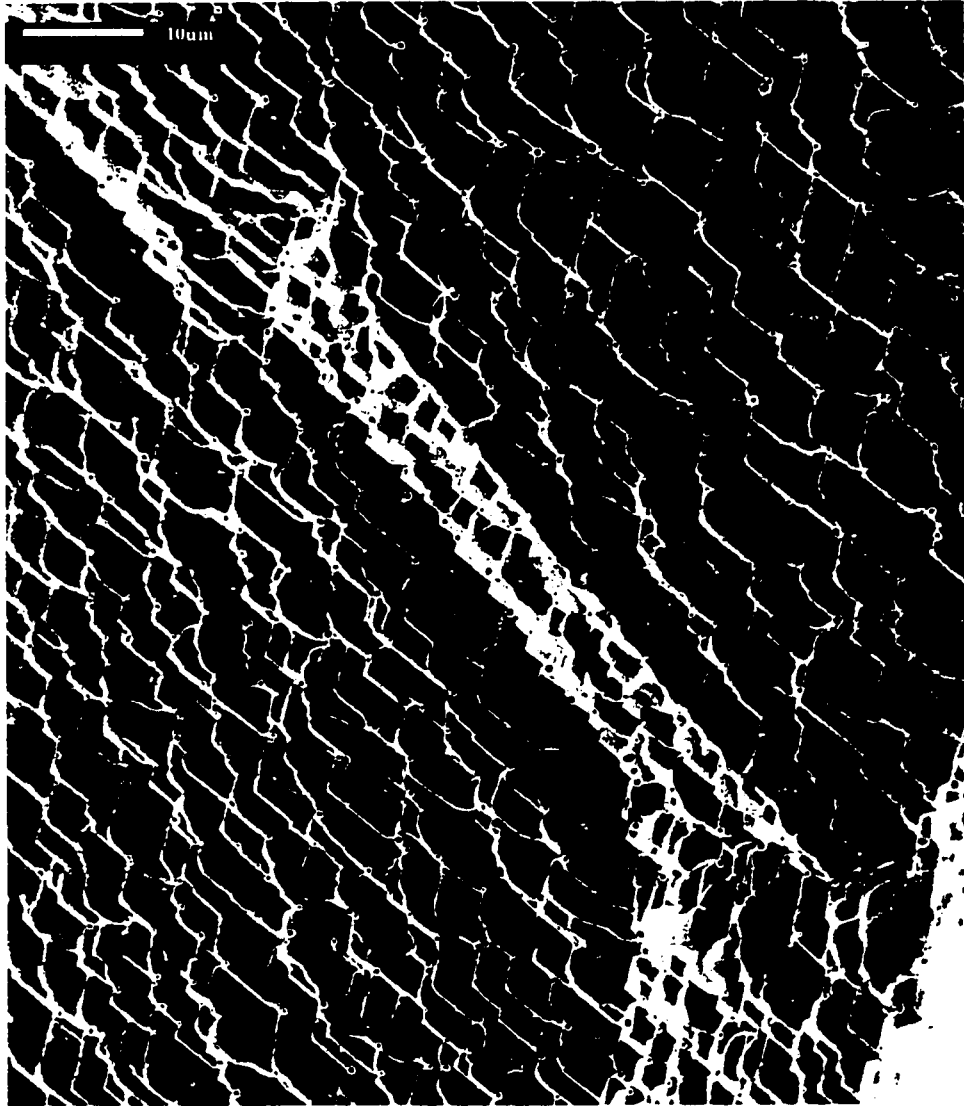


Figure 3.13 High Magnification Electron Microscope Image of a Fractured Concentrated Material Edge Prior to Sublimination for Membrane Concentrate Frozen at the Initial Freezing Temperature -2 degrees Celsius (Photo #2)

were not ruptured to suggest freezing did not occur instantaneously (Figure 3.14).

Distilled water was frozen and used as a control to distinguish between the presence of concentrated material observed in ice samples before and after sublimation. Figure 3.15 is an electron microscope image of a fractured ice surface comprised entirely of frozen distilled water. The appearance of fractures were produced during sample preparation. Shown in Figure 3.16 is a high magnification electron microscope image of the fractured ice specimen showing its characteristic surface morphology.

Tests were also conducted to investigate the changes that occurred to the concentrated material from instantaneously freezing the membrane concentrate by exposing it to the freezing temperature of liquid nitrogen (-190 °C). Shown in Figure 3.17 is an overview of a fractured ice specimen surface showing the concentrated material produced by instantaneous freezing (< 15 seconds). A high magnification electron microscope image of a single fractured wafer edge reveals the thickness and surface texture of the wafer-like material (Figure 3.18). From examination of this figure it can be seen that instantaneous freezing produced high concentrations of very thin, compact wafer-like zones of material arranged in sheet like patterns. The thickness of the wafer-like zones were less than 0.5 μm . These very thin zones of concentrated material were not observed in ice matrices extracted from the frozen concentrate during the freeze-thaw experiments at the initial freezing temperatures investigated.



Figure 3.14 Extreme High Magnification Electron Microscope Image of a Fractured Concentrated Material Edge Showing its Pore Morphology for Membrane Concentrate Frozen at the Initial Freezing Temperature -2 degrees Celsius

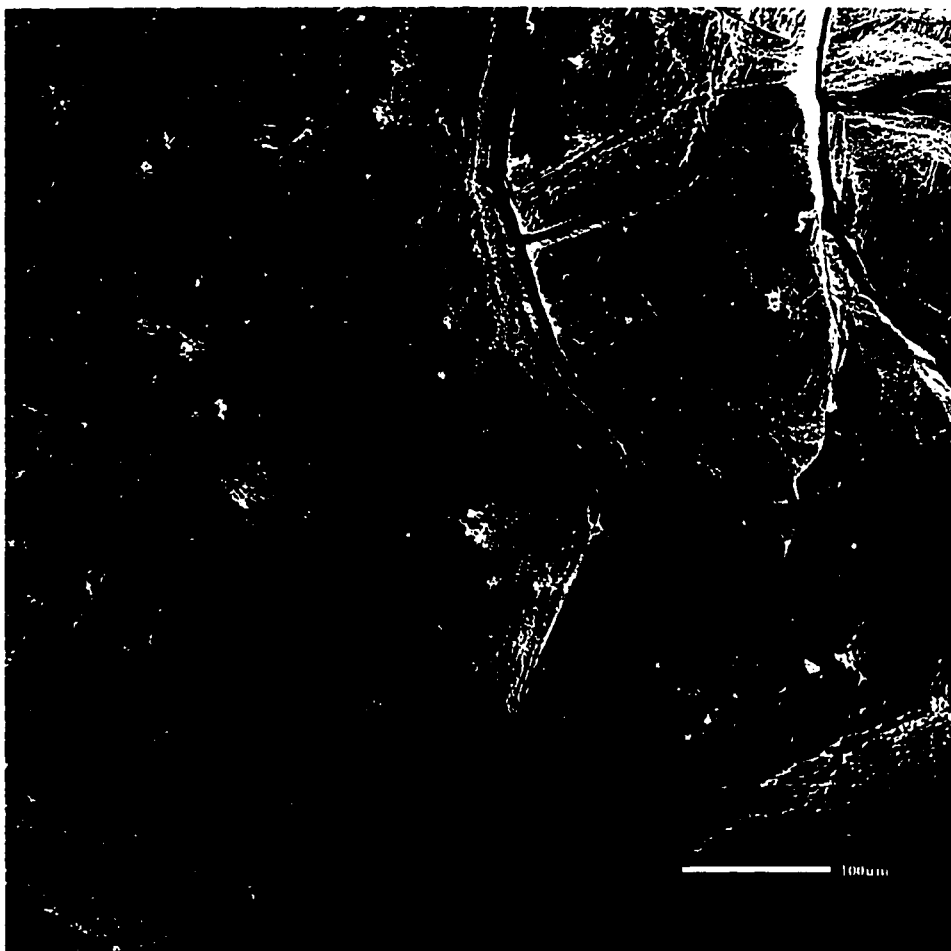


Figure 3.15 Electron Microscope Photograph of a Fractured Ice Specimen Surface Produced by Freezing Distilled Water at the Initial Freezing Temperature -15 degrees Celsius

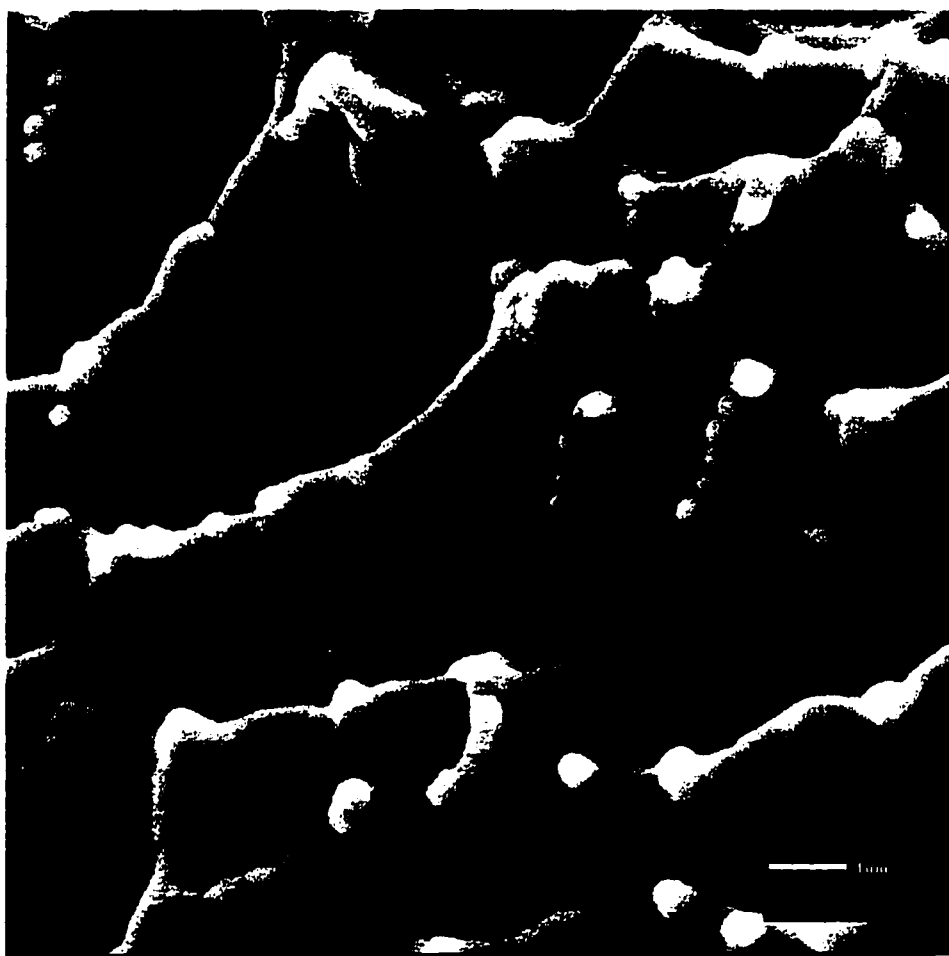


Figure 3.16 High Magnification Electron Microscope Image Showing the Surface Morphology of Frozen Distilled Water



Figure 3.17 Electron Microscope Photograph of a Fractured Ice Specimen Surface Produced by Instantaneously Freezing Membrane Concentrate in Liquid Nitrogen



Figure 3.18 High Magnification Electron Microscope Image of a Fractured Concentrated Material Edge Produced by Instantaneously Freezing Membrane Concentrate in Liquid Nitrogen

3.5.2.1.2 FILTER PAPER SPECIMENS

Filter paper specimens were prepared for examination of the concentrated material's thawed morphological properties. Sample preparation comprised of melting a fixed volume of ice on top of 0.8 μm cellulose filter paper while allowing the melt water to freely seep through the paper. Samples were not filtered under a vacuum to minimize disruption to the structural integrity of the concentrated material. The volume of ice applied to the filter paper was equivalent to approximately 1 mL of liquid. Following gravity filtration, the filter papers were removed and placed to dry in a desiccator for approximately 12 hours before analysis by SEM. Figure 3.19 is an electron microscope image of a clean membrane filter paper surface. Closer examination by SEM reveals the pore structure of the clean membrane filter paper (Figure 3.20).

The filter paper was carefully cut using surgical scissors and mounted on aluminum stubs using adhesive tape. Following mounting, samples were double sputter coated in an Edwards Sputter Coater (Model S150B) with gold to achieve a total thickness of 100 Angstroms. SEM analysis was conducted at 5 KV.

3.5.3 FREEZING POINT DETERMINATION

3.5.3.1 EXPERIMENTAL SAMPLES

The freezing point of an aqueous solution is directly related to the concentration of its water soluble constituents. If one or more substances are dissolved in water, the freezing point will be lowered in direct proportion to the molarity of the solution. The sectioning and chemical

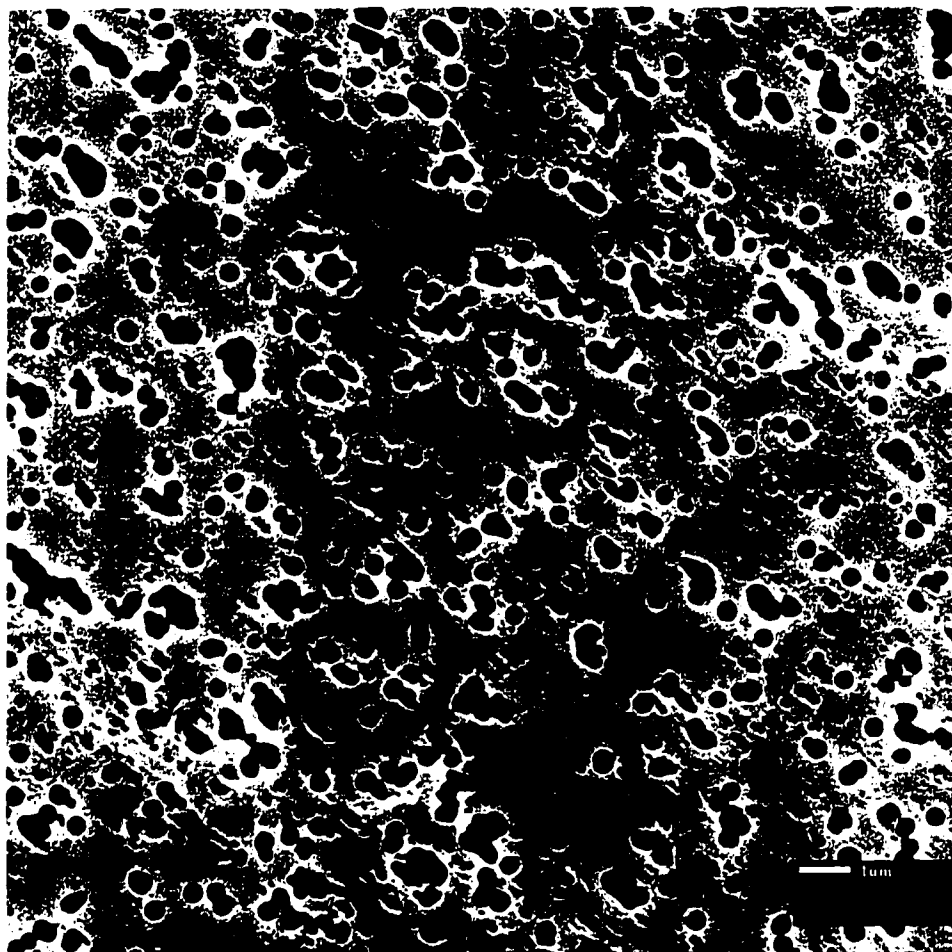


Figure 3.19 Electron Microscope Photograph of a Clean Membrane Filter Paper Surface

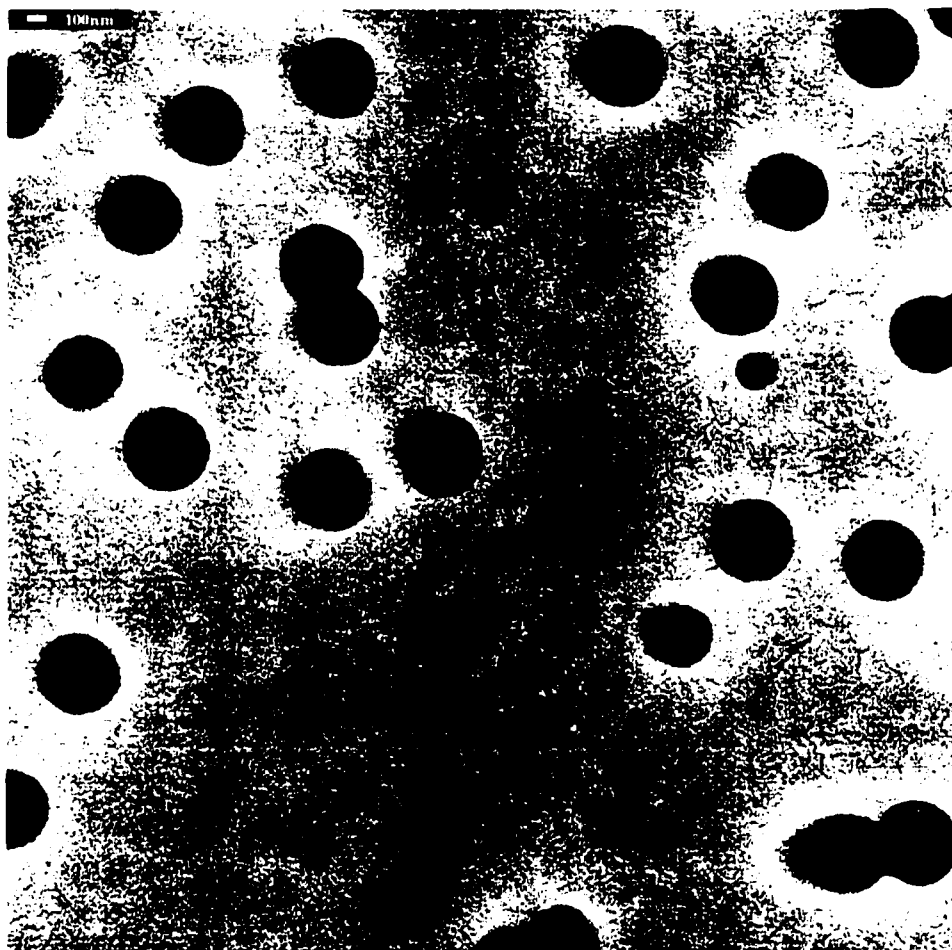


Figure 3.20 High Magnification Electron Microscope Image of a Clean Filter Paper Surface Showing its Pore Morphology

analysis of columns of frozen effluent showed the experimental water's constituents were concentrated in the direction of freezing, with the degree of concentration dependent on the freezing rate. To understand the change in the liquid's freezing point with respect to depth during freezing, samples of each experimental water were deliberately concentrated and the freezing point measured using the cryoscope. Different concentration strengths of each experimental water were produced by heating the effluent using a hot plate to a maximum temperature of 65 °C and allowing a portion of the effluent's water to evaporate. Boiling temperatures were avoided to minimize the loss of volatile organics. The cryoscope was used to measure the freezing point of different concentration strengths of each experimental water. Results from these tests were used to derive Figures 3.21 and 3.22. From examination of these figures it can be seen that the freezing point decreased very minimally for large increases in color concentration regardless of experimental water type. This would indicate the constituent matter of the effluent contributes only minimally to the constitutional undercooling of the solution during freezing.

3.5.3.2 CRYOMATIC CRYOSCOPE INSTRUMENT

Freezing point determination was performed using the Advanced Cryomatic Milk Cryoscope 4C2 instrument from Advanced Instruments Inc. The freezing point result was reported in degrees Celsius Hortvet (°H).

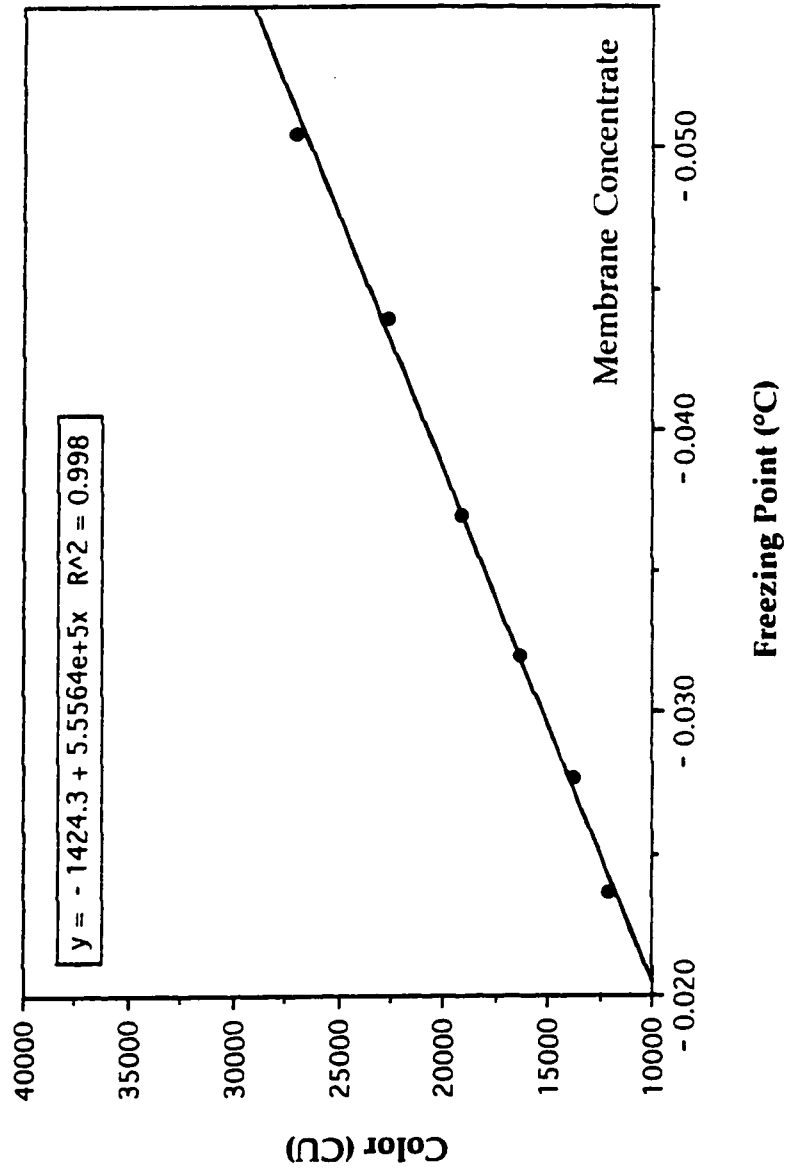


Figure 3.21 Plot of Freezing Point With Respect to Different Concentration Strengths of Membrane Concentrate

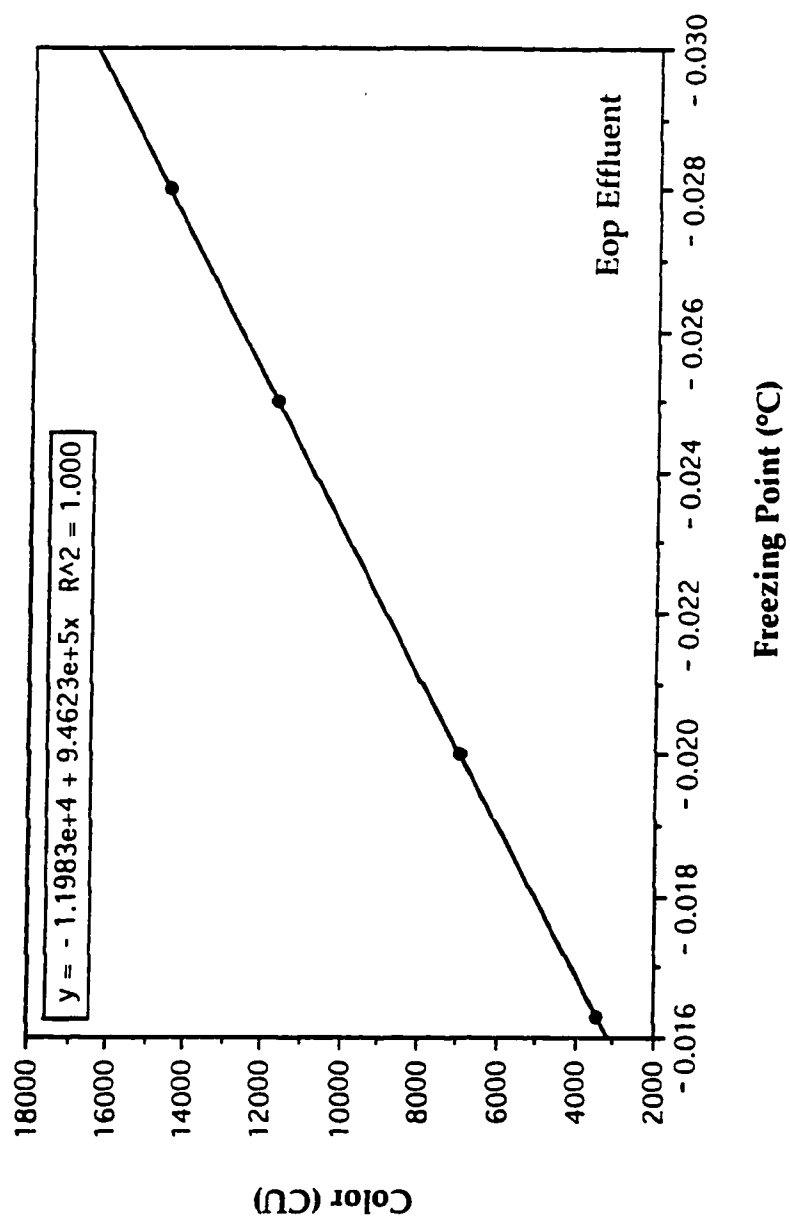


Figure 3.22 Plot of Freezing Point With Respect to Different Concentration Strengths of Eop Effluent

Equation 3.1 was used to convert the freezing point from degrees Celsius Hortvet to degrees Celsius (Prentice, 1973):

$$^{\circ}\text{C} = 0.96418 ^{\circ}\text{H} + 0.00085 \quad (3.1)$$

All determinations were conducted in duplicate.

3.5.4 X-RAY PHOTOELECTRON SPECTROSCOPY

X-ray photoelectron spectroscopy was used for chemical analysis of precipitates observed on filter paper samples. The procedure involved directing X-ray photons onto the sample surface to cause the ejection of an atomic core electron for every photon absorbed. Identification of the element was determined by measurement of the binding energy of one or more orbital electrons. The intensity of the measured signal was a function of the amount or concentration of the element present on the surface.

Filter paper samples were analyzed using the X-ray and Imaging Microanalysis System (IMIX) manufactured by Princeton Gamma-Tech, Inc. X-ray analysis was conducted at 20 KV.

3.5.5 SIZE FRACTIONATION BY ULTRAFILTRATION

Membrane concentrate was size fractionated to allow examination of the morphology of particular size fractions frozen unidirectionally. A Minitan Acrylic Ultrafiltration System by Millipore Direct was used to size fractionate the alkaline extraction stage membrane concentrate.

3.6 EXPERIMENTAL APPARATUS

3.6.1 UNIDIRECTIONAL FREEZING APPARATUS

Unidirectional freezing experiments were conducted in a cold storeroom at 4 °C using four of the experimental apparatuses shown in Figure 3.23. Four sets of apparatuses were constructed of polyurethane to the dimensions shown below. Inserted inside at the base of the 100 mm diameter by 200 mm deep cylindrical hole of the sample location was a glycol contraction bag designed to relieve the tremendous pressures that develop during phase change from a liquid to a solid. Tests conducted at the liquid depth of 250 mm required modification to the apparatuses to increase the depth of the sample compartment by an additional 100 mm. Freezing of the sample was initiated from the top down to simulate natural freezing by use of a specially designed aluminum freezing plate. The sample was placed in a 2 litre capacity plastic bag inside the apparatus and the freezing plate placed on top inside the bag for contact with the liquid. Chilled glycol was continuously circulated through the aluminum plate with the temperature of the glycol controlled by a refrigeration system. The temperature of the chilled glycol was adjustable to enable establishing a desired initial freezing temperature between the range of 0 °C to -25 °C, within an relative accuracy of ± 0.5 °C. To obtain an initial freezing temperature set point of -25 °C the experimental apparatus was placed inside a freezer adjusted to produce an inside environmental temperature of between -0.5 °C to -1 °C. Thermosisters with a accuracy of ± 0.5 °C were placed against the plastic bag at different elevations inside the apparatus to record both the freezing and thawing isotherms (samples

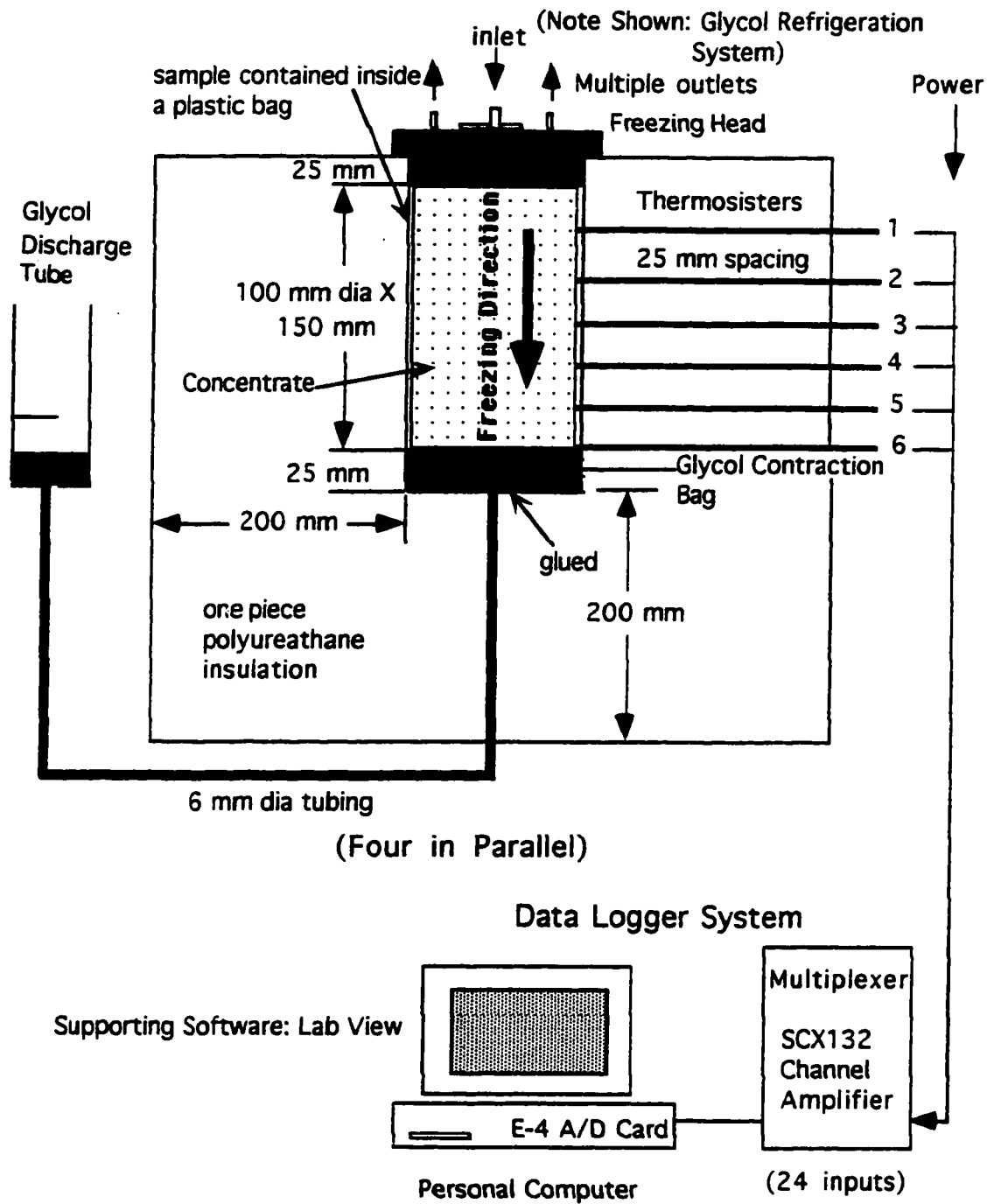


Figure 3.23 Unidirectional Freezing Apparatus

thawed top down only). Temperature data was collected at one minute intervals using a data logger supported by Lab View® software. The temperature of the experimental waters prior to freezing was 4 °C, the same temperature at which the water was stored.

A total of four freezing apparatuses were constructed and connected to the data logger. During experimental testing it was found a single refrigeration unit using separate freezing heads could operate in parallel a maximum of two freezing apparatuses at any one time, while producing equivalent freezing rates.

The thermosisters of each freezing apparatus were checked routinely throughout the study for their operation by comparing thermosister readings to air and liquid temperatures measured by a thermometer. Thermosister readings were found to be in agreement with temperature values measured by a thermometer to within ± 0.5 °C.

City of Edmonton drinking water was initially used to commission each experimental apparatus to ensure the freezing and thawing isotherms were similar that multiple runs could be conducted and accurately compared while using all four apparatuses. From examination of Figure 3.24 it can be seen that the freezing isotherms for identical freezing conditions were not significantly different among the experimental apparatuses enabling the use of all four freezing apparatus for comparison of runs. Frozen ice columns spiked with food coloring dye were also visually examined to confirm the direction of freezing. Frozen samples pulled to examine dye concentration distribution showed the dye was unidirectionally concentrated and distributed throughout the ice

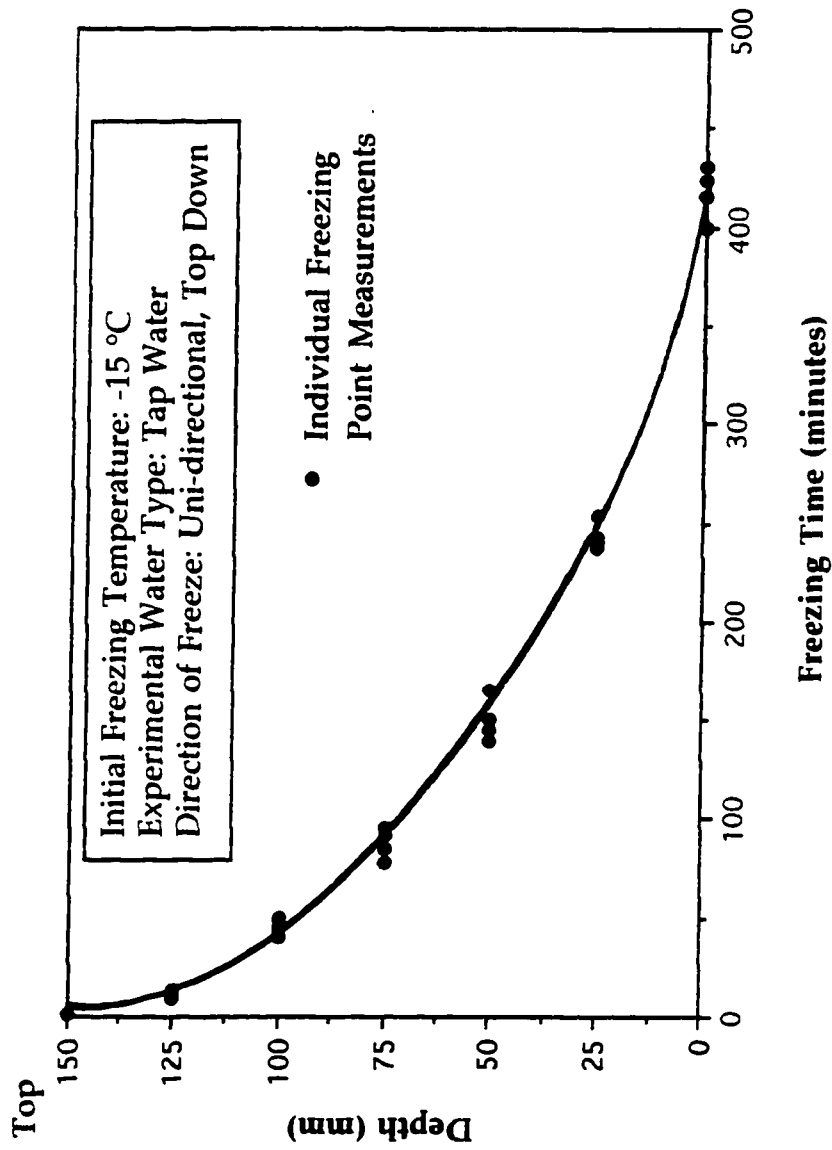


Figure 3.24 Plot Showing the Comparison of the Freezing Curves for Each Experimental Apparatus Representing the Freezing of City of Edmonton Drinking Water at the Initial Freezing Temperature -15 °C

matrix at the bottom of the ice column. The equal distribution of dye over the cross section of the ice column indicated ice crystal growth occurred primarily in the downward vertical direction.

3.6.2 EXPERIMENTAL APPARATUS FOR STABILITY TESTS AND SAMPLE THAWING

The experimental apparatus shown in Figure 3.25 was used to conduct stability tests and tests to simulate thawing predominantly from the bottom up consisted of 100 mm diameter by either 200 mm or 250 mm deep polyethylene cylinders. The wall thickness of the polyethylene cylinders were 50 mm thick. The base of the cylinders consisted of 50 mm thick stainless steel bases. These cylinders were nearly identical in size to the sample holder of the freezing apparatus so that ice columns could be removed and placed directly into these cylinders for evaluation of different rates of thawing.

3.7 EXPERIMENTAL PROCEDURES AND PROTOCOLS

3.7.1 SAMPLE COLLECTION

Frozen and thawed, composite and location specific samples were collected of the experimental waters during their freeze-thaw experiments. Summarized in the proceeding sections are descriptions of the methods and types of samples collected for chemical determination.

3.7.1.1 FROZEN SAMPLES

Frozen composite and location specific samples were collected of the experimental waters following freezing. Sample collection comprised of

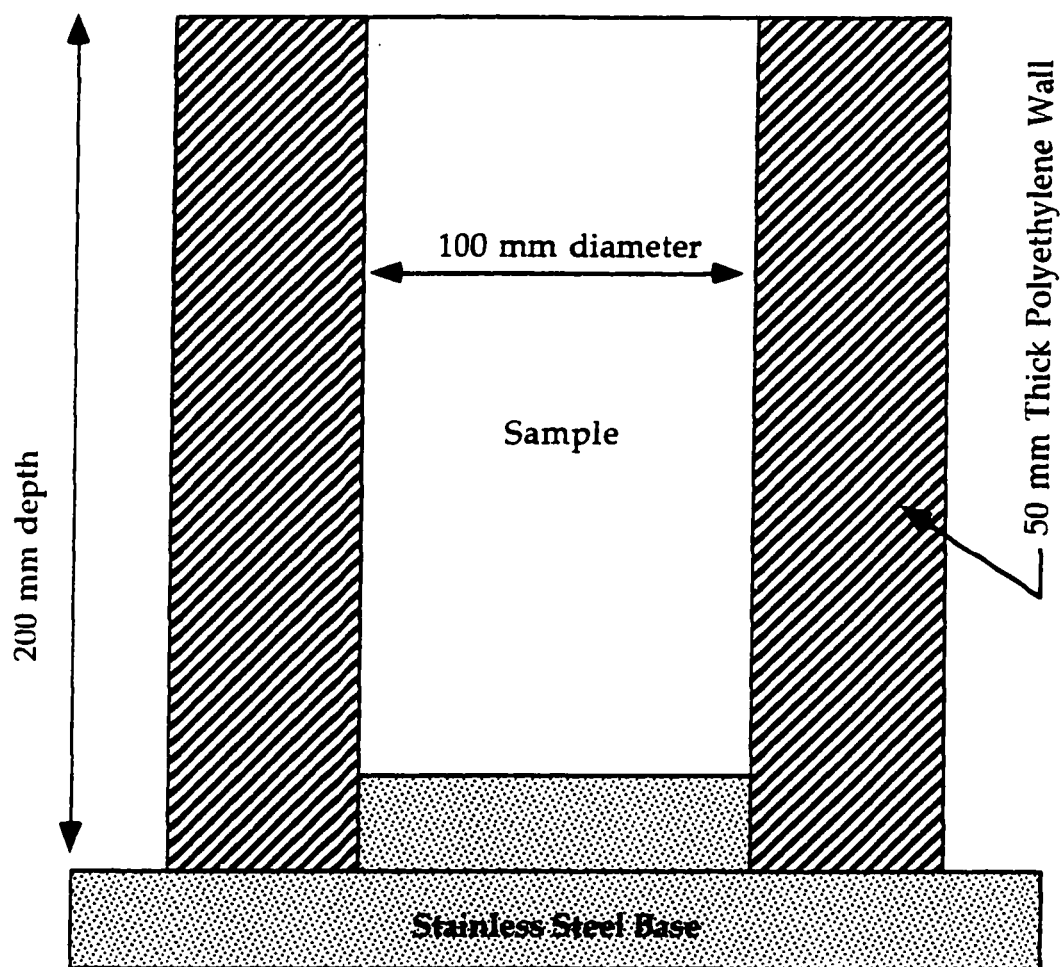


Figure 3.25 Experimental Thawing and Stability Apparatus

sectioning the ice column of each experimental water type at its different experimental freezing temperatures using a band saw located in a cold storeroom. The band saw prior to and after each ice sectioning was cleaned with alcohol and distilled water. Collection of frozen composite samples consisted of sectioning the ice column into three volume sizes (i.e., top 35 % frozen volume, middle 35 % frozen volume, and bottom 30 % frozen volume). Collection of location specific samples consisted of sectioning the ice column into 25 mm thick by 100 mm diameter ice sections. Following sample collection, ice samples were placed in borosilicate glass sample containers, sealed, and allowed to thaw at room temperature (24 °C).

3.7.1.2 LIQUID SAMPLES

Liquid composite and selective samples were collected of the experimental waters following thawing. Prior to sample collection, the liquid depth was measured and recorded using a calibrated ruler. The collection of liquid composite samples consisted of siphoning off the thawed treated experimental water into three composite volumes (i.e., top 35 % liquid volume, middle 35 % liquid volume, bottom 30 % liquid volume) using a 6 mm diameter Tigon tubing. The volume collected was discharged into a graduated cylinder during sample collection to monitor that the correct volume fraction had been obtained. The collection of selective samples was by pipette. A 25 mL capacity pipette was inserted into the sample center at different depths following which sample portions representative of 25 mm thick liquid layers were slowly removed. The initial liquid depth and the depths at which each sample were collected was recorded with respect to the initial unsampled depth. Sampling was conducted from the top down. This method of selective sampling was

more accurate than attempting to siphon 25 mm thick liquid depths. Careful attention was paid not to disturb the liquid at the point of collection during sampling.

3.7.2 METHODS OF THAWING

Two methods of thawing the frozen effluent were investigated; from the top down or from predominantly the bottom up. Thawing of ice columns from the top down were conducted in the freezing apparatus by placement of a programmable heater above the ice column at a fixed distance of 75 mm from the ice surface. The programmable heater was programmed for the initial thawing temperature. Thawing was complete and the sample collected when the entire liquid volume had reached a constant liquid temperature equal to the initial thawing temperature. Ice columns thawed from the top down were prevented from floating during thawing. Data to measure the thawing rate was recorded by thermosisters linked to a data logger.

Ice columns thawed from predominantly the bottom up were first removed and placed in the thawing apparatus described in section 3.6.1. To remove the ice columns from the freezing apparatus a rope net was positioned between the plastic sample bag and the inside wall of the apparatus underneath the glycol contraction bag. The rope net was installed in such a manner so as not to inhibit the function of the thermosisters. To remove the ice column, the glycol contraction bag was first drained. Following this the sample was pulled vertically from the freezing apparatus using the pull net. The plastic bag was removed and the sample placed inside the thawing apparatus. The diameter of the freezing

apparatus was designed to be marginally smaller than that of the sample holder of the thawing apparatus to ensure a tight fit. Thawing was conducted from all directions in a temperature controlled room. In filming the thawing process, it was found that the ice column thawed more quickly in the vertical direction than from the horizontal direction and that this was attributed to differences in the materials of construction for the thawing apparatus. In this method of thawing the ice was allowed to float, allowing the melt water flow pattern to be in the downward direction.

3.7.3 MELT WATER FLOW PATTERN DYE STUDIES

Dye studies using a food dye were conducted to examine the melt water flow patterns associated to different methods of thawing and thawing temperatures. Make-up of the stock dye solution consisted of diluting 1 mL of standard food dye (red in color) into 1000 mL of distilled water. Distilled water was then used as the experimental water and frozen unidirectionally in a clear Plexiglas cylinder identical in size and construction to the thawing apparatus. The dye solution was added to the experimental water following freezing. To add the dye solution, several 6 mm diameter holes were carefully drilled into the ice column for a depth equal to $\frac{2}{3}$ (approximately 100 mm) the total depth. A surgical needle was then used to inject the dye solution into the drilled holes after which the ice column was re-frozen unidirectionally. Melting of ice columns containing dye were conducted to examine the flow pattern of the melt water for when the ice column was thawed from predominantly the bottom up at the thawing temperatures 4 °C and 24 °C. For comparison, dye studies were also conducted to examine the melt water flow pattern

for when the ice column was thawed from the top down at a temperature of 24 °C. All thawing tests were conducted in a temperature controlled room.

3.7.4 CYCLED FREEZE-THAW EXPERIMENTS

Cycled freeze-thaw experiments were conducted to investigate the additional color removal that would be obtained in the upper liquid portion of membrane concentrate treated repeatedly by freeze-thaw. The freeze-thaw conditions selected were those experimental set points that provided for the best results. The initial freezing temperatures investigated were -2 °C and -15 °C. The liquid depth selected was 150 mm. Frozen concentrate samples were thawed from the bottom up at a temperature of 24 °C. The maximum number of freeze-thaw cycles investigated were 3 cycles. Thawed composite samples were collected following each cycle in accordance to section 3.7.1.2. All runs were conducted in triplicate.

3.8 EXPERIMENTAL DESIGN

3.8.1 SELECTION OF MEASUREMENT

3.8.1.1 ALKALINE EXTRACTION STAGE EFFLUENT

Color was selected as the parameter that would be measured to evaluate treatment performance by freeze-thaw of alkaline extraction stage effluent. Depicted in Figures 3.26 to 3.28 are the correlations of color with respect to its corresponding COD, total alkalinity, and TDS concentrations. Examination of these figures shows color can be used to accurately predict

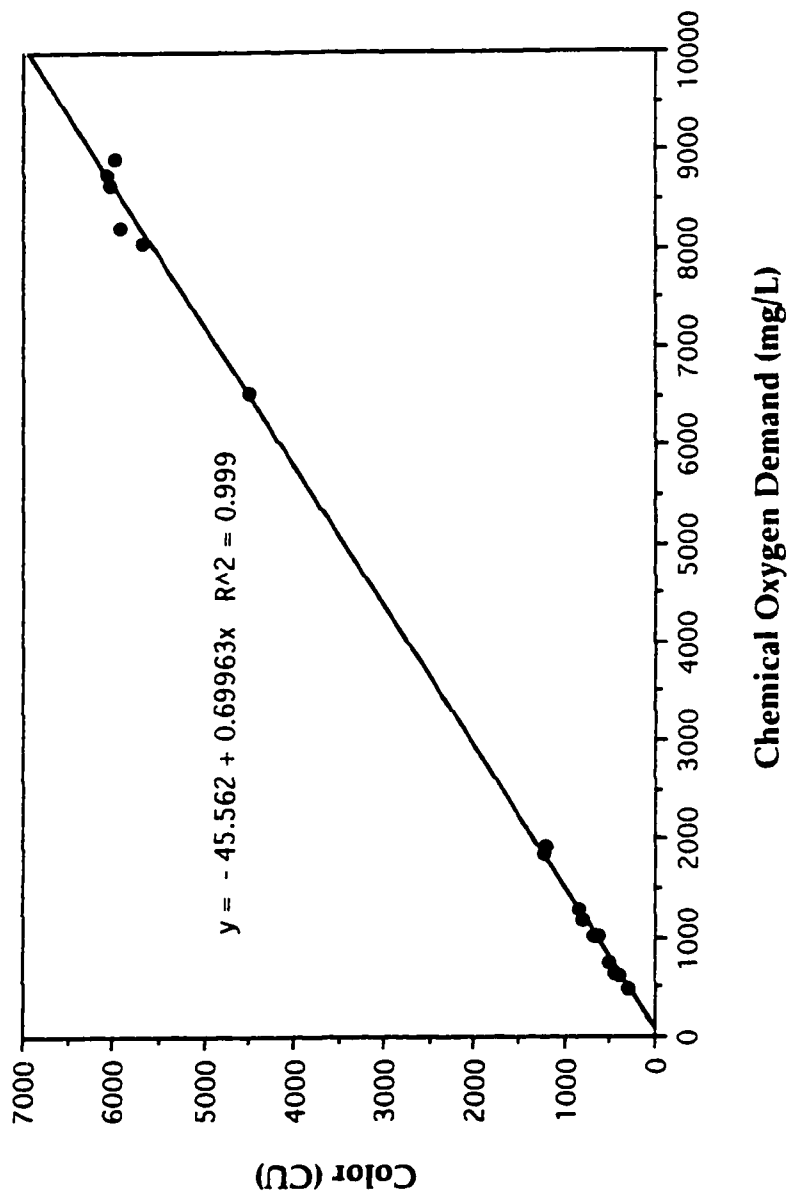


Figure 3.26 Plot Correlating Color to Chemical Oxygen Demand for Eop Effluent Treated by Freeze-thaw Under Different Freezing and Thawing Conditions

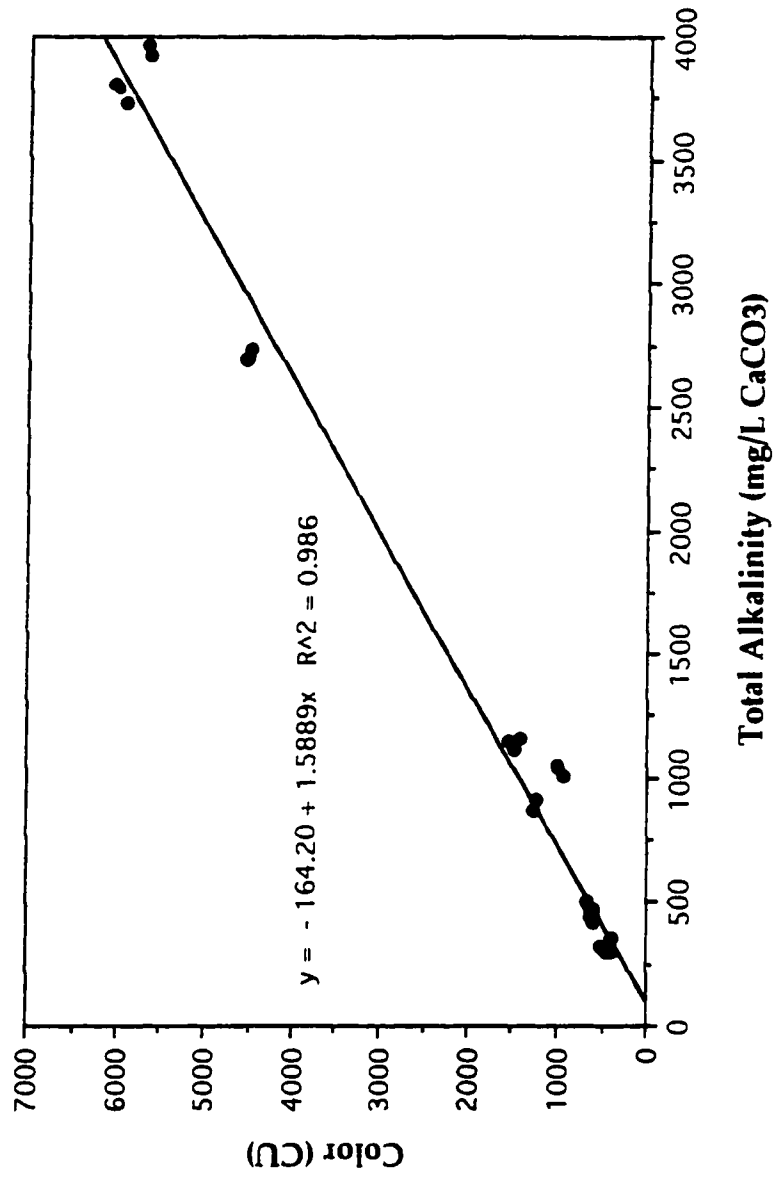


Figure 3.27 Plot Correlating Color to Total Alkalinity for Eop Effluent
Treated by Freeze-thaw Under Different Freezing and Thawing
Conditions

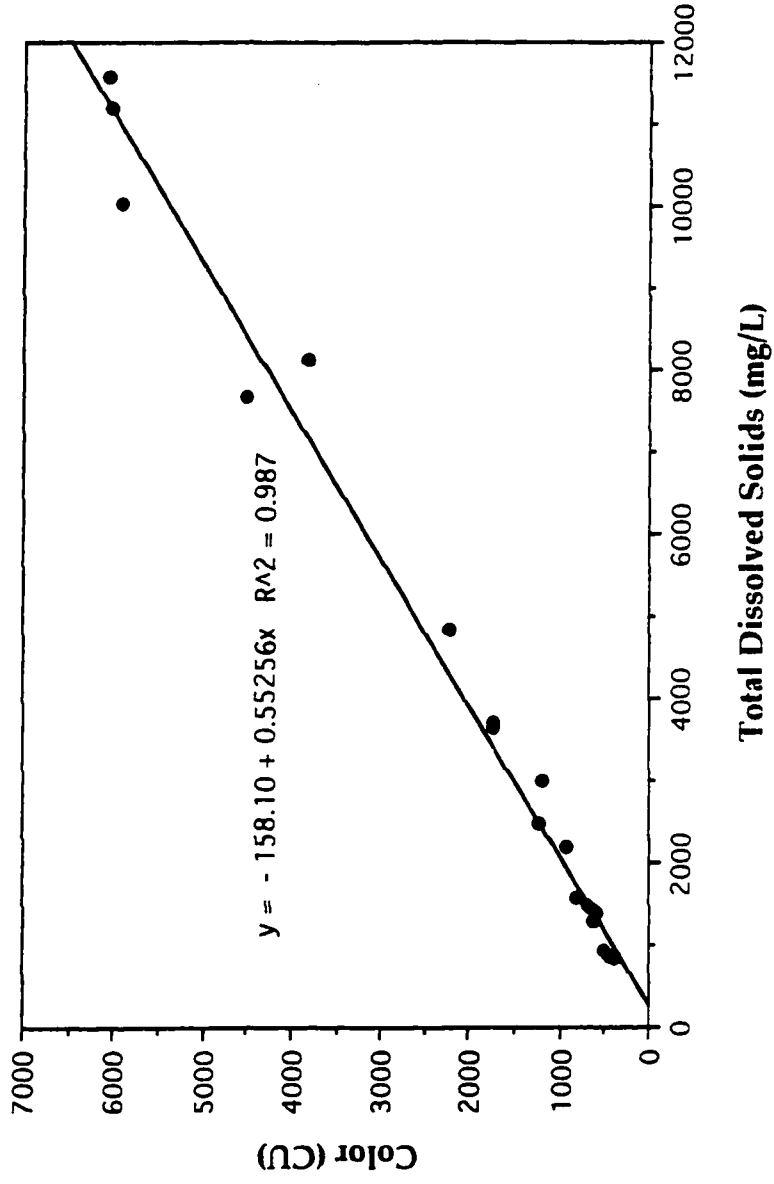


Figure 3.28 Plot Correlating Color to Total Dissolved Solids for Eop Effluent Treated by Freeze-thaw Under Different Freezing and Thawing Conditions

COD, total alkalinity, and TDS over the range of concentrations concerned. The coefficient of linear correlation for color with respect to COD, total alkalinity, and TDS were 0.999, 0.986, and 0.987, respectively.

Tests were also conducted to determine if the color concentration in the top 70 % liquid volume could be accurately calculated from averaging the measured values for the top and middle composite sample portions. Summarized in Table 3.7 is the statistical data comparing the calculated color derived from averaging the measured top and middle color concentration of the composite samples to the actual color concentration produced by mixing the top and middle composite samples. Table 3.7 shows the calculated and measured color concentrations representative of the color in the top 70 % liquid volume were not significantly different using the two tailed Paired t-test at a 95 % confidence limit. Based on this, the color concentration in the top 70 % liquid volume was in most cases determined by averaging the color concentrations measured in the top and middle composite sample portions.

3.8.1.2 ALKALINE EXTRACTION STAGE MEMBRANE CONCENTRATE

Similarly, color was selected as the parameter that would be measured to evaluate treatment performance by freeze-thaw of membrane concentrate. Depicted in Figures 3.29 to 3.31 are correlations of color with respect to its corresponding COD, total alkalinity, and TDS concentrations. Examination of these figures shows color can be used to accurately predict COD, total alkalinity, and TDS over the range of concentrations concerned.

Table 3.7 Summary of Statistical Data Comparing the Sample Means of the Calculated and Measured Color Concentrations of the Top 70 % Liquid Volume Using the Paired t-Test

Run	Calculated Color (CU)	Measured Color (CU)	d_i	\bar{d}	s_d	t-test Value	Critical Value	Conclusion
Run 1								
1	863	875	-12	29.0	19.313	2.601	4.303	accept H_0
2	900	950	-50					
3	875	900	-25					
Run 2								
1	1140	1180	-40	23.3	28.868	1.400	4.303	accept H_0
2	1180	1220	-40					
3	1140	1130	+10					
Run 3								
1	1580	1550	+30	10.0	52.915	0.327	4.303	accept H_0
2	1600	1650	-50					
3	1650	1600	+50					

null hypothesis: $\mu_1 = \mu_2$, two tailed Paired-difference test, $\alpha = 0.05$, two degrees of freedom, $t = d(n)^{1/2}/s_d$

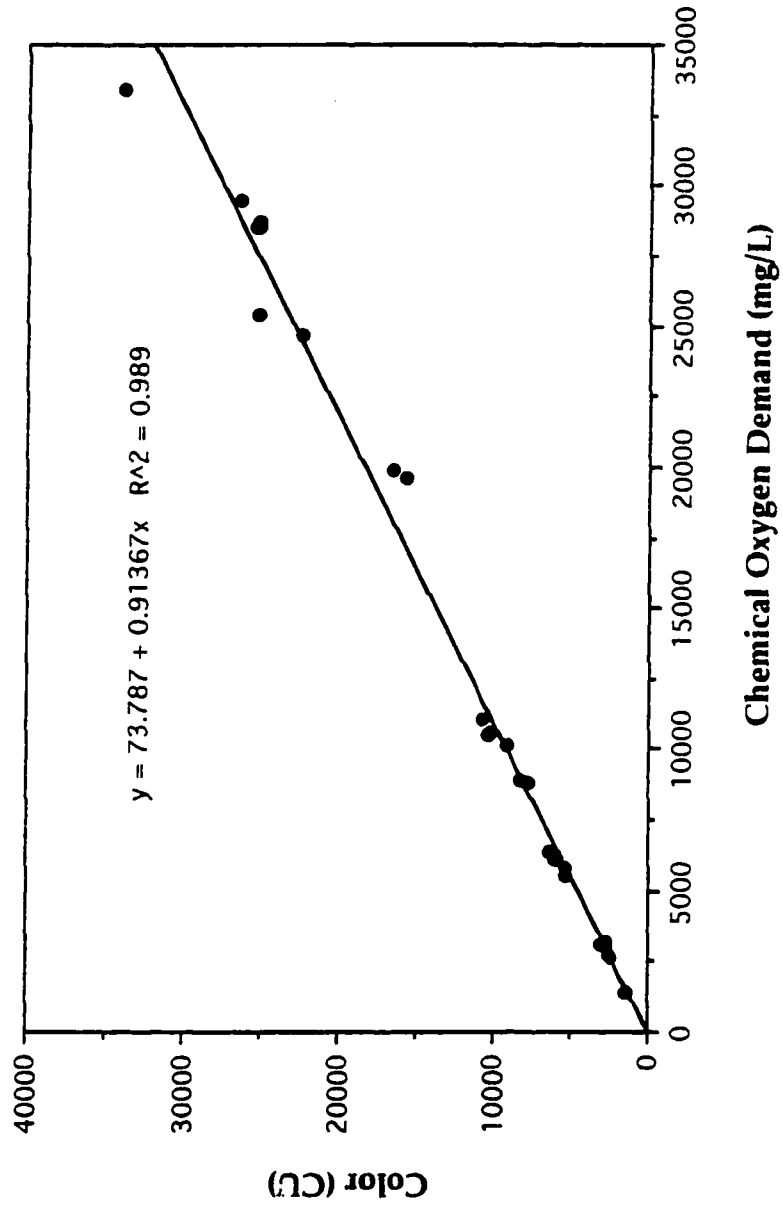


Figure 3.29 Plot Correlating Color to Chemical Oxygen Demand for Membrane Concentrate Treated by Freeze-thaw Under Different Freezing and Thawing Conditions

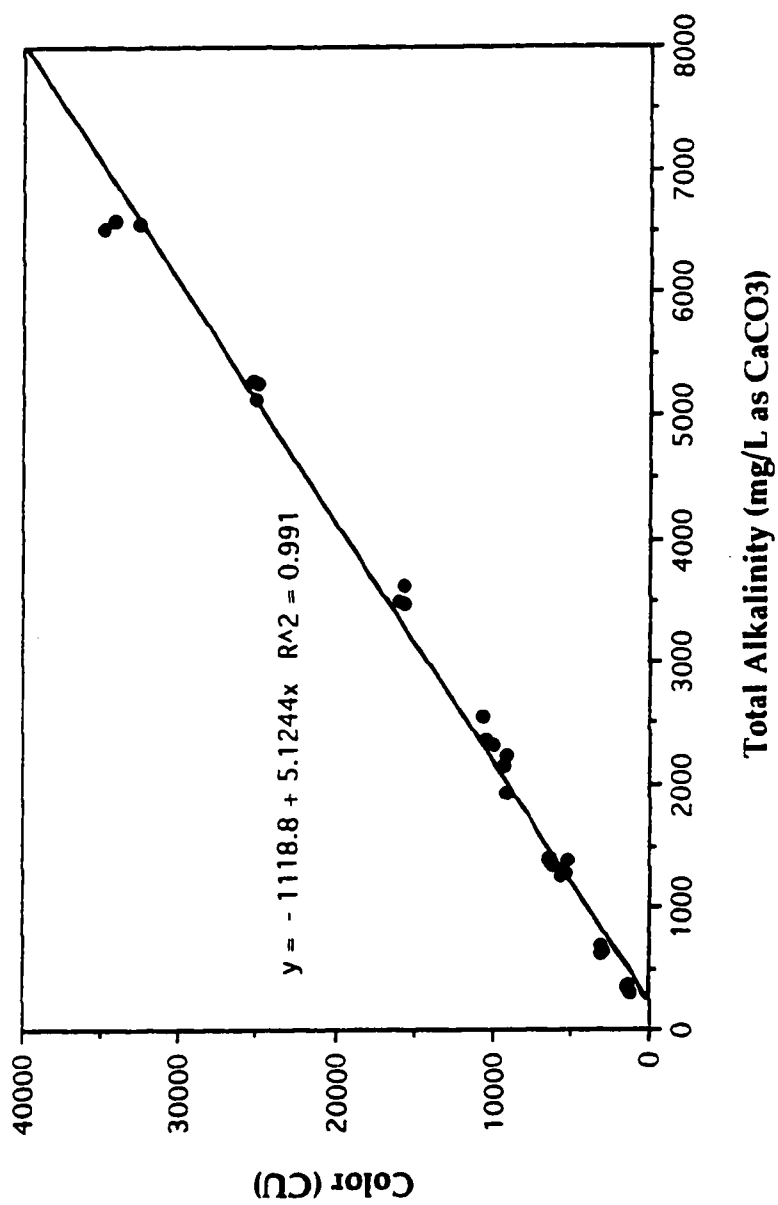


Figure 3.30 Plot Correlating Color to Total Alkalinity for Membrane Concentrate Treated by Freeze-thaw Under Different Freezing and Thawing Conditions

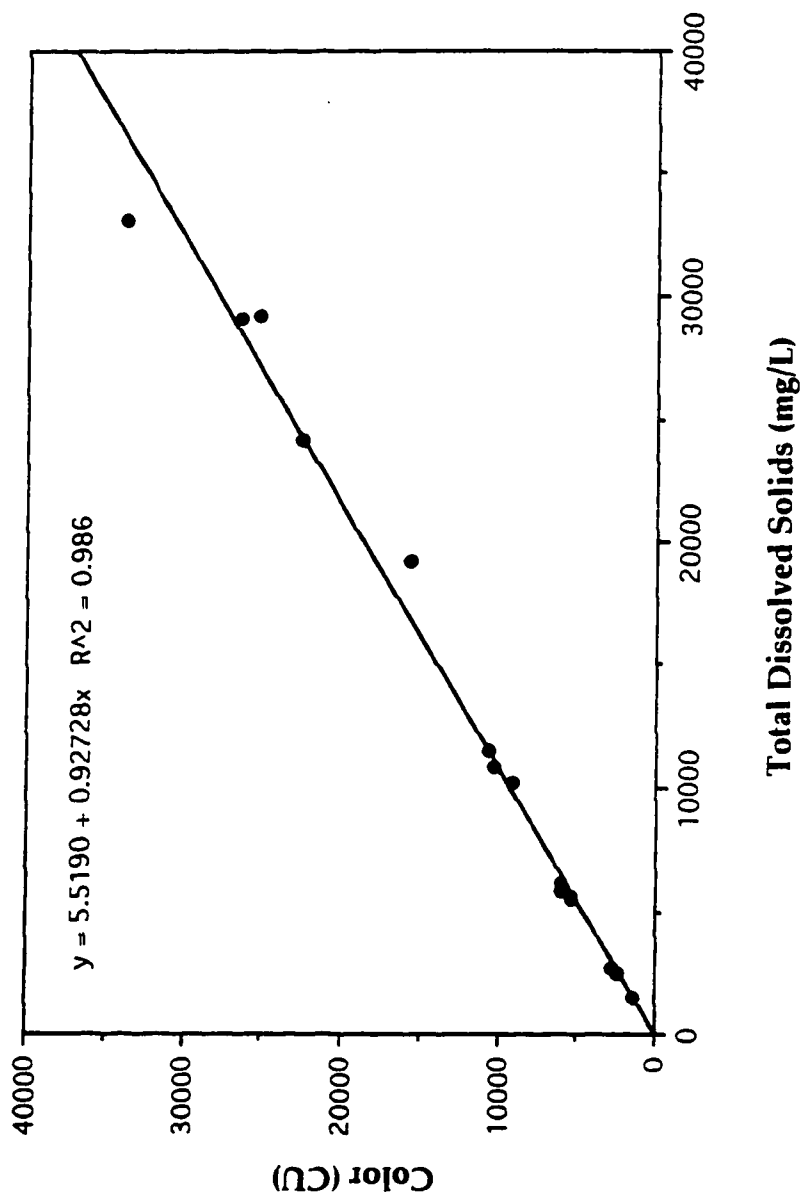


Figure 3.31 Plot Correlating Color to Total Dissolved Solids for Membrane Concentrate Treated by Freeze-thaw Under Different Freezing and Thawing Conditions

The coefficient of linear correlation for color with respect to COD, total alkalinity, and TDS were 0.989, 0.991 and 0.988, respectively.

To limit the amount of chemical analysis, comparative tests were conducted to determine the difference between calculating the average color concentration of the top and middle composite samples versus mixing the two and measuring the resultant color concentration. Summarized in Table 3.8 is the statistical data comparing the calculated color derived from averaging the measured top and middle color concentration of the composite samples to the actual color concentration produced by mixing the top and middle composite samples. Examination of this table shows that calculated and measured color concentrations representative of the color in the top 70 % liquid volume were not significantly different using the two tailed Paired t-test at a 95 % confidence limit. Based on this the color concentration in the top 70 % liquid volume was in most cases determined by averaging the color concentrations measured in the top and middle composite sample portions.

3.8.2 FACTORIAL DESIGNS

Individual factorial experiments were conducted to examine the effect of four quantitative variables on treatment performance with respect to each experimental water type. The quantitative variables investigated were: initial freezing temperature, storage temperature, storage time, and thawing temperature. Summarized below in Tables 3.9 to 3.10 are the factorial designs for each experimental water type. The fixed variables applied in each factorial design are summarized in Table 3.11. The selection of these fixed variables were based on experimental studies

Table 3.8 Summary of Statistical Data Comparing the Sample Means of the Calculated and Measured Color Concentration of the Top 70 % Liquid Volume Using the Paired t-Test

Run	Calculated Color (CU)	Measured Color (CU)	d_i	\bar{d}	s_d	t-test Value	Critical Value	Conclusion
Run 1								
1	9730	9750	-20	6.7	32.145	0.361	4.303	accept H_0
2	9770	9800	-30					
3	9580	9550	+30					
Run 2								
1	5270	5300	-30	6.7	32.145	0.361	4.303	accept H_0
2	5340	5360	-20					
3	5200	5170	+30					
Run 3								
1	4130	4120	+10	0.0	26.450	0.000	4.303	accept H_0
2	4280	4310	-30					
3	4350	4330	+20					

null hypothesis: $\mu_1 = \mu_2$, two tailed Paired-difference test, $\alpha = 0.05$, two degrees of freedom, $t = \bar{d}(n)^{1/2}/s_d$

Table 3.9 2⁴ Factorial Design Matrix for the Alkaline Extraction Stage Membrane Concentrate

Quantitative Variables	Levels
Initial Freezing Temperature (°C)	-2 °C & -15 °C
Thawing Temperature (°C)	+4 °C & +24 °C
Storage Temperature (°C)	-2 °C & -15 °C
Storage Time (days)	0, 30, 60, & 90 days

Table 3.10 2⁴ Factorial Design Matrix for the Alkaline Extraction Stage Effluent

Quantitative Variables	Levels
Initial Freezing Temperature (°C)	-2 °C & -15 °C
Thawing Temperature (°C)	+4 °C & +24 °C
Storage Temperature (°C)	-2 °C & -15 °C
Storage Time (days)	0, 30, 60, & 90 days

Table 3.11 Fixed Variables Applied in Each Factorial Design

Fixed Variables	Setpoint
Liquid Depth (mm)	150 mm
Concentration Strength	Stock Experimental Water
Method of Thawing	Bottom-up
Freeze-thaw Cycles	1

conducted to examine the relative importance of each variable with respect to treatment performance. The fixed variables selected were found to be relatively unimportant over the range of interest or found to adversely affect treatment performance that the set points arbitrarily chosen for these variables were those which would produce the best results under different freeze-thaw conditions. The measured response was color concentration in the top 70 % liquid volume. All experimental runs were conducted as a minimum in duplicate.

3.9 ISOTHERM DATA

3.9.1 FREEZING ISOTHERM DATA

The freezing curves presented herein were approximated using freezing isotherm data and the experimental water's original freezing point. Tests were conducted to determine the degree in change in freezing point of the effluent with respect to its depth during freezing by sampling to measure the change in chemical composition with respect to depth of the frozen effluent brought about by freezing. The changes in the frozen effluent's color concentration with respect to depth were shown using Figures 3.21 and 3.22 to result in only minimal decreases in the effluent's freezing point. The maximum estimated change in freezing point was 0.09 °C or less depending on the effluent type and depth. These changes were not significant that the change in freezing point with respect to depth could accurately be detected by the thermosisters. Consequently, to approximate the freezing curves at their initial freezing temperatures an average freezing point was assumed over the entire depth of the sample

with the value selected being the experimental water's original freezing point.

Although they are an approximation of the freezing rate with respect to the sample's depth, the freezing curves were used primarily as a check for comparing duplicate run conditions. Duplicate run conditions were only compared when the freezing curves were shown to be similar. The freezing curves plotted are the average of six experimental runs. The average estimated time to completely freeze the effluent as determined from the freezing curve was the time period for the entire sample to undergo a phase change from a liquid to solid.

3.9.1.1 ALKALINE EXTRACTION STAGE EFFLUENT

3.9.1.1.1 INITIAL FREEZING TEMPERATURE: -2 °C

Figure 3.32 is an approximation of the freezing curve representative of unidirectionally freezing Eop effluent at the initial freezing temperature -2 °C. The average estimated time period to completely freeze the Eop effluent unidirectionally was approximately 3,270 minutes (2.27 days).

3.9.1.1.2 INITIAL FREEZING TEMPERATURE: -15 °C

Figure 3.33 is an approximation of the freezing curve representative of unidirectionally freezing Eop effluent at the initial freezing temperature -15 °C. The average estimated time period to completely freeze the Eop effluent unidirectionally was approximately 461 minutes (0.32 days).

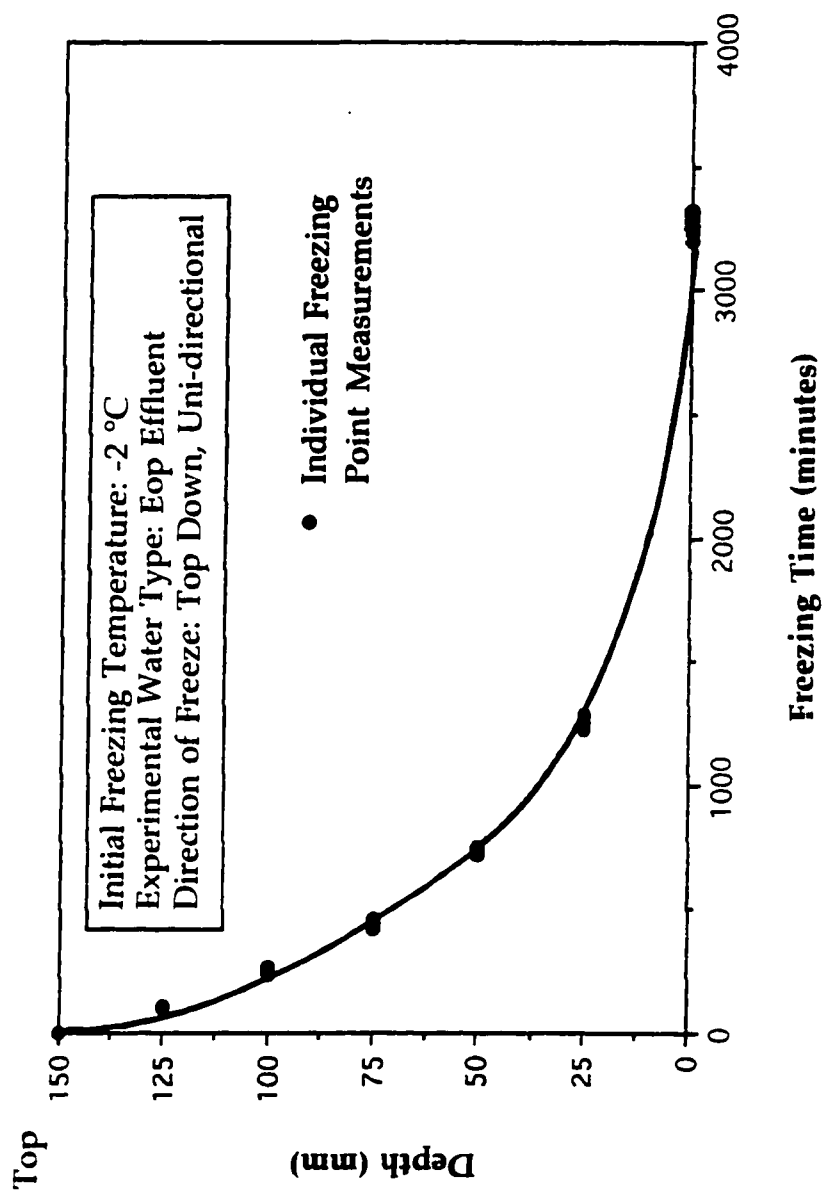


Figure 3.32 Freezing Curve Representative of Freezing Eop Effluent at the Initial Freezing Temperature -2 °C

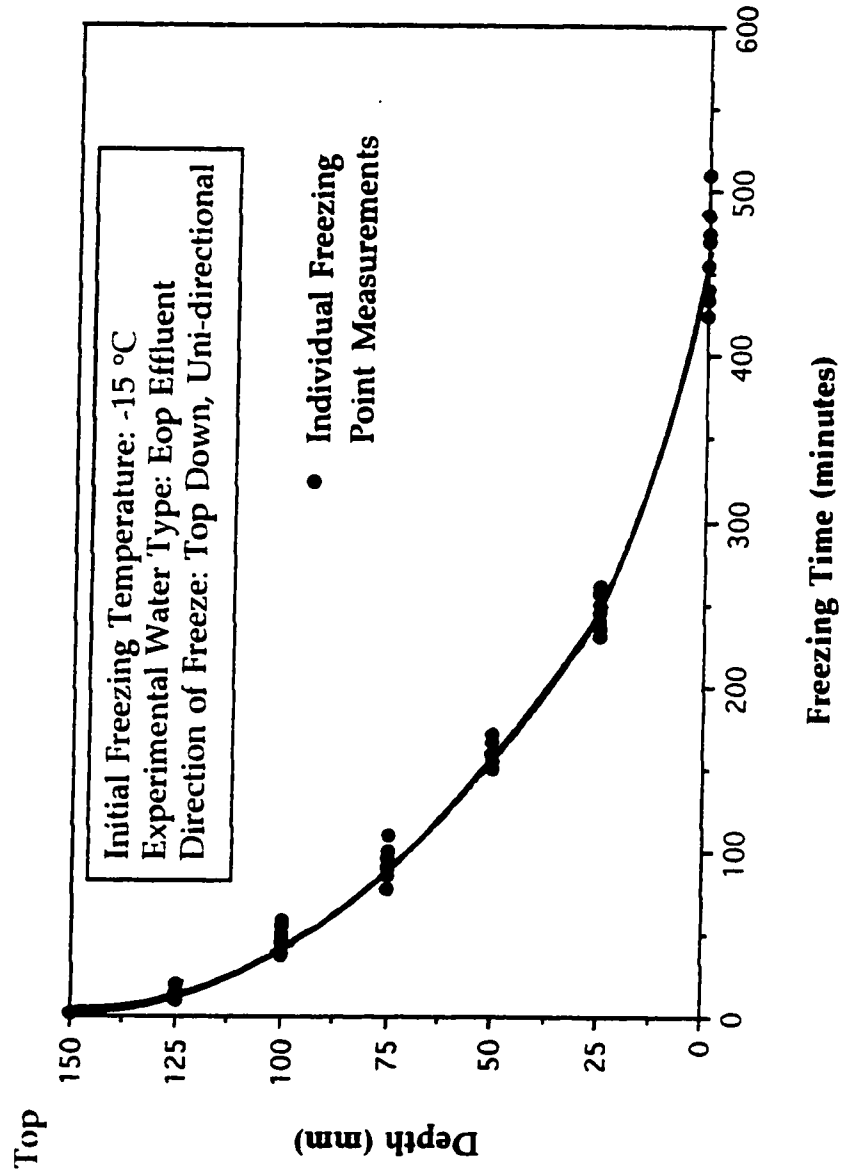


Figure 3.33 Freezing Curve Representative of Freezing Eop Effluent at the Initial Freezing Temperature -15 °C

3.9.1.1.3 INITIAL FREEZING TEMPERATURE: -25 °C

Figure 3.34 is an approximation of the freezing curve representative of unidirectionally freezing Eop effluent at the initial freezing temperature -25 °C. The average estimated time period to completely freeze the Eop effluent unidirectionally was approximately 229 minutes (0.16 days).

3.9.1.2 ALKALINE EXTRACTION STAGE MEMBRANE CONCENTRATE

3.9.1.2.1 INITIAL FREEZING TEMPERATURE: -2 °C

Figure 3.35 is an approximation of the freezing curve representative of freezing unidirectionally membrane concentrate at the initial freezing temperature -2 °C. The average estimated time period to completely freeze the membrane concentrate was approximately 3,450 minutes (2.39 days).

3.9.1.2.2 INITIAL FREEZING TEMPERATURE: -15 °C

Figure 3.36 is an approximation of the freezing curve representative of freezing unidirectionally membrane concentrate at the initial freezing temperature -15 °C. The average estimated time period to completely freeze the membrane concentrate unidirectionally was approximately 476 minutes (0.33 days).

3.9.1.2.3 INITIAL FREEZING TEMPERATURE: -25 °C

Figure 3.37 is an approximation of the freezing curve representative of freezing unidirectionally membrane concentrate at the initial freezing temperature -25 °C. The average estimated time period to completely freeze the membrane concentrate unidirectionally was approximately 245 minutes (0.17 days).

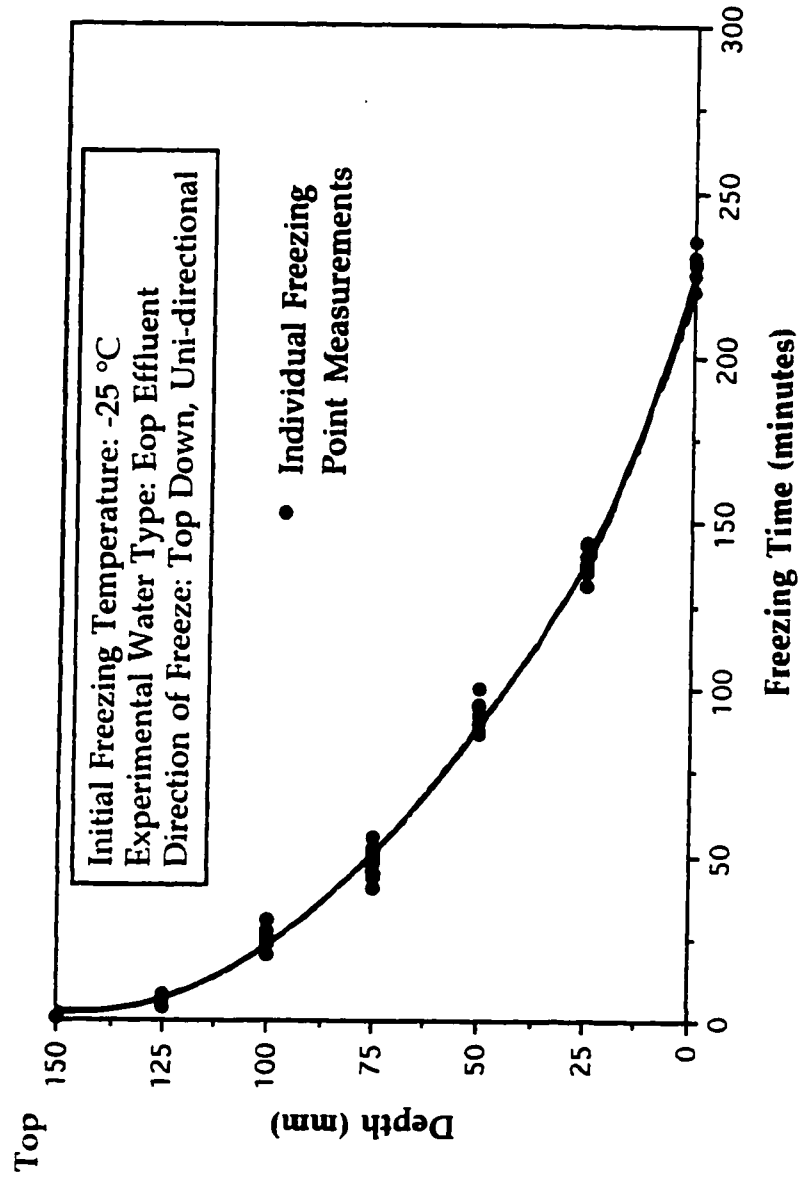


Figure 3.34 Freezing Curve Representative of Freezing Eop Effluent at the Initial Freezing Temperature -25 °C

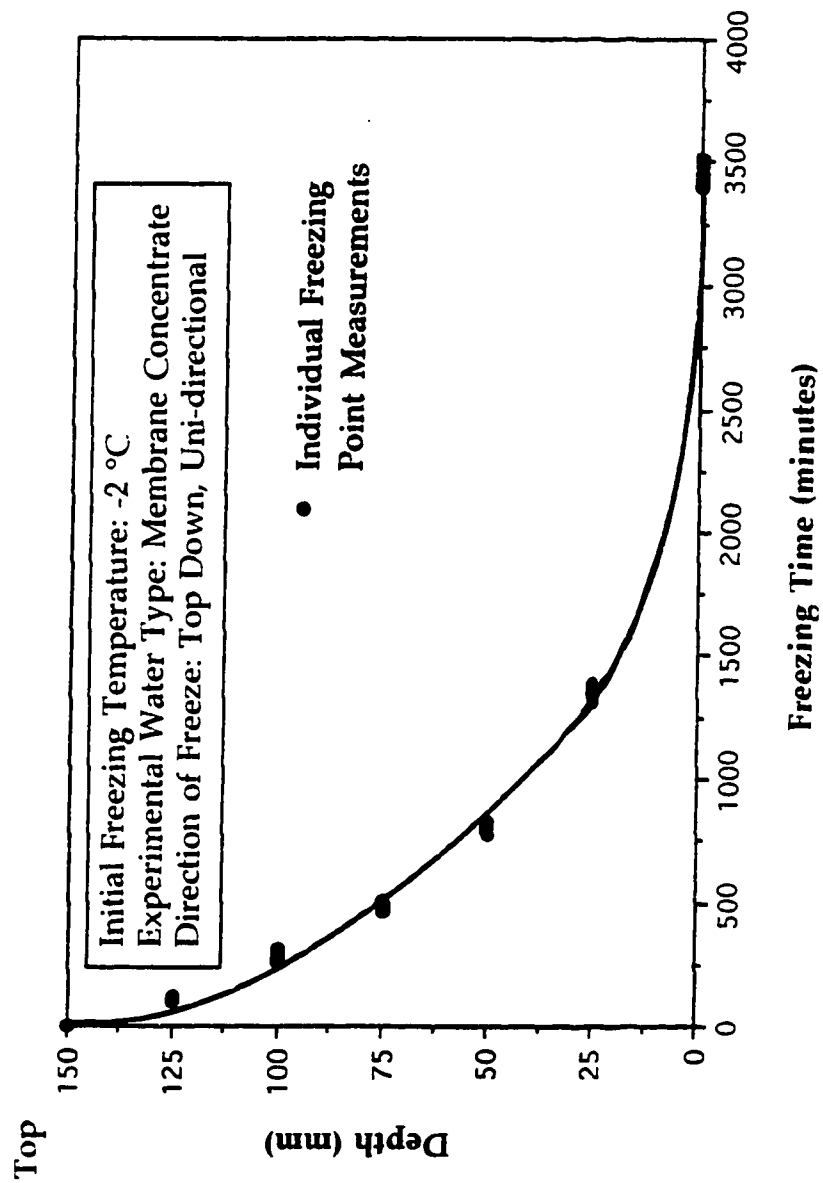


Figure 3.35 Freezing Curve Representative of Freezing Membrane Concentrate at the Initial Freezing Temperature -2 °C

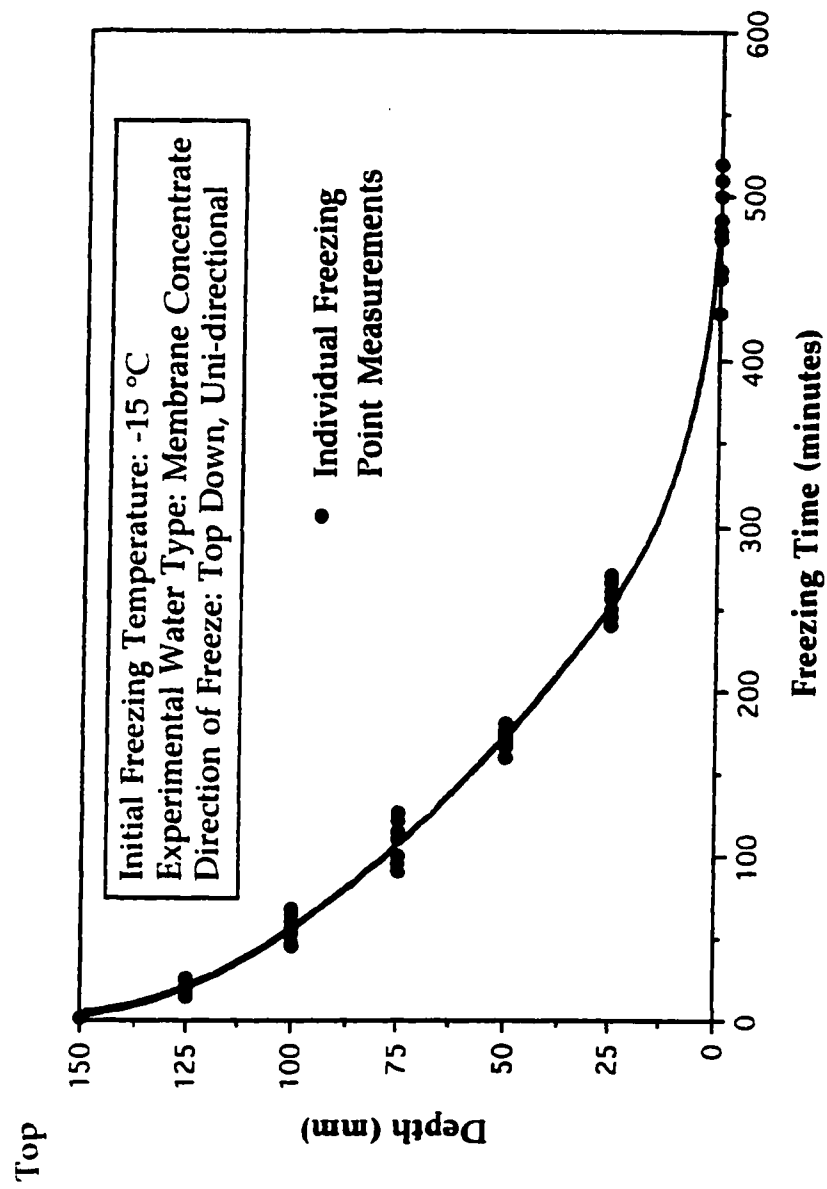


Figure 3.36 Freezing Curve Representative of Freezing Membrane Concentrate at the Initial Freezing Temperature -15 °C

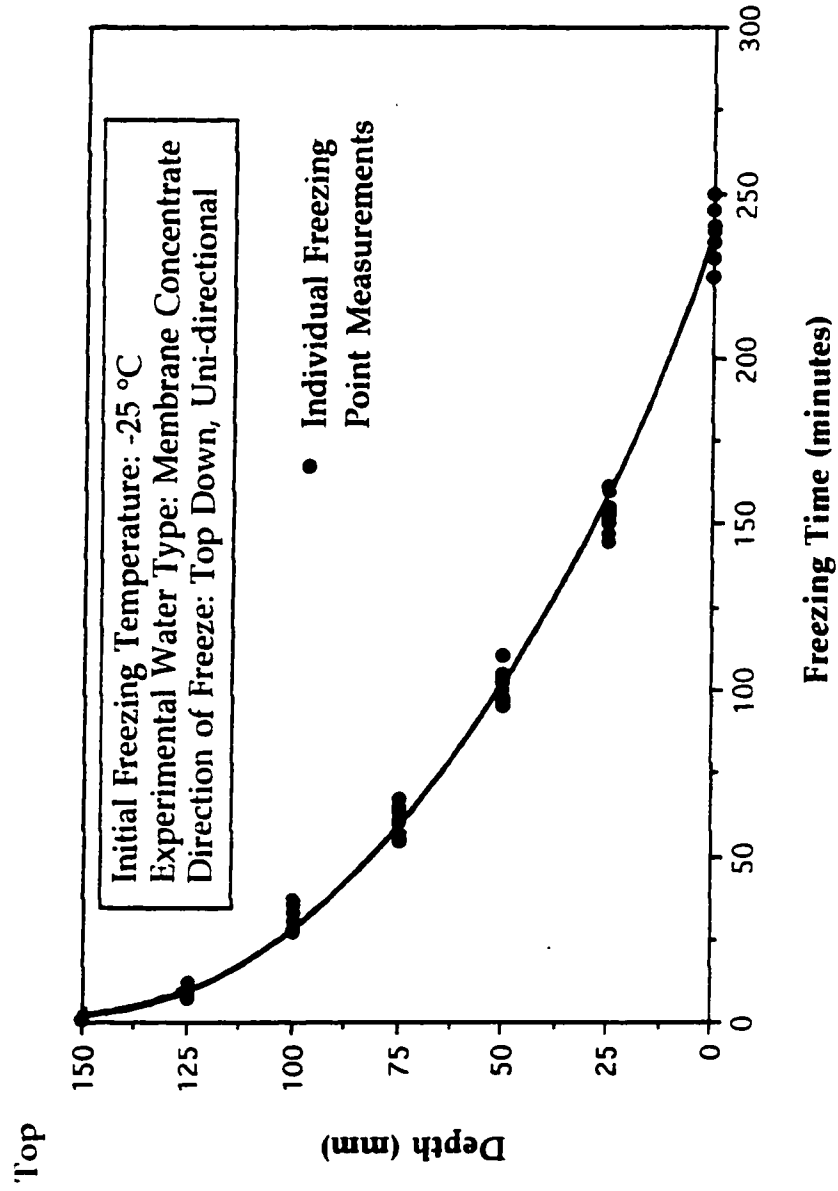


Figure 3.37 Freezing Curve Representative of Freezing Membrane Concentrate at the Initial Freezing Temperature -25 °C

3.9.2 THAWING ISOTHERM DATA

Tabulated are the thawing times for frozen samples thawed bottom up and top down. Thawing was considered complete when the entire thawed liquid volume had reached a constant temperature equal to the initial thawing temperature. The time periods recorded were reported to the nearest half hour.

3.9.2.1 ALKALINE EXTRACTION STAGE EFFLUENT

Summarized in Table 3.12 are the time periods required to completely thaw 150 mm deep by 100 mm diameter frozen Eop ice columns from predominantly the bottom up with respect to their different initial freezing and thawing temperatures. Examination of this table shows the respective thawing times were similar between each thawing temperature at the different initial freezing temperatures. As expected, the thawing times were reported to increase as the thawing temperature decreased. Table 3.12 shows the average increase in thawing time for Eop effluent was between 74.9 hours to 79.9 hours from having decreased the thawing temperature from 24 °C to 4 °C at the different initial freezing temperatures. As expected increasing the column depth from 150 mm to 250 mm increased the thawing time. Table 3.13 shows the additional increase in thawing time was between 4.9 hours to 6.3 hours at the different initial freezing temperatures in comparison to the shallower liquid depth.

Table 3.12 Thawing Times for Eop Effluent Thawed Predominantly From
the Bottom up Between the Temperature Range 4 °C to 24 °C

Experimental Setpoint	Average (hours)*	Range (hours)
Initial Freezing Temperature: -2 °C		
Thawing Temperature		
24 °C	12.7	12.0 to 13.0
15 °C	29.3	28.5 to 30.0
4 °C	88.3	87.0 to 89.5
Initial Freezing Temperature: -15 °C		
Thawing Temperature		
24 °C	13.9	13.0 to 15.0
15 °C	29.9	29.0 to 31.0
4 °C	88.8	87.0 to 90.0
Initial Freezing Temperature: -25 °C		
Thawing Temperature		
24 °C	15.6	15.0 to 16.5
15 °C	29.8	28.5 to 31.5
4 °C	95.5	94.0 to 97.0

* average of 8 values, liquid depth: 150 mm

Table 3.13 Thawing Times for Eop Effluent Thawed Predominantly From
the Bottom up at a Temperature of 24 °C for a Liquid Depth of 250 mm

Experimental Setpoint	Average (hours)*	Range (hours)
Initial Freezing Temperature: -2 °C		
Thawing Temperature		
24 °C	19.0	18.5 to 19.5
Initial Freezing Temperature: -15 °C		
Thawing Temperature		
24 °C	19.8	19.5 to 20.0
Initial Freezing Temperature: -25 °C		
Thawing Temperature		
24 °C	20.5	20.0 to 21.0

* average of 2 values, liquid depth: 250 mm

3.9.2.2 ALKALINE EXTRACTION STAGE MEMBRANE CONCENTRATE

Summarized in Table 3.14 are the average time periods required to completely thaw 150 mm deep by 100 mm diameter membrane concentrate ice columns from predominantly the bottom up with respect to their different initial freezing and thawing temperatures. Examination of this table shows the respective thawing times were similar between each thawing temperature at the different initial freezing temperatures. Reported to increase were the thawing times as the thawing temperature decreased. Table 3.14 shows the average increase in thawing time for membrane concentrate at their different initial freezing temperatures was between 76.8 hours to 80.4 hours for decreases in the thawing temperature from 24 °C to 4 °C. As expected increasing the column depth from 150 mm to 250 mm increased the thawing time. Table 3.15 shows the increase in thawing time was between 5.4 hours to 7.9 hours at the different initial freezing temperatures.

Table 3.14 Thawing Times for Membrane Concentrate Thawed Predominantly
From the Bottom up Between the Temperature Range 4 °C to 24 °C

Experimental Setpoint	Average (hours)*	Range (hours)
Initial Freezing Temperature: -2 °C		
Thawing Temperature		
24 °C	12.1	11.5 to 12.5
15 °C	28.5	28.0 to 29.5
4 °C	88.9	88.0 to 90.0
Initial Freezing Temperature: -15 °C		
Thawing Temperature		
24 °C	14.0	13.5 to 14.5
15 °C	30.1	29.0 to 31.0
4 °C	91.5	90.0 to 93.0
Initial Freezing Temperature: -25 °C		
Thawing Temperature		
24 °C	15.4	15.0 to 16.0
15 °C	30.5	30.0 to 31.0
4 °C	95.8	94.0 to 97.0

* average of 8 values, liquid depth: 150 mm

**Table 3.15 Thawing Times for Membrane Concentrate Thawed Predominantly
From the Bottom up at a Temperature of 24 °C for a Liquid Depth
of 250 mm**

Experimental Setpoint	Average (hours)*	Range (hours)
Initial Freezing Temperature: -2 °C		
Thawing Temperature 24 °C	20.0	19.5 to 20.5
Initial Freezing Temperature: -15 °C		
Thawing Temperature 24 °C	20.3	20.0 to 20.5
Initial Freezing Temperature: -25 °C		
Thawing Temperature 24 °C	20.8	20.5 to 21.0

* average of 2 values, liquid depth: 250 mm

4.0 UNIDIRECTIONAL FREEZE-THAW STUDIES

Presented in this chapter are experimental results from unidirectional freeze-thaw studies conducted to treat alkaline extraction stage effluent and membrane concentrate. As part of this investigation individual variables were examined to determine their relative significance with respect to process performance.

4.1 PROCEDURES

Unidirectional freeze-thaw experiments were conducted in accordance to section 3.6. Sample collection and analyses were conducted in accordance to sections 3.7 and 3.5.

4.2 RESULTS AND DISCUSSION

4.2.1 CONSTITUENT CONCENTRATION AND REMOVAL BY FREEZE-THAW

Conducted under ideal conditions freeze-thaw can be employed in a manner similar to that which would occur naturally to effectively treat alkaline extraction stage effluents derived from kraft pulp mill operations. Plotted in Figures 4.1 and 4.2 are the average percent color removals from the top 70 % liquid fraction with respect to initial freezing temperature in the treatment of alkaline extraction stage effluent and membrane concentrate. From examination of these figures it can be seen that the method by which the ice was thawed substantially affected treatment performance. The color removals, irrespective of initial freezing temperature and effluent type, were significantly higher in samples thawed predominantly from the bottom up compared to samples thawed

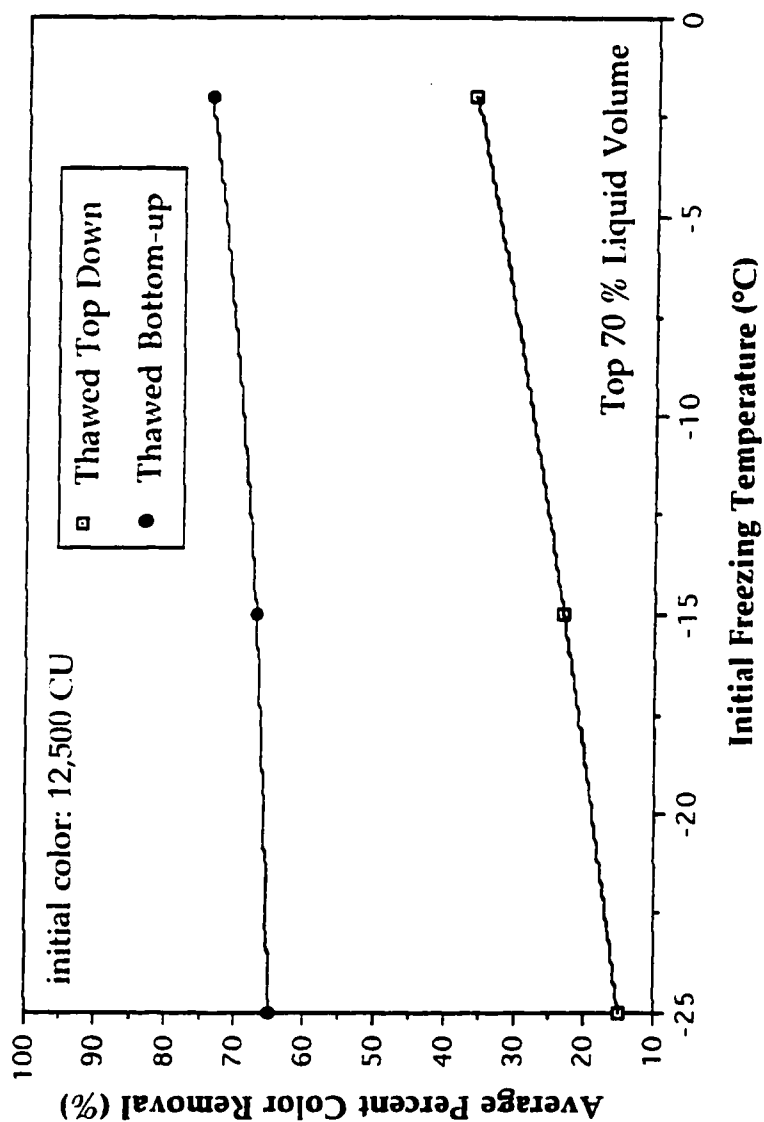


Figure 4.1 Plot of Average Percent Color Removal in the Top 70 % Liquid Volume with Respect to Initial Freezing Temperature for Membrane Concentrate Thawed Top Down and Bottom up at 24 °C Immediately After Being Frozen up at 24 °C

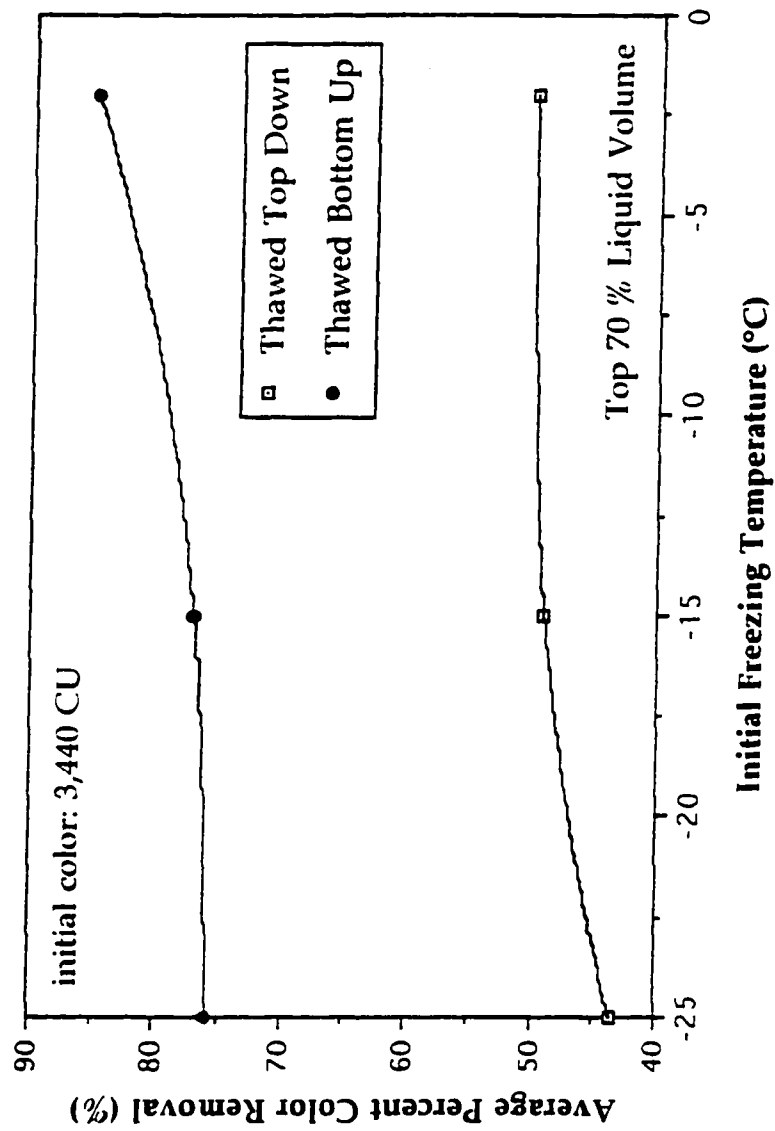


Figure 4.2 Plot of Average Percent Color Removal in the Top 70 % Liquid Volume with Respect to Initial Freezing Temperature for Eop Effluent Thawed Top Down and Bottom up at 24 °C Immediately After Being Frozen

top down. The differences in the average percent color removals in the top 70 % liquid fraction between samples thawed top down versus bottom up in the treatment of membrane concentrate were 37.4 %, 44.1 %, and 49.9 % at the initial freezing temperatures -2 °C, -15 °C, and -25 °C, respectively. Similarly, for alkaline extraction stage effluent the average percent differences in color removal were 34.0 %, 27.4 %, and 24.8 % at the initial freezing temperatures -2 °C, -15 °C, and -25 °C, respectively. In addition, the general tendency of the data, irrespective of the method of thawing and effluent type, was color removal increased with initial freezing temperature.

The difference in the average percent color removals in the top 70 % liquid fraction with respect to the method of thawing can be attributed to several factors. In ice columns thawed from the top down the ice was prevented from floating. Where as in ice columns thawed from predominantly the bottom up the ice was allowed to float throughout the thawing process. The resultant differences between the two methods are believed attributed to how the concentrated material was released from the ice matrix during thawing. During thawing, because of differences in density, the concentrated material was the first to thaw followed by the ice directly surrounding it. Ice columns thawed from the bottom up permitted the escape of the concentrated material allowing it to settle aided by the flow of melt water. Where as ice columns thawed from the top down as conducted in this study did not permit complete separation of the concentrated material from the ice. Believed to have occurred was the concentrated material settled on top of the thawing ice at the ice/liquid

interface only to be subjected to the constant disturbances created by the melt water.

Differences between the average percent color removals with respect to initial freezing temperature for each effluent type were believed to be directly related to the physical properties of the concentrated material produced during freezing. Plotted in Figures 4.3 to 4.4 are the average percent color removals from the top 70 % liquid fraction with respect to the average thickness of the concentrated material as determined by SEM for each experimental water type. From examination of these figures it can be seen, irrespective of effluent type, that the average percent color removal increased with the thickness of the concentrated material. The differences of which were believed to be in part, attributed to the fragile nature of the concentrated material. The concentrated material was found to be very susceptible to break-up from simple mixing to indicate it was not really a floc per say, but more likely a mixture of stable and dissolved matter together with precipitated and flocculated matter, all of which was compressed and dehydrated from freezing. Believed was that the concentrated material produced at the colder initial freezing temperatures was more susceptible to dissolution. Firstly, because of the relative increase in surface area of the concentrated material over which there can occur greater diffusion. The concentrated material produced at the colder initial freezing temperatures was thinner and more numerous in the ice matrix. Secondly, because of the relative differences that would be expected in the settling rate of the concentrated material. It was believed the thinner the concentrated material the more slowly it settled during

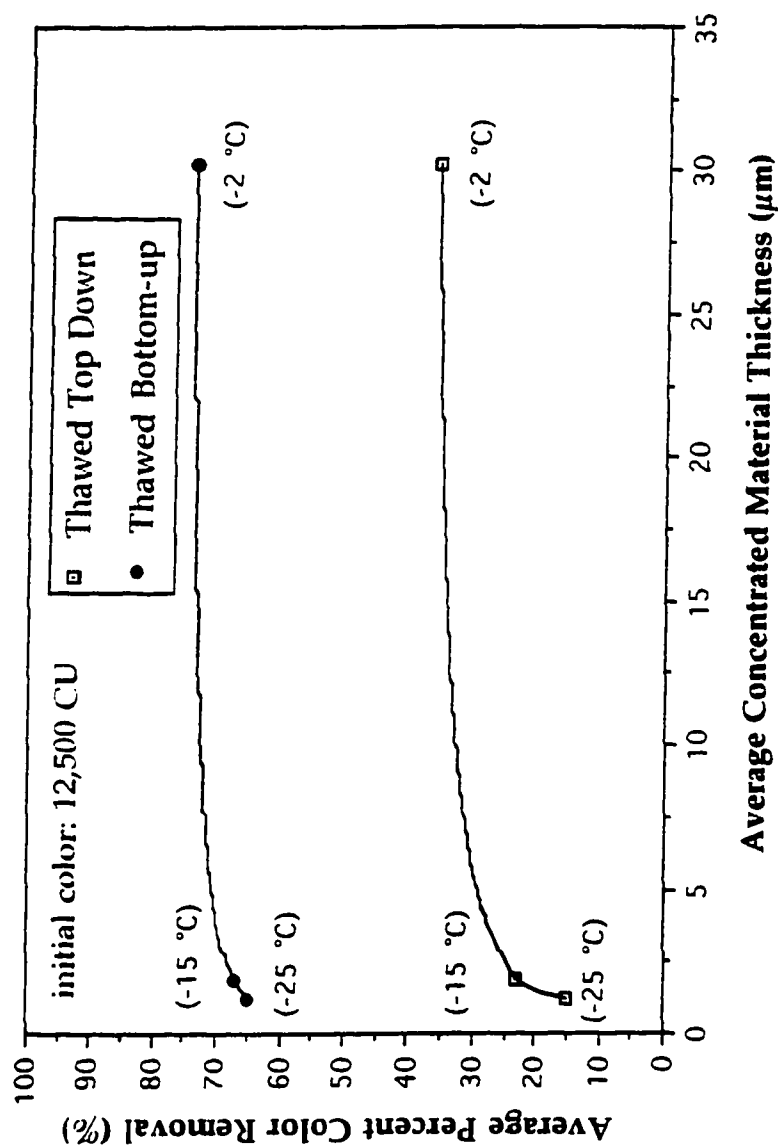


Figure 4.3 Plot of Average Percent Color Removal in the Top 70 % Liquid Volume with Respect to Material Thickness (Top Sample Specimens) for Membrane Concentrate Thawed Top Down and Bottom up at 24 $^{\circ}\text{C}$ Immediately After Being Frozen

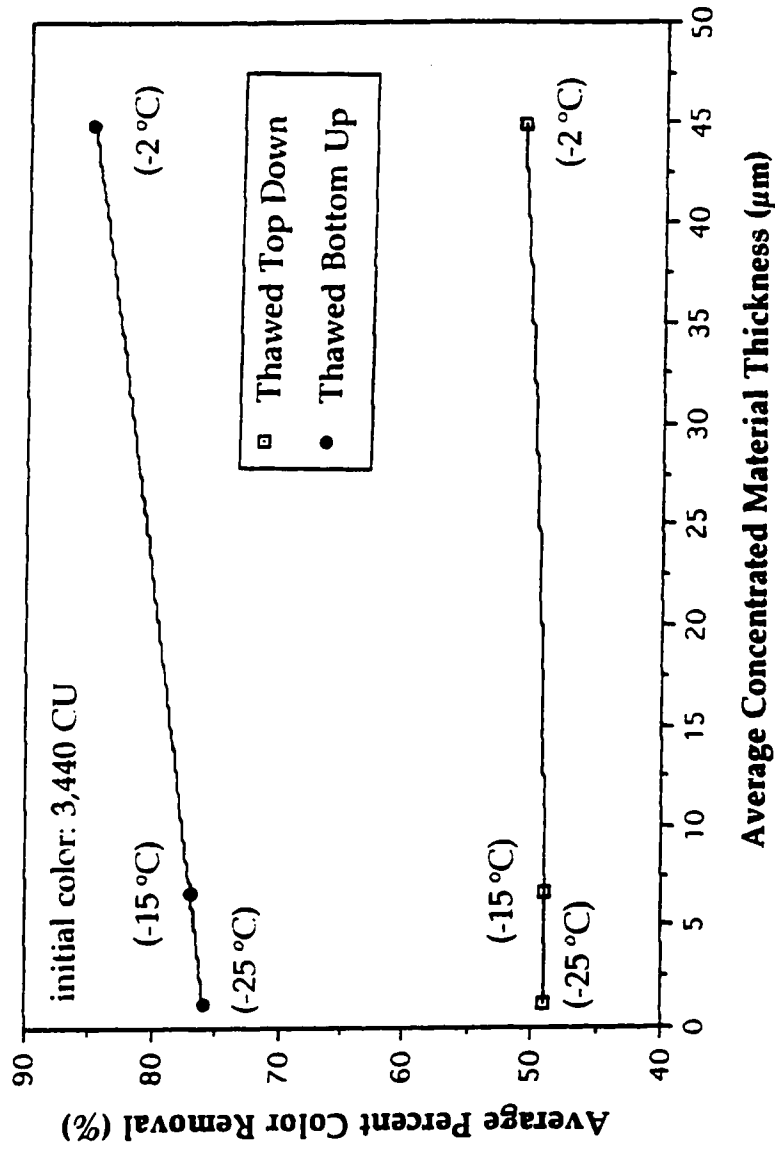


Figure 4.4 Plot of Average Percent Color Removal in the Top 70 % Liquid Volume with Respect to Material Thickness (Top Sample Specimens) for Eop Effluent Thawed Top Down and Bottom-up at 24 °C Immediately After Being Frozen

which it was in longer contact with the bulk solution for diffusion to occur.

4.2.2 PROCESS VARIABLES AND THEIR RELATIVE SIGNIFICANCE

Presented in this section are the experimental results from examination of the process variables; rate of thawing, storage temperature, storage time, liquid depth, and cycle freeze-thaw.

4.2.2.1 RATE OF THAWING

Rate of thawing was investigated because of the belief that melt water can assist in the concentration and settlement of the concentrated material during thawing. Plotted in Figures 4.5 and 4.6 are the average percent color removals from the top 70 % liquid fraction with respect to thawing temperature and method of thawing for each experimental water frozen at their different initial freezing temperatures. The general tendency of the data, irrespective of effluent type, was the average percent color removal increased with thawing temperature for ice columns thawed from predominantly the bottom up. For example, in the case of membrane concentrate the average increases in percent color removal for the initial freezing temperatures -2 °C, -15 °C, and -25 °C from increasing the thawing temperature from 4 °C to 24 °C were 6.3 %, 8.3 %, and 7.5 %, respectively. In addition, the average percent color removals increased with respect to the initial freezing temperature (Figure 4.7).

The general tendency of the data, irrespective of effluent type, was the average percent color removal decreased with thawing temperature for ice columns thawed top down. For example, for membrane concentrate

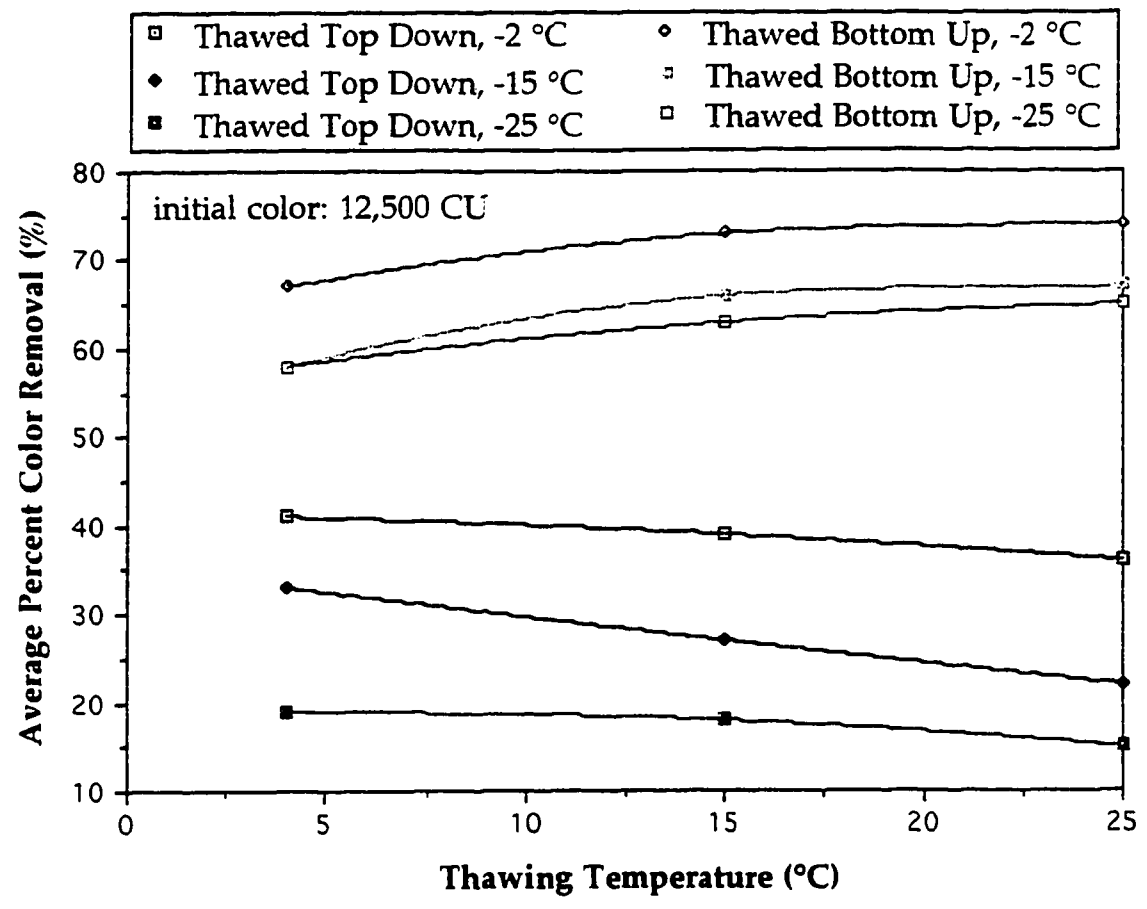


Figure 4.5 Plot of Average Percent Color Removal in the Top 70 % Liquid Volume with Respect to Thawing Temperature for Membrane Concentrate Thawed Top Down and Bottom up for Different Initial Freezing Temperatures

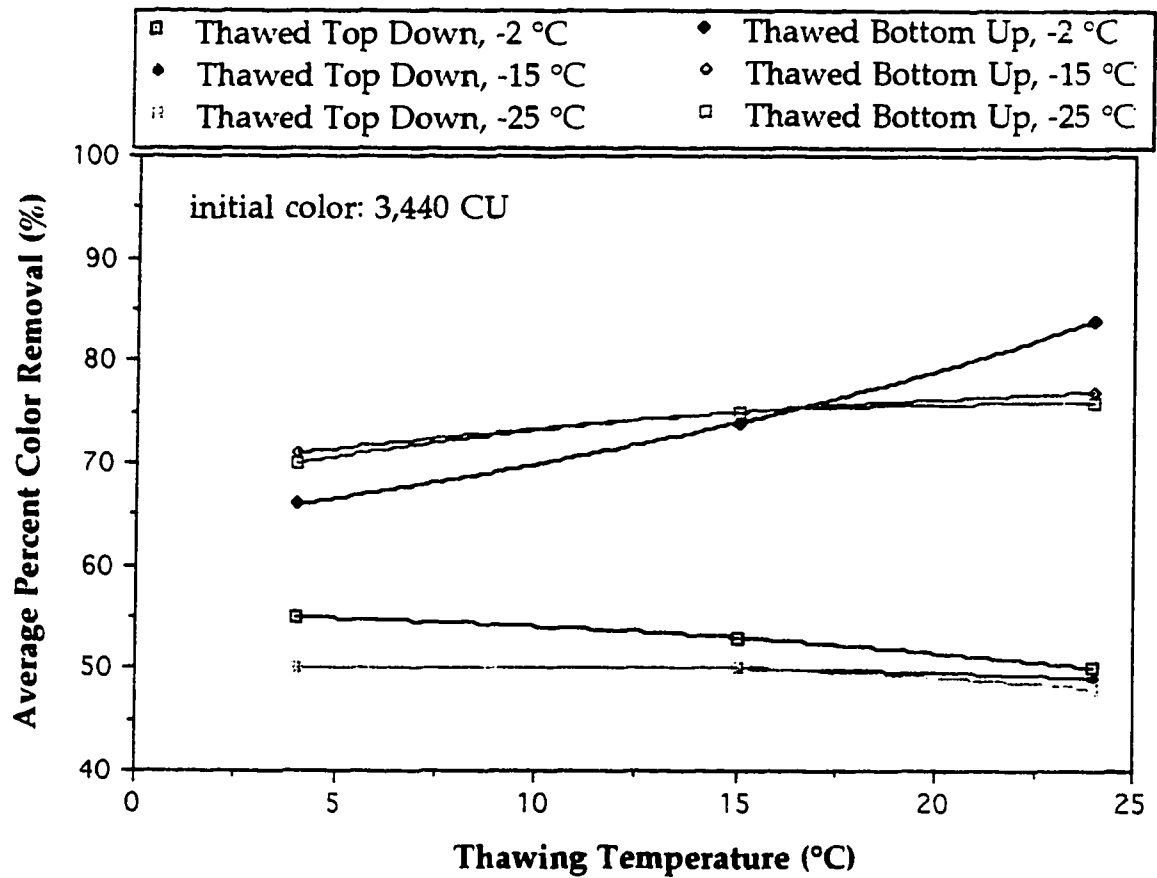


Figure 4.6 Plot of Average Percent Color Removal in the Top 70 % Liquid Volume with Respect to Thawing Temperature for Eop Effluent Thawed Top Down and Bottom up for Different Initial Freezing Temperatures

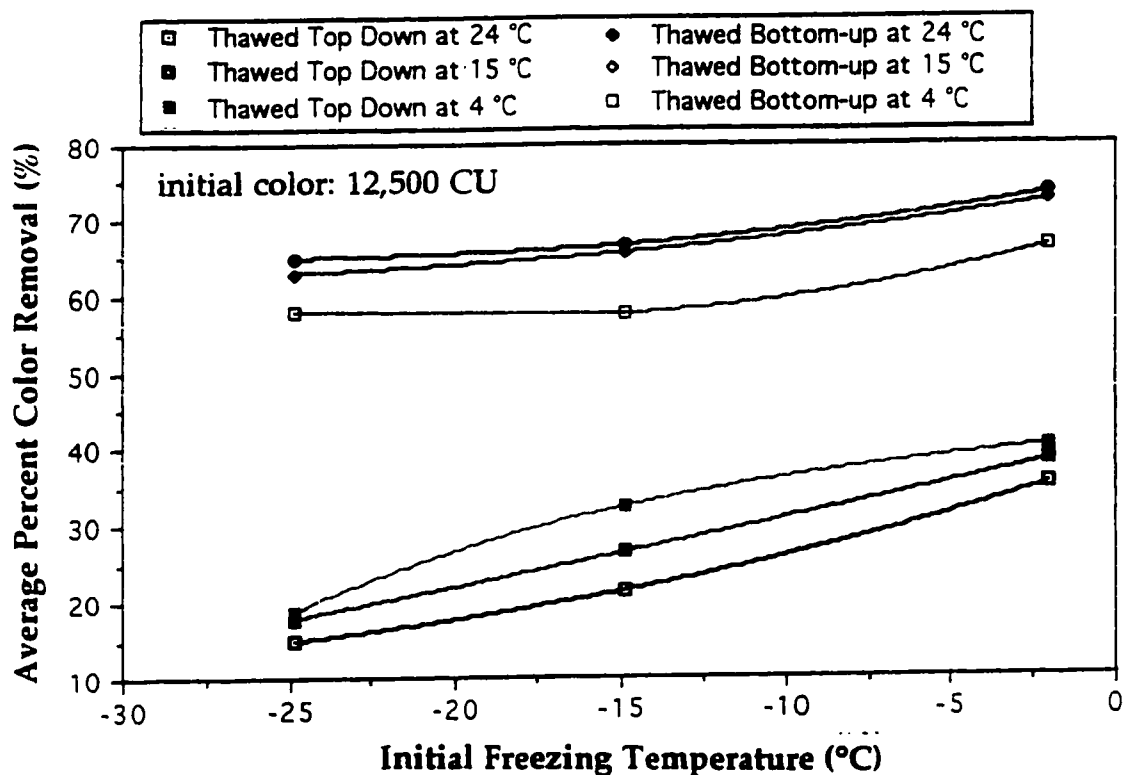


Figure 4.7 Plot of Average Percent Color Removal in the Top 70 % Liquid Volume with Respect to Initial Freezing Temperature for Membrane Concentrate Thawed Top Down and Bottom up at 24 °C

the average increases in percent color removal for the initial freezing temperatures -2°C , -15°C , and -25°C from increasing the thawing temperature from 4°C to 24°C were 5.0 %, 10.7 %, and 3.8 %, respectively. Similarly, the average percent color removals were shown to increase with initial freezing temperature (Figure 4.8). Analysis of variance and the Duncan Multiple Range Test were used to determine which means were significantly different at a 95 % confidence limit. The results of this analysis are presented in Appendix A. In the case of membrane concentrate, the general tendency of the data, irrespective of the method of thawing, was that there were significant differences between most all pairs of means, with exception of sometimes the mean comparisons associated with the very cold thawing temperatures. For Eop effluent a similar tendency was observed, except the pairs of means representative of samples thawed top down were not significantly different.

The rate at which the ice column was thawed greatly affected treatment performance. However, the manner in which it affected treatment performance was dependent on the method of thawing (top down versus bottom up). Rate of thawing affects the melt water flow pattern which in turn was believed to affect constituent removal. Figures 4.9 and 4.10 are the melt water flow patterns as conceptualized from dye studies for ice columns thawed from the bottom up. Melt water under rapid rates of thawing (24°C) was observed in dye studies to flow downward in almost a vertical pattern to concentrate the dye solution at the bottom. At slow rates of thawing (4°C) the melt water was observed to accumulate directly under the melting ice to form a highly concentrated zone. This highly concentrated zone was observed to disperse

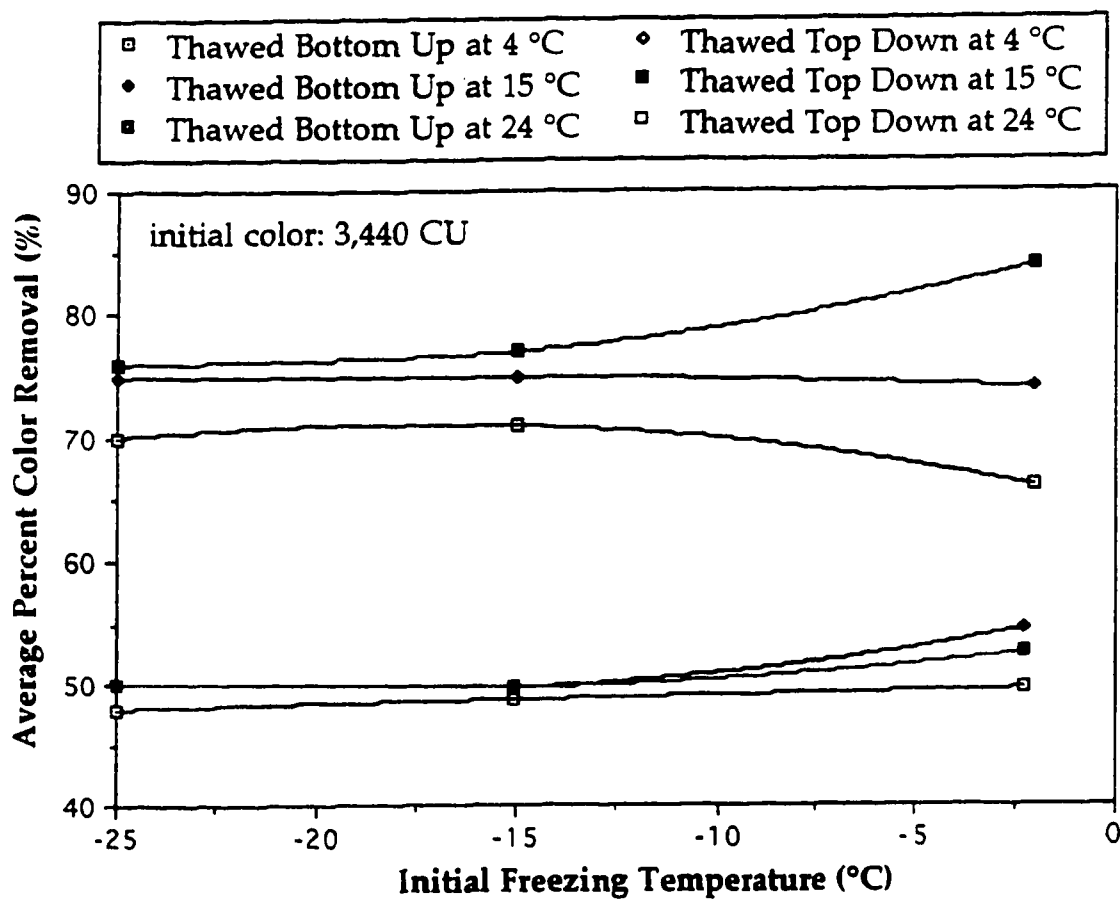


Figure 4.8 Plot of Average Percent Color Removal in the Top 70 % Liquid Volume with Respect to Initial Freezing Temperature for Eop Effluent Thawed Top Down and Bottom-up at 24 °C

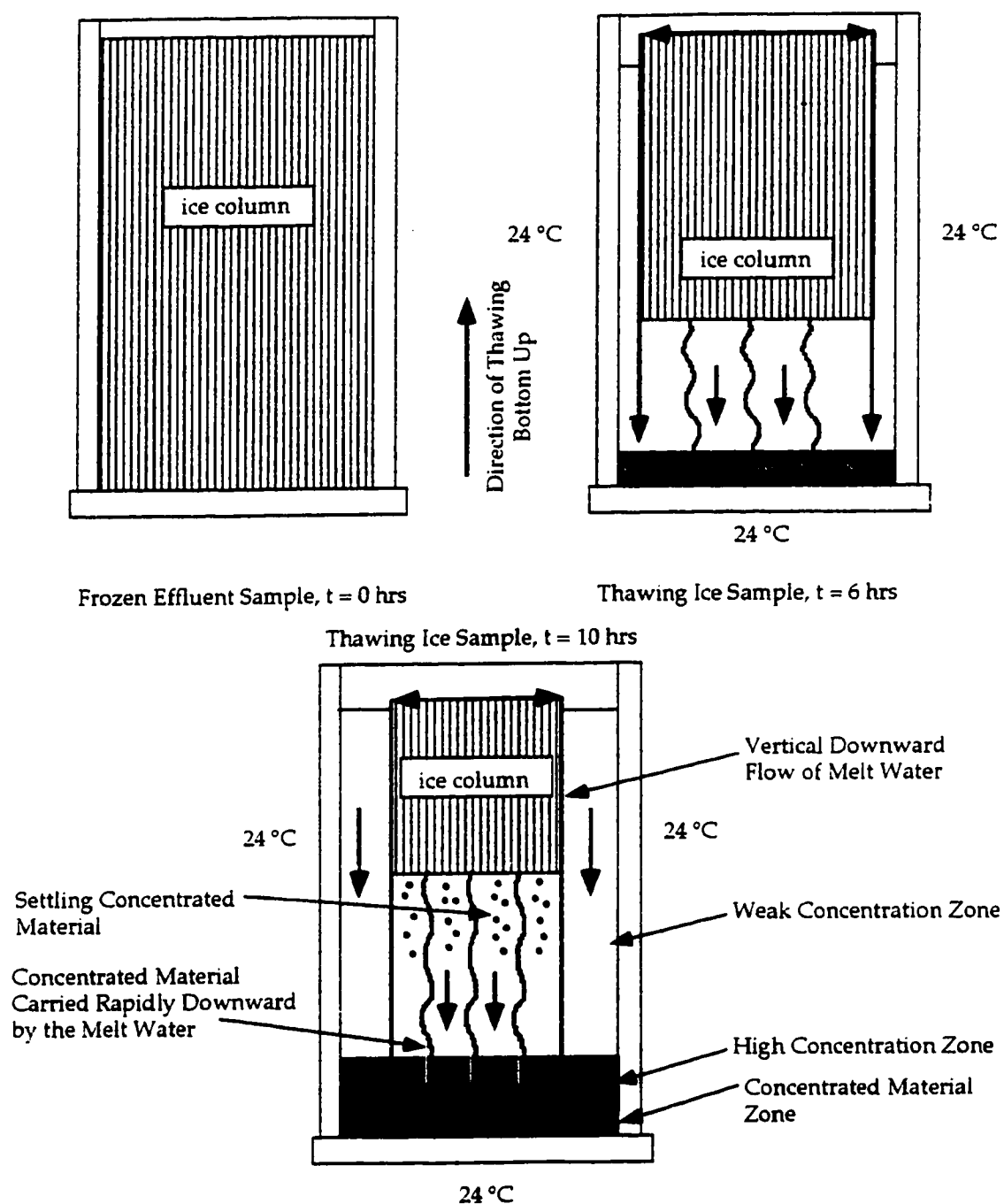


Figure 4.9 Melt Water Flow Pattern As Observed in Dye Studies in Melting Ice From the Bottom-up at 24 °C

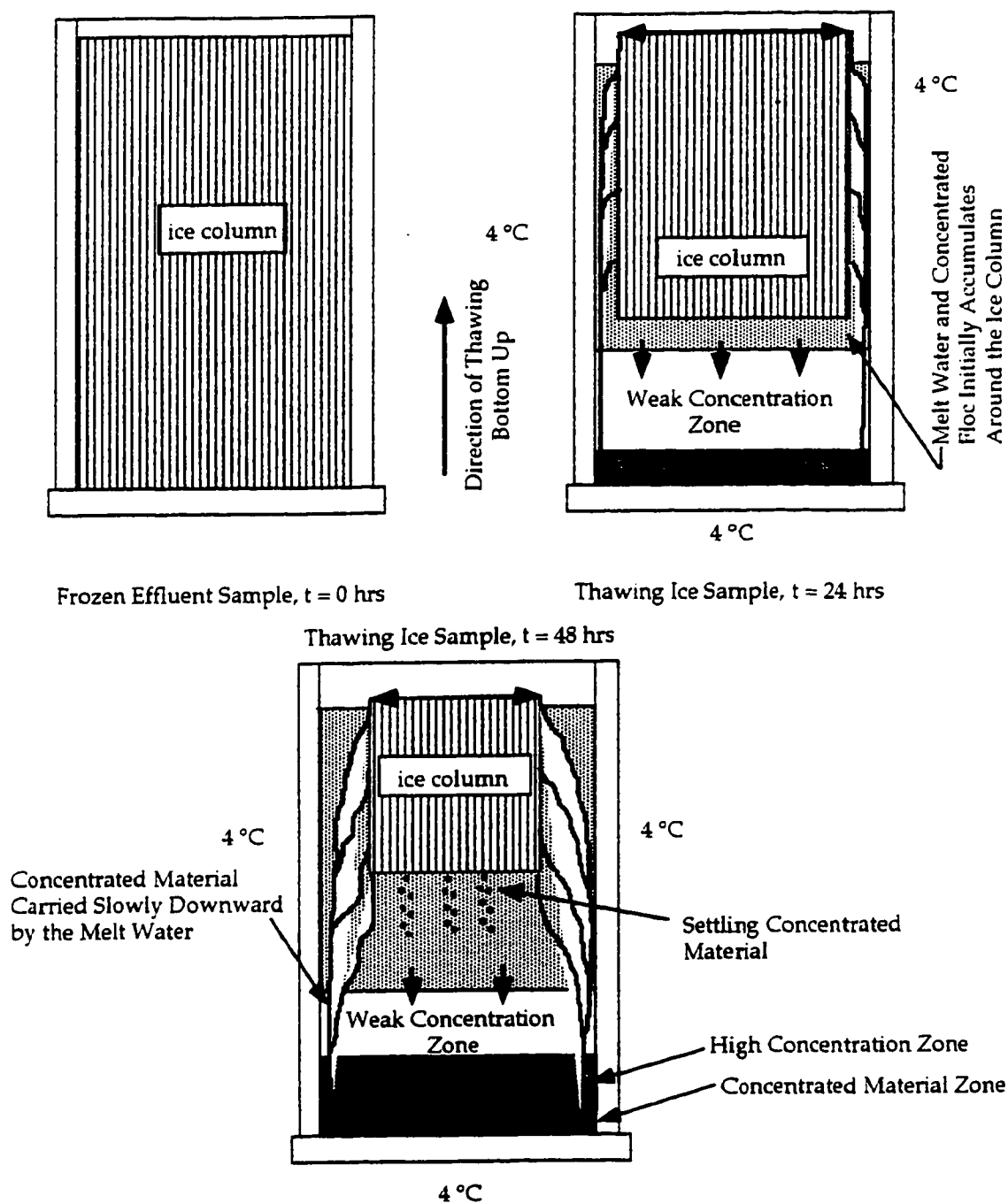


Figure 4.10 Melt Water Flow Pattern As Observed in Dye Studies in Melting Ice From the Bottom-up at 4 °C

horizontally, while diffusing only very slowly downwards. The differences in melt water flow patterns were attributed to differences in densities with respect to different temperature liquids at different depths. At high rates of thawing the melt water as it warmed was of higher density to the liquid below it. Whereas at low rates of thawing (4 °C) the melt water as it warmed was of lower density than the water below it. The higher average percent color removals associated with the higher rates of thawing were believed to be attributed to the effect the melt water flow pattern can have on the concentration and settlement of concentrated material produced during freezing.

Thawing of the ice column from the top down in which the ice was prevented from floating produced a melt water flow pattern opposite to that observed in samples thawed bottom up. Figure 4.11 shows the melt water flow pattern as conceptualized from dye studies in melting the ice column from the top down at a temperature of 24 °C. At high thawing temperatures, melt water at 0 °C is quickly displaced by warmer, more denser water, causing it to travel upward to the immediate surface, exposing the concentrated material that settles at the ice/liquid interface to a constant level of disturbance. At colder thawing temperatures, the melt water is expected to travel much slower reducing substantially the disturbances to the concentrated material. In either case, thawing the ice column from the top down produced unacceptable results in regards to constituent removal.

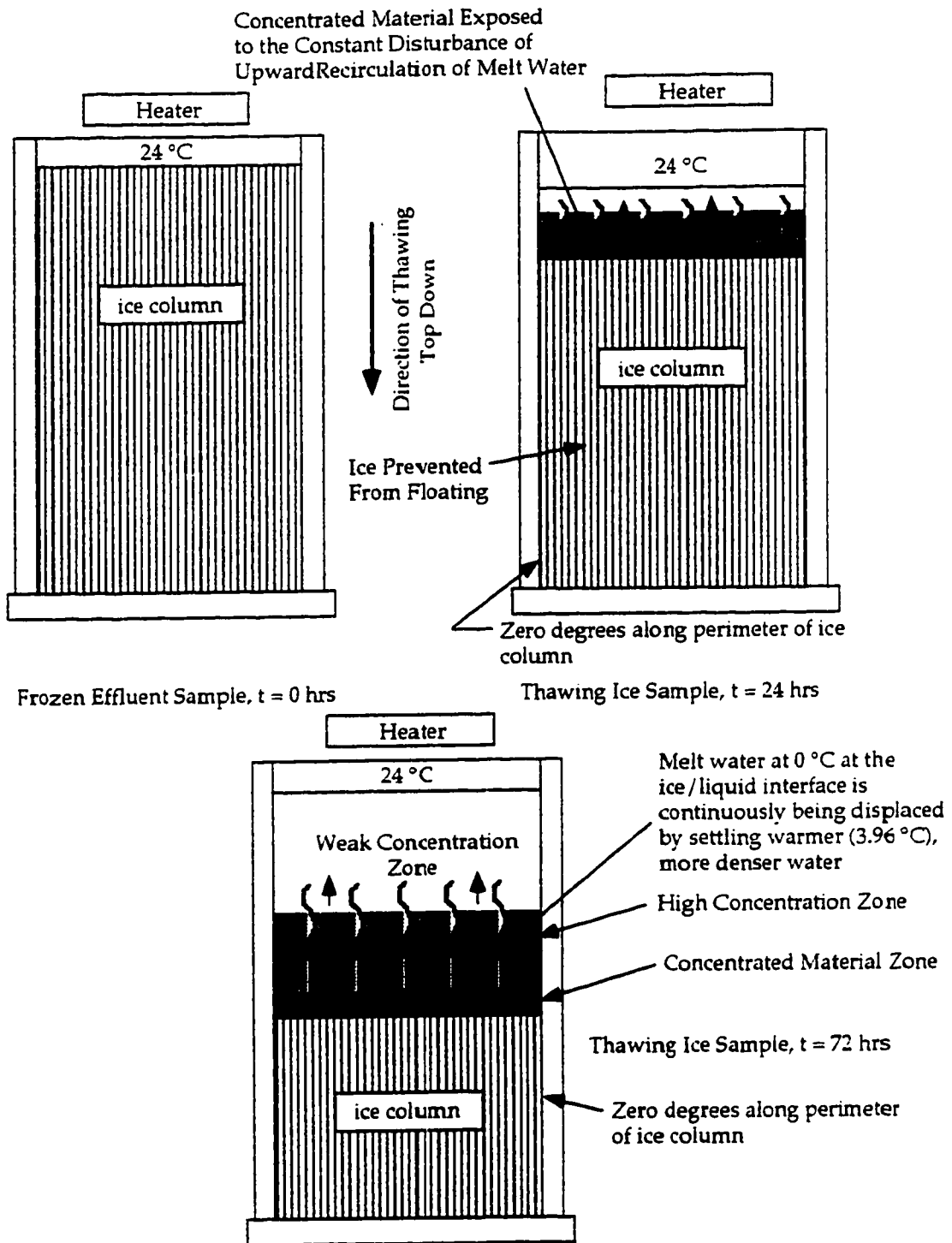


Figure 4.11 Melt Water Flow Pattern As Observed in Dye Studies in Melting Ice From the Top Down at 24 °C

4.2.2.2 STORAGE TEMPERATURE AND STORAGE TIME

Storage temperature and storage time were investigated because of the belief that dehydration of the concentrated material over time while frozen will enhance treatment performance. Plotted in Figures 4.12 to 4.19 are the average percent color removals in the top 70 % liquid volume with respect to storage time and storage temperature for alkaline extraction stage effluent and membrane concentrate thawed predominantly from the bottom up at temperatures 4 °C and 24 °C. The general tendency of the data was prolonged storage times, irrespective of effluent type, enhanced treatment performance only when the frozen effluent was stored at temperatures lower than the initial freezing temperature. For membrane concentrate the average percent color removals (Figure 4.12) in samples thawed bottom up at 24 °C were reported to increase from 73.5 % to a maximum of 77.5 % (difference of 4.0 %) from decreasing the storage temperature from -2 °C to -15 °C over a 90 day storage period when the initial freezing temperature was -2 °C. Similarly, at a thawing temperature of 4 °C the average percent color removal increased from 66.9 % to 68.8 %, for a maximum difference of 1.9 % (Figure 4.14). At storage temperatures equal or higher than the initial freezing temperatures the average percent change in color removal, although marginally different, were not significant with respect to the sample thawed immediately after being frozen.

The Student's t distribution was used to test the hypotheses that sample means with respect to the different storage temperatures were significantly different at a 95 % confidence limit. This test procedure is particularly suited for very small independent samples in which the

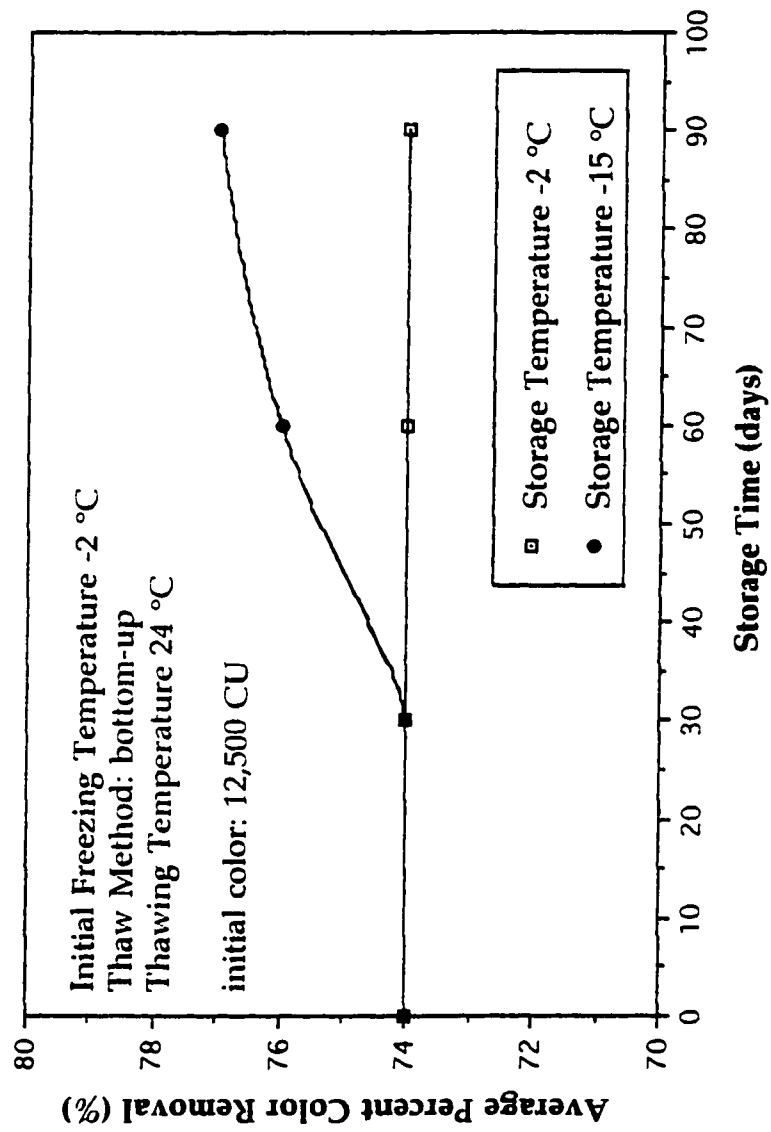


Figure 4.12 Plot of Average Percent Color Removal with Respect to Storage Time and Storage Temperature for Membrane Concentrate Frozen at the Initial Freezing Temperature -2 °C (Thawed Bottom Up at 24 °C)

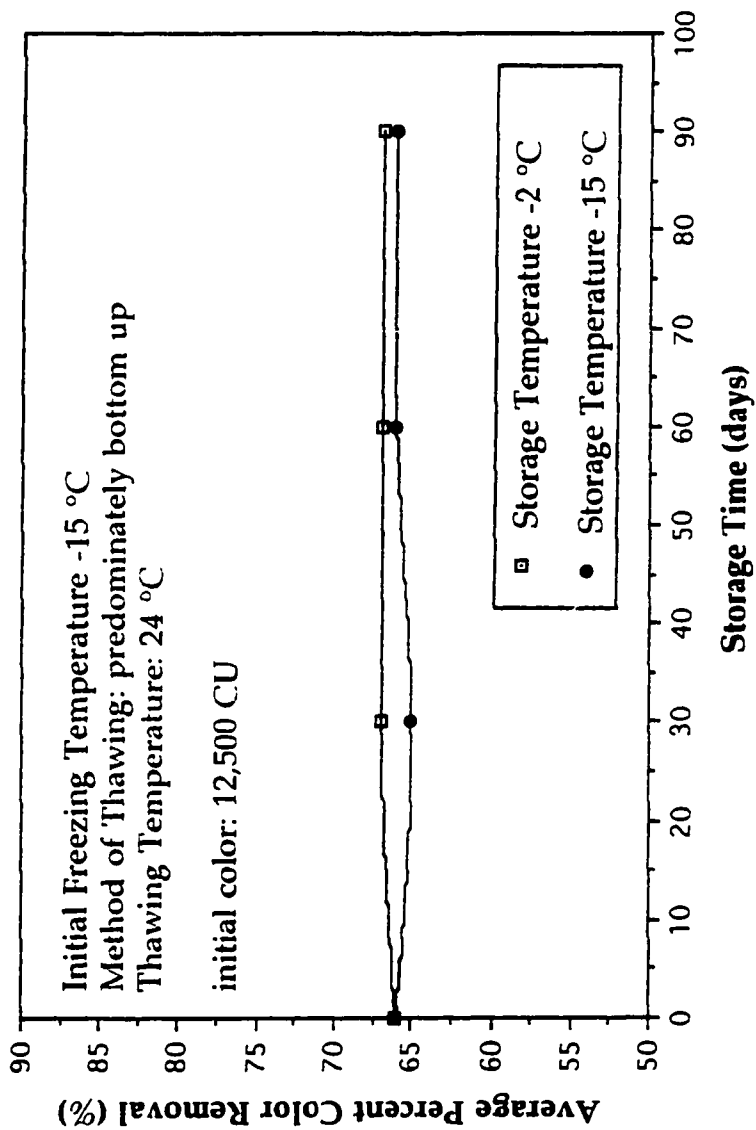


Figure 4.13 Plot of Average Percent Color Removal with Respect to Storage Time and Storage Temperature for Membrane Concentrate Frozen at the Initial Freezing Temperature -15 °C (Thawed Bottom Up at 24 °C)

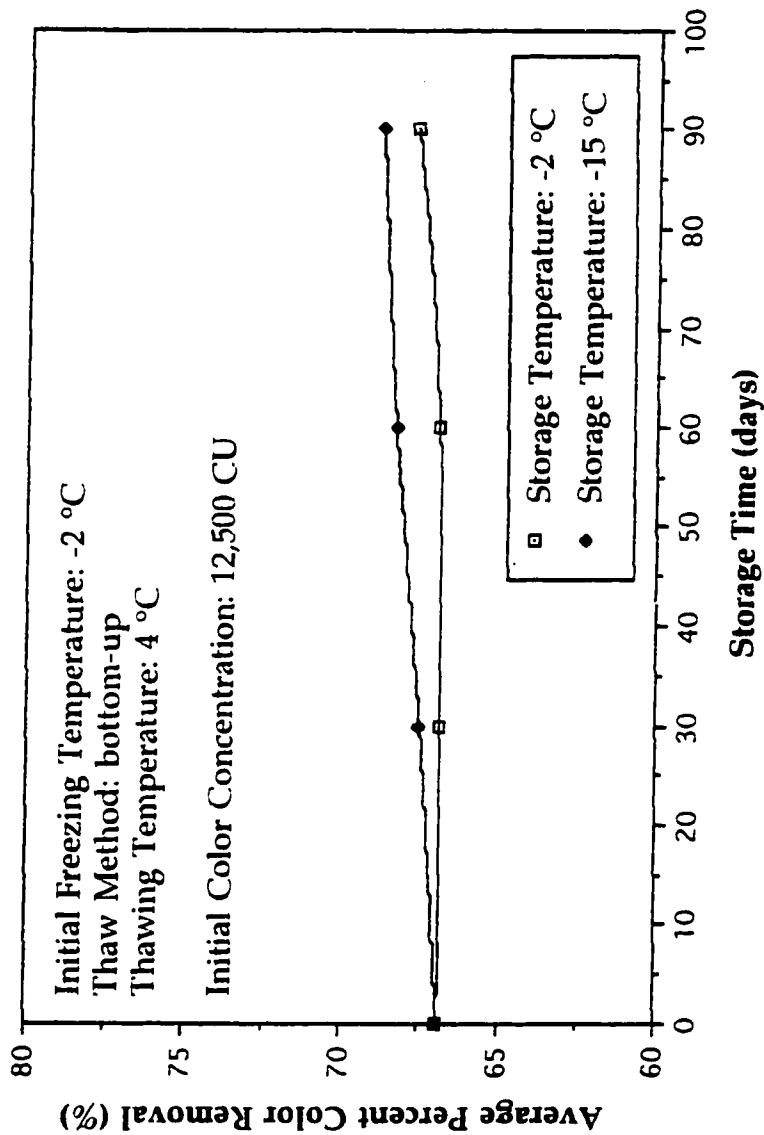


Figure 4.14 Plot of Average Percent Color Removal with Respect to Storage Time and Storage Temperature for Membrane Concentrate Frozen at the Initial Freezing Temperature -2 °C (Thawed Bottom Up at 4 °C)

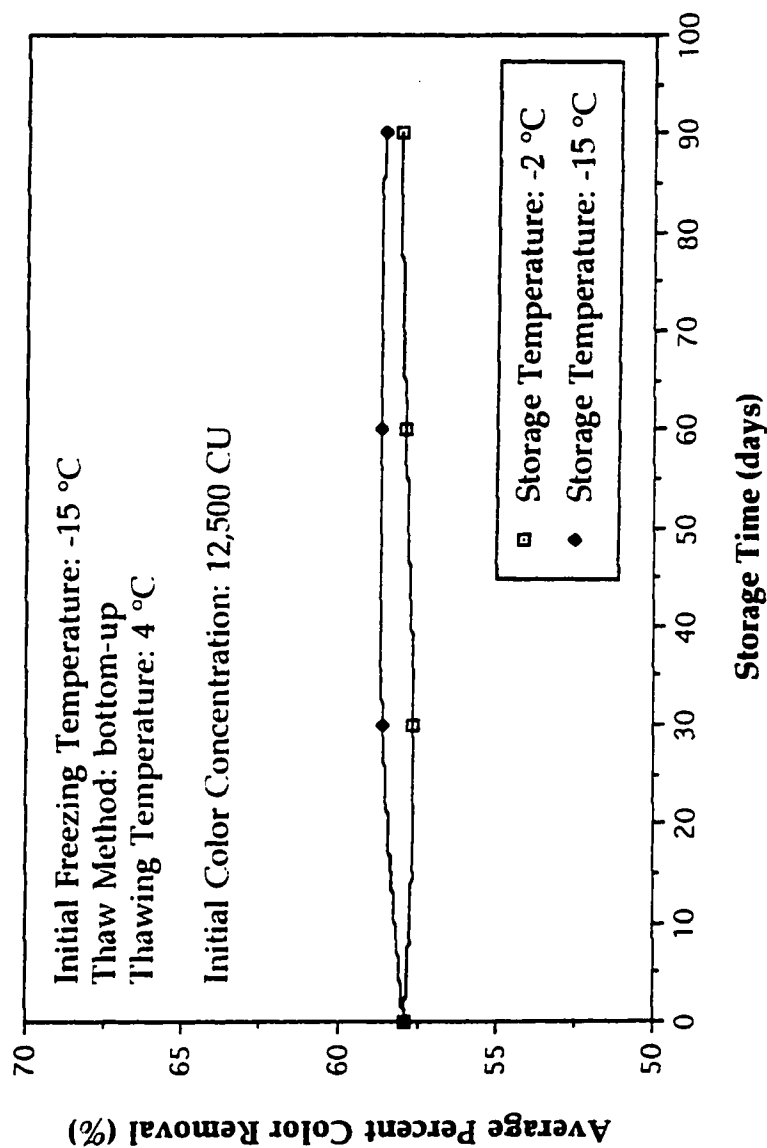


Figure 4.15 Plot of Average Percent Color Removal with Respect to Storage Time and Storage Temperature for Membrane Concentrate
Frozen at the Initial Freezing Temperature -15 °C (Thawed Bottom Up at 4 °C)

variances are unknown but are assumed equal. Summarized in Tables 4.1 to 4.4 are the results from having statistically compared the sample means using a two tailed Student t-test for membrane concentrate frozen at the initial freezing temperatures -2°C and -15°C , followed by their storage at different temperatures. It can be concluded from examination of these tables that the hypotheses in which it was proposed that the sample means were equal for the different storage temperatures were untrue. Storage of samples of membrane concentrate frozen at the initial freezing temperature -2°C at the colder temperature -15°C for periods of one month or longer produced significantly higher color removals. Similar results were also observed under the same freeze/storage conditions at the thawing temperature 4°C . Examination of these tables shows the average percent change in color removal for different storage times and temperatures were in most instances significantly different for membrane concentrate frozen at the initial freezing temperature -2°C and thawed bottom up at 4°C .

Storage of membrane concentrate frozen at the initial freezing temperature -15°C at different storage temperatures between the time period 0 to 90 days did not significantly improve color removal in the top 70 % liquid volume following thawing at the temperatures 4°C and 24°C . Tables 4.2 and 4.4 shows using the two tailed Student t-test that the average percent color removals in the top and middle sample portions were not significantly different for the storage temperatures -2°C and -15°C at a 95 % confidence limit.

Storage time did not significantly enhance color removal in the

Table 4.1 Tests of Hypotheses for the Different Storage Temperatures -2 °C and -15 °C for Membrane Concentrate Frozen at the Initial Freezing Temperature -2 °C (Thawed Bottom Up at 24 °C)

Storage Time (days)	Sample Volume (35 %)	Storage Temperature (°C)		Pooled Estimate	Test Statistic	Conclusion
		-2 °C	-15 °C			
30	top	1260 (15.00)	1230 (25.00)	20.616	1.455	accept H_0
	middle	5480 (25.00)	5230 (25.00)	25.000	10.000	reject H_0
60	top	1320 (25.00)	1100 (60.00)	45.962	4.787	reject H_0
	middle	5430 (35.00)	5240 (60.00)	49.117	3.868	accept H_0
90	top	1270 (60.00)	910 (75.00)	67.915	5.301	reject H_0
	middle	5350 (55.00)	4730 (125.00)	95.566	6.488	reject H_0

Student t value: $t_{2,0.025} = 4.303$, (?) - sample variance, $H_0: \mu_1 = \mu_2$

Table 4.2 Tests of Hypotheses for the Different Storage Temperatures -2 °C and -15 °C for Membrane Concentrate Frozen at the Initial Freezing Temperature -15 °C (Thawed Bottom Up at 24 °C)

Storage Time (days)	Sample Volume (35 %)	Storage Temperature (°C)		Pooled Estimate	Test Statistic	Conclusion
		-2 °C	-15 °C			
30	top	2350 (95.00)	2370 (90.00)	92.534	0.216	accept H_0
	middle	6060 (80.00)	6260 (80.00)	80.000	2.500	accept H_0
60	top	2370 (80.00)	2280 (75.00)	77.540	1.161	accept H_0
	middle	6050 (160.00)	6220 (65.00)	122.117	1.392	accept H_0
90	top	2360 (145.00)	2230 (75.00)	115.434	1.126	accept H_0
	middle	6010 (120.00)	6200 (100.00)	110.454	1.720	accept H_0

Student t value: $t_{2,0.025} = 4.303$, (?) - sample variance, $H_0: \mu_1 = \mu_2$

Table 4.3 Tests of Hypotheses for the Different Storage Temperatures -2 °C and -15 °C for Membrane Concentrate Frozen at the Initial Freezing Temperature -2 °C (Thawed Bottom Up at 4 °C)

Storage Time (days)	Sample Volume (35 %)	Storage Temperature (°C)		Pooled Estimate	Test Statistic	Conclusion
		-2 °C	-15 °C			
30	top	2590 (30.00)	2550 (40.00)	35.355	1.131	accept H_0
	middle	5690 (40.00)	5560 (45.00)	42.573	3.054	accept H_0
60	top	2650 (60.00)	2470 (20.00)	28.504	6.315	reject H_0
	middle	5630 (45.00)	5460 (25.00)	36.401	4.670	reject H_0
90	top	2550 (35.00)	2390 (25.00)	30.414	5.261	reject H_0
	middle	5530 (35.00)	5420 (30.00)	32.596	3.375	accept H_0

Student t value: $t_{2,0.025} = 4.303$, (?) - sample variance, $H_0: \mu_1 = \mu_2$

Table 4.4 Tests of Hypotheses for the Different Storage Temperatures -2 °C and -15 °C for Membrane Concentrate Frozen at the Initial Freezing Temperature -15 °C (Thawed Bottom Up at 4 °C)

Storage Time (days)	Sample Volume (35 %)	Storage Temperature (°C)		Pooled Estimate	Test Statistic	Conclusion
		-2 °C	-15 °C			
30	top	2810 (45.00)	2740 (20.00)	34.821	1.436	accept H_0
	middle	7810 (55.00)	7590 (30.00)	44.300	4.966	reject H_0
60	top	2770 (20.00)	2700 (45.00)	34.821	2.010	accept H_0
	middle	7750 (40.00)	7630 (25.00)	33.354	3.600	accept H_0
90	top	2750 (5.00)	2780 (15.00)	11.180	2.683	accept H_0
	middle	7750 (55.00)	7660 (45.00)	50.249	1.791	accept H_0

Student t value: $t_{2,0.025} = 4.303$, (?) - sample variance, $H_0: \mu_1 = \mu_2$

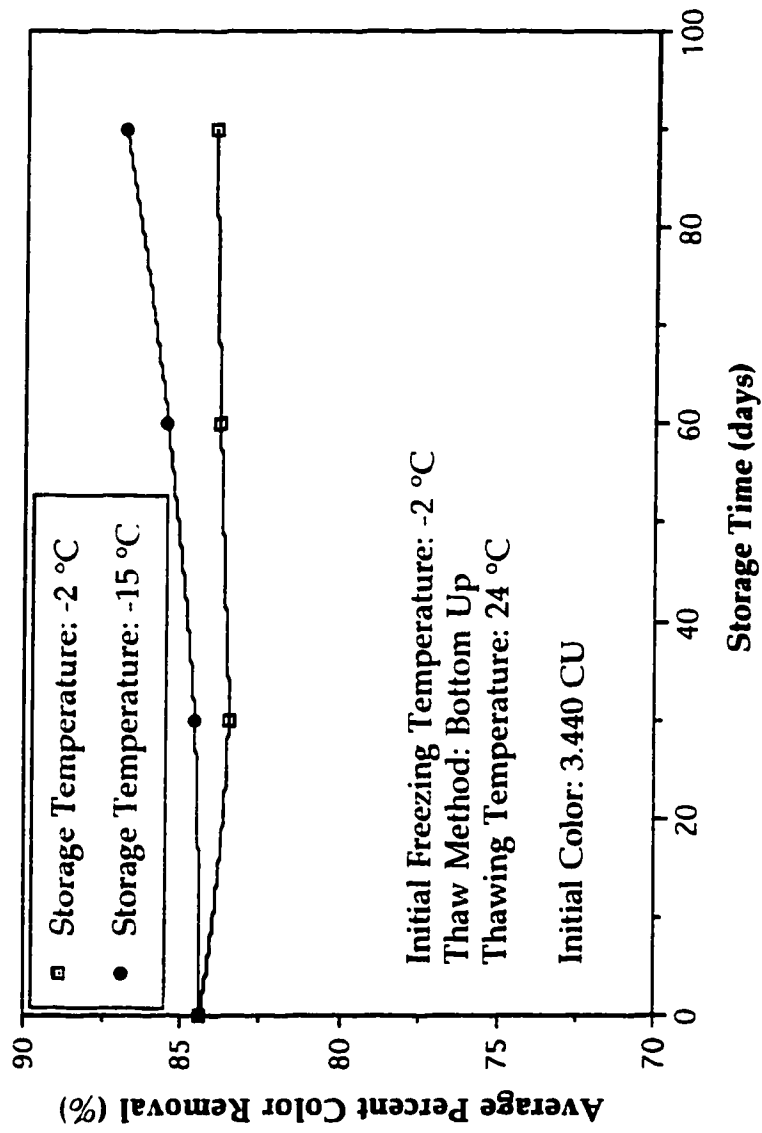


Figure 4.16 Plot of Average Percent Color Removal with Respect to Storage Time and Storage Temperature for Eop Effluent Frozen at the Initial Freezing Temperature -2 °C (Thawed Bottom Up at 24 °C)

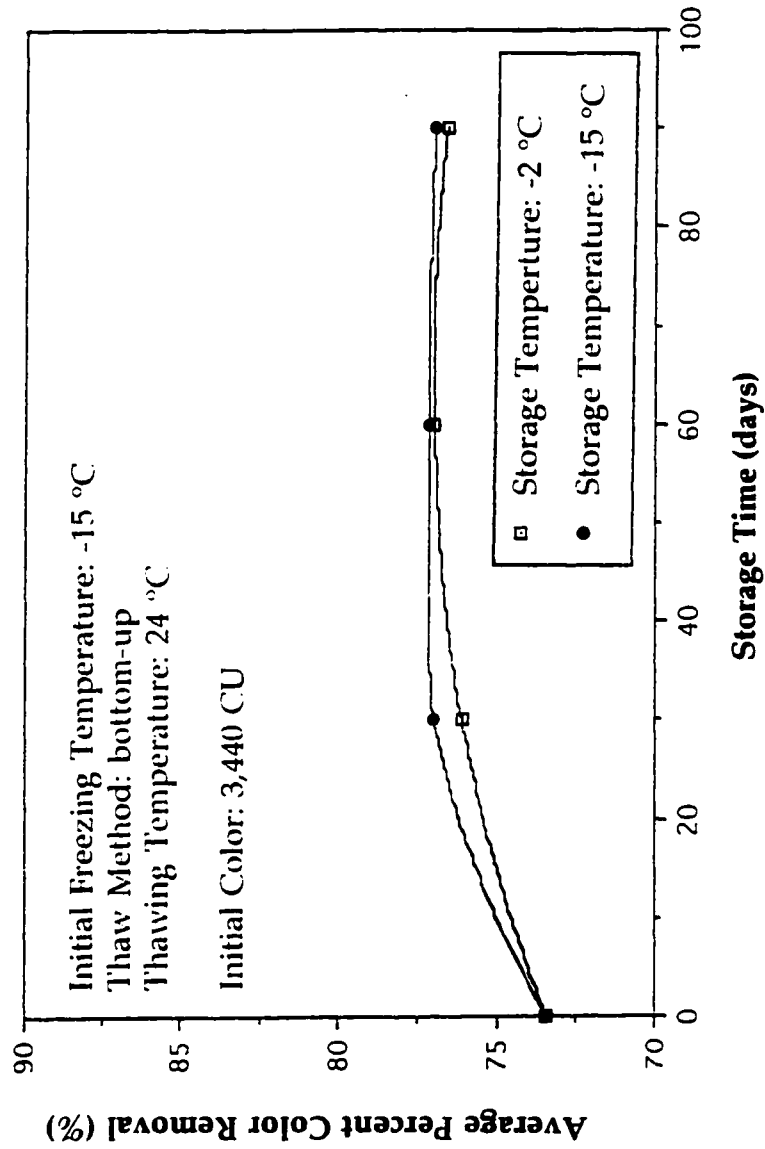


Figure 4.17 Plot of Average Percent Color Removal with Respect to Storage Time and Storage Temperature for Eop Effluent Frozen at the Initial Freezing Temperature -15 °C (Thawed Bottom Up at 24 °C)

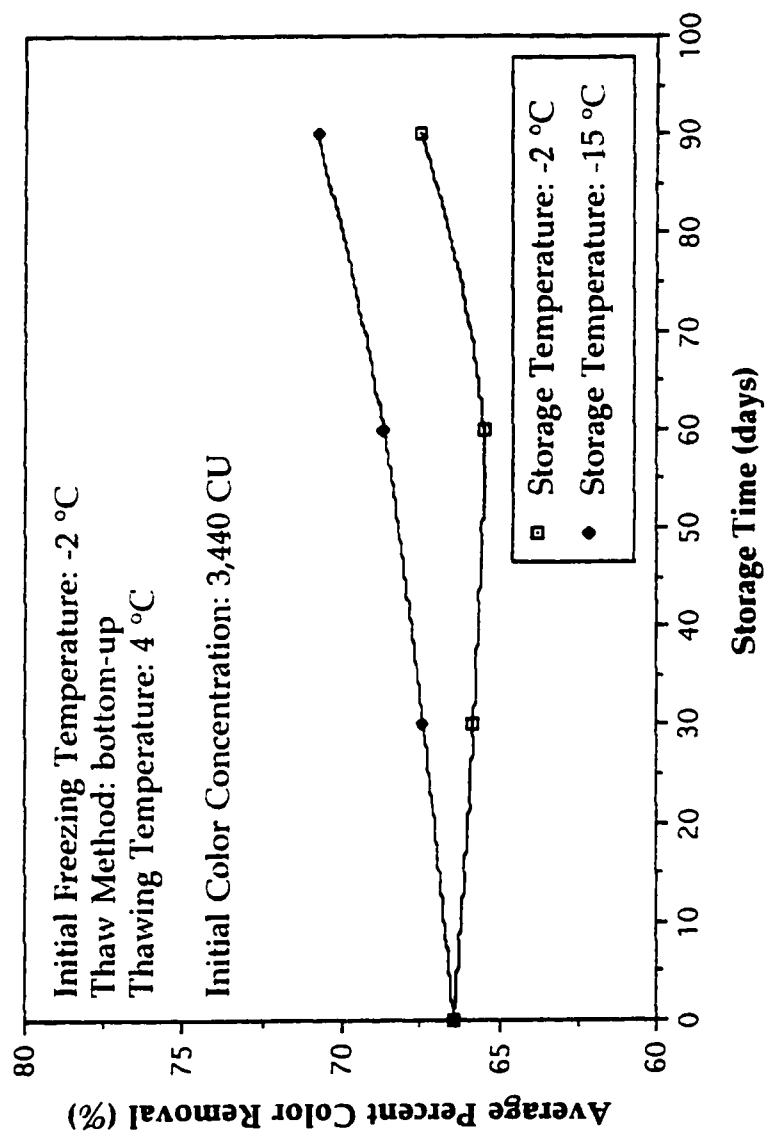


Figure 4.18 Plot of Percent Color Removal with Respect to Storage Time and Storage Temperature for Eop Effluent Frozen at the Initial Freezing Temperature -2 °C (Thawed Bottom Up at 4 °C)

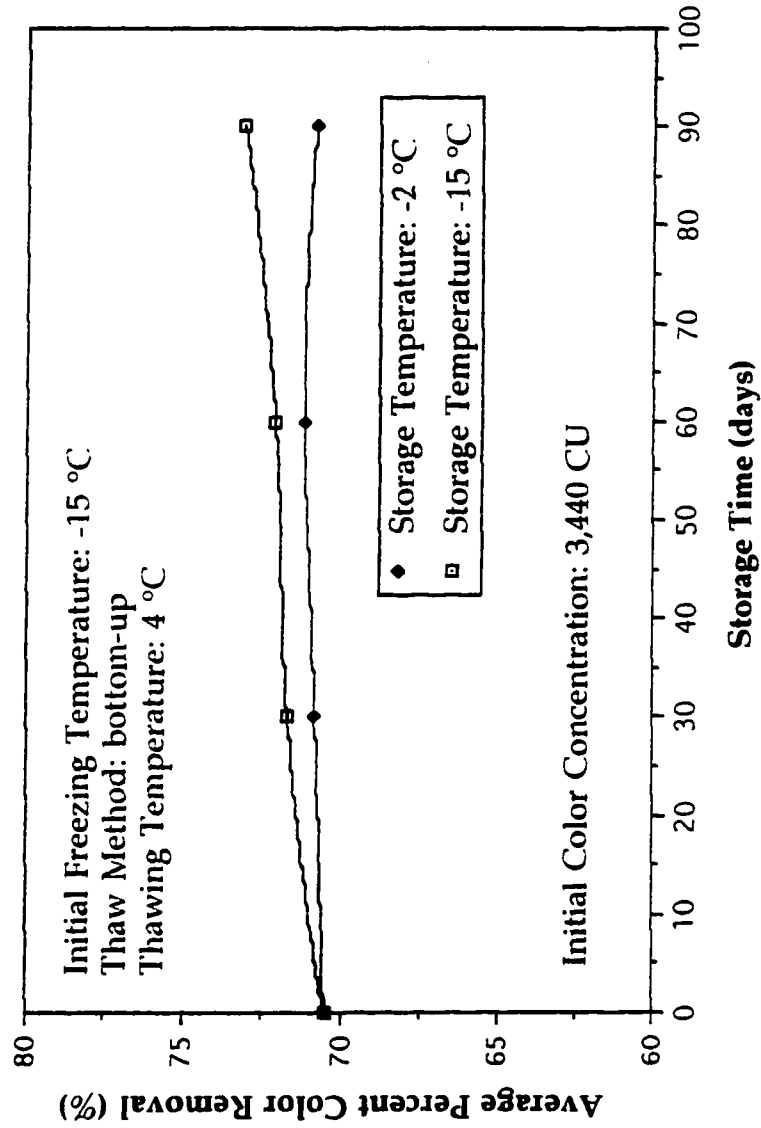


Figure 4.19 Plot of Percent Color Removal with Respect to Storage Time and Storage Temperature for Eop Effluent Frozen at the Initial Freezing Temperature -15 °C (Thawed Bottom Up at 4 °C)

treatment of Eop effluent as observed for membrane concentrate. Although the average percent color removals in the top 70 % liquid volume were reported to increase over time for frozen Eop effluent stored at temperatures equal or lower than its initial freezing temperature, statistically the differences were not significant at a 95 % confidence limit. At storage temperatures above the initial freezing temperature the average percent color removals remained unchanged or decreased marginally with respect to samples thawed immediately after being frozen. Tables 4.5 to 4.8 are the results from having statistically compared the sample means using the two tailed Student's t-test for Eop effluent frozen at the initial freezing temperatures -2 °C and -15 °C, followed by their storage at different temperatures. It can be concluded from examination of these tables that the hypotheses in which it was proposed that the sample means were equal for the different storage temperatures was in part true for samples thawed predominantly from the bottom up for when the storage temperatures were equal or lower than their initial freezing temperature following extended periods of storage.

4.2.2.3 LIQUID DEPTH

Liquid depth was investigated with the belief that small changes in liquid depth will not substantially affect treatment performance.

4.2.2.3.1 ALKALINE EXTRACTION STAGE MEMBRANE CONCENTRATE

Data from selectively sampling the frozen and thawed membrane concentrate during and following freeze-thaw with respect to color are

Table 4.5 Tests of Hypotheses for the Different Storage Temperatures -2 °C and -15 °C for Eop Effluent Frozen at the Initial Freezing Temperature -2 °C (Thawed Bottom Up at 24 °C)

Storage Time (days)	Sample Volume (35 %)	Storage Temperature (°C)		Pooled Estimate	Test Statistic	Conclusion
		-2 °C	-15 °C			
30	top	445 (15.00)	400 (10.00)	12.745	3.530	accept H_0
	middle	685 (15.00)	660 (10.00)	12.748	1.961	accept H_0
60	top	435 (15.00)	360 (10.00)	12.748	5.883	reject H_0
	middle	680 (30.00)	640 (10.00)	22.361	1.790	accept H_0
90	top	425 (15.00)	290 (20.00)	17.678	7.637	reject H_0
	middle	675 (15.00)	610 (20.00)	17.678	3.677	accept H_0

Student t value: $t_{2,0.025} = 4.303$, (?) - sample variance, $H_0: \mu_1 = \mu_2$

Table 4.6 Tests of Hypotheses for the Different Storage Temperatures -2 °C and -15 °C for Eop Effluent Frozen at the Initial Freezing Temperature -15 °C (Thawed Bottom Up at 24 °C)

Storage Time (days)	Sample Volume (35 %)	Storage Temperature (°C)		Pooled Estimate	Test Statistic	Conclusion
		-2 °C	-15 °C			
30	top	640 (10.00)	615 (15.00)	12.748	1.961	accept H_0
	middle	1000 (20.00)	970 (25.00)	22.638	1.325	accept H_0
60	top	620 (10.00)	600 (10.00)	10.000	2.000	accept H_0
	middle	965 (15.00)	965 (15.00)	0.000	0.000	accept H_0
90	top	630 (10.00)	603 (7.00)	8.631	3.128	accept H_0
	middle	980 (20.00)	973 (7.00)	14.983	0.467	accept H_0

Student t value: $t_{2,0.025} = 4.303$, (?) - sample variance, $H_0: \mu_1 = \mu_2$

Table 4.7 Tests of Hypotheses for the Different Storage Temperatures -2 °C and -15 °C for Eop Effluent Frozen at the Initial Freezing Temperature -2 °C (Thawed Bottom Up at 4 °C)

Storage Time (days)	Sample Volume (35 %)	Storage Temperature (°C)		Pooled Estimate	Test Statistic	Conclusion
		-2 °C	-15 °C			
30	top	840 (30.00)	765 (45.00)	38.242	1.961	accept H_0
	middle	1510 (20.00)	1530 (25.00)	22.638	0.883	accept H_0
60	top	875 (25.00)	675 (25.00)	25.000	8.000	reject H_0
	middle	1510 (50.00)	1480 (30.00)	41.231	0.728	accept H_0
90	top	788 (13.00)	630 (20.00)	16.867	9.367	reject H_0
	middle	1450 (40.00)	1380 (35.00)	37.583	1.863	accept H_0

Student t value: $t_{2,0.025} = 4.303$, (?) - sample variance, $H_0: \mu_1 = \mu_2$

Table 4.8 Tests of Hypotheses for the Different Storage Temperatures -2 °C and -15 °C for Eop Effluent Frozen at the Initial Freezing Temperature -15 °C (Thawed Bottom Up at 4 °C)

Storage Time (days)	Sample Volume (35 %)	Storage Temperature (°C)		Pooled Estimate	Test Statistic	Conclusion
		-2 °C	-15 °C			
30	top	720 (30.00)	735 (15.00)	23.717	0.632	accept H_0
	middle	1230 (25.00)	1280 (25.00)	25.000	2.000	accept H_0
60	top	705 (5.00)	735 (25.00)	18.028	1.664	accept H_0
	middle	1210 (20.00)	1230 (5.00)	14.577	1.372	accept H_0
90	top	680 (10.00)	745 (55.00)	39.528	1.644	accept H_0
	middle	1170 (10.00)	1260 (15.00)	12.748	7.060	reject H_0

Student t value: $t_{2,0.025} = 4.303$, (?) - sample variance, $H_0: \mu_1 = \mu_2$

presented and discussed. The color distributions were compared to determine the differences with respect to initial freezing temperature, method of thawing, and liquid depth. Also determined was the degree of color removal attributed to freezing alone. Liquid depth was also investigated for its relative significance and possible inclusion into the factorial design as an independent variable.

The entrapment of constituents in the upper top portion of the ice column increased as the initial freezing temperature decreased. The difference between the resultant color distributions for the frozen concentrate and concentrate thawed top down in the upper liquid portion increased as the initial freezing temperature decreased, with the color values reported as being higher in samples thawed top down. The general tendency, irrespective of initial freezing temperature, was thawing the frozen concentrate from the bottom up provided additional color removal than that achieved by freezing alone. The amount of additional color removal obtained increased with initial freezing temperature. Differences between color distributions for the different initial liquid depths for frozen concentrate thawed bottom up were either the same or if different in value with respect to depth were approximately equal in regards to the overall resultant composite color concentration for the same percent liquid volumes.

Treatment performance reported for the liquid depths 150 mm and 250 mm, irrespective of initial freezing temperature, were not substantially different for concentrate thawed predominantly from the bottom up. Having shown the relative unimportance of this variable between the initial freezing temperatures -2 °C to -15 °C (the selected

boundary range for modeling) its inclusion in the empirical model as an independent variable was not considered.

4.2.2.3.1 INITIAL FREEZING TEMPERATURE: -2 °C

Shown in Figure 4.20 are the color distributions produced at the initial freezing temperature -2 °C with respect to depth for frozen membrane concentrate and for concentrate thawed top down and bottom up at a thawing temperature of 24 °C. The color distributions associated with the top 70 % liquid volume were not substantially different between membrane concentrate frozen at the initial freezing temperature -2 °C and membrane concentrate frozen and then thawed top down at a temperature of 24 °C. At this initial freezing temperature, thawing the membrane concentrate from the top down did not result in any further additional color removal in the top 70 % liquid portion than that initially achieved by freezing. For example, the color concentration in the top 70 % liquid volume of the concentrate thawed top down was measured to range from a minimum 4,050 CU to a maximum of 6,500 CU. Similarly, the color concentration in the top 70 % volume fraction of the frozen concentrate was measured to range from a minimum 3,570 CU to a maximum 5,240 CU. Oppositely, thawing the frozen concentrate from the bottom up at a temperature of 24 °C in which the ice column was allowed to float resulted in additional color removal than that initially achieved by freezing alone. Under these circumstances, the color concentration in the top 70 % liquid volume was measured to range from a minimum 825 CU to a maximum of 6,700 CU.

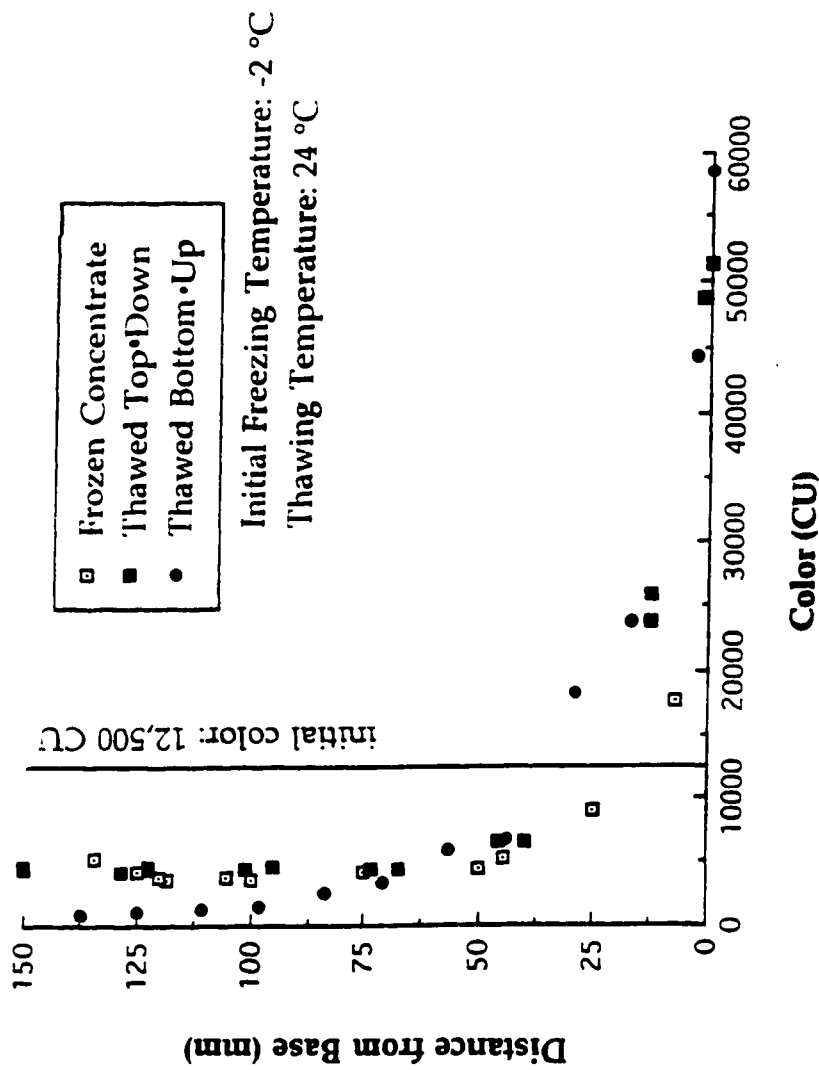


Figure 4.20 Color Distribution with Respect to Depth for Frozen Membrane Concentrate and for Concentrate Thawed Top Down and Bottom Up at a Thawing Temperature of 24 °C for an Initial Freezing Temperature of -2 °C.

Figure 4.21 are the color distributions produced when freezing membrane concentrate to a uniform temperature of $-2\text{ }^{\circ}\text{C}$ versus freezing the concentrate frozen to a non-uniform temperature with respect to its frozen depth. In both cases the initial freezing rates were similar with the only difference being that one sample was thawed before reaching its initial freezing temperature of $-2\text{ }^{\circ}\text{C}$. The frozen concentrate sample thawed prematurely was done so when the temperature in the bottom of its ice column had reached $-1\text{ }^{\circ}\text{C}$. From examination of this figure it can be seen that the color distributions were not substantially different. This indicates that the difference in time between when samples were frozen and thawed were not significant to have the parameter storage time at this initial freezing temperature significantly affect treatment performance.

Plotted in Figure 4.22 are the color distributions for different liquid depths of membrane concentrate frozen at the initial freezing temperature $-2\text{ }^{\circ}\text{C}$ following which the samples were immediately thawed from the bottom up at a temperature of $24\text{ }^{\circ}\text{C}$. Examination of this figure shows the volume reduction to achieve an equivalent treated effluent quality from freeze-thaw was not substantially different between liquid depths. Increasing the liquid depth from 150 mm to 250 mm shifted the resultant color distribution curve vertically upwards, to produce a color concentration range in the top 70 % liquid volume that was approximately equal to the lower liquid depths. For example, the color concentration range in the top 70 % liquid volume for a liquid depth of 150 mm was measured to range from 825 CU to 6,700 CU. Similarly, the color concentration for the 250 mm liquid depth was measured to range from 1,280 CU to 6,500 CU. The shape of the distribution curves were not

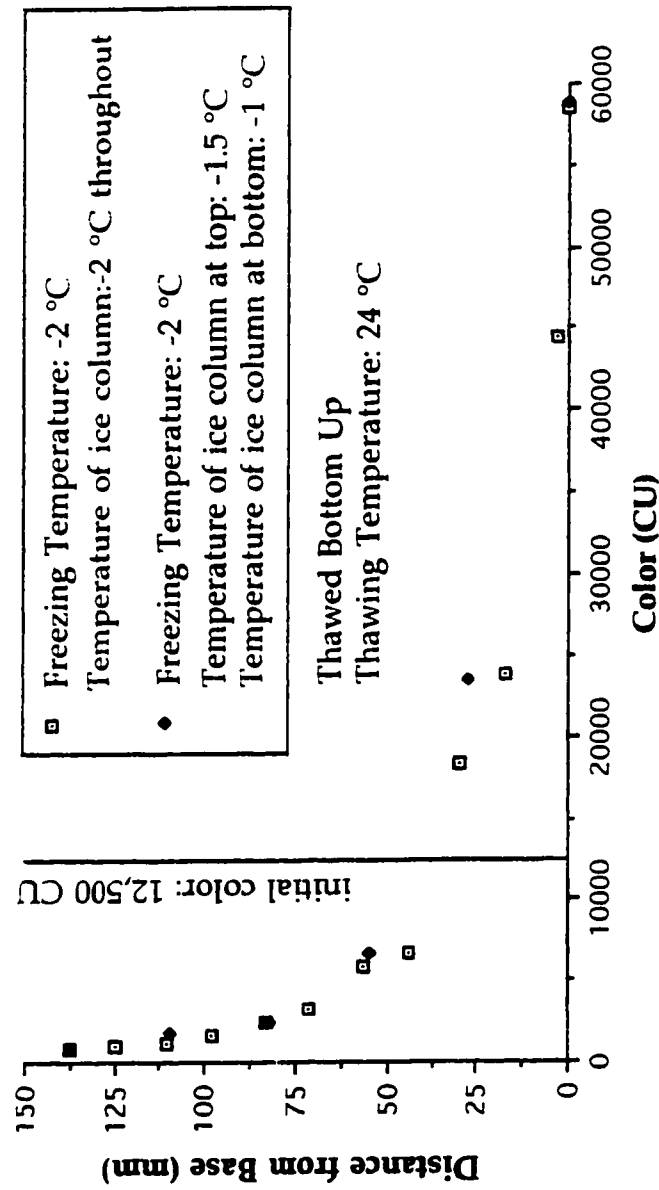


Figure 4.21 Color Distribution with Respect to Depth for Membrane Concentrate Frozen to Different Temperatures and Thawed Bottom Up at a Thawing Temperature of 24 °C for an Initial Freezing Temperature of -2 °C

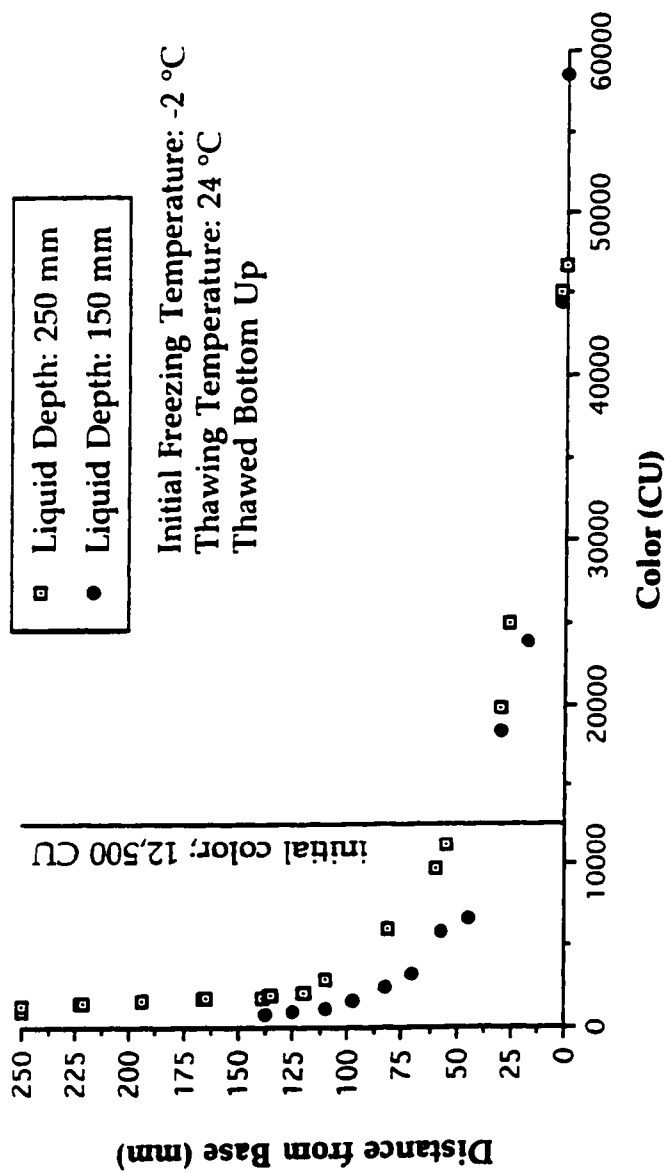


Figure 4.22 Comparison of Color Distributions with Respect to Depth for Membrane Concentrate of Different Liquid Depths Frozen at the Initial Freezing Temperature -2 °C and Thawed Bottom Up at a Temperature of 24 °C

substantially different to suggest the composite samples representative of the top 70 % liquid volume for these different liquid depths would not be substantially different. Therefore the relative significance of the data was that varying the liquid depth between 150 mm to 250 mm does not substantially affect treatment performance in terms of the resultant color concentration that can be anticipated in a particular liquid volume at this initial freezing temperature.

4.2.2.3.2 INITIAL FREEZING TEMPERATURE: -15 °C

Shown in Figure 4.23 are the color distributions produced at the initial freezing temperature -15 °C with respect to depth for frozen membrane concentrate and for concentrate thawed top down and bottom up at a thawing temperature of 24 °C. The color distributions associated with the top 70 % liquid volume were shown to differ between the frozen membrane concentrate and the concentrate frozen and thawed top down. Thawing the membrane concentrate from the top down in which the ice was prevented from floating reduced the overall color removal in the top liquid portion with respect to that achieved by freezing alone. For example, the color concentration in the top 70 % liquid volume of the concentrate thawed top down averaged 9,700 CU. Similarly, the color concentration in the top 70 % volume fraction of the frozen concentrate was measured to range from a minimum 6,500 CU to a maximum 10,400 CU. Thawing the frozen concentrate from the bottom up at a temperature of 24 °C in which the ice column was allowed to float resulted in additional color removal than that initially achieved by freezing. Under these circumstances, the color concentrations in the top 70 % liquid volume were measured to range from a minimum 1,290 CU to a

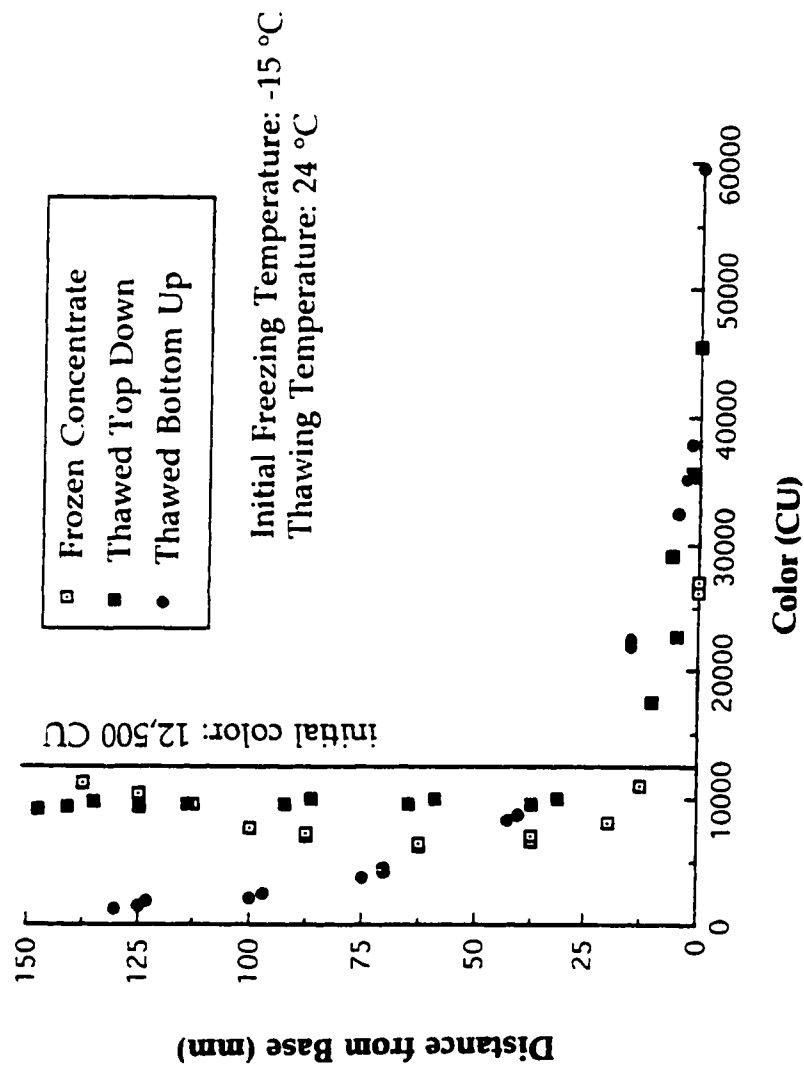


Figure 4.23 Color Distribution with Respect to Depth for Frozen Membrane Concentrate and for Concentrate Thawed Top-Down and Bottom-Up at a Thawing Temperature of 24 °C for an Initial Freezing Temperature of -15 °C

maximum 8,200 CU. In comparison to the warmer initial freezing temperature, the data suggests method of thawing adversely affects treatment performance more and that was attributed to how the concentrated material is released from the ice matrix during thawing.

Shown in Figure 4.24 are the color distributions that are produced when freezing the membrane concentrate to an uniform temperature of -14.5°C versus freezing the concentrate frozen but to a non-uniform temperature with respect to its frozen depth. In both cases the initial freezing rates were similar with the only difference being that one sample was thawed before reaching a constant frozen temperature of -15°C . This frozen concentrate sample was thawed when the bottom of its ice column had reached a temperature of -5°C , while the corresponding top column temperature was -9.6°C . From examination of this figure it can be seen that the color distributions were not substantially different. In studies conducted to investigate storage time it was concluded that time frozen does not significantly affect treatment performance when the storage temperature was -15°C or warmer for samples frozen at the initial freezing temperature -15°C .

Plotted in Figure 4.25 are the color distributions for partially and completely frozen membrane concentrate thawed bottom up at a temperature of 24°C . From examination of this figure it can be seen that the color distributions were not substantially different for the portions that were frozen.

Shown in Figure 4.26 are the color distributions for different liquid depths of membrane concentrate frozen at the initial freezing temperature

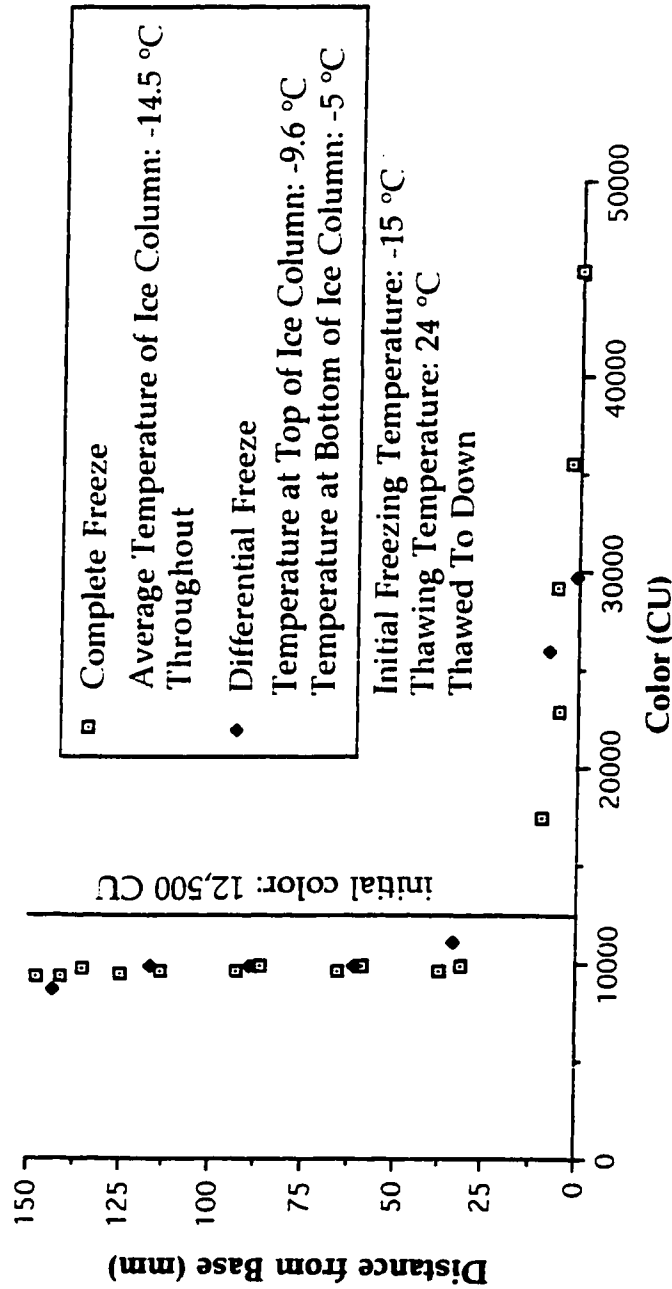


Figure 4.24 Color Distribution with Respect to Depth for Membrane Concentrate Frozen to Different Temperatures and Thawed Bottom-Up at a Thawing Temperature of 24 °C for an Initial Freezing Temperature of -15 °C

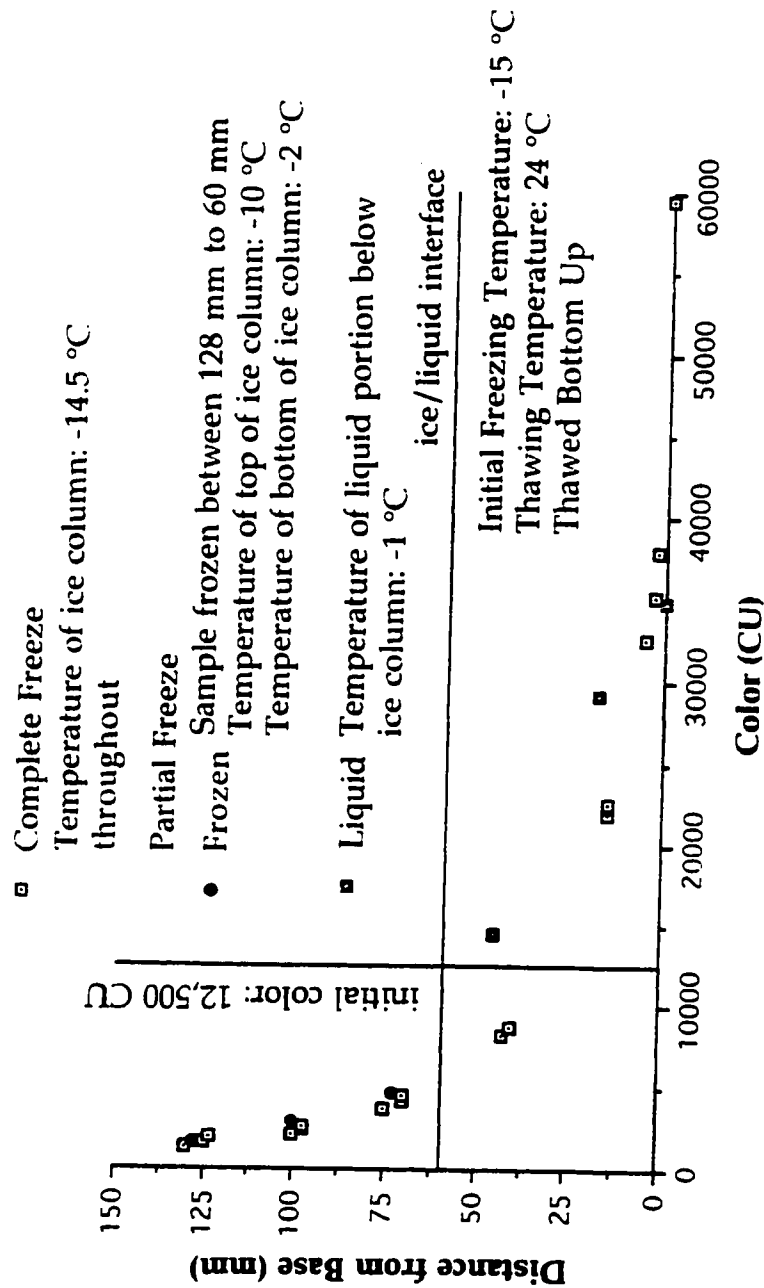


Figure 4.25 Color Distribution with Respect to Depth for Completely and Partially Frozen Membrane Concentrate Thawed Bottom Up at a Thawing Temperature of 24 °C for an Initial Freezing Temperature of -15 °C

-15 °C following which the samples were immediately thawed from the bottom up at a temperature of 24 °C. Examination of this figure shows the color distributions were not substantially different between the two liquid depths. The relative significance of this data was that it further demonstrates the unimportance of liquid depth with respect to treatment performance at cold initial freezing temperatures.

4.2.2.3.3 INITIAL FREEZING TEMPERATURE: -25 °C

Plotted in Figure 4.27 are the color distributions produced at the initial freezing temperature -25 °C for frozen membrane concentrate and for concentrate thawed top down and bottom up at a temperature of 24 °C. Examination of this figure shows there was a substantial difference between the color distributions between the frozen concentrate and the concentrate thawed top down, much more than that observed at the warmer initial freezing temperature. For example, the color concentration in the top 70 % liquid volume of the concentrate thawed top down averaged 10,400 CU. Whereas the color concentrations in the top 70 % volume fraction of the frozen concentrate were measured to range from a minimum 6,060 CU to a maximum 11,300 CU. Thawing the frozen concentrate from the bottom up provided for additional color removal than that achieved by freezing alone. Under these circumstances, the color concentrations in the top 70 % liquid volume were measured to range from a minimum 1,620 CU to a maximum 7,500 CU. However, the general tendency of the data was the additional color removal achieved by thawing the concentrate from the bottom up decreased as the initial freezing temperature decreased.

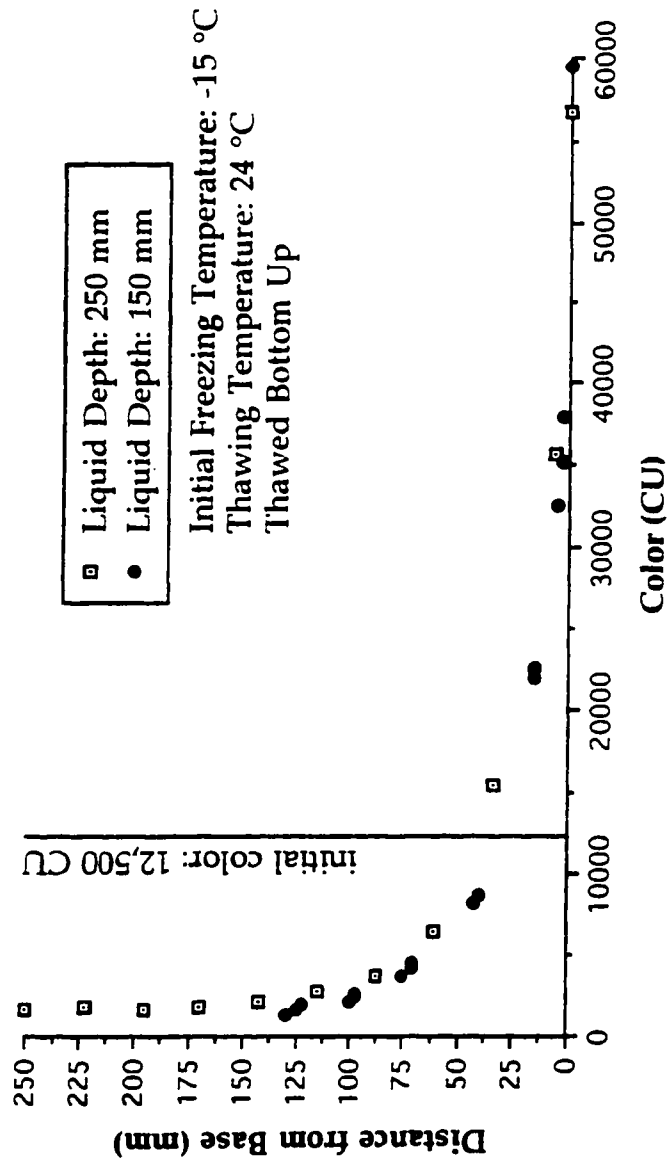


Figure 4.26 Comparison of Color Distributions with Respect to Depth for Membrane Concentrate of Different Liquid Depths Frozen at the Initial Freezing Temperature -15 °C and Thawed Bottom Up at a Temperature of 24 °C

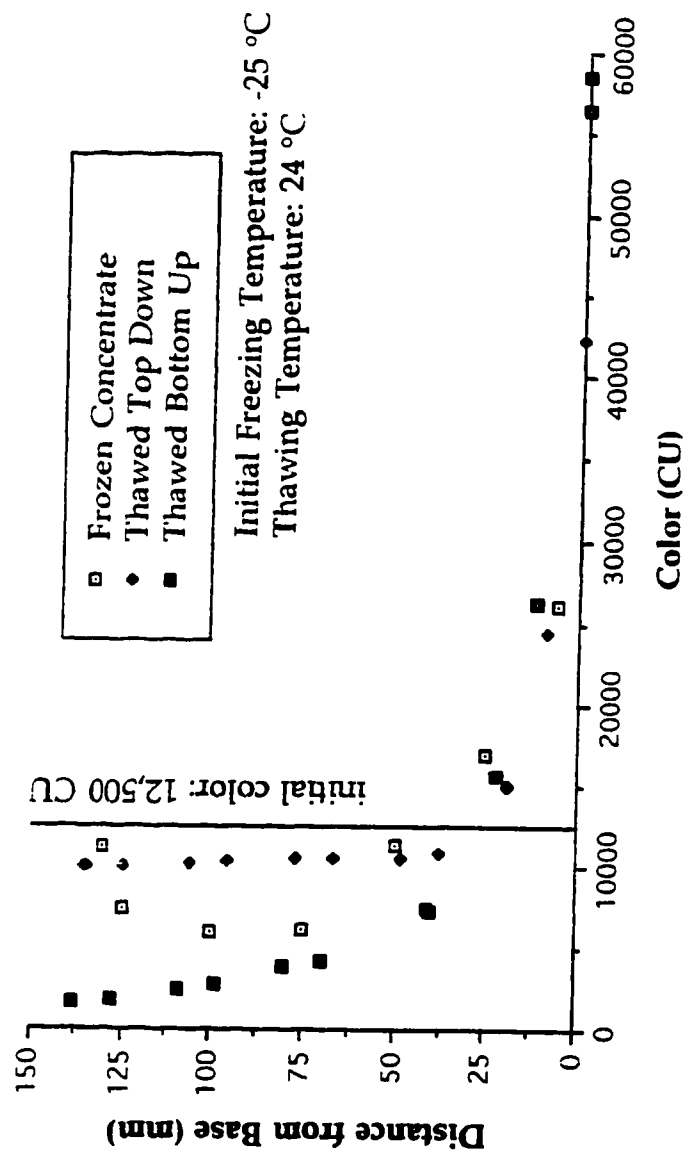


Figure 4.27 Color Distribution with Respect to Depth for Frozen Membrane Concentrate and for Concentrate Thawed Top-Down and Bottom Up at a Thawing Temperature of 24 °C for an Initial Freezing Temperature of -25 °C

Shown in Figure 4.28 are the color distributions for different liquid depths of membrane concentrate frozen at the initial freezing temperature -25°C and thawed bottom up at a temperature of 24°C . Examination of this figure shows the color distributions as being marginally different between the two liquid depths. The color distribution for the liquid depth 250 mm was higher and paralleled the distribution curve for the lower liquid depth. Increasing the liquid depth from 150 mm to 250 mm shifted the resultant color distribution curve vertically upwards, to produce a color concentration range in the top 70 % liquid volume that was approximately equal for the two liquid depths. The color concentrations in the top 70 % liquid volume for a liquid depth of 150 mm were measured to range from 1,620 CU to 7,500 CU. Whereas the color concentrations for the 250 mm liquid depth were measured to range from 1,740 CU to 5,500 CU. The shape of the distribution curves were not substantially different to suggest the composite samples representative of the top 70 % liquid volume for these different liquid depths would not be substantially different. The relative significance of the data was that varying the liquid depth between 150 mm to 250 mm does not substantially affect treatment performance in terms of the resultant color concentration that can be anticipated in a particular liquid volume at this initial freezing temperature.

4.2.2.3.2 ALKALINE EXTRACTION STAGE EFFLUENT

Data from sampling the frozen and thawed Eop effluent during and following freeze-thaw with respect to color are presented and discussed. The general tendencies observed for the data were similar to that reported

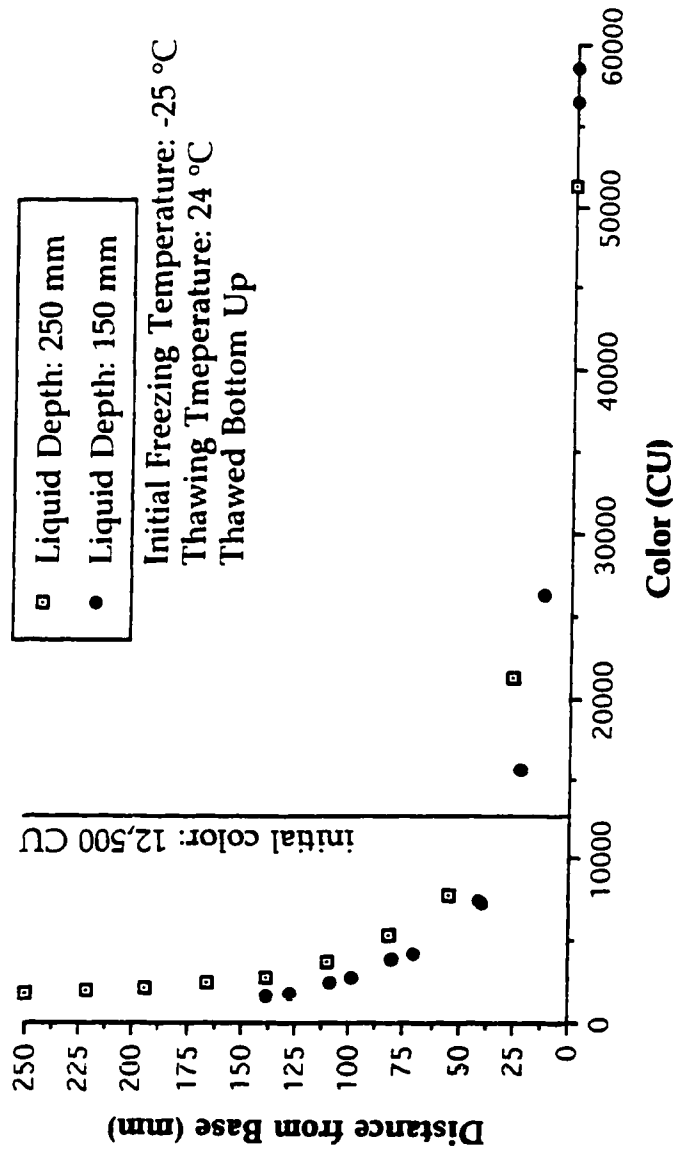


Figure 4.28 Comparison of Color Distributions with Respect to Depth for Membrane Concentrate of Different Liquid Depths Frozen at the Initial Freezing Temperature -25 °C and Thawed Bottom Up at a Temperature of 24 °C

for the membrane concentrate. The entrapment of constituents in the upper top ice column portion increased as the initial freezing temperature decreased. Thawing the frozen effluent from the bottom up provided for additional color removal in the upper volume fraction compared to that achieved by freezing, with the magnitude decreasing with initial freezing temperature. Thawing the frozen effluent from the top down decreased the overall color removal with respect to the frozen sample in the upper volume fraction, with the magnitude increasing with decreasing initial freezing temperature. Increasing the liquid depth to 250 mm decreased marginally the overall color removal in the upper liquid fraction in comparison with the lower liquid depth, with the magnitude increasing with decreasing initial freezing temperature.

4.2.2.3.2.1 INITIAL FREEZING TEMPERATURE: -2 °C

Plotted in Figure 4.29 are the color distributions produced at the initial freezing temperature -2 °C for frozen Eop effluent and effluent thawed top down and bottom up at a temperature of 24 °C. Examination of this figure shows the color distributions were not substantially different between the frozen effluent and the effluent sample thawed top down. However, thawing the effluent from the bottom up provided for additional color removal beyond that achieved by freezing alone.

Shown in Figure 4.30 are the color distributions for different liquid depths of Eop effluent frozen at the initial freezing temperature -2 °C and thawed bottom up at a temperature of 24 °C. Examination of this figure shows the color distributions for the different liquid depths were not substantially different. This indicates that liquid depth for the range

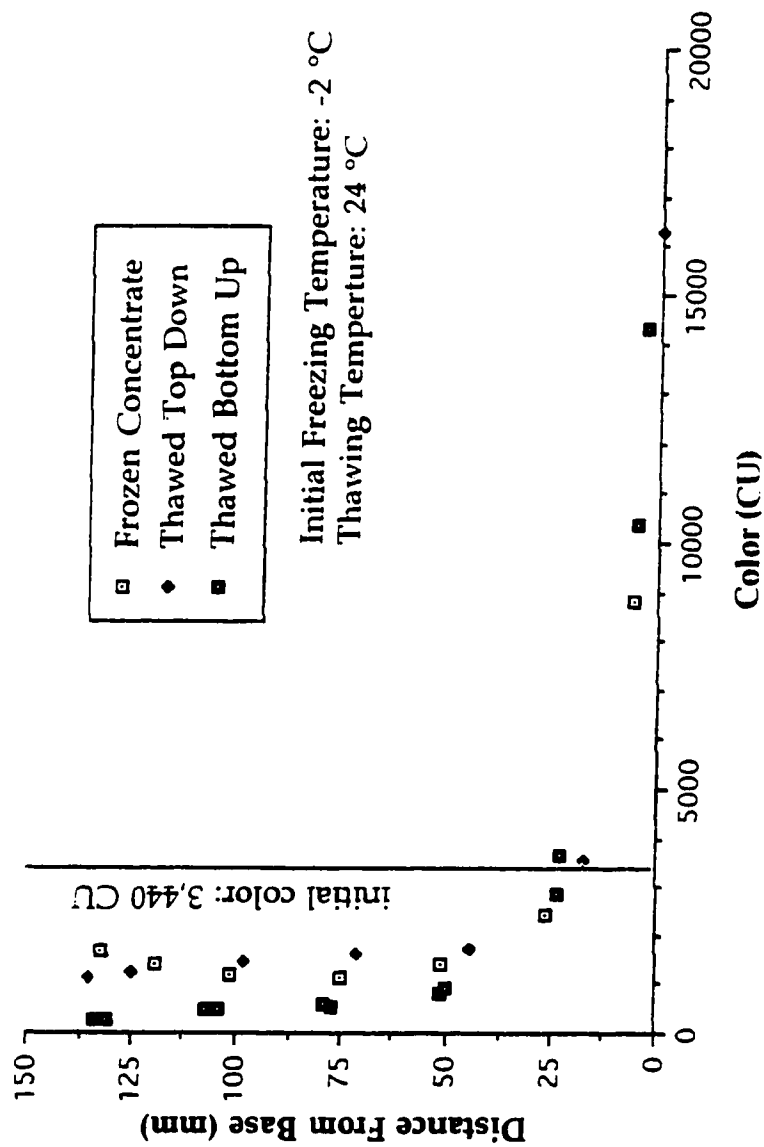


Figure 4.29 Color Distribution with Respect to Depth for Frozen Eop Effluent and for Effluent Thawed Top-Down and Bottom Up at a Thawing Temperature of 24 °C for an Initial Freezing Temperature of -2 °C

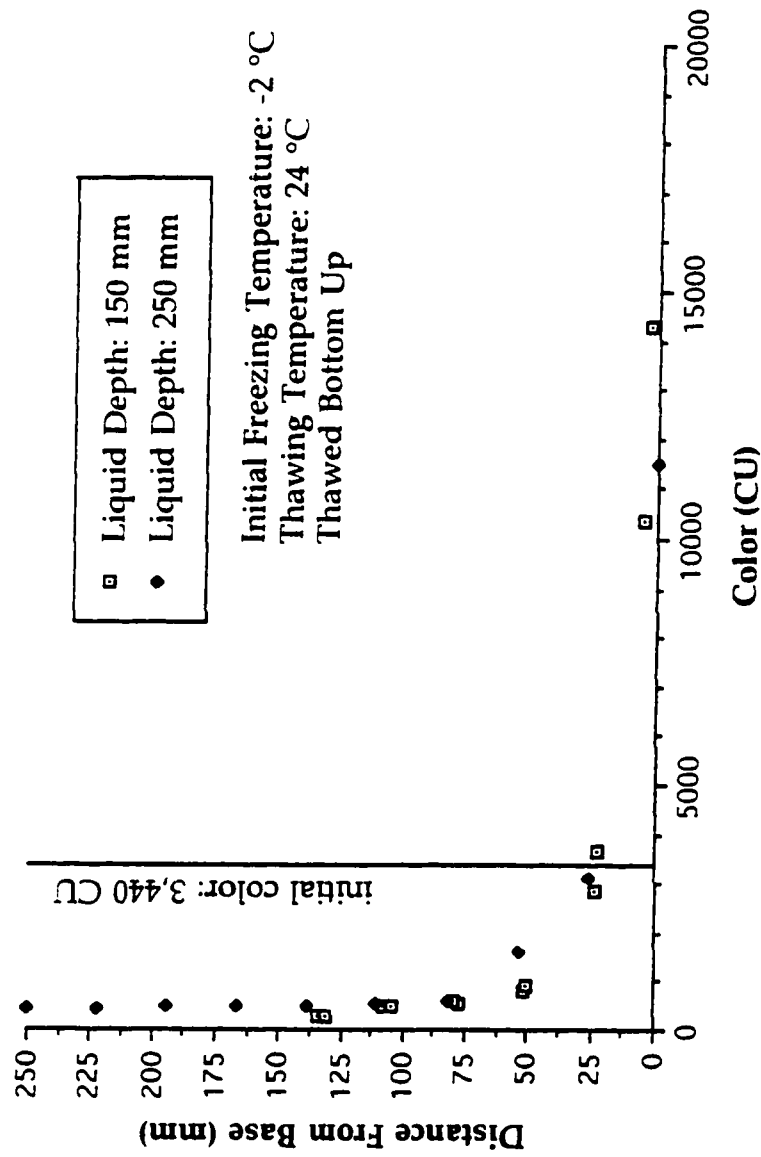


Figure 4.30 Comparison of Color Distributions with Respect to Depth for
Eop Effluent of Different Liquid Depths Frozen at the
Initial Freezing Temperature -2 °C and Thawed Bottom
Up at a Temperature of 24 °C

investigated would not contribute significantly to treatment performance at this initial freezing temperature.

4.2.2.3.2.2 INITIAL FREEZING TEMPERATURE: -15 °C

Plotted in Figure 4.31 are the color distributions for frozen Eop effluent and effluent thawed top down and bottom up at a temperature of 24 °C for an initial freezing temperature of -15 °C. The color distributions were not substantially different, particularly in the upper volume portion, between the frozen effluent and effluent samples thawed top down and bottom up.

Shown in Figure 4.32 are the color distributions for different liquid depths of Eop effluent frozen at the initial freezing temperature -15 °C and thawed bottom up at a temperature of 24 °C. The color distribution for the initial liquid depth 150 mm was marginally lower in comparison to the higher liquid depth.

4.2.2.3.2.3 INITIAL FREEZING TEMPERATURE: -25 °C

Plotted in Figure 4.33 are the color distributions for frozen Eop effluent and effluent thawed top down and bottom up at a temperature of 24 °C for an initial freezing temperature of -25 °C. Examination of this figure shows the color distributions were substantially different between the frozen effluent and the effluent sample thawed top down. The color distribution for the effluent sample thawed top down was substantially higher in comparison to the frozen concentrate. However, thawing the effluent from the bottom up provided for additional color removal producing values above that achieved by freezing alone.

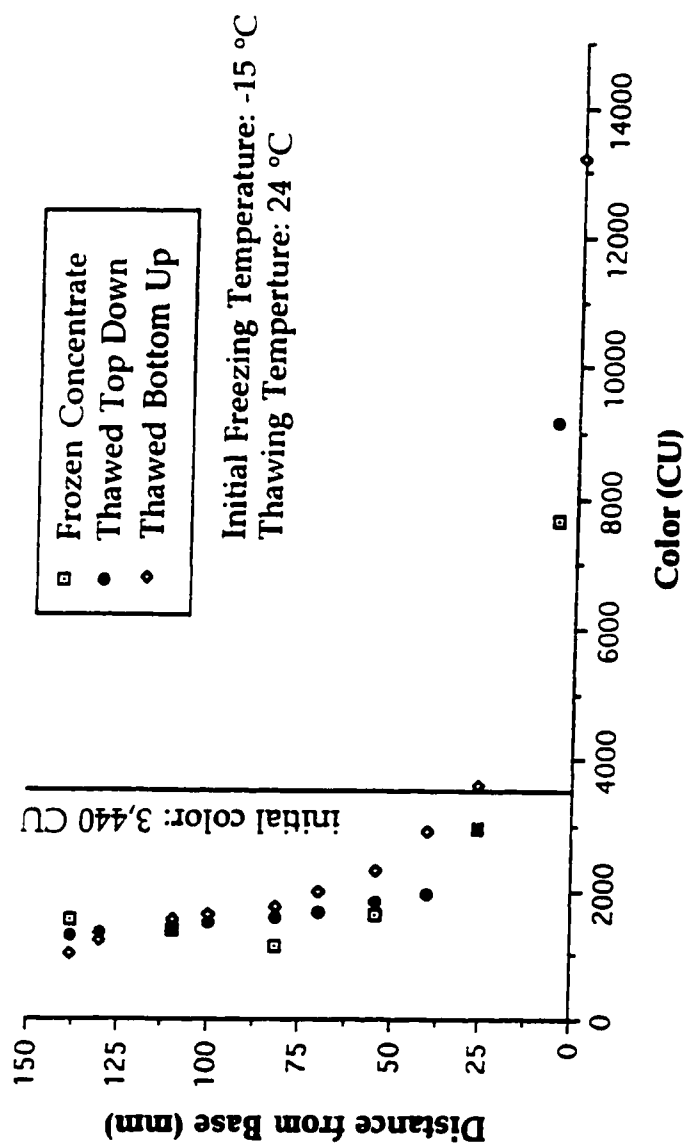


Figure 4.31 Color Distribution with Respect to Depth for Frozen Eop Effluent and for Effluent Thawed Top Down and Bottom Up at a Thawing Temperature of 24 °C for an Initial Freezing Temperature of -15 °C

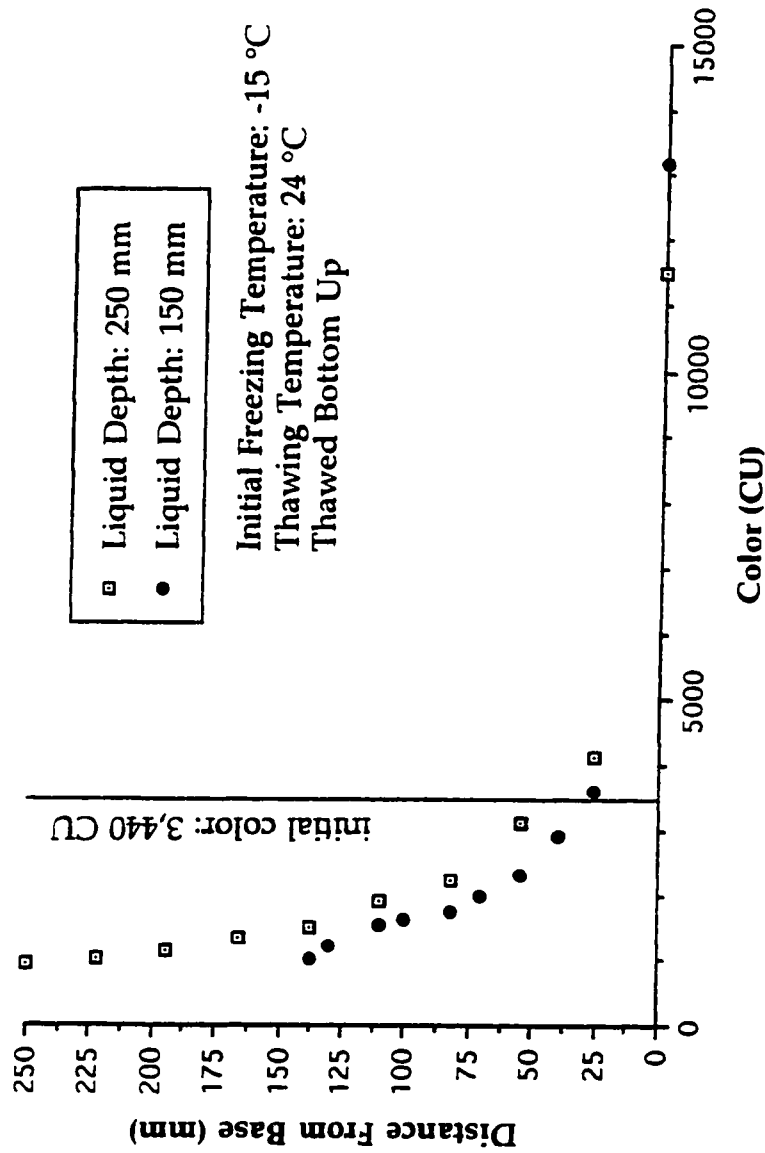


Figure 4.32 Comparison of Color Distributions with Respect to Depth for Eop Effluent of Different Liquid Depths Frozen at the Initial Freezing Temperature -15 °C and Thawed Bottom Up at a Temperature of 24 °C

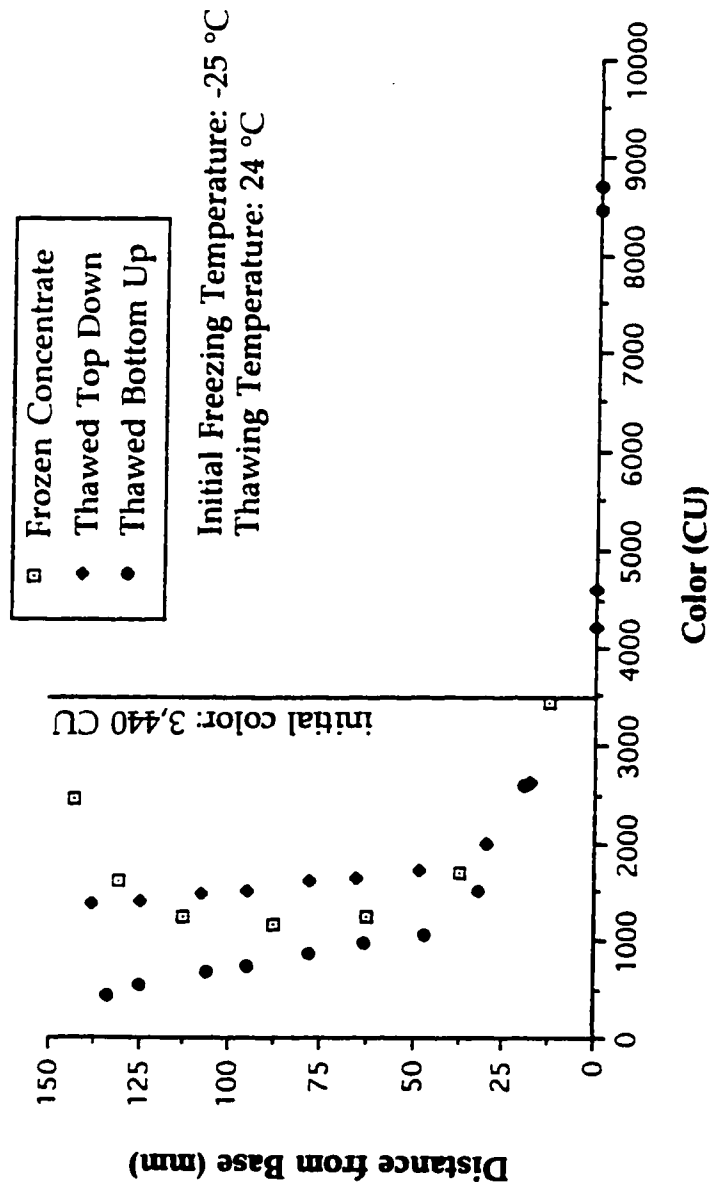


Figure 4.33 Color Distribution with Respect to Depth for Frozen Eop
Effluent and for Effluent Thawed Top-Down and Bottom
Up at a Thawing Temperature of 24 °C for an Initial
Freezing Temperature of -25 °C

Shown in Figure 4.34 are the color distributions for different liquid depths of Eop effluent frozen at the initial freezing temperature -25°C and thawed bottom up at a temperature of 24°C . The general tendency of the data was similar to that observed at the initial freezing temperature -15°C . The color distribution for the initial liquid depth of 150 mm was marginally lower in comparison to the higher liquid depth (250 mm).

4.2.2.4 FREEZE CONCENTRATION

Composite samples were collected of the frozen effluent for comparison to thawed composite samples to determine constituent removal by freeze concentration.

Common general tendencies observed with respect to the data for each experimental water type included the following; color removal attributed to freezing was reported to decrease with decreasing initial freezing temperature. For example, the average percent color removal in the top 70 % liquid volume for the frozen Eop effluent decreased from 59.3 % at an initial freezing temperature of -2°C to 50.4 % at an initial freezing temperature of -25°C . Similarly, for membrane concentrate the average percent color removal decreased from 67.0 % to 24.2 %, respectively. In all cases, thawing the frozen samples from predominantly the bottom up provided for additional color removal, with the magnitude increasing with thawing temperature. Whereas thawing the frozen samples from the top down produced in most cases color removals lower than that achieved by freezing, with the magnitude increasing with decreasing thawing temperature.

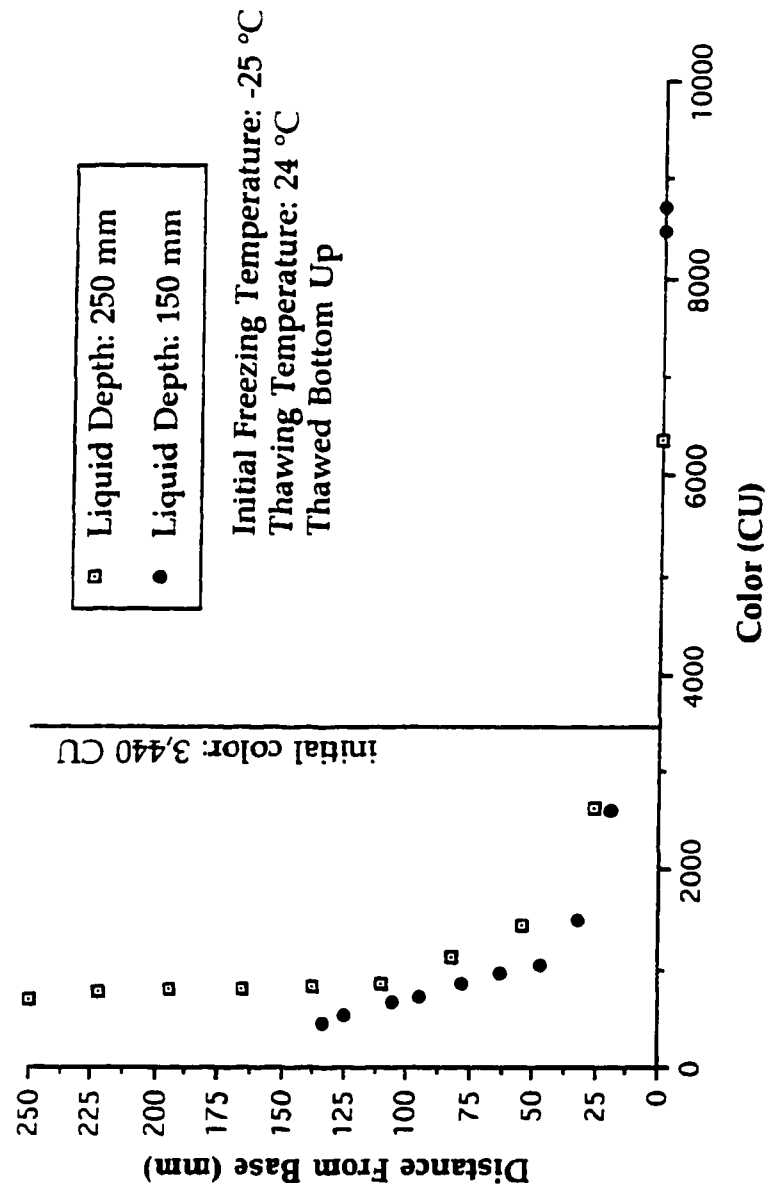


Figure 4.34 Comparison of Color Distributions with Respect to Depth for
Eop Effluent of Different Liquid Depths Frozen at the
Initial Freezing Temperature -25 °C and Thawed Bottom
Up at a Temperature of 24 °C

4.2.2.4.1 ALKALINE EXTRACTION STAGE MEMBRANE CONCENTRATE

Plotted in Figures 4.35 to 4.37 are the average percent color removals for the top 70 % volume portion with respect to thawing and initial freezing temperature for frozen and thawed membrane concentrate composite samples. The average percent color removals, irrespective of initial freezing temperature, for samples thawed top down were substantially lower than the removal rates reported for the frozen concentrate. At the initial freezing temperature -2°C the average percent differences with respect to the frozen concentrate ranged from 27.4 % to 32.4 %. Similarly, at initial freezing temperatures -15°C and -25°C the average percent differences were reported to range from a maximum of 10.3 % and from 5.2 % to 9.0 %, respectively. Oppositely, the average percent color removals, irrespective of initial freezing temperature, for samples thawed bottom up were substantially higher than the removal rates for the frozen concentrate. At the initial freezing temperature -2°C the maximum percent difference in comparison to the frozen concentrate was 5 % at the highest thawing temperature investigated (24°C). Similarly, at initial freezing temperatures -15°C and -25°C the average percent differences were reported to range from 25.4 % to 33.8 % and 38.2 % to 40.9 %, respectively.

4.2.2.4.2 ALKALINE EXTRACTION STAGE EFFLUENT

The experimental results obtained in treatment of Eop effluent were similar to that observed for membrane concentrate with respect to the general tendency of the data.

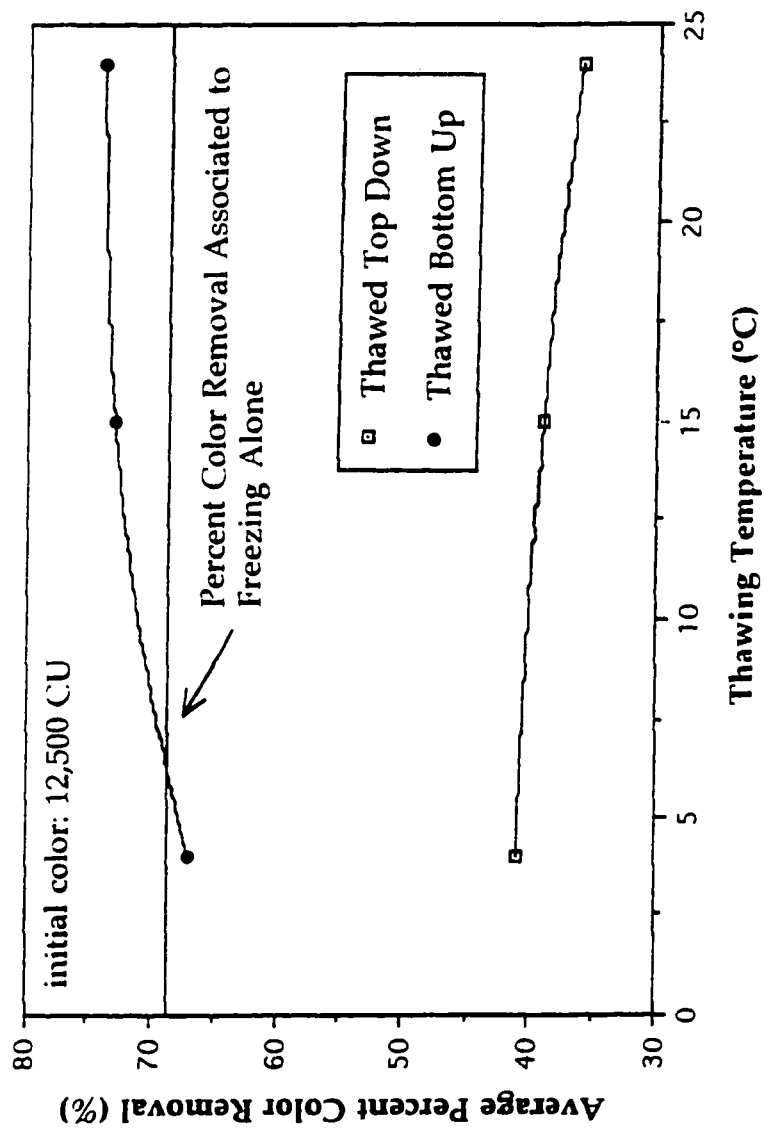


Figure 4.35 Plot of Average Percent Color Removal in the Top 70 % Liquid Volume with Respect to Thawing Temperature for Frozen and Thawed Membrane Concentrate Frozen at the Initial Freezing Temperature -2 °C

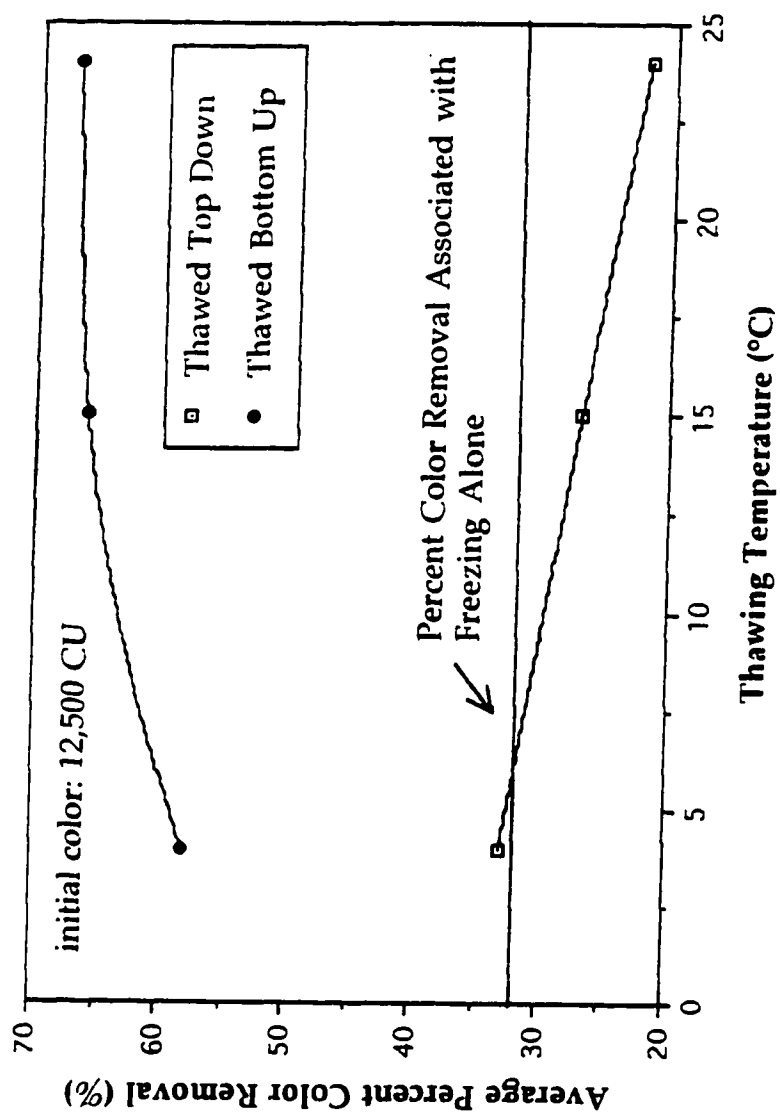


Figure 4.36 Plot of Average Percent Color Removal in the Top 70 % Liquid Volume with Respect to Thawing Temperature for Frozen and Thawed Membrane Concentrate Frozen at the Initial Freezing Temperature -15 °C

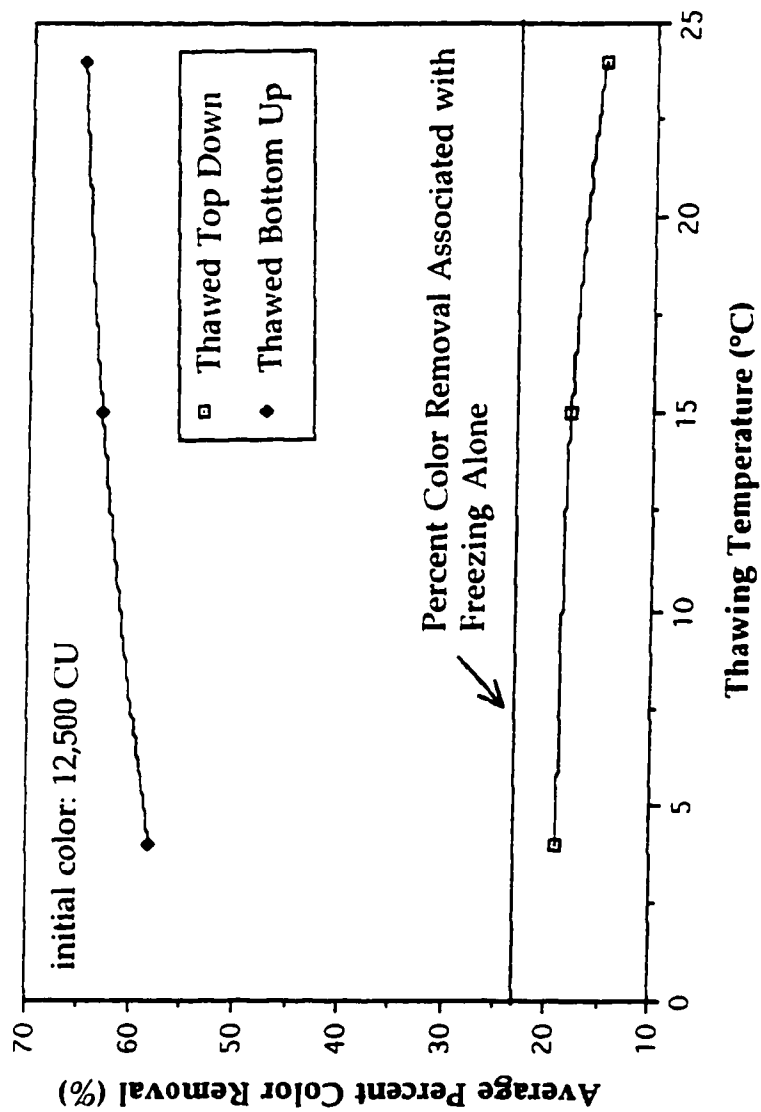


Figure 4.37 Plot of Average Percent Color Removal in the Top 70 % Liquid Volume with Respect to Thawing Temperature for Frozen and Thawed Membrane Concentrate Frozen at the Initial Freezing Temperature -25 °C

Plotted in Figures 4.38 to 4.40 are the average percent color removals for the top 70 % volume portion with respect to thawing and initial freezing temperature for frozen and thawed Eop composite samples. The average percent color removals, irrespective of initial freezing temperature, for samples thawed bottom up were substantially higher than the removal rates for frozen samples. At the initial freezing temperature -2°C the average percent differences were reported to range from 7.2 % to 25.1 %. Similarly, at initial freezing temperatures -15°C and -25°C the average percent differences were reported to range from 15.3 % to 21.6 % and 19.5 % to 25.8 %, respectively. In all cases the percent differences increased with thawing temperature. Oppositely, the average percent color removals, irrespective of initial freezing temperature, for samples thawed top down were substantially lower than the removal rates for frozen concentrate. At the initial freezing temperature -2°C the average percent differences were reported to range from 4.3 % to 8.9 %, respectively. Similarly, at initial freezing temperatures -15°C and -25°C the average percent differences were reported to range from 4.8 % to 5.8 % and 0.8 % to 2.0 %, respectively. The percent differences decreased with thawing temperature.

4.2.2.5 CYCLED FREEZE-THAW

Cycled freeze-thaw improved color removal. However, the additional removals were very small, with the magnitude of the percent changes decreasing with the number of freeze-thaw cycles and with decreasing initial freezing temperature.

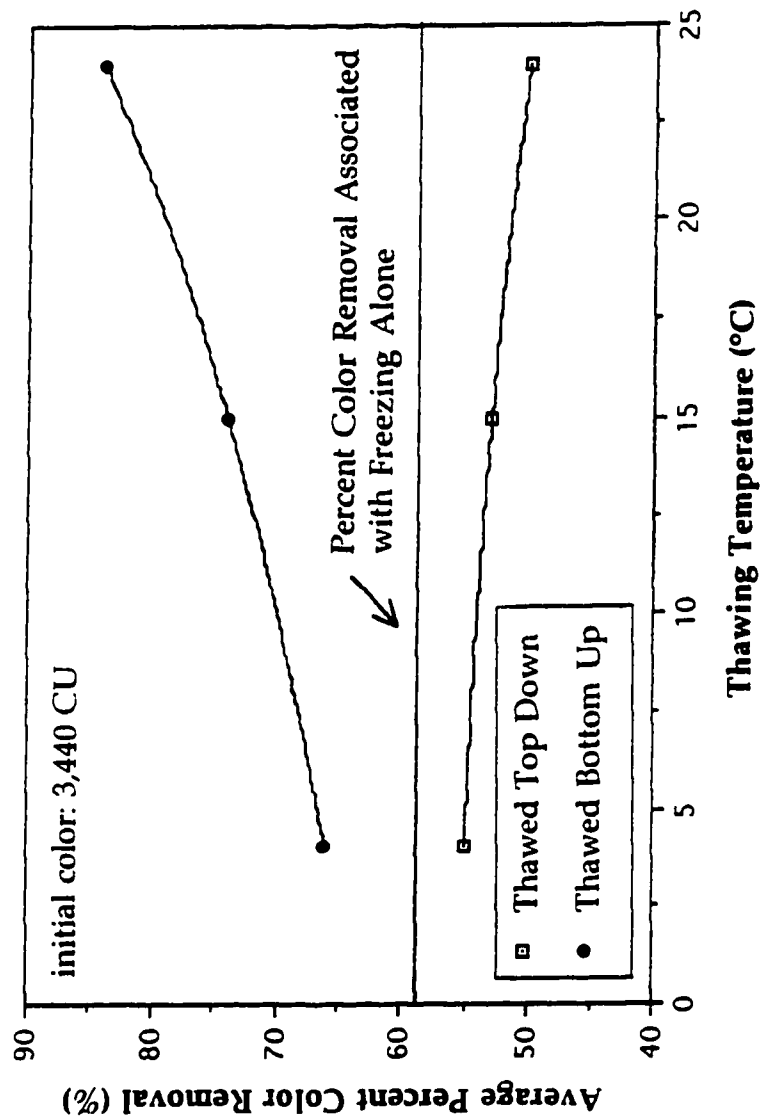


Figure 4.38 Plot of Average Percent Color Removal in the Top 70 % Liquid Volume with Respect to Thawing Temperature for Frozen and Thawed Eop Effluent Frozen at the Initial Freezing Temperature -2 °C

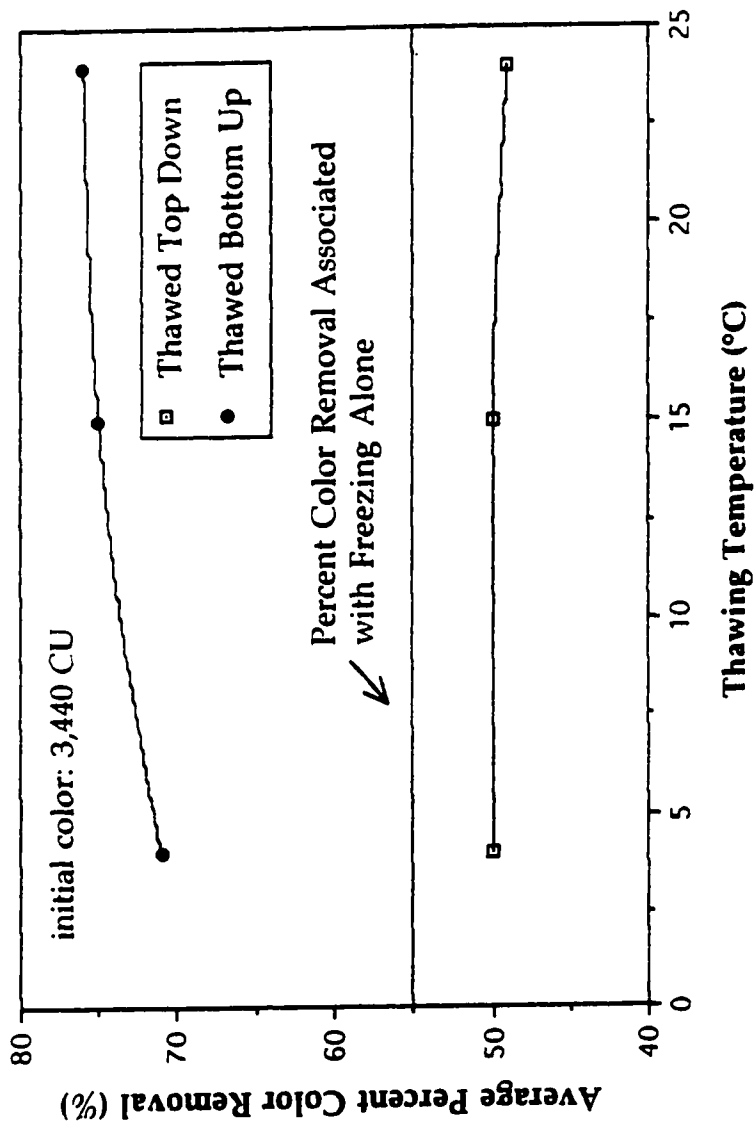


Figure 4.39 Plot of Average Percent Color Removal in the Top 70 % Liquid Volume with Respect to Thawing Temperature for Frozen and Thawed Eop Effluent Frozen at the Initial Freezing Temperature -15 °C

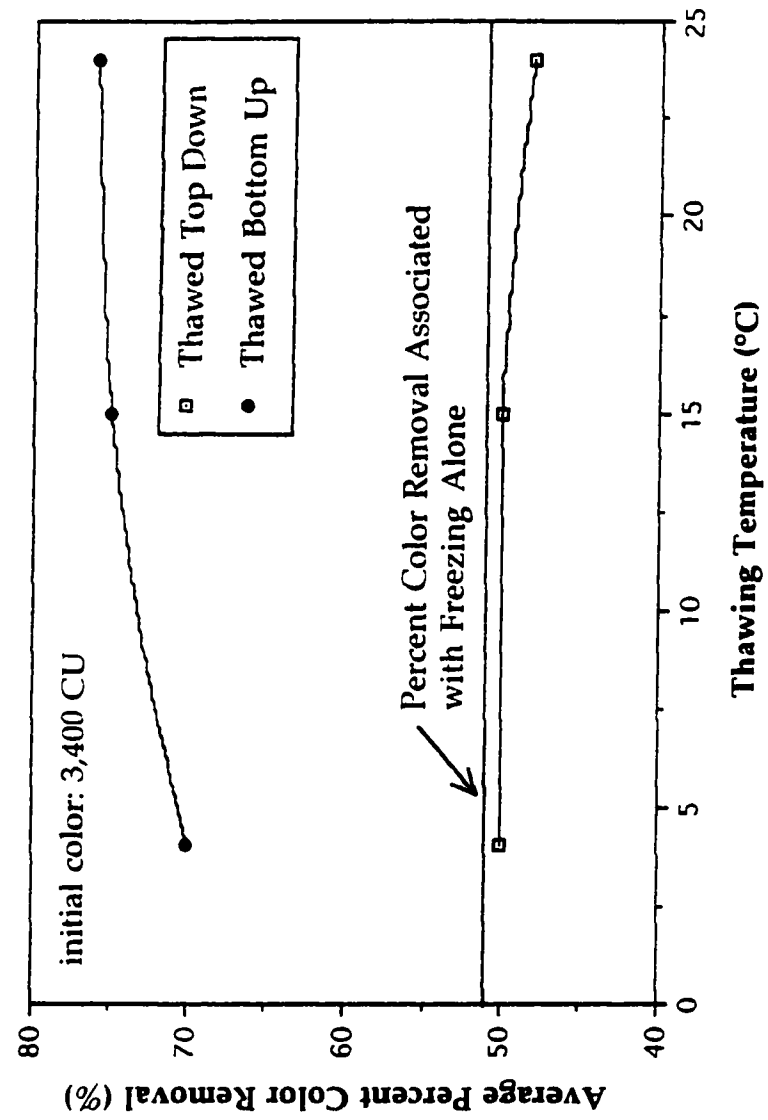


Figure 4.40 Plot of Average Percent Color Removal in the Top 70 % Liquid Volume with Respect to Thawing Temperature for Frozen and Thawed Eop Effluent Frozen at the Initial Freezing Temperature -25 °C

The data presented herein shows that treatment performance was not adversely affected under conditions of multiple freeze-thaw provided that thawing occurs in a manner similar to that observed to produce optimum results as identified in earlier experiments.

4.2.2.5.1 INITIAL FREEZING TEMPERATURE: -2 °C

Plotted in Figure 4.41 are the average percent color removals with respect to the top, middle, and combined upper liquid portions for membrane concentrate treated repeatedly by freeze-thaw at the initial freezing temperature -2 °C. Examination of this figure shows the highest degree of color removal (73.2 %) from the upper liquid portion occurred following one cycle of freeze-thaw. Additional freeze-thaw cycles thereafter were observed to improve color removal with the magnitude of the increase decreasing with the number of freeze-thaw cycles. The average percent increase in color removals in the top 70 % liquid volume were reported to range from 1.4 % to 3.2 % following three cycles of freeze-thaw. Analysis of variance and the Duncan Multiple Range Test were used to determine if the number of freeze-thaw cycles were significantly different at a 95 % confidence limit. The results of this analysis are presented in Appendix A. From the analysis it can be seen that there were significant differences between all pairs of means with the exception of cycle 2 and 3. At this initial freezing temperature cycle freeze-thaw was shown as one method of obtaining a superior treated effluent quality.

4.2.2.5.2 INITIAL FREEZING TEMPERATURE: -15 °C

Plotted in Figure 4.42 are the average percent color removals with respect to the top, middle, and combined upper liquid portions for

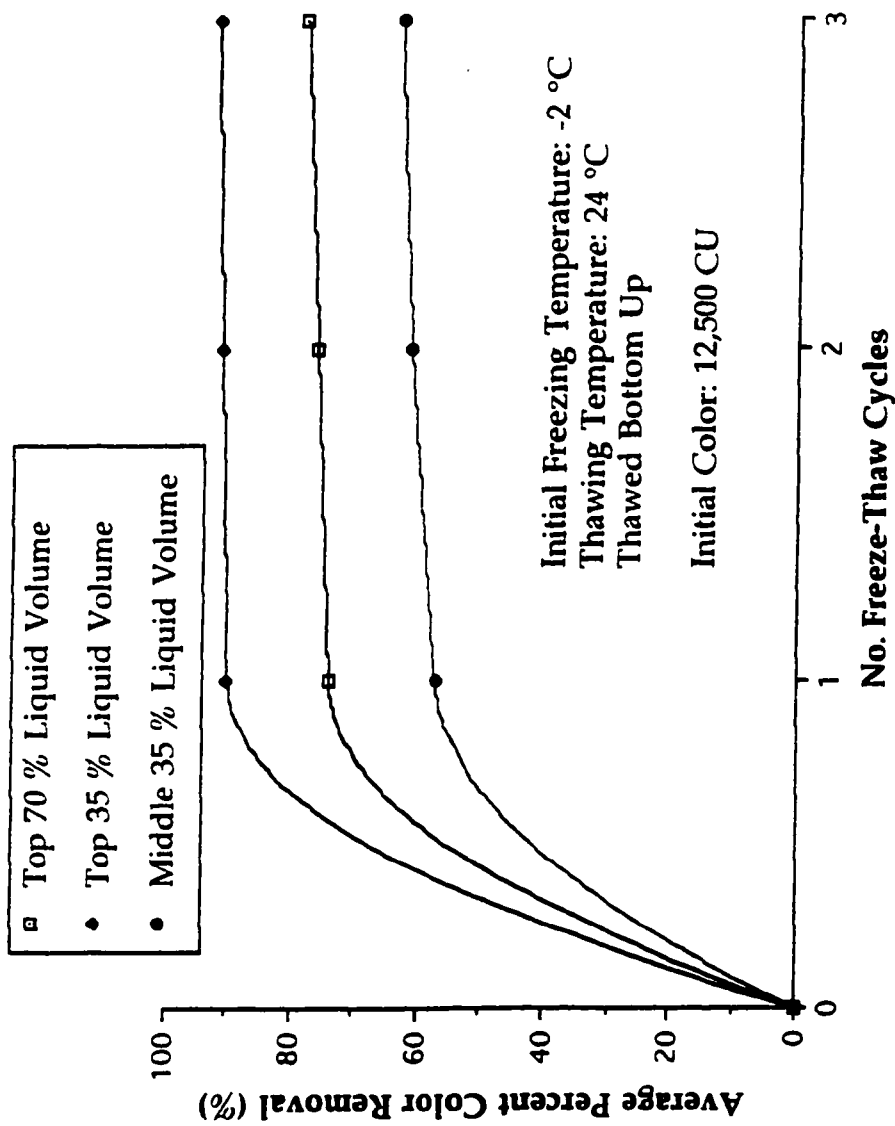


Figure 4.41 Plot of Average Percent Color Removal in Various Liquid Fractions with respect to the Number of Freeze-thaw Cycles for Membrane Concentrate Frozen at the Initial Freezing Temperature -2 °C

membrane concentrate treated repeatedly by freeze-thaw at the initial freezing temperature -15 °C. The average percent color removals increased with the number of freeze-thaw cycles. Figure 4.42 shows the average percent increases in color removal ranged from 1.6 % to 1.9 %, with the magnitude of the increase decreasing with the number of freeze-thaw cycles. Analysis of variance and the Duncan Multiple Range Test were used to determine if the number of freeze-thaw cycles were significantly different at a 95 % confidence limit. The results of this analysis are presented in Appendix A. From the analysis it can be seen that there were significant differences between all pairs of means to indicate cycle freeze-thaw improves treatment performance.

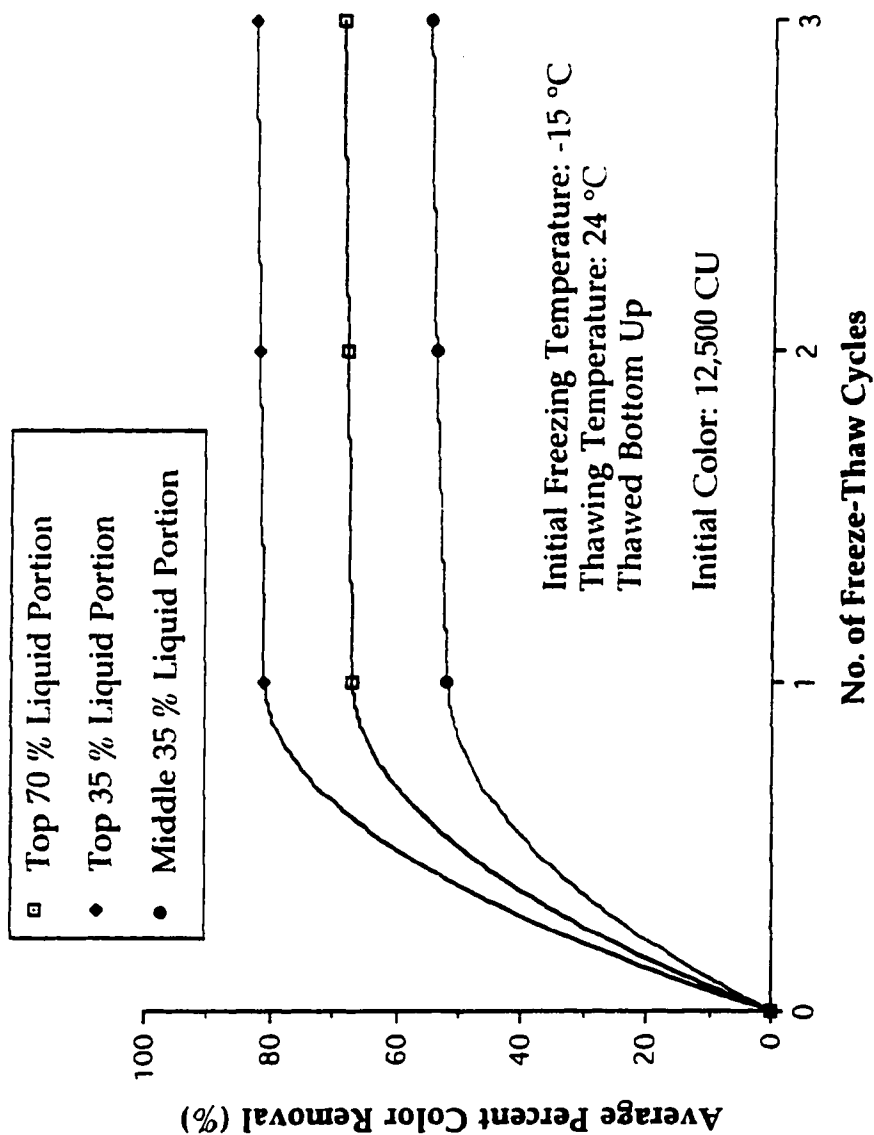


Figure 4.42 Plot of Average Percent Color Removal in Various Liquid Fractions with respect to the Number of Freeze-thaw Cycles for Membrane Concentrate Frozen at the Initial Freezing Temperature -15 °C

5.0 SCANNING ELECTRON MICROSCOPY STUDIES

Presented in this chapter are the scanning electron microscopy results conducted to visually characterize the changes that occurs to the effluent's constituent material under different freeze-thaw conditions.

5.1 PROCEDURE

5.1.1 ICE SPECIMEN COLLECTION

Ice specimens for visual characterization of its concentrated material produced during freezing were collected from each experimental water frozen at different initial freezing temperatures. The initial freezing temperatures investigated were -2 °C, -15 °C, and -25 °C, respectively. The size of the sample population selected for characterization of the concentrated material at its different initial freezing temperatures were 3 independent ice specimen samples for each experimental run condition. Ice specimens were collected from the top and bottom portions of the ice column of frozen membrane concentrate and from only the top portion of frozen Eop effluent. The sample location depths were 50 mm and 100 mm from the top of the ice column. Ice samples were collected by first sectioning the ice column at the sample depth, followed by the cutting out of a 3 mm by 3 mm by 6 mm deep ice specimen from the center of the column. The ice specimen was positioned in the specimen holder of the SEM instrument to ensure the fractured surface represented the cross sectional area perpendicular to the direction of freezing. Preparation of ice specimens for examination by SEM was accordance to the method described in Section 3.5.2.1.1. Measurement of the thickness of the concentrated material was facilitated from the use of high magnification

electron microscopy of single fractured wafer edges coupled with the use of the tools bar of the Microsoft® Photoshop software. The relative accuracy of this method of measurement was +/- 0.1 μm .

5.1.2 METHOD OF MEASUREMENT

To properly understand and compare the results between ice specimens from the same ice column or of the same run setting, the thickness of the wafer-like structure of the concentrated material were plotted with respect to its frequency distributions. The mean, median, mode, and sample variance were calculated for each sample set for comparison of the measures of dispersion. Thickness measurements were randomly taken of the concentrated material from a minimum of 10 separate independent surface locations for each ice specimen for physical characterization. The thickness value presented for each independent sample location was an average of three measurements taken along the length of the concentrated material to determine its average width. Excluded from measurement was intersection points for the initial freezing temperature -2 °C where wafers were observed to join. These cross sectional areas were observed by SEM in some cases to contain substantial amounts of constituent material. All experimental test settings for SEM characterization were conducted in triplicate at separate random times.

5.2 CROSS SECTIONAL MORPHOLOGY OF FROZEN CONCENTRATED MATERIAL

Presented in this chapter are the scanning electron microscopy results from having examined the morphology of frozen concentrated

material produced by unidirectionally freezing alkaline extraction stage membrane concentrate and Eop effluent at different initial freezing temperatures.

5.2.1 ALKALINE EXTRACTION STAGE MEMBRANE CONCENTRATE

5.2.1.1 INITIAL FREEZING TEMPERATURE: -2 °C

The frozen state physical properties of the concentrated material produced by freezing membrane concentrate at the initial freezing temperature -2 °C consisted of thick, porous wafer-like structures arranged in "honey comb or box" like patterns. The concentrated material was observed to extend vertically into the ice column parallel with the direction of freezing. Cross sectional sectioning of the concentrated material showed it to be highly porous and variable in width. Contained within the material's structure were numerous small pores which prior to sublimation were filled with ice (Figure 5.1). Believed was that this porosity was the result of the freezing process and was not created during preparation of the ice specimen for SEM analysis. Figure 5.1 is a high magnification electron microscope image of the concentrated material prior to sublimation. No fractures along the zone of the concentrated material of this sample were visible nor in that of other samples examined to suggest the isolated pockets of ice present within the material existed prior to preparation of the sample for SEM analysis. This assumption was in part, based on the fact that had this porosity not existed prior to sample preparation, one would have expected fractures to have formed along the zone of concentrated material for unconstrained ice specimens caused from the rapid expansion of the freezing of the free available water. In

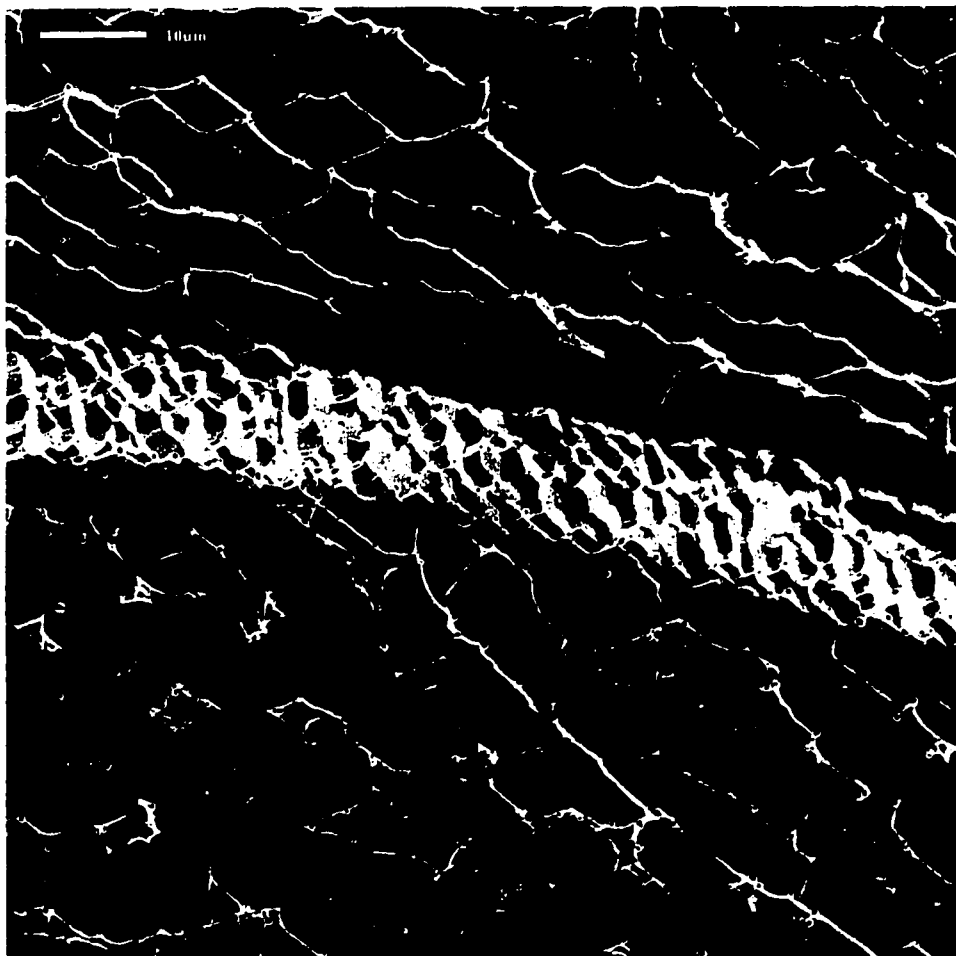


Figure 5.1 High Magnification Electron Microscope Image of the Concentrated Material Prior to Sublimation for Membrane Concentrate Frozen at the Initial Freezing Temperature -2 degrees Celsius

addition, the instantaneous freezing of the sample by submerging it in liquid nitrogen would have likely precluded the high degree of separation observed following sublimation. Instead, what appears to have occurred during freezing was the formation of small isolated pockets of ice crystals from the freezing of the free available water contained within the highly concentrated material zones.

Characteristic of the top and bottom ice specimens were the orientation of the concentrated material within the ice matrix. Examination of Figures 5.2 and 5.3 shows the concentrated material to have arranged itself in "honey comb or box" like patterns. This type of pattern arrangement was observed only at the initial freezing temperature -2 °C. That which will be shown in the proceeding sections was the concentrated material not only increase in quantity, but rearrange themselves to form sheet like patterns at the colder initial freezing temperatures.

5.2.1.1.1 TOP SAMPLE LOCATION RESULTS

Tables 5.1 to 5.3 are frequency tables of the concentrated material thickness as measured in ice specimens collected from three independent samples representing the top ice portion of membrane concentrate frozen at the initial freezing temperature -2 °C. Table 5.4 is a summary of the information derived from examination of the three independent sample sets by SEM. The calculated means and sample variances ranged from 28.7 μm to 31.3 μm and from 18.74 μm to 20.32 μm , respectively. The two-tailed Student t-test was used to show that the individual means were not



Figure 5.2 Electron Microscope Photograph of the Concentrated Material Contained Within the Ice Matrix for an Ice Specimen Collected from the Top Ice Column Portion for Membrane Concentrate Frozen at the Initial Freezing Temperature -2 degrees Celsius



Figure 5.3 Electron Microscope Photograph of the Concentrated Material Contained Within the Ice Matrix for an Ice Specimen Collected from the Bottom Ice Column Portion for Membrane Concentrate Frozen at the Initial Freezing Temperature -2 degrees Celsius

significantly different at a 95 % confidence limit (Table 5.5). The calculated average thickness of the concentrated material for the combined data of sample sets 1, 2, and 3 as observed in the top portion of the ice column was $30.2\ \mu\text{m}$, with a sample variance and range of $18.51\ \mu\text{m}$ and $9.2\ \mu\text{m}$ to $68.4\ \mu\text{m}$, respectively.

High magnification electron microscope images of fractured edges of concentrated material are shown in Figure 5.4. Examination of this figure shows the frozen state physical properties of the concentrated material were similar among the different sample sets. Although variable in their thickness, a common physical characteristic of the concentrated material observed was in regards to their shape and porosity. The concentrated material was highly porous and wafer-like in appearance.

5.2.1.12 BOTTOM SAMPLE LOCATION RESULTS

Presented in graphical form by way of frequency histograms (Figures 5.5 to 5.7) are the measured thicknesses of the concentrated material as observed in ice specimens collected from three independent samples representing the bottom ice portion of membrane concentrate frozen at the initial freezing temperature $-2\ ^\circ\text{C}$. Table 5.6 is a summary of the information derived from examination of the three independent sample sets. The calculated means and sample variances ranged from $25.6\ \mu\text{m}$ to $26.4\ \mu\text{m}$ and from $13.09\ \mu\text{m}$ to $15.12\ \mu\text{m}$, respectively. The two-tailed Student t-test was used to show the individual means from the three independent samples were not significantly different at a 95 % confidence limit (Table 5.7). The calculated average thickness of the concentrated

Table 5.1 Data Representing the Average Thickness of the Concentrated Material Produced in the Top Sample Portion of the Ice Column for Membrane Concentrate Frozen at the Initial Freezing Temperature -2 °C, Sample Set #1

Concentrated Material Thickness (μm)	Relative Frequency
9.5	0.1
14.3	0.1
15.9	0.1
18.2	0.1
21.5	0.1
25.6	0.1
36.8	0.1
42.7	0.1
56.8	0.1
65.0	0.1

Mean: 30.7 μm , Median: 23.5 μm , Sample Size: 10

Table 5.2 Data Representing the Average Thickness of the Concentrated Material Produced in the Top Sample Portion of the Ice Column for Membrane Concentrate Frozen at the Initial Freezing Temperature -2 °C, Sample Set #2

Concentrated Material Thickness (μm)	Relative Frequency
8.5	0.1
13.6	0.1
15.3	0.1
16.4	0.1
20.0	0.1
21.0	0.1
36.8	0.1
40.5	0.1
46.8	0.1
68.4	0.1

Mean: 28.7 μm , Median: 20.5 μm , Sample Size: 10

Table 5.3 Data Representing the Average Thickness of the Concentrated Material Produced in the Top Sample Portion of the Ice Column for Membrane Concentrate Frozen at the Initial Freezing Temperature -2 °C, Sample Set #3

Concentrated Material Thickness (μm)	Relative Frequency
8.5	0.1
14.5	0.1
15.0	0.1
17.8	0.1
19.5	0.1
19.8	0.1
43.6	0.1
52.3	0.1
59.1	0.1
61.4	0.1

Mean: 31.3 μm , Median: 19.7 μm , Sample Size: 10

Table 5.4 Summary of Statistical Data for Sample Sets 1, 2, and 3 (Initial Freezing Temperature -2 °C, Top Sample)

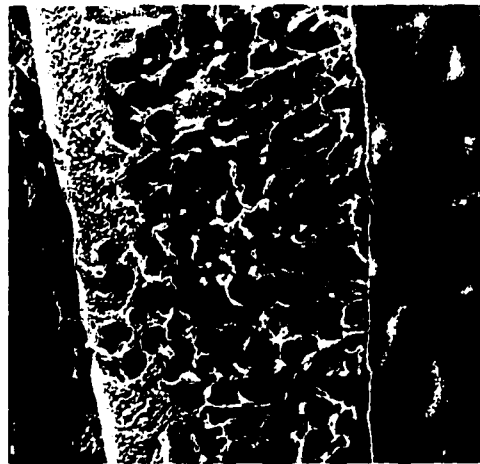
Sample Set*	Mean (μm)	Mean Deviation (μm)	Sample Variance (μm)	Range (μm)
1	30.7	15.8	19.01	10.0 to 65.3
2	28.7	15.4	18.74	9.4 to 68.4
3	31.3	18.2	20.32	9.2 to 59.6

* - sample set size equal to 10

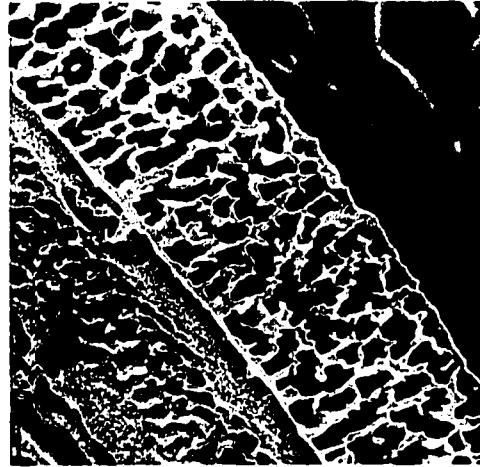
Table 5.5 Tests of Hypotheses for Sample Sets 1, 2, and 3 (Initial Freezing Temperature -2 °C, Top Sample)

Null Hypothesis	Computed Test Statistic*	$t_{(0.025, 18)}$	Conclusion
$\mu_{\text{set1}} = \mu_{\text{set2}}$	0.24	2.093	accept as equal
$\mu_{\text{set1}} = \mu_{\text{set3}}$	0.07	2.093	accept as equal
$\mu_{\text{set2}} = \mu_{\text{set3}}$	0.30	2.093	accept as equal

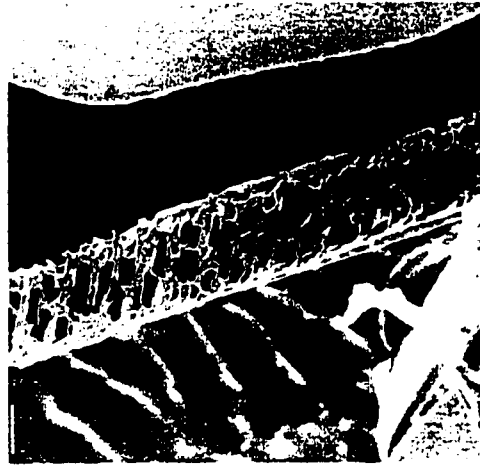
* sample variances unknown but assumed equal



(a) Sample Set #1 (bar = 1 micron)



(b) Sample Set #2 (bar = 1 micron)



(c) Sample Set #3 (bar = 10 microns)

Figure 5.4 Collection of High Magnification Electron Microscope Images of Fractured Concentrated Material Edges Produced by Freezing Membrane Concentrate at the Initial Freezing Temperature -2 degrees Celsius (Top Sample Portion)

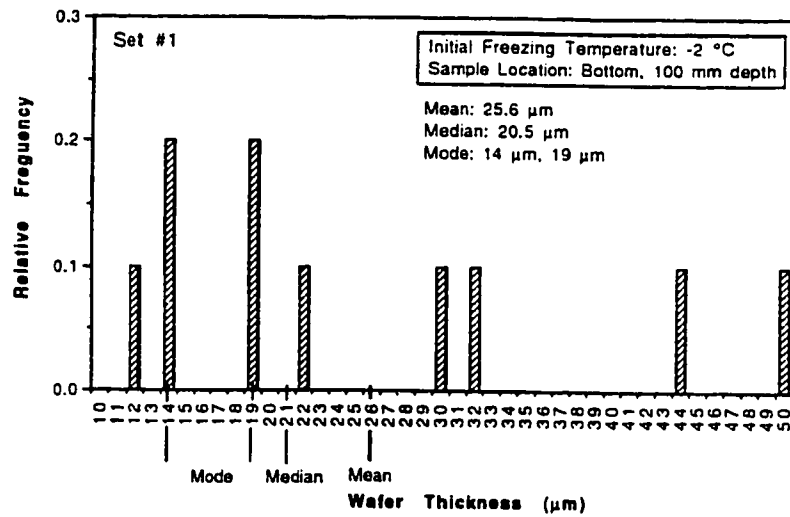


Figure 5.5 Data Representing the Average Thickness of the Concentrated Material Produced in the Bottom Sample Portion of the Ice Column for Membrane Concentrate Frozen at the Initial Freezing Temperature -2 °C, Sample Set #1

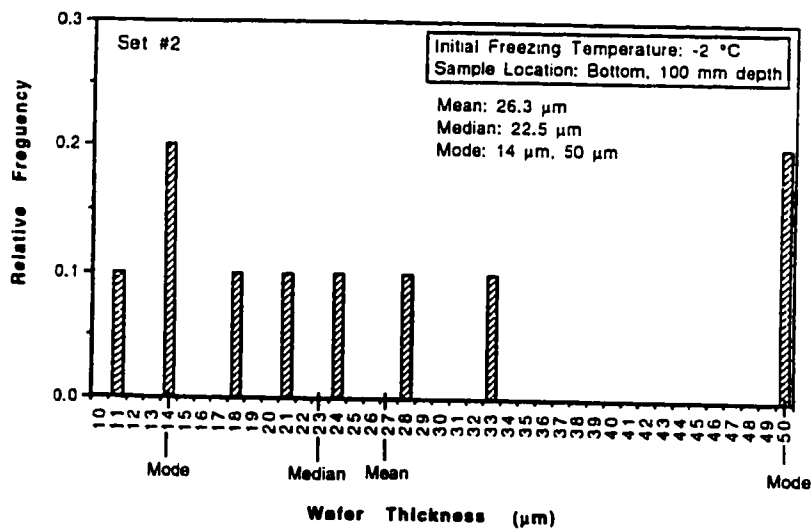


Figure 5.6 Data Representing the Average Thickness of the Concentrated Material Produced in the Bottom Sample Portion of the Ice Column for Membrane Concentrate Frozen at the Initial Freezing Temperature -2 °C, Sample Set #2

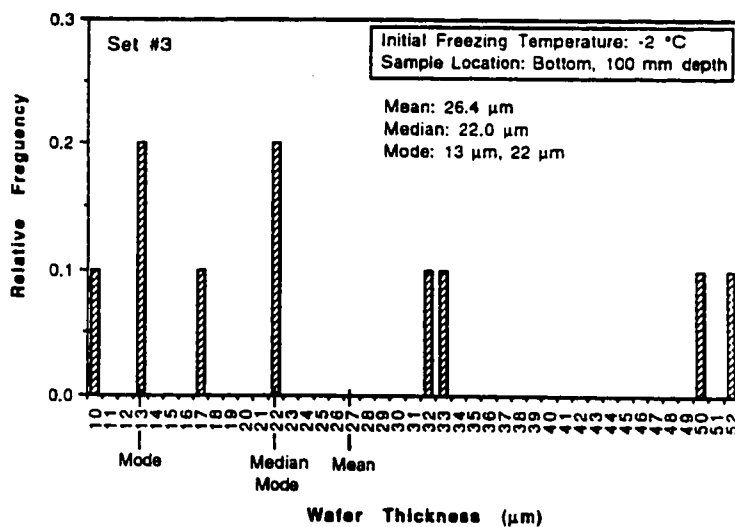


Figure 5.7 Data Representing the Average Thickness of the Concentrated Material Produced in the Bottom Sample Portion of the Ice Column for Membrane Concentrate Frozen at the Initial Freezing Temperature -2 °C, Sample Set #3

Table 5.6 Summary of Statistical Data for Sample Sets 1, 2, and 3
(Initial Freezing Temperature -2 °C, Bottom Sample)

Sample Set*	Mean (μm)	Mean Deviation (μm)	Sample Variance (μm)	Range (μm)
1	25.6	10.7	13.09	14.1 to 50.2
2	26.3	11.2	14.16	11.3 to 50.6
3	26.4	12.3	15.12	10.2 to 52.1

* - sample set size equal to 10

material for the combined data of sample sets 1, 2, and 3 as observed in the bottom portion of the ice column was $26.1 \mu\text{m}$, with a sample variance and range of $13.32 \mu\text{m}$ and $10.2 \mu\text{m}$ to $52.1 \mu\text{m}$, respectively. The two-tailed Student t-test was used to show the individual means from the top and bottom sample sets were not significantly different at a 95 % confidence limit (Table 5.8).

High magnification electron microscope images of single fractured edges of concentrated material are shown in Figure 5.8. Although similar in appearance to the concentrated material observed in the top sample portion of the ice column, the porosity of the concentrated material collected from the bottom tended to differ with respect to its cross sectional density. The pores appeared to be larger and arranged along the perimeter of the material edge with larger amounts of mass concentrated in the center as compared to the pore structure for the concentrated material collected from the top.

5.2.1.2 INITIAL FREEZING TEMPERATURE: -15°C

The frozen state physical properties of the concentrated material produced by freezing membrane concentrate at the initial freezing temperature -15°C consisted of thin, dense wafer-like structures arranged in "sheet" like patterns. The concentrated material was observed to extend vertically into the ice matrix parallel with the direction of freezing. Cross sectional sampling of the concentrated material showed it to be thin, very compact and generally of uniform width. Figure 5.9 shows the concentrated material to have arranged itself into long parallel continuous

Table 5.7 Tests of Hypotheses for Sample Sets 1, 2, and 3
(Initial Freezing Temperature -2 °C, Bottom Sample)

Null Hypothesis	Computed Test Statistic*	$t_{(0.025, 18)}$	Conclusion
$\mu_{\text{set1}} = \mu_{\text{set2}}$	0.11	2.093	accept as equal
$\mu_{\text{set1}} = \mu_{\text{set3}}$	0.13	2.093	accept as equal
$\mu_{\text{set2}} = \mu_{\text{set3}}$	0.02	2.093	accept as equal

* sample variances unknown but assumed equal

Table 5.8 Tests of Hypotheses Concerning the Difference in Means
Between the Top and Bottom Sample Locations
(Initial Freezing Temperature -2 °C)

Null Hypothesis	Computed Test Statistic*	$Z_{0.025}$	Conclusion
$\mu_{\text{top}} = \mu_{\text{bottom}}$	0.99	1.96	accept as equal

* sample variances unknown but assumed equal, sample set size: 30



(a) Sample Set #1 (bar = 10 microns)



(b) Sample Set #2 (bar = 10 microns)



(c) Sample Set #3 (bar = 10 microns)

Figure 5.8 Collection of High Magnification Electron Microscope Images of Fractured Concentrated Material Edges Produced by Freezing Membrane Concentrate at the Initial Freezing Temperature -2 degrees Celsius (Bottom Sample Portion)



(a) Top Sample Portion (bar = 100 microns)



(b) Bottom Sample Portion (bar = 100 microns)

Figure 5.9 Collection of Electron Microscope Photographs of Concentrated Material Contained Within the Ice Matrix of Ice Specimens Collected from the Top and Bottom Ice Column Portions for Membrane Concentrate Frozen at the Initial Freezing Temperature -15 degrees Celsius

sheets. The distance between these sheets as measured in the top and bottom ice specimens are summarized in Table 5.9. The measured distance (within $\pm 1 \mu\text{m}$) between the zones of concentrated material were reported to differ with respect to sample location with a higher spacing observed in bottom ice specimens. The average spacing between the concentrated material in the bottom sample portion was $192 \mu\text{m}$ for a range of $133 \mu\text{m}$ to $300 \mu\text{m}$, respectively. The reported spacing in the top ice specimens was much lower, with the average distance being $117 \mu\text{m}$ for a range of $67 \mu\text{m}$ to $165 \mu\text{m}$. The difference in material spacing can be attributed to differences in freezing rate and particle entrapment. Sectioning of frozen concentrate samples showed particle entrapment to differ with respect to depth with the lowest concentrations found at mid point of the ice column close to where bottom samples were collected.

5.2.1.2.1 TOP SAMPLE LOCATION RESULTS

Presented in graphical form by way of frequency histograms (Figures 5.10 to 5.12) are the measured thicknesses of the concentrated material as observed in ice specimens collected from three independent samples representing the top ice portion of membrane concentrate frozen at the initial freezing temperature -15°C . Examination of the concentrated material by SEM showed it to be thin, highly compact wafer-like structures with no visible porosity. Table 5.10 is a summary of the information derived from examination of the three independent sample sets by SEM. The calculated means and sample variances ranged from $1.7 \mu\text{m}$ to $2.1 \mu\text{m}$ and from $0.68 \mu\text{m}$ to $1.13 \mu\text{m}$, respectively. The two-tailed Student t-test was used to show the individual means were not significantly different at

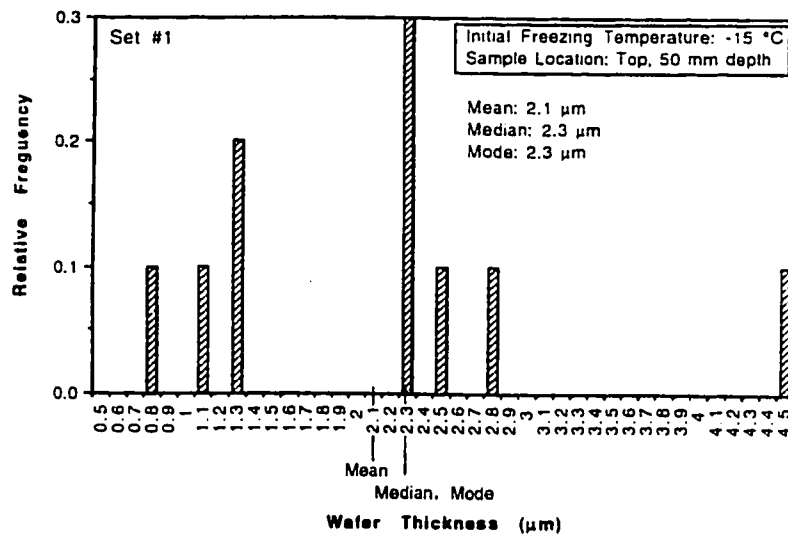


Figure 5.10 Data Representing the Average Thickness of the Concentrated Material Produced in the Top Sample Portion of the Ice Column for Membrane Concentrate Frozen at the Initial Freezing Temperature -15 °C, Sample Set #1

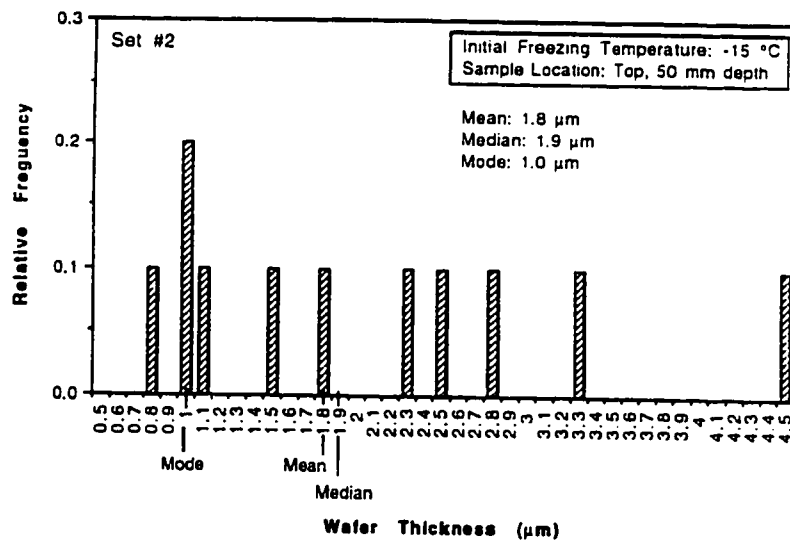


Figure 5.11 Data Representing the Average Thickness of the Concentrated Material Produced in the Top Sample Portion of the Ice Column for Membrane Concentrate Frozen at the Initial Freezing Temperature -15 °C, Sample Set #2

Table 5.9 Summary of Statistical Data Concerning the Distances Between the Concentrated Material as Measured in the Top and Bottom Ice Columns for Membrane Concentrate Frozen at the Initial Freezing Temperature -15 °C

Top Sample Location		
Mean (μm)	Sample Variance (μm)	Range (μm)
117	25.1	67 to 165
Bottom Sample Location		
Mean (μm)	Sample Variance (μm)	Range (μm)
192	41.3	133 to 300

Sample Size: 25

Table 5.10 Summary of Statistical Data for Sample Sets 1, 2, and 3
(Initial Freezing Temperature -15 °C, Top Sample)

Sample Set*	Mean (μm)	Mean Deviation (μm)	Sample Variance (μm)	Range (μm)
1	2.1	0.8	1.13	0.8 to 4.5
2	1.8	0.7	0.93	0.8 to 3.3
3	1.7	0.6	0.68	0.8 to 2.8

* - sample set size equal to 10

a 95 % confidence limit (Table 5.11). The calculated average thickness of the concentrated material for the combined data of sample sets 1, 2, and 3 as observed in the top portion of the ice column was 1.9 μm , with a sample variance and range of 0.92 μm and 0.8 μm to 4.5 μm , respectively.

High magnification electron microscope images of single fractured edges of the concentrated material are shown in Figure 5.13. These photographs revealed the concentrated material's highly compact wafer-like structure.

5.2.1.2.2 BOTTOM SAMPLE LOCATION RESULTS

Presented in graphical form by way of frequency histograms (Figures 5.14 to 5.16) are the measured thicknesses of the concentrated material as observed in ice specimens collected from three independent samples representing the bottom ice portion of membrane concentrate frozen at the initial freezing temperature -15 °C. Table 5.12 is a summary of the information derived from examination of the three independent sample sets by SEM. The calculated means and sample variances ranged from 1.6 μm to 2.2 μm and from 0.61 μm to 1.03 μm , respectively. The two-tailed Student t-test was used to show that the individual means were not significantly different at a 95 % confidence limit (Table 5.13). The calculated average thickness of the concentrated material for the combined data of sample sets 1, 2, and 3 as observed in the bottom portion of the ice column was 1.9 μm , with a sample variance and range of 0.88 μm and 0.8 μm to 4.8 μm , respectively. The two-tailed Student t-test was used to show

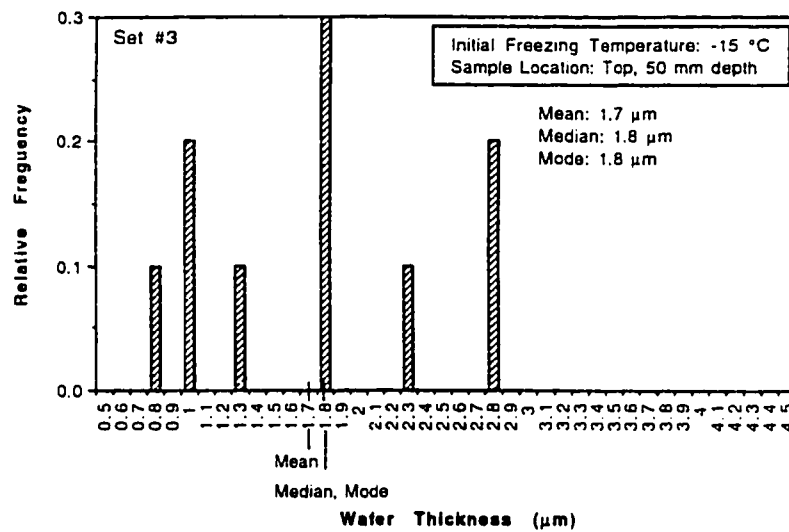


Figure 5.12 Data Representing the Average Thickness of the Concentrated Material Produced in the Top Sample Portion of the Ice Column for Membrane Concentrate Frozen at the Initial Freezing Temperature -15 °C, Sample Set #3

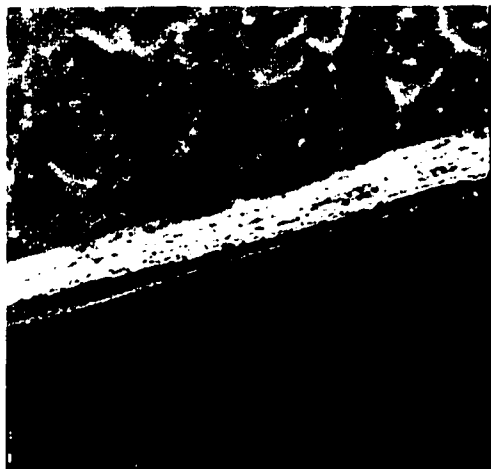
Table 5.11 Tests of Hypotheses for Sample Sets 1, 2, and 3
(Initial Freezing Temperature -15 °C, Top Sample)

Null Hypothesis	Computed Test Statistic*	$t_{(0.025, 18)}$	Conclusion
$\mu_{\text{set1}} = \mu_{\text{set2}}$	0.67	2.093	accept as equal
$\mu_{\text{set1}} = \mu_{\text{set3}}$	0.97	2.093	accept as equal
$\mu_{\text{set2}} = \mu_{\text{set3}}$	0.28	2.093	accept as equal

* sample variances unknown but assumed equal



(a) Sample Set #1 (bar = 1 micron)



(b) Sample Set #2 (bar = 1 micron)



(c) Sample Set #3 (bar = 1 micron)

Figure 5.13 Collection of High Magnification Electron Microscope Images of Fractured Concentrated Material Edges Produced by Freezing Membrane Concentrate at the Initial Freezing Temperature -15 degrees Celsius (Top Sample Portion)

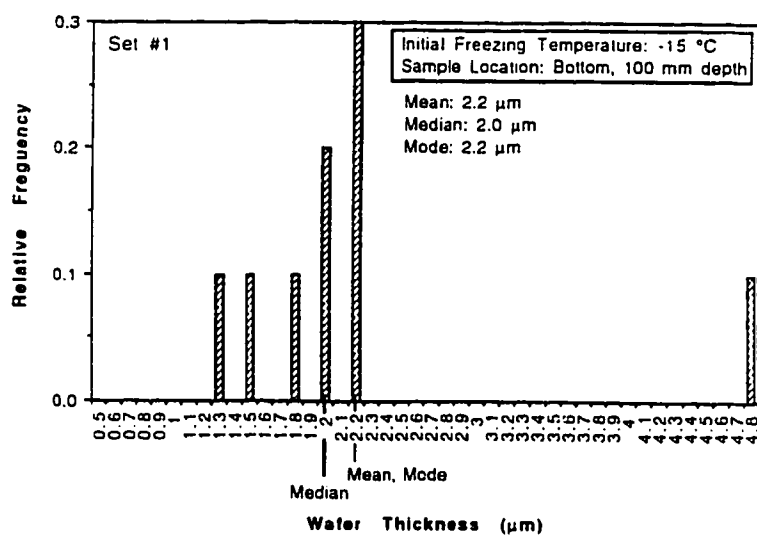


Figure 5.14 Data Representing the Average Thickness of the Concentrated Material Produced in the Bottom Sample Portion of the Ice Column for Membrane Concentrate Frozen at the Initial Freezing Temperature -15 °C, Sample Set #1

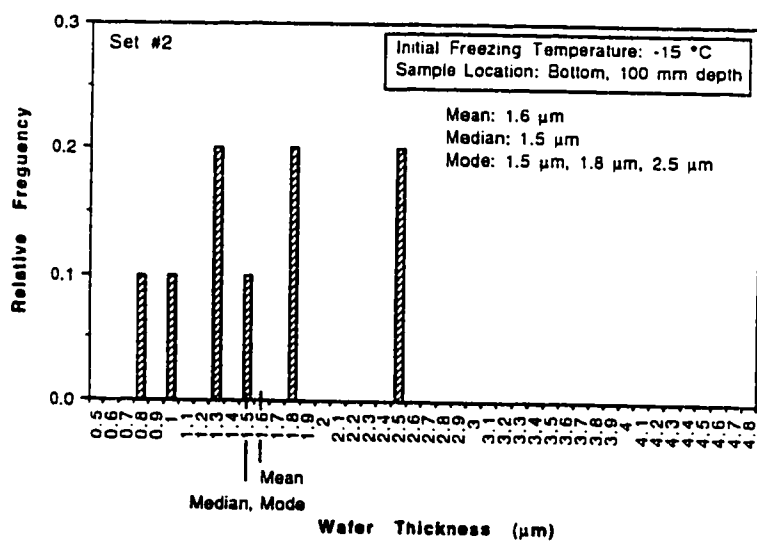


Figure 5.15 Data Representing the Average Thickness of the Concentrated Material Structures Produced in the Bottom Sample Portion of the Ice Column for Membrane Concentrate Frozen at the Initial Freezing Temperature -15 °C, Sample Set #2

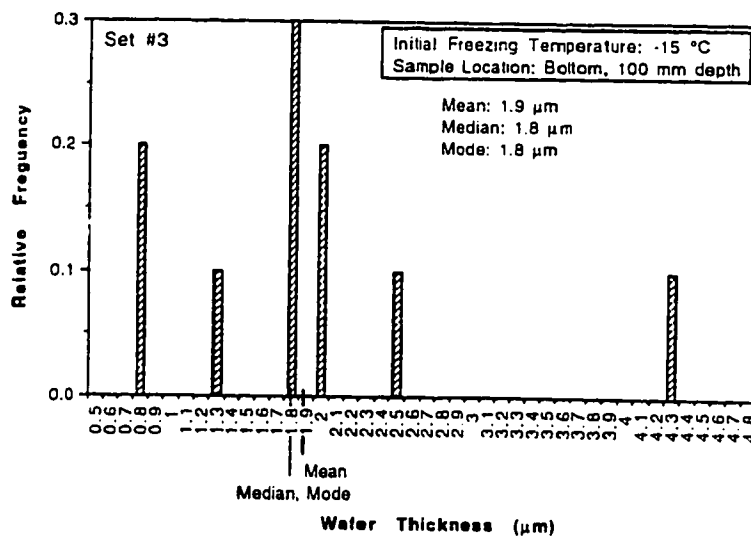


Figure 5.16 Data Representing the Average Thickness of the Concentrated Material Produced in the Bottom Sample Portion of the Ice Column for Membrane Concentrate Frozen at the Initial Freezing Temperature -15 °C, Sample Set #3

Table 5.12 Summary of Statistical Data for Sample Sets 1, 2, and 3
(Initial Freezing Temperature -15 °C, Bottom Sample)

Sample Set*	Mean (μm)	Mean Deviation (μm)	Sample Variance (μm)	Range (μm)
1	2.2	0.5	1.03	1.3 to 4.8
2	1.6	0.4	0.61	0.8 to 2.5
3	1.9	0.6	1.04	0.8 to 4.3

* - sample set size equal to 10

that the average thickness of the concentrated material from the top and bottom sample locations were not significantly different at a 95 % confidence limit (Table 5.14).

High magnification scanning electron microscope images of single fractured edges of concentrated material are shown in Figure 5.17. The SEM results were similar to that reported for the top sample specimens.

5.2.1.3 INITIAL FREEZING TEMPERATURE: -25 °C

The frozen state physical properties of the concentrated material produced by freezing membrane concentrate at the initial freezing temperature -25 °C were similar to that reported for the initial freezing temperature -15 °C. Although slightly thinner, cross sectional sampling of the concentrated material showed them also to be thin, very compact and of uniform width. Other notable differences were with respect to surface texture. The surface texture of the concentrated material appeared to be visibly smoother. Similarities were with respect to orientation pattern of the concentrated material. Figure 5.18 shows the concentrated material to have arranged themselves into long continuous equally spaced sheets.

5.2.1.3.1 TOP SAMPLE LOCATION RESULTS

Presented in graphical form by way of frequency histograms (Figures 5.19 to 5.21) are the measured thicknesses of the concentrated material as observed in ice specimens collected from three independent samples representing the top ice portion of membrane concentrate frozen at the initial freezing temperature -25 °C. Table 5.15 is a summary of the

Table 5.13 Tests of Hypotheses Concerning the Difference in Means
for Sample Sets 1, 2, and 3
(Initial Freezing Temperature -15 °C, Bottom Sample)

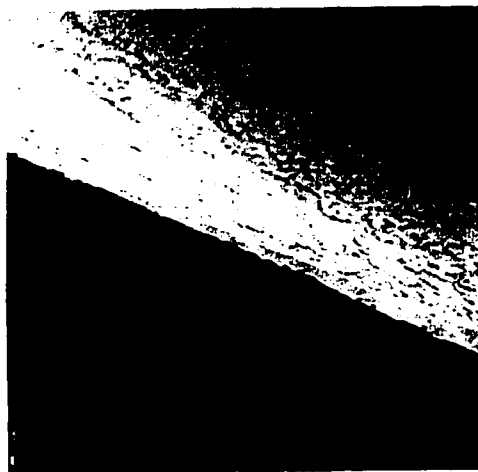
Null Hypothesis	Computed Test Statistic*	$t_{(0.025, 18)}$	Conclusion
$\mu_{\text{set1}} = \mu_{\text{set2}}$	1.63	2.093	accept as equal
$\mu_{\text{set1}} = \mu_{\text{set3}}$	0.67	2.093	accept as equal
$\mu_{\text{set2}} = \mu_{\text{set3}}$	0.81	2.093	accept as equal

* sample variances unknown but assumed equal

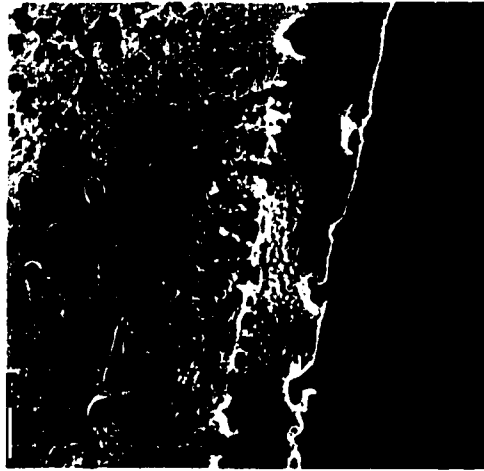
Table 5.14 Tests of Hypotheses Concerning the Difference in Means
Between the Top and Bottom Sample Locations
(Initial Freezing Temperature -15 °C)

Null Hypothesis	Computed Test Statistic*	$Z_{0.025}$	Conclusion
$\mu_{\text{top}} = \mu_{\text{bottom}}$	0.00	1.96	accept as equal

* sample variances unknown but assumed equal, sample set size: 30



(a) Sample Set #1 (bar = 1 micron)



(b) Sample Set #2 (bar = 1 micron)



(c) Sample Set #3 (bar = 1 micron)

Figure 5.17 Collection of High Magnification Electron Microscope Images of Fractured Concentrated Material Edges Produced by Freezing Membrane Concentrate at the Initial Freezing Temperature -15 degrees Celsius (Bottom Sample Portion)



(a) Top Sample Portion (bar = 10 microns)



(b) Bottom Sample Portion (bar = 100 microns)

Figure 5.18 Collection of Electron Microscope Photographs of Concentrated Material Contained Within the Ice Matrix of Ice Specimens Collected from the Top and Bottom Ice Column Portions for Membrane Concentrate Frozen at the Initial Freezing Temperature -25 degrees Celsius

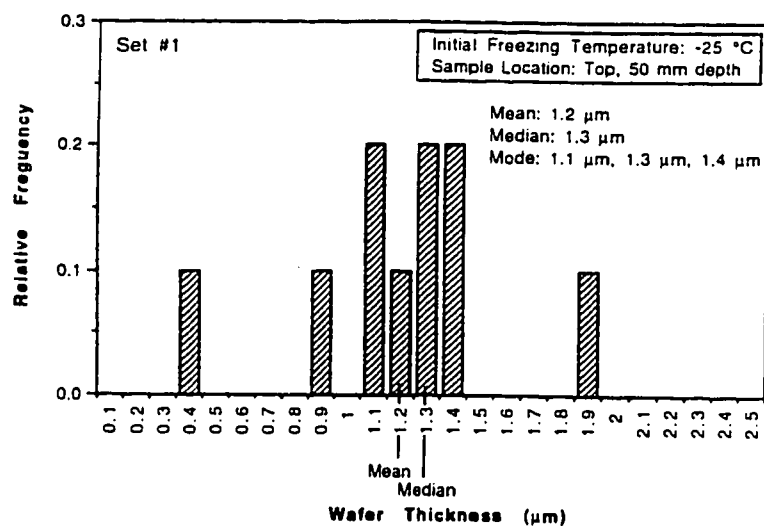


Figure 5.19 Data Representing the Average Thickness of the Concentrated Material Produced in the Top Sample Portion of the Ice Column for Membrane Concentrate Frozen at the Initial Freezing Temperature -25 °C, Sample Set #1

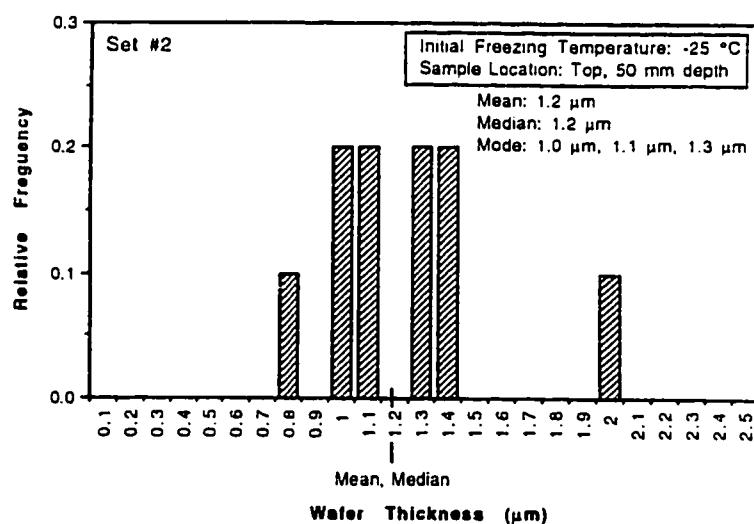


Figure 5.20 Data Representing the Average Thickness of the Concentrated Material Produced in the Top Sample Portion of the Ice Column for Membrane Concentrate Frozen at the Initial Freezing Temperature -25 °C, Sample Set #2

information derived from examination of the three independent sample sets by SEM. The calculated means and sample variances ranged from 1.2 μm to 1.3 μm and from 0.29 μm to 0.41 μm , respectively. The two-tailed Student t-test was used to show that the individual means were not significantly different at a 95 % confidence limit (Table 5.16). The calculated average thickness of the concentrated material for the combined data of sample sets 1, 2, and 3 as observed in the top portion of the ice column was 1.2 μm , with a sample variance and range of 0.31 μm and 0.4 μm to 2.0 μm , respectively.

High magnification scanning electron microscope images of single fractured edges of the concentrated material are shown in Figure 5.22. The SEM photographs revealed the concentrated material's highly compact wafer-like structure.

5.2.1.3.2 BOTTOM SAMPLE LOCATION RESULTS

Presented in graphical form by way of frequency histograms (Figures 5.23 to 5.25) are the measured thicknesses of the concentrated material as observed in ice specimens collected from three independent samples representing the bottom ice portion of membrane concentrate frozen at the initial freezing temperature -25 °C. Table 5.17 is a summary of the information derived from examination of for the three independent sample sets by SEM. The calculated means and sample variances ranged from 1.0 μm to 1.2 μm and from 0.60 μm to 0.73 μm , respectively. The two-tailed Student t-test was used to show that the individual means were not significantly different at a 95 % confidence limit (Table 5.18). The

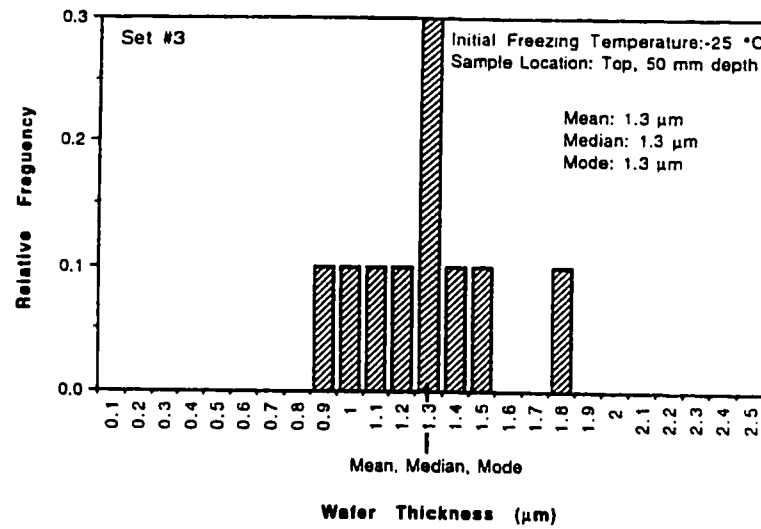


Figure 5.21 Data Representing the Average Thickness of the Concentrated Material Produced in the Top Sample Portion of the Ice Column for Membrane Concentrate Frozen at the initial Freezing Temperature -25 °C, Sample Set #3

Table 5.15 Summary of Statistical Data for Sample Sets 1, 2, and 3
(Initial Freezing Temperature -25 °C, Top Sample)

Sample Set*	Mean (μm)	Mean Deviation (μm)	Sample Variance (μm)	Range (μm)
1	1.2	0.3	0.41	0.4 to 1.9
2	1.2	0.3	0.30	0.8 to 2.0
3	1.3	0.2	0.29	0.9 to 1.8

* - sample set size equal to 10

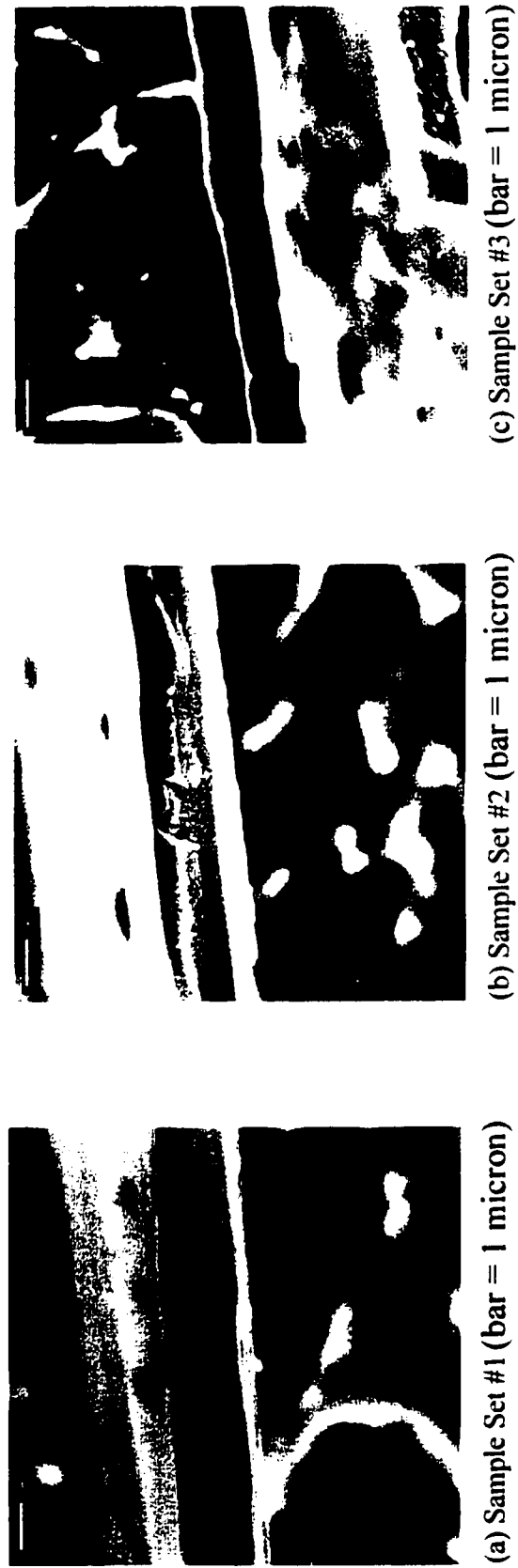


Figure 5.22 Collection of High Magnification Electron Microscope Images of Fractured Concentrated Material Edges Produced by Freezing Membrane Concentrate at the Initial Freezing Temperature -25 degrees Celsius (Top Sample Portion)

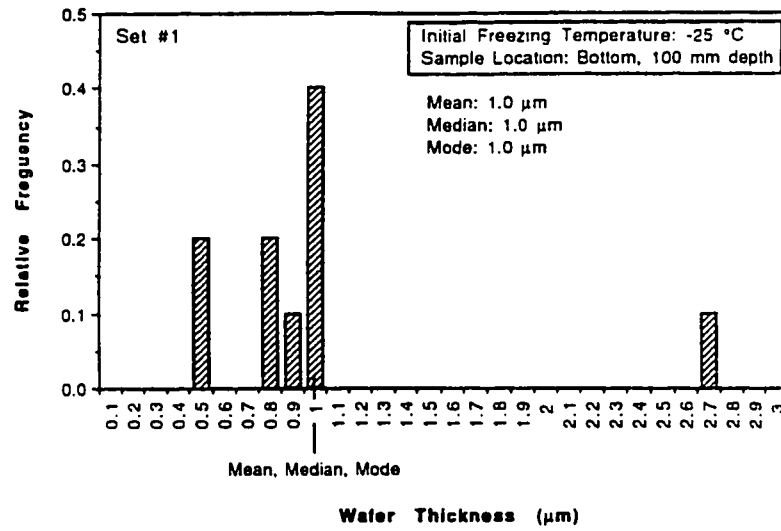


Figure 5.23 Data Representing the Average Thickness of the Concentrated Material Produced in the Bottom Sample Portion of the Ice Column for Membrane Concentrate Frozen at the Initial Freezing Temperature -25 °C, Sample Set #1

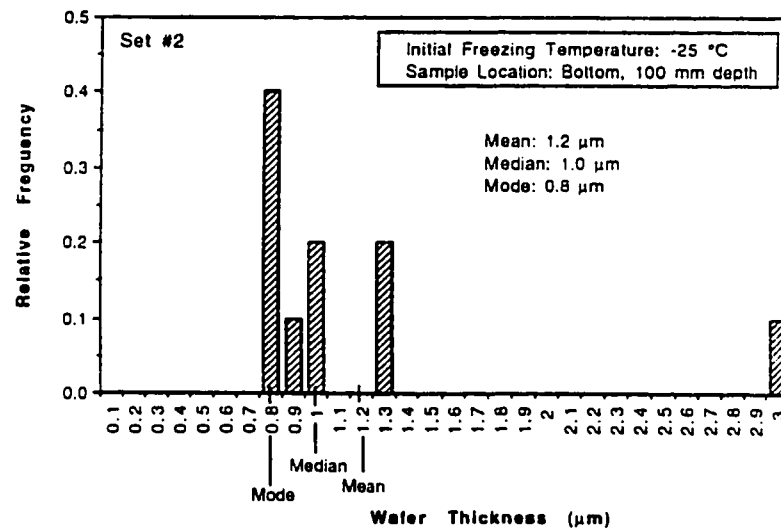


Figure 5.24 Data Representing the Average Thickness of the Concentrated Material Produced in the Bottom Sample Portion of the Ice Column for Membrane Concentrate Frozen at the Initial Freezing Temperature -25 °C, Sample Set #2

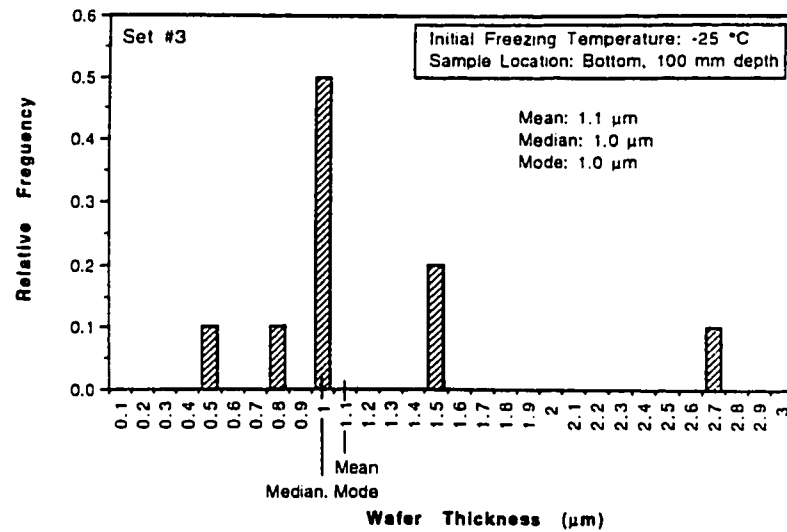


Figure 5.25 Data Representing the Average Thickness of the Concentrated Material Produced in the Bottom Sample Portion of the Ice Column for Membrane Concentrate Frozen at the Initial Freezing Temperature -25 °C, Sample Set #3

Table 5.16 Tests of Hypotheses Concerning the Difference in Means of Sample Sets 1, 2, and 3
(Initial Freezing Temperature -25 °C, Top Sample)

Null Hypothesis	Computed Test Statistic*	$t_{(0.025, 18)}$	Conclusion
$\mu_{\text{set1}} = \mu_{\text{set2}}$	0.00	2.093	accept as equal
$\mu_{\text{set1}} = \mu_{\text{set3}}$	0.63	2.093	accept as equal
$\mu_{\text{set2}} = \mu_{\text{set3}}$	0.75	2.093	accept as equal

* sample variances unknown but assumed equal

calculated average thickness of the concentrated material for the combined data of sample sets 1, 2, and 3 as observed in the bottom portion of the ice column was 1.1 μm , with a sample variance and range of 0.61 μm and 0.5 μm to 3.0 μm , respectively. The two-tailed Student t-test was used to show that the individual means were not significantly different at a 95 % confidence limit (Table 5.19).

High magnification electron microscope images of fractured edges of concentrated material are shown in Figure 5.26. The SEM photographs revealed the concentrated material's very thin, highly compact wafer-like structure.

5.2.1.4 INITIAL FREEZING TEMPERATURE VERSUS THE THICKNESS OF THE CONCENTRATED MATERIAL

Changes that occurred to the thickness of the concentrated material with respect to initial freezing temperature are shown in Figure 5.27 for the alkaline extraction stage membrane concentrate. Examination of this figure shows the thickness of the concentrated material increasing with initial freezing temperature. Analysis of variance and the Duncan Multiple Range Test were used to determine which average thicknesses for the top and bottom sample portions were significantly different at a 95 % confidence limit. The results of this analysis are presented in Appendix B. Analysis of the data showed the average thickness of the concentrated material produced at the initial freezing temperature -2 °C to be significantly different for the top and bottom sample portions in comparison to material thicknesses produced at the colder initial freezing temperatures -15 °C and -25 °C. In the case of the bottom sample portion

Table 5.17 Summary of Statistical Data for Sample Sets 1, 2, and 3
(Initial Freezing Temperature -25 °C, Bottom Sample)

Sample Set*	Mean (μm)	Mean Deviation (μm)	Sample Variance (μm)	Range (μm)
1	1.0	0.3	0.60	0.5 to 2.7
2	1.2	0.4	0.73	0.8 to 3.0
3	1.1	0.4	0.61	0.5 to 2.7

* - sample set size equal to 10

Table 5.18 Tests of Hypotheses Concerning the Difference in Means
of Sample Sets 1, 2, and 3
(Initial Freezing Temperature -25 °C, Bottom Sample)

Null Hypothesis	Computed Test Statistic*	$t_{(0.025, 18)}$	Conclusion
$\mu_{\text{set1}} = \mu_{\text{set2}}$	0.69	2.093	accept as equal
$\mu_{\text{set1}} = \mu_{\text{set3}}$	0.03	2.093	accept as equal
$\mu_{\text{set2}} = \mu_{\text{set3}}$	0.34	2.093	accept as equal

* sample variances unknown but assumed equal

Table 5.19 Tests of Hypotheses Concerning the Difference in Means
Between the Top and Bottom Sample Locations
(Initial Freezing Temperature -25 °C)

Null Hypothesis	Computed Test Statistic*	$Z_{0.025}$	Conclusion
$\mu_{\text{top}} = \mu_{\text{bottom}}$	0.80	1.96	accept as equal

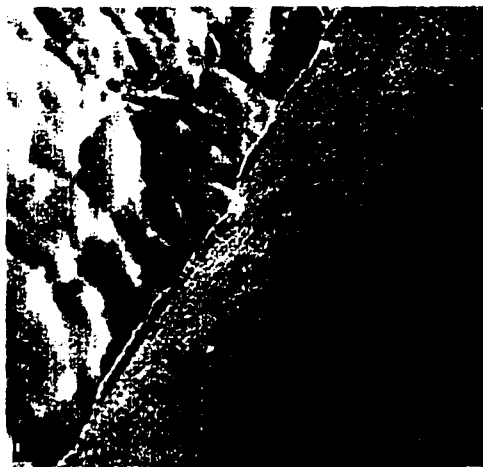
* sample variances unknown but assumed equal, sample set size: 30



(a) Sample Set #1 (bar = 1 micron)



(b) Sample Set #2 (bar = 1 micron)



(c) Sample Set #3 (bar = 1 micron)

Figure 5.26 Collection of High Magnification Electron Microscope Images of Fractured Concentrated Material Edges Produced by Freezing Membrane Concentrate at the Initial Freezing Temperature -25 degrees Celsius (Bottom Sample Portion)

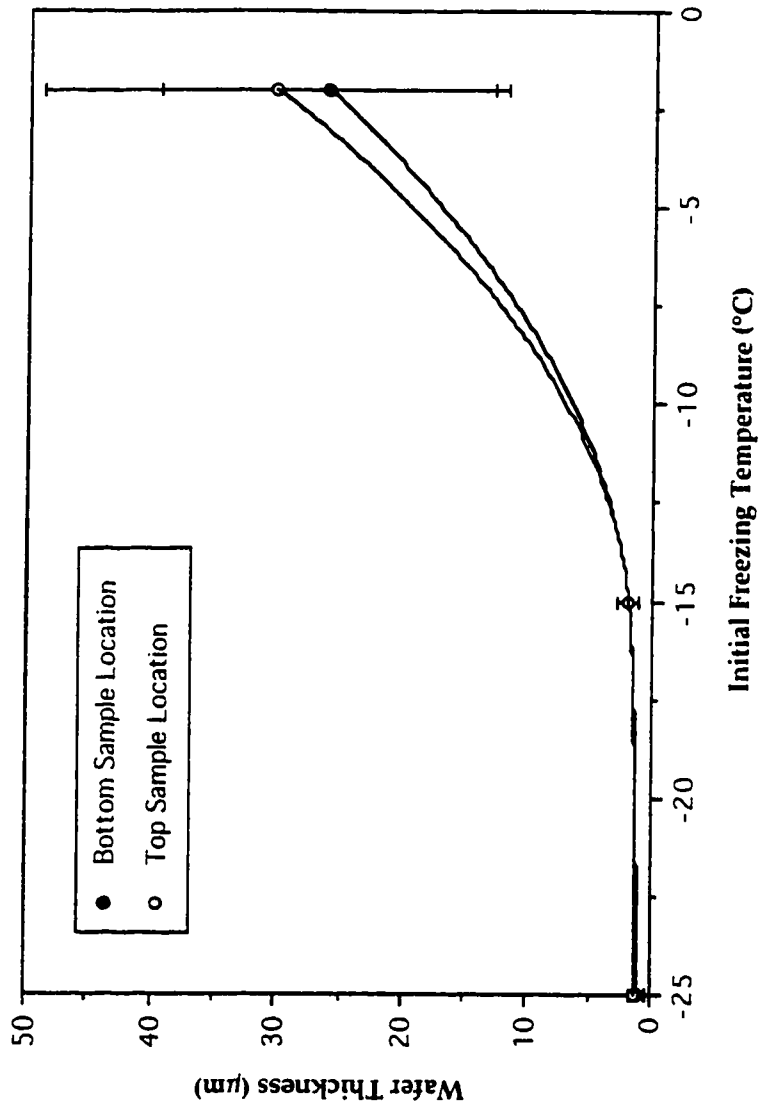


Figure 5.27 Plot of Average Concentrated Material Thickness with Respect to Initial Freezing Temperature for Membrane Concentrate

the material thickness produced at the initial freezing temperature -15°C was significantly different than the material thickness produced at the initial freezing temperature -25°C .

In the proceeding sections it was shown that the thickness of the concentrated material can significantly affect separation efficiency. Also the chemical nature of the concentrated material can affect the relative importance of some independent variables. For example, the thick, highly porous concentrated material typical of the warmer initial freezing temperature (-2°C) was more likely to be affected by the independent variables storage time and storage temperature through mechanical compression of the material over the course of freezing its likely higher concentration of free available water.

5.2.2 ALKALINE EXTRACTION STAGE EFFLUENT

5.2.2.1 INITIAL FREEZING TEMPERATURE: -2°C

The concentrated material that was characteristic of the Eop effluent unidirectionally frozen at the initial freezing temperature -2°C was observed to arrange itself into "honey comb or box" like patterns within the ice matrix. Figure 5.28 is an electron microscope image of a fractured ice specimen surface collected from the top portion of the ice column. This ice specimen was sublimed in accordance to section 3.5.2.1.1 to expose the orientation of the concentrated material. The arrangement pattern shown was similar to that observed for the membrane concentrate frozen at the same initial freezing temperature. Further examination of this figure shows the "honey comb" structures were similar in width, but variable in



Figure 5.28 Electron Microscope Photograph of Concentrated Material Contained Within the Ice Matrix for an Ice Specimen Collected from the Top Ice Column Portion for Eop Effluent Frozen at the Initial Freezing Temperature -2 degrees Celsius

length. Summarized in Table 5.20 are the average dimensions (width and length) of the "honey comb or box like" structures.

5.2.2.1.1 TOP SAMPLE LOCATION RESULTS

Presented in graphical form by way of frequency distributions (Figures 5.29 to 5.31) are the measured thicknesses of the concentrated material observed in ice specimens collected from three independent samples of the top ice portion for Eop effluent frozen at the initial freezing temperature -2 °C. Table 5.21 is a summary of the information derived from examination of the three independent sample sets by SEM. The calculated means and sample variances ranged from 43.2 μm to 47.9 μm and from 18.90 μm to 22.61 μm , respectively. The two-tailed Student t-test was used to show that the individual means were not significantly different at a 95 % confidence limit (Table 5.22). The calculated average thickness of the concentrated material for the combined data of sample sets 1, 2, and 3 as observed in the top portion of the ice column was 44.9 μm , with a sample variance and range of 19.61 μm and 20.1 μm to 80.1 μm , respectively.

High magnification electron microscope images of fractured edges of concentrated material are shown in Figure 5.32. The concentrated material was of higher porosity in comparison to that observed in concentrated material for the membrane concentrate. Attributed to differences in effluent type and concentration, the significance of this increased porosity was the likelihood of this material being more susceptible to break-up upon thawing.

Table 5.20 Summary of Statistical Data Concerning the Cross Sectional Dimensions of the "Honey Comb" Pattern Characteristic of Eop Effluent Frozen at the Initial Freezing Temperature -2 °C

Width (μm)			Length (μm)		
Mean	Variance	Range	Mean	Variance	Range
214	19	183 to 233	483	200	250 to 867

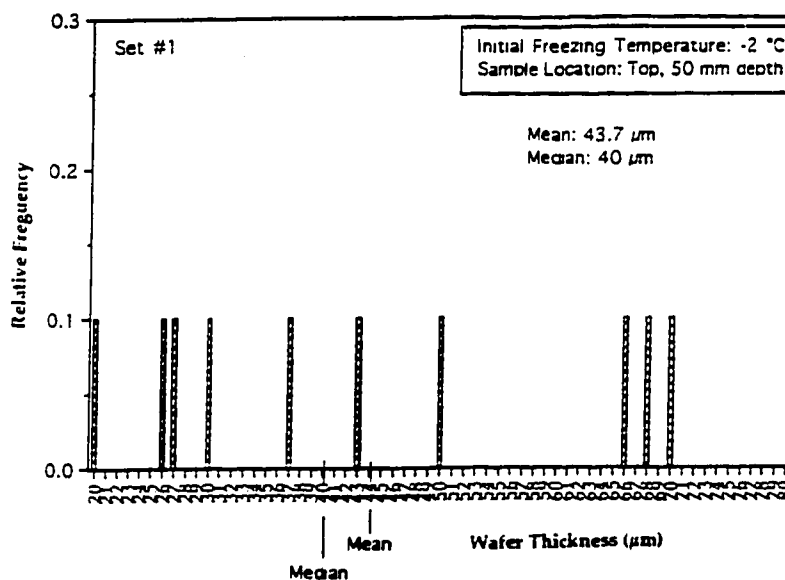


Figure 5.29 Data Representing the Average Thickness of the Concentrated Material Produced in the Top Sample Portion of the Ice Column for Eop Effluent Frozen at the Initial Freezing Temperature -2 °C, Sample Set #1

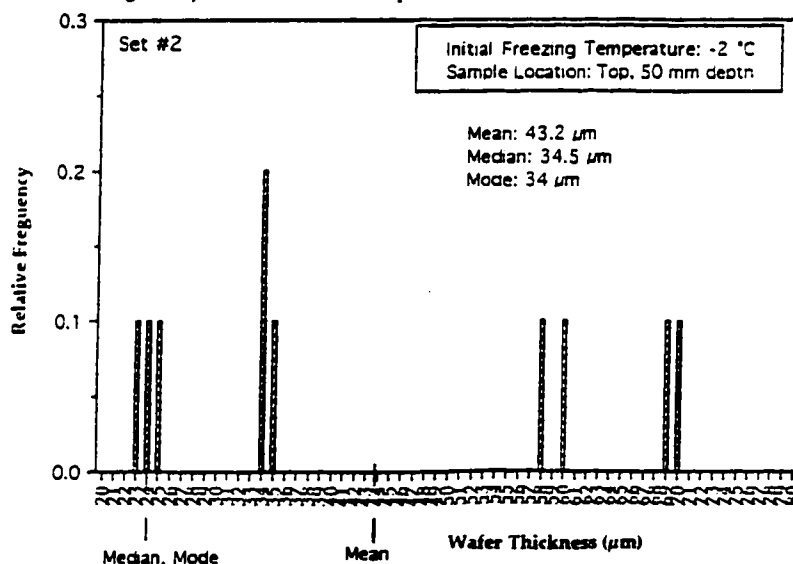


Figure 5.30 Data Representing the Average Thickness of the Concentrated Material Produced in the Top Sample Portion of the Ice Column for Eop Effluent Frozen at the Initial Freezing Temperature -2 °C, Sample Set #2

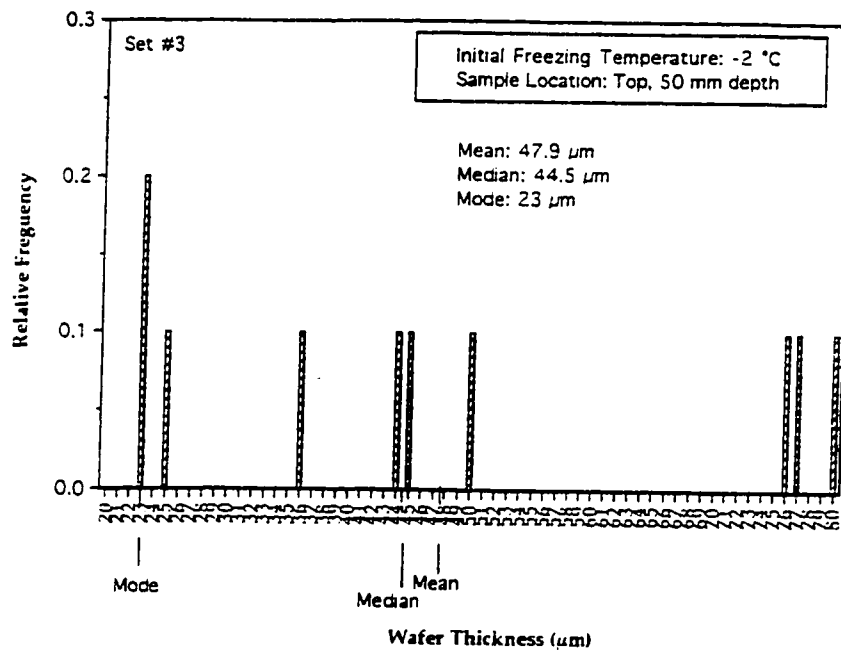


Figure 5.31 Data Representing the Average Thickness of the Concentrated Material Produced in the Top Sample Portion of the Ice Column for Eop Effluent Frozen at the Initial Freezing Temperature -2 °C, Sample Set #3

Table 5.21 Summary of Statistical Data for Sample Sets 1, 2, and 3
(Initial Freezing Temperature -2 °C, Top Sample)

Sample Set*	Mean (μm)	Mean Deviation (μm)	Sample Variance (μm)	Range (μm)
1	43.7	15.8	18.90	20.1 to 70.4
2	43.2	16.8	18.93	23.3 to 70.7
3	47.9	18.3	22.61	23.5 to 80.1

* - sample set size equal to 10

Table 5.22 Tests of Hypotheses Concerning the Difference in Means
Between Sample Sets 1, 2, and 3
(Initial Freezing Temperature -2 °C, Top Sample)

Null Hypothesis	Computed Test Statistic*	$t_{(0.025, 18)}$	Conclusion
$\mu_{\text{set1}} = \mu_{\text{set2}}$	0.12	2.093	accept as equal
$\mu_{\text{set1}} = \mu_{\text{set3}}$	0.27	2.093	accept as equal
$\mu_{\text{set2}} = \mu_{\text{set3}}$	0.16	2.093	accept as equal

* sample variances unknown but assumed equal



Figure 5.32 Collection of High Magnification Electron Microscope Images of Fractured Concentrated Material Edges Produced by Freezing Eop Effluent at the Initial Freezing Temperature -2 degrees Celsius (Top Sample Portion)

5.2.2.2 INITIAL FREEZING TEMPERATURE: -15 °C

The concentrated material characteristic of the Eop effluent frozen at the initial freezing temperature -15 °C was observed to arrange themselves into long continuous sheets of wafers oriented parallel and at relatively equal distances with respect to each other. Figure 5.33 is an electron microscope image of a fractured ice specimen surface sublimed to expose the orientation of the concentrated material.

5.2.2.2.1 TOP SAMPLE LOCATION RESULTS

Presented in tabular form are the frequency distributions (Tables 5.23 to 5.25) of the measured thicknesses of the concentrated material observed in ice specimens collected from three independent samples representative of the top ice portion for Eop effluent frozen at the initial freezing temperature -15 °C. Table 5.26 is a summary of the information derived from examination of the three independent sample sets by SEM. The calculated means and sample variances ranged from 5.9 μm to 7.3 μm and from 5.11 μm to 7.04 μm , respectively. The two-tailed Student t-test was used to show that the means were not significantly different at a 95 % confidence limit (Table 5.27). The combined calculated average thickness of the concentrated material for the combined data of sample sets 1, 2, and 3 as observed in the top portion of the ice column was 6.7 μm , with a sample variance and range of 5.11 μm and 0.7 μm to 16.5 μm , respectively.

High magnification electron microscope images of fractured edges of concentrated material are shown in Figure 5.34. Examination of this figure shows the concentrated material to be thin, very compact wafer-like structures, with no visible porosity. Their physical appearance were



Figure 5.33 Electron Microscope Photograph of Concentrated Material Contained Within the Ice Matrix for an Ice Specimen Collected from the Top Ice Column Portion for Eop Effluent Frozen at the Initial Freezing Temperature -15 degrees Celsius

Table 5.23 Data Representing the Average Thickness of the Concentrated Material Produced in the Top Sample Portion of the Ice Column for Eop Effluent Frozen at the Initial Freezing Temperature 15 °C, Sample Set #1

Sample Number	Measured Thickness (μm)	Relative Frequency
1	0.7	0.1
2	2.5	0.1
3	3.5	0.1
4	4.0	0.1
5	5.2	0.1
6	6.7	0.1
7	7.3	0.1
8	11.1	0.1
9	15.8	0.1
10	16.5	0.1

sample set size: 10

Table 5.24 Data Representing the Average Thickness of the Concentrated Material Produced in the Top Sample Portion of the Ice Column for Eop Effluent Frozen at the Initial Freezing Temperature 15 °C, Sample Set #2

Sample Number	Measured Thickness (μm)	Relative Frequency
1	0.7	0.1
2	2.5	0.1
3,4	3.5	0.2
5	4.2	0.1
6	5.5	0.1
7	6.7	0.1
8	12.2	0.1
9	14.2	0.1
10	15.0	0.1

sample set size: 10

Table 5.25 Data Representing the Average Thickness of the Concentrated Material Produced in the Top Sample Portion of the Ice Column for Eop Effluent Frozen at the Initial Freezing Temperature 15 °C, Sample Set #3

Sample Number	Measured Thickness (μm)	Relative Frequency
1	0.7	0.1
2	2.8	0.1
3	3.3	0.1
4	3.8	0.1
5	4.0	0.1
6	4.5	0.1
7	6.7	0.1
8	7.2	0.1
9	15.0	0.1
10	15.8	0.1

sample set size: 10

Table 5.26 Summary of Statistical Data for Sample Sets 1, 2, and 3 (Initial Freezing Temperature -15 °C, Top Sample)

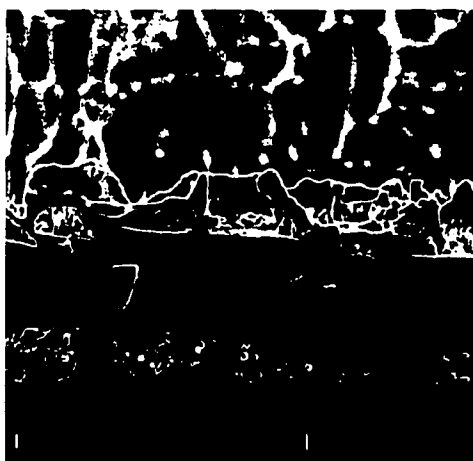
Sample Set*	Mean (μm)	Mean Deviation (μm)	Sample Variance (μm)	Range (μm)
1	7.3	3.9	7.04	0.7 to 16.5
2	6.8	4.2	5.13	0.7 to 15.0
3	5.9	3.6	5.11	0.7 to 15.8

* - sample set size equal to 10

Table 5.27 Tests of Hypotheses Concerning the Difference in Means Between Sample Sets 1, 2, and 3 (Initial Freezing Temperature -15 °C, Top Sample)

Null Hypothesis	Computed Test Statistic*	$t_{(0.025, 18)}$	Conclusion
$\mu_{\text{set1}} = \mu_{\text{set2}}$	0.18	2.093	accept as equal
$\mu_{\text{set1}} = \mu_{\text{set3}}$	0.51	2.093	accept as equal
$\mu_{\text{set2}} = \mu_{\text{set3}}$	0.39	2.093	accept as equal

* sample variances unknown but assumed equal



(a) Sample Set #1 (bar = 1 micron)



(b) Sample Set #2 (bar = 1 micron)



(c) Sample Set #3 (bar = 1 micron)

Figure 5.34 Collection of High Magnification Electron Microscope Images of Fractured Concentrated Material Edges Produced by Freezing Eop Effluent at the Initial Freezing Temperature -15 degrees Celsius (Top Sample Portion)

similar to that of the slightly thinner concentrated material observed for membrane concentrate frozen at the same initial freezing temperature.

5.2.2.3 INITIAL FREEZING TEMPERATURE: -25 °C

The concentrated material characteristic of Eop effluent frozen at the initial freezing temperature -25 °C was observed to arrange themselves into long broken sheets of wafers oriented parallel with each other (Figure 5.35). Unlike the concentrated material observed for the membrane concentrate, the wafer-like structures for the lower concentration strength Eop effluent were discontinuous along their length. The distance between zones of concentrated material were measured to range from 100 μm to 150 μm .

5.2.2.3.1 TOP SAMPLE LOCATION RESULTS

Presented in graphical form by way of frequency histograms (Figures 5.36 to 5.38) are the measured thicknesses of the concentrated material observed in ice specimens collected from three independent samples of the top ice portion for Eop effluent frozen at the initial freezing temperature -25 °C. Table 5.28 is a summary of the information derived from examination of the three independent sample sets by SEM. The calculated means were the same for each sample set for a value of 1.2 μm . The sample variances were reported to range from 0.40 μm to 0.53 μm . The two-tailed Student t-test was used to show that the results were not significantly different at a 95 % confidence limit (Table 5.29). The calculated average thickness of the concentrated material for the combined data of sample sets 1, 2, and 3 as observed in the top portion of the ice



Figure 5.35 Electron Microscope Photograph of Concentrated Material Contained Within the Ice Matrix for an Ice Specimen Collected from the Top Ice Column Portion for Eop Effluent Frozen at the Initial Freezing Temperature -25 degrees Celsius

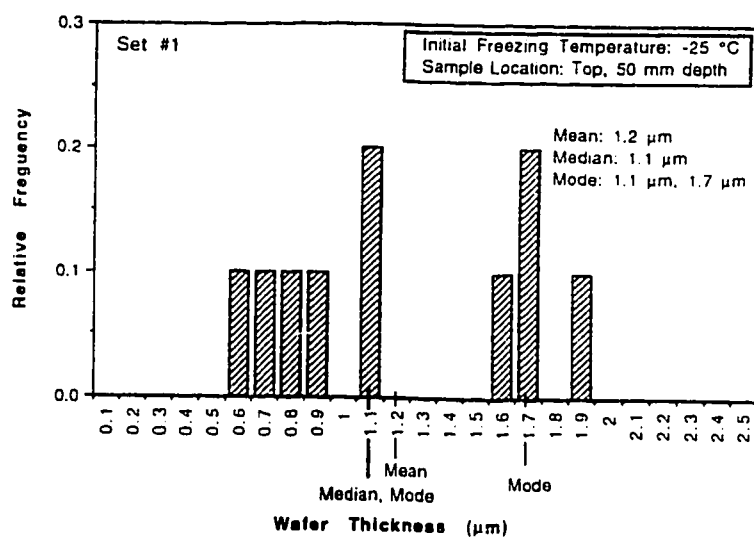


Figure 5.36 Data Representing the Average Thickness of the Concentrated Material Produced in the Top Sample Portion of the Ice Column for Eop Effluent Frozen at the Initial Freezing Temperature -25 °C, Sample Set #1

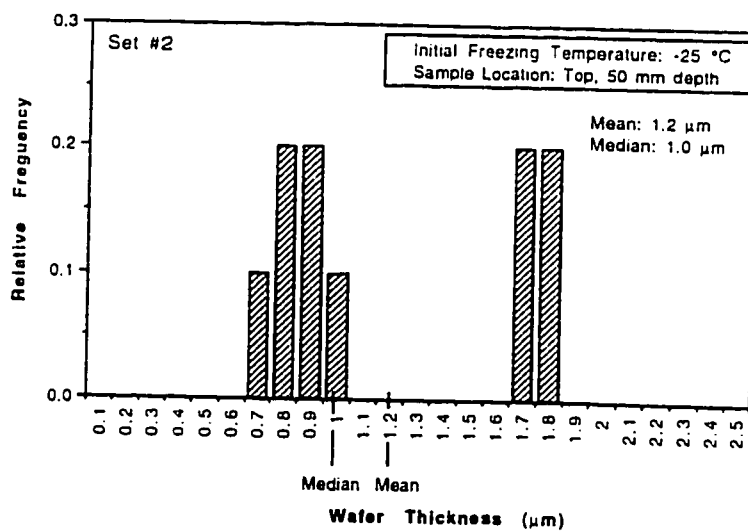


Figure 5.37 Data Representing the Average Thickness of the Concentrated Material Produced in the Top Sample Portion of the Ice Column for Eop Effluent Frozen at the Initial Freezing Temperature -25 °C, Sample Set #2

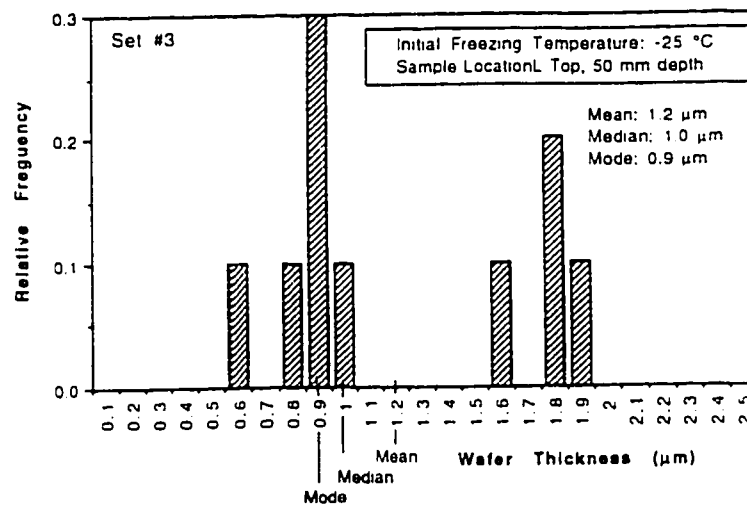


Figure 5.38 Data Representing the Average Thickness of the Concentrated Material Produced in the Top Sample Portion of the Ice Column for Eop Effluent Frozen at the Initial Freezing Temperature -25 °C, Sample Set #3

Table 5.28 Summary of Statistical Data for Sample Sets 1, 2, and 3
(Initial Freezing Temperature -25 °C, Top Sample)

Sample Set*	Mean (μm)	Mean Deviation (μm)	Sample Variance (μm^2)	Range (μm)
1	1.2	0.4	0.53	0.6 to 1.9
2	1.2	0.4	0.50	0.7 to 1.8
3	1.2	0.4	0.40	0.6 to 1.9

* - sample set size equal to 10

Table 5.29 Tests of Hypotheses Concerning the Difference in Means Between Sample Sets 1, 2, and 3
(Initial Freezing Temperature -25 °C, Top Sample)

Null Hypothesis	Computed Test Statistic*	$t_{(0.025, 18)}$	Conclusion
$\mu_{\text{set1}} = \mu_{\text{set2}}$	0.00	2.093	accept as equal
$\mu_{\text{set1}} = \mu_{\text{set3}}$	0.00	2.093	accept as equal
$\mu_{\text{set2}} = \mu_{\text{set3}}$	0.00	2.093	accept as equal

* - sample variances unknown but assumed equal

column was 1.2 μm , with a sample variance and range of 0.51 μm and 0.6 μm to 1.9 μm , respectively.

High magnification electron microscope images of single fractured edges of concentrated material are shown in Figure 5.39. The concentrated material consisted of thin, very compact zones of wafer-like structures. The surface texture of these structures were very smooth.

5.2.2.4 INITIAL FREEZING TEMPERATURE VERSUS THE THICKNESS OF THE CONCENTRATED MATERIAL

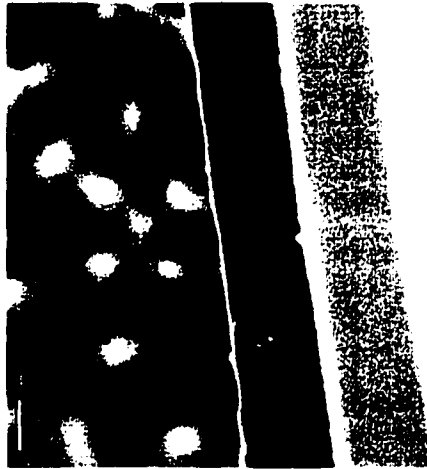
Changes that occurred to the thickness of the concentrated material with respect to initial freezing temperature are shown in Figure 5.40 for the alkaline extraction stage effluent. Similarly, the thickness of concentrated material increased with initial freezing temperature. Analysis of variance and the Duncan Multiple Range Test were used to determine which average thicknesses for the top sample portions were significantly different at a 95 % confidence limit. The results of this analysis are presented in Appendix B. From the analysis it was shown that there are significant differences between all pairs of means representing the average material thicknesses produced at the different initial freezing temperatures.

5.3 MORPHOLOGY OF THE CONCENTRATED MATERIAL FOLLOWING THAWING

Studies were conducted to examine the morphology of the concentrated material in its thawed state. The objective of which was to identify any floc like structures. The concentrated material examined were



(a) Sample Set #1 (bar = 1 micron)



(b) Sample Set #2 (bar = 1 micron)



(c) Sample Set #3 (bar = 1 micron)

Figure 5.39 Collection of High Magnification Electron Microscope Images of Fractured Concentrated Material Edges Produced by Freezing Eop Effluent at the Initial Freezing Temperature -15 degrees Celsius (Top Sample Portion)

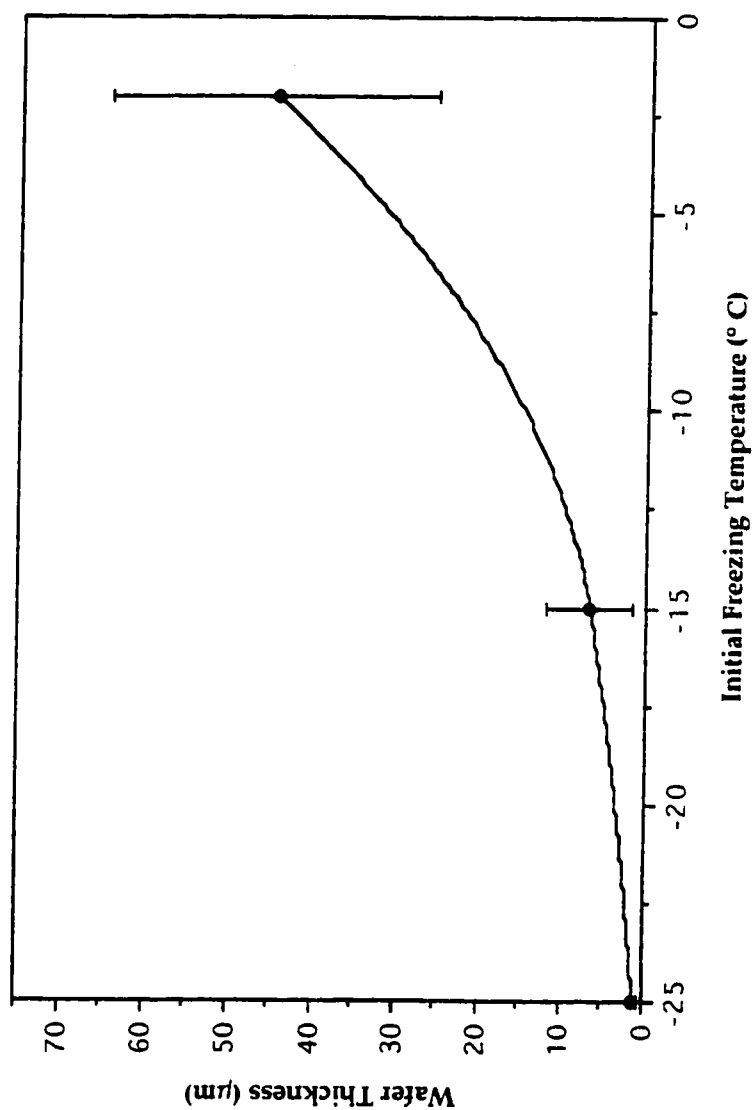


Figure 5.40 Plot of Average Concentrated Material Thickness with Respect to Initial Freezing Temperature for Eop Effluent

those produced from freezing membrane concentrate at the initial freezing temperatures -2 °C and -15 °C.

5.3.1 PROCEDURE

The experimental procedure used was that described in section 3.5.2.1.2 Filter Paper Specimens. Ice specimens examined were collected from membrane concentrate frozen at the initial freezing temperatures -2 °C and -15 °C. The volume of the ice specimen thawed was equivalent to approximately 1 mL. Control samples consisted of the analysis of a clean filter paper surface and filter paper to which 1 mL of liquid raw untreated membrane concentrate was applied.

5.3.2 RESULTS AND DISCUSSION

Small samples of ice were allowed to melt directly onto filter paper in an attempt identify the concentrated material's thawed morphological properties. To avoid any unnecessary disturbances, ice samples were allowed to thaw and drain freely through the filter paper at room temperature (24 °C). The filter apparatus was not operated under a vacuum during melting to avoid destroying what structures survived the melting process. The appearance of the concentrated material in its thawed physical state was observed to differ with respect to initial freezing temperature. Concentrated material produced at the initial freezing temperature -15 °C did not retain its physical structure during thawing. Examination of the concentrated material in its thawed physical state as shown in Figures 5.41 and 5.42 shows the material having dissipated into a fine layer of organic mass with there being no apparent floc like structures. High magnification electron microscope images taken of the thawed

concentrated material as shown in Figures 5.43 and 5.44 shows the only identifiable structures left remaining on the filter paper were circular precipitates. X-ray defraction of these circular substances (Figure 5.45) identified them as being calcium carbonate precipitate coated with a small amount of organic residue. Aside from the presence of precipitate, the surface appearance of the filter paper was not substantially different from that observed for the control representative of an equivalent volume of liquid raw untreated membrane concentrate (Figure 5.46). In comparison to the clean filter sample (Figure 5.47) the organic constituents were observed to fill the pore structure of the filter paper.

Very different results were observed in the examination of the thawed concentrated material produced at the initial freezing temperature -2°C (Figure 5.48). Figures 5.49 to 5.50 are high magnification electron microscope images taken of the thawed material produced at the initial freezing temperature -2°C . Examination of these figures shows the thawed concentrated material to have retained a large portion of its physical structure produced during freezing. The structure was floc like in appearance. Measurement of the suspended solids concentrations in the bottom sample portions of ice samples thawed bottom up for different freeze-thaw conditions showed the initial freezing temperature -2°C as having the highest concentration. The settled material was comprised of a white precipitate and from tests was believed to be calcium carbonate. The results are plotted in Figure 5.51. The results presented add substantial insight into the nature of the concentrated material produced at the different initial freezing temperatures. From SEM examination it can be concluded that the concentrated material is not a floc per say but is

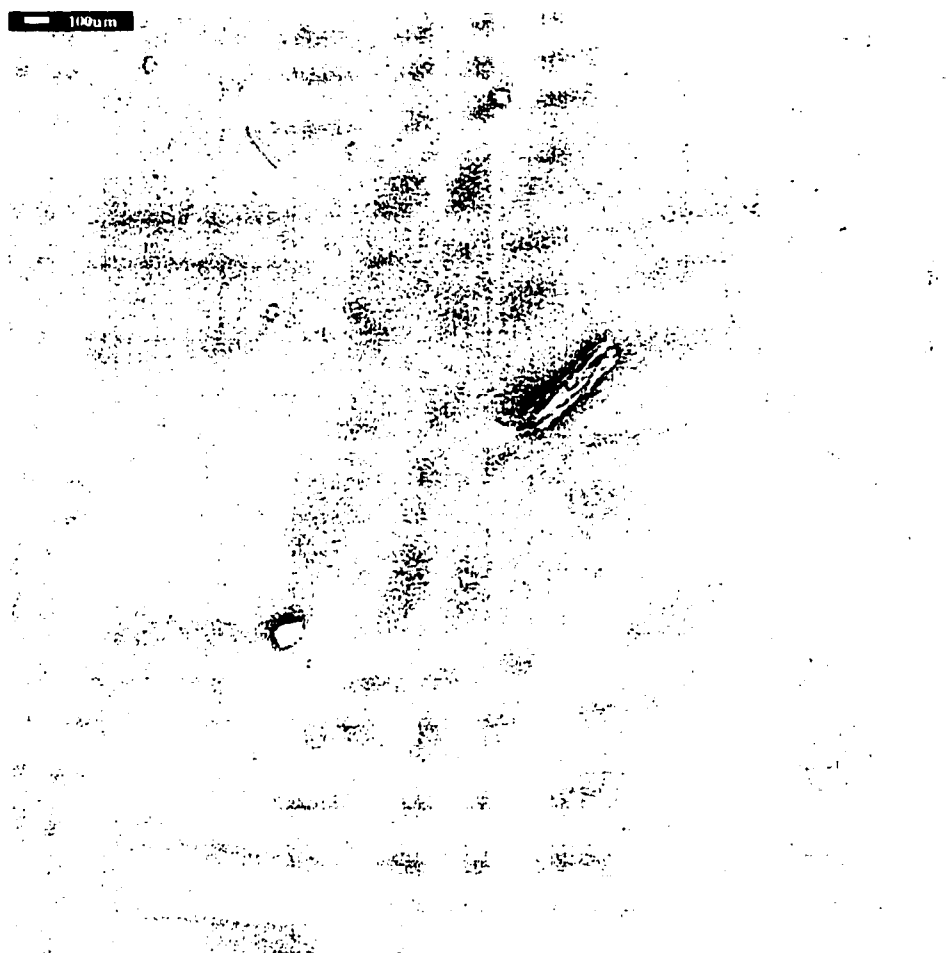


Figure 5.41 Electron Microscope Photograph of the Concentrated Material Retained on the Filter Paper After Thawing Membrane Concentrate Frozen at the Initial Freezing Temperature -15 degrees Celsius

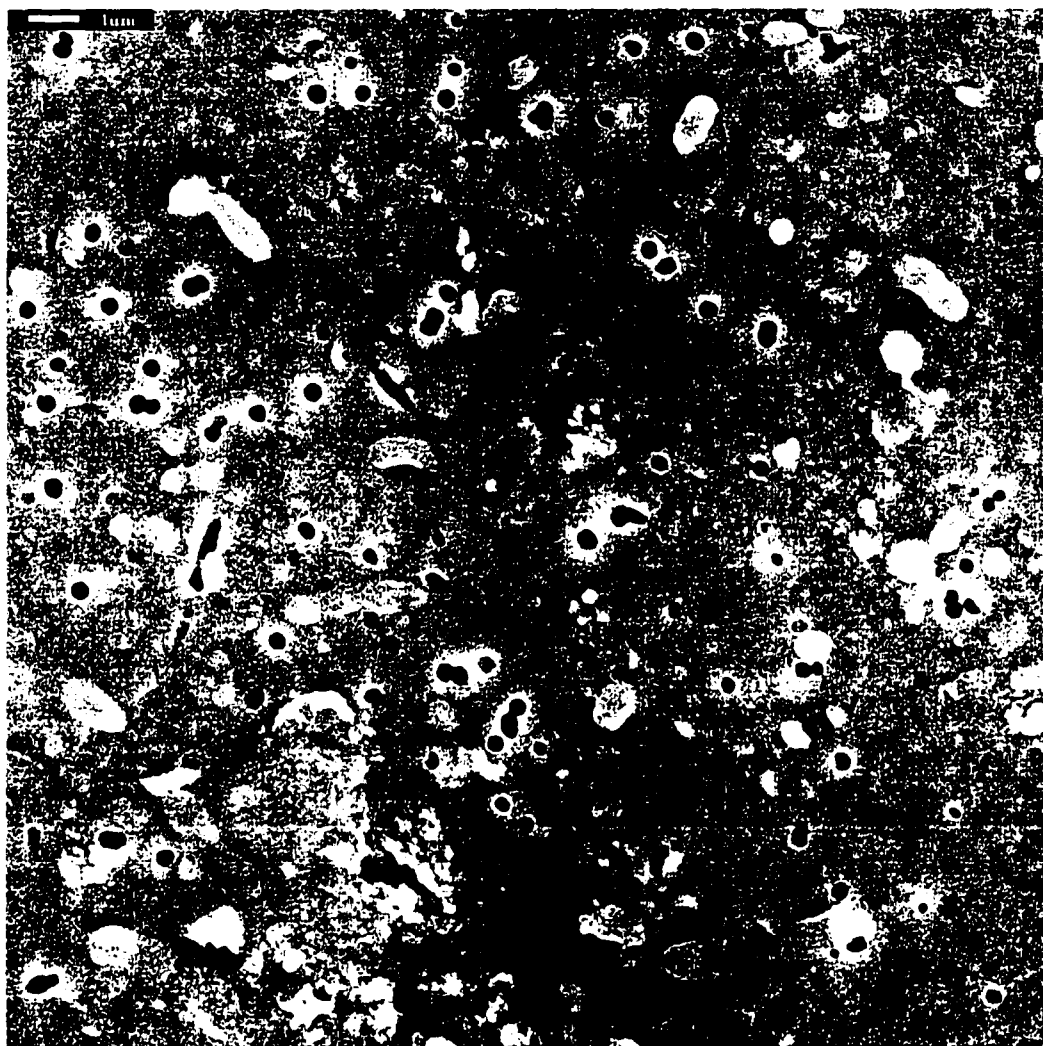


Figure 5.42 High Magnification Electron Microscope Image Showing the Morphology of the Concentrated Material Retained on the Filter Paper After Thawing Membrane Concentrate Frozen at the Initial Freezing Temperature -15 degrees Celsius

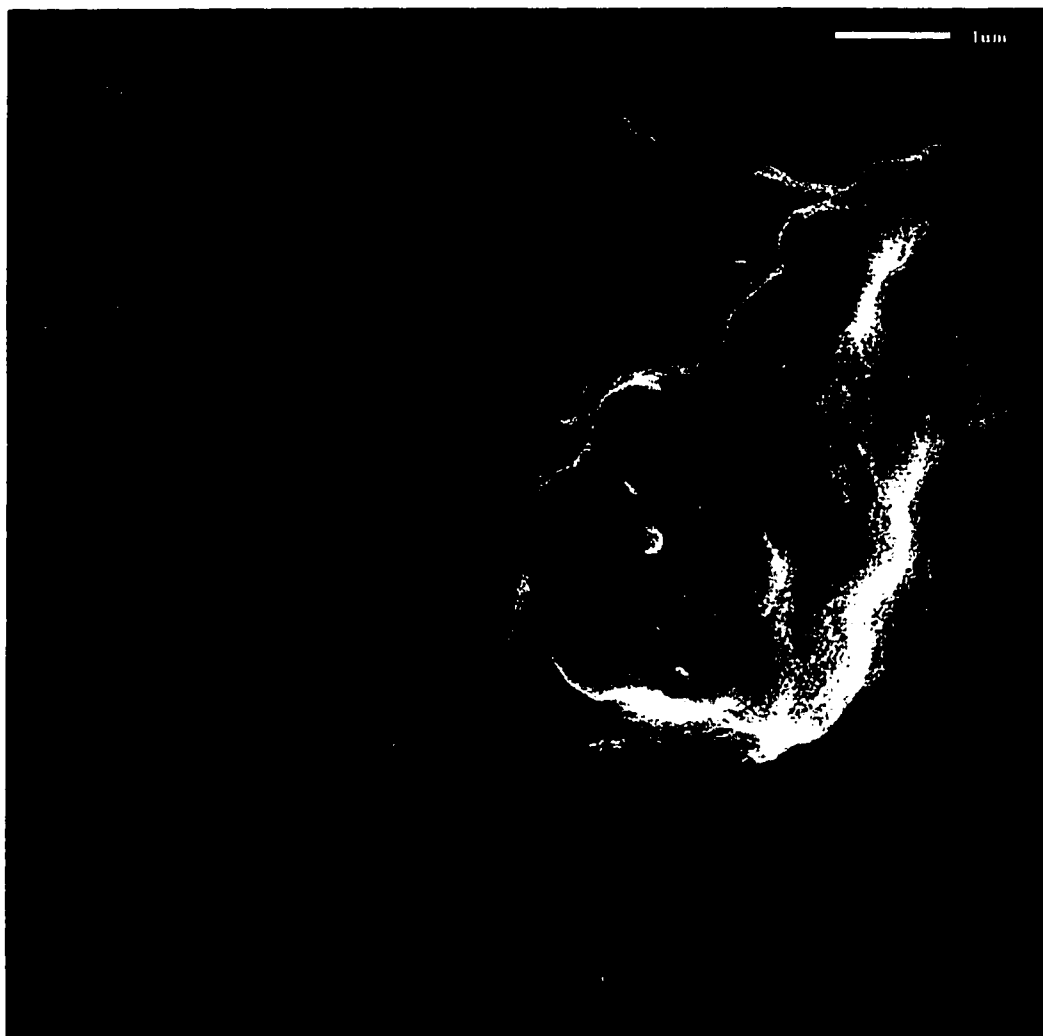


Figure 5.43 High Magnification Electron Microscope Image Showing the Morphology of the Concentrated Material Retained on the Filter Paper After Thawing Membrane Concentrate Frozen at the Initial Freezing Temperature -15 degrees Celsius

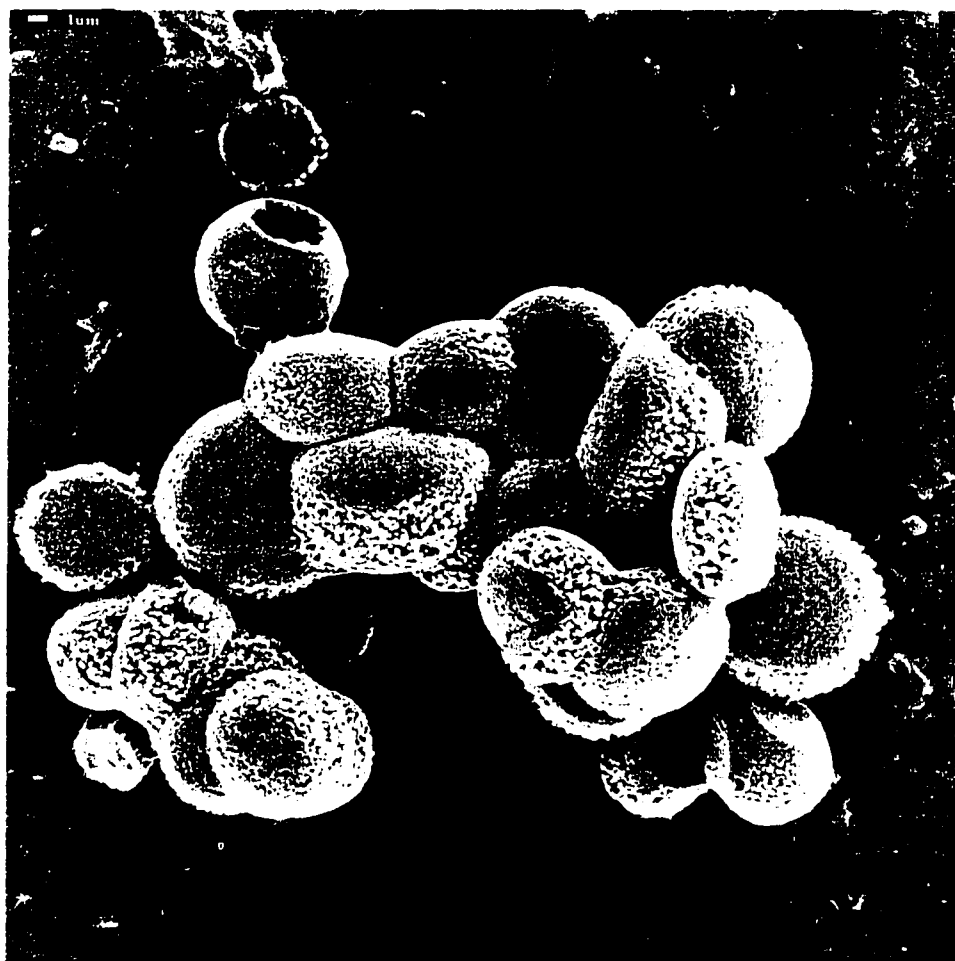


Figure 5.44 High Magnification Electron Microscope Image Showing the Morphology of the Concentrated Material Retained on the Filter Paper After Thawing Membrane Concentrate Frozen at the Initial Freezing Temperature -15 degrees Celsius (Extreme Close-up)

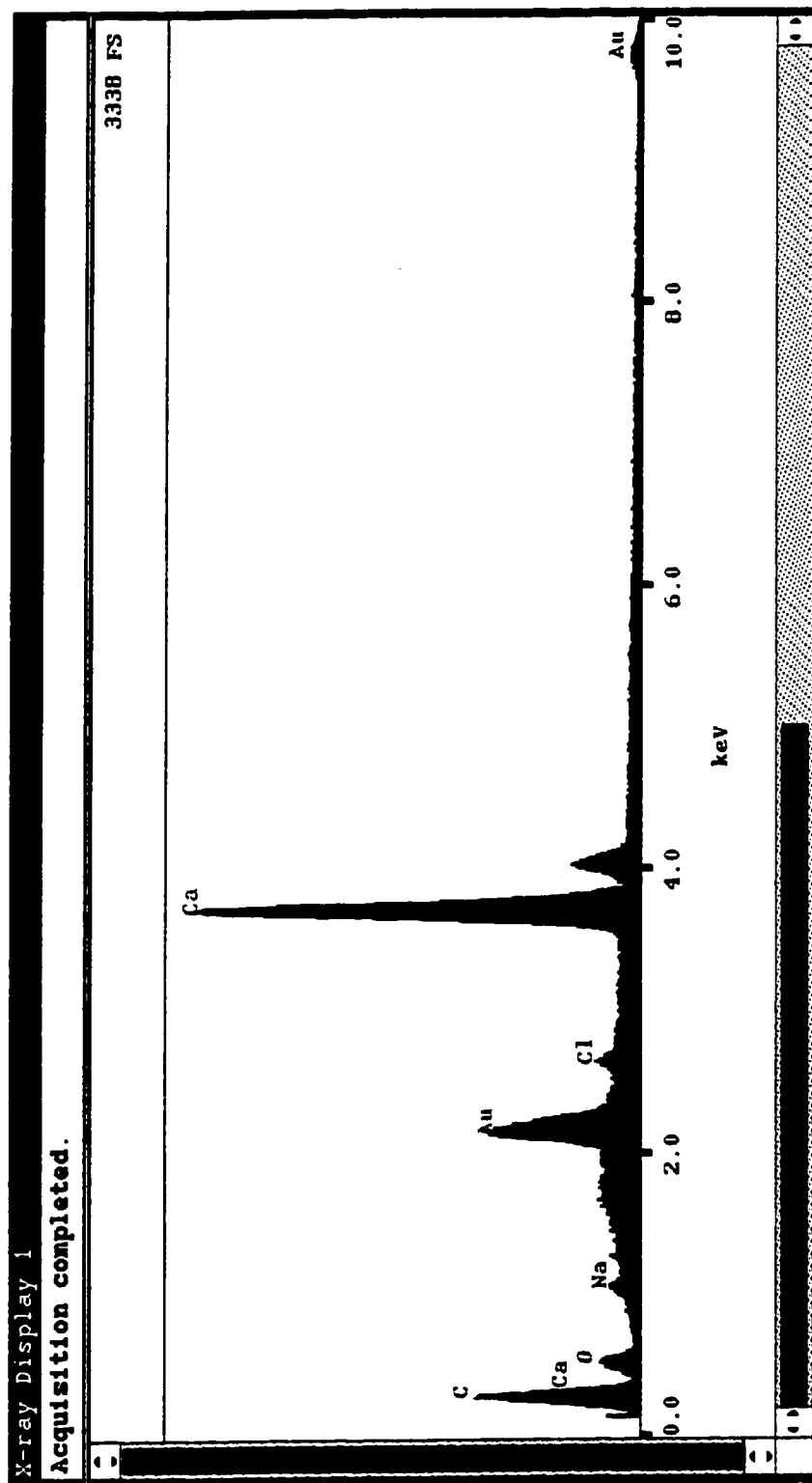


Figure 5.45 X-ray Diffraction Results of Precipitate Found Associated with the Concentrated Material Found on Filter Paper Samples After the Thawing of Membrane Concentrate

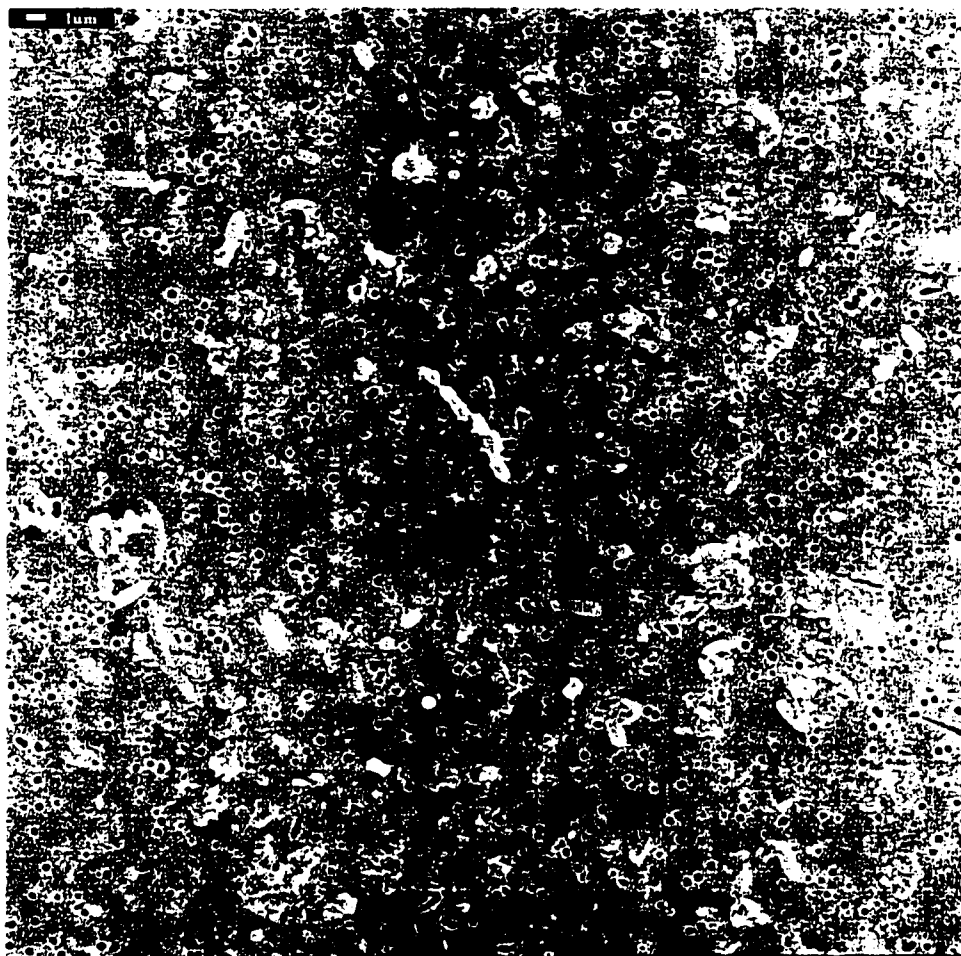


Figure 5.46 Electron Microscope Photograph of a Filter Paper Surface to Which Untreated Membrane Concentrate was Applied

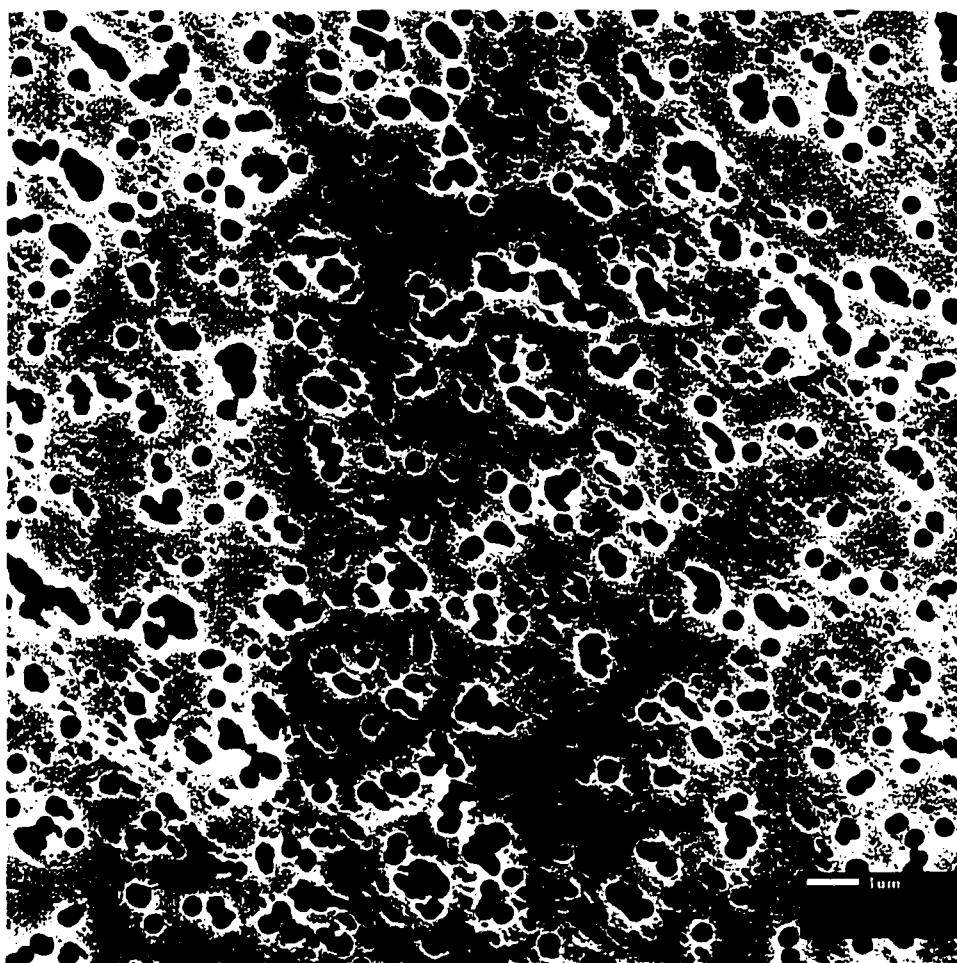


Figure 5.47 Electron Microscope Photograph of a Clean Filter Paper Sample - Control



Figure 5.48 Electron Microscope Photograph of the Concentrated Material Retained on the Filter Paper After Thawing Membrane Concentrate Frozen at the Initial Freezing Temperature -2 degrees Celsius

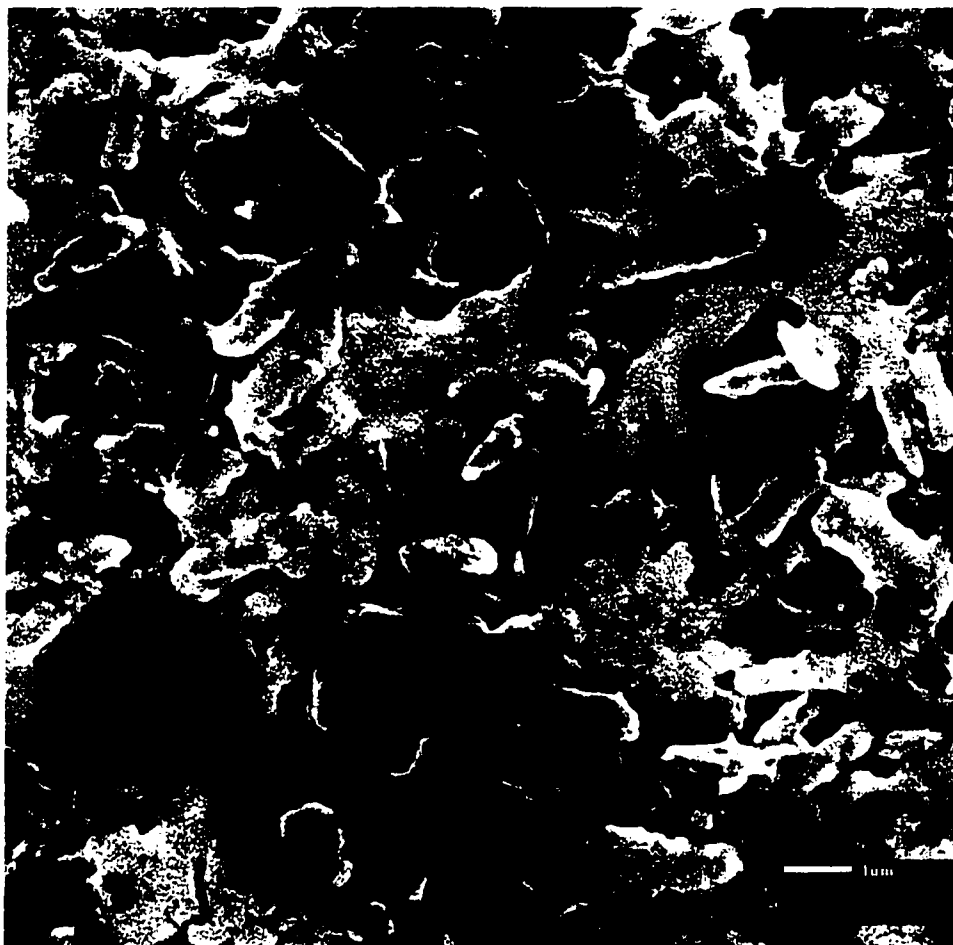


Figure 5.49 High Magnification Electron Microscope Image Showing the Morphology of the Concentrated Material Retained on the Filter Paper After Thawing Membrane Concentrate Frozen at the Initial Freezing Temperature -2 degrees Celsius



Figure 5.50 High Magnification Electron Microscope Image Showing the Morphology of the Concentrated Material Retained on the Filter Paper After Thawing Membrane Concentrate Frozen at the Initial Freezing Temperature -2 degrees Celsius (Extreme Close-up)

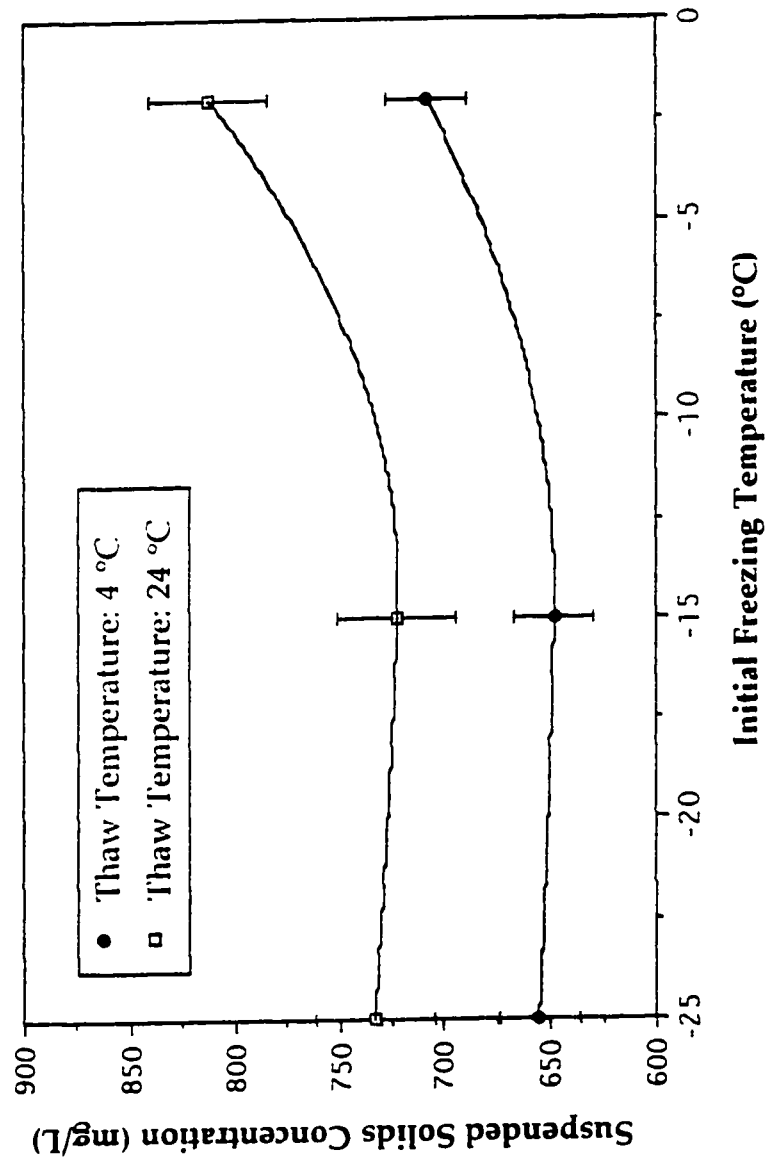


Figure 5.51 Plot of Suspended Solids Concentration with Respect to Different Freeze-thaw Conditions for Membrane Concentrate

comprised of a mixture of stable and coagulated material. Stable material includes dissolved and colloidal organic material. That which will be shown in the stability studies is the concentrated material dissolves back into solution over time.

5.4 CHANGES IN THE CONCENTRATED MATERIAL'S PHYSICAL PROPERTIES WITH RESPECT TO CONCENTRATION

Concentration was studied for its influence on the physical properties of the concentrated material produced by freezing different dilutions of the alkaline extraction stage membrane concentrate at different initial freezing temperatures. The initial freezing temperatures studied were -2°C and -15°C . The alkaline extraction stage membrane concentrate dilution ratios investigated were 0 %, 50 %, 66 %, 75 %, and 80 %, respectively.

5.4.1 PROCEDURE

Millipore distilled water was used to dilute the alkaline extraction stage membrane concentrate for make-up of the experimental waters. Following preparation, the experimental waters were unidirectionally frozen at their desired initial freezing temperatures using the experimental apparatus described in section 3.6.1. Ice specimens for examination by SEM were collected in accordance to section 3.7.1.2 from the center top portion of the ice column at a depth of 50 mm from the top.

5.4.2 RESULTS AND DISCUSSION

5.4.2.1 INITIAL FREEZING TEMPERATURE: -2 °C

Tabulated and graphically presented in Figures 5.52 to 5.53 and Table 5.30 are the frequency distributions representing the cross sectional thickness of the concentrated material produced by freezing different concentration strengths of alkaline extraction stage membrane concentrate at the initial freezing temperature -2 °C. Summarized in Table 5.31 is a summary of the information derived from examination of the different concentrate dilutions by SEM. Changes that occurred to the thickness of the concentrated material with respect to percent dilution are shown in Figure 5.54. The average thickness of the concentrated material decreased with respect to percent dilution. In addition, the sample variance associated with each dilution also decreased. The slope of the curve was shown to have rapidly decreased at the 66 % dilution. At dilutions beyond 66 %, the concentrated material observed in ice matrices did not resemble the wafer like structure typically observed for the stock solution. At the 75 % dilution the concentrated material appeared as strands rather than as continuous wafers as observed at the lower percent dilutions. Analysis of variance and the Duncan Multiple Range Test were used to determine which average thicknesses for the different percent dilutions were significantly different at a 95 % confidence limit. The results of this analysis are presented in Appendix B. From the analysis it was shown that there are significant differences between all pairs of means representing the average material thicknesses produced at the different percent dilutions.

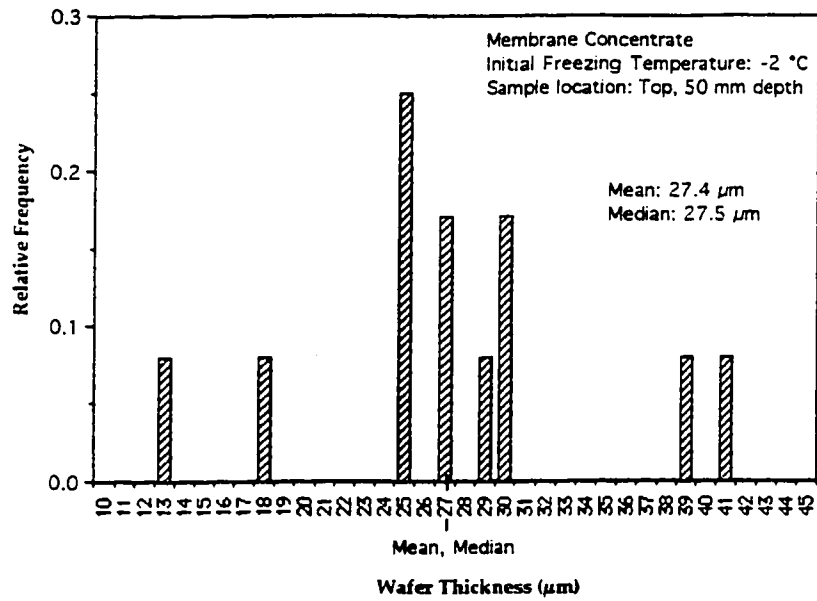


Figure 5.52 Frequency Histogram Showing the Measure of Dispersion of the Concentrated Material Thickness for Membrane Concentrate Frozen at the Initial Freezing Temperature -2 °C

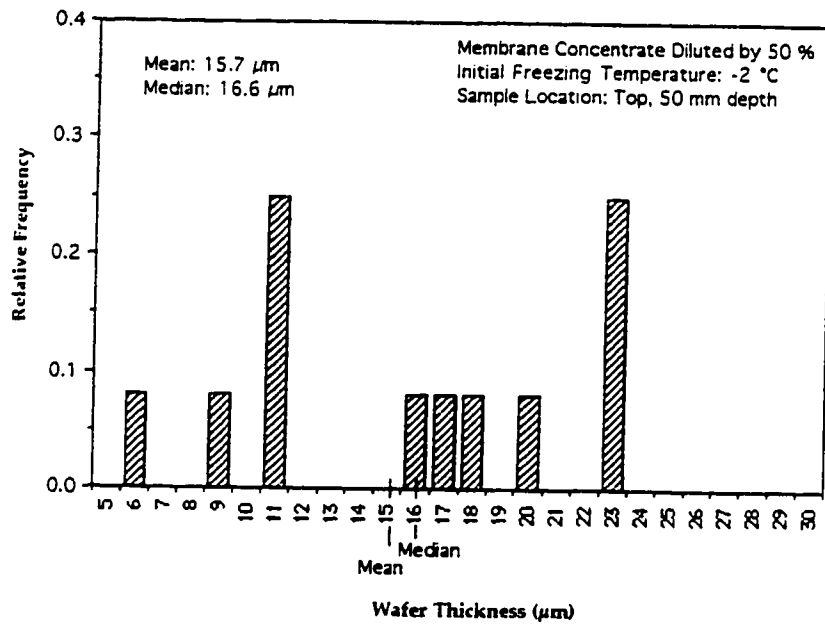


Figure 5.53 Frequency Histogram Showing the Measure of Dispersion of the Concentrated Material Thickness for Membrane Concentrate Diluted by 50 % and Frozen at the Initial Freezing Temperature -2 °C

Table 5.30 Summary of Data Showing the Measure of Dispersion of the Concentrated Material Thickness for Membrane Concentrate Diluted by 66 % and Frozen at the Initial Freezing Temperature -2 °C

Concentrated Material Thickness (μm)	Relative Frequency
0.9	0.08
1.0	0.08
1.1	0.08
1.5	0.08
1.6	0.17
1.8	0.17
2.7	0.17
3.2	0.08
4.5	0.08

Mean: 2.0 μm , Median: 1.7 μm , Mode: 1.6 μm , 1.8 μm , 2.7 μm

Table 5.31 Summary of Statistical Data Concerning the Concentrated Material Thickness for Membrane Concentrate of Different Dilutions Frozen at the Initial Freezing Temperature -2 °C

Percent Dilution*	Mean (μm)	Sample Variance (μm)	Range (μm)
Undiluted (0 %)	27.4	7.57	12.7 to 40.9
50 %	15.7	4.25	5.9 to 23.2
66 %	2.0	1.10	0.9 to 4.5

* - sample set size equal to 12

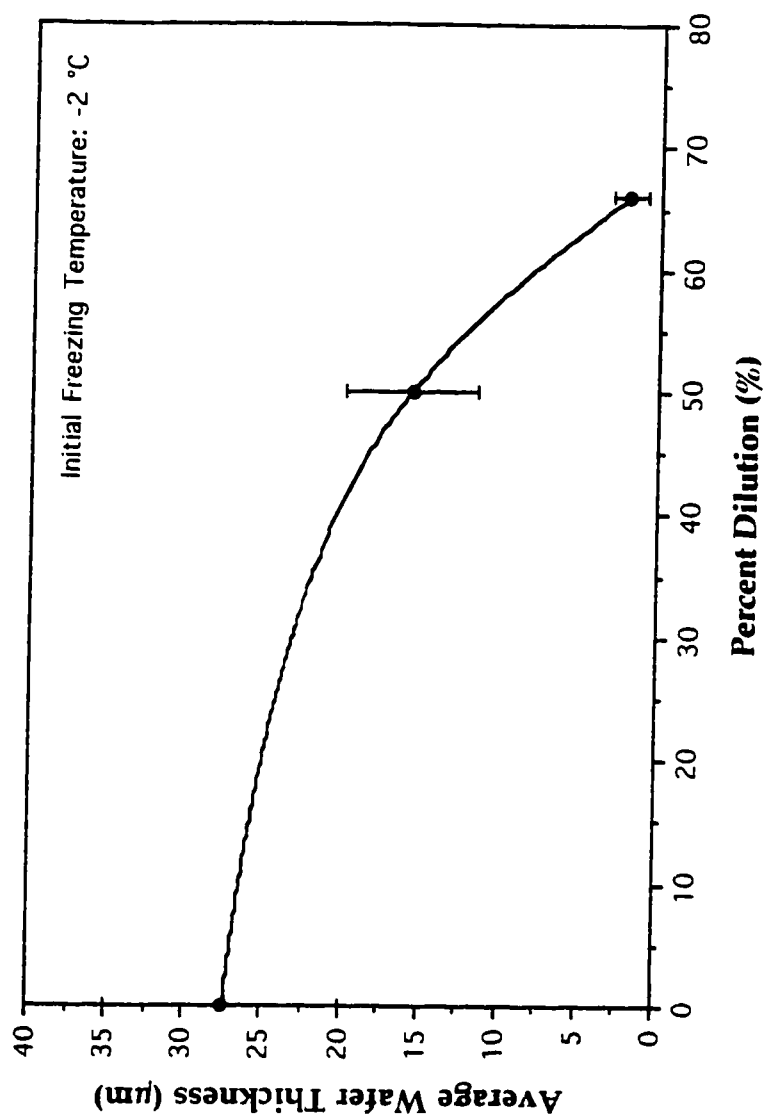


Figure 5.54 Plot of Average Concentrated Material Thickness Versus Percent Dilution for Different Concentration Strengths of Membrane Concentrate Frozen at the Initial Freezing Temperature -2 °C

Also observed, aside from changes in thickness, were differences with respect to orientation and density. High magnification electron microscope images of fractured ice surfaces for each concentrate dilution are shown in Figures 5.55 to 5.58. The orientation of the wafers were reported to change with respect to dilution from "honey comb" like structures to continuous wafers arranged as sheets (Figure 5.59) to finally individual strands (Figure 5.60). The morphology of the concentrated material did not appear to differ with respect to the material observed for the undiluted concentrate until above a 50 % dilution (corresponding to a color concentration 6,250 CU) at which point the material observed resembled that reported at the colder initial freezing temperatures. In addition, the removal efficiencies obtained by freeze-thaw are not anticipated to vary for a concentrate with a color concentration between 12,500 CU to 6,250 CU. This suggests that the empirical model developed using the results obtained when the measured response is expressed in percent color removal will be valid for membrane concentrations with a initial color between the dilution ranges of 0 (corresponding color 12,500 CU) to 50 % (corresponding color 6,250 CU). At dilution ratios above 50 % (corresponding color <6,250 CU) concentration will likely be required to be included as an independent variable in the model as the concentrated material produced at the initial freezing temperature -2 °C at these dilutions were substantially different with respect to the undiluted concentrate.

5.4.2.2 INITIAL FREEZING TEMPERATURE: -15 °C

Represented below in Figures 5.61 to 5.64 are the frequency

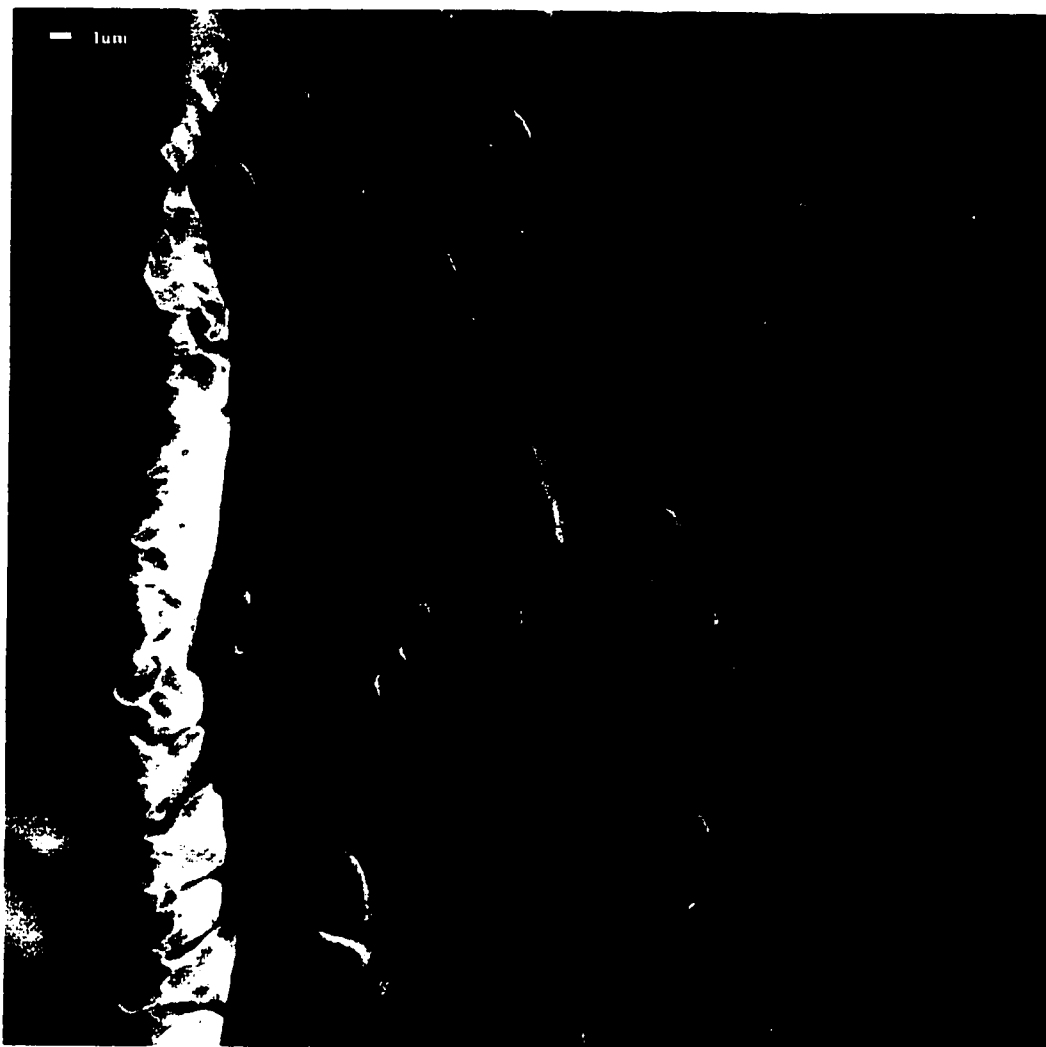


Figure 5.55 High Magnification Electron Microscope Image of a Fractured Concentrated Material Edge Produced by Freezing Membrane Concentrate at the Initial Freezing Temperature -2 degrees Celsius

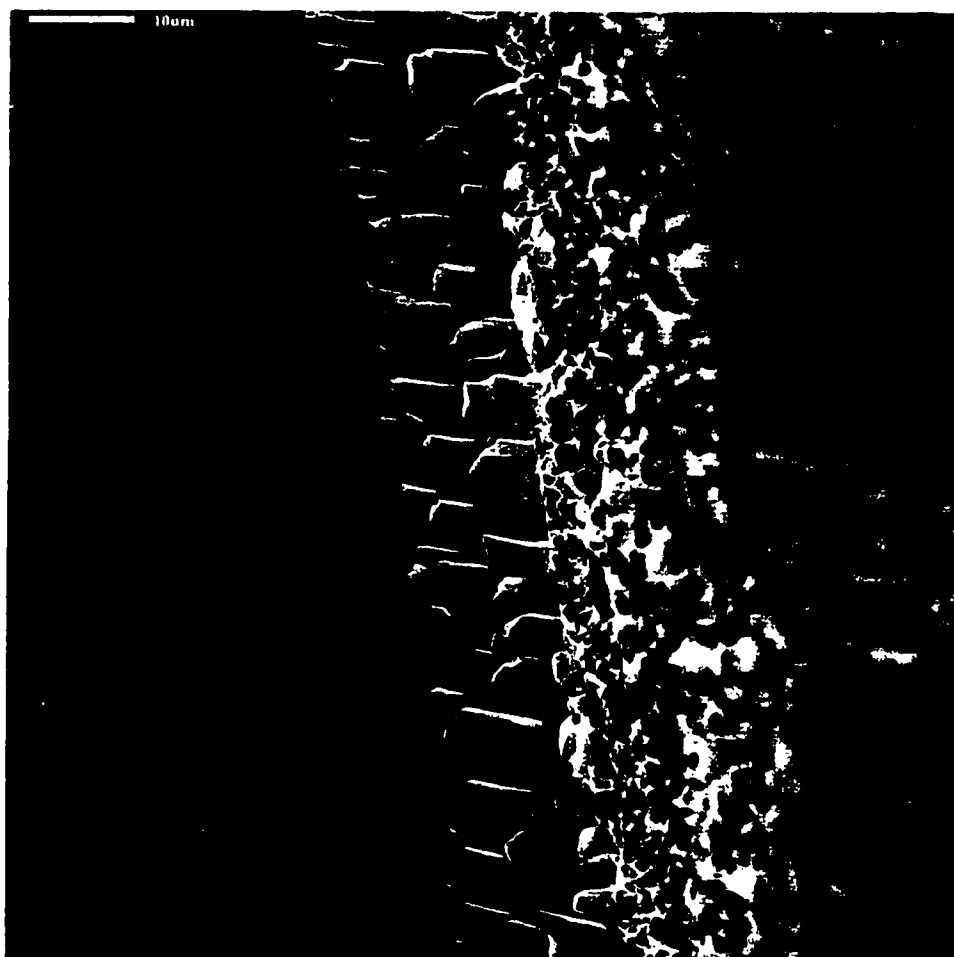


Figure 5.56 High Magnification Electron Microscope Image of a Fractured Concentrated Material Edge Produced by Freezing Membrane Concentrate Diluted to 50 % at the Initial Freezing Temperature -2 degrees Celsius

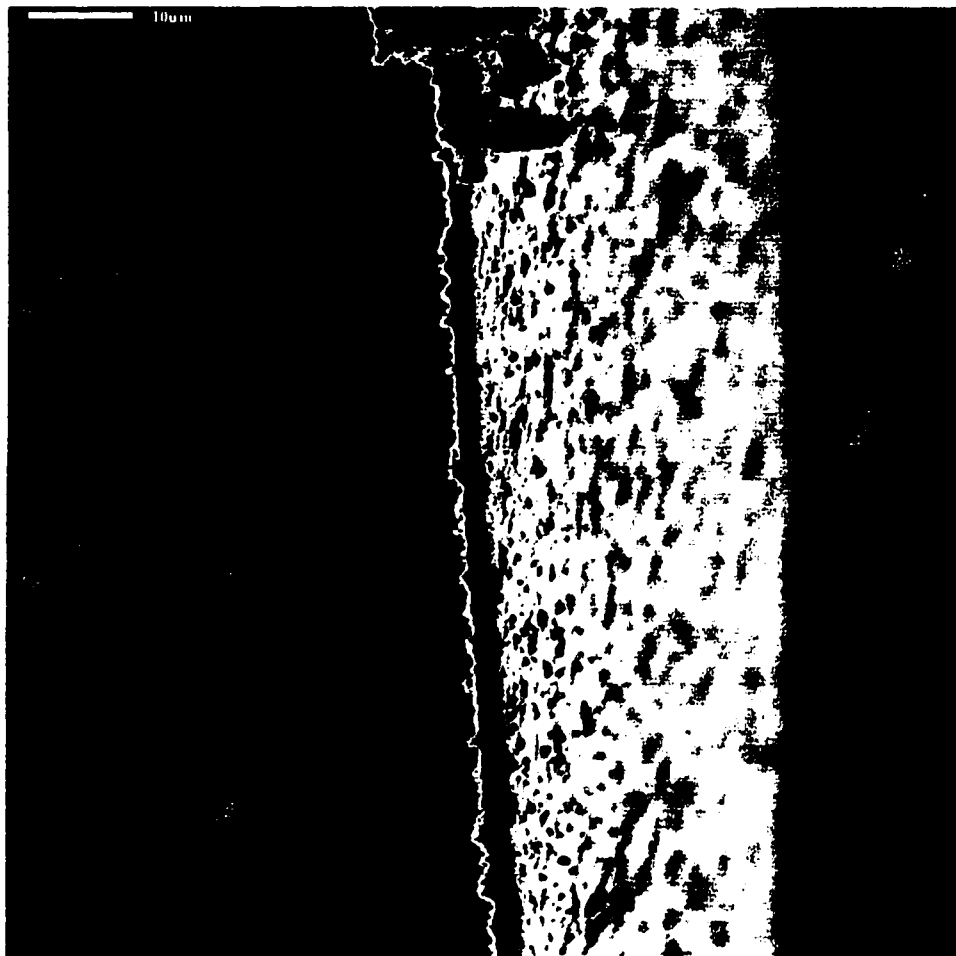


Figure 5.57 High Magnification Electron Microscope Image of a Fractured Concentrated Material Edge Produced by Freezing Membrane Concentrate Diluted to 66 % at the Initial Freezing Temperature -2 degrees Celsius



Figure 5.58 High Magnification Electron Microscope Image of a Fractured Concentrated Material Edge Produced by Freezing Membrane Concentrate Diluted to 75 % at the Initial Freezing Temperature -2 degrees Celsius



Figure 5.59 Electron Microscope Photograph of Concentrated Material Contained Within the Ice Matrix for an Ice Specimen Collected from the Top Ice Column Portion Produced by Freezing Membrane Concentrate Diluted to 50 % at the Initial Freezing Temperature -2 degrees Celsius

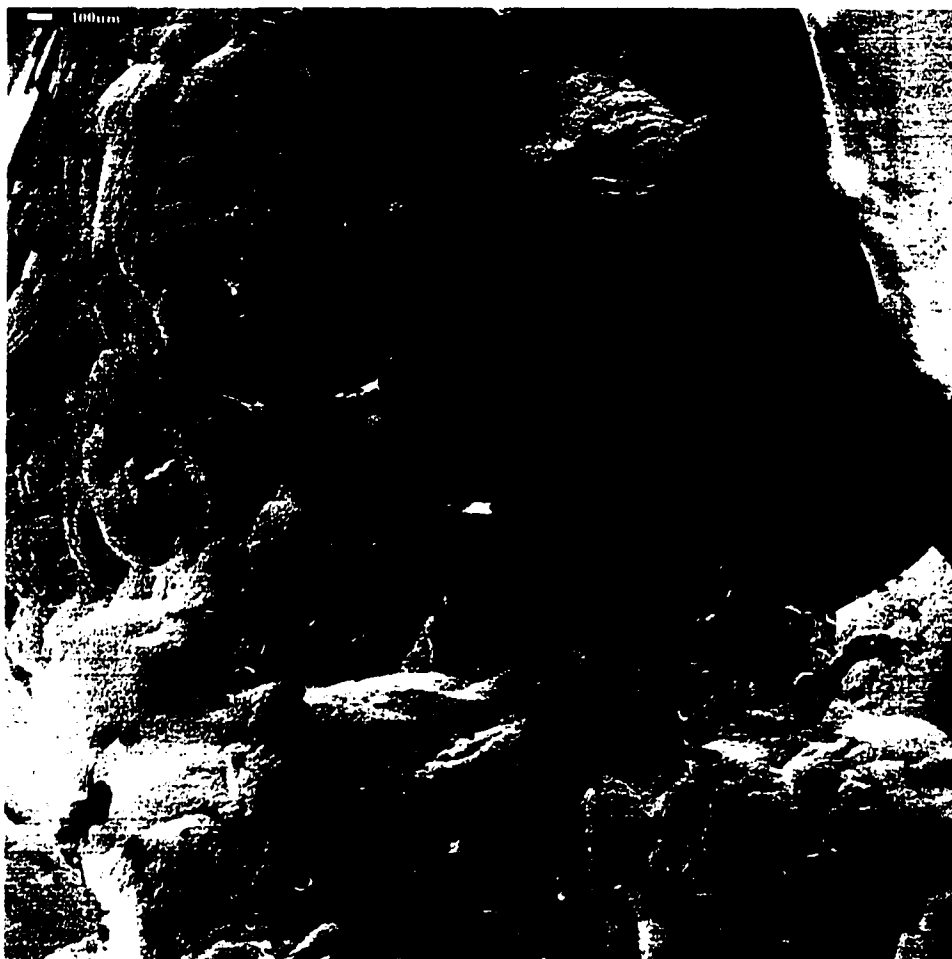


Figure 5.60 Electron Microscope Photograph of Concentrated Material Contained Within the Ice Matrix for an Ice Specimen Collected from the Top Ice Column Portion Produced by Freezing Membrane Concentrate Diluted to 75 % at the Initial Freezing Temperature -2 degrees Celsius

histograms for the measures of dispersion of the cross sectional thickness of the concentrated material produced by freezing different concentration strengths of the alkaline extraction stage membrane concentrate at the initial freezing temperature -15°C . Summarized in Table 5.32 is a summary of the information derived from examination of the cross sectional thicknesses of the concentrated material at each concentrate dilution. Changes that occurred to the thickness of the concentrated material with respect to percent dilution are shown in Figure 5.65. The average thickness of the concentrated material decreased linearly with respect to percent dilution. The decrease ranged from $1.9\text{ }\mu\text{m}$ for the undiluted concentrate to an average thickness of $0.7\text{ }\mu\text{m}$ for a dilution ratio of 75 %. High magnification electron microscope images of single fractured concentrated material edges showing the change with respect to percent dilution are shown in Figures 5.66 to 5.70. Similarly, the data suggests that the independent variable concentration can be neglected as a factor in the model that substantially affects the thickness of the concentrated material for membrane concentrations with a initial color between the dilution ranges of 0 (corresponding color 12,500 CU) to 50 % (corresponding color 6,250 CU). At a dilution of 50 % the resultant average thickness of the concentrated material was still within the range reported for the undiluted concentrate. At dilution ratios above 50 % (corresponding color $<6250\text{ CU}$) concentration will likely be required to be included as a variable in the model as the material produced at the initial freezing temperature -15°C at these dilutions will be substantially thinner with respect to the undiluted concentrate.

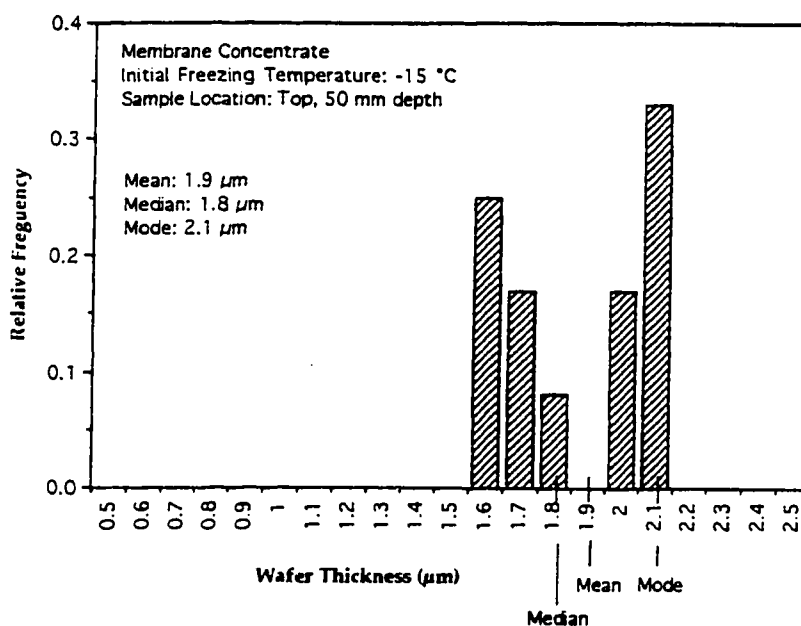


Figure 5.61 Frequency Histogram Showing the Measure of Dispersion of the Concentrated Material Thickness for Membrane Concentrate Frozen at the Initial Freezing Temperature -15 °C

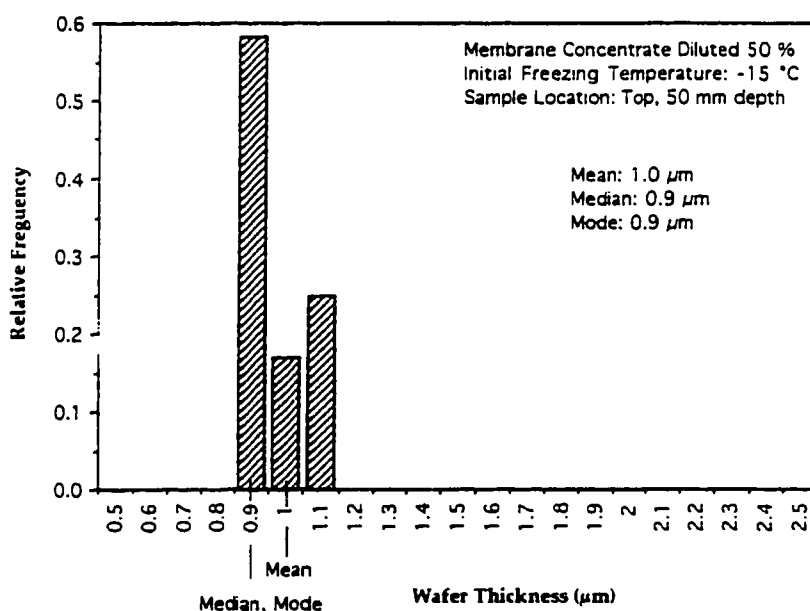


Figure 5.62 Frequency Histogram Showing the Measure of Dispersion of the Concentrated Material Thickness for Membrane Concentrate Diluted by 50 % and Frozen at the Initial Freezing Temperature -15 °C

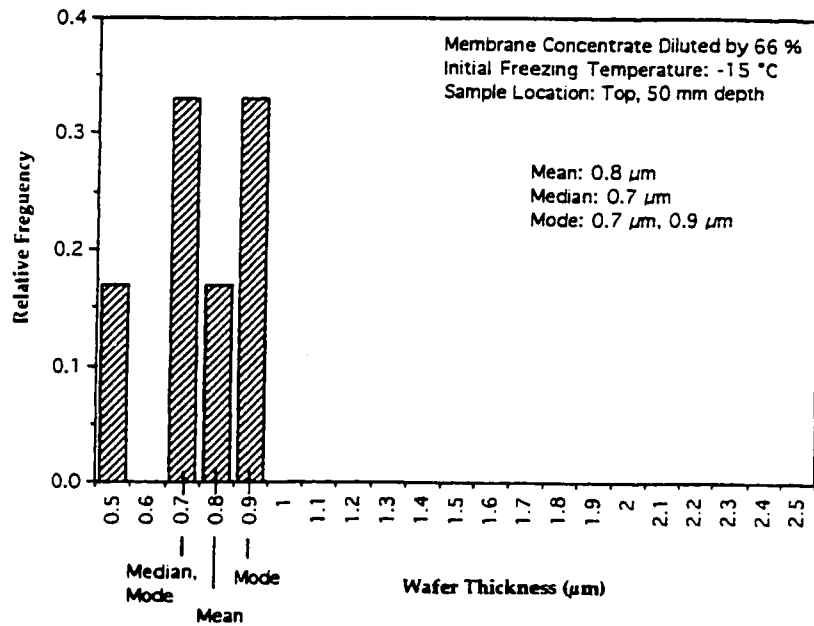


Figure 5.63 Frequency Histogram Showing the Measure of Dispersion of the Concentrated Material Thickness for Membrane Concentrate Diluted by 66 % and Frozen at the Initial Freezing Temperature -15 °C

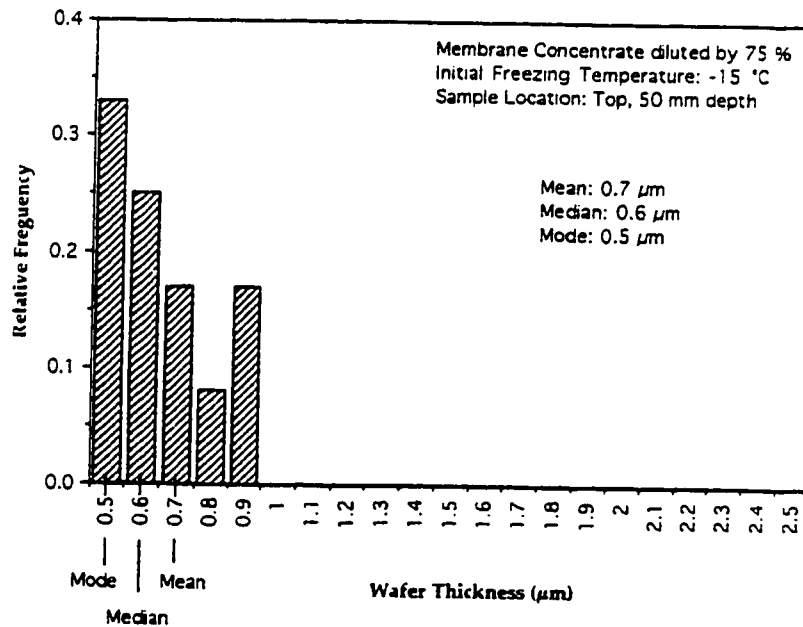


Figure 5.64 Frequency Histogram Showing the Measure of Dispersion of the Concentrated Material Thickness for Membrane Concentrate Diluted by 75 % and Frozen at the Initial Freezing Temperature -15 °C

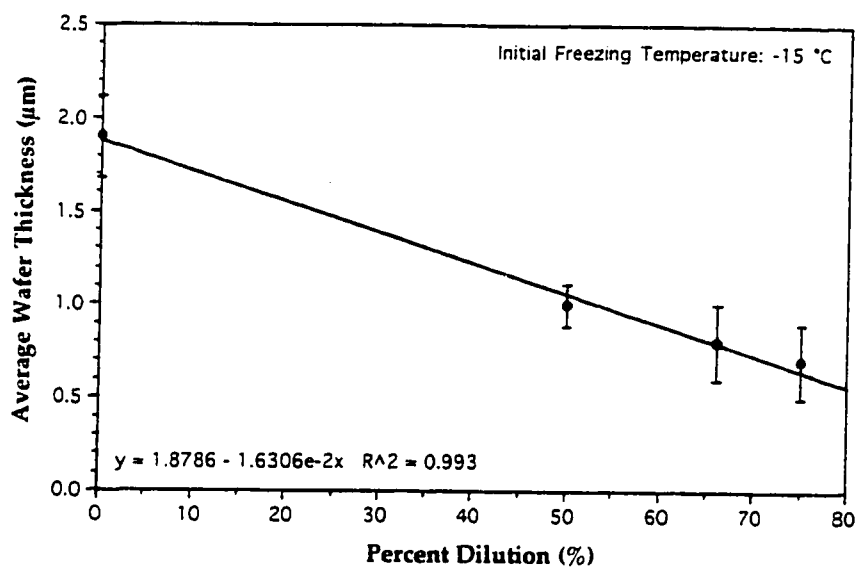


Figure 5.65 Plot of Percent Dilution Versus Average Concentrate Material Thickness (Initial Freezing Temperature -15, Top Sample)

Table 5.32 Summary of Statistical Data for the Thickness of the Concentrated Material for Different Dilutions of Membrane Concentrate Frozen at the Initial Freezing Temperature -15 °C

Percent Dilution*	Mean (μm)	Sample Variance (μm)	Range (μm)
Undiluted (0 %)	1.9	0.22	1.6 to 2.1
50 %	1.0	0.11	0.9 to 1.1
66 %	0.8	0.20	0.5 to 0.9
75 %	0.7	0.20	0.5 to 0.9

* - sample set size equal to 12

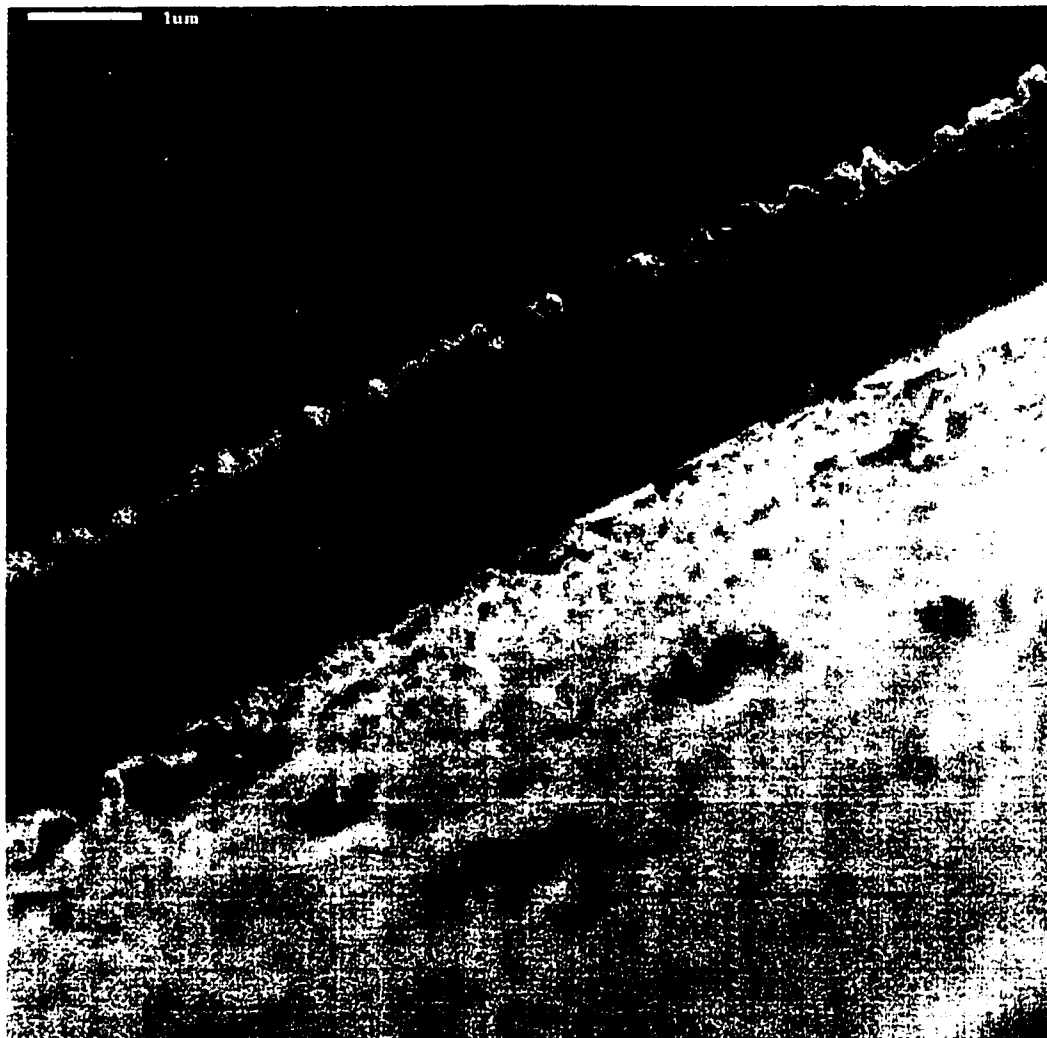


Figure 5.66 High Magnification Electron Microscope Image of a Fractured Concentrated Material Edge Produced by Freezing Membrane Concentrate at the Initial Freezing Temperature -15 degrees Celsius

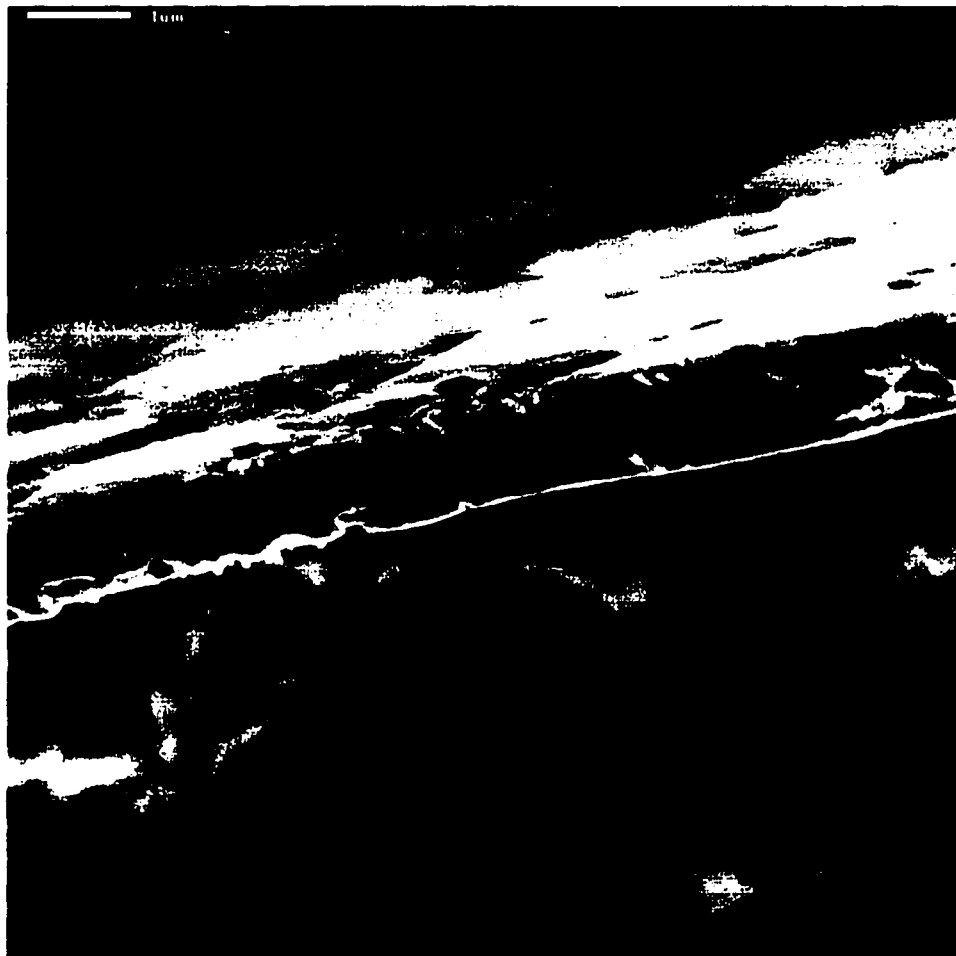


Figure 5.67 High Magnification Electron Microscope Image of a Fractured Concentrated Material Edge Produced by Freezing Membrane Concentrate Diluted to 50 % at the Initial Freezing Temperature -15 degrees Celsius

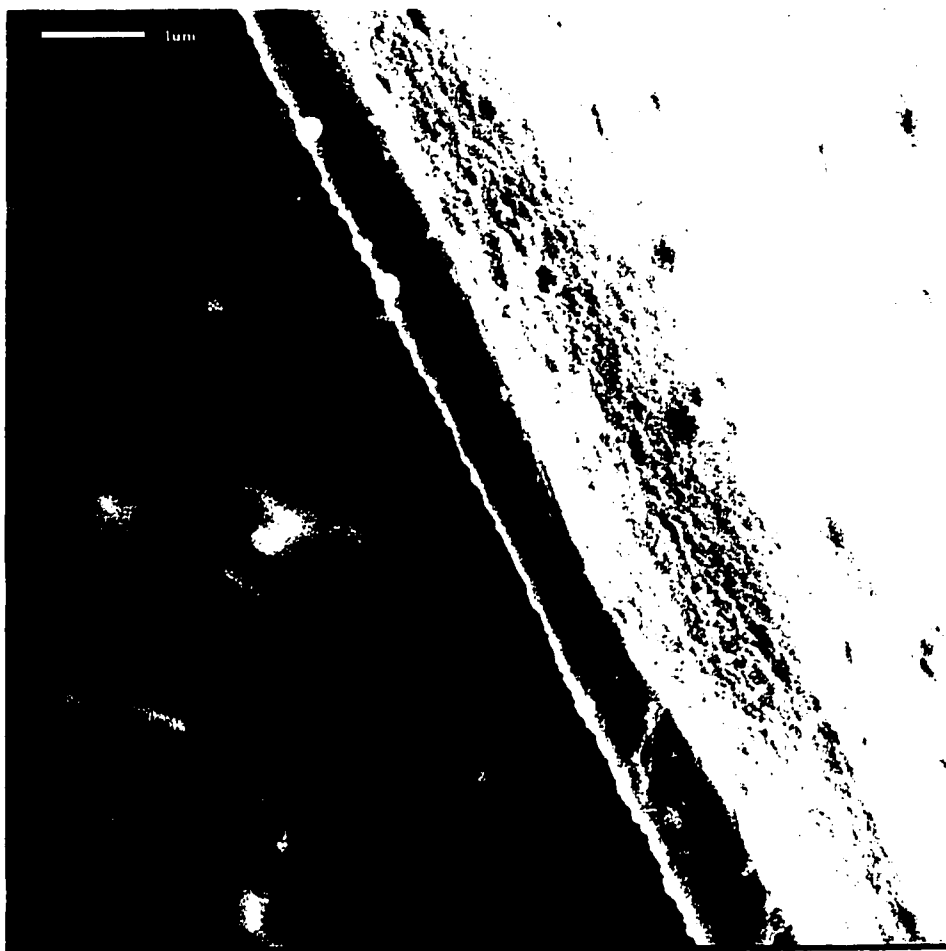


Figure 5.68 High Magnification Electron Microscope Image of a Fractured Concentrated Material Edge Produced by Freezing Membrane Concentrate Diluted to 66 % at the Initial Freezing Temperature -15 degrees Celsius

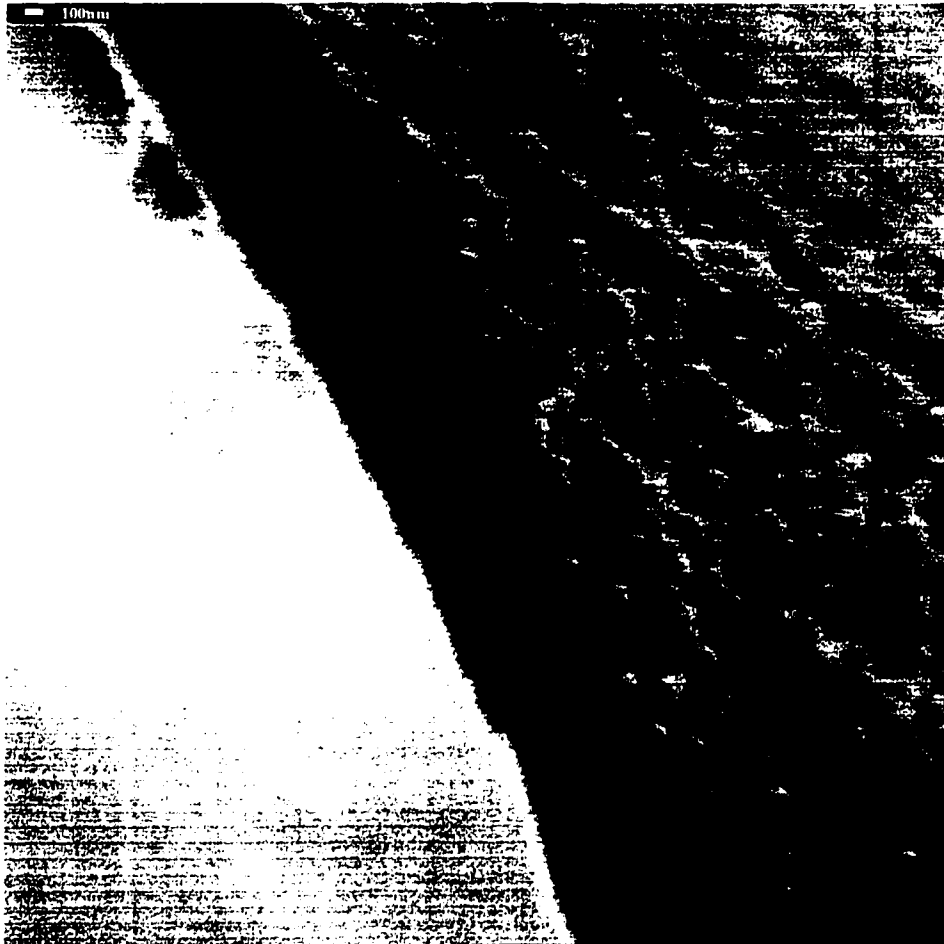


Figure 5.69 High Magnification Electron Microscope Image of a Fractured Concentrated Material Edge Produced by Freezing Membrane Concentrate Diluted to 75 % at the Initial Freezing Temperature -15 degrees Celsius

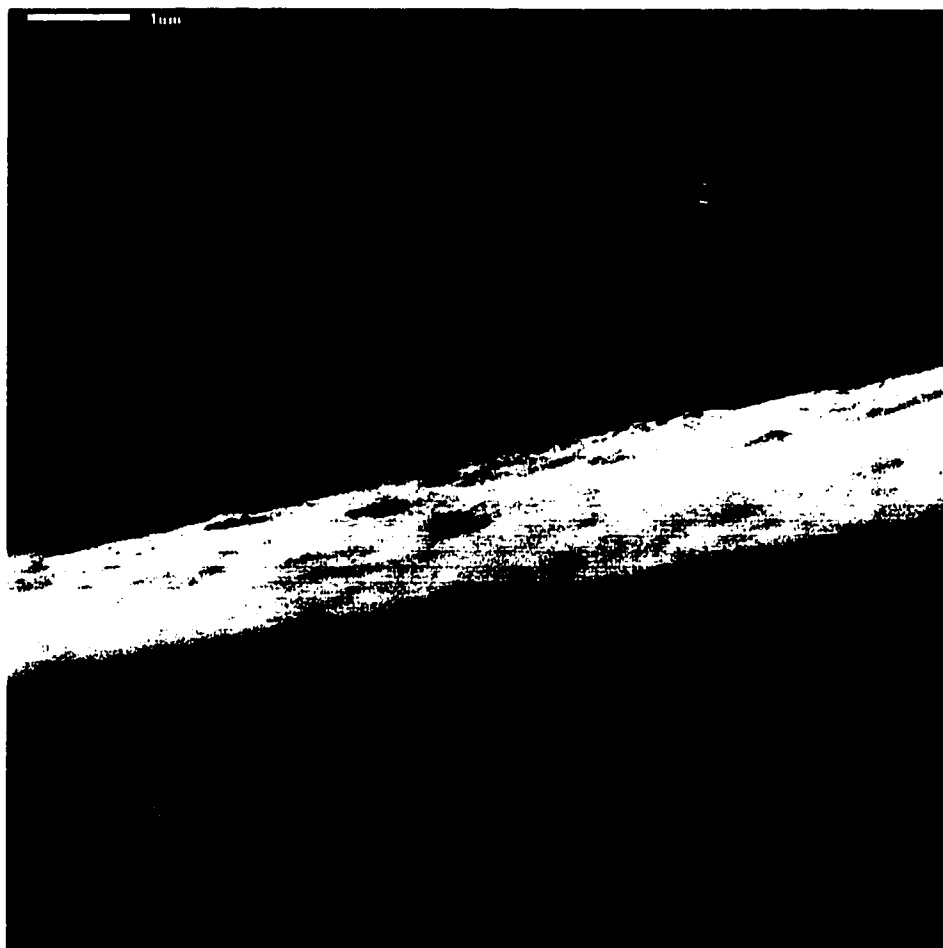


Figure 5.70 High Magnification Electron Microscope Image of a Fractured Concentrated Material Edge produced by Freezing Membrane Concentrate Diluted to 80 % at the Initial Freezing Temperature -15 degrees Celsius

Analysis of variance and the Duncan Multiple Range Test were used to determine which average thicknesses for the different percent dilutions were significantly different at a 95 % confidence limit. The results of this analysis are presented in Appendix B. From the analysis it was shown that there are significant differences between all pairs of means with the exception of those average material thicknesses produced at the 66 % dilutions and higher. Average thicknesses reported for concentrate dilutions beyond 66 % were not significantly different even though the electron microscope images showed there having occurred additional changes with respect to the material's density and spacing.

Also observed, aside from changes in thickness, were changes with respect to the quantity of the wafers and the overall spacing between them. Shown in Figures 5.71 to 5.74 are electron microscope images of the fractured ice surface showing the density and spacing between the concentrated material for the different concentrate dilutions. The spacing between the material increased with respect to dilution, as well as there was a decrease in density. The orientation of the material with respect each other did not change. Summarized in Table 5.33 are the calculated means, sample variances and ranges in spacing with respect to the different concentrate dilutions. The wafer spacing was measured to increase from an average of 122 μm for the undiluted concentrate to an average of 256 μm for the dilution ratio 75 %.

Dilution of the concentrate was not reported to substantially change the effluent's original freezing point. Summarized in Table 5.34 are the freezing point values for the different concentrate dilutions. Diluting the



Figure 5.71 Electron Microscope Photograph of a Fractured Ice Specimen Surface Produced by Freezing Membrane Concentrate Diluted to 50 % at the Initial Freezing temperature -15 degrees Celsius



Figure 5.72 Electron Microscope Photograph of a Fractured Ice Specimen Surface Produced by Freezing Membrane Concentrate Diluted to 66 % at the Initial Freezing Temperature -15 degrees Celsius



Figure 5.73 Electron Microscope Photograph of a Fractured Ice Specimen Surface Produced by Freezing Membrane Concentrate Diluted to 75 % at the Initial Freezing Temperature -15 degrees Celsius



Figure 5.74 Electron Microscope Photograph of a Fractured Ice Specimen Surface Produced by Freezing Membrane Concentrate Diluted to 80 % at the Initial Freezing Temperature -15 degrees Celsius

Table 5.33 Summary of Statistical Data Concerning the Difference in Spacing Between the Concentrated Material for Different Dilutions of Membrane Concentrate Frozen at the Initial Freezing Temperature -15 °C

Percent Dilution*	Mean (μm)	Sample Variance (μm)	Range (μm)
0 % Undiluted	122	7.6	100 to 133
50 %	171	16.1	150 to 200
66 %	182	45.7	133 to 250
75 %	256	24.5	217 to 333

*sample set size: 12

Table 5.34 Freezing Point Values for the Diluted Membrane Concentrate Solutions

Percent Dilution*	Freezing Point (°H)	Freezing Point (°C)
Undiluted (0 %)	0.0237	0.0237
50 %	0.0121	0.0125
66 %	0.0082	0.0088
75 %	0.0059	0.0065

concentrate by 75 % was measured to decrease the freezing point depression of the undiluted concentrate by 0.017 °C.

The effect concentration has on treatment performance was investigated by diluting the membrane concentrate with distilled water followed by unidirectional freezing of the diluted solutions. The initial work presented focused on determining the changes that occurs to the morphology of the concentrated material with respect to concentrate concentration. The second part of these experiments were to determine the applicable minimum concentration limit, if any, for the concentrate which if exceeded cannot be effectively treated by freeze-thaw. Initial work presented thus far suggests that high removal efficiencies can be obtained for effluents of low and high constituent concentrations provided that freeze-thaw is conducted at the optimum conditions. That is slow freezing rates coupled with long storage times at cold temperatures followed by rapid thawing are required to obtain high removal efficiencies, regardless of concentration. Tests conducted at the optimum conditions on Eop effluent and membrane concentrate produced high removal efficiencies with respect to color (>73 % in the top 70 % liquid volume) regardless of their variable concentrations. The difference in separation efficiencies between the two effluents, neglecting the differences in their organic size distributions, were similar with the higher removals associated with the lower concentration Eop effluent.

Summarized in Table 5.35 are the average percent color removals in the top 70 % liquid fraction for various dilutions of membrane concentrate unidirectionally frozen at the initial freezing temperature -2 °C. All samples were thawed bottom up at a temperature of 24 °C. From

examination of this table it can be seen that the magnitude of the percent color removal began to decrease below the dilution ratio of 50 %. Between the dilution range of 0 to 51 % the average percent color removals were similar, even though the initial and final color concentrations were substantially different. The relative significance of this information is that within a particular color concentration, which for membrane concentrate was between zero to 51 % dilution (corresponding to a color concentration of between 12,500 CU to 6,130 CU), the anticipated percent color removals would not be substantially different to suggest that concentration can be neglected as a parameter in the modeling. However, color concentrations below 6,130 CU requires concentration be included as an independent variable in the regression model.

5.5 SIZE FRACTIONATION AND PHYSICAL PROPERTIES OF THE CONCENTRATED MATERIAL

Membrane concentrate was size fractionated to separate its low and high molecular weight fractions to determine the effect concentration and molecular size has on the morphology of the concentrated material produced during freezing.

5.5.1 PROCEDURE

A Minitan Acrylic Ultrafiltration System by Millipore Direct was used to size fractionate the alkaline extraction stage membrane concentrate. The concentrate's constituents were concentrated into two size fractions; those salts and organics with a molecular weight of approximately < 5000 Daltons, and those organics with a molecular weight of approximately > 5000 Daltons.

5.5.2 RESULTS AND DISCUSSION

Summarized in Table 5.36 are the chemical compositions of each relative size fraction for membrane concentrate processed to isolate its low and high molecular weight compounds. As expected a majority of the constituents in the membrane concentrate were larger than the approximate molecular weight size 5000 Daltons.

The electron microscope images presented are for having frozen each size fraction of the membrane concentrate unidirectionally at the initial freezing temperature -15 °C. Ice specimens were collected from the top and bottom portions of each ice column. The morphology of the concentrated material collected from the top portion of the ice column representing the above 5000 MW fraction was string-like in appearance with no apparent pattern or orientation (Figure 5.75). High magnification electron microscope image (Figure 5.76) of this concentrated material revealed it as being comprised of very fine, interconnected smooth strands of material. The morphology of the concentrated material collected from the top portion of the ice column representing the below 5000 MW fraction was substantially different. Figures 5.77 and 5.78 shows the concentrated material to be "disk" like in appearance with their size observed to vary. Absent was the appearance of thin string-like strands as observed for the high molecular weight fraction.

The morphology of the concentrated material collected from the bottom portion of the ice column was substantially different between fractions in comparison to that observed in top samples. Figure 5.79 shows the concentrated material representative of the above 5000 MW fraction to

Table 5.35 Average Percent Color Removals in the Top 70 % Liquid Fraction for Various Dilutions of Membrane Concentrate Frozen Unidirectionally at the Initial Freezing Temperature -2 °C and Thawed bottom up at 24 °C

Percent Dilution (%)	Final pH	Initial Color (CU)	Final Color* (CU)	Average Percent Color Removal (%)
stock, no dilution	9.65	12,500	3,350	73
51 %	8.65	6,130	1,470	76
78 %	7.95	2,780	1,130	60
90 %	7.45	1,300	780	40

* Average color concentration in the top 70 % liquid fraction, All runs conducted in duplicate

Table 5.36 Chemical Composition of the Membrane Concentrate and its Low and High Molecular Weight Fractions

Concentrate Type	Color (CU)*	Total Dissolved Solids (mg/L)*	Chemical Oxygen Demand (mg/L)*
Eop Membrane Concentrate	13,300	14,300	14,500
Eop Concentrate (> 5000 MW)	21,100	18,500	19,200
Eop Concentrate (< 5000 MW)	2,150	6,120	6,560

* - average value



Figure 5.75 Electron Microscope Photograph of the Concentrated Material Structure Observed for the Above 5000 MW Fraction for Membrane Concentrate Frozen at the Initial Freezing Temperature -15 degrees Celsius (Top Sample Portion)



Figure 5.76 High Magnification Electron Microscope Image of the Concentrated Material Representative of the Above 5000 MW Fraction (Top Sample Portion)

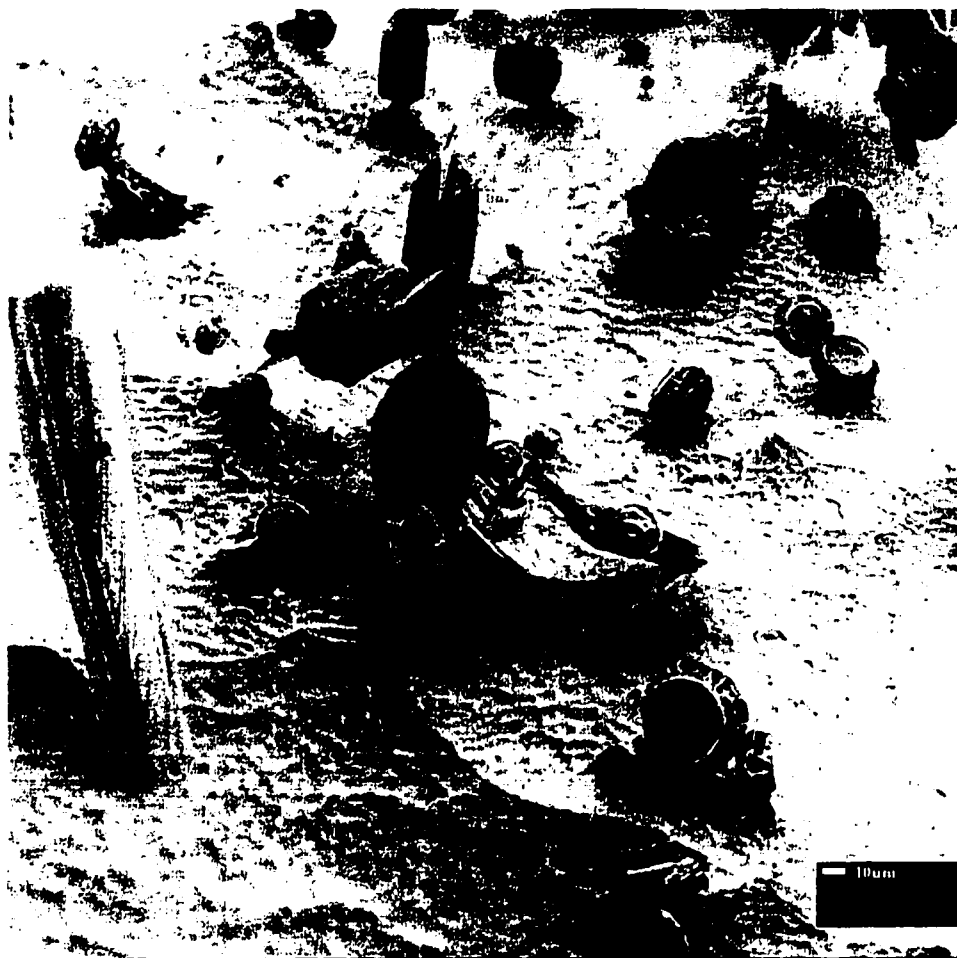


Figure 5.77 Electron Microscope Photograph of the Concentrated Material Structure Observed for the Below 5000 MW Fraction for Membrane Concentrate frozen at the Initial Freezing Temperature -15 degrees Celsius (Top Sample Portion)

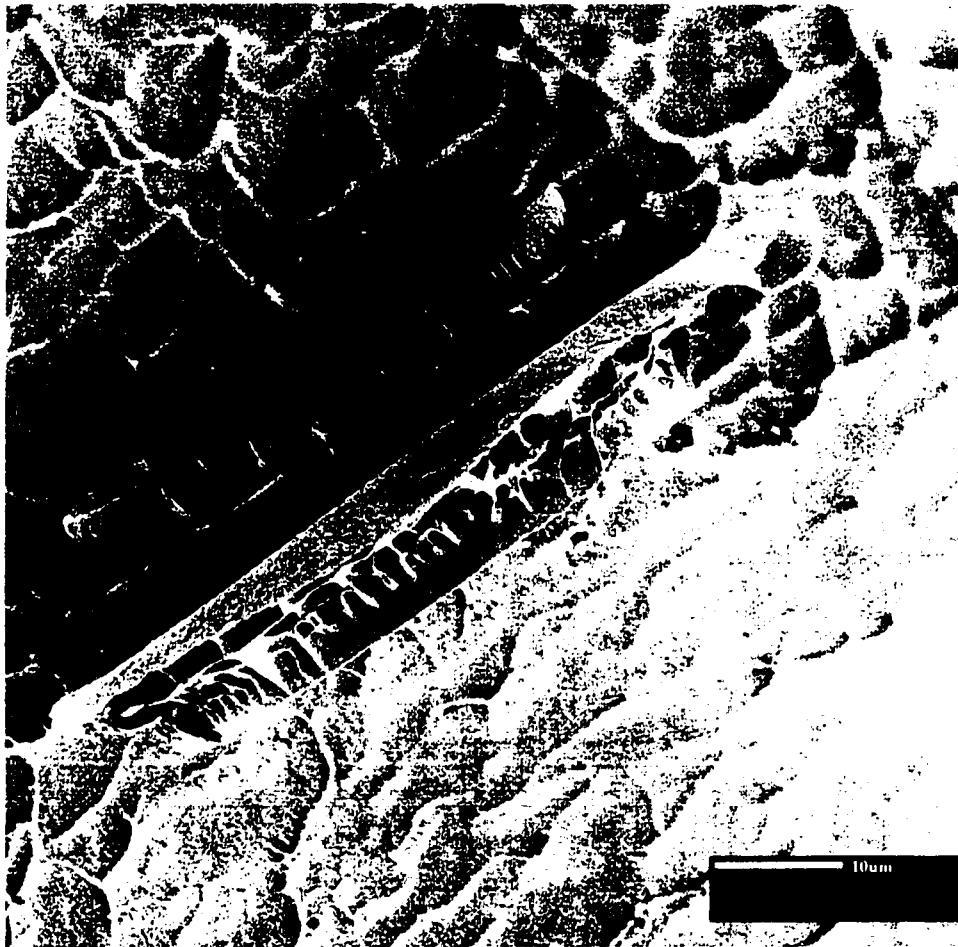


Figure 5.78 High Magnification Electron Microscope Image of the Concentrated Material Representative of the Below 5000 MW Fraction (Top Sample Portion)



Figure 5.79 Electron Microscope Photograph of the Concentrated Material Structure observed for the Above 5000 MW fraction for Membrane Concentrate Frozen at the Initial Freezing Temperature -15 degrees Celsius (Bottom Sample Portion)

be less strand like in appearance. Instead, the concentrated material was more wafer-like in appearance. Similarly, Figure 5.80 shows the concentrated material representative of the below 5000 MW fraction also to be wafer-like in appearance, with there being fewer disk like shaped structures present. High magnification electron microscope images of the surface morphology of the wafer-like concentrated material (bottom samples) shows the below 5000 MW fraction to have a fine, smooth surfaced texture (Figure 5.81). Oppositely, the wafer-like structures produced from the high molecular weight fraction were pitted and rough looking (Figure 5.82). The wafer-like structures representative of the raw concentrate had a surface morphology that resembled something in between the low and high molecular weight fractions (Figure 5.83).

The morphological differences in regards to shape between the concentrated material produced with respect to the different effluent fractions were believed to be due to concentration differences. The shape of the concentrated material for the low concentration, low molecular weight fraction were disk like in appearance. Where as, the shape of the concentrated material for the high strength, high molecular weight fraction were wafer like in appearance. The data suggests that the high molecular weight material was more amenable to forming continuous interconnected concentrated material during freezing. Morphological differences in regards to surface texture were believed to be the related to organic type and size. The low molecular weight organics were observed to produce a smooth surface versus the rough looking texture produced by the high molecular weight organics.



Figure 5.80 Electron Microscope Photograph of the Concentrated Material Structure observed for the Below 5000 MW fraction for Membrane Concentrate Frozen at the Initial Freezing Temperature -15 degrees Celsius (Bottom Sample Portion)



Figure 5.81 High Magnification Electron Microscope Image of the Concentrated Material Surface Morphology Representative of the Above 5000 MW Fraction (Bottom Sample Portion)

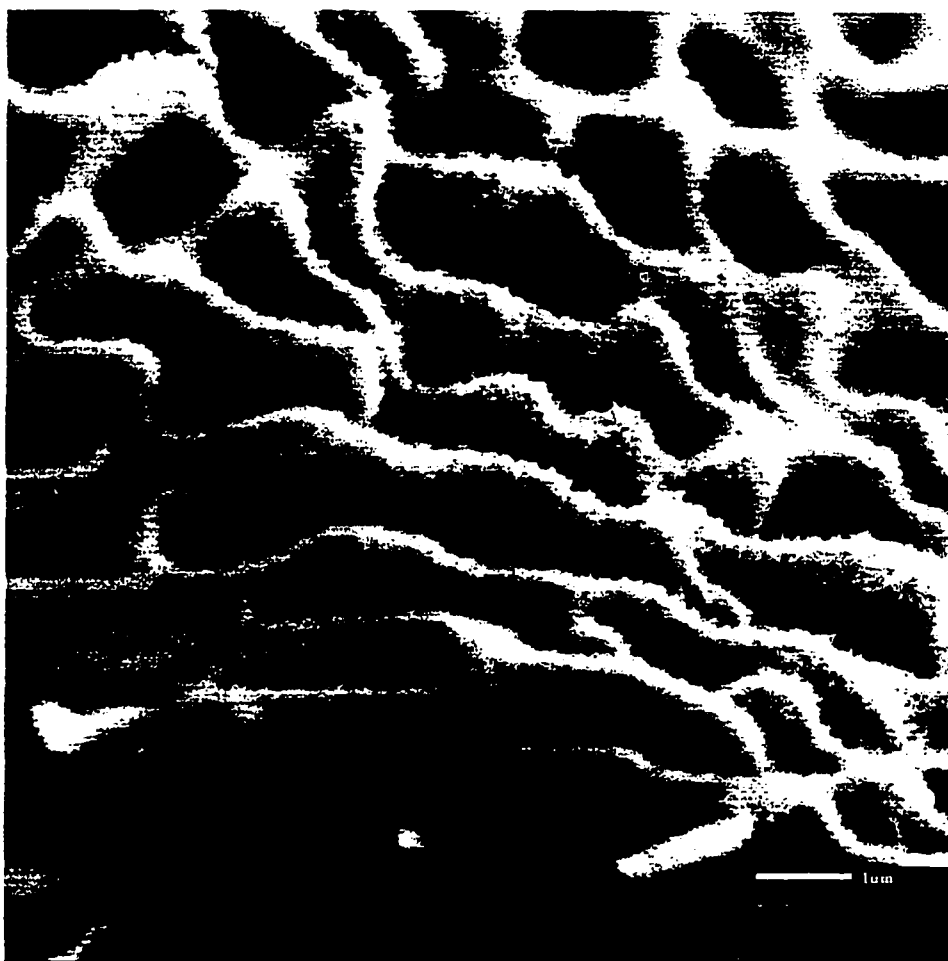


Figure 5.82 High Magnification Electron Microscope Image of the Concentrated Material Surface Morphology Representative of the Below 5000 MW Fraction (Bottom Sample Portion)

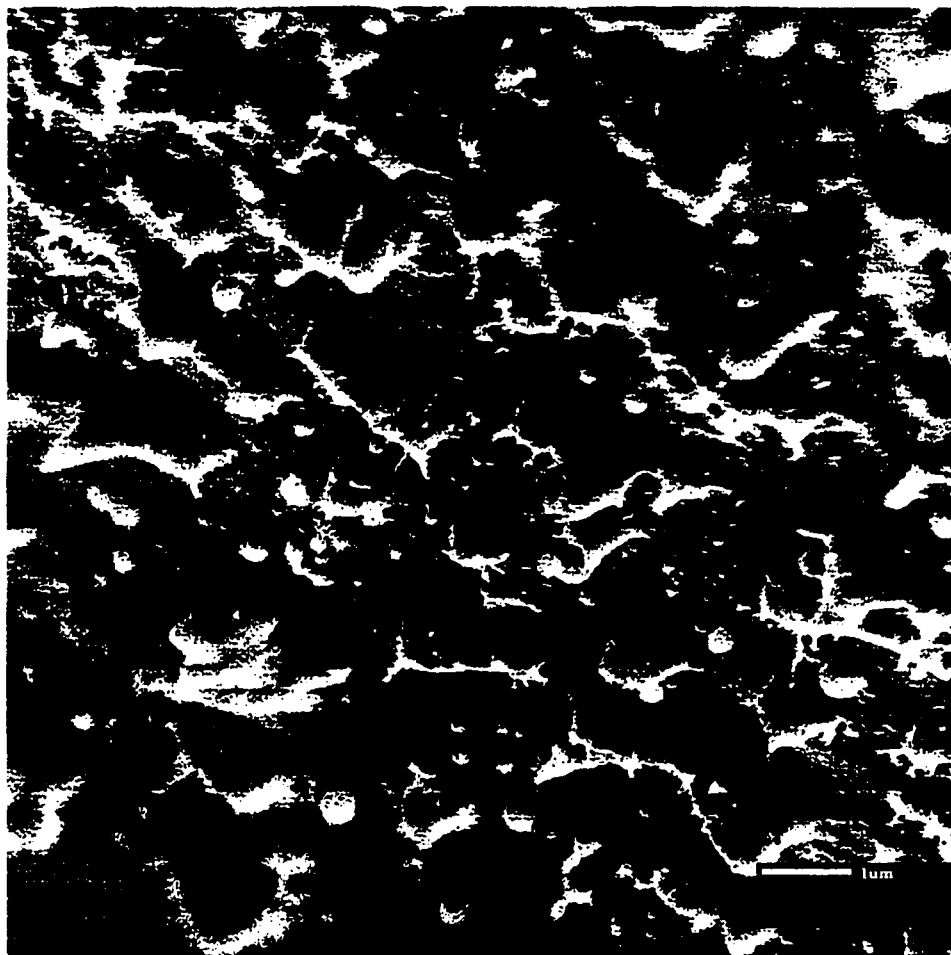


Figure 5.83 High Magnification Electron Microscope Image of the Concentrated Material Surface Morphology Representative of the Membrane Concentrate (Bottom Sample Portion)

6.0 POSTULATED MECHANISMS OF REMOVAL BY FREEZE-THAW

Based on experimental evidence from this study it was postulated that when membrane concentrate or Eop effluent freezes from the surface down, ice crystals build downward in the form of needles. These needles seek available free water molecules for growth by projecting down and outward into the concentrate. As the ice needles thrust into the concentrate, they push aside the contaminants, always seeking more free water molecules for continued growth. Figure 6.1 shows that as the water in the upper layer of the concentrate begins to freeze (b), it creates a thin, upper layer of ice from which ice needles originate (c). During freezing heat is released during cooling with the change of phase. The shape of the needle like projections of the growing ice crystals stem from the variable solute concentration at the ice/liquid interface and the effect it has on causing planar interface breakdown into arrays of cellular projections. Mullins and Sekerka (1964) observed the instability related to the freezing of NaCl as causing the ice to grow in the form of thin planes separated by regions of concentrated brine. This type of phenomena was observed for both experimental water types in which thin planes separated by concentrated material were visible only at the very cold initial freezing temperatures ($\leq -15\text{ }^{\circ}\text{C}$) to suggest that during freezing the ice crystal growth in a temperature gradient, was sufficient to inhibit the nucleation of new crystals for their continuous downward vertical growth. As the ice needles grow, they thrust both downward and outward to concentrate the effluent's constituents into thin highly concentrated zones of concentrate. The outward growth of the ice needles were observed to differ with respect to the initial freezing temperature. At warm initial freezing temperatures

Freeze Concentration of the Constituent Material to
Produce the Wafer-like Structures As Seen From the Side

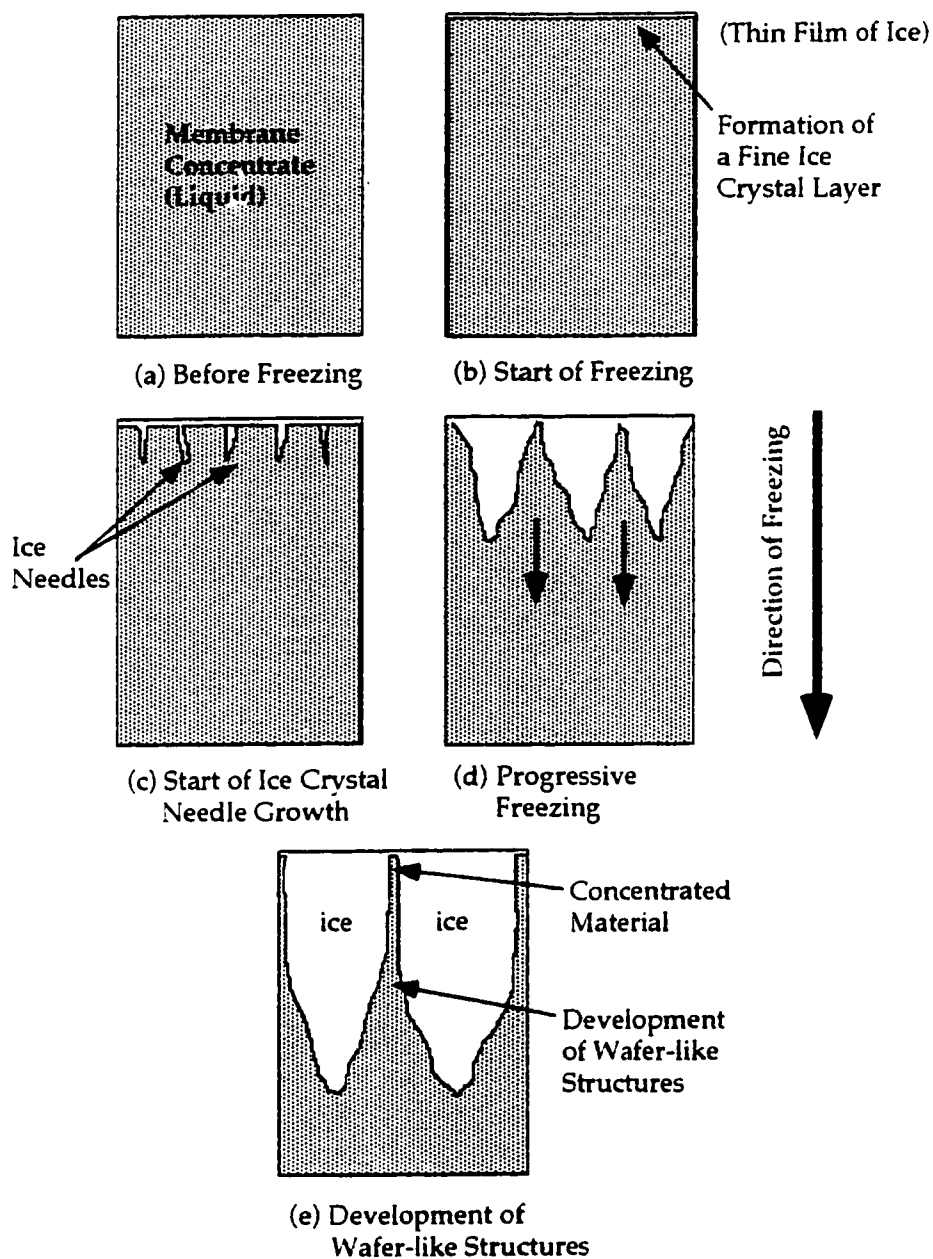


Figure 6.1 Conceptual Model for High Strength Pulp Mill Effluent Freezing

(-2 °C) the ice needles were observed to uniformly grow outwards in a radial pattern. Whereas at the very cold initial freezing temperatures (< -15 °C) the ice needles were observed to grow predominantly in one direction resulting in the sheet like patterns observed. The downward growth of the ice needles into the concentrate was in an uniform fashion (d). This observation was based on the removal of partially frozen concentrate samples where it was observed that the ice front advances in a relatively uniform, orderly fashion. As the ice growth continues, the constituents of the effluent are compressed into thin zones of concentrate to produce zones of fragile concentrated material arranged in "sheet or honey comb" like patterns, depending on the initial freezing temperature, as observed by SEM. In time, the ice crystals dehydrate the captured concentrated material, further compressing the constituents into more compact wafers. It is through this mechanical compression that the constituents are mechanically coagulated with a variety of physico-chemical reactions (electrostatic interactions, adsorption, charge neutralization, and precipitation) occurring. Changing water chemistry within this zone over time affects both the solubility and stability of the constituent matter. Mechanical coagulation occurs from the compression of the double layer of the colloidal organics by indifferent electrolytes. The increase in ionic strength reduces the thickness of the particle's diffuse layer to decrease the repulsive interactions between particles. The result is the disappearance of the activation energy barrier between same charged particles allowing the domination of attractive interactions by Van der Waals forces. Changing solubility will also cause the precipitation of dissolved salts and organics during which constituent material can become entrapped through enmeshment in a precipitate. The

result was the formation of a cohesive concentrated material that was comprised of dissolved, colloidal, and coagulated material. Postulated was that the concentrated material produced during freezing was comprised of a complex mixture of thermodynamically stable and unstable colloids, precipitates and dissolved inorganic/organic matter. Unstable colloids are irreversible. Where as stable colloids are reversible. Mechanical concentration and compression of stable and unstable colloids to cause their contact can increase their rate of aggregation during freezing to form fragile flocs. Postulated was that the stable colloids become entrapped amongst the complex mixture during freezing which ultimately allows for their removal from the bulk solution upon rapid thawing. The dissolved and stable colloid fractions were however, not stable and over time "untangle" themselves from the complex mixture to diffuse back into the bulk solution.

Release of the concentrated material for its removal from the bulk solution was favored by thawing the ice mass from the bottom up. Postulated was the concentrated material was the first component in the ice matrix to thaw followed by the ice surrounding the material and along the ice/liquid interface. When this occurs the highly compact, dehydrated concentrated material is released where it settles under its own density with the rate possibly assisted by the melt water depending on the thawing temperature. At high rates of thawing the melt water flow was predominantly in the downward vertical direction where it greatly increased the removal rate of the material. The increase of which was attributed to differences in the densities between the warming of the melt water and the bulk solution.

6.1 CONCEPTUAL MODEL THAT EXPLAINS EFFLUENT FREEZING AT THE INITIAL FREEZING TEMPERATURE -2 °C

Figure 6.2 conceptualizes, looking from the surface down, the series of transitions that are believed to occur to the constituents of each experimental water as the free available water freezes over the course of freezing to produce the "honey comb" like patterns observed in SEM studies at the initial freezing temperature -2 °C. Unlike that observed at the colder initial freezing temperatures, the slow rate of freezing associated with the warmer initial freezing temperature -2 °C resulted in a much different cross sectional arrangement for the concentrated material. The development of "honey comb" like patterns versus the "sheet" like patterns observed at the colder initial freezing temperatures can be explained by the effect freezing rate has on particle migration. Previous work by others showed the opportunity for particles to be pushed and concentrated at greater distances by the ice-liquid interface before being entrapped by the ice increases with the slower rates of freezing. From examination of SEM images it was observed that the ice crystal growth occurred in all directions perpendicular to its growth producing large diameter ice needles that projected vertically into the ice column. The circular like diameter ice needles suggests the solute concentration, although variable with depth, was relatively uniform around the perimeter of the ice needle. Particle entrapment occurred only when the liquid is no longer able to diffuse into the growing solid behind the concentration of particles.

Particle migration of a different nature was also observed to have occurred locally within the zone of concentrated material. From SEM

Slow Freeze Concentration of the Constituent Material
in the Effluent As Seen From the Surface



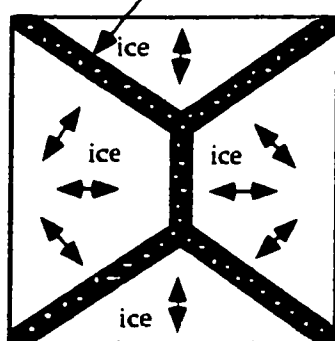
(a) Before Freezing



(b) Start of Ice Crystal Growth

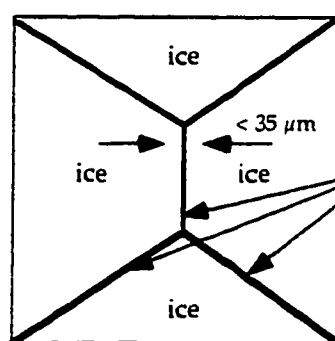
Initial Ice Crystal
Formation Occurs
to Form Circular Ice
Needles to Produce
a "Honey Comb
or Box" like Pattern

Internal segregation of the free
available water inside the wafer



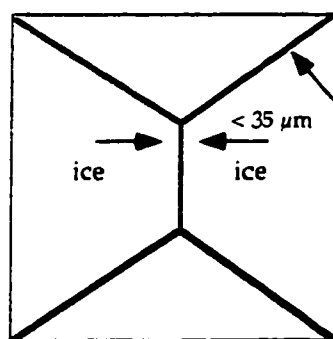
(c) Progressive Freeze
Concentration

Concentrated Material



(d) Effluent Frozen

Thick, Porous
Wafer-like Structures



(e) Mechanical Compression
And Dehydration Over
Time of the Concentrated
Material

Mechanical Compression of
the Concentrated Material
From the Freezing of the Free
Available Water

Figure 6.2 Steps Describing the Formation of the Concentrated Material
Observed at the Initial Freezing Temperature -2°C

photographs it was observed that the free available water contained in the highly concentrated zone of material freezes to further segregate the constituents within the zone producing a highly porous wafer like structure. Unknown exactly was how the ice crystal growth within the zone of concentrated material was initiated. However it is postulated that the appearance of small ice crystals in the wafer structure occurs by nucleation. This is supported by the fact that the ice crystals do not extend to great distances into the wafer structures.

6.2 CONCEPTUAL MODEL THAT EXPLAINS EFFLUENT FREEZING AT THE INITIAL FREEZING TEMPERATURES -15 °C AND -25 °C

At the initial freezing temperatures -15 °C and -25 °C the free available water in the membrane concentrate froze to concentrate the constituents into organized, well structured patterns of thin concentrated zones. Figure 6.3 conceptualizes, looking from the surface down, the series of transitions that are believed to occur to the constituents as the free available water freezes. Following the formation of a thin, upper ice crystal layer, arrays of cellular ice crystal needles are projected downward into the concentrate (b). These ice needles grow both downward and outward. With the nucleation of new crystals inhibited, the ice crystals grow continuously and longitudinally over large distances forming long continuous sheets. The formation of these long continuous planes of ice causes the constituents to be concentrated into thin wafer-like structures that were oriented parallel and at approximately equal distances from each other (c) & (d). The distance between wafers were a function of the concentrate's concentration and freezing rate.

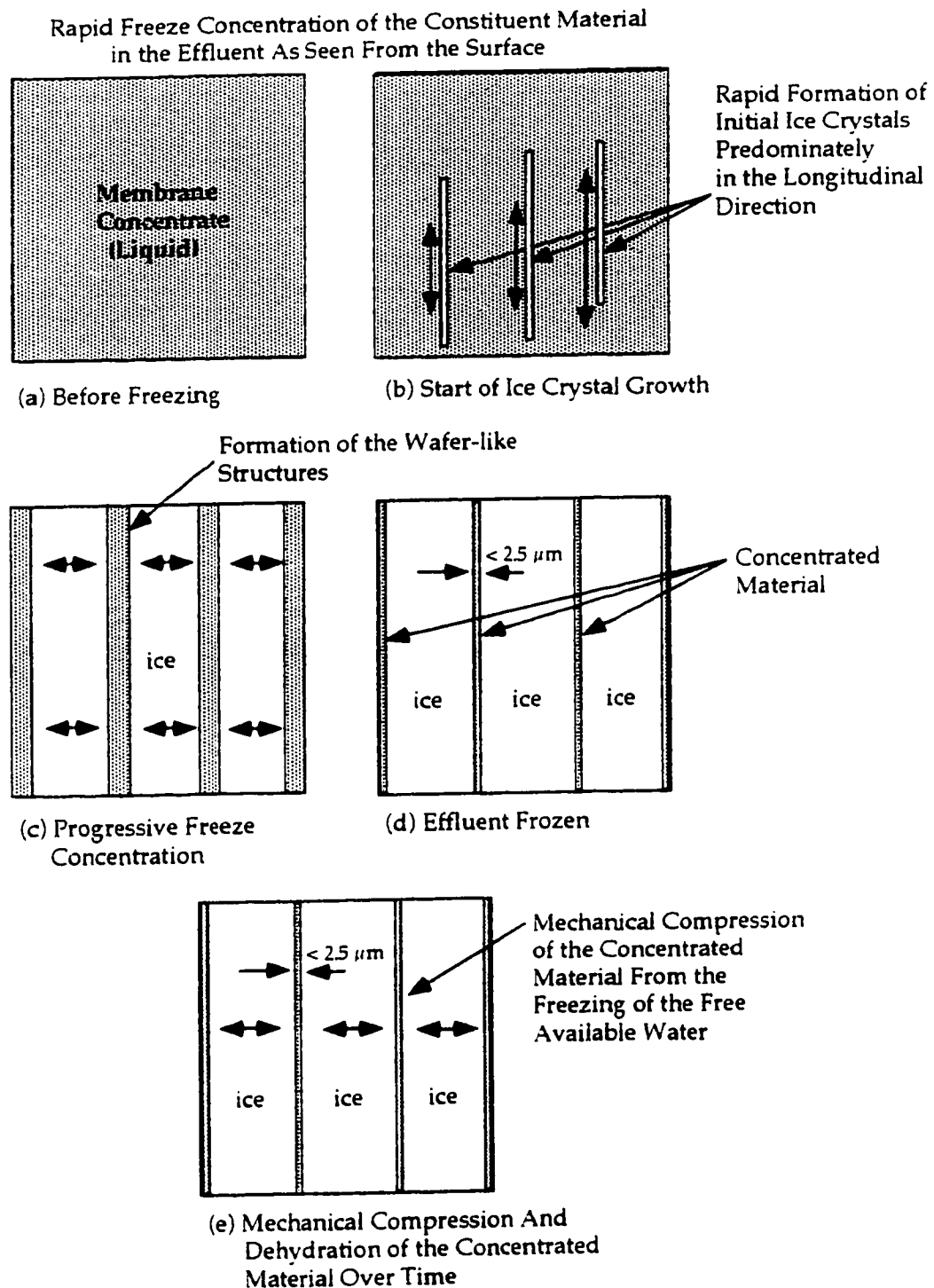


Figure 6.3 Steps Describing the Development of the Concentrated Material Observed at the Initial Freezing Temperatures -15 and -25 °C

7.0 CONCENTRATED MATERIAL STABILITY STUDIES

7.1 PROCEDURE

Experimental studies were conducted to examine the stability of the concentrated material over time for each experimental water following treatment by freeze-thaw to determine the tendency of the settled material to dissolve back into the bulk solution. Following treatment by freeze-thaw samples were sealed, covered to prevent the transmission of light and allowed to stand undisturbed at a room temperature of 24 °C for a period of approximately 4 weeks. Composite samples were collected in duplicate at the following time intervals: 3 days, 1 week, 2 weeks, and 4 weeks. Controls comprising of the untreated effluent were allowed to stand undisturbed for 4 weeks during which they were sampled at the same intervals as given above for color to determine the percent change with respect to time. The purpose of the controls were to determine the change in color due to sample degradation possibility from post precipitation and biological activity.

7.2 RESULTS AND DISCUSSION

The data collected from stability studies was used to develop an operational relationship which then could be used by operations to determine the drain time for the upper liquid fraction to achieve a desired performance level. This operational relationship is applicable only when the freezing bed is designed to recover the relatively clear effluent by drawing it via a weir system. The upper liquid fraction represents the top 70 % liquid volume of the thawed treated effluent. Multiple linear regression analysis was used utilizing the variable selection technique of

stepwise regression to develop models that represent the functional relationship given below for each experimental water type.

$$t_D = k f(C_t/C_o, T_F) \quad (7.1)$$

where;

t_D = time to drain supernatant after thawing, (hours)

k = constant

C_t/C_o = color concentration ratio

C_t = color concentration in the top 70 % liquid
volume at time t , (CU)

C_o = initial color concentration, (CU)

T_F = initial freezing temperature, (°C)

The models developed are valid only under the following conditions.

<u>Independent Variables</u>	<u>Range</u>
Initial freezing temperature	-2 °C to -15 °C
Method of thaw	Bottom-up
Liquid depth	150 mm
Thawing temperature	24 °C
Number of freeze-thaw cycles	1

7.2.1 ALKALINE EXTRACTION STAGE MEMBRANE CONCENTRATE

The concentrated material removed by freeze-thaw was observed to diffuse back into the bulk solution over time. The rate of color dispersion was reported to differ with respect to the initial freezing temperature. The

general tendency of the data was the rate of color dispersion increased as the initial freezing temperature increased, of which the differences can be attributed to several factors. The most important was the difference in the concentration gradients between the bottom liquid portions representative of the material removed and concentrated by freeze-thaw. The highest percentage of waste constituents removed and concentrated in the bottom sample portion by freeze-thaw was at the initial freezing temperature -2°C . A second possible factor, although it could not be accurately measured relates to breakup of the concentrated material during thawing. In preceding sections it was shown decreasing the initial freezing temperature decreased the overall thickness of the concentrated material produced during freezing. This resulted in what appeared in SEM studies of thawed ice samples to produce a correspondingly increase in the fragility of the concentrated material. Postulated was break-up attributes to the rate of diffusion of the concentrated material back into solution (i.e., the time period required for the concentrated material to mechanically break-up or "untangle" itself under quiescent conditions). Thirdly, relates to biological degradation of the effluent in which chemical transformations are carried out by living microorganisms. Biological degradation was observed to affect the Eop effluent more so than the membrane concentrate over the same time period. For example, the color concentration in the Eop effluent was reported to decrease by significant amounts over time. Where as the color concentration in the membrane concentrate was reported to increase by significant amounts over time. The effect of which may be related to differences in concentration, molecular weight, and the ratio of soluble to colloidal/suspended organic matter between each effluent type. The membrane concentrate was also

comprised primarily of large molecular weight organics which when broken down through biological activity can increase the effluent's color intensity.

Summarized in Table 7.1 are the regression results (Appendix C). Tests on the individual regression coefficients showed that all the variables contributed significantly to the model. The adjusted coefficient of multiple determination R^2 was 0.997 to indicate that about 99.70 % of the variability in the changes reported for the top 70 % sample portion with respect to time were explained using the independent variables: initial freezing temperature and color concentration ratio. Residual analysis was performed on each independent variable to judge the model's adequacy. From examination of Figures 7.1 to 7.3 it can be seen that there were no severe deviations from normality. The operational model designed to predict the time period following treatment for when to drain to obtain a desired effluent quality in the top 70 % liquid fraction is depicted in equation 7.2.

$$t_D = -649.490 + 2603.607 C_R + 8.294 T_F + 21.476 C_R T_F \quad (7.2)$$

where;

t_D = time period when to drain the top 70 % liquid fraction,
(hours)

$C_R = C_t / C_o$, $C_o = 12,500$ CU

T_F = initial freezing temperature ($^{\circ}\text{C}$)

Table 7.1 Best Multiple Linear Regression Model as Determined by Stepwise Regression Representing the Desired Drain Time to Begin Collection of the Treated Effluent for Membrane Concentrate Treated by Freeze-thaw

Independent Variable	Coefficient	Standard Error	Standard Coefficient	Tolerance	T	P (two-tailed test)
Constant	-649.409	21.693	0.000	N/A	-29.753	0.000
Color Concentration Ratio	2603.607	58.207	1.192	0.251	44.730	0.000
Freezing Temperature	8.294	2.101	0.199	0.070	3.948	0.001
Color Concentration Ratio* Freezing Temperature	21.476	5.025	0.267	0.046	4.274	0.001

Dependent Variable: Desired Drain Time (hours)

Multiple R: 0.999, Squared Multiple R: 0.0997, Adjusted Squared Multiple R: 0.997

Source	SUM-OF-SQUARES	DEGREES OF FREEDOM	MEAN-SQUARES	F-RATIO	P
REGRESSION	1465175.619	3	488391.873	1864.566	0.000
RESIDUAL	4190.931	16	261.933		

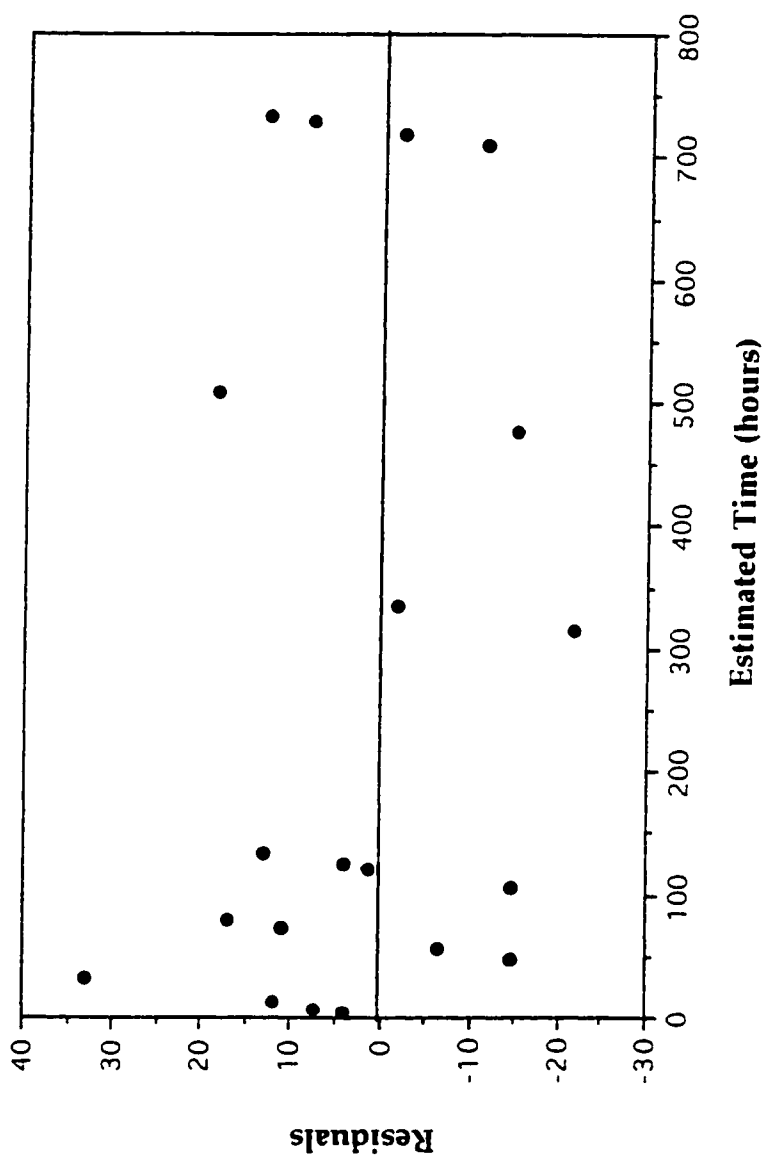


Figure 7.1 Plot of Residuals Against Estimated Time for Concentrate Stability Produced From Freeze-thaw of Membrane Concentrate

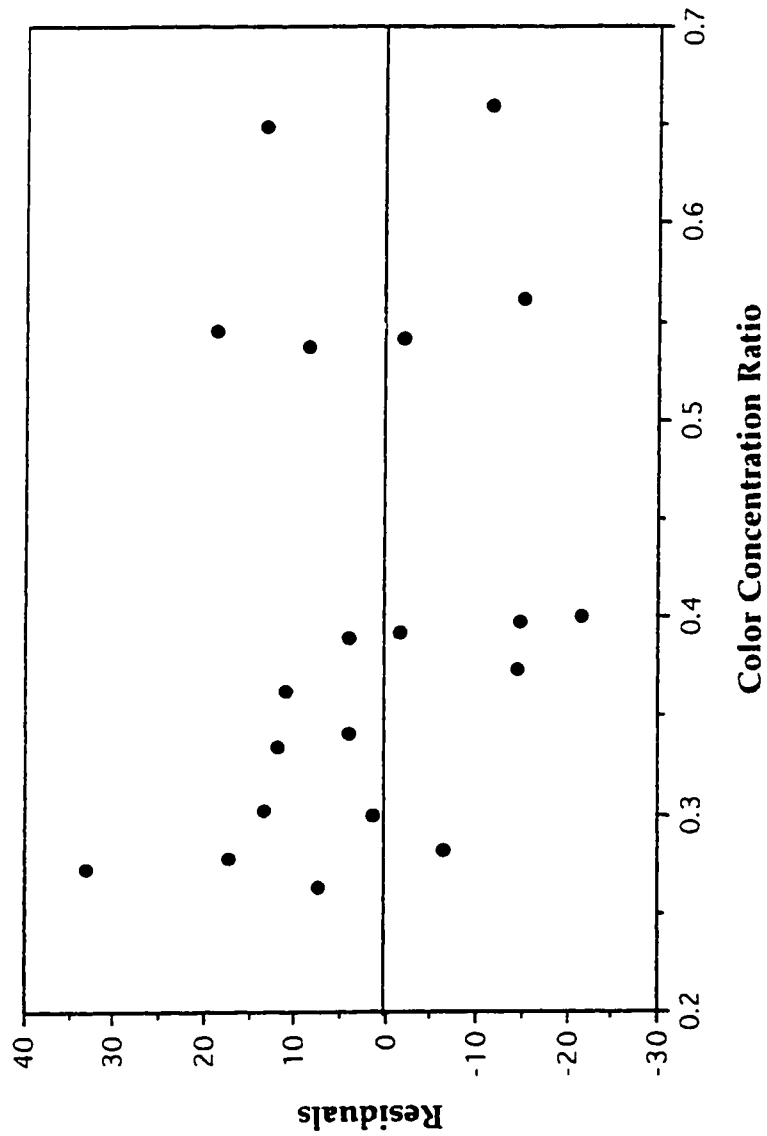


Figure 7.2 Plot of Residuals Against Color Concentration Ratio for Concentrate Stability Produced From Freeze-thaw of Membrane Concentrate

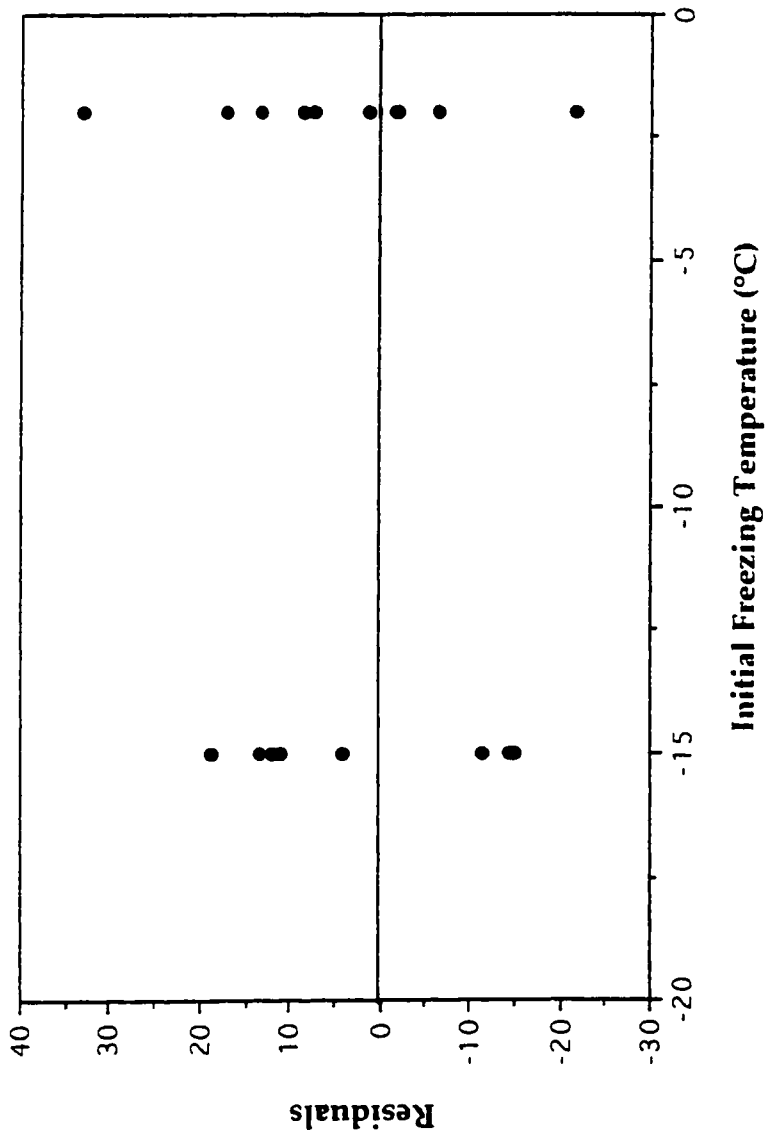


Figure 7.3 Plot of Residuals Against Initial Freezing Temperature for Concentrate Stability Produced From Freeze-thaw of Membrane Concentrate

7.2.1.1 CONTROL

Plotted in Figure 7.4 are the color concentrations for the different liquid fractions with respect to time for the untreated sample left to stand undisturbed at room temperature (24 °C). Figure 7.4 shows the color concentration having changed over time with it first measured to have increased in the bottom liquid fraction. The color concentration was measured to increase by a maximum of 500 CU in the bottom liquid fraction over approximately a 4 week time period, with the overall color concentration in the control sample reported to increase by 400 CU. The reported change in color concentrations for the different liquid fractions can be attributed to biological activity. For example, the membrane concentrate was comprised primarily of high molecular weight (> 8000) color bodies which are known to resist biological degradation. However, when broken down the increase observed was not unlike that reported in other studies where color intensity was actually reported to increase during biological treatment. Color bodies with molecular weights around 5,600 have been reported as being responsible for the largest portion of the color measured.

7.2.1.2 INITIAL FREEZING TEMPERATURE: -2 °C

Plotted in Figures 7.5 to 7.6 are the color concentrations for different liquid fractions left to stand undisturbed with respect to time for membrane concentrate treated by freeze-thaw at the initial freezing temperature -2 °C. The change in color concentration over time for each liquid fraction occurred under quiescent conditions. Because of biological

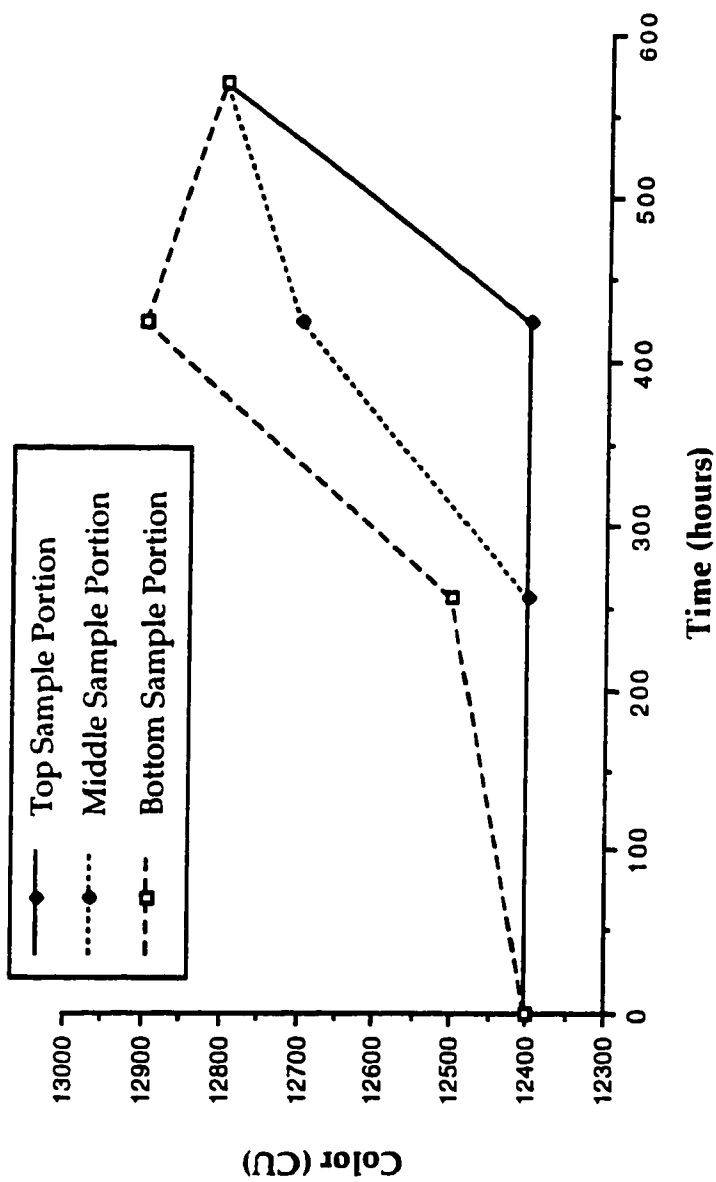


Figure 7.4 Change in Color Concentration in the Top, Middle, and Bottom Sample Portions of the Control Sample Over Time

degradation, Fick's second law by itself, which incorporates the equation of continuity, cannot be used to explain the rate of color dispersion.

The rate of color dispersion occurred predominantly in one direction only, with the mass diffusing from the bottom up into the bulk solution to suggest the concentrated material produced during freezing was not entirely a floc and that the floc produced was reversible. Conducting a simple mass balance reveals a majority of the color was accounted for when adding up of all three liquid fractions at time zero which suggests simple agitation from chemical analysis was sufficient to break-up and resuspend the concentrated constituent material. It also indicates the material was poorly compressed during freezing in which there did not occur a substantial decrease in color from possible precipitation and flocculation as observed for the more compact concentrated material zones produced at the colder initial freezing temperatures. Examination of Table 7.2 shows the resultant color concentrations as actually decreasing with time which may be attributed to biological degradation of the weakly concentrated effluent fractions and from post chemical precipitation. Post chemical precipitation occurred and was more pronounced in highly concentrated effluent fractions at this initial freezing temperature than at any other. The type of precipitate included substantial amounts of calcium carbonate which may have enmeshed organic material during precipitation. The relationship between color and time was linear with a almost perfect positive correlation (R^2 values ranged from 0.996 to 1.000), regardless of liquid fraction.

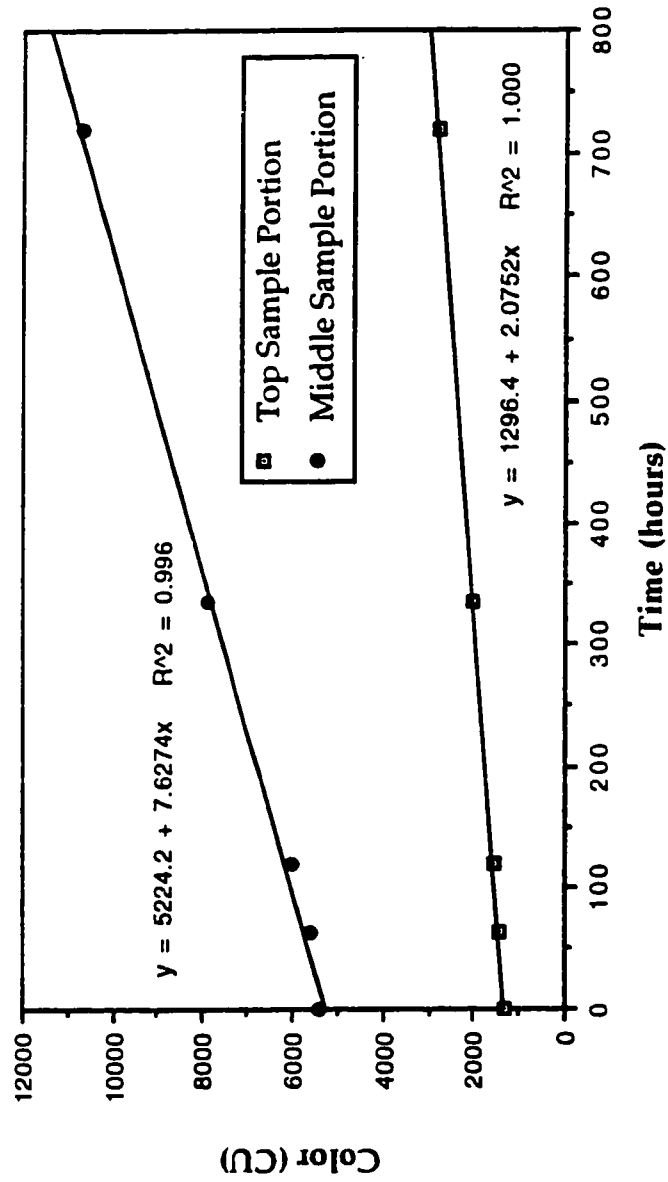


Figure 7.5 Plot of Change in Color Concentration in the Top and Middle Sample Portions with Respect to Time for Membrane Concentrate Frozen at the Initial Freezing Temperature -2 °C, Thawed Bottom Up at 24 °C and Then Left to Stand Undisturbed at 24 °C

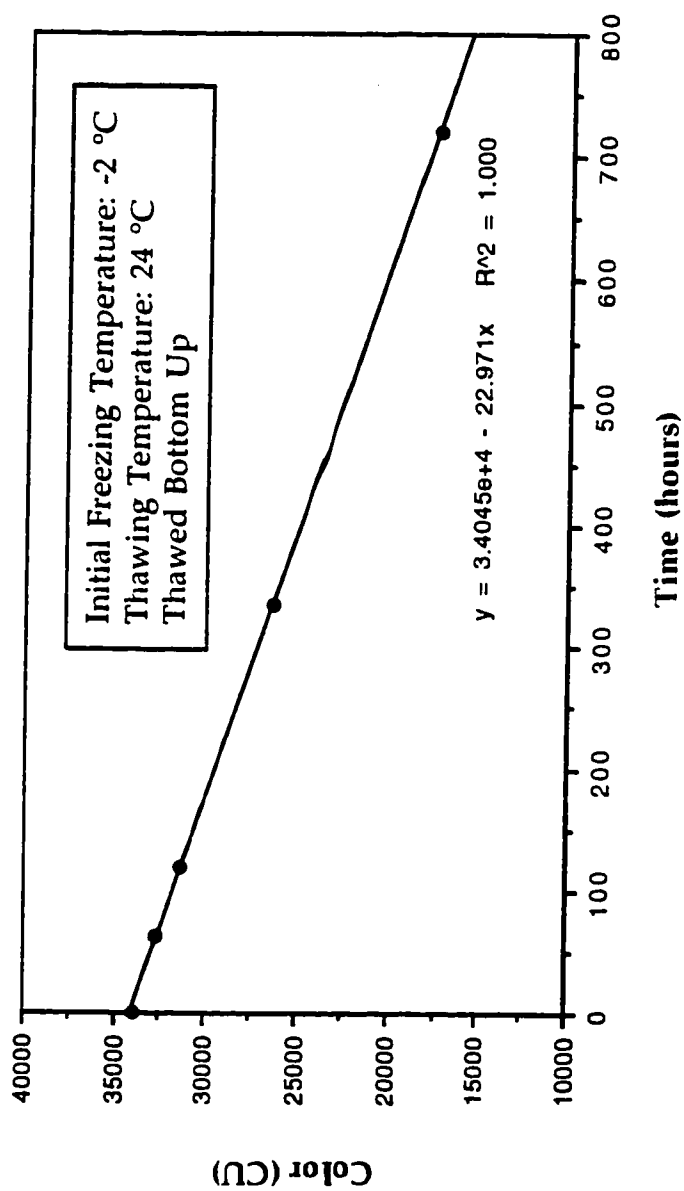


Figure 7.6 Plot of Change in Color Concentration in the Bottom Sample Portions with Respect to Time for Membrane Concentrate Frozen at the Initial Freezing Temperature -2 °C, Thawed Bottom Up at 24 °C and Then Left to Stand Undisturbed at 24 °C

7.2.1.3 INITIAL FREEZING TEMPERATURE: -15 °C

Plotted in Figures 7.7 to 7.8 are the color concentrations for different liquid fractions left undisturbed with respect to time for membrane concentrate treated by freeze-thaw at the initial freezing temperature -15 °C. The relationships observed for color with respect to time were similar to that reported for the initial freezing temperature -2 °C with the primary differences being in regards to the rate of color dispersion. The calculated slopes representing the decrease in color concentration in the bottom sample portions were -22.97 at the freezing temperature -2 °C and -6.19 at the freezing temperature -15 °C, respectively. The rate of color dispersion was approximately 3.7 times lower than that calculated for the initial freezing temperature -2 °C. A simple mass balance reveals a good majority of the color was accounted for when adding up of all three liquid fractions at time zero. However, the overall mass was lower than that reported for the raw to suggest the possible precipitation of color bodies from the production of highly compact zones of concentrated material during freezing. From examination of Table 7.3 the resultant color concentrations can be seen as increasing with time. This was opposite to that observed at the initial freezing temperature -2 °C with the differences likely attributed to post chemical precipitation having occurred more at the warmer initial freezing temperature. The increase in color can also be attributed to increased biological degradation in the top liquid fraction to potentially increase color from the breakdown of its higher percentage of high molecular weight compounds. It may also be attributed to a fraction of the color causing material not as being easily untangleable from its compact

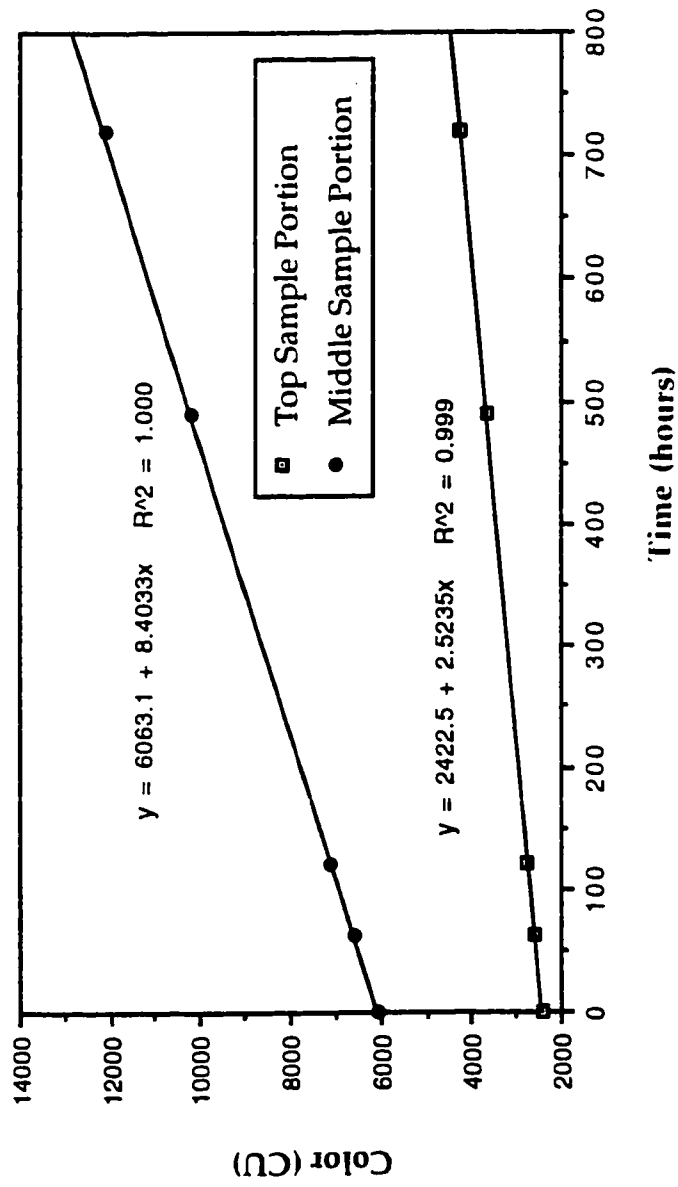


Figure 7.7 Plot of Change in Color Concentration in the Top and Middle Sample Portions with Respect to Time for Membrane Concentrate Frozen at the Initial Freezing Temperature -15 °C, Thawed Bottom Up at 24 °C and Then Left to Stand Undisturbed at 24 °C

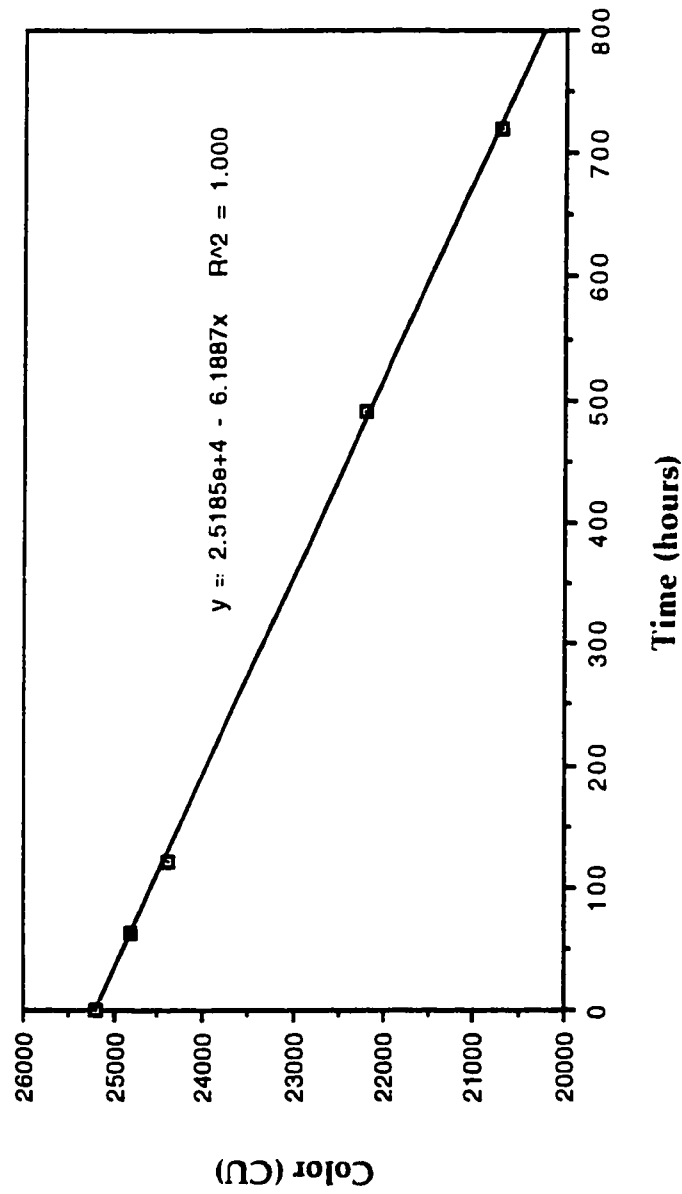


Figure 7.8 Plot of Change in Color Concentration in the Bottom Sample Portions with Respect to Time for Membrane Concentrate Frozen at the Initial Freezing Temperature -15 °C, Thawed Bottom Up at 24 °C and Then Left to Stand Undisturbed at 24 °C

Table 7.2 **Change in Treated Effluent Color Concentration with Respect to Time for Membrane Concentrate Left to Stand Undisturbed Following Freeze-thaw (Initial Freezing Temperature -2 °C, Thaw Bottom-up at 24 °C)**

Parameter	Time (hours)				
	0	62.5	119.5	335.5	720
Resultant Color Concentration (CU)*	12,400	12,300	12,100	11,400	9,800
Percent Difference with Respect to Raw (%)	-0.8	-1.6	-3.2	-9.1	-21.6

* Average Values, Sample Set Size: 3, Raw Effluent Color: 12,400 CU, minus sign indicates a decrease with respect to raw

Table 7.3 **Change in Treated Effluent Color Concentration with Respect to Time for Membrane Concentrate Left to Stand Undisturbed Following Freeze-thaw (Initial Freezing Temperature -15 °C, Thaw Bottom-up at 24 °C)**

Parameter	Time (hours)				
	0	63	120	491	720
Resultant Color Concentration (CU)*	10,500	10,600	10,800	11,500	11,900
Percent Difference with Respect to Raw (%)	-16.0	-15.2	-13.6	-8.0	-4.8

* Average Values, Sample Set Size: 3, Raw Effluent Color: 12,400 CU, minus sign indicates a decrease with respect to raw

concentrated material structure as maybe for the more highly porous material structure produced at the initial freezing temperature -2 °C.

7.2.2 ALKALINE EXTRACTION STAGE EFFLUENT

Similar to that observed for the membrane concentrate, the constituents removed as a concentrated material by freeze-thaw were reported over time to diffuse back into the bulk solution. The biological degradation rate to the control sample over time at room temperature was substantially higher than that observed for the more concentrated membrane concentrate. In the case of membrane concentrate the color concentration was reported to increase in the upper liquid fraction over time. Whereas for the Eop effluent the color concentration in the upper liquid fraction was reported to decrease over time. The difference of which may be in part related to the size distribution of the organics and their biodegradability. In either case, the rate of biological degradation was substantial to have greatly influenced the resultant color concentrations associated with each liquid fraction.

Summarized in Table 7.4 are the regression results (Appendix D). Tests on the individual regression coefficients showed that all the variables contributed significantly to the model. The adjusted coefficient of multiple determination R^2 was 0.972 to indicate that about 97.20 % of the variability in the changes reported in the top 70 % sample portion with respect to time were explained using the independent variables: initial freezing temperature and the color concentration ratio. Residual analysis was performed on each independent variable to judge the model's adequacy. From examination of Figures 7.9 to 7.11 it can be seen that there

Table 7.4 Best Multiple Linear Regression Model as Determined by Stepwise Regression Representing the Desired Drain Time to Begin Collection of the Treated Effluent for Eop Effluent Treated by Freeze-thaw

Independent Variable	Coefficient	Standard Error	Standard Coefficient	Tolerance	T	P (two-tailed test)
Constant	-198.633	38.403	0.000	N/A	-5.172	0.000
Color Concentration Ratio	1929.426	132.210	0.956	0.341	14.594	0.000
Freezing Temperature	28.840	4.492	0.739	0.111	6.421	0.000
Color Concentration Ratio* Freezing Temperature	-31.677	13.115	-0.341	0.074	-2.415	0.028

Dependent Variable: Desired Time to Begin Draining (hours)

Multiple R: 0.988, Squared Multiple R: 0.0977, Adjusted Squared Multiple R: 0.972

Source	SUM-OF-SQUARES	DEGREES OF FREEDOM	MEAN-SQUARES	F-RATIO	P
REGRESSION	1257530.598	3	419176.866	222.194	0.000
RESIDUAL	30184.602	16	1886.538		

were no severe deviations with respect to normality. The operational model designed to predict the time period when to drain following treatment to obtain a desired effluent quality in the top 70 % liquid fraction is depicted in equation 7.3.

$$t_D = -198.633 + 1929.426 C_r + 28.840 T_F - 31.677 C_r T_F \quad (7.3)$$

where;

t_D = time period when to drain the top 70 % liquid fraction,
(hours)

$C_r = C_t / C_o$, $C_o = 3,440$ CU

T_F = initial freezing temperature (°C)

7.2.2.1 CONTROL

Plotted in Figure 7.12 are the color concentrations for the different liquid fractions with respect to time for the untreated sample left to stand undisturbed at room temperature (24 °C). The color concentration in the control sample was reported to uniformly decrease for a maximum change of 1,470 CU over approximately a four week time period. The decrease in color concentration was likely from biological degradation or from natural color flocculation of the sample over time.

7.2.2.2 INITIAL FREEZING TEMPERATURE: -2 °C

Plotted in Figures 7.13 to 7.14 are the color concentrations for the different liquid fractions left undisturbed with respect to time for Eop effluent treated by freeze-thaw at the initial freezing temperature of -2 °C. Similar to that observed for the membrane concentrate, the change in color with respect to time for each liquid fraction can be described by a

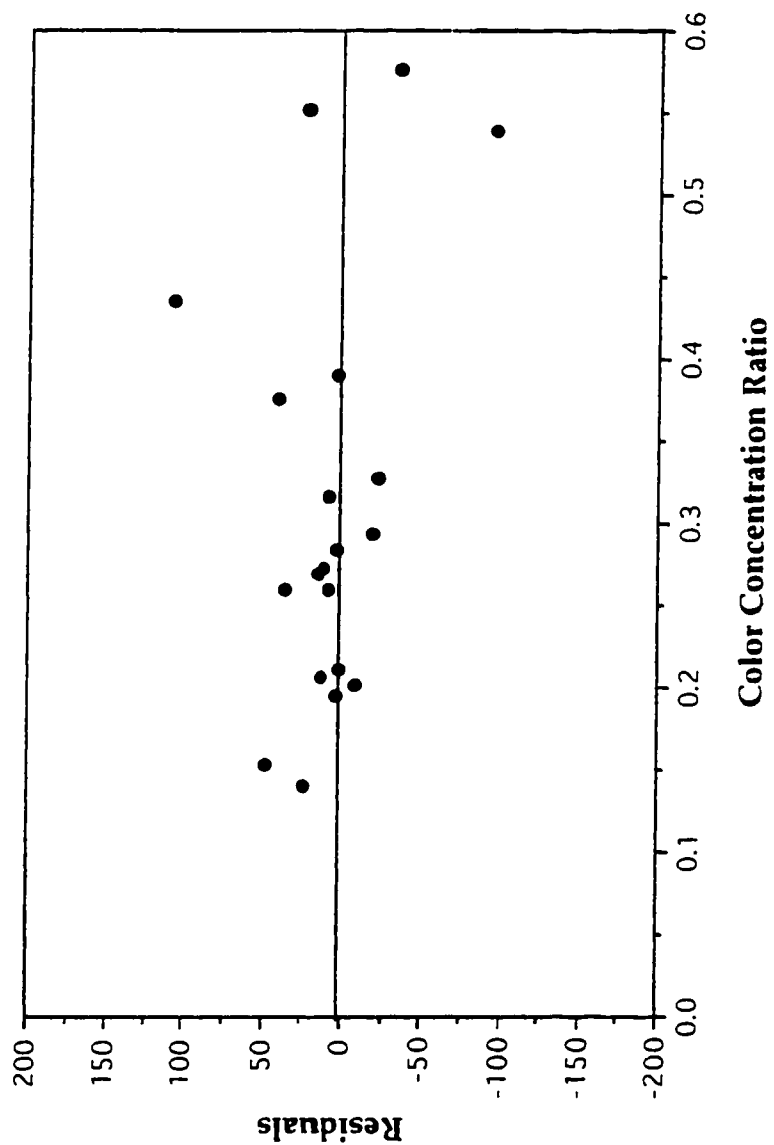


Figure 7.9 Plot of Residuals Against Color Concentration Ratio for Concentrate Stability Produced From Freeze-thaw of Eop Effluent

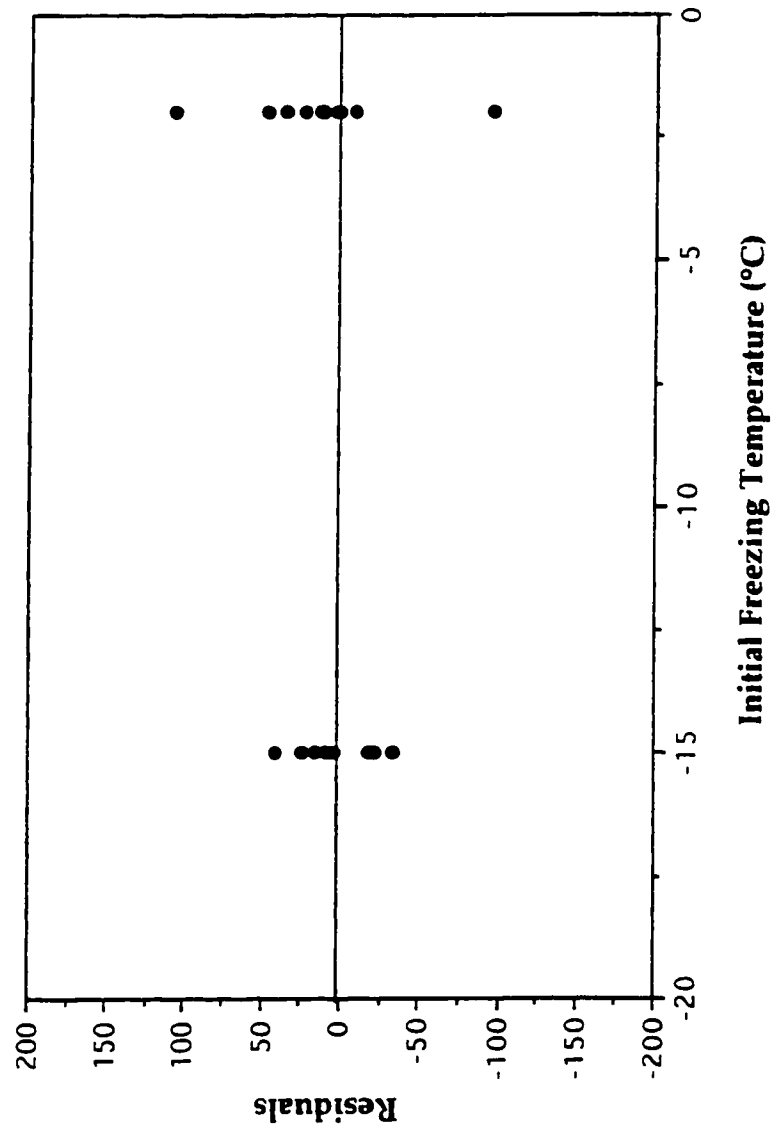


Figure 7.10 Plot of Residuals Against Initial Freezing Temperature for Concentrate Stability Produced From Freeze-thaw of Eop Effluent

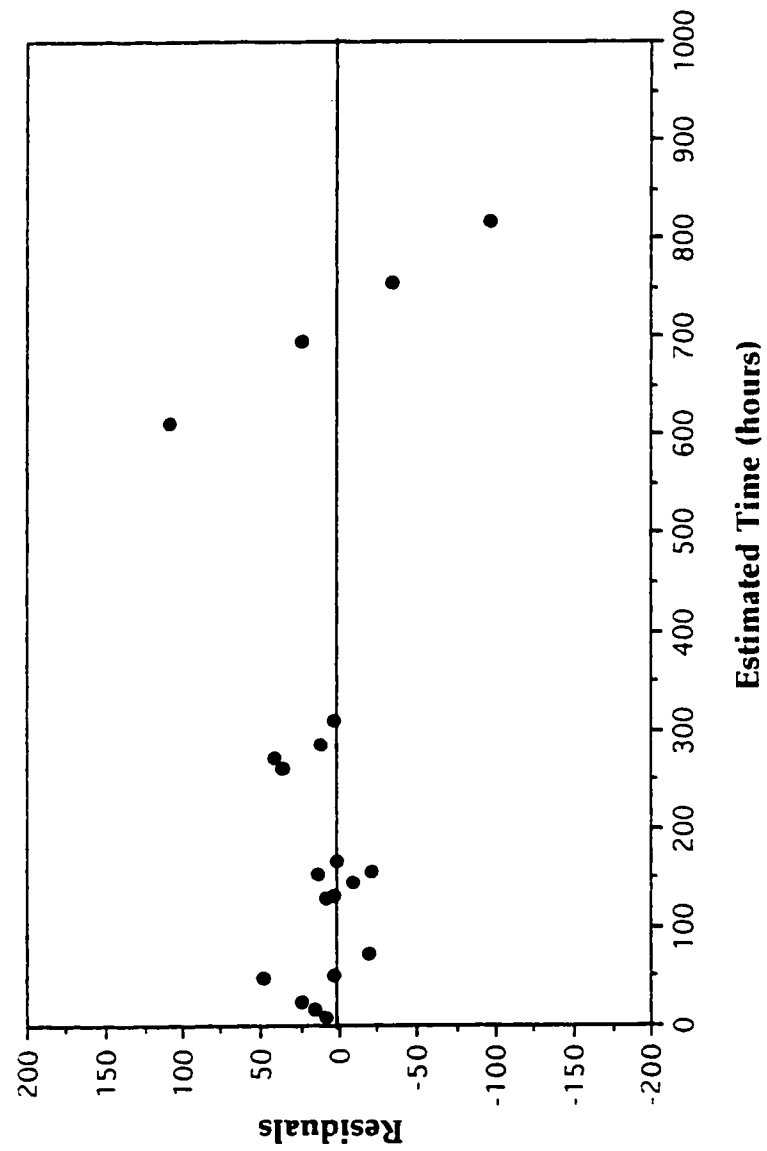


Figure 7.11 Plot of Residuals Against Estimated Time for Concentrate Stability Produced From Freeze-thaw of Eop Effluent

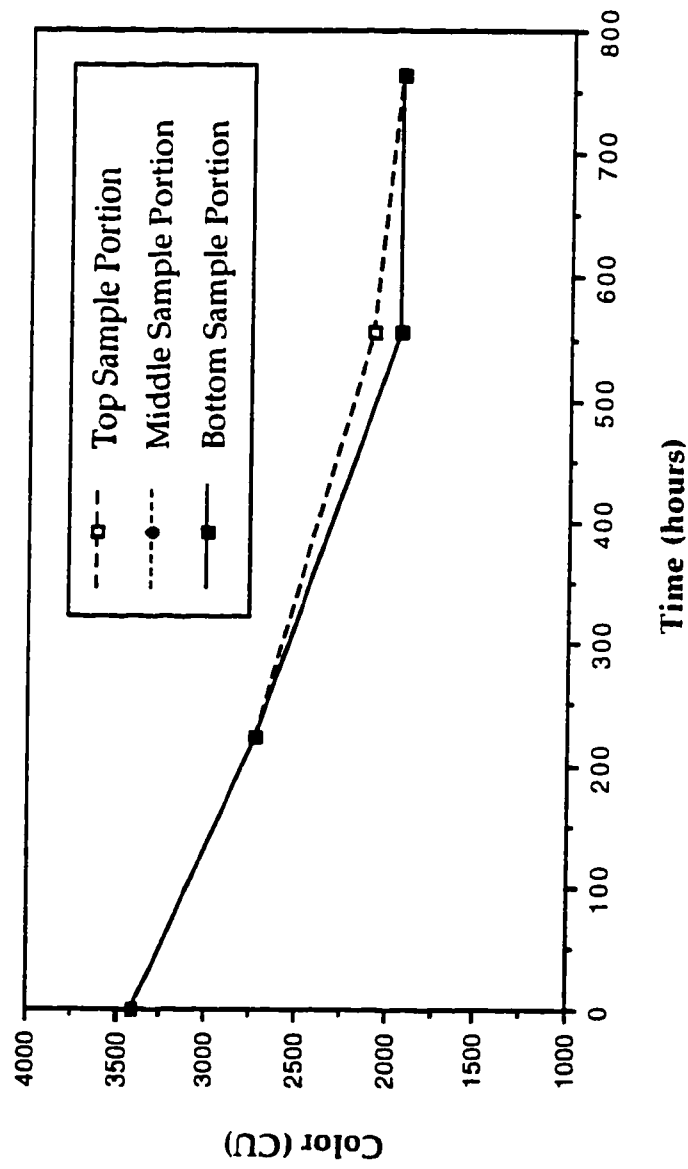


Figure 7.12 Change in Color Concentration in the Top, Middle, and Bottom Sample Portions of the Control Sample Over Time

linear relationship. Similarly, conducting a simple mass balance reveals a good majority of the color was accounted for when adding up of all three liquid fractions at time zero. From examination of Table 7.5 the resultant color concentrations can be seen as increasing with time. This indicates that the concentrated material produced was not entirely comprised of flocs per say, but rather a mixture of dissolved and stable organic matter together with flocculated and precipitated organic and inorganic material.

7.2.2.3 INITIAL FREEZING TEMPERATURE: -15 °C

Plotted in Figures 7.15 to 7.16 are the color concentrations for the different liquid fractions left undisturbed with respect to time for Eop effluent treated by freeze-thaw at the initial freezing temperature of -15 °C. The calculated slopes representing the change in color in the bottom sample portions were -1.85 at the initial freezing temperature -2 °C and -0.31 at the initial freezing temperature -15 °C. The rate of color dispersion was approximately 6.0 times lower than that calculated for the initial freezing temperature -2 °C. Conducting a simple mass balance reveals a good majority of the color was accounted for when adding up of all three liquid fractions at time zero. From examination of Table 7.6 the resultant color concentration can be seen as increasing with time. This again indicates that the concentrated material produced was not entirely comprised of flocs per say, but rather a mixture of dissolved and stable organic matter together with flocculated and precipitated organic and inorganic material.

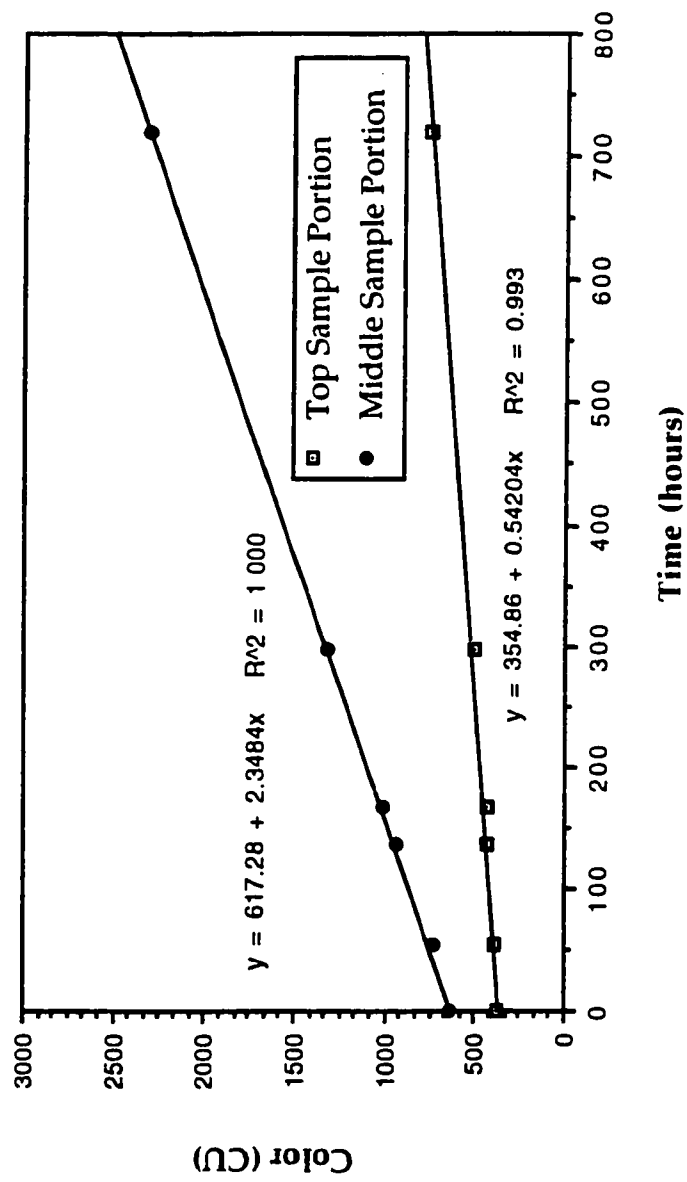


Figure 7.13 Plot of Change in Color Concentration in the Top and Middle Sample Portions with Respect to Time for Eop Effluent Frozen at the Initial Freezing Temperature -2 °C, Thawed Bottom Up at 24 °C and Then Left to Stand Undisturbed at 24 °C

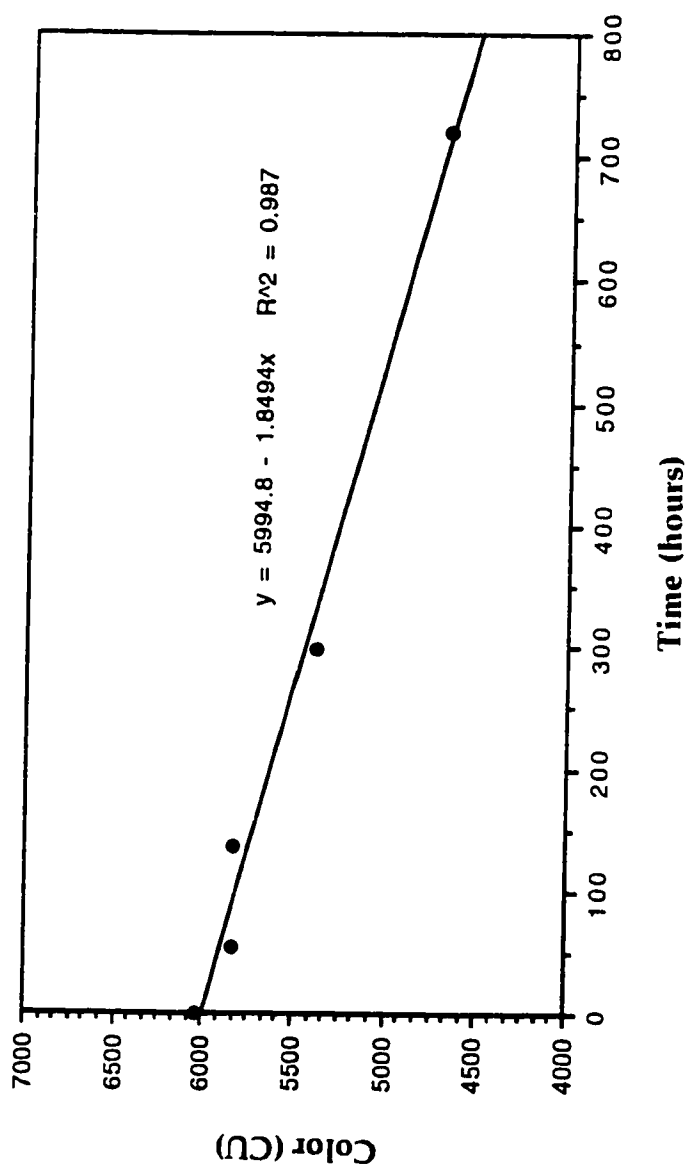


Figure 7.14 Plot of Change in Color Concentration in the Bottom

Sample Portions with Respect to Time for Eop Effluent

Frozen at the Initial Freezing Temperature -2 °C, Thawed

Bottom Up at 24 °C and Then Left to Stand Undisturbed at 24 °C

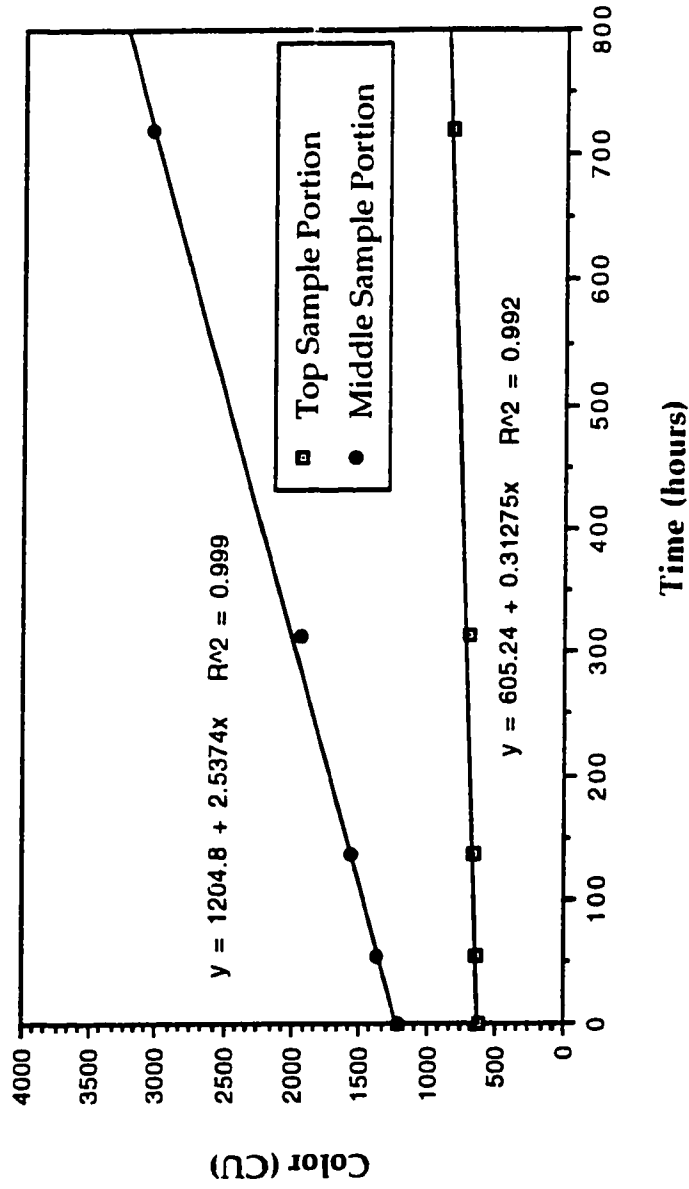


Figure 7.15 Plot of Change in Color Concentration in the Top and Middle Sample Portions with Respect to Time for Eop Effluent Frozen at the Initial Freezing Temperature -15 °C, Thawed Bottom Up at 24 °C and Then Left to Stand Undisturbed at 24 °C

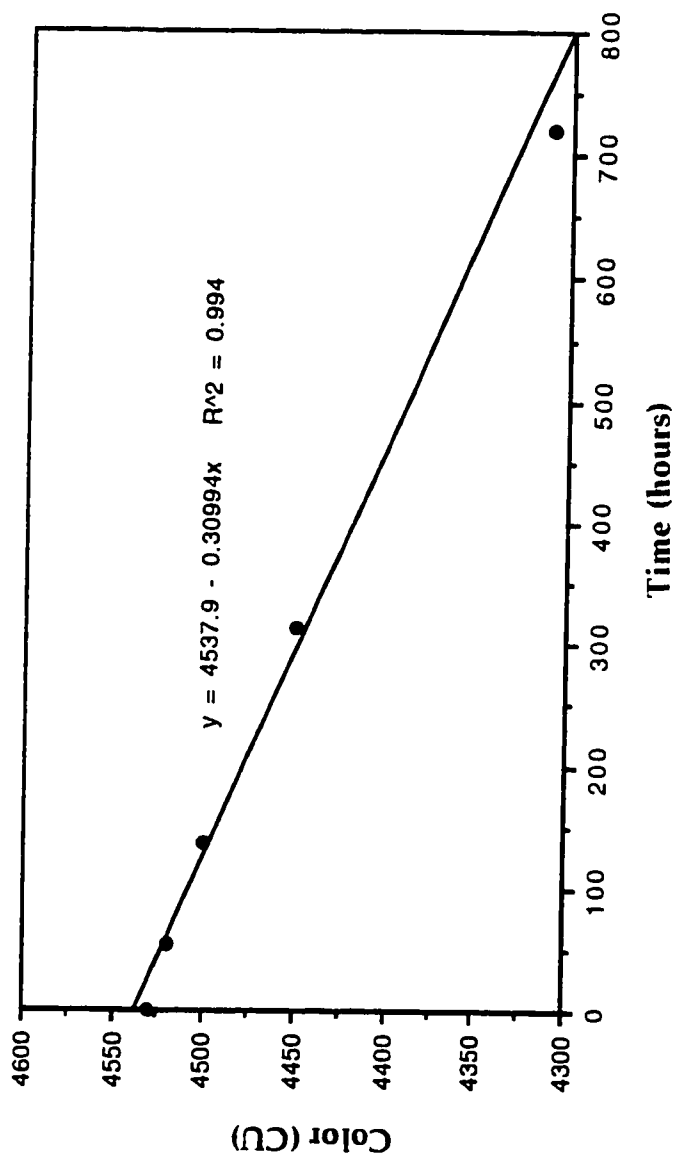


Figure 7.16 Plot of Change in Color Concentration in the Bottom
Sample Portions with Respect to Time for Eop Effluent
Frozen at the Initial Freezing Temperature -15 °C, Thawed
Bottom Up at 24 °C and Then Left to Stand Undisturbed at 24 °C

Table 7.5 Change in Treated Effluent Color Concentration with Respect to Time for Eop Effluent Left to Stand Undisturbed Following Freeze-thaw (Initial Freezing Temperature -2 °C, Thaw Bottom-up at 24 °C)

Parameter	Time (hours)				
	0	54	136	298	720
Resultant Color Concentration (CU)*	2,100	2,200	2,220	2,260	2,470
Percent Difference with Respect to Raw (%)	-39.0	-36.0	-35.5	-34.3	-28.2

* Average Values, Sample Set Size: 3, Raw Effluent Color: 3,440 CU, minus sign indicates a decrease with respect to raw

Table 7.6 Change in Treated Effluent Color Concentration with Respect to Time for Eop Effluent Left to Stand Undisturbed Following Freeze-thaw (Initial Freezing Temperature -15 °C, Thaw Bottom-up at 24 °C)

Parameter	Time (hours)				
	0	55	136	313	720
Resultant Color Concentration (CU)*	1,990	2,050	2,130	2,260	2,650
Percent Difference with Respect to Raw (%)	-42.2	-40.4	-38.1	-34.3	-22.9

* Average Values, Sample Set Size: 3, Raw Effluent Color: 3,440 CU, minus sign indicates a decrease with respect to raw

8.0 FREEZE LAYERING STUDIES

8.1 PROCEDURE

Experiments to simulate freezing in layers were conducted at the experimental conditions that provided for the best results for each experimental water type. The initial freezing temperatures investigated were -2 °C, -15 °C, and -25 °C, respectively. All frozen samples were thawed bottom up at a temperature of 24 °C. Freezing in layers was conducted in 125 mm lifts, with the freezing of the first layer performed followed by the addition and freezing of the second layer on top of the first. The initial liquid temperatures of each effluent prior to freezing was 4 °C.

8.2 RESULTS AND DISCUSSION

Experimental tests were conducted to evaluate the benefit of conducting freeze-thaw by layering versus single liquid depths. The manner in which the effluent would freeze in a freezing pond can be described by water's unusual property. The density of water is a function of temperature and its maximum density occurs near 4 °C. In freezing the effluent from the top down, the surface water loses its heat, becomes more dense and sinks. This process occurs until all the water in the freezing bed is at 3.96 °C, when the density is at its maximum. Further cooling produces a lighter layer of water at the top. The lighter layer grows in depth with cooling until the effluent at the top has lost enough heat to cause ice production. Under quiescent conditions, a thin surface film of ice develops. The rate of freezing of the water to the underside of the ice sheet is a function of how effective the latent heat of fusion released by freezing can be conducted upward. The rate of thermal growth of the ice cover is

governed by the heat exchange at the top and bottom surfaces and heat conduction in the ice cover. Heat conduction across the top surface will depend on air temperature, wind velocity, humidity, and short- and long-wave radiation. Heat conduction at the bottom surface depends on water temperature and temperature of the freezing bed. Heat conduction in the ice depends on its thermal conductivities with respect to its depth.

Freezing and thawing indices have been developed for calculation of freezing and thawing depths, particularly for soils. Several equations are available with the original work by Neumann serving as a basis for development of the empirical models by Berggren and Stefan. In particular, a modified Stefan equation was developed specifically to solve the thawing depth of a multiple layer system. Equations of this nature can be used as operational tools to predict the freezing and thawing depth of a single and multiple layer system under different climatic conditions which in turn can be used to regulate the maximum number of layers. An important parameter that is not taken into account by the above indices is the temperature of the waste effluent. Pulp mill effluents are high in temperature (65 °C) and will as result cause thawing of the immediate top portion of the frozen layer over which the new layer of effluent is applied. Unknown is to what depth there will occur additional thawing in the frozen layer immediately below the newly applied layer. Before such indices can be applied additional field work is required to simulate freeze layering at the effluent temperatures anticipated for the process.

The layering results presented were derived from freezing each experimental water in 125 mm lifts with the initial temperature of these liquids equal to their storage temperatures (4 °C). Because the storage

temperature was close to the maximum density of water, laboratory unidirectional freezing experiments did not simulate the concentration effects that would occur from density changes as the liquid cools. Substantial thawing of the layer below from the application of a high temperature effluent is likely to have an adverse effect on the end supernatant quality. This is based on the fact substantial heating from the top simulates thawing from the top down which was reported in preceding sections to adversely affect treatment performance.

8.2.1 ALKALINE EXTRACTION STAGE MEMBRANE CONCENTRATE

Layering was not observed to substantially improve treatment performance. The general tendency of the data was layering marginally improved treatment performance only at the lower initial freezing temperatures in which the color concentrations were reported as being marginally lower. The results are in part explained by the fragility of the concentrated material. Layering conducted in thin layers at low initial freezing temperatures was believed to have reduced the degree of disturbance to the concentrated material during thawing by reducing the contact time of the material has with the bulk solution before it is removed.

8.2.1.1 INITIAL FREEZING TEMPERATURE: -2 °C

Plotted in Figure 8.1 are the color distributions with respect to liquid depth for membrane concentrate frozen in single and multiple layers at the initial freezing temperature -2 °C. The color distributions were not

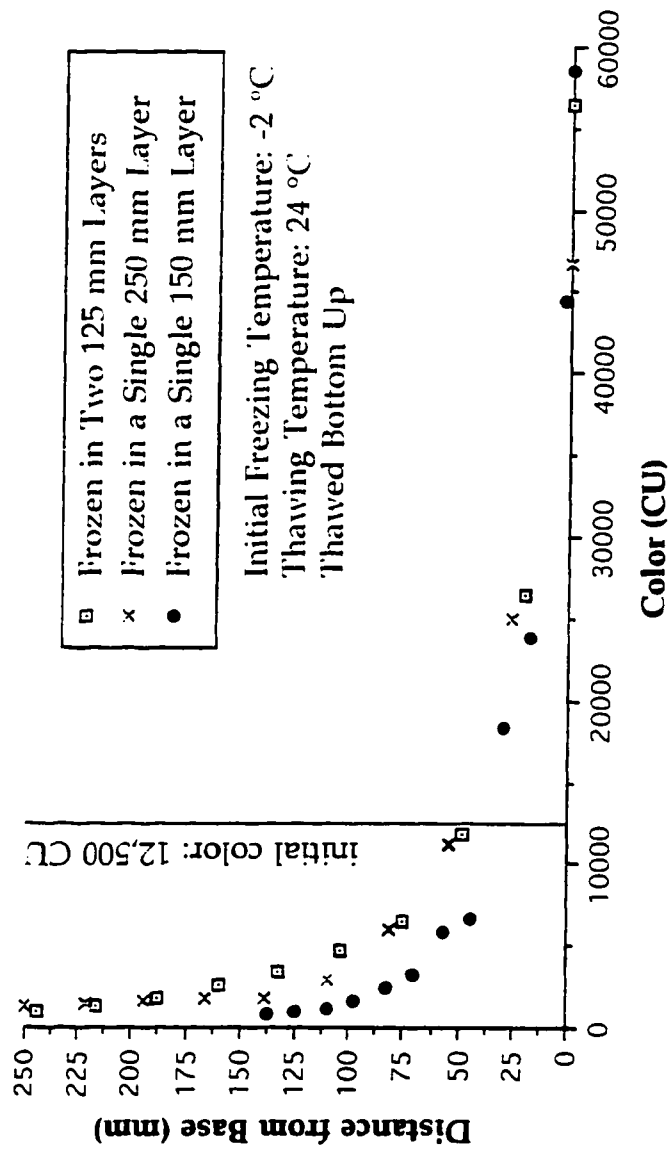


Figure 8.1 Plot Showing the Comparison Between Color Distributions for Membrane Concentrate Frozen in Single and Multiple Layers for Different Liquid Depths at the Initial Freezing Temperature -2 °C

substantially different with respect to concentrate samples treated in multiple layers of 125 mm liquid depths versus samples treated in single layers of 250 mm liquid depths. Those points along the curves in which the data began to deviate was at the interface of the first and second layer for samples treated by layering and that this was probably the result of superficial melting of the top layer caused by the addition of the second layer. The color distribution associated with the single 150 mm liquid depth was lower than the distributions reported for layering and deeper liquid depths (250 mm).

8.2.1.2 INITIAL FREEZING TEMPERATURE: -15 °C

Plotted in Figure 8.2 are the color distributions with respect to liquid depth for membrane concentrate frozen in single and multiple layers at the initial freezing temperature -15 °C. The color distributions were not substantially different with respect to concentrate samples treated in multiple layers of 125 mm liquid depths versus samples treated in single layers of 150 mm and 250 mm liquid depths.

8.2.1.3 INITIAL FREEZING TEMPERATURE: -25 °C

Plotted in Figure 8.3 are the color distributions with respect to liquid depth for membrane concentrate frozen in single and multiple layers at the initial freezing temperature -25 °C. The color distribution was marginally lower for concentrate frozen in multiple layers of 125 mm liquid depths in comparison to concentrate frozen at a single liquid depth of 250 mm. The color distributions were not substantially different for concentrate frozen in multiple layers of 125 mm liquid depths versus single layers of 150 mm liquid depths.

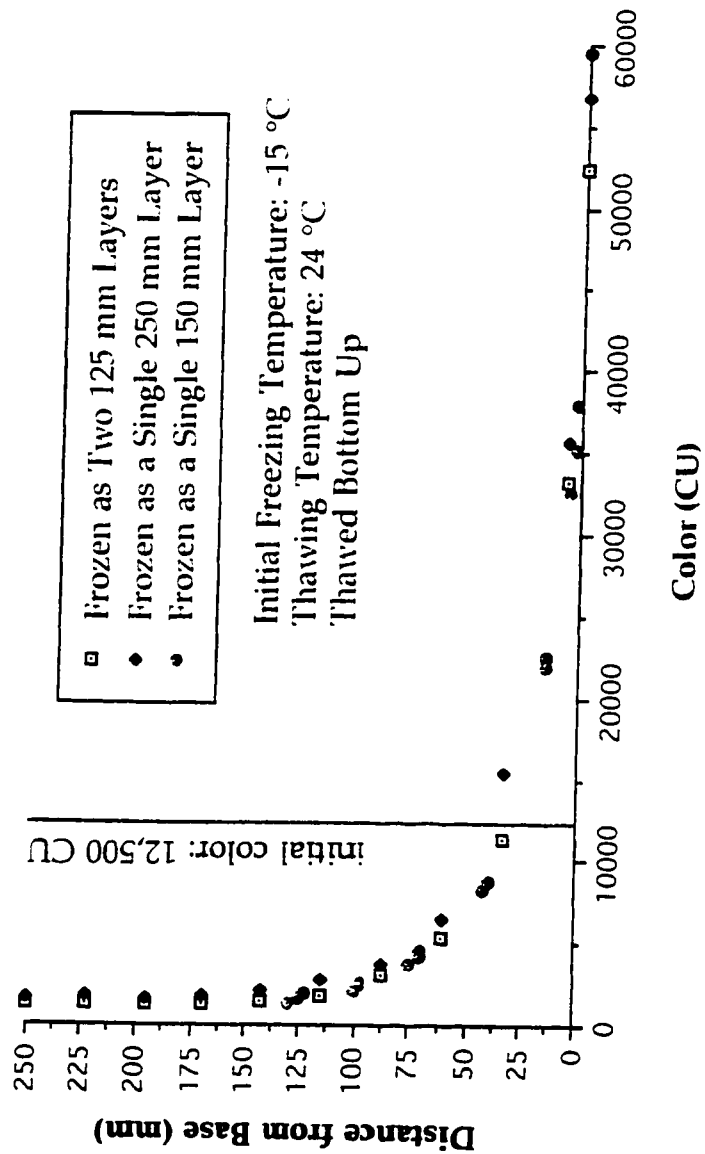


Figure 8.2 Plot Showing the Comparison Between Color Distributions for Membrane Concentrate Frozen in Single and Multiple Layers for Different Liquid Depths at the Initial Freezing Temperature -15 °C

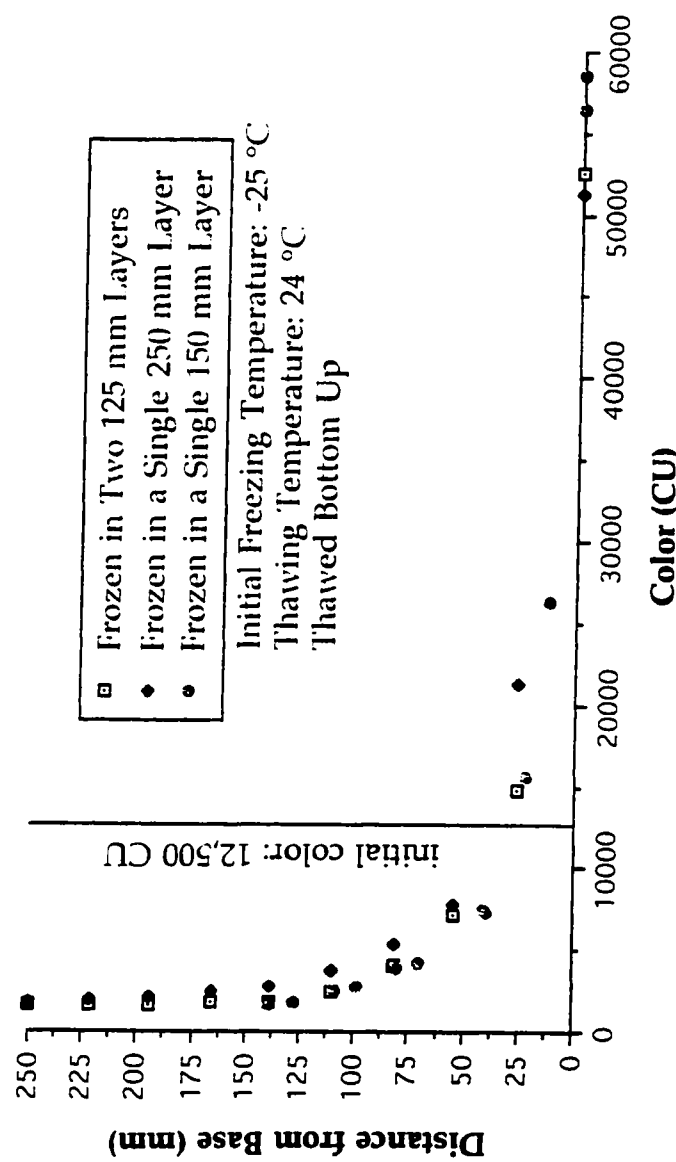


Figure 8.3 Plot Showing the Comparison Between Color Distributions for Membrane Concentrate Frozen in Single and Multiple Layers for Different Liquid Depths at the Initial Freezing Temperature -25 °C

8.2.2 ALKALINE EXTRACTION STAGE EFFLUENT

Layering was observed to have a more beneficial effect on color removal by freeze-thaw of Eop effluent than reported for membrane concentrate. The general tendency of the data was layering improved treatment performance at the lower initial freezing temperatures in which the color concentrations decreased with respect to deeper liquid depths. However, at low initial freezing temperatures (≤ -15 °C) the color distributions were not substantially different between samples frozen in multiple layers of 125 mm liquid depths and samples frozen in single 150 mm liquid depths. The results can be in part explained by the fragility of the concentrated material. Layering conducted at low initial freezing temperatures was believed to have reduced the degree of disturbance to the concentrated material during thawing.

8.2.2.1 INITIAL FREEZING TEMPERATURE: -2 °C

Plotted in Figure 8.4 are the color distributions with respect to liquid depth for Eop effluent frozen in single and multiple layers at the initial freezing temperature -2 °C. The general tendency of the data at this initial freezing temperature was similar to that reported for the membrane concentrate at the same initial freezing temperature. The color distributions were not substantially different with respect to Eop samples treated in multiple layers of 125 mm liquid depths versus samples treated in a single layer of 250 mm liquid depth. The only points along the curves in which the data began to deviate were those close to the interface of the first and second layer for samples treated by layering and that this was likely the result of superficial melting of the top first layer caused

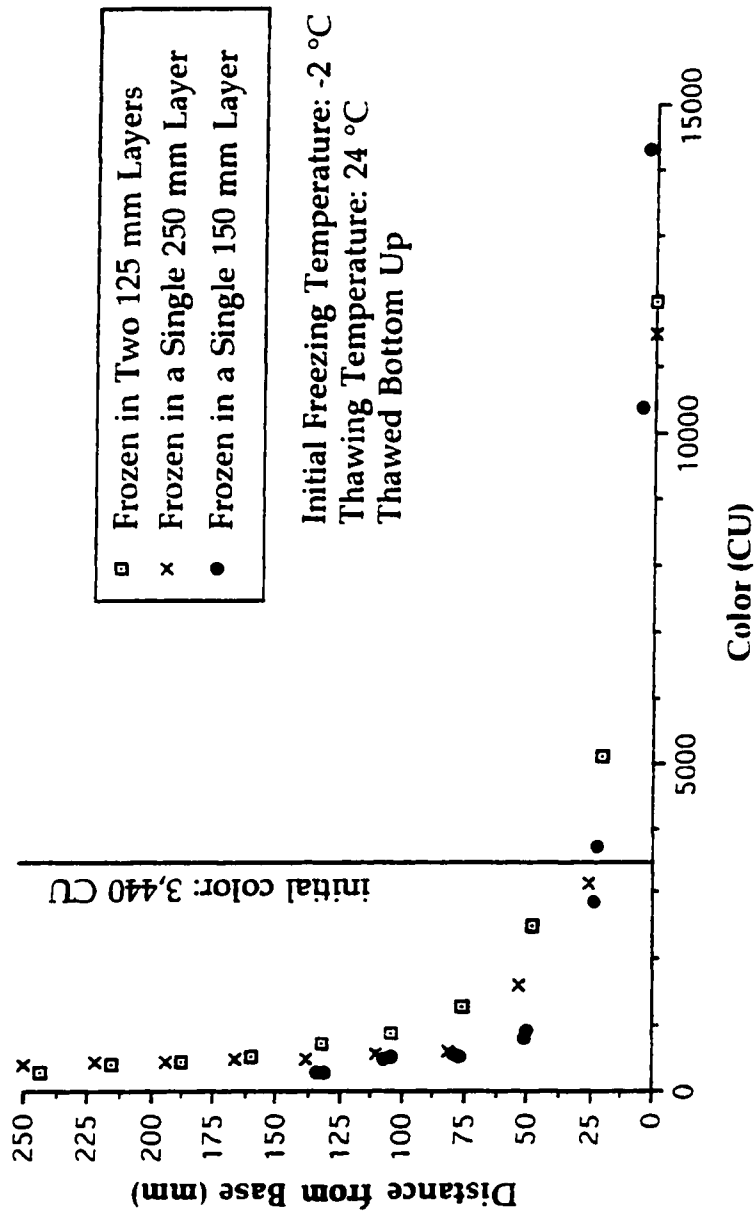


Figure 8.4 Plot Showing the Comparison Between Color Distributions for Eop Effluent Frozen in Single and Multiple Layers for Different Liquid Depths at the Initial Freezing Temperature -2 °C

by the addition of the second layer. The color distribution associated with the single 150 mm liquid depth was lower than the distributions reported for layering and the deeper liquid depths.

8.2.2.2 INITIAL FREEZING TEMPERATURE: -15 °C

Plotted in Figure 8.5 are the color distributions with respect to liquid depth for Eop effluent frozen in single and multiple layers at the initial freezing temperature -15 °C. The color distribution was marginally lower for Eop frozen in multiple layers of 125 mm liquid depths versus a single 250 mm liquid depth. Also similar were the color distributions for Eop frozen in multiple and single layers of 125 mm and 150 mm liquid depths.

8.2.2.3 INITIAL FREEZING TEMPERATURE: -25 °C

Plotted in Figure 8.6 are the color distributions with respect to liquid depth for Eop effluent frozen in single and multiple layers at the initial freezing temperature -25 °C. The general tendency of the data at this initial freezing temperature was similar to that observed for the initial freezing temperature of -15 °C. The color distribution was marginally lower for Eop frozen in multiple layers of 125 mm liquid depths versus a single 250 mm liquid depth. Also similar were the color distributions for Eop frozen in multiple and single layers of 125 mm to 150 mm liquid depths.

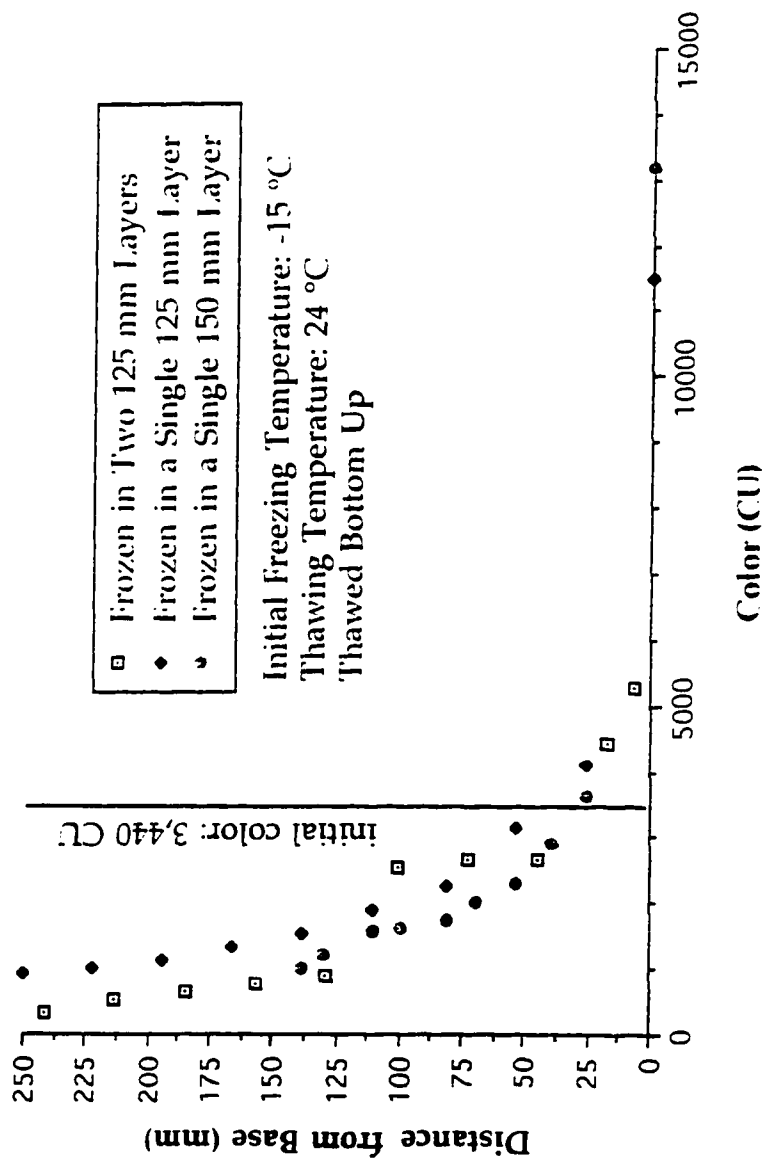


Figure 8.5 Plot Showing the Comparison Between Color Distributions for Eop Effluent Frozen in Single and Multiple Layers for Different Liquid Depths at the Initial Freezing Temperature -15 °C

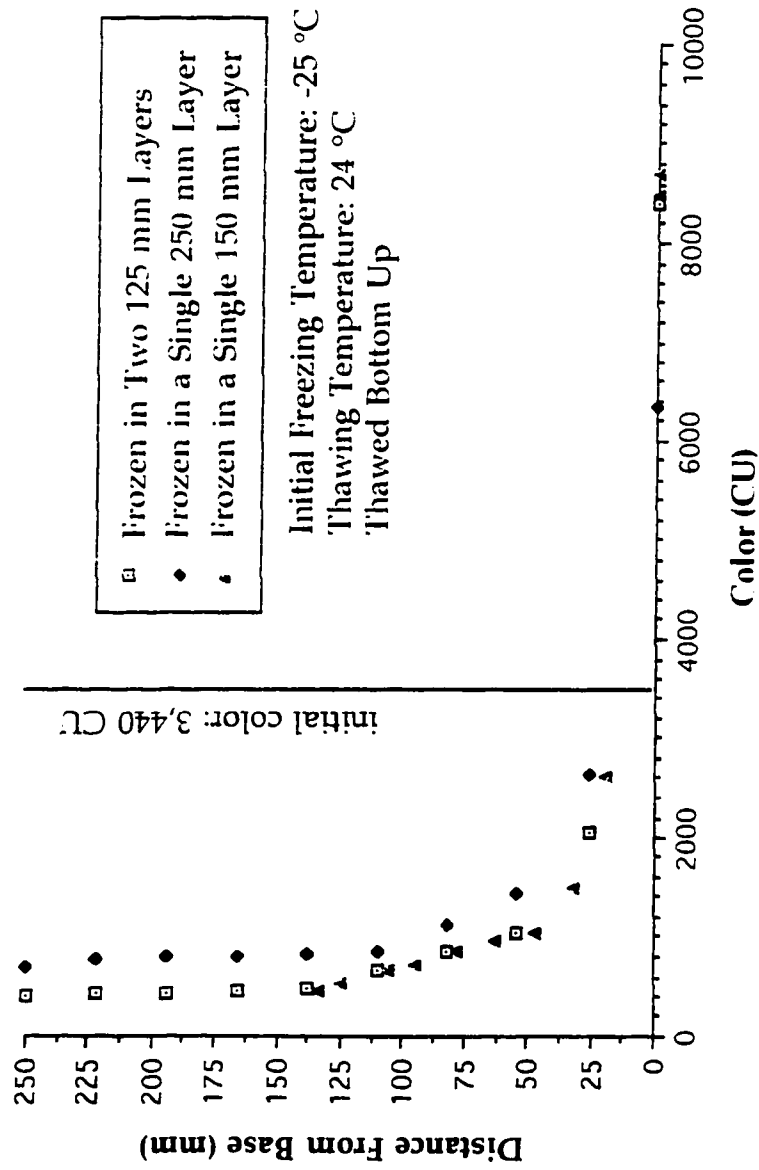


Figure 8.6 Plot Showing the Comparison Between Color Distributions for Eop Effluent Frozen in Single and Multiple Layers for Different Liquid Depths at the Initial Freezing Temperature -25 °C

9.0 EMPIRICAL MODEL DEVELOPMENT

Empirical models are applicable in circumstances whereby the mechanisms underlying the process are too complicated or not well enough understood to allow an exact model to be postulated from theory. In the case of freeze-thaw for the treatment of pulp mill membrane concentrates, the interaction of the physical and chemical mechanisms capable of causing separation are varied and complex, making the use of theoretical models not possible. Model building is an iterative sequence. Factorial designs were used to facilitate the discovery of similarities and simplifications and thus assisted in the process of model building. These experimental designs were also used to provide estimates of the "effects" of the changes.

9.1 FACTORIAL DESIGN

Separate factorial experiments were initially conducted for each experimental water type to investigate the quantitative variables: initial freezing temperature, method of thawing, thawing temperature, storage time, and storage temperature. Boundary points were then selected and the factorial experiments combined to develop an empirical relationship to predict the color concentration in the top 70 % liquid fraction for each effluent type following treatment by freeze-thaw.

9.2 BOUNDARY SELECTION AND MODEL LIMITATIONS

Utilizing results from the preceding sections boundary parameter set points were selected from which multiple linear regression analyses were performed to statistically model the freeze-thaw process for each

experimental water type. Method of thawing was identified as the most important parameter in achieving high color removals in the upper liquid fraction. Consistently observed for frozen samples thawed top down in which the ice was prevented from floating was the overall color removals in the top 70 % liquid volume were very low (≤ 40.8 %). So low were the removals with respect to the untreated effluents that thawing the effluents from the top down would not, from an operational point of view, produce acceptable results to warrant the use of this technology. Therefore with respect to method of thawing to achieve acceptable results the process would have to be operated to promote melting of the ice from the bottom up. This will require the system to be designed to modify the natural process of thawing by the introduction of heat. Waste heat resulting from the discharge of high temperature effluents is a logical heat source which for the pulp mill represents a source of pollution. Natural thawing is a mix of melting from the top and bottom of the ice. However, the introduction of heat below the ice mass is necessary to establish the appropriate melt water flow pattern and the release of the concentrated material entrapped within the ice matrix. In the model, thawing temperature therefore relates to the temperature applied at the bottom of the ice mass to cause melting. Under these circumstances, thawing temperature was deemed a controllable process parameter. A broad range of thawing temperatures were investigated. The thawing temperatures that were independently studied were 4 °C, 15 °C, and 24 °C, respectively. The range of thawing temperatures considered as boundary set points in the models were the between the temperature range 4 °C to 24 °C. High thawing temperatures were considered in part because of the on-site waste heat source available in the discharge of high temperature effluents which

may be used to thaw the ice mass from the bottom up. To take advantage of this waste heat, the effluent would be prior to freezing pumped through an underground pipe network located underneath the freezing ponds. The purpose of which would be to heat the ground below the frozen mass to cause melting from the bottom up and to allow the ice to eventually break away to float. Because of high expected waste stream effluent temperatures (65 °C) an upper boundary limit of 24 °C was selected for the independent variable thawing temperature.

The range of initial freezing temperatures investigated as part of this study were from -2 °C to -25 °C. The boundary set points selected for the independent variable initial freezing temperature was between -2 °C and -15 °C. Data presented in the preceding chapters showed that treatment performance did not significantly change for initial freezing temperatures below -15 °C in samples thawed from the bottom up. Therefore the lower boundary set point selected for initial freezing temperature was -15 °C. However, in reality outside temperatures colder than -15 °C can occur for very cold regions. The storage temperature range investigated was between the temperatures -2 °C and -15 °C. The same boundary set points were used for storage temperature as used for the independent variable initial freezing temperature.

The range of storage times investigated were from 0 to 90 days. Independent results showed that if storage temperature was to be considered a parameter then a storage time of greater than 30 days was necessary for the results to be significant. For example, in the case of membrane concentrate, storage times below 30 days were not observed to significantly affect treatment performance. However, it is anticipated that

the process will be operated by means of layering in which thin layers of effluent will be frozen from the top down on top of existing frozen layers. This would likely be required to conserve land space and to take advantage of the positive effect storage time can have on treatment performance. Therefore the upper boundary limit selected for storage time was 90 days.

Liquid depth was not included as an independent variable in the regression analyses. Data presented in preceding chapters showed liquid depth to be relatively unimportant between range of 150 mm to 250 mm. The color removals for each experimental water type were either not substantially different or in the case of the warmer initial freezing temperature (-2°C) the percent color removals associated with the equivalent volume fractions were not substantially different. Therefore the models that are developed can be assumed to be valid between a liquid depth of 150 mm to 250 mm.

Concentration was not included as an independent variable in the regression analyses. Experimental studies conducted to examine the effect of concentration on the concentrated material morphology showed for membrane concentrate, the general characteristics of the material remained relatively unchanged (within 1 standard deviation of the thickness observed for the stock solution) between the dilutions strengths 0 % (stock concentrate) to 50 %. These dilution strengths correspond to a concentrate with a color concentration between 6,250 CU to 12,500 CU. The concentrated material produced between this dilution range at the initial freezing temperatures -2°C and -15°C were not substantially different with respect the undiluted sample in regards to shape, porosity, and thickness. Therefore the empirical model developed to predict treatment

efficiency when expressed as percent color removal would be valid for the above color range for concentrates derived from the same effluent source using similar membrane technology (i.e., molecular weight cutoff of around 8000). Dilution studies were not conducted on the Eop effluent as this waste stream concentration was not expected to vary greatly in the context of kraft pulp mill operations.

9.3 ANALYSIS OF VARIANCE FOR EACH EXPERIMENTAL WATER TYPE

Presented below are the analysis of variance tables conducted to test the equality of the parameters: initial freezing temperature, thawing temperature, storage temperature, and storage time with respect to each effluent type. These parameters were statistically examined at their boundary set points to determine their effect on the measured color concentration contained in the top 70 % liquid volume of each effluent type following treatment by freeze-thaw.

9.3.1 ALKALINE EXTRACTION STAGE MEMBRANE CONCENTRATE

From examination of the F ratio values in Table 9.1 it can be concluded that the single level interactions: initial freezing temperature, thawing temperature, storage time, and storage temperature at the set points investigated significantly affected the resultant color concentration in the top 70 % liquid volume of the treated concentrate for a 95 % confidence limit. Similarly, the two level interactions that significantly affected the resultant color concentration in the upper liquid portion were:

Table 9.1 Analysis of Variance Table for Membrane Concentrate Frozen and Thawed Under Different Freeze-thaw Conditions

Effect	SUM-OF-SQUARES	Degrees of Freedom (n-1)	Mean-Square	F-Ratio	P
<u>Main Effects</u>					
Initial Freezing Temperature	0.184846E+08	1	0.184846E+08	5172.220	0.000
Thawing Temperature	0.134460E+08	1	0.134460E+08	3762.344	0.000
Storage Time	149763.672	3	49921.224	13.969	0.000
Storage Temperature	214484.766	1	214484.766	60.015	0.000
<u>Two-Factor Interactions</u>					
Freezing Temperature * Thawing Temperature	121191.016	1	121191.016	33.911	0.000
Freezing Temperature * Storage Time	69407.422	3	23135.807	6.474	0.002
Freezing Temperature * Storage Temperature	91884.766	1	91884.766	25.710	0.000
Thawing Temperature* Storage Time	21798.047	3	7266.016	2.033	0.129
Thawing Temperature* Storage Temperature	244.141	1	244.141	0.068	0.795
Storage Time* Storage Temperature	25285.547	3	8428.516	2.358	0.090
<u>Three-Factor Interaction</u>					
Freezing Temperature* Thawing Temperature* Storage Time	9779.297	3	3259.766	0.912	0.446
Freezing Temperature* Thawing Temperature* Storage Temperature	65344.141	1	65344.141	18.284	0.000
Freezing Temperature* Storage Temperature* Storage Time	42060.547	3	14020.182	3.923	0.017
Thawing Temperature* Storage Temperature* Storage Time	34488.672	3	11496.224	3.217	0.036
<u>Four-Factor Interaction</u>					
Freezing Temperature * Thawing Temperature * Storage Time* Storage Temperature	11663.672	3	3887.891	1.088	0.368
Error	114362.500	32	3573.828		

initial freezing temperature * thawing temperature, initial freezing temperature * storage time, and initial freezing temperature * storage temperature. Similarly, the three level interactions that significantly affected the resultant color concentration in the upper liquid portion were: initial freezing temperature * thawing temperature * storage temperature, initial freezing temperature * storage temperature * storage time, and thawing temperature * storage time * storage temperature. The remaining two, three, and four level interactions not discussed in Table 9.1 were not reported to significantly affect treatment performance.

9.3.2 ALKALINE EXTRACTION STAGE EFFLUENT

From examination of the F ratio values in Table 9.2 it can be concluded that the single level interactions: initial freezing temperature, thawing temperature, storage time, and storage temperature at the set points investigated significantly affected the resultant color concentration in the top 70 % liquid volume of the treated Eop effluent for a 95 % confidence limit. Similarly, the two level interactions that significantly affected the resultant color concentration in the upper liquid portion were: initial freezing temperature * thawing temperature, initial freezing temperature * storage time, initial freezing temperature * storage temperature, thawing temperature * storage time, thawing temperature * storage temperature, and storage time * storage temperature. The remaining three, and four level interactions presented in Table 9.2 were not reported to significantly affect treatment performance.

Table 9.2 Analysis of Variance Table for Eop Effluent Frozen and Thawed Under Different Freeze-thaw Conditions

Effect	SUM-OF-SQUARES	Degrees of Freedom (n-1)	Mean-Square	F-Ratio	P
<u>Main Effects</u>					
Initial Freezing Temperature	59963.766	1	59963.766	94.086	0.000
Thawing Temperature	2526907.641	1	2526907.641	3964.846	0.000
Storage Time	20730.172	3	6910.057	10.842	0.000
Storage Temperature	32715.766	1	32715.766	51.333	0.000
<u>Two-Factor Interactions</u>					
Freezing Temperature * Thawing Temperature	680418.766	1	680418.766	1067.611	0.000
Freezing Temperature * Storage Time	7842.797	3	2614.266	4.102	0.014
Freezing Temperature * Storage Temperature	4048.141	1	4048.141	6.352	0.017
Thawing Temperature * Storage Time	8072.672	3	2690.891	4.222	0.013
Thawing Temperature * Storage Temperature	2929.516	1	2929.516	4.597	0.040
Storage Time * Storage Temperature	7769.547	3	2589.849	4.064	0.015
<u>Three-Factor Interaction</u>					
Freezing Temperature * Thawing Temperature * Storage Time	946.547	3	315.516	0.495	0.688
Freezing Temperature * Storage Temperature * Storage Time	3822.172	3	1274.057	1.999	0.134
Thawing Temperature * Storage Temperature * Storage Time	972.047	3	324.016	0.508	0.679
<u>Four-Factor Interaction</u>					
Freezing Temperature * Thawing Temperature * Storage Time * Storage Temperature	3170.922	3	1056.974	1.658	0.196
Error	20394.500	32	637.328		

9.4 MULTIPLE LINEAR REGRESSION MODELING

9.4.1 ALKALINE EXTRACTION STAGE MEMBRANE CONCENTRATE

Multiple linear regression analysis was performed on the laboratory data produced in the treatment of membrane concentrate by freeze-thaw. The independent variables considered in the analysis were those interactions shown to significantly affect treatment performance in the table of analysis of variance. Summarized in Table 9.3 are the regression results.

Tests on the individual regression coefficients showed that the interactions: initial freezing temperature, thawing temperature, storage time, storage temperature, initial freezing temperature * thawing temperature, initial freezing temperature * thawing temperature * storage temperature, initial freezing temperature * storage time * storage temperature, and thawing temperature * storage time * storage temperature contributed significantly to the model. The variables that did not contribute significantly to the model were the interactions; initial freezing temperature * storage temperature, and initial freezing temperature * storage time. The above testing of the individual regression coefficients suggests the model might be more effective with the deletion of these interactions. The adjusted coefficient of multiple determination R^2 was 0.990 to indicate that about 99.00 % of the variability in the measured color concentration in the top 70 % liquid volume was explained by using the independent variables: initial freezing temperature, thawing temperature, storage time, and storage temperature. A normal plot of the individual effects with respect to probability shows the

Table 9.3 Multiple Linear Regression Model for Prediction of the Color Concentration in the Top 70 %
Liquid Fraction of Membrane Concentrate Treated by Freeze-thaw

Independent Variable	Coefficient	Standard Error	Standard Coefficient	Tolerance	T	P (two-tailed test)
Constant	4237.453	43.536	0.000	N/A	97.333	0.000
Freezing Temperature	-87.603	4.423	-0.794	0.098	-19.807	0.000
Thawing Temperature	-37.620	1.674	-0.525	0.289	-22.479	0.000
Storage Time	-1.747	0.504	-0.082	0.283	-3.468	0.001
Storage Temperature	12.369	2.615	0.112	0.280	4.730	0.000
Freezing Temperature*	1.075	0.186	0.211	0.119	5.781	0.000
Thawing Temperature*						
Freezing Temperature*	-0.056	0.056	-0.036	0.122	-1.001	0.322
Storage Time						
Freezing Temperature*	-0.197	0.380	-0.024	0.071	-0.518	0.607
Storage Temperature						
Freezing Temperature*	0.048	0.015	0.113	0.133	3.266	0.002
Thawing Temperature*						
Storage Temperature*						
Freezing Temperature*	0.009	0.004	0.073	0.136	2.148	0.036
Storage Temperature*						
Time						
Thawing Temperature*	0.007	0.002	0.081	0.249	3.239	0.002
Storage Temperature*						
Time						

Dependent Variable: Color concentration in the top 70 % liquid volume following treatment by freeze-thaw

Multiple R: 0.996, Squared Multiple R: 0.992, Adjusted Squared Multiple R: 0.990

Source	SUM-OF-SQUARES	DEGREES OF FREEDOM	MEAN-SQUARES	F-RATIO	P
REGRESSION	0.3262791E+08	10	3262788.945	630.051	0.000
RESIDUAL	274466.405	53	5178.611		
(Lack of Fit)	158103.905	21	7528.757	2.07	
(Pure Error)	116362.500	32	3636.328		

F(0.025, 21, 32) = 2.19

estimates; initial freezing temperature, thawing temperature and storage temperature as having deviated from the straight line (Figure 9.1). From this we can conclude that these effects cannot be easily explained as chance occurrences.

Residual analysis was performed on each independent variable to judge the model's adequacy. From examination of Figures 9.2 to 9.6 it can be seen that there were no severe deviations from normality. To check the model's lack of fit, the pure error sum of squares was calculated. The lack of fit sum of squares was calculated by subtracting the pure error sum of squares from the residual sum of squares. Using this information the F_o statistic was calculated and compared to the table value. Since $F_{(0.025, 21, 32)} > F_o$ in Table 9.3 we must accept the hypothesis that the tentative model adequately describes the data. The model is depicted in equation 9.1.

The empirical relationship developed to predict the resultant color concentration in the top 70 % liquid fraction following treatment of membrane concentrate by freeze-thaw is as follows:

$$\begin{aligned}
 y = & 4237.453 - 87.603 T_F - 37.620 T_T - 1.747 S_i + 12.369 S_T \\
 & + 1.075 T_F T_T - 0.056 T_T S_i - 0.197 T_F S_i + 0.048 T_F T_T S_T \\
 & + 0.009 T_F S_i S_T + 0.007 T_T S_i S_T
 \end{aligned} \quad (9.1)$$

where;

y = estimated color concentration in the top 70 % liquid volume, CU

T_F = Initial Freezing Temperature, °C

T_T = Thawing Temperature, °C

S_i = Storage Time, days

S_T = Storage Temperature, °C

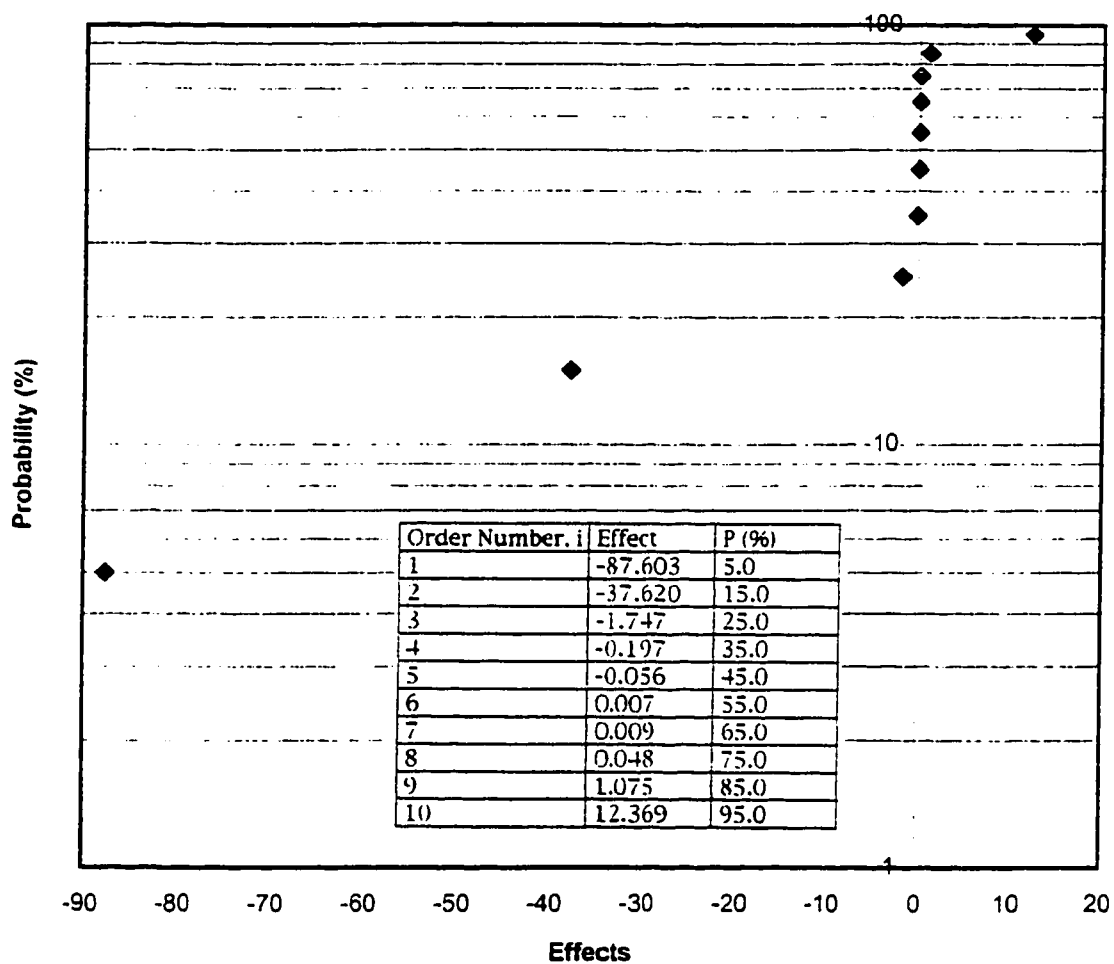


Figure 9.1 Normal Plot of Effects for the Regression Model Developed for the Membrane Concentrate

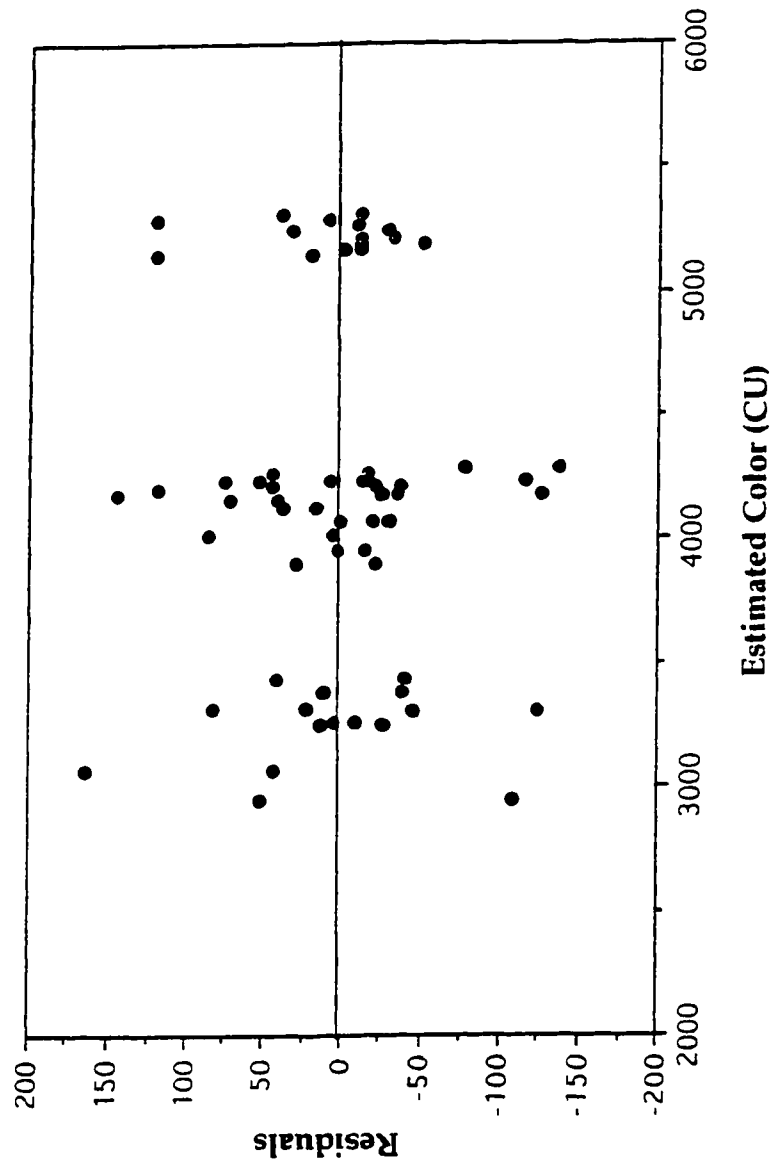


Figure 9.2 Plot of Residuals Against Estimated Color

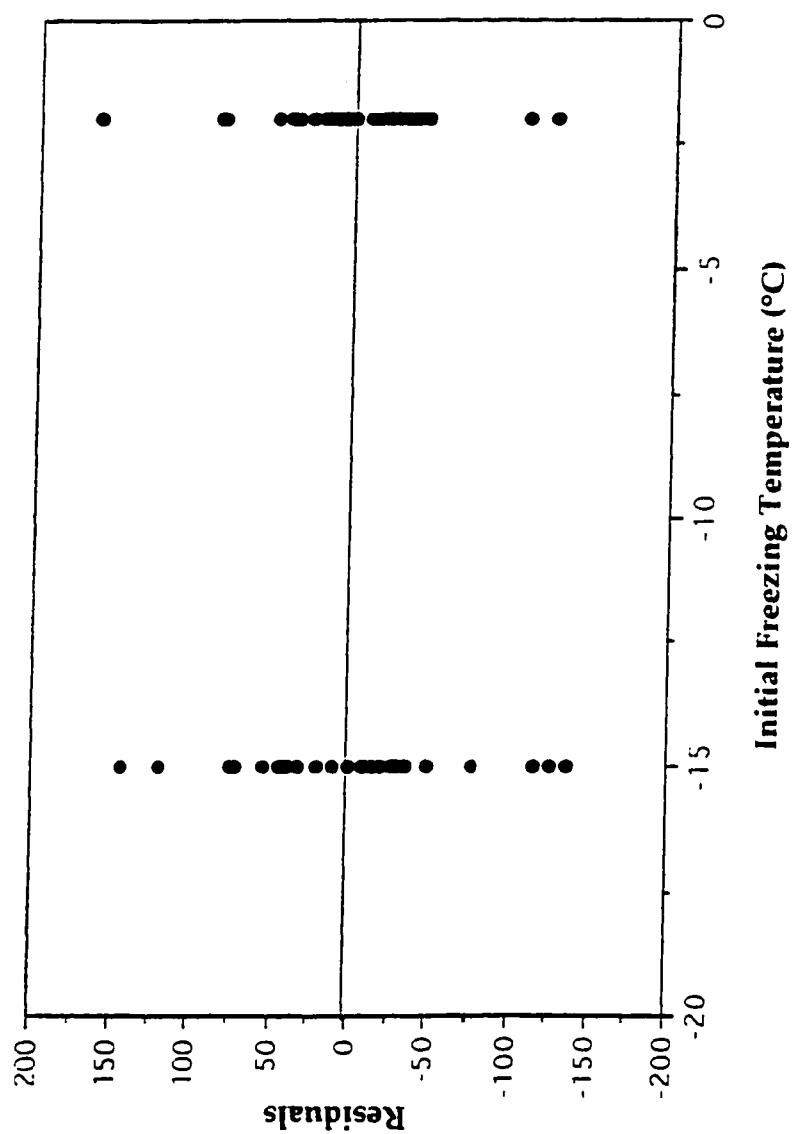


Figure 9.3 Plot of Residuals Against Initial Freezing Temperature

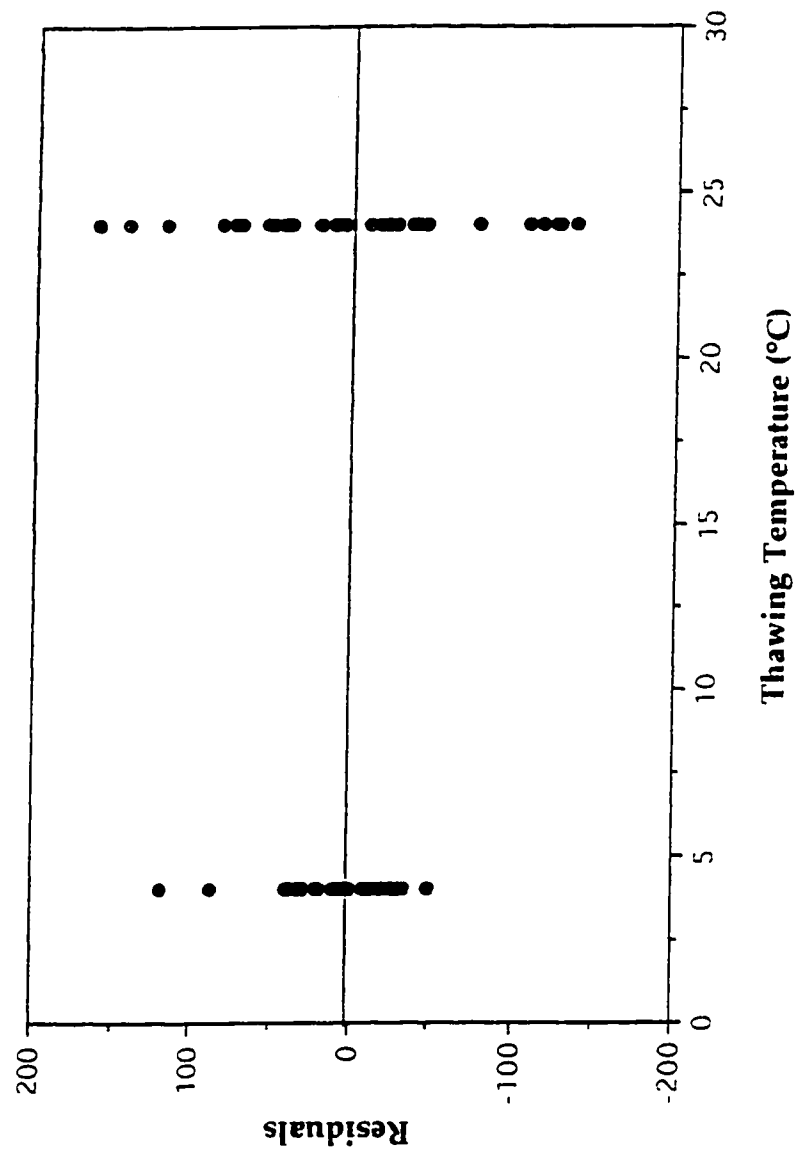


Figure 9.4 Plot of Residuals Against Thawing Temperature

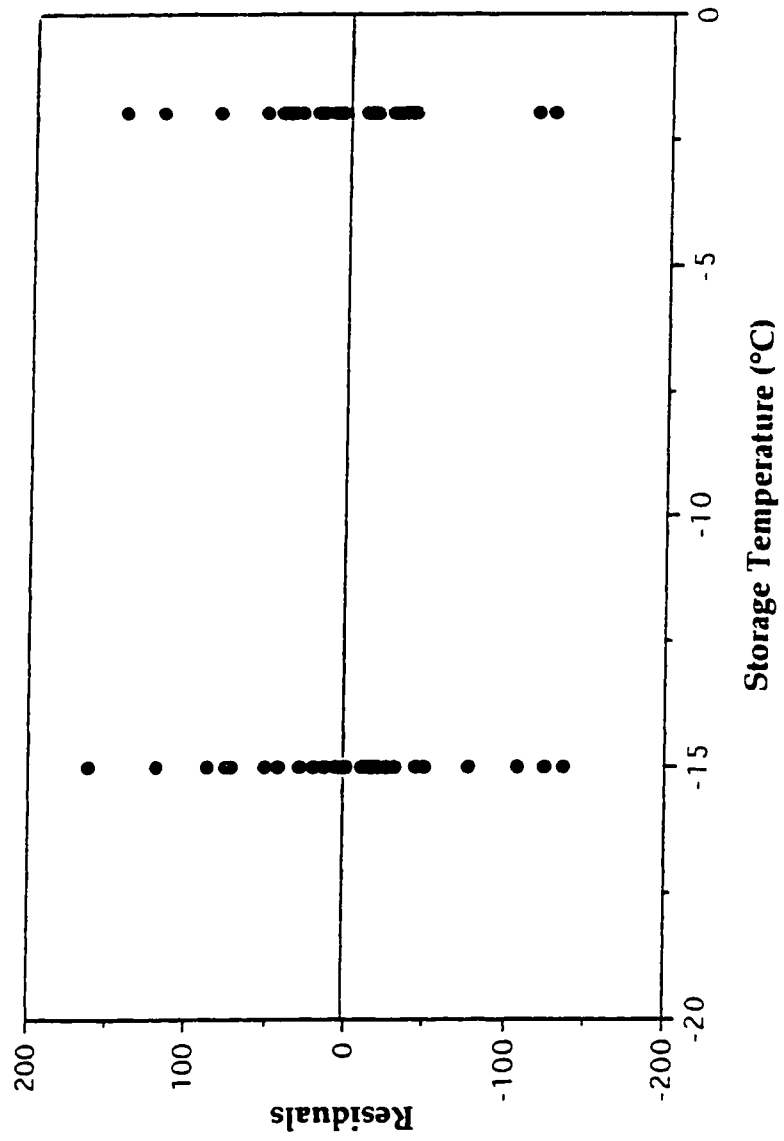


Figure 9.5 Plot of Residuals Against Storage Temperature

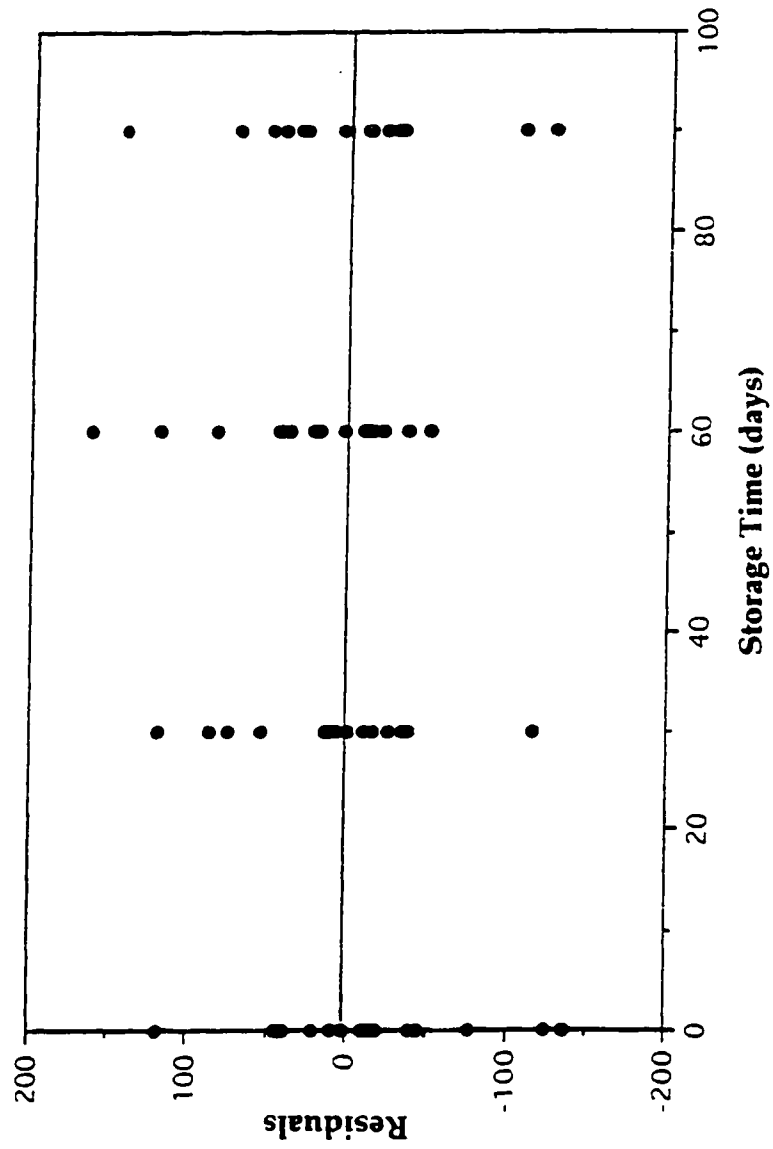


Figure 9.6 Plot of Residuals Against Storage Time

Although the above model adequately describes the data the inclusion of two and three level interactions unnecessarily makes model's use as an operational tool difficult. Stepwise regression was used as a variable selection technique to conclude the best regression equation. The computer results of this stepwise regression are given in Appendix E. The best regression is summarized in Table 9.4. Interactions deleted as part of the stepwise analysis were initial freezing temperature * storage time, and initial freezing temperature * storage temperature. A revised normal plot of the individual effects with respect to probability shows the results did not change with the estimates; initial freezing temperature, thawing temperature and storage temperature deviating from the straight line (Figure 9.7). Deletion of these terms did not change the adjusted coefficient of multiple determination R^2 . Residual analysis was performed on each independent variable to judge the model's adequacy. From examination of Figures 9.8 to 9.12 it can be seen that there were no severe deviations from normality. To check the model's lack of fit, the lack of fit sum of squares was recalculated by subtracting the pure error sum of squares from the residual sum of squares. Using this information the F_o statistic was calculated and compared to the table value. Since $F_{(0.025, 24, 32)} > F_o$ in Table 9.4 we cannot reject the hypothesis that the tentative model adequately describes the data. The best regression model is depicted in equation 9.2.

$$y = 4232.061 - 87.997 T_F - 37.696 T_T - 1.380 S_i + 13.676 S_T \quad (9.2) \\ + 1.009 T_F T_T + 0.040 T_F T_T S_T + 0.011 T_F S_i S_T + 0.006 T_T S_i S_T$$

where;

y = estimated color concentration in the top 70 % liquid volume, CU

T_F = Initial Freezing Temperature, °C

T_T = Thawing Temperature, °C

S_i = Storage Time, days

S_T = Storage Temperature, °C

9.4.2 ALKALINE EXTRACTION STAGE EFFLUENT

Multiple linear regression analysis was performed on the laboratory data produced in the treatment of Eop effluent by freeze-thaw. The independent variables considered in the analysis were those interactions shown to significantly affect treatment performance in the analysis of variance table. Summarized in Table 9.5 are the regression results.

Tests on the individual regression coefficients showed that all the interactions with the exception of thawing temperature * storage temperature contributed significantly to the model. The above testing of the individual regression coefficients suggests the model might be more effective with the deletion of the interaction thawing temperature * storage temperature. The adjusted coefficient of multiple determination R^2 was 0.986 to indicate that about 98.60 % of the variability in the measured color concentration in the top 70 % liquid volume was explained by using the independent variables: initial freezing temperature, thawing temperature, storage time and storage temperature. A normal plot of the individual effects with respect to probability shows the estimates; initial freezing temperature, storage temperature, thawing temperature, storage time and initial freezing temperature * thawing

Table 9.4 Best Multiple Linear Regression Model as Determined by Stepwise Regression for Prediction of the

Color Concentration in the Top 70 % Liquid Fraction of Membrane Concentrate Treated by Freeze-thaw

Independent Variable	Coefficient	Standard Error	Standard Coefficient	Tolerance	T	P (two-tailed test)
Constant	4232.061	37.209	0.000	N/A	113.739	0.000
Freezing Temperature	-87.997	2.609	-0.798	0.282	-33.732	0.000
Thawing Temperature	-37.696	1.626	-0.526	0.307	-23.181	0.000
Storage Time	-1.380	0.373	-0.065	0.519	-3.704	0.000
Storage Temperature	13.676	1.998	0.124	0.481	6.846	0.000
Freezing Temperature*	1.009	0.166	0.198	0.148	6.061	0.000
Thawing Temperature						
Freezing Temperature*	0.040	0.011	0.094	0.241	3.677	0.001
Thawing Temperature* Storage Temperature						
Freezing Temperature*	0.011	0.003	0.082	0.343	3.823	0.000
Storage Time* Storage Temperature						
Thawing Temperature*	0.006	0.002	0.079	0.340	3.662	0.001
Storage Time* Storage Temperature						

Dependent Variable: Color concentration in the top 70 % liquid volume following treatment by freeze-thaw

Multiple R: 0.996, Squared Multiple R: 0.0991, Adjusted Squared Multiple R: 0.990

Source	SUM-OF-SQUARES	DEGREES OF FREEDOM	MEAN-SQUARES	F-RATIO	P
REGRESSION	0.326170E+08	8	4077122.998	785.788	0.000
RESIDUAL	285371.878	55	5188.580		
(Lack of Fit)	169009.378	23	7348.234	2.02	
(Pure Error)	116362.500	32	3636.328		

 $F_{(0.025, 23, 32)} = 2.14$

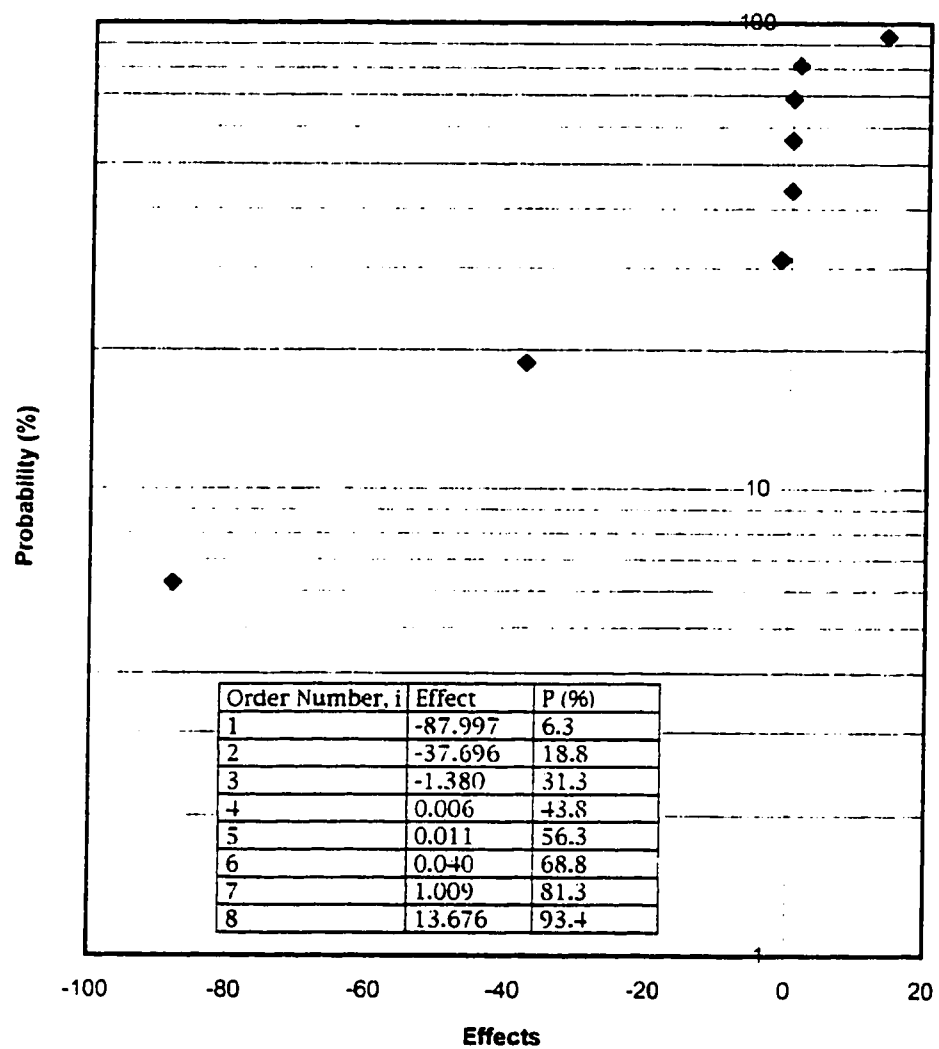


Figure 9.7 Normal Plot of Effects for the Revised Regression Model Developed for the Membrane Concentrate

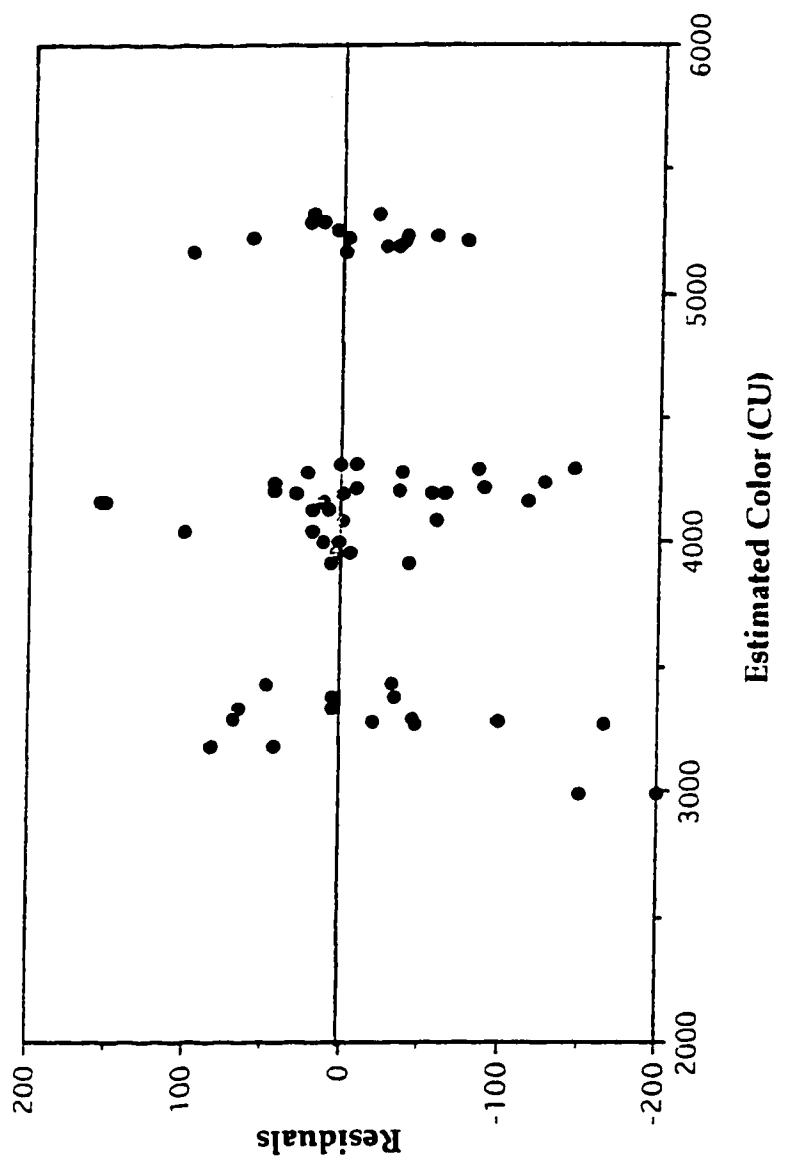


Figure 9.8 Plot of Residuals Against Estimated Color for the Revised Model (Membrane Concentrate)

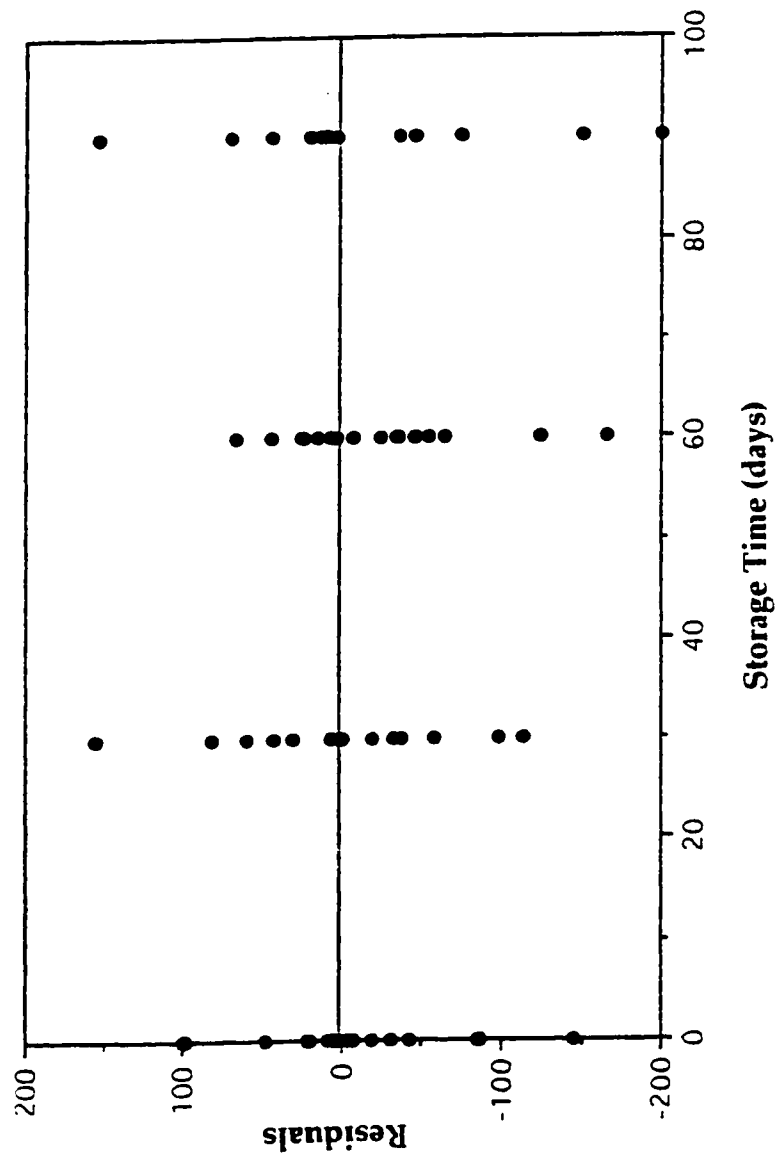


Figure 9.9 Plot of Residuals Against the Independent Variable Storage Time for the Revised Model (Membrane Concentrate)

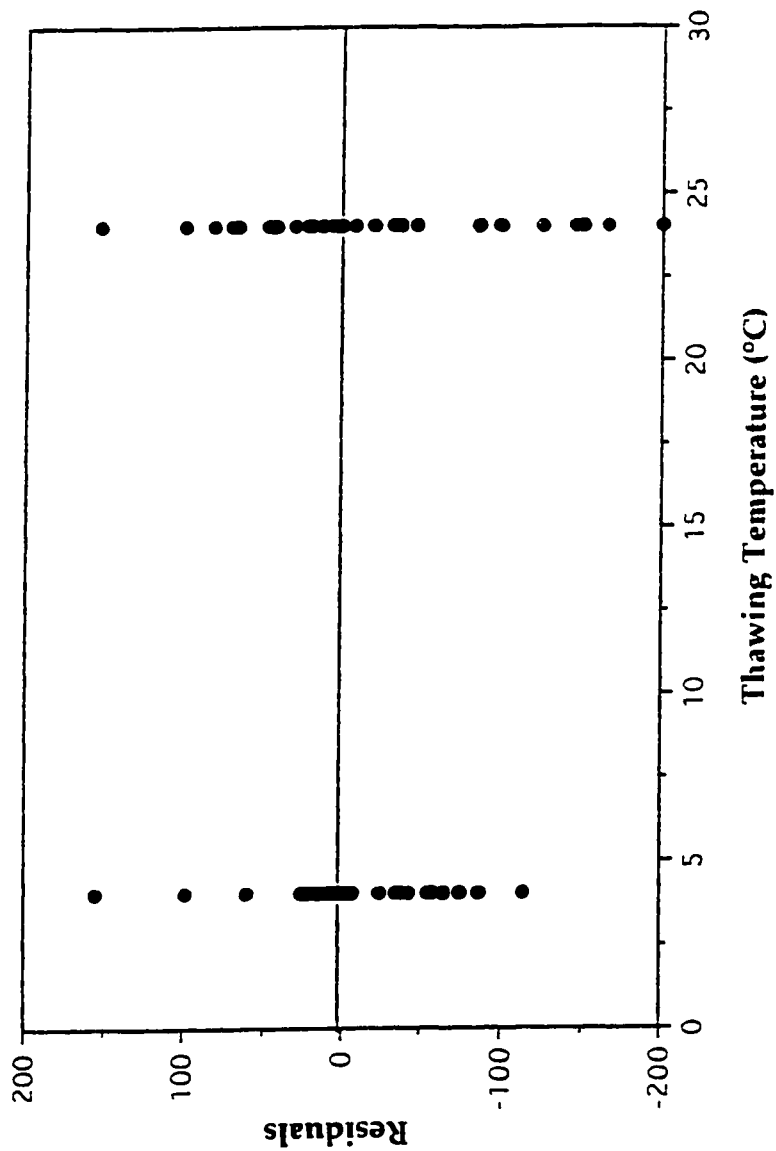


Figure 9.10 Plot of Residuals Against the Independent Variable Thawing Temperature for the Revised Model (Membrane Concentrate)

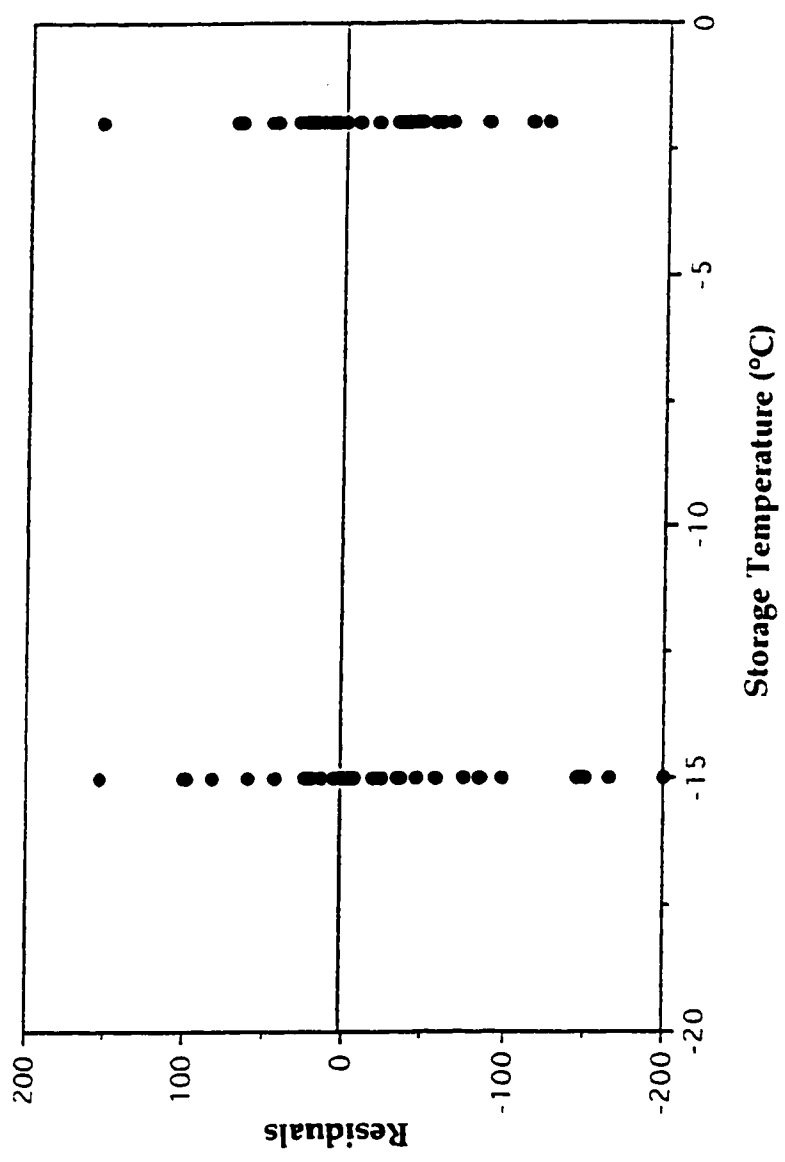


Figure 9.11 Plot of Residuals Against the Independent Variable Storage Temperature for the Revised Model (Membrane Concentrate)

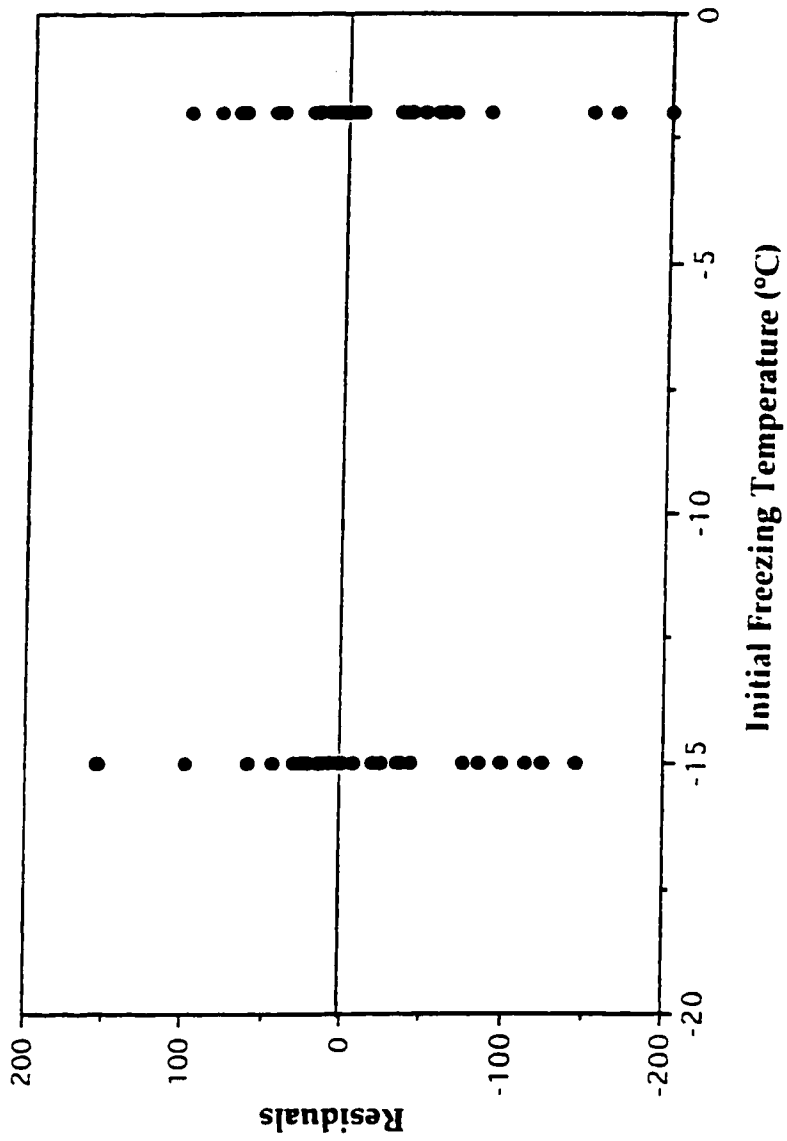


Figure 9.12 Plot of Residuals Against the Independent Variable Initial Freezing Temperature for the Revised Model (Membrane Concentrate)

Table 9.5 Multiple Linear Regression Model for Prediction of the Color Concentration in the Top 70 % Liquid Fraction of Eop Effluent Treated by Freeze-thaw

Independent Variable	Coefficient	Standard Error	Standard Coefficient	Tolerance	T	P (two-tailed test)
Constant	1378.123	17.714	0.000	N/A	77.800	0.000
Freezing Temperature	20.606	1.322	0.583	0.155	15.587	0.000
Thawing Temperature	-35.676	0.843	-1.552	0.161	-42.342	0.000
Storage Time	-0.805	0.254	-0.117	0.157	-3.164	0.003
Storage Temperature	4.290	1.322	0.121	0.155	3.245	0.002
Freezing Temperature*	-1.586	0.056	-0.969	0.214	-30.520	0.000
Thawing Temperature*	0.032	0.010	0.102	0.210	3.171	0.003
Storage Time	-0.033	0.015	-0.067	0.222	-2.161	0.035
Freezing Temperature*	-0.104	0.052	-0.064	0.214	-2.003	0.050
Storage Temperature	0.050	0.015	0.101	0.222	3.220	0.002
Freezing Temperature*	0.188	0.088	0.073	0.226	2.354	0.022
Storage Temperature						

Dependent Variable: Color concentration in the top 70 % liquid volume following treatment by freeze-thaw

Multiple R: 0.994, Squared Multiple R: 0.0989, Adjusted Squared Multiple R: 0.986

Source	SUM-OF-SQUARES	DEGREES OF FREEDOM	MEAN-SQUARES	F-RATIO	P
REGRESSION	3343121.506	10	334312.151	457.677	0.000
RESIDUAL	38714.103	53	730.455		
(Lack of Fit)	20772.25	21	989.155	1.587	
(Pure Error)	19944.500	32	623.266		

$F_{(0.025, 21, 32)} = 2.19$

temperature as having deviated from the straight line (Figure 9.13). From this we can conclude that these effects cannot be explained as chance occurrences. In the test for significance of regression $F_o > F_{(0.025, 10, 53)}$ to reject the hypothesis that at least one of the independent variables contributes significantly to the model.

Residual analysis was performed on each independent variable to judge the model adequacy. From examination of Figures 9.14 to 9.18 it can be seen that there were no severe deviations from normality. To check the model's lack of fit, the pure error sum of squares was calculated. The lack of fit sum of squares was calculated by subtracting the pure error sum of squares from the residual sum of squares. Using this information the F_o statistic was calculated and compared to the table value. Since F_o was $< F_{(0.025, 21, 32)}$ in Table 9.5 we cannot reject the hypothesis that the tentative model adequately describes the data. The model is depicted in equation 9.3.

The empirical relationship developed to predict the resultant color concentration in the top 70 % liquid fraction following treatment of Eop effluent by freeze-thaw is as follows (equation 9.3):

$$y = 1378.123 + 20.606 T_F - 35.676 T_T - 0.805 S_i + 4.290 S_T - 1.586 T_F T_T \\ + 0.032 T_T S_i - 0.033 T_F S_i - 0.104 T_T S_T + 0.188 T_F S_T + 0.050 S_i S_T$$

where;

y = estimated color concentration in the top 70 % liquid volume, CU

T_F = Initial Freezing Temperature, °C

T_T = Thawing Temperature, °C

S_i = Storage Time, days

S_T = Storage Temperature, °C

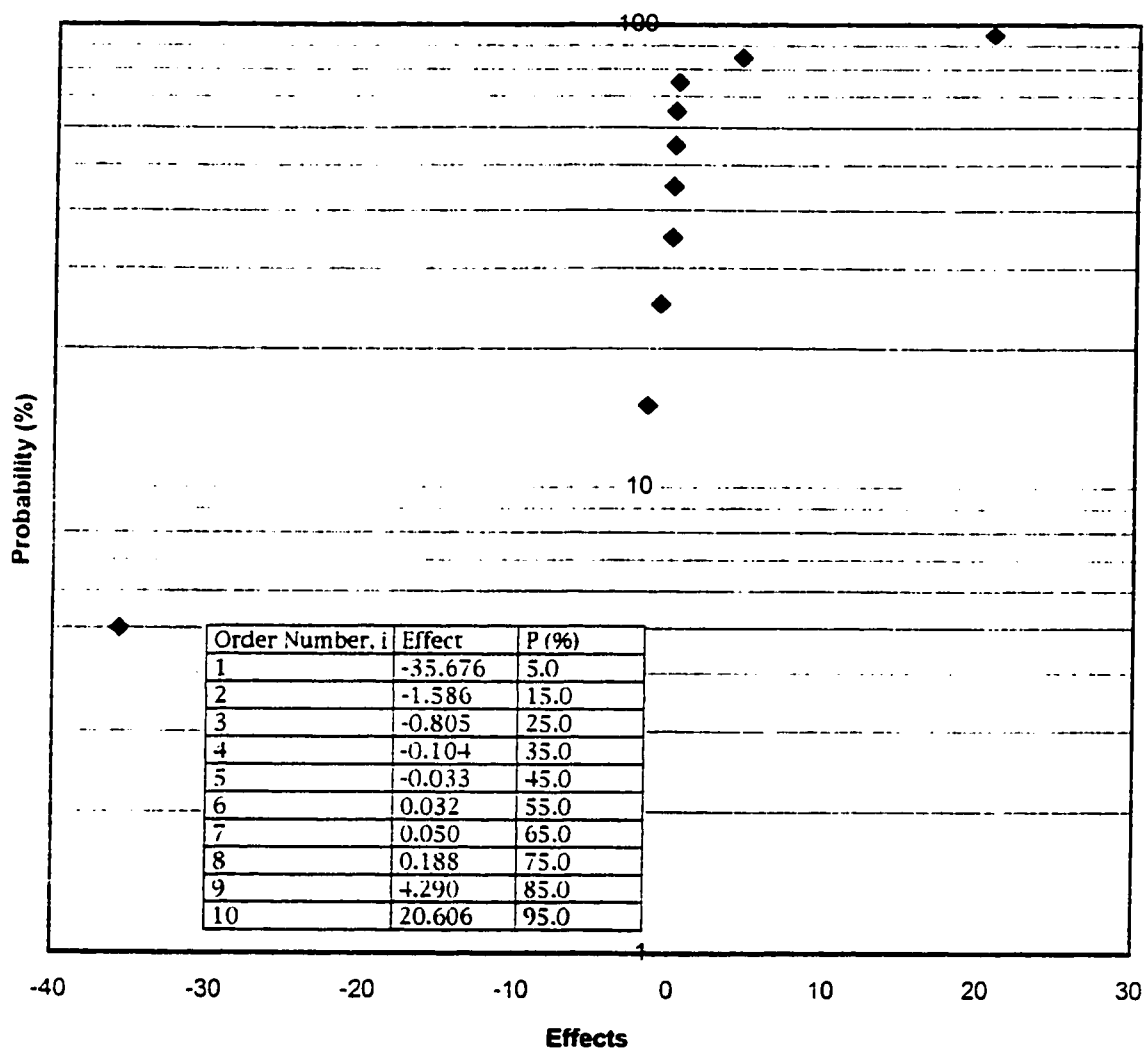


Figure 9.13 Normal Plot of Effects for the Regression Model Developed for the Eop Effluent

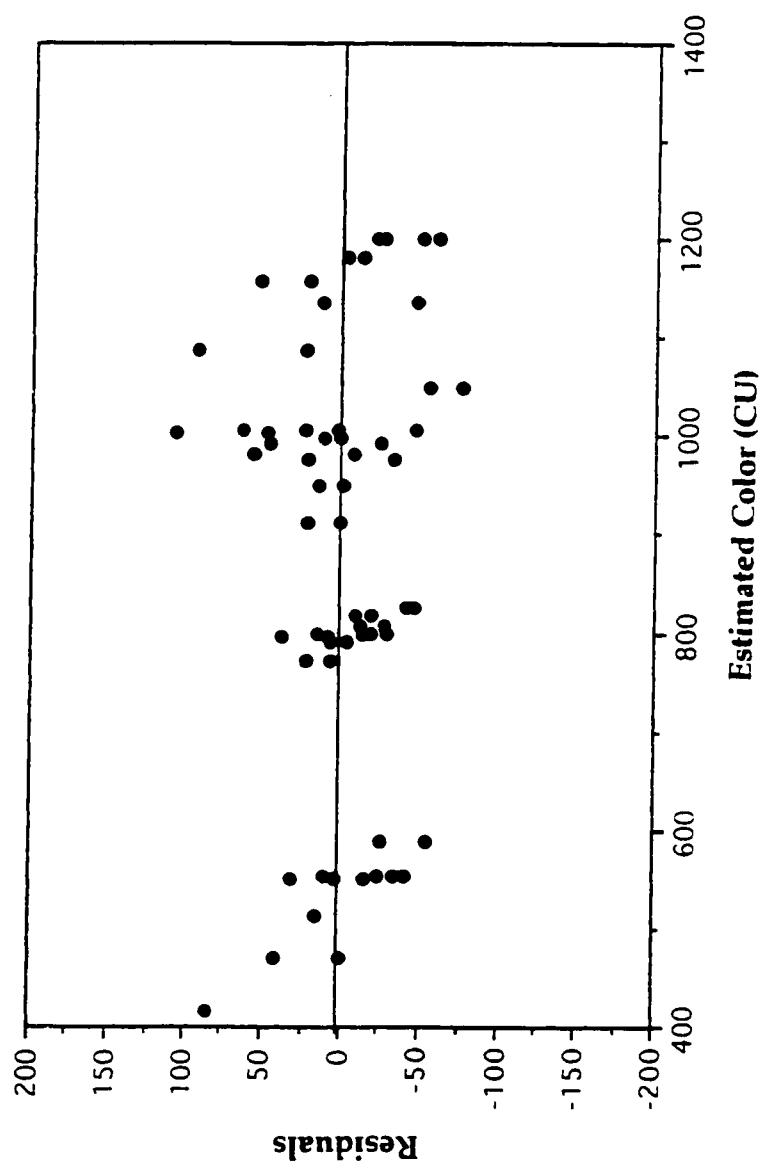


Figure 9.14 Plot of Residuals Against Estimated Color

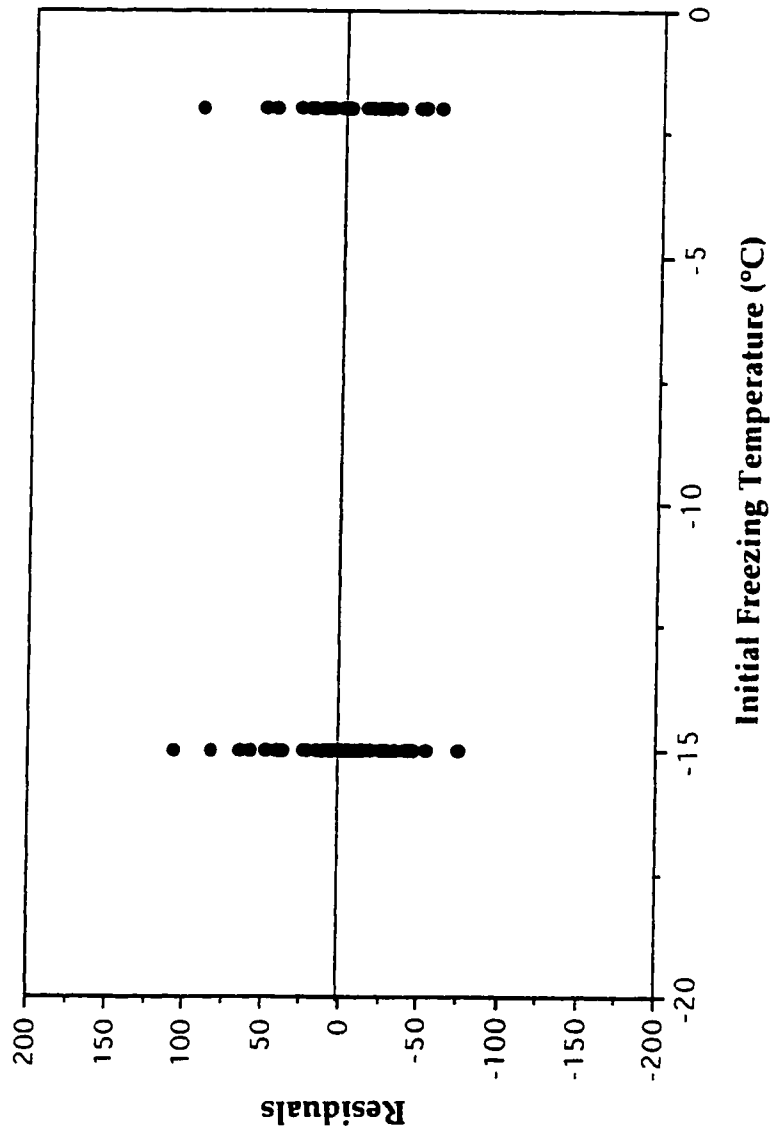


Figure 9.15 Plot of Residuals Against Initial Freezing Temperature

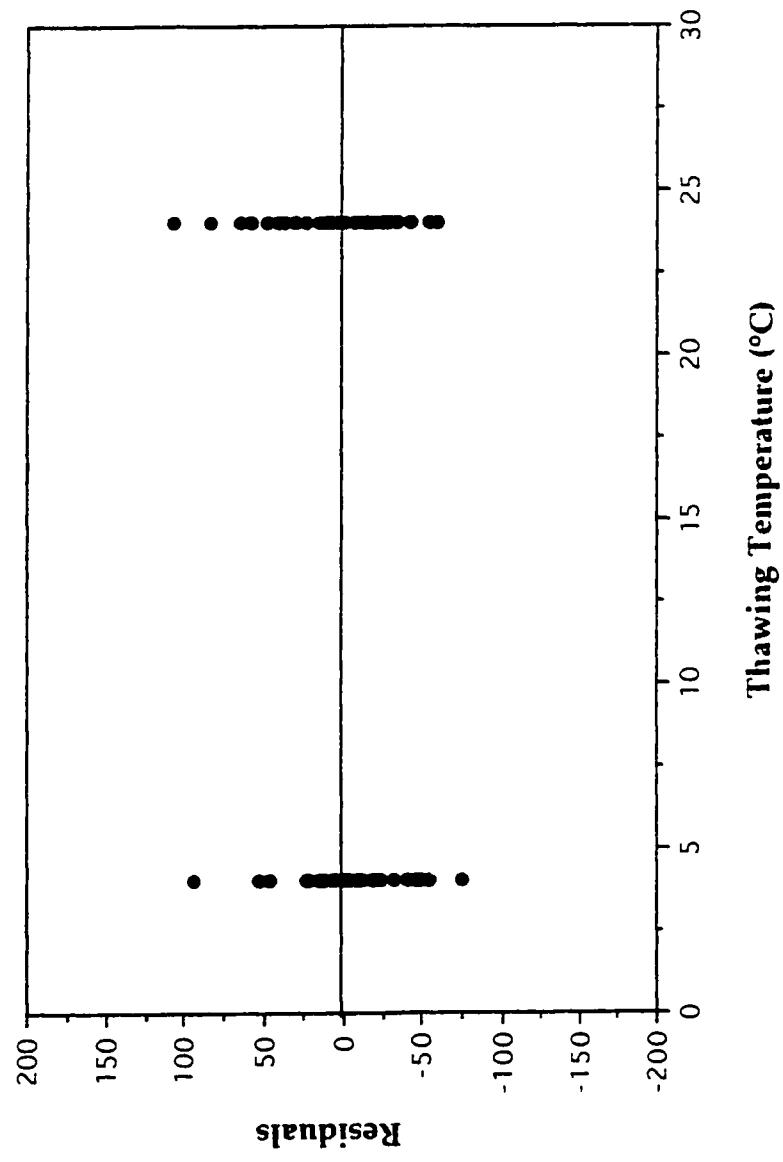


Figure 9.16 Plot of Residuals Against Thawing Temperature

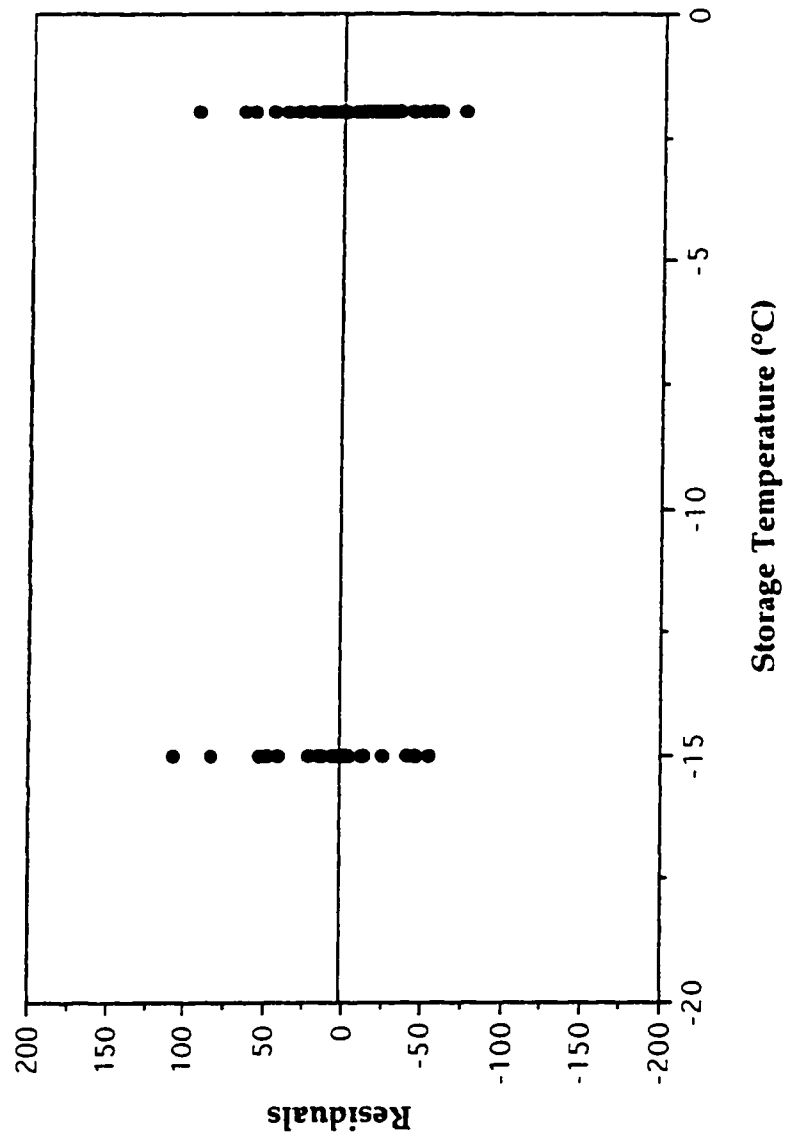


Figure 9.17 Plot of Residuals Against Storage Temperature

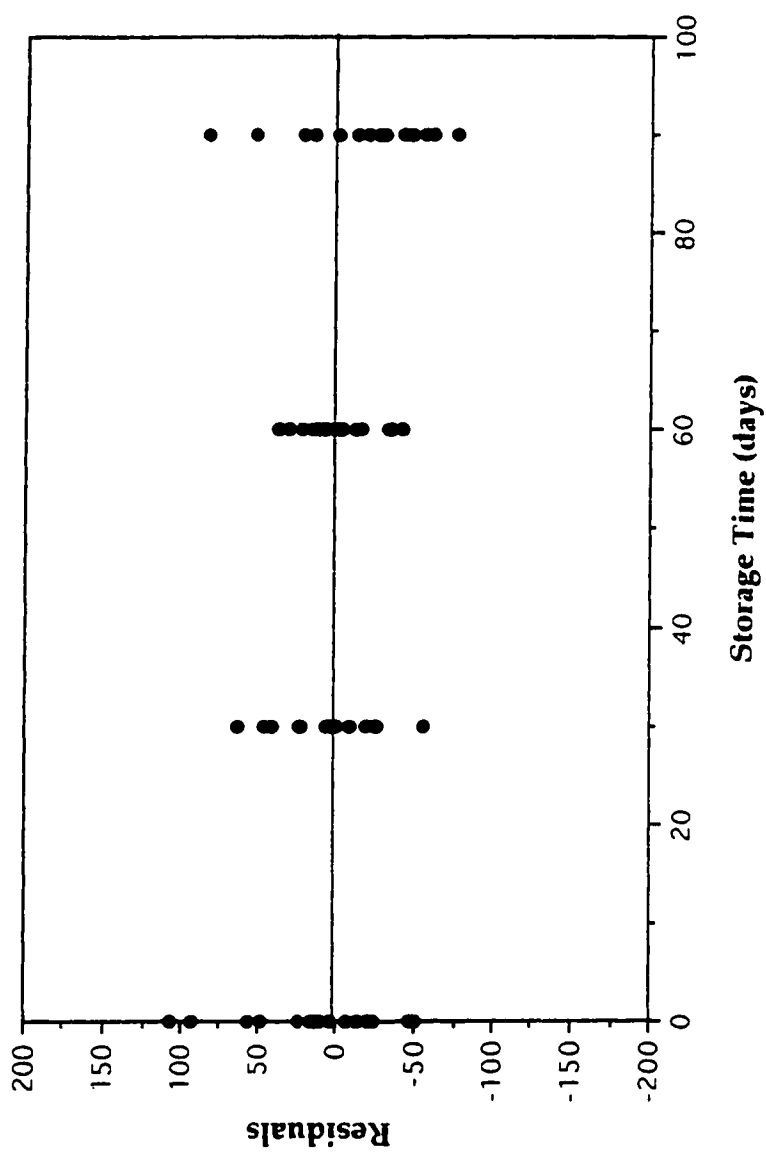


Figure 9.18 Plot of Residuals Against Storage Time

Although the above model adequately describes the data the inclusion of two level interactions unnecessarily makes model's use as an operational tool difficult. Stepwise regression was used as a variable selection technique to conclude the best regression equation. The computer results of this stepwise regression are given in Appendix F. The best regression is summarized in Table 9.6. Interactions deleted as part of the stepwise analysis were storage temperature, initial freezing temperature * storage temperature, and thawing temperature * storage temperature. A revised normal plot of the individual effects with respect to probability shows the estimates; initial freezing temperature, thawing temperature, and initial freezing temperature * thawing temperature as not having fallen on the straight line (Figure 9.19). From this we can conclude that these effects cannot be explained as chance occurrences. Deletion of these terms reduced the adjusted coefficient of multiple determination R^2 from 0.986 to 0.984. Residual analysis was performed on each independent variable to judge the model adequacy. From examination of Figures 9.20 to 9.24 it can be seen that there were no severe deviations from normality. To check the model's lack of fit, the lack of fit sum of squares was recalculated by subtracting the pure error sum of squares from the residual sum of squares. Using this information the F_0 statistic was calculated and compared to the table value. Since F_0 was $< F_{(0.025, 24, 32)}$ in Table 9.6 we cannot reject the hypothesis that the tentative

Table 9.6 Best Multiple Linear Regression Model as Determined by Stepwise Regression for Prediction of the Color Concentration in the Top 70 % Liquid Fraction of Eop Effluent Treated by Freeze-thaw

Independent Variable	Coefficient	Standard Error	Standard Coefficient	Tolerance	T	P (two-tailed test)
Constant	1341.658	14.702	0.000	N/A	91.254	0.000
Freezing Temperature	19.006	1.218	0.537	0.210	15.610	0.000
Thawing Temperature	-34.791	0.770	-1.513	0.222	-45.162	0.000
Storage Time	-0.655	0.249	-0.096	0.189	-2.637	0.011
Freezing Temperature* Thawing Temperature	-1.586	0.056	-0.969	0.214	-28.425	0.000
Thawing Temperature* Storage Time	0.032	0.011	0.102	0.210	2.953	0.005
Freezing Temperature* Storage Time	-0.033	0.017	-0.067	0.222	-2.013	0.049
Storage Time* Storage Temperature	0.068	0.010	0.136	0.621	6.790	0.000

Dependent Variable: Color concentration in the top 70 % liquid volume following treatment by freeze-thaw

Multiple R: 0.993, Squared Multiple R: 0.0986, Adjusted Squared Multiple R: 0.984

Source	SUM-OF-SQUARES	DEGREES OF FREEDOM	MEAN-SQUARES	F-RATIO	P
REGRESSION	3334676.418	7	476382.345	565.688	0.000
RESIDUAL	47159.192	56	842.128		
(Lack of fit)	29214.692	24	1217.279	1.95	
(Pure Error)	19944.500	32	623.266		

F(0.025, 24,32) = 2.12

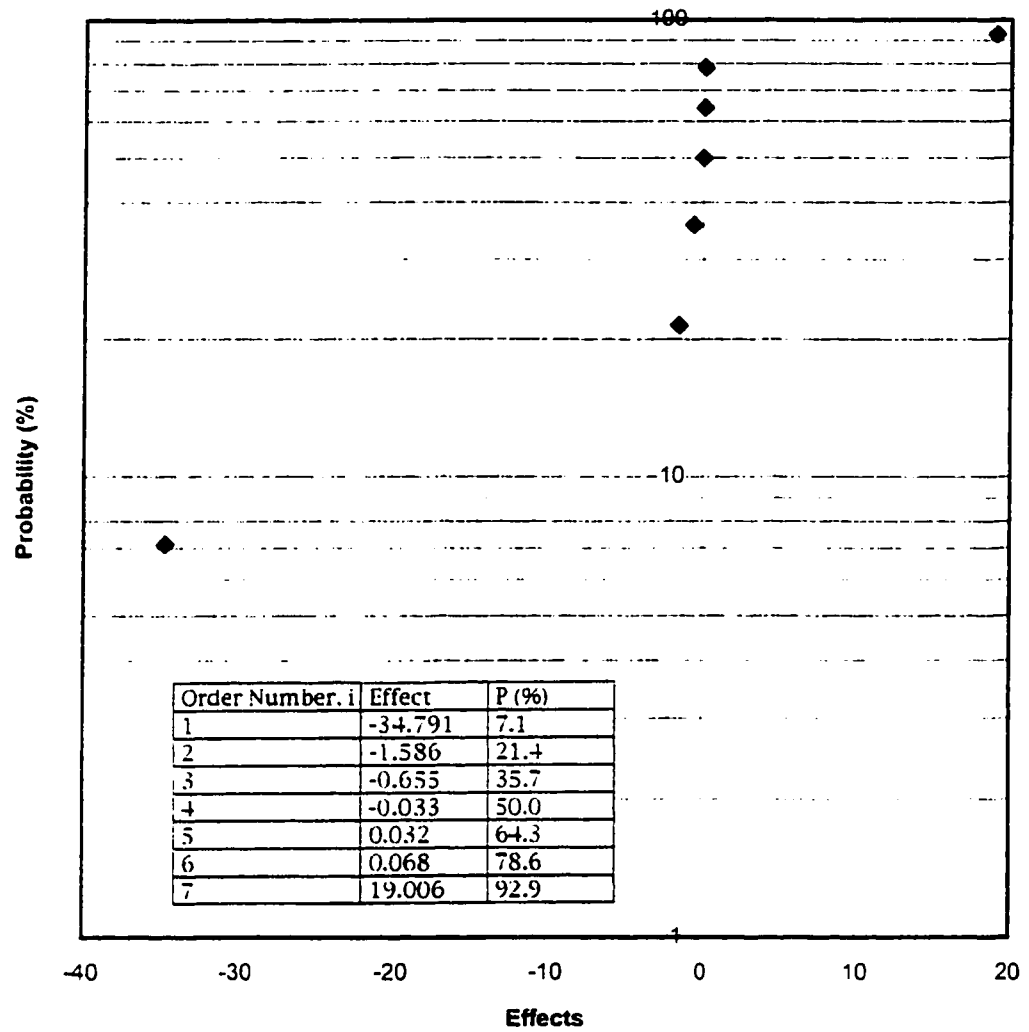


Figure 9.19 Normal Plot of Effects for the Revised Regression Model
Developed for the Eop Effluent

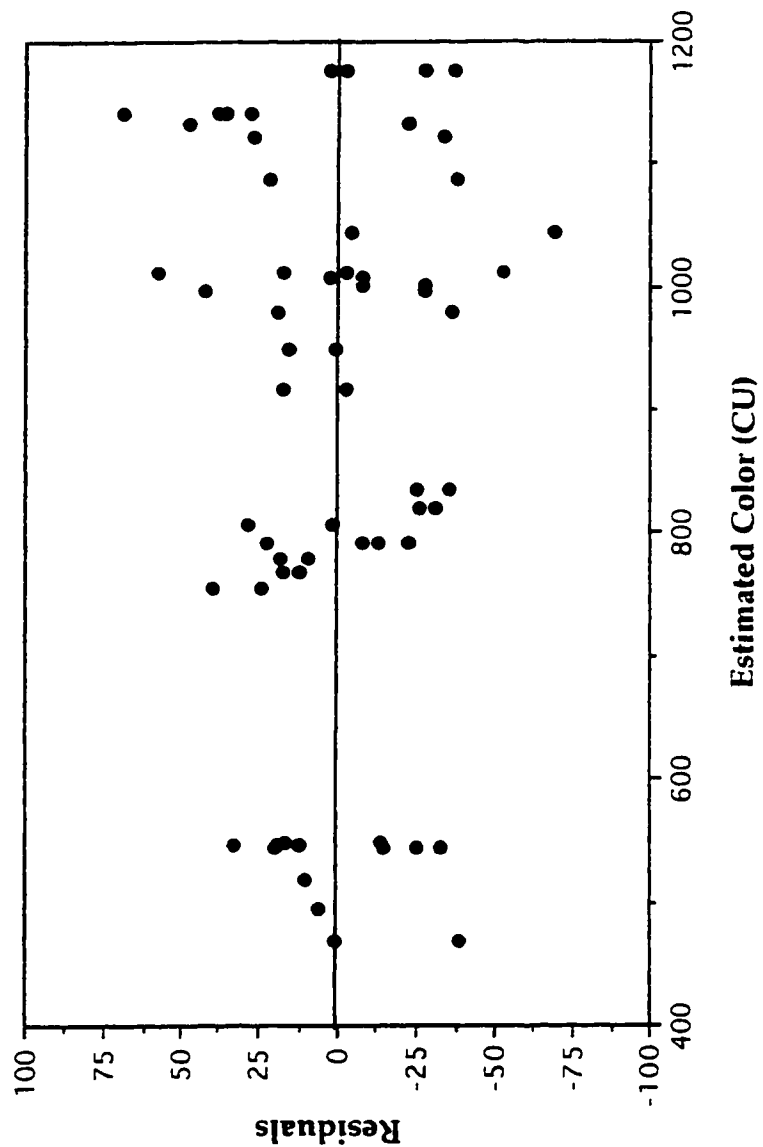


Figure 9.20 Plot of Residuals Against Estimated Color for the Revised Model (Eop Effluent)

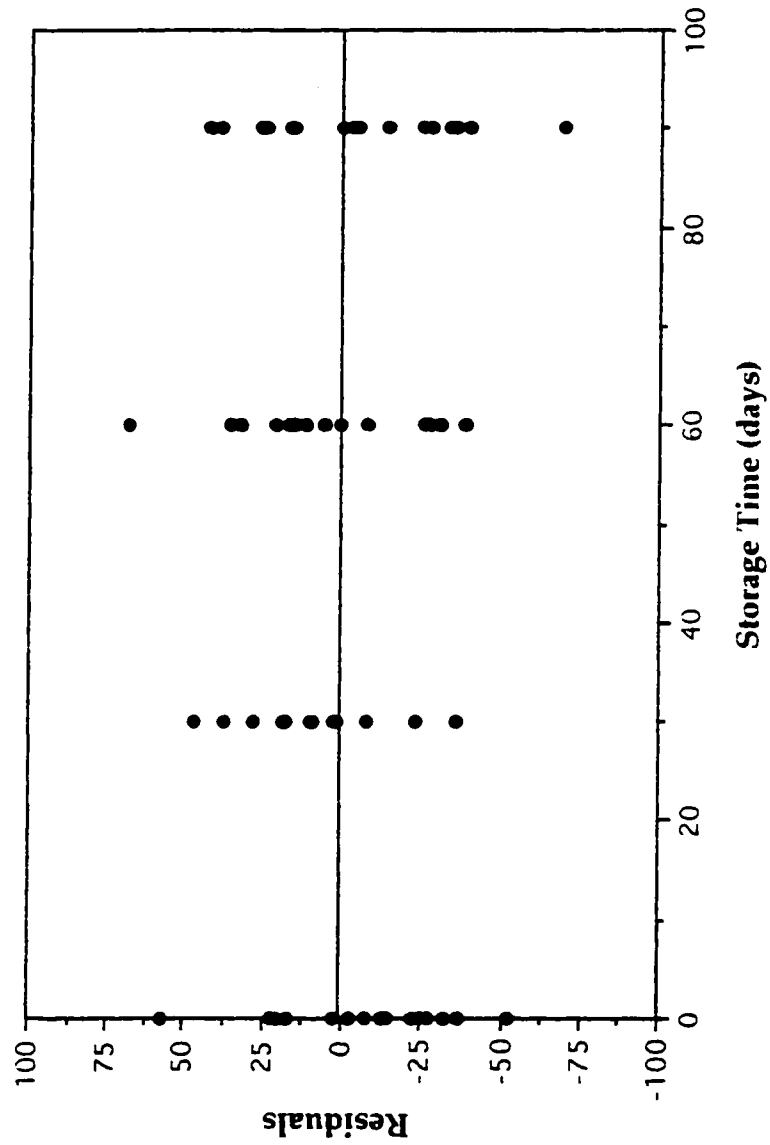


Figure 9.21 Plot of Residuals Against the Independent Variable Storage Time for the Revised Model (Eop Effluent)

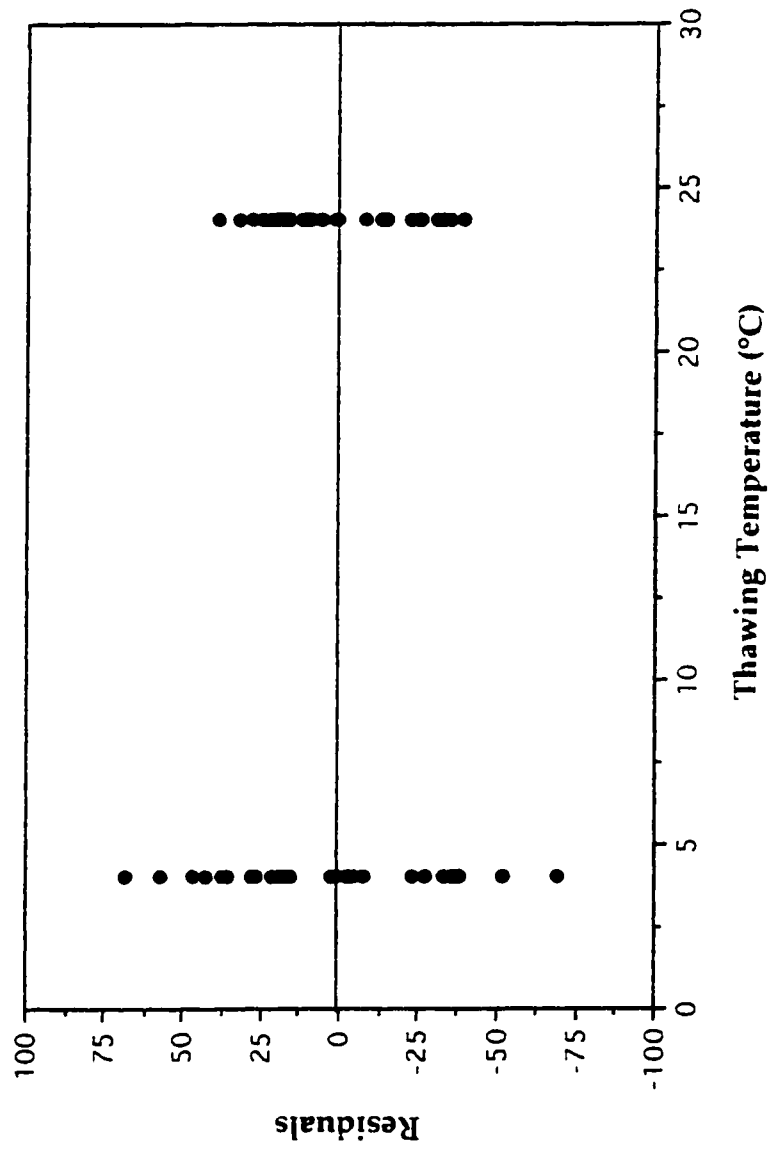


Figure 9.22 Plot of Residuals Against the Independent Variable Thawing Temperature for the Revised Model (Eop Effluent)

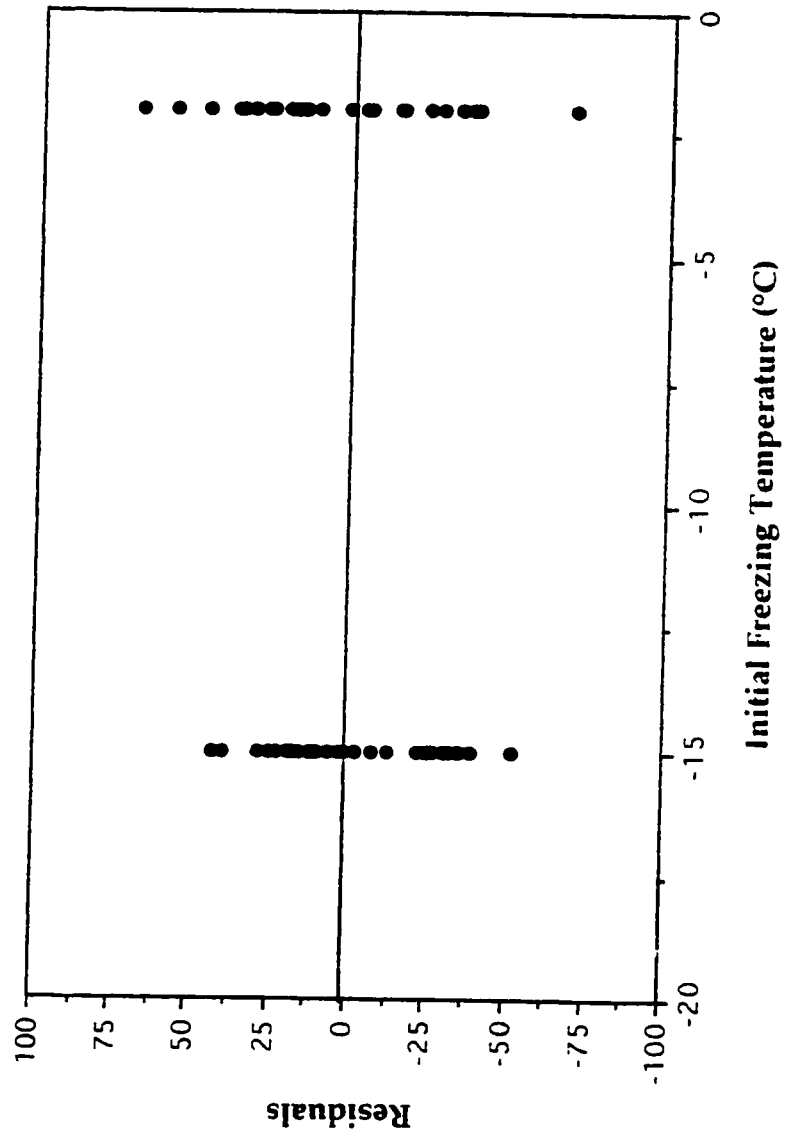


Figure 9.24 Plot of Residuals Against the Independent Variable Initial Freezing Temperature for the Revised Model (Eop Effluent)

model adequately describes the data. The best regression model is depicted in equation 9.4.

$$y = 1341.658 + 19.006 T_F - 34.791 T_T - 0.655 S_i - 1.586 T_F T_T + 0.032 T_T S_i - 0.033 T_F S_i + 0.068 S_i S_T \quad (9.4)$$

where;

y = estimated color concentration in the top 70 % liquid volume, CU

T_F = Initial Freezing Temperature, °C

T_T = Thawing Temperature, °C

S_i = Storage Time, days

S_T = Storage Temperature, °C

9.5 MODEL TESTING

The best empirical models developed for each experimental water type were checked for their prediction of new observations at different experimental set points from those used in modeling.

9.5.1 ALKALINE EXTRACTION STAGE MEMBRANE CONCENTRATE

The best empirical model (equation 9.2) was tested at an experimental set point other than that used in the development of the model to check its prediction of new observations. Summarized in Table 9.7 are actual values compared to predicted values by the new model. The actual data used represents the resultant color concentration in the top 70 % liquid volume in which the experimental set points were: initial freezing temperature -5 °C, thawing temperature 24 °C, storage time 0, and storage temperature equal to the initial freezing temperature. Examination

of Table 9.7 shows the model was a good predictor of the actual color concentration measured in the upper liquid portion of the run setting taken between the boundary set points of the model. Residuals at the initial freezing temperature -5°C were calculated to range from 78 CU to 192 CU.

9.5.2 ALKALINE EXTRACTION STAGE EFFLUENT

The best empirical model (equation 9.4) was tested at two different experimental set points to check the model's prediction of new observations. Summarized in Table 9.8 are actual values compared to predicted values by the new model. The actual data used represents the resultant color concentration in the top 70 % liquid volume in which the experimental set points were: initial freezing temperature -5°C and -10°C , thawing temperature 24°C , storage time 0, and storage temperature equal to the initial freezing temperatures. Examination of Table 9.8 shows the model was a good predictor of the actual color concentration measured in the upper liquid portion of run settings taken between the boundary set points of the model. Residuals at the initial freezing temperature -5°C were calculated to range from 8 CU to 57 CU, for a corresponding range in percent difference between 1.3 % to 9.5 %. At the initial freezing temperature -10°C the residuals were calculated to range from 48 CU to 71 CU, for a corresponding range in percent differences from between 6.4 % to 9.2 %.

Table 9.7 Prediction of New Observations Using the Best Regression
Model Developed From the Membrane Concentrate Data

Experimental Setting	Actual Measured Value (CU)*	Predicted Value (CU)	Residuals	Percent Difference (%)
Freezing Temperature = -5 °C Thawing Temperature = 24 °C Storage Time = 0 days Storage Temperature = -5 °C	3680	3600	78	2.1
Freezing Temperature = -5 °C Thawing Temperature = 24 °C Storage Time = 0 days Storage Temperature = -5 °C	3410	3600	-192	5.3

* color concentration in the top 70 % liquid volume

Table 9.8 Prediction of New Observations Using the Best Regression Model Developed From the Eop Data

Experimental Setting	Actual Measured Value (CU)*	Predicted Value (CU)	Residuals (CU)	Percent Difference (%)
Freezing Temperature = -10 °C Thawing Temperature = 24 °C Storage Time = 0 days Storage Temperature = -10 °C	768	697	71	9.2
Freezing Temperature = -10 °C Thawing Temperature = 24 °C Storage Time = 0 days Storage Temperature = -10 °C	745	697	48	6.4
Freezing Temperature = -5 °C Thawing Temperature = 24 °C Storage Time = 0 days Storage Temperature = -5 °C	545	602	-57	9.5
Freezing Temperature = -5 °C Thawing Temperature = 24 °C Storage Time = 0 days Storage Temperature = -5 °C	610	602	8	1.3

* color concentration in the top 70 % liquid volume

10.0 OVERALL SUMMARY AND CONCLUSIONS

The research identified a new field of application for freeze-thaw as a waste treatment process for the management of high strength effluents derived from kraft pulp mill operations. Freeze-thaw was shown that it can effectively treat effluents that are comprised of dissolved and colloidal organic matter which through concentration and mechanical coagulation by freezing can be efficiently settled and removed from the bulk solution upon thawing to allow the collection of a relatively clear supernatant. Although the focus of this research was on kraft pulp mill effluents, it is likely that this method of treatment is also suitable for other waste effluents whose constituents are amenable to removal by mechanical coagulation using freezing.

Alkaline extraction stage effluent and concentrates there of are waste streams that are well suited for treatment by freeze-thaw. The primary mechanisms postulated as being responsible for removal of the effluent's constituent matter by freeze-thaw were based on a series of experiments conducted to examine the concentrated material in its frozen and thawed physical state. Found was there occurs a series of mechanisms that work consecutively to concentrate and settle the constituents of the waste effluent as a concentrated material. It was postulated that separation initially begins to occur in the cooling of the liquid during freezing through settlement of more dense liquid layers as water approaches its maximum density during cooling. This was followed by the development of a fine layer of ice on the liquid surface, from which ice needles began to grow. The rate of freezing determines the cross sectional morphology of these ice needles. Slow rates of freezing produces circular ice needles,

where as high rates of freezing causes the ice needles to rapidly grow predominantly in one direction to form the sheet like pattern observed in SEM studies. The variable solute concentration around the perimeter of the ice needles causes them to grow predominantly downward, parallel with the direction of freezing pushing aside the liquid's constituents in search of new water molecules. Over time these ice needles grow outward to slowly concentrate the constituents to form highly concentrated zones of concentrate. Changing water chemistry within these zones over time affects the both the solubility and stability of the constituent matter. Mechanical coagulation occurs during freezing from the compression of the double layer of the colloidal organics by indifferent electrolytes. The increase in ionic strength reduces the thickness of the particle's diffuse layer to decrease the repulsive interactions between particles. The result is the lowering of the activation energy barrier between same charged particles allowing the domination of attractive interactions by Van der Waals forces. Changing solubility will also cause the precipitation of dissolved salts and organics during which constituent material can become entrapped through enmeshment in a precipitate. The result was the formation of a cohesive concentrated material that is comprised of a mixture of stable and coagulated material.

During the course of freezing the ice/liquid interface advances downward from unidirectional freezing to also concentrate the liquid's constituents. Precipitates produced from these water quality changes may settle under the forces of gravity. The rate of freezing changes with respect to depth, however the changes in freezing point were not substantial to alter the morphology of the concentrated material associated to that initial

freezing temperature. Freezing acts to bring together for contact the effluent's constituents. Once frozen the constituents of the effluent are entrapped in thin, highly concentrated zones. The result was the initial formation of zones of concentrated material. Believed was this concentrated material is comprised of a mixture of compounds consisting of thermodynamically stable and unstable colloids, precipitates, and dissolved matter. Unstable colloids are irreversible. Aggregation of unstable colloids can occur as result of electrostatic interactions (Van der Waals forces) and/or by adsorption and charge neutralization. Postulated was aggregation of these colloids coupled with mechanical compression of the concentrated material from the freezing of the free available water over time entraps the stable dissolved and colloid fraction within this complex mixture allowing for their initial removal from the bulk solution upon thawing. The ability of the process to remove the stable dissolved and colloid fractions entrapped within the concentrated material was in part dependent on the rate of thawing. For example, rapid rates of thawing reduces the material's contact time with the bulk solution for there to occur diffusion of the stable fraction back into solution. Laboratory studies showed the settled concentrated material was not entirely stable and would diffuse back into solution over time. Believed was that over time the stable dissolved and colloid fraction "untangles" itself from the concentrated material to diffuse back into solution. Consequently the immediate collection of the resultant clear effluent produced by freeze-thaw was important in obtaining high treatment efficiencies.

The operating parameters that were reported to provide the best results were for the most part, representative of conditions that prevail

naturally in cold climate areas. High color removals in excess of 73 % with respect to the untreated membrane concentrate were achieved in the top 70 % liquid volume for when the effluent was frozen very slowly and rapidly thawed from predominantly from the bottom up. A total of seven independent variables were studied for their effect on treatment performance. The most important was the independent variable method of thawing. The method by which the frozen effluent was thawed proved crucial in whether or not freeze-thaw could effectively treat the effluent to concentrate and ultimately reduce the liquid volume of waste constituents requiring disposal. As part of the investigation, the frozen effluent was thawed in one of two directions, top down or predominantly from the bottom up. Ice columns that were thawed top down were done in such a manner to prevent the ice from floating so as to study the effect of melt water and the release of the concentrated material from the ice matrix. Ice columns thawed predominantly from the bottom up were done so to deliberately float the ice. The results of this comparison showed melt water and its flow pattern plays an important role in the concentration and settlement of the concentrated material produced during freezing. The method by which the concentrated material was released from the ice matrix was also important. Thawing of the ice column from the bottom up released the concentrated material enabling it to settle and be carried downward with the melt water. Thawing the frozen effluent from the bottom up was conducive to establishing a melt water flow that was in the downward vertical direction which assisted in the concentration and settlement of fragile concentrated material in the bottom portion of the thawed liquid fraction. So different were the removal efficiencies between the two methods of thawing that as part of the treatment process it was

made mandatory that the ice must always be melted from predominantly the bottom up.

The independent variable that was identified as being the second most important process parameter was initial freezing temperature. Initial freezing temperature plays an important role in determining the morphology of the concentrated material produced during freezing. Crucial in achieving high color removals from the upper liquid fraction was for the production of thick, cohesive structures of concentrated material, which in SEM studies was observed to occur at the warmer initial freezing temperatures. The best results were associated with the highest initial freezing temperature -2°C . At colder initial freezing temperatures ($\leq -15^{\circ}\text{C}$) the concentrated material produced during freezing was observed to substantially change. The concentrated material decreased in thickness and the zones of material were more numerous as the initial freezing temperature decreased. Studies conducted to investigate the concentrated material's fragility showed material concentrated at the colder initial freezing temperatures was less likely to retain their frozen state physical properties under conditions of moderate disturbance produced during thawing. Material concentrated at the initial freezing temperature -2°C were on the other hand better able to retain a good percentage of their frozen state physical structure following thawing.

Another independent variable that was identified as being important was thawing temperature. The rate at which the ice formation was melted was observed in dye studies to affect the melt water flow pattern. High thawing rates typically provided for the best results when all other parameter settings were held constant. At high thawing rates the

melt water was observed to flow in a downward vertical pattern which served to quickly thaw to release and concentrate the concentrated material minimizing its contact time for diffusion back into the upper liquid fraction. As well it offered the path of least amount of disturbance to minimize break-up of the concentrated material during thawing. Decreasing the thawing rate to a temperature close to the value where the effluent was at its maximum density affected substantially the downward flow rate of the melt water to reduce color removal in samples thawed bottom up. In dye studies the melt water was observed to concentrate directly under the ice, dispersing more in the horizontal direction than in the downward vertical direction.

Other independent variables observed to affect treatment performance, although to a much lesser degree, were storage time and storage temperature. Increasing the time period over which the frozen effluent was kept frozen improved separation efficiency. However, the greatest improvements occurred when the storage temperature was adjusted to below the initial freezing temperature over its storage time. The general tendency of the data was the magnitude of the improvement from adjustment of the storage temperature increased with the lower the storage temperature was with respect to the initial freezing temperature. This observation was likely attributed to differences between the mass of the concentrated material and the amount of free available water contained within.

Other variables that were evaluated and found to be relatively unimportant over the model range were liquid depth and concentration. Selective sampling of the thawed effluents with respect to depth showed

the color distribution curves were not substantially different between the liquid depths 150 mm and 250 mm at the initial freezing temperatures -15 °C and -25 °C. The color values with respect to depth were however different at the initial freezing temperature -2 °C. At this initial freezing temperature increasing the liquid depth from 150 mm to 250 mm shifted the color distribution curve up and to the right, with the reported color values being slightly higher for the deeper liquid depth. However, calculation of the overall composite color concentration corresponding to the top 70 % liquid portion showed the average color concentrations between the two liquid depths were not that very different. Based on this it was concluded that over the range of liquid depths studied, depth was relatively unimportant and therefore excluded as an independent variable in development of the model. In addition, freezing was shown that it could be conducted in multiple layers without adversely affecting treatment performance. Additional work however is required to determine if a maximum liquid depth exists before which the freezing rate in the bottom liquid layer portion would be substantially affected to alter the morphology of the concentrated material produced during freezing. Also required is to determine the maximum number of layers that can be frozen in series without adversely affecting treatment performance during thawing.

Concentration was investigated for how it affects the morphology of concentrated material produced during freezing. Results of the study showed substantial dilution (> 50 %) corresponding to a color concentration below 6,250 CU of the membrane concentrate was required before there was a significant change in material thickness and structure in

comparison to that observed in freezing the raw concentrate, particularly at the warmer initial freezing temperature. Based on this the percent color removals obtained with respect to the raw by freeze-thaw were not anticipated to change substantially for concentrates with color concentrations between 6,250 CU to 12,500 CU.

Concentration was also studied for how it affects treatment performance using membrane concentrate diluted with distilled water to achieve various dilutions. Initial work conducted suggested that high removal efficiencies can be obtained for effluents of moderate and high constituent concentrations provided that freeze-thaw was conducted at its optimum conditions. That is slow freezing rates coupled with long storage times at cold temperatures followed by rapid thawing were required to obtain high removal efficiencies, regardless of concentration. This initial work was confirmed in dilution studies whereby the membrane concentrate was shown to have a minimum color concentration limit, below which concentration would have to be included as an independent variable in the model. For membrane concentrates derived from the alkaline extraction stage effluent the minimum concentration limit was around 6,130 CU. Therefore the empirical model developed for the membrane concentrate when expressed as percent color removal can be assumed valid over a board concentration range.

The empirical models developed by others are for the application of freeze-thaw in the conditioning of sludges. They have been developed as operational tools that provide no information about treatment efficiency, rather they allow the operator to select process parameters that will guarantee the freezing or thawing of the sludge. The approach taken in

this study was to develop an empirical model for each experimental water type to predict color concentration within the top 70 % liquid volume which then can be used by operations to predict treatment performance and to allow for control those climatic conditions that are not conducive to achieving high separation efficiencies. Analysis of variance and stepwise multi-linear regression analyses were used for model development. The empirical models developed for each experimental water were not entirely the same with respect to the individual coefficients that could not be explained as chance occurrences. For example, in the case of membrane concentrate the individual coefficients that could not be explained by chance occurrences were initial freezing temperature, thawing rate, storage time, and storage temperature. For the Eop effluent, the individual coefficients that could not be explained by chance occurrences were initial freezing temperature, storage time, and thawing temperature. The absence of storage temperature as an important independent variable in the model developed for the Eop effluent was in part, related to the porosity of the concentrated material produced during freezing. Although the thickness of the concentrated material between the two effluent types were relatively the same, the material produced in freezing Eop effluent was much more porous. More highly porous concentrated material may be more susceptible to diffusion back into solution. The amount of material mass and free available water within the concentrated mass appears to be important factors which define the importance of these variables. It is the belief that the importance of storage temperature as an independent variable increases with concentration at the warmer initial freezing temperatures, particularly for very high strength liquid waste streams where the structural integrity of the

concentrated material can be significantly strengthened through mechanical compression brought about by long storage periods.

11.0 CONCEPTUAL ENGINEERING DESIGN

Independent variables that significantly affect treatment performance by freeze-thaw were identified in the preceding sections. Controllable process variables were thawing temperature, storage time, and thaw direction. Non-controllable variables were initial freezing temperature and storage temperature. Other controllable process variables found to affect treatment performance to a much lesser degree were liquid depth and number of freeze-thaw cycles. Utilizing all of the data presented a conceptual design for conducting freeze-thaw of high strength kraft pulp mill effluents was proposed by way of freezing ponds. Important operational considerations that must be taken into account when sizing the freezing pond are disturbances to the liquid body during and following thawing created by climatic conditions. In laboratory tests it was found that any substantial mixing of the treated effluent would readily resuspended the settled material after which it would not resettle. Locating the freezing ponds indoor in an unheated building would be the best solution to eliminate disturbances related to the elements. It would also increase operational control of the thawing process and eliminate operational problems related to snow fall. Substantial snow fall on top of the freezing ponds can act to dilute the concentration of new effluents applied on top existing frozen layers. This would be of particular concern for low strength effluents such as the alkaline extraction stage effluent where substantial dilution can significantly affect the type of concentrated material produced during freezing. In addition, substantial snow fall accumulation on top of a layer during its freezing can cause ice flooding by submerging the initial ice cover during the freezing process. Unknown is

what effect this will have on treatment performance. Also of particular concern is sunlight exposure and the effect it can have on the frozen mass and the thawed treated effluent. Operating the process in the absence of sunlight will minimize surface melting during storage of the frozen mass. Surface melting is however not as serious in terms of its effect on treatment performance as would biological activity or algae growth brought about by sunlight exposure during and following thawing. Given that the process performs well at high thawing temperatures, warm thawed liquid temperatures combined with sunlight exposure can lead to substantial algae growth if the effluents were not immediately collected. Algae growth can create operational problems with respect to separation of the various treated liquid fractions.

Efficient operation of the process requires multiple freezing ponds. To take advantage of the waste heat discharged with the effluent to initiate and control thawing would require conducting the freezing and thawing process simultaneously using multiple beds. That is before an effluent is discharged into a bed for freezing its heat would be transferred into a medium to cause and control the rate of thaw of the frozen effluent contained in another freezing bed. Utilizing the effluent's high discharge temperature to initiate and control thawing also reduces the adverse effect heat would have on existing frozen layers when conducting layer freezing. For example, failure to remove the heat can simulate thawing from the top down of existing frozen layers during layer freezing which in laboratory experiments was observed to resuspend material concentrated by freezing alone.

The freeze-thaw conditions required to obtain optimum performance are slow freezing, followed by long storage times at cold temperatures after which high thawing temperatures are introduced to thaw the ice mass from the bottom up. The conceptual design proposed takes into account promoting those conditions that favor the above. That is the primary design components have multiple purposes. Rapid thawing of the ice mass from the bottom up is crucial for the release of the concentrated material and for establishment of the melt water flow pattern conducive to its fast removal. To achieve thawing from the bottom up utilizing waste heat from the effluent being discharged it is proposed that the effluent be pumped into an underground distribution network located within a high thermal conductive zone immediately below the frozen ice mass. The recommended method of installation for the distribution system is to have it located below the bed in which it is separated from the ice mass by an impermeable barrier designed for leak control. The impermeable barrier can consist of a synthetic liner such as high density polyethylene liner of sufficient thickness to resist ice damage. In the design of the distribution system it is important to optimize heat conduction. Provisions will have to be included in the design to drain the distribution system following thawing when the network is not in use to avoid freezing. Given this requirement, the distribution system can also be used during freezing to maintain cold temperatures in the lowest bottom portion of the frozen ice mass taking advantage of the positive effects cold storage temperatures can have on treatment performance. Consequently, the distribution system serves multiple purposes in the operation of the freezing bed. During thawing the distribution system conveys the heat source required to initiate and maintain melting. During freezing, the

system is drained and operated under a vacuum to draw cold air through the network to lower the temperature of the ice mass in the bottom of the freezing bed. This will maintain a temperature gradient within the freezing bed to assist layer freezing and to allow operating the bed at colder than normal freezing temperatures.

Recovery of the relatively clear effluent can be achieved in one of several ways. One method is to have installed inside the bed fixed adjustable weirs to allow drainage of the clear effluent following treatment. Adjustable weirs or the ability to alter the liquid depth is required for treatment of different strength waste effluents or to response to changing climatic conditions. For example, changing the liquid depth can slow down the time period to freeze the liquid layer during periods of cold temperatures. If adjustable weir plates are used then their design and operation are of particular importance. To avoid resuspending the settled material, it is important to withdraw the clear treated effluent slowly. Rapid removal of the effluent can adversely affect the effluent quality collected. Collection of the clear treated effluent in this manner should only be conducted after thawing, until such time work is conducted to investigate the advantages of recovering the liquid during thawing. The concentrated material must be allowed to escape from the ice matrix into a water medium and settle before discharge to ensure proper treatment. Design and spacing of the collection weirs is important as they can act to interfere with the melt water flow. The actual weir design should be similar to adjustable weir plates that can be manually adjusted down for collection of the upper treated effluent portion. Alternatively, a more simple method for collecting the relatively clear effluent is to drain the

bottom portion of the thawed liquid fraction during thawing. The relatively clear effluent would be left after which it would be collected. Crucial in the success of this process is the thawing the ice at a temperature that has the melt water flowing vertically downwards. The freezing beds should also be gradually sloped to allow for drainage and collection of the thawed or residual liquid fraction.

12.0 RECOMMENDATIONS AND FUTURE WORK

Additional work is required to expand the boundary set points of the models developed herein. Most notable is additional work is required to better evaluate the effect concentration has on treatment performance. Unknown for the variety of effluent types that can be anticipated for kraft mill operations is what are the concentration limits which if exceeded freeze-thaw can not be used to effectively treat these effluents. Postulated was that concentration determines among other things the importance of the independent variables storage time and storage temperature. It is believed that the more concentrated the effluent the more effective freeze-thaw will be in the separation the constituent material from the bulk solution. Work in this area can be used to expand the models to include concentration as an independent variable so as to allow for the prediction of treatment performance for varying strength liquid waste streams of similar chemical composition.

Additional work is also required to fully characterize the physical changes that occurs to the concentrated material during freezing, storage, and thawing. Absent in the work of this study were tests designed to determine the physical changes to the concentrated material within the ice matrix during long periods of storage. This information would provide additional insight into the removal mechanisms of the concentrated material and the establishment of more accurate operating protocols for treatment of particular liquid waste stream types.

Understanding better the fundamentals behind the process, work can now proceed with how to best apply this technology in the treatment

of liquid waste streams comprised primarily of complex dissolved/colloidal organics of which are amenable to separation by mechanical coagulation. Detailed engineering design followed by pilot testing on a small scale basis are required to confirm laboratory data and to progress engineering design. In particular, field testing is required to investigate and optimize the method of process operation. For example, work is required to determine the optimum liquid depth and the maximum number of layers that can be frozen in series at any one time without adversely affecting treatment performance. Freeze-thaw layering also needs to be conducted at liquid temperatures anticipated for the effluents to determine if liquid temperature adversely affects treatment performance. Other methods such as effluent collection during and after thawing or ice shaving also need to be evaluated for their benefits. For example, it would be useful to evaluate the benefits of collecting the melt water during thawing with respect to treatment performance. This information can be used in the development of more elaborate operational protocols for optimization of the process.

Finally, further study is needed to evaluate freeze-thaw for the treatment of other industrial wastewaters that are comprised primarily of organics to strengthen the conclusion of this work that effluents amenable to separation by mechanical coagulation can be effectively treated by freeze-thaw.

13.0 REFERENCES

- APHA-AWWA-WPCF. 1989. Standard methods for the examination of water and wastewater. 17 th edition. Denver, Colo.
- Baker, R. A. 1969. Trace organic contaminant concentrations by freezing - III. Ice washing. Wat. Res., 3: 717-730.
- Baker, R. A. 1967. Trace organic contaminant concentrations by freezing - I. Low inorganic aqueous solutions. Wat. Res., 1: 61-77.
- Barduhn, A. J., Rose, A., Sweeny, R. F. 1963. A study of freezing and gas hydrate formation. Env. Hlth. Series U. S. Public Health Service. AWTR-4-Report No. 999-WT-4.
- Barnes, H. T. 1928. Ice Engineering, Renouf Publishing Co. Ltd., Montreal.
- Benn, D., Doe, P. W. 1969. The disposal of sludge by freezing and thawing process. Filtr. Sep., 8: 383-389.
- Bolling, G. F., Tiller, W. A. 1961. Growth from the melt: cellular interface morphology. J. Appl. Phys., 31: 2040-2045.
- Box, G. E. P., Hunter, W. G., Hunter, J. S. 1978. Statistics for Experimenters: An introduction to design, data analysis, and model building. John Wiley & Sons, New York, USA. 653 p.
- Chalmers, B. 1959. How water freezes. Scient. Am., 200: 114-122.
- Chang, I. L., Lee, D. J. 1998. Ternary expression stage in biological sludge dewatering. Wat. Res., 32(3): 905-914.
- Cheng, C-Y., Updergraff, D. M., Ross, L. W. 1970. Sludge dewatering by high-rate freezing at small temperature differences. Envir. Sci. Technol. 4: 1145-1147.
- Cisse, J., Bolling, G. F. 1971. A study of the trapping and rejection of insoluble particles during the freezing of water. J. Crystal Growth., 10: 67-76.
- Clements, G. S., Stephenson, R. J., Regan, C. J. 1950. Sludge dewatering by freezing with added chemicals. J. Inst. Sewage Purification., 4: 318 322.

- Cook, T. E., Farmer, F. A., Reid, J., Rowbottom, R. 1973. The effect of pulp and paper mill effluents on the taste and odour of the receiving water and the fish therein. Pulp and Paper Magazine of Canada, 74: 97-106.
- Corte, A. 1962. Vertical migration of particles in front of a moving freezing plane. J. Geophys. Res., 67: 1085-1090.
- Egan, C. J., Davis, H. E. 1982. Concentration of black liquor by freeze-crystallization. Proceedings of Technical Association of the Pulp and Paper Industry. San. Francisco. September 13-16, 1982, Book III, pp 471-479.
- English, A. C., Dole, M. 1950. Diffusion of sucrose in supersaturated solutions. J. A. C. S., 72: 3261-3267.
- Environment Canada. 1979. Natural freeze-thaw sludge conditioning and dewatering. Technology Development Report EPS 4-WP-79-1.
- Ezekwo, G., Tong, H. M., Gryte, C. C. 1980. On the mechanism of dewatering colloidal aqueous solutions by freeze-thaw processes. Water Res., 14: 1079-1088.
- Farrell, J. B. 1971. A status report on the utilization of freezing in dewatering of sludges. From the Proceedings of the XIIth International Congress of Refrigeration. Washington, D.C., Vol. 1, pp 739-743.
- Farrell, J. B., Smith, J. E., Dean, R. B., Grossman, E., Grant, O. L. 1970. Natural freezing for dewatering of aluminum hydroxide sludges. J. Am. Water Works Ass., 62: 787-791.
- Fremont, H., Kleper, M. H. 1980. Kraft mill effluent color removal by ultrafiltration. From the Proceedings of the 35 th Industrial Waste Conference. Purdue University, pp 114-131.
- Gross, G. W. 1965. The Workman-Reynolds effect and ionic transfer processes at the ice-solution interface. J. Geophys. Res., 70: 2291-2300.
- Halde, R. 1979. Concentration of impurities by progressive freezing. Water Res. 14: 575-580.
- Hadzeriga, P. 1972. Treatment of phosphate rock slimes by freezing. U.S. Patent 3,681,931.
- Harrison, J. D., Tiller, W. A. 1963. Ice interface morphology developed during freezing. J. Appl. Phys., 34: 3349-3355.

- Hoekstra, P. Miller, R. D. 1967. On the mobility of water molecules in the transition layer between ice and a solid surface. J. Colloid Interface Sci. 25: 166-173.
- Johnson, W. E. 1976. State-of-the-art of freezing processes, their potential and future. Desalination., 19: 349-358.
- Katuscak, S., Hrvik, A., Mahdalik, M., 1971. Ozonation of lignin. Part 1. Activation of lignin with ozone. Paper Och Tra., 9: 519-524
- Khazanie, R. 1986. Elementary statistics: In a world of applications. Scott, Foresman and Company, London, England. Second Edition. 562 p.
- Knocke, W. R., Trahern, P. 1989. Freeze-thaw conditioning of chemical and biological sludges. Wat. Res., 23: 35-42.
- Kovacs, T. G., Voss, R. H. 1986. Factors influencing the effect of bleached kraft mill effluents on drinking water quality. Wat. Res., 20: 1185-1191.
- Kringstad, K. P., Lindstrom, K. 1984. Spent liquors from pulp bleaching. Environ. Sci. Technol., 18(8): 236A-249A
- Kuo, V., Wilcox, A. 1973. Removal of particles by solidification. Ind. Engng. Chem. Process & Design Development., 12: 376-379.
- Logsdon, G., Edgerley, E. 1971. Sludge dewatering by freezing. J. Am. Wat. Wks. Ass., 63: 734-740.
- Martel, C. J., 1998. Natural dewatering of alum sludge in freezing beds. Ninth International Conference on Cold Regions Engineering, Duluth, Minnesota, September 27-30, 1998, pgs 282-291.
- Martel, C. J., Affleck, R., Yushuk, M. 1998. Operational parameters for mechanical freezing of alum sludge. Wat. Res., 32: 2646-2654.
- Moulton, L. K. 1969. Prediction of the depth of frost penetration: a review of the literature. Report No. 5, West Virginia University, Morgantown.
- Mullins, W. W., Sekerka, R. F. 1964. Stability of planar interface during the solidification of a dilute binary alloy. J. Appl. Phys., 35: 444-451.
- Murphy, J. M., Bolmer, P. W. 1973. Freezing and melting treatment of red mud slurries to aid solid separation. U.S. Patent 3,714,792.
- Oleneva, G. E. 1973. Formation of ice crystals in starch. Kh. Tekhn. Khteau., 7: 42-44.

- Parker, J. P., Collins, A. G. 1997. Feasibility study on freeze/thaw conditioning of pulp mill waste activated sludge. J. Cold Regions Engineering., 11: 245-251.
- Parker, J. P., Collins, A. G., Dempsey, J. P. 1998. Effects of freezing rate, solids content, and curing time on freeze/thaw conditioning of water treatment residuals. Environ. Sci. Technol., 32: 383-387.
- Parungo, F. P., Lodge, J. P. 1965. Molecular structure and ice nucleation of some organics. J. Met., 22: 309-313.
- Penman, A., Van Es, D. W. 1973. Winnipeg freezes sludge, slashes disposal costs 10 fold. Civil Engng. - ASCE., 43,(11): 65-67.
- Powell, R. L., Barduhn, A. J. 1965. Separation of dissolved solids from wastewater by eutectic freezing. Presented A. I. Ch. E. National Meeting, Houston, Texas, Feb 7-11.
- Prentice, J. 1973. Freezing point determination. Analyst., 103, 12-69
- Randall, C. W., Ali Khan, M. Z., Stephens, N. T., 1975. Waste activated sludge conditioning by direct slurry freezing. Wat. Res., 9: 917-925.
- Smith, M. A., Furgason, R. R., 1976. Use of ozone in the treatment of kraft pulp mill liquid wastes. Part 2. Biodegradation. Second Int. Symp. on Ozone Technology, Proc., 309 - 320.
- Smith, V. G., Tiller, N. A., Rutter, R. W. 1955. Mathematical analysis of solute redistribution during solidification. Can. J. Phys., 33: 723-745.
- Stanczyk, H. M., Field, L., Collins, E. W. 1971. Dewatering of Florida phosphate slime by freezing techniques. U.S. Bureau of Mines. Report 7250.
- Stanley, S. J., Smith, D. W. 1991. Reduction of ice thickness on northern water reserviors. J. Cold Regions Engineering., ASCE, 5: 106-124.
- Taber, S. 1930. The mechanics of frost heaving. J. Geol., 58(4): 303.
- Tilsworth, T., Murphy, R. S., Garinger, L. E., Wagner, J. 1972. Freeze conditioning of waste activated sludge. Proceedings of the Twenty-Seventh Industrial Waste Conference, Purdue University, Lafayette, Indiana: 486-491.
- Uhlmann, D. R., Chalmers, B., Jackson, K. A. 1964. Interaction between particles and a solid liquid interface. J. Appl. Phys., 35: 2986-2993.

- Vesilind, P. A., Martel, C. J. 1991. Freezing of water and wastewater sludges. Jour. of Environ. Engineering., 116: 854-862.
- Vesilind, P. A. 1991. Agitation and filterability of freeze/thawed sludge. J. Cold Regions Engng., ASCE, 5(2): 77-83.
- Vesilind, P. A. 1990. Sludge freezing in shallow layers. Jour. of Environ. Engineering., 116: 646-650.
- Vincent, H., Kuo, S., Wicox, W. R. 1973. Removal of particles by solidification. Ind. Eng. Chem. Process. Des. Develop., 12: 376-379.
- Wood, G. R., Walton, A. G. 1969. Kinetics of ice nucleation from water and electrolyte solutions. Office of Saline Water Research and Development. Progress Report No. 500. 171 p.
- Workman, E. J., Reynolds, S. E. 1950. Electrical phenomena occurring during the freezing of dilute aqueous solutions and their possible relationship to thunderstorm electricity. Phys. Rev., 78: 254-259.

APPENDIX A

ANALYSIS OF VARIANCE AND DUNCAN MULTIPLE RANGE TEST RESULTS

CHAPTER 4

UNIDIRECTIONAL FREEZE-THAW STUDIES

MEMBRANE CONCENTRATE AND E_{op} EFFLUENT

Analysis of Variance and Duncan Multiple Range Test
Membrane Concentrate, Initial Freezing Temperature -2 °C, Thawed
Bottom up

Analysis of Variance

Dependent Variable: Color in the top 70 % liquid fraction

Levels: 4 °C, 15 °C, and 24 °C

Source	SUM-OF-SQUARES	Degrees of Freedom (n-1)	Mean-Square	F-Ratio	P
Thawing Temperature (°C)	1098405.556	2	549202.778	47.849	0.000
Error	68866.667	6	11477.778		

Means:

$\mu_1 = 4140$ CU (Thawing Temperature 4 °C)

$\mu_2 = 3460$ CU (Thawing Temperature 15 °C)

$\mu_3 = 3350$ CU (Thawing Temperature 24 °C)

Duncan Multiple Range Test

$n = 3$

$N = 9$

degrees freedom = 6

$$S_{yi} = (MS_E/n)^{1/2} = 61.854$$

$$R_2 = (2,6)S_{yi} = 3.46(61.854) = 214.015$$

$$R_3 = (3,6)S_{yi} = 3.58(61.854) = 221.437$$

1 vs 3 = 4140 - 3350 = 790 > 221.437 significant

1 vs 2 = 4140 - 3460 = 680 > 214.015 significant

2 vs 3 = 3460 - 3350 = 110 < 214.015 not significant

Analysis of Variance and Duncan Multiple Range Test
Membrane Concentrate, Initial Freezing Temperature -15 °C, Thawed
Bottom up

Analysis of Variance

Dependent Variable: Color in the top 70 % liquid fraction

Levels: 4 °C, 15 °C, and 24 °C

Source	SUM-OF-SQUARES	Degrees of Freedom (n-1)	Mean-Square	F-Ratio	P
Thawing Temperature (°C)	2088955.556	2	1044477.778	118.392	0.000
Error	52933.333	6	8822.222		

Means:

$\mu_1 = 5260$ CU (Thawing Temperature 4 °C)

$\mu_2 = 4250$ CU (Thawing Temperature 15 °C)

$\mu_3 = 4220$ CU (Thawing Temperature 24 °C)

Duncan Multiple Range Test

$n = 3$

$N = 9$

degrees freedom = 6

$$S_{yi} = (MS_E/n)^{1/2} = 54.229$$

$$R_2 = (2,6)S_{yi} = 3.46(54.229) = 187.631$$

$$R_3 = (3,6)S_{yi} = 3.58(54.229) = 194.140$$

1 vs 3 = 5260 - 4220 = 1040 > 194.140 significant

1 vs 2 = 5260 - 4250 = 1010 > 187.631 significant

2 vs 3 = 4250 - 4220 = 30 < 187.631 not significant

Analysis of Variance and Duncan Multiple Range Test
Membrane Concentrate, Initial Freezing Temperature -25 °C, Thawed
Bottom up

Analysis of Variance

Dependent Variable: Color in the top 70 % liquid fraction

Levels: 4 °C, 15 °C, and 24 °C

Source	SUM-OF-SQUARES	Degrees of Freedom (n-1)	Mean-Square	F-Ratio	P
Thawing Temperature (°C)	1400155.556	2	700077.778	103.121	0.000
Error	40733.333	6	6788.889		

Means:

$\mu_1 = 5300$ CU (Thawing Temperature 4 °C)

$\mu_2 = 4670$ CU (Thawing Temperature 15 °C)

$\mu_3 = 4360$ CU (Thawing Temperature 24 °C)

Duncan Multiple Range Test

$n = 3$

$N = 9$

degrees freedom = 6

$$S_{yi} = (MS_E/n)^{1/2} = 47.571$$

$$R_2 = (2,6)S_{yi} = 3.46(47.571) = 164.600$$

$$R_3 = (3,6)S_{yi} = 3.58(47.571) = 170.304$$

1 vs 3 = 5300 - 4360 = 940 > 170.304 significant

1 vs 2 = 5300 - 4670 = 630 > 164.600 significant

2 vs 3 = 4670 - 4360 = 310 > 164.600 significant

Analysis of Variance and Duncan Multiple Range Test
Membrane Concentrate, Initial Freezing Temperature -2 °C, Thawed
Top Down

Analysis of Variance

Dependent Variable: Color in the top 70 % liquid fraction
Levels: 4 °C, 15 °C, and 24 °C

Source	SUM-OF-SQUARES	Degrees of Freedom (n-1)	Mean-Square	F-Ratio	P
Thawing Temperature (°C)	651466.667	2	325733.333	35.839	0.000
Error	54533.333	6	9088.889		

Means:

$\mu_1 = 7400$ CU (Thawing Temperature 4 °C)
 $\mu_2 = 7630$ CU (Thawing Temperature 15 °C)
 $\mu_3 = 8030$ CU (Thawing Temperature 24 °C)

Duncan Multiple Range Test

$n = 3$

$N = 9$

degrees freedom = 6

$$S_{y_i} = (MS_E/n)^{1/2} = 55.042$$

$$R_2 = (2,6)S_{y_i} = 3.46(55.042) = 190.445$$

$$R_3 = (3,6)S_{y_i} = 3.58(55.042) = 197.050$$

3 vs 1 = $8030 - 7400 = 630 > 197.050$ significant

3 vs 2 = $8030 - 7630 = 400 > 190.445$ significant

2 vs 1 = $7630 - 7400 = 230 > 190.445$ significant

Analysis of Variance and Duncan Multiple Range Test
Membrane Concentrate, Initial Freezing Temperature -15 °C, Thawed
Top Down

Analysis of Variance

Dependent Variable: Color in the top 70 % liquid fraction

Levels: 4 °C, 15 °C, and 24 °C

Source	SUM-OF-SQUARES	Degrees of Freedom (n-1)	Mean-Square	F-Ratio	P
Thawing Temperature (°C)	2825866.667	2	1412933.333	70.686	0.000
Error	119933.333	6	19988.889		

Means:

$\mu_1 = 8390$ CU (Thawing Temperature 4 °C)

$\mu_2 = 9200$ CU (Thawing Temperature 15 °C)

$\mu_3 = 9740$ CU (Thawing Temperature 24 °C)

Duncan Multiple Range Test

$n = 3$

$N = 9$

degrees freedom = 6

$$S_{yi} = (MS_E/n)^{1/2} = 81.627$$

$$R_2 = (2,6)S_{yi} = 3.46(81.627) = 282.429$$

$$R_3 = (3,6)S_{yi} = 3.58(81.627) = 292.225$$

3 vs 1 = 9740 - 8390 = 1350 > 292.225 significant

3 vs 2 = 9740 - 9200 = 540 > 282.429 significant

2 vs 1 = 9200 - 8390 = 810 > 282.429 significant

Analysis of Variance and Duncan Multiple Range Test
Membrane Concentrate, Initial Freezing Temperature -25 °C, Thawed
Top Down

Analysis of Variance

Dependent Variable: Color in the top 70 % liquid fraction
Levels: 4 °C, 15 °C, and 24 °C

Source	SUM-OF-SQUARES	Degrees of Freedom (n-1)	Mean-Square	F-Ratio	P
Thawing Temperature (°C)	526666.667	2	263333.333	29.625	0.001
Error	53333.333	6	8888.889		

Means:

$\mu_1 = 10100$ CU (Thawing Temperature 4 °C)
 $\mu_2 = 10200$ CU (Thawing Temperature 15 °C)
 $\mu_3 = 10600$ CU (Thawing Temperature 24 °C)

Duncan Multiple Range Test

$n = 3$
 $N = 9$
degrees freedom = 6

$$S_{y_i} = (MS_E/n)^{1/2} = 54.433$$

$$R_2 = (2,6)S_{y_i} = 3.46(54.433) = 188.338$$

$$R_3 = (3,6)S_{y_i} = 3.58(54.433) = 194.870$$

3 vs 1 = 10600 - 10100 = 500 > 194.870 significant
3 vs 2 = 10600 - 10200 = 400 > 188.338 significant
2 vs 1 = 10200 - 10100 = 100 < 188.338 not significant

Analysis of Variance and Duncan Multiple Range Test
Eop, Initial Freezing Temperature -2 °C, Thawed
Bottom up

Analysis of Variance

Dependent Variable: Color in the top 70 % liquid fraction

Levels: 4 °C, 15 °C, and 24 °C

Source	SUM-OF-SQUARES	Degrees of Freedom (n-1)	Mean-Square	F-Ratio	P
Thawing Temperature (°C)	1618884.222	2	809442.111	1890.238	0.000
Error	2569.333	6	428.222		

Means:

$\mu_1 = 1160$ CU (Thawing Temperature 4 °C)

$\mu_2 = 880$ CU (Thawing Temperature 15 °C)

$\mu_3 = 536$ CU (Thawing Temperature 24 °C)

Duncan Multiple Range Test

$n = 3$

$N = 9$

degrees freedom = 6

$$S_{yi} = (MS_E/n)^{1/2} = 11.947$$

$$R_2 = (2,6)S_{yi} = 3.46(11.947) = 41.337$$

$$R_3 = (3,6)S_{yi} = 3.58(11.947) = 42.770$$

1 vs 3 = 1160 - 536 = 624 > 42.770 significant

1 vs 2 = 1160 - 880 = 280 > 41.337 significant

2 vs 3 = 880 - 536 = 344 > 41.337 significant

Analysis of Variance and Duncan Multiple Range Test
Eop, Initial Freezing Temperature -15 °C, Thawed
Bottom up

Analysis of Variance

Dependent Variable: Color in the top 70 % liquid fraction

Levels: 4 °C, 15 °C, and 24 °C

Source	SUM-OF-SQUARES	Degrees of Freedom (n-1)	Mean-Square	F-Ratio	P
Thawing Temperature (°C)	61550.000	2	30775.000	14.252	0.005
Error	12956.000	6	2159.333		

Means:

$\mu_1 = 1020$ CU (Thawing Temperature 4 °C)

$\mu_2 = 869$ CU (Thawing Temperature 15 °C)

$\mu_3 = 799$ CU (Thawing Temperature 24 °C)

Duncan Multiple Range Test

$n = 3$

$N = 9$

degrees freedom = 6

$$S_{yi} = (MS_E/n)^{1/2} = 26.829$$

$$R_2 = (2,6)S_{yi} = 3.46(26.829) = 92.827$$

$$R_3 = (3,6)S_{yi} = 3.58(26.829) = 96.048$$

1 vs 3 = 1020 - 799 = 221 > 96.048 significant

1 vs 2 = 1020 - 869 = 151 > 92.827 significant

2 vs 3 = 869 - 799 = 70 < 92.827 not significant

Analysis of Variance and Duncan Multiple Range Test
Eop, Initial Freezing Temperature -25 °C, Thawed
Bottom up

Analysis of Variance

Dependent Variable: Color in the top 70 % liquid fraction

Levels: 4 °C, 15 °C, and 24 °C

Source	SUM-OF-SQUARES	Degrees of Freedom (n-1)	Mean-Square	F-Ratio	P
Thawing Temperature (°C)	78116.667	2	39058.333	34.517	0.001
Error	6789.333	6	1131.556		

Means:

$\mu_1 = 1035$ CU (Thawing Temperature 4 °C)

$\mu_2 = 872$ CU (Thawing Temperature 15 °C)

$\mu_3 = 819$ CU (Thawing Temperature 24 °C)

Duncan Multiple Range Test

$n = 3$

$N = 9$

degrees freedom = 6

$$S_{yi} = (MSE/n)^{1/2} = 19.421$$

$$R_2 = (2,6)S_{yi} = 3.46(19.421) = 67.197$$

$$R_3 = (3,6)S_{yi} = 3.58(19.421) = 69.527$$

1 vs 3 = 1035 - 819 = 216 > 69.527 significant

1 vs 2 = 1035 - 872 = 163 > 67.197 significant

2 vs 3 = 872 - 819 = 53 < 67.197 not significant

Analysis of Variance and Duncan Multiple Range Test
Eop, Initial Freezing Temperature -2 °C, Thawed Top Down

Analysis of Variance

Dependent Variable: Color in the top 70 % liquid fraction

Levels: 4 °C, 15 °C, and 24 °C

Source	SUM-OF-SQUARES	Degrees of Freedom (n-1)	Mean-Square	F-Ratio	P
Thawing Temperature (°C)	36688.889	2	18344.444	6.070	0.036
Error	18133.333	6	3022.222		

Means:

$\mu_1 = 1560$ CU (Thawing Temperature 4 °C)

$\mu_2 = 1610$ CU (Thawing Temperature 15 °C)

$\mu_3 = 1710$ CU (Thawing Temperature 24 °C)

Duncan Multiple Range Test

$n = 3$

$N = 9$

degrees freedom = 6

$$S_{yi} = (MS_E/n)^{1/2} = 31.740$$

$$R_2 = (2,6)S_{yi} = 3.46(31.740) = 109.820$$

$$R_3 = (3,6)S_{yi} = 3.58(31.740) = 113.629$$

$$3 \text{ vs } 1 = 1710 - 1560 = 150 > 113.629 \text{ significant}$$

$$3 \text{ vs } 2 = 1710 - 1610 = 100 < 109.820 \text{ not significant}$$

$$2 \text{ vs } 1 = 1610 - 1560 = 50 < 109.820 \text{ not significant}$$

Analysis of Variance and Duncan Multiple Range Test
Eop, Initial Freezing Temperature -15 °C, Thawed Top Down

Analysis of Variance

Dependent Variable: Color in the top 70 % liquid fraction

Levels: 4 °C, 15 °C, and 24 °C

Source	SUM-OF-SQUARES	Degrees of Freedom (n-1)	Mean-Square	F-Ratio	P
Thawing Temperature (°C)	1755.556	2	877.778	2.324	0.179
Error	2266.667	6	377.778		

Means:

$\mu_1 = 1710$ CU (Thawing Temperature 4 °C)

$\mu_2 = 1720$ CU (Thawing Temperature 15 °C)

$\mu_3 = 1740$ CU (Thawing Temperature 24 °C)

Duncan Multiple Range Test

$n = 3$

$N = 9$

degrees freedom = 6

$$S_{yi} = (MS_E/n)^{1/2} = 11.222$$

$$R_2 = (2,6)S_{yi} = 3.46(11.222) = 38.828$$

$$R_3 = (3,6)S_{yi} = 3.58(11.222) = 40.175$$

3 vs 1 = 1740 - 1710 = 30 < 40.175 not significant

3 vs 2 = 1740 - 1720 = 20 < 38.828 not significant

2 vs 1 = 1720 - 1710 = 10 < 38.828 not significant

Analysis of Variance and Duncan Multiple Range Test
Eop, Initial Freezing Temperature -25 °C, Thawed Top Down

Analysis of Variance

Dependent Variable: Color in the top 70 % liquid fraction

Levels: 4 °C, 15 °C, and 24 °C

Source	SUM-OF-SQUARES	Degrees of Freedom (n-1)	Mean-Square	F-Ratio	P
Thawing Temperature (°C)	2466.667	2	1233.333	0.677	0.543
Error	10933.333	6	1822.222		

Means:

$\mu_1 = 1740$ CU (Thawing Temperature 4 °C)

$\mu_2 = 1740$ CU (Thawing Temperature 15 °C)

$\mu_3 = 1780$ CU (Thawing Temperature 24 °C)

Duncan Multiple Range Test

$n = 3$

$N = 9$

degrees freedom = 6

$$S_{yi} = (MS_E/n)^{1/2} = 24.646$$

$$R_2 = (2,6)S_{yi} = 3.46(24.646) = 85.274$$

$$R_3 = (3,6)S_{yi} = 3.58(24.646) = 88.233$$

3 vs 1 = 1780 - 1740 = 40 < 88.233 not significant

3 vs 2 = 1780 - 1740 = 40 < 85.274 not significant

2 vs 1 = 1740 - 1740 = 0 < 85.274 not significant

Analysis of Variance and Duncan Multiple Range Test
Membrane Concentrate, Cycle Freeze-thaw, Initial Freezing
Temperature -2 °C

Analysis of Variance

Dependent Variable: Color in the top 70 % liquid fraction

Levels: 1, 2, and 3 cycles

Source	SUM-OF-SQUARES	Degrees of Freedom (n-1)	Mean-Square	F-Ratio	P
Cycle Freeze-thaw	500216.667	2	250108.333	23.713	0.001
Error	63283.333	6	10547.222		

Means:

$\mu_1 = 3350$ CU (Cycle 1)

$\mu_2 = 2960$ CU (Cycle 2)

$\mu_3 = 2790$ CU (Cycle 3)

Duncan Multiple Range Test

$n = 3$

$N = 9$

degrees freedom = 6

$$S_{y_i} = (MS_E/n)^{1/2} = 59.294$$

$$R_2 = (2,6)S_{y_i} = 3.46(59.294) = 205.157$$

$$R_3 = (3,6)S_{y_i} = 3.58(59.294) = 212.273$$

1 vs 3 = 3350 - 2790 = 560 > 212.273 significant

1 vs 2 = 3350 - 2960 = 390 > 205.157 significant

2 vs 3 = 2960 - 2790 = 170 < 205.157 not significant

Analysis of Variance and Duncan Multiple Range Test
Membrane Concentrate, Cycle Freeze-thaw, Initial Freezing
Temperature -15 °C

Analysis of Variance

Dependent Variable: Color in the top 70 % liquid fraction

Levels: 1, 2, and 3 cycles

Source	SUM-OF-SQUARES	Degrees of Freedom (n-1)	Mean-Square	F-Ratio	P
Cycle Freeze-thaw	281866.667	2	140933.333	29.845	0.001
Error	28333.333	6	4722.222		

Means:

$$\mu_1 = 4220 \text{ CU (Cycle 1)}$$

$$\mu_2 = 4000 \text{ CU (Cycle 2)}$$

$$\mu_3 = 3790 \text{ CU (Cycle 3)}$$

Duncan Multiple Range Test

$$n = 3$$

$$N = 9$$

$$\text{degrees freedom} = 6$$

$$S_{yi} = (MS_E/n)^{1/2} = 39.675$$

$$R_2 = (2,6)S_{yi} = 3.46(39.675) = 137.276$$

$$R_3 = (3,6)S_{yi} = 3.58(39.675) = 142.037$$

$$1 \text{ vs } 3 = 4220 - 3790 = 430 > 142.037 \text{ significant}$$

$$1 \text{ vs } 2 = 4220 - 4000 = 220 > 137.276 \text{ significant}$$

$$2 \text{ vs } 3 = 4000 - 3790 = 210 > 137.276 \text{ significant}$$

APPENDIX B

ANALYSIS OF VARIANCE AND DUNCAN MULTIPLE RANGE TEST RESULTS

CHAPTER 5

SCANNING ELECTRON MICROSCOPY STUDIES

MEMBRANE CONCENTRATE AND E_{op} EFFLUENT

Analysis of Variance and Duncan Multiple Range Test
Membrane Concentrate, Concentrated Material Thickness Versus Initial
Freezing Temperature (Top)

Analysis of Variance

Dependent Variable: Cross sectional thickness

Levels: -2 °C, -15 °C, and -25 °C

Source	SUM-OF-SQUARES	Degrees of Freedom (n-1)	Mean-Square	F-Ratio	P
Freezing Temperature (°C)	1646.069	2	823.034	1299.528	0.000
Error	3.800	6	0.633		

Means:

$\mu_1 = 1.2 \mu\text{m}$ (Freezing Temperature -25 °C)

$\mu_2 = 1.9 \mu\text{m}$ (Freezing Temperature -15 °C)

$\mu_3 = 30.2 \mu\text{m}$ (Freezing Temperature -2 °C)

Duncan Multiple Range Test

$n = 3$

$N = 9$

degrees freedom = 6

$$S_{yi} = (MS_E/n)^{1/2} = 0.459$$

$$R_2 = (2,6)S_{yi} = 3.46(0.459) = 1.588$$

$$R_3 = (3,6)S_{yi} = 3.58(0.459) = 1.643$$

$$1 \text{ vs } 3 = 30.2 - 1.2 = 29.0 > 1.643 \text{ significant}$$

$$1 \text{ vs } 2 = 30.2 - 1.9 = 28.2 > 1.588 \text{ significant}$$

$$2 \text{ vs } 3 = 1.9 - 1.2 = 0.7 < 1.588 \text{ not significant}$$

Analysis of Variance and Duncan Multiple Range Test
Membrane Concentrate, Concentrated Material Thickness Versus Initial
Freezing Temperature (Bottom)

Analysis of Variance

Dependent Variable: Cross sectional thickness

Levels: -2 °C, -15 °C, and -25 °C

Source	SUM-OF-SQUARES	Degrees of Freedom (n-1)	Mean-Square	F-Ratio	P
Freezing Temperature (°C)	1211.280	2	605.640	6265.241	0.000
Error	0.580	6	0.097		

Means:

$\mu_1 = 1.1 \mu\text{m}$ (Freezing Temperature -25 °C)

$\mu_2 = 1.9 \mu\text{m}$ (Freezing Temperature -15 °C)

$\mu_3 = 26.1 \mu\text{m}$ (Freezing Temperature -2 °C)

Duncan Multiple Range Test

$n = 3$

$N = 9$

degrees freedom = 6

$$S_{yi} = (MS_E/n)^{1/2} = 0.180$$

$$R_2 = (2,6)S_{yi} = 3.46(0.180) = 0.623$$

$$R_3 = (3,6)S_{yi} = 3.58(0.180) = 0.644$$

$$1 \text{ vs } 3 = 26.1 - 1.1 = 25.0 > 0.644 \text{ significant}$$

$$1 \text{ vs } 2 = 26.1 - 1.9 = 24.2 > 0.623 \text{ significant}$$

$$2 \text{ vs } 3 = 1.9 - 1.1 = 0.8 > 0.623 \text{ significant}$$

Analysis of Variance and Duncan Multiple Range Test
Eop, Concentrated Material Thickness Versus Initial Freezing
Temperature

Analysis of Variance

Dependent Variable: Cross sectional thickness

Levels: -2 °C, -15 °C, and -25 °C

Source	SUM-OF-SQUARES	Degrees of Freedom (n-1)	Mean-Square	F-Ratio	P
Freezing Temperature (°C)	3406.827	2	1703.413	713.057	0.000
Error	14.333	6	2.389		

Means:

$\mu_1 = 1.2 \mu\text{m}$ (Freezing Temperature -25 °C)

$\mu_2 = 6.7 \mu\text{m}$ (Freezing Temperature -15 °C)

$\mu_3 = 44.9 \mu\text{m}$ (Freezing Temperature -2 °C)

Duncan Multiple Range Test

$n = 3$

$N = 9$

degrees freedom = 6

$$S_{yi} = (MS_E/n)^{1/2} = 0.892$$

$$R_2 = (2,6)S_{yi} = 3.46(0.892) = 3.086$$

$$R_3 = (3,6)S_{yi} = 3.58(0.892) = 3.193$$

$$1 \text{ vs } 3 = 44.9 - 1.2 = 43.7 > 3.193 \text{ significant}$$

$$1 \text{ vs } 2 = 44.9 - 6.7 = 38.2 > 3.086 \text{ significant}$$

$$2 \text{ vs } 3 = 6.7 - 1.2 = 5.5 > 3.086 \text{ significant}$$

Analysis of Variance and Duncan Multiple Range Test
Membrane Concentrate, Dilution Study, Initial Freezing
Temperature -2 °C

Analysis of Variance

Dependent Variable: Concentrate material thickness

Levels: 0 %, 50 %, and 66 %

Source	SUM-OF-SQUARES	Degrees of Freedom (n-1)	Mean-Square	F-Ratio	P
Dilution (%)	3855.935	2	1927.968	61.720	0.000
Error	1030.833	33	31.237		

Means:

$$\mu_1 = 27.4 \mu\text{m}$$

$$\mu_2 = 15.7 \mu\text{m}$$

$$\mu_3 = 2.0 \mu\text{m}$$

Duncan Multiple Range Test

$$n = 3$$

$$N = 36$$

$$\text{degrees freedom} = 33$$

$$S_{yi} = (MS_E/n)^{1/2} = 3.227$$

$$R_2 = (2,33)S_{yi} = 2.88(3.227) = 9.294$$

$$R_3 = (3,33)S_{yi} = 3.03(3.227) = 9.778$$

$$1 \text{ vs } 3 = 27.4 - 2.0 = 25.4 > 9.778 \text{ significant}$$

$$1 \text{ vs } 2 = 27.4 - 15.7 = 11.7 > 9.294 \text{ significant}$$

$$2 \text{ vs } 3 = 15.7 - 2.0 = 13.7 > 9.294 \text{ significant}$$

Analysis of Variance and Duncan Multiple Range Test
Membrane Concentrate, Dilution Study, Initial Freezing
Temperature -15 °C

Analysis of Variance

Dependent Variable: Concentrate material thickness

Levels: 0 %, 50 %, and 66 %

Source	SUM-OF-SQUARES	Degrees of Freedom (n-1)	Mean-Square	F-Ratio	P
Dilution (%)	11.083	3	3.694	148.679	0.000
Error	1.093	44	0.025		

Means:

$$\mu_1 = 1.9 \mu\text{m}$$

$$\mu_2 = 1.0 \mu\text{m}$$

$$\mu_3 = 0.8 \mu\text{m}$$

$$\mu_4 = 0.7 \mu\text{m}$$

Duncan Multiple Range Test

$$n = 4$$

$$N = 48$$

$$\text{degrees freedom} = 44$$

$$S_{y_i} = (MS_E/n)^{1/2} = 0.079$$

$$R_2 = (2,44)S_{y_i} = 2.86(0.079) = 0.226$$

$$R_3 = (3,44)S_{y_i} = 3.01(0.079) = 0.238$$

$$R_4 = (4,44)S_{y_i} = 3.10(0.079) = 0.245$$

$$1 \text{ vs } 4 = 1.9 - 0.7 = 1.2 > 0.245 \text{ significant}$$

$$1 \text{ vs } 3 = 1.9 - 0.8 = 1.1 > 0.238 \text{ significant}$$

$$1 \text{ vs } 2 = 1.9 - 1.0 = 0.9 > 0.226 \text{ significant}$$

$$2 \text{ vs } 4 = 1.0 - 0.7 = 0.3 > 0.238 \text{ significant}$$

$$2 \text{ vs } 3 = 1.0 - 0.8 = 0.2 < 0.226 \text{ not significant}$$

$$3 \text{ vs } 4 = 0.8 - 0.7 = 0.1 < 0.226 \text{ not significant}$$

APPENDIX C

STEPWISE REGRESSION ANALYSIS STABILITY RESULTS

MEMBRANE CONCCENTRATE

TUE 10/11/98 10:56:50 PM

SYSTAT VERSION 5.0
COPYRIGHT, 1990-1992
SYSTAT, INC.

Welcome to SYSTAT!
WORKSPACE CLEAR FOR CREATING NEW DATASET
SYSTAT FILE VARIABLES AVAILABLE TO YOU ARE:
TIME CONC FREEZE

TUE 10/11/98 10:57:28 PM C:\SYSTATW5\STABEPT1.SYS

DEPENDENT VARIABLE TIME

MINIMUM TOLERANCE FOR ENTRY INTO MODEL = .010000

FORWARD STEPWISE WITH ALPHA-TO-ENTER= .150 AND ALPHA-TO-REMOVE= .150

STEP # 0 R= .000 RSQUARE= .000

VARIABLE	COEFFICIENT	STD ERROR	STD COEF	TOLERANCE	F	'P'
----------	-------------	-----------	----------	-----------	---	-----

IN

1 CONSTANT

OUT	PART. CORR
-----	------------

2 CONC	0.927	.	.	.1E+01	109.696	0.000
3 FREEZE	-0.057	.	.	.1E+01	0.059	0.811
4 FREEZE*CONC	-0.362	.	.	.1E+01	2.711	0.117

STEP # 1 R= .927 RSQUARE= .959

TERM ENTERED: CONC

VARIABLE	COEFFICIENT	STD ERROR	STD COEF	TOLERANCE	F	'P'
----------	-------------	-----------	----------	-----------	---	-----

IN

1 CONSTANT

2 CONC	2024.111	193.259	0.927	.1E+01	109.696	0.000
--------	----------	---------	-------	--------	---------	-------

OUT	PART. CORR
-----	------------

3 FREEZE	0.978	.	.	0.82264	375.336	0.000
4 FREEZE*CONC	0.980	.	.	0.53625	408.614	0.000

STEP # 2 R= .997 RSQUARE= .994

TERM ENTERED: FREEZE*CONC

VARIABLE	COEFFICIENT	STD ERROR	STD COEF	TOLERANCE	F	'P'
----------	-------------	-----------	----------	-----------	---	-----

IN

1 CONSTANT

2 CONC	2771.213	54.273	1.269	0.53625	.26E+04	0.000
4 FREEZE*CONC	40.449	2.001	0.502	0.53625	408.614	0.000

OUT	PART. CORR
-----	------------

3 FREEZE	0.702	.	.	0.07022	15.584	0.001
----------	-------	---	---	---------	--------	-------

STEP # 3 R= .999 RSQUARE= .997

TERM ENTERED: FREEZE

VARIABLE	COEFFICIENT	STD ERROR	STD COEF	TOLERANCE	F	'P'
----------	-------------	-----------	----------	-----------	---	-----

IN

1	CONSTANT						
2	CONC	2603.607	58.207	1.192	0.25094	.20E+04	0.000
3	FREEZE	8.294	2.101	0.199	0.07022	15.584	0.001
4	FREEZE*CONC	21.476	5.025	0.267	0.04576	18.263	0.001

OUT

PART. CORR

none

THE SUBSET MODEL INCLUDES THE FOLLOWING PREDICTORS:

CONSTANT
 CONC
 FREEZE
 FREEZE*CONC

DEP VAR: TIME N: 20 MULTIPLE R: 0.999 SQUARED MULTIPLE R: 0.997
 ADJUSTED SQUARED MULTIPLE R: .997 STANDARD ERROR OF ESTIMATE: 16.184

VARIABLE	COEFFICIENT	STD ERROR	STD COEF	TOLERANCE	T	P(2 TAIL)
CONSTANT	-649.409	21.693	0.000	.	-29.936	0.000
CONC	2603.607	58.207	1.192	0.251	44.730	0.000
FREEZE	8.294	2.101	0.199	0.070	3.948	0.001
FREEZE*CONC	21.476	5.025	0.267	0.046	4.274	0.001

ANALYSIS OF VARIANCE

SOURCE	SUM-OF-SQUARES	DF	MEAN-SQUARE	F-RATIO	P
REGRESSION	1465175.619	3	488391.873	1864.566	0.000
RESIDUAL	4190.931	16	261.933		

APPENDIX D

STEPWISE REGRESSION ANALYSIS STABILITY RESULTS

Eop EFFLUENT

Welcome to SYSTAT!
 WORKSPACE CLEAR FOR CREATING NEW DATASET
 SYSTAT FILE VARIABLES AVAILABLE TO YOU ARE:
 TIME CONC FREEZE

WED 11/11/98 12:27:53 AM C:\SYSTATW5\STABEOP.SYS

DEPENDENT VARIABLE TIME

MINIMUM TOLERANCE FOR ENTRY INTO MODEL = .010000

FORWARD STEPWISE WITH ALPHA-TO-ENTER= .150 AND ALPHA-TO-REMOVE= .150

STEP # 0 R= .000 RSQUARE= .000

VARIABLE	COEFFICIENT	STD ERROR	STD COEF	TOLERANCE	F	'P'
----------	-------------	-----------	----------	-----------	---	-----

IN

1 CONSTANT

OUT	PART. CORR
-----	------------

2 CONC	0.881	.	.	.1E+01	62.452	0.000
3 FREEZE	0.039	.	.	.1E+01	0.027	0.972
4 FREEZE*CONC	-0.310	.	.	.1E+01	1.915	0.193

STEP # 1 R= .881 RSQUARE= .776

TERM ENTERED: CONC

VARIABLE	COEFFICIENT	STD ERROR	STD COEF	TOLERANCE	F	'P'
----------	-------------	-----------	----------	-----------	---	-----

IN

1 CONSTANT

2 CONC	1777.963	224.983	0.881	.1E+01	62.452	0.000
--------	----------	---------	-------	--------	--------	-------

OUT	PART. CORR
-----	------------

3 FREEZE	0.926	.	.	0.83225	101.907	0.000
4 FREEZE*CONC	0.791	.	.	0.55390	28.368	0.000

STEP # 2 R= .984 RSQUARE= .968

TERM ENTERED: FREEZE

VARIABLE	COEFFICIENT	STD ERROR	STD COEF	TOLERANCE	F	'P'
----------	-------------	-----------	----------	-----------	---	-----

IN

1 CONSTANT

2 CONC	2174.687	95.952	1.078	0.83225	513.670	0.000
3 FREEZE	18.738	1.856	0.480	0.83225	101.907	0.000

OUT	PART. CORR
-----	------------

4 FREEZE*CONC	-0.517	.	.	0.07365	5.834	0.028
---------------	--------	---	---	---------	-------	-------

STEP # 3 R= .988 RSQUARE= .977

TERM ENTERED: FREEZE*CONC

VARIABLE	COEFFICIENT	STD ERROR	STD COEF	TOLERANCE	F	'P'
----------	-------------	-----------	----------	-----------	---	-----

```

IN
---
1 CONSTANT
2 CONC          1929.426      132.210      0.956 0.34131  212.974  0.000
3 FREEZE        28.840       4.492       0.739 0.11066   41.226  0.000
4 FREEZE*CONC   -31.677      13.115     -0.341 0.07365    5.834  0.028

OUT          PART. CORR
---
      none

```

THE SUBSET MODEL INCLUDES THE FOLLOWING PREDICTORS:

```

CONSTANT
CONC
FREEZE
FREEZE*CONC

```

```

DEF VAR:      TIME      N:      20  MULTIPLE R: 0.988  SQUARED MULTIPLE R: 0.977
ADJUSTED SQUARED MULTIPLE R: .972  STANDARD ERROR OF ESTIMATE: 43.434

```

VARIABLE	COEFFICIENT	STD ERROR	STD COEF	TOLERANCE	T	P(2 TAIL)
CONSTANT	-198.633	38.403	0.000	.	-5.172	0.000
CONC	1929.426	132.210	0.956	0.341	14.594	0.000
FREEZE	28.840	4.492	0.739	0.111	6.421	0.000
FREEZE*CONC	-31.677	13.115	-0.341	0.074	-2.415	0.028

ANALYSIS OF VARIANCE

SOURCE	SUM-OF-SQUARES	DF	MEAN-SQUARE	F-RATIO	P
REGRESSION	1257530.598	3	419176.866	221.194	0.000
RESIDUAL	30184.602	16	1886.538		

APPENDIX E

STEPWISE REGRESSION ANALYSIS RESULTS

MEMBRANE CONCENTRATE

SYSTAT VERSION 5.0
COPYRIGHT, 1990-1992
SYSTAT, INC.

Welcome to SYSTAT!

WORKSPACE CLEAR FOR CREATING NEW DATASET
SYSTAT FILE VARIABLES AVAILABLE TO YOU ARE:

COLOR	FREEZE	THAW	TYPE	EFFLUENT
TIME	TEMP			

MON 9/11/98 10:12:44 PM A:\EOPTYP1F.SYS

DEPENDENT VARIABLE COLOR

MINIMUM TOLERANCE FOR ENTRY INTO MODEL = .010000

FORWARD STEPWISE WITH ALPHA-TO-ENTER= .150 AND ALPHA-TO-REMOVE= .150

STEP # 0 R= .000 RSQUARE= .000

VARIABLE	COEFFICIENT	STD ERROR	STD COEF TOLERANCE	F	'P'
----------	-------------	-----------	--------------------	---	-----

IN

1 CONSTANT

OUT

PART. CORR

2 FREEZE	-0.750	.	.1E+01	79.489	0.000
3 THAW	-0.639	.	.1E+01	42.847	0.000
4 TIME	-0.064	.	.1E+01	0.258	0.613
5 TEMP	0.081	.	.1E+01	0.407	0.526
6 FREEZE*THAW	-0.071	.	.1E+01	0.311	0.579
7 FREEZE*TIME	-0.453	.	.1E+01	16.040	0.000
8 FREEZE*TEMP	0.441	.	.1E+01	14.980	0.000
9 *TEMP	0.042	.	.1E+01	0.108	0.744
10 *TEMP	0.307	.	.1E+01	6.467	0.013
11 *TEMP	0.355	.	.1E+01	8.920	0.004

STEP # 1 R= .750 RSQUARE= .562

TERM ENTERED: FREEZE

VARIABLE	COEFFICIENT	STD ERROR	STD COEF TOLERANCE	F	'P'
----------	-------------	-----------	--------------------	---	-----

IN

1 CONSTANT

2 FREEZE	-82.680	9.274	-0.750 .1E+01	79.489	0.000
----------	---------	-------	---------------	--------	-------

OUT

PART. CORR

3 THAW	-0.966	.	.1E+01	844.042	0.000
4 TIME	-0.097	.	.1E+01	0.582	0.448
5 TEMP	0.122	.	.1E+01	0.921	0.341
6 FREEZE*THAW	0.823	.	0.58031	127.867	0.000
7 FREEZE*TIME	0.039	.	0.60089	0.094	0.760
8 FREEZE*TEMP	-0.048	.	0.61312	0.143	0.706
9 *TEMP	-0.512	.	0.79062	21.654	0.000
FREEZE*TIME					

```

10 *TEMP          -0.049      .      . 0.79882    0.145    0.704
    THAW*TIME
11 *TEMP          0.536      .      . .1E+01    24.556    0.000

```

STEP # 2 R= .985 RSQUARE= .970
TERM ENTERED: THAW

VARIABLE	COEFFICIENT	STD ERROR	STD COEF	TOLERANCE	F	'P'
IN						

1 CONSTANT						
2 FREEZE	-82.680	2.427	-0.750	.1E+01	.12E+04	0.000
3 THAW	-45.836	1.578	-0.639	.1E+01	844.042	0.000
OUT						
PART. CORR						

4 TIME	-0.375	.	.	.1E+01	9.791	0.003
5 TEMP	0.470	.	.	.1E+01	16.994	0.000
6 FREEZE*THAW	0.353	.	.	0.21413	8.549	0.005
7 FREEZE*TIME	0.151	.	.	0.60089	1.406	0.240
8 FREEZE*TEMP	-0.186	.	.	0.61312	2.160	0.147
FREEZE*THAW						
9 *TEMP	-0.209	.	.	0.60794	2.748	0.103
FREEZE*TIME						
10 *TEMP	-0.188	.	.	0.79882	2.195	0.144
THAW*TIME						
11 *TEMP	0.503	.	.	0.81263	20 323	0.000

STEP # 3 R= .989 RSQUARE= .978
TERM ENTERED: THAW*TIME
*TEMP

VARIABLE	COEFFICIENT	STD ERROR	STD COEF	TOLERANCE	F	'P'
IN						

1 CONSTANT						
2 FREEZE	-82.680	2.115	-0.750	.1E+01	.15E+04	0.000
3 THAW	-42.860	1.525	-0.598	0.81263	789.686	0.000
THAW*TIME						
11 *TEMP	0.008	0.002	0.096	0.81263	20.323	0.000
OUT						
PART. CORR						

4 TIME	-0.164	.	.	0.74893	1.627	0.207
5 TEMP	0.285	.	.	0.73573	5.213	0.026
6 FREEZE*THAW	0.409	.	.	0.21413	11.825	0.001
7 FREEZE*TIME	-0.062	.	.	0.50570	0.225	0.637
8 FREEZE*TEMP	0.024	.	.	0.51088	0.034	0.854
FREEZE*THAW						
9 *TEMP	0.026	.	.	0.48174	0.040	0.843
FREEZE*TIME						
10 *TEMP	0.208	.	.	0.46505	2.673	0.107

STEP # 4 R= .991 RSQUARE= .982
TERM ENTERED: FREEZE*THAW

VARIABLE	COEFFICIENT	STD ERROR	STD COEF	TOLERANCE	F	'P'
IN						

1 CONSTANT						
2 FREEZE	-92.053	3.350	-0.835	0.33784	755.278	0.000
3 THAW	-37.169	2.170	-0.518	0.34006	293.374	0.000
6 FREEZE*THAW	0.669	0.195	0.131	0.21413	11.825	0.001
THAW*TIME						
11 *TEMP	0.008	0.002	0.096	0.81263	23.990	0.000
OUT						
PART. CORR						

4 TIME	-0.179	.	.	0.74893	1.930	0.170

5 TEMP	0.312	.	. 0.73573	6.262	0.015
7 FREEZE*TIME	-0.068	.	. 0.50570	0.266	0.608
8 FREEZE*TEMP	0.026	.	. 0.51088	0.040	0.841
FREEZE*THAW					
9 *TEMP	0.271	.	. 0.37491	4.601	0.036
FREEZE*TIME					
10 *TEMP	0.228	.	. 0.46505	3.184	0.080

STEP # 5 R= .992 RSQUARE= .983
TERM ENTERED: TEMP

VARIABLE	COEFFICIENT	STD ERROR	STD COEF	TOLERANCE	F	'P'
IN						

1 CONSTANT						
2 FREEZE	-92.053	3.209	-0.835	0.33784	822.643	0.000
3 THAW	-38.042	2.108	-0.531	0.33075	325.563	0.000
5 TEMP	5.442	2.175	0.049	0.73573	6.262	0.015
6 FREEZE*THAW	0.669	0.187	0.131	0.21413	12.879	0.001
THAW*TIME						
11 *TEMP	0.005	0.002	0.068	0.59787	9.598	0.003
OUT						
PART. CORR						

4 TIME	-0.323	.	. 0.65875		6.639	0.013
7 FREEZE*TIME	0.015	.	. 0.47150		0.013	0.911
8 FREEZE*TEMP	0.410	.	. 0.22624		11.539	0.001
FREEZE*THAW						
9 *TEMP	0.537	.	. 0.27216		23.079	0.000
FREEZE*TIME						
10 *TEMP	0.337	.	. 0.43385		7.290	0.009

STEP # 6 R= .994 RSQUARE= .988
TERM ENTERED: FREEZE*THAW
*TEMP

VARIABLE	COEFFICIENT	STD ERROR	STD COEF	TOLERANCE	F	'P'
IN						

1 CONSTANT						
2 FREEZE	-92.053	2.731	-0.835	0.33784	.11E+04	0.000
3 THAW	-37.298	1.801	-0.520	0.32830	428.880	0.000
5 TEMP	10.906	2.172	0.099	0.53408	25.204	0.000
6 FREEZE*THAW	1.147	0.187	0.225	0.15377	37.504	0.000
FREEZE*THAW						
9 *TEMP	0.056	0.012	0.133	0.27216	23.079	0.000
THAW*TIME						
11 *TEMP	0.007	0.002	0.092	0.55775	22.663	0.000
OUT						
PART. CORR						

4 TIME	-0.265	.	. 0.63420		4.230	0.044
7 FREEZE*TIME	-0.073	.	. 0.46219		0.296	0.588
8 FREEZE*TEMP	0.080	.	. 0.12446		0.363	0.549
FREEZE*TIME						
10 *TEMP	0.287	.	. 0.41908		5.014	0.029

STEP # 7 R= .995 RSQUARE= .989
TERM ENTERED: FREEZE*TIME
*TEMP

VARIABLE	COEFFICIENT	STD ERROR	STD COEF	TOLERANCE	F	'P'
IN						

1 CONSTANT						
2 FREEZE	-89.672	2.846	-0.813	0.29069	992.717	0.000
3 THAW	-36.579	1.770	-0.510	0.31750	427.039	0.000
5 TEMP	11.537	2.119	0.105	0.52462	29.657	0.000
6 FREEZE*THAW	1.107	0.182	0.217	0.15226	37.000	0.000

*TEMP	0.006	0.002	0.079	0.340	3.662	0.001
-------	-------	-------	-------	-------	-------	-------

ANALYSIS OF VARIANCE

SOURCE	SUM-OF-SQUARES	DF	MEAN-SQUARE	F-RATIO	P
REGRESSION	.326170E+08	8	4077122.998	785.788	0.000
RESIDUAL	285371.878	55	5188.580		

APPENDIX F**STEPWISE REGRESSION ANALYSIS RESULTS****Eop EFFLUENT**

SYSTAT VERSION 5.0
COPYRIGHT, 1990-1992
SYSTAT, INC.

Welcome to SYSTAT!

WORKSPACE CLEAR FOR CREATING NEW DATASET
SYSTAT FILE VARIABLES AVAILABLE TO YOU ARE:

COLOR	FREEZE	THAW	TYPE	EFFLUENT
TIME	TEMP			

SAT 7/11/98 10:52:06 PM A:\EOPFINAL.SYS

DEP VAR: COLOR N: 64 MULTIPLE R: 0.994 SQUARED MULTIPLE R: 0.989
ADJUSTED SQUARED MULTIPLE R: .986 STANDARD ERROR OF ESTIMATE: 27.027

VARIABLE	COEFFICIENT	STD ERROR	STD COEF TOLERANCE	T	P(2 TAIL)
CONSTANT	1378.123	17.714	0.000	77.800	0.000
FREEZE	20.606	1.322	0.583	15.587	0.000
THAW	-35.676	0.843	-1.552	-42.342	0.000
TIME	-0.805	0.254	-0.117	-3.164	0.003
TEMP	4.290	1.322	0.121	3.245	0.002
FREEZE*THAW	-1.586	0.052	-0.969	-30.520	0.000
FREEZE*TIME	-0.033	0.015	-0.067	-2.161	0.035
FREEZE*TEMP	0.188	0.080	0.073	2.354	0.022
THAW*TIME	0.032	0.010	0.102	3.171	0.003
THAW*TEMP	-0.104	0.052	-0.064	-2.003	0.050
TIME*TEMP	0.050	0.015	0.101	3.220	0.002

ANALYSIS OF VARIANCE

SOURCE	SUM-OF-SQUARES	DF	MEAN-SQUARE	F-RATIO	P
REGRESSION	3343121.506	10	334312.151	457.677	0.000
RESIDUAL	38714.103	53	730.455		

SAT 7/11/98 10:52:32 PM A:\EOPFINAL.SYS

DEPENDENT VARIABLE COLOR

MINIMUM TOLERANCE FOR ENTRY INTO MODEL = .010000

FORWARD STEPWISE WITH ALPHA-TO-ENTER= .150 AND ALPHA-TO-REMOVE= .150

STEP # 0 R= .000 RSQUARE= .000

VARIABLE	COEFFICIENT	STD ERROR	STD COEF TOLERANCE	F	'P'
----------	-------------	-----------	--------------------	---	-----

IN

1 CONSTANT

OUT

PART. CORR

2 FREEZE	-0.133	.	.1E+01	1.119	0.294
3 THAW	-0.864	.	.1E+01	183.253	0.000
4 TIME	-0.073	.	.1E+01	0.328	0.569
5 TEMP	0.098	.	.1E+01	0.606	0.439
6 FREEZE*THAW	0.229	.	.1E+01	3.439	0.068
7 FREEZE*TIME	-0.054	.	.1E+01	0.184	0.669
8 FREEZE*TEMP	0.038	.	.1E+01	0.090	0.765
9 THAW*TIME	-0.557	.	.1E+01	27.853	0.000

10 THAW*TEMP	0.573	.	.	.1E+01	30.334	0.000
11 TIME*TEMP	0.129	.	.	.1E+01	1.051	0.309

STEP # 1 R= .864 RSQUARE= .747
TERM ENTERED: THAW

VARIABLE	COEFFICIENT	STD ERROR	STD COEF	TOLERANCE	F	'P'
IN						

1 CONSTANT						
3 THAW	-19.870	1.468	-0.864	.1E+01	183.253	0.000
OUT						
PART. CORR						

2 FREEZE	-0.265	.	.	.1E+01	4.601	0.036
4 TIME	-0.144	.	.	.1E+01	1.297	0.259
5 TEMP	0.196	.	.	.1E+01	2.427	0.124
6 FREEZE*THAW	-0.734	.	.	0.63382	71.269	0.000
7 FREEZE*TIME	-0.108	.	.	.1E+01	0.723	0.399
8 FREEZE*TEMP	0.076	.	.	.1E+01	0.352	0.555
9 THAW*TIME	-0.064	.	.	0.62185	0.247	0.621
10 THAW*TEMP	0.125	.	.	0.63382	0.971	0.328
11 TIME*TEMP	0.257	.	.	.1E+01	4.306	0.042

STEP # 2 R= .940 RSQUARE= .883
TERM ENTERED: FREEZE*THAW

VARIABLE	COEFFICIENT	STD ERROR	STD COEF	TOLERANCE	F	'P'
IN						

1 CONSTANT						
3 THAW	-26.319	1.262	-1.145	0.63382	434.718	0.000
6 FREEZE*THAW	-0.759	0.090	-0.464	0.63382	71.269	0.000
OUT						
PART. CORR						

2 FREEZE	0.842	.	.	0.33784	146.527	0.000
4 TIME	-0.213	.	.	.1E+01	2.838	0.097
5 TEMP	0.288	.	.	.1E+01	5.429	0.023
7 FREEZE*TIME	0.462	.	.	0.73573	16.288	0.000
8 FREEZE*TEMP	-0.505	.	.	0.74382	20.534	0.000
9 THAW*TIME	-0.094	.	.	0.62185	0.530	0.469
10 THAW*TEMP	0.184	.	.	0.63382	2.110	0.152
11 TIME*TEMP	0.378	.	.	.1E+01	10.009	0.002

STEP # 3 R= .983 RSQUARE= .966
TERM ENTERED: FREEZE

VARIABLE	COEFFICIENT	STD ERROR	STD COEF	TOLERANCE	F	'P'
IN						

1 CONSTANT						
2 FREEZE	17.499	1.446	0.495	0.33784	146.527	0.000
3 THAW	-33.354	0.899	-1.451	0.36900	.14E+04	0.000
6 FREEZE*THAW	-1.586	0.084	-0.969	0.21413	356.410	0.000
OUT						
PART. CORR						

4 TIME	-0.394	.	.	.1E+01	10.859	0.002
5 TEMP	0.534	.	.	.1E+01	23.588	0.000
7 FREEZE*TIME	0.208	.	.	0.60089	2.677	0.107
8 FREEZE*TEMP	-0.310	.	.	0.61312	6.288	0.015
9 THAW*TIME	-0.174	.	.	0.62185	1.834	0.181
10 THAW*TEMP	0.342	.	.	0.63382	7.811	0.007
11 TIME*TEMP	0.701	.	.	.1E+01	57.164	0.000

STEP # 4 R= .991 RSQUARE= .983
TERM ENTERED: TIME*TEMP

VARIABLE	COEFFICIENT	STD ERROR	STD COEF	TOLERANCE	F	'P'
IN						

1 CONSTANT						
2 FREEZE	17.499	1.039	0.495	0.33784	283.686	0.000
3 THAW	-33.354	0.646	-1.451	0.36900	.27E+04	0.000
6 FREEZE*THAW	-1.586	0.060	-0.969	0.21413	690.034	0.000
11 TIME*TEMP	0.064	0.008	0.129	.1E+01	57.164	0.000

OUT	PART. CORR

4 TIME	0.067
5 TEMP	0.165
7 FREEZE*TIME	-0.217
8 FREEZE*TEMP	0.068
9 THAW*TIME	0.288
10 THAW*TEMP	-0.031

STEP # 5 R= .992 RSQUARE= .984
TERM ENTERED: THAW*TIME

VARIABLE	COEFFICIENT	STD ERROR	STD COEF	TOLERANCE	F	'P'
IN						

1 CONSTANT						
2 FREEZE	17.499	1.003	0.495	0.33784	304.169	0.000
3 THAW	-34.137	0.711	-1.485	0.28393	.23E+04	0.000
6 FREEZE*THAW	-1.586	0.058	-0.969	0.21413	739.857	0.000
9 THAW*TIME	0.017	0.008	0.055	0.46572	5.260	0.025
11 TIME*TEMP	0.075	0.009	0.151	0.74893	62.796	0.000

OUT	PART. CORR

4 TIME	-0.228
5 TEMP	0.034
7 FREEZE*TIME	-0.078
8 FREEZE*TEMP	0.182
10 THAW*TEMP	-0.145

STEP # 6 R= .992 RSQUARE= .985
TERM ENTERED: TIME

VARIABLE	COEFFICIENT	STD ERROR	STD COEF	TOLERANCE	F	'P'
IN						

1 CONSTANT						
2 FREEZE	17.499	0.986	0.495	0.33784	315.290	0.000
3 THAW	-34.791	0.791	-1.513	0.22173	.19E+04	0.000
4 TIME	-0.371	0.210	-0.054	0.28005	3.121	0.083
6 FREEZE*THAW	-1.586	0.057	-0.969	0.21413	766.908	0.000
9 THAW*TIME	0.032	0.011	0.102	0.21008	8.278	0.006
11 TIME*TEMP	0.068	0.010	0.136	0.62083	43.759	0.000

OUT	PART. CORR

5 TEMP	0.170
7 FREEZE*TIME	-0.260
8 FREEZE*TEMP	0.118
10 THAW*TEMP	-0.075

STEP # 7 R= .993 RSQUARE= .986
TERM ENTERED: FREEZE*TIME

VARIABLE	COEFFICIENT	STD ERROR	STD COEF	TOLERANCE	F	'P'
IN						

1 CONSTANT						

2	FREEZE	19.006	1.218	0.537	0.21008	243.677	0.000
3	THAW	-34.791	0.770	-1.513	0.22173	.20E+04	0.000
4	TIME	-0.655	0.249	-0.096	0.18937	6.951	0.011
6	FREEZE*THAW	-1.586	0.056	-0.969	0.21413	807.975	0.000
7	FREEZE*TIME	-0.033	0.017	-0.067	0.22173	4.052	0.049
9	THAW*TIME	0.032	0.011	0.102	0.21008	8.721	0.005
11	TIME*TEMP	0.068	0.010	0.136	0.62083	46.102	0.000

OUT PART. CORR

5	TEMP	0.176	.	0.35714	1.766	0.189
8	FREEZE*TEMP	0.122	.	0.36441	0.834	0.365
10	THAW*TEMP	-0.078	.	0.36402	0.336	0.564

THE SUBSET MODEL INCLUDES THE FOLLOWING PREDICTORS:

CONSTANT
FREEZE
THAW
TIME
FREEZE*THAW
FREEZE*TIME
THAW*TIME
TIME*TEMP

DEP VAR: COLOR N: 64 MULTIPLE R: 0.993 SQUARED MULTIPLE R: 0.986
ADJUSTED SQUARED MULTIPLE R: .984 STANDARD ERROR OF ESTIMATE: 29.019

VARIABLE	COEFFICIENT	STD ERROR	STD COEF	TOLERANCE	T	P(2 TAIL)
CONSTANT	1341.658	14.702	0.000	.	91.254	0.000
FREEZE	19.006	1.218	0.537	0.210	15.610	0.000
THAW	-34.791	0.770	-1.513	0.222	-45.162	0.000
TIME	-0.655	0.249	-0.096	0.189	-2.637	0.011
FREEZE*THAW	-1.586	0.056	-0.969	0.214	-28.425	0.000
FREEZE*TIME	-0.033	0.017	-0.067	0.222	-2.013	0.049
THAW*TIME	0.032	0.011	0.102	0.210	2.953	0.005
TIME*TEMP	0.068	0.010	0.136	0.621	6.790	0.000

ANALYSIS OF VARIANCE

SOURCE	SUM-OF-SQUARES	DF	MEAN-SQUARE	F-RATIO	P
REGRESSION	3334676.418	7	476382.345	565.688	0.000
RESIDUAL	47159.192	56	842.128		

APPENDIX G**COMPOSITE RESULTS****ALKALINE EXTRACTION STAGE MEMBRANE CONCENTRATE**

Composite Results
Initial Freezing Temperature -2 °C
Thawed Top Down at a Thawing Temperature 24 °C

Sample Location	Initial Freezing Temperature -2 °C								
	Top (35 %)			Middle (35 %)			Bottom (30 %)		
	μ	s	range	μ	s	range	μ	s	range
Color (CU)	5360	100.0	5250 to 5450	10700	310.0	10400 to 11000	22500	260.0	22300 to 22800
COD (mg/L)	5810	216.0	5600 to 6030	11100	255.0	10800 to 11300	24700	529.0	24100 to 25100
pH	9.59	0.04	9.55 to 9.62	9.56	0.03	9.54 to 9.59	9.59	0.02	9.47 to 9.53
Total Alkalinity (mg/L CaCO ₃)	1200	66.0	1130 to 1260	2090	75.0	2010 to 2160	5060	70.0	4940 to 5150
Total Suspended Solids (mg/L)	13	2.3	12 to 16	15	2.2	12 to 16	318	50.5	272 to 372
Turbidity (NTU)	8.8	2.81	7.0 to 12.0	5.2	0.20	5.0 to 5.4	5.7	1.00	4.5 to 6.4
Total Dissolved Solids (mg/L)	5530	185.1	5320 to 5670	11500	667.4	10700 to 11900	24200	122.3	24100 to 24300
Volatile Suspended Solids (mg/L)	12	4.00	8 to 16	12	4.0	8 to 16	165	194.1	132 to 200

μ - mean, s - sample variance

Composite Results
Initial Freezing Temperature -2 °C
Thawed Top Down at a Thawing Temperature 15 °C

Sample Location	Initial Freezing Temperature -2 °C								
	Top (35 %)			Middle (35 %)			Bottom (30 %)		
	μ	s	range	μ	s	range	μ	s	range
Color (CU)	5060	45.83	5010 to 5100	10200	158.1	10000 to 10300	22600	40.82	22500 to 22700
COD (mg/L)	5420	76.49	5350 to 5500	10900	158.1	10800 to 11100	24500	158.21	24300 to 24600
pH	9.56	0.022	9.55 to 9.59	9.57	0.016	9.55 to 9.58	9.51	0.016	9.50 to 9.53
Total Alkalinity (mg/L CaCO ₃)	1190	50.74	1150 to 1250	2100	25.50	2080 to 2130	5220	76.49	5000 to 5200
Total Suspended Solids (mg/L)	12	0.00	12	11	2.3	8 to 12	298	7.6	290 to 305
Turbidity (NTU)	10	0.79	9.5 to 11	5.1	0.32	4.9 to 5.5	4.2	0.26	4.0 to 4.5
Total Dissolved Solids (mg/L)	5440	42.43	5380 to 5510	10900	255.0	10700 to 11200	24500	200.0	24300 to 24700
Volatile Suspended Solids (mg/L)	9	2.3	8 to 12	11	2.4	8 to 12	225	25.0	200 to 250

μ - mean, s - sample variance

Composite Results
Initial Freezing Temperature -2 °C
Thawed Top Down at a Thawing Temperature 4 °C

Sample Location	Initial Freezing Temperature -2 °C								
	Top (35 %)			Middle (35 %)			Bottom (30 %)		
	μ	s	range	μ	s	range	μ	s	range
Color (CU)	4860	81.55	4800 to 4950	9940	77.78	9850 to 10000	22500	360.6	22100 to 22600
COD (mg/L)	5230	49.50	5150 to 5300	10300	200.0	10100 to 10500	24500	255.0	24300 to 24800
pH	9.58	0.036	9.55 to 9.62	9.54	0.007	9.53 to 9.54	9.53	0.007	9.51 to 9.53
Total Alkalinity (mg/L CaCO ₃)	1110	32.40	1090 to 1150	2060	38.24	2025 to 2100	5310	36.06	5280 to 5350
Total Suspended Solids (mg/L)	8	0.00	8	7	2.3	4 to 8	336	33.29	298 to 360
Turbidity (NTU)	5.5	0.25	5.3 to 5.8	4.1	0.16	4.0 to 4.3	3.9	0.30	3.6 to 4.2
Total Dissolved Solids (mg/L)	5210	65.57	5150 to 5280	10400	255.0	10100 to 10600	24600	300.0	24300 to 24800
Volatile Suspended Solids (mg/L)	8	0.00	8	7	2.3	4 to 8	192	21.7	172 to 225

μ - mean, s - sample variance

Composite Results
Initial Freezing Temperature -2 °C
Thawed Bottom up at a Thawing Temperature 24 °C

Sample Location	Initial Freezing Temperature -2 °C								
	Top (35 %)			Middle (35 %)			Bottom (30 %)		
	μ	s	range	μ	s	range	μ	s	range
Color (CU)	1310	149	1140 to 1420	5390	190	5210 to 5590	33900	735	32700 to 34900
COD (mg/L)	1440	125	1310 to 1560	5490	170	5320 to 5660	33400	778	32500 to 34000
pH	9.50	0.04	9.47 to 9.55	9.49	0.02	9.47 to 9.51	9.40	0.01	9.38 to 9.41
Total Alkalinity (mg/L CaCO ₃)	332	30	300 to 360	1310	69	1260 to 1390	6560	32	6520 to 6580
Total Suspended Solids (mg/L)	11	2.3	8 to 12	5	2.3	4 to 8	812	50.1	764 to 864
Turbidity (NTU)	13	1.1	12 to 14	4.4	1.1	3.1 to 5.2	3.5	0.4	3.2 to 4.0
Total Dissolved Solids (mg/L)	1480	152	1280 to 1590	5620	151	5460 to 5760	33100	644	32400 to 33600
Volatile Suspended Solids (mg/L)	9	2.3	8 to 12	5.3	2.3	4 to 8	375	24.1	352 to 400

μ - mean, s - sample variance

Composite Results
Initial Freezing Temperature -2 °C
Thawed Bottom up at a Thawing Temperature 15 °C

Sample Location	Initial Freezing Temperature -2 °C								
	Top (35 %)			Middle (35 %)			Bottom (30 %)		
	μ	s	range	μ	s	range	μ	s	range
Color (CU)	1500	45.28	1450 to 1540	5410	96.41	5300 to 5480	31200	200.0	31000 to 31400
COD(mg/L)	1520	90.83	1440 to 1620	5490	22.36	5460 to 5520	32400	406.2	32000 to 32800
pH	9.47	0.012	9.46 to 9.48	9.49	0.010	9.49 to 9.50	9.39	0.012	9.38 to 9.41
Total Alkalinity (mg/L CaCO ₃)	318	22.55	295 to 340	1350	50.00	1300 to 1400	6380	35.36	6350 to 6420
Total Suspended Solids (mg/L)	9	2.3	8 to 12	7	2.3	4 to 8	720	22.9	690 to 740
Turbidity (NTU)	13	1.00	13 to 15	4.8	0.25	4.5 to 5.0	4.2	0.22	4.0 to 4.5
Total Dissolved Solids (mg/L)	1500	60.00	1440 to 1560	5810	36.06	5780 to 5850	32200	353.6	31800 to 32500
Volatile Suspended Solids (mg/L)	8	0.00	8	7	2.3	4 to 8	333	8.7	325 to 345

μ - mean, s - sample variance

Composite Results
Initial Freezing Temperature -2 °C
Thawed Bottom up at a Thawing Temperature 4 °C

Sample Location	Initial Freezing Temperature -2 °C								
	Top (35 %)			Middle (35 %)			Bottom (30 %)		
	μ	s	range	μ	s	range	μ	s	range
Color (CU)	2610	160.9	2480 to 2790	5670	148.7	5480 to 5950	30100	291.5	29800 to 30300
COD(mg/L)	2740	196.1	2560 to 2950	5620	163.7	5480 to 5800	32100	160.8	30300 to 33300
pH	9.40	0.017	9.38 to 9.41	9.39	0.026	9.36 to 9.41	9.37	0.017	9.35 to 9.38
Total Alkalinity (mg/L CaCO ₃)	675	30.09	656 to 710	1460	75.17	1370 to 1500	5980	75.17	5900 to 6050
Total Suspended Solids (mg/L)	4	0.00	4	9	2.4	8 to 12	708	18.9	695 to 730
Turbidity (NTU)	7.0	1.80	5.0 to 8.5	1.9	0.26	1.6 to 2.1	3.2	0.35	2.8 to 3.5
Total Dissolved Solids (mg/L)	2850	108.2	2760 to 2970	6110	113.8	6020 to 6240	30000	781.0	29500 to 30900
Volatile Suspended Solids (mg/L)	4	0.00	4	9	2.4	8 to 12	312	7.7	305 to 320

μ - mean, s - sample variance

Composite Results
Initial Freezing Temperature -15 °C
Thawed Top Down at a Thawing Temperature 24 °C

Sample Location	Initial Freezing Temperature -15 °C								
	Top (35 %)			Middle (35 %)			Bottom (30 %)		
	μ	s	range	μ	s	range	μ	s	range
Color (CU)	9180	64.0	9130 to 9250	10300	308	10000 to 10600	15700	158.1	15600 to 15900
COD(mg/L)	10100	203	9920 to 10300	10500	300	10200 to 10800	19600	600	19000 to 20200
pH	9.64	0.01	9.64 to 9.66	9.66	0.01	9.65 to 9.67	9.68	0.03	9.65 to 9.70
Total Alkalinity (mg/L CaCO ₃)	2100	104	1930 to 2220	2420	148	2320 to 2550	3530	82	3470 to 3620
Total Suspended Solids (mg/L)	9	2.3	8 to 12	12	0.00	12	348	12.0	336 to 360
Turbidity (NTU)	3.2	0.5	2.7 to 3.6	3.3	0.8	2.4 to 3.9	2.7	0.2	2.4 to 2.9
Total Dissolved Solids (mg/L)	10200	212	10000 to 10400	10900	200	10700 to 11100	19300	1044	18100 to 20000
Volatile Suspended Solids (mg/L)	9	2.3	8 to 12	12	0.00	12	216	20.0	196 to 236

μ - mean, s - sample variance

Composite Results
Initial Freezing Temperature -15 °C
Thawed Top Down at a Thawing Temperature 15 °C

Sample Location	Initial Freezing Temperature -15 °C								
	Top (35 %)			Middle (35 %)			Bottom (30 %)		
	μ	s	range	μ	s	range	μ	s	range
Color (CU)	8290	135.3	8420 to 8920	10100	127.5	9950 to 10200	16400	353.6	16100 to 16800
COD(mg/L)	8920	76.49	8850 to 9000	10400	158.1	10300 to 10600	19900	200.0	19700 to 20100
pH	9.59	0.021	9.57 to 9.61	9.57	0.007	9.57 to 9.58	9.57	0.017	9.55 to 9.58
Total Alkalinity (mg/L CaCO ₃)	1960	45.28	1910 to 2000	2410	35.36	2380 to 2450	3550	45.28	3510 to 3600
Total Suspended Solids (mg/L)	8	0.00	8	11	2.3	8 to 12	368	16.1	350 to 380
Turbidity (NTU)	2.9	0.16	2.8 to 3.1	2.0	0.01	1.9 to 2.1	3.5	0.55	3.1 to 4.1
Total Dissolved Solids (mg/L)	9000	133.2	8890 to 9150	10400	100.0	10300 to 10500	19800	200.0	19600 to 20000
Volatile Suspended Solids (mg/L)	8	0.00	8	11	2.4	8 to 12	226	9.08	218 to 236

μ - mean, s - sample variance

Composite Results
Initial Freezing Temperature -15 °C
Thawed Top Down at a Thawing Temperature 4 °C

Sample Location	Initial Freezing Temperature -15 °C								
	Top (35 %)			Middle (35 %)			Bottom (30 %)		
	μ	s	range	μ	s	range	μ	s	range
Color (CU)	7390	101.2	7210 to 7530	9390	242.7	9120 to 9590	17900	264.6	17700 to 18200
COD (mg/L)	7980	136.6	7890 to 8140	9720	436.2	9340 to 10300	20200	212.1	20000 to 20400
pH	9.55	0.07	9.54 to 9.55	9.58	0.012	9.57 to 9.59	9.55	0.017	9.54 to 9.57
Total Alkalinity (mg/L CaCO ₃)	1840	30.82	1810 to 1870	2310	32.40	2290 to 2350	3690	41.83	3640 to 3720
Total Suspended Solids (mg/L)	5	2.3	4 to 8	11	2.3	8 to 12	447	15.3	430 to 460
Turbidity (NTU)	1.5	0.21	1.3 to 1.7	1.2	0.07	1.1 to 1.2	10	1.00	9 to 11
Total Dissolved Solids (mg/L)	7880	57.0	7820 to 7930	9950	71.6	9850 to 10100	16900	255.0	16700 to 17200
Volatile Suspended Solids (mg/L)	5	2.3	4 to 8	9	2.4	8 to 12	255	13.2	245 to 270

μ - mean, s - sample variance

Composite Results
Initial Freezing Temperature -15 °C
Thawed Bottom Up at a Thawing Temperature 24 °C

Sample Location	Initial Freezing Temperature -15 °C								
	Top (35 %)			Middle (35 %)			Bottom (30 %)		
	μ	s	range	μ	s	range	μ	s	range
Color (CU)	2410	16	2390 to 2420	6030	153	5900 to 6200	25200	158.1	25100 to 25400
COD (mg/L)	2640	203	2580 to 2720	6070	125	5950 to 6200	28700	1725	27200 to 30600
pH	9.67	0.02	9.65 to 9.69	9.67	0.03	9.65 to 9.70	9.61	0.01	9.60 to 9.63
Total Alkalinity (mg/L CaCO ₃)	544	7	536 to 548	1370	70	1300 to 1440	5260	145	5100 to 5360
Total Suspended Solids (mg/L)	12	4.0	8 to 16	9	2.3	8 to 12	722	65.3	647 to 768
Turbidity (NTU)	15	1.0	14 to 16	3.2	0.9	2.1 to 3.9	4.8	2.1	2.4 to 6.4
Total Dissolved Solids (mg/L)	2500	12	2490 to 2510	6180	163	6000 to 6320	29200	100	29100 to 29300
Volatile Suspended Solids (mg/L)	12	4.0	8 to 16	9	2.3	8 to 12	216	20.0	196 to 236

μ - mean, s - sample variance

Composite Results
Initial Freezing Temperature -15 °C
Thawed Bottom Up at a Thawing Temperature 15 °C

Sample Location	Initial Freezing Temperature -15 °C								
	Top (35 %)			Middle (35 %)			Bottom (30 %)		
	μ	s	range	μ	s	range	μ	s	range
Color (CU)	2520	104.2	2400 to 2600	5980	125.9	5850 to 6100	25400	158.1	25300 to 25600
COD (mg/L)	2730	125.1	2600 to 2850	6260	145.8	6100 to 6380	28500	400.0	28100 to 28900
pH	9.51	0.016	9.49 to 9.53	9.55	0.010	9.54 to 9.56	9.56	0.012	9.55 to 9.57
Total Alkalinity (mg/L CaCO ₃)	566	9.54	556 to 575	1295	32.79	1260 to 1325	5120	45.83	5080 to 5170
Total Suspended Solids (mg/L)	5	2.3	4 to 8	7	2.3	4 to 8	608	17.56	690 to 625
Turbidity (NTU)	15	1.2	14 to 16	6.3	0.82	5.6 to 7.2	4.5	0.07	4.5 to 4.6
Total Dissolved Solids (mg/L)	2720	75.49	2650 to 2800	6390	115.3	6300 to 6520	28400	158.1	28200 to 28500
Volatile Suspended Solids (mg/L)	5	2.3	4 to 8	7	2.3	4 to 8	190	9.2	180 to 198

μ - mean, s - sample variance

Composite Results
Initial Freezing Temperature -15 °C
Thawed Bottom up at a Thawing Temperature 4 °C

Sample Location	Initial Freezing Temperature -15 °C								
	Top (35 %)			Middle (35 %)			Bottom (30 %)		
	μ	s	range	μ	s	range	μ	s	range
Color (CU)	2780	70.36	2710 to 2850	7740	101.5	7630 to 7830	25200	100.0	25100 to 25300
COD (mg/L)	3160	65.19	3100 to 3230	8780	65.57	8710 to 8840	28500	255.0	28200 to 28700
pH	9.48	0.016	9.46 to 9.49	9.52	0.021	9.50 to 9.54	9.56	0.016	9.54 to 9.57
Total Alkalinity (mg/L CaCO ₃)	676	17.62	660 to 695	1840	30.00	1810 to 1870	5550	45.28	5510 to 5600
Total Suspended Solids (mg/L)	5	2.3	4 to 8	7	2.3	4 to 8	648	23.6	630 to 675
Turbidity (NTU)	10	0.7	9 to 10	5.3	0.16	5.1 to 5.4	4.4	0.25	4.1 to 4.6
Total Dissolved Solids (mg/L)	3070	75.17	3000 to 3150	8450	87.46	8380 to 8550	26700	158.1	26500 to 26800
Volatile Suspended Solids (mg/L)	5	2.3	4 to 8	7	2.3	4 to 8	67	16.1	55 to 85

μ - mean, s - sample variance

Composite Results
Initial Freezing Temperature -25 °C
Thawed Top Down at a Thawing Temperature 24 °C

Sample Location	Initial Freezing Temperature -25 °C								
	Top (35 %)			Middle (35 %)			Bottom (30 %)		
	μ	s	range	μ	s	range	μ	s	range
Color (CU)	10200	122	10100 to 10300	11000	158.1	10900 to 11200	13900	265	13600 to 14100
COD (mg/L)	10500	71	10500 to 10600	11300	71	11200 to 11300	14100	173	13900 to 14200
pH	9.66	0.01	9.65 to 9.67	9.65	0.01	9.65 to 9.66	9.66	0.02	9.65 to 9.68
Total Alkalinity (mg/L CaCO ₃)	2380	35	2350 to 2420	2700	16	2690 to 2720	3200	25	3170 to 3220
Total Suspended Solids (mg/L)	9	2.3	8 to 12	12	0.00	12	307	13	295 to 320
Turbidity (NTU)	3.1	0.1	2.9 to 3.2	2.5	0.5	2.1 to 3.1	5.5	0.3	5.2 to 5.7
Total Dissolved Solids (mg/L)	10300	158.1	10100 to 10400	11100	71	11000 to 11100	14200	71	14100 to 14200
Volatile Suspended Solids (mg/L)	9	2.3	8 to 12	12	0.00	12	202	7.6	195 to 210

μ - mean, s - sample variance

Composite Results
Initial Freezing Temperature -25 °C
Thawed Top Down at a Thawing Temperature 15 °C

Sample Location	Initial Freezing Temperature -25 °C								
	Top (35 %)			Middle (35 %)			Bottom (30 %)		
	μ	s	range	μ	s	range	μ	s	range
Color (CU)	9780	66.71	9720 to 9850	10700	200.0	10500 to 10900	14000	158.1	13900 to 14200
COD (mg/L)	9980	107.0	9890 to 10100	10900	158.1	10800 to 11100	14200	40.82	14100 to 14300
pH	9.60	0.01	9.59 to 9.61	9.57	0.012	9.56 to 9.58	9.58	0.007	9.57 to 9.58
Total Alkalinity (mg/L CaCO ₃)	2360	52.92	2300 to 2400	2720	40.62	2680 to 2760	3250	35.36	3210 to 3280
Total Suspended Solids (mg/L)	9	2.3	8 to 12	9	2.3	8 to 12	328	16.1	310 to 340
Turbidity (NTU)	2.6	0.23	2.4 to 2.9	2.1	0.20	1.9 to 2.3	4.1	0.20	3.9 to 4.3
Total Dissolved Solids (mg/L)	10000	79.06	9950 to 10100	10900	173.2	10800 to 11100	14200	100.0	14100 to 14300
Volatile Suspended Solids (mg/L)	9	2.3	8 to 12	9	2.3	8 to 12	212	12.5	198 to 221

μ - mean, s - sample variance

Composite Results
Initial Freezing Temperature -25 °C
Thawed Bottom Up at a Thawing Temperature 4 °C

Sample Location	Initial Freezing Temperature -25 °C								
	Top (35 %)			Middle (35 %)			Bottom (30 %)		
	μ	s	range	μ	s	range	μ	s	range
Color (CU)	3060	80.93	2990 to 3150	7540	50.50	7490 to 7590	25000	100.0	24900 to 25100
COD (mg/L)	3200	80.0	3120 to 3280	7410	52.92	7350 to 7450	25200	40.82	25100 to 25300
pH	9.45	0.007	9.45 to 9.46	9.42	0.012	9.41 to 9.43	9.40	0.010	9.39 to 9.41
Total Alkalinity (mg/L CaCO ₃)	663	24.67	636 to 680	1370	40.77	1325 to 1400	5150	50.00	5100 to 5200
Total Suspended Solids (mg/L)	5	2.3	4 to 8	8	0.00	8	655	22.9	630 to 675
Turbidity (NTU)	8.9	0.50	8.4 to 9.3	5.6	0.50	5.1 to 6.1	3.9	0.32	3.5 to 4.1
Total Dissolved Solids (mg/L)	3260	36.10	3230 to 3300	7410	45.28	7360 to 7450	25300	200.0	25100 to 25500
Volatile Suspended Solids (mg/L)	5	2.3	4 to 8	8	0.00	8	392	10.4	380 to 400

μ - mean, s - sample variance

Composite Results
Initial Freezing Temperature -25 °C
Thawed Bottom Up at a Thawing Temperature 24 °C

Sample Location	Initial Freezing Temperature -25 °C								
	Top (35 %)			Middle (35 %)			Bottom (30 %)		
	μ	s	range	μ	s	range	μ	s	range
Color (CU)	2780	36	2740 to 2810	5940	40	5900 to 5980	26400	158.1	26200 to 26500
COD (mg/L)	3030	104	2950 to 3150	6060	95	5950 to 6130	29500	354	29100 to 29800
pH	9.45	0.02	9.43 to 9.48	9.39	0.01	9.38 to 9.43	9.43	0.02	9.40 to 9.45
Total Alkalinity (mg/L CaCO ₃)	597	13	580 to 610	1330	31	1300 to 1360	5100	50	5050 to 5150
Total Suspended Solids (mg/L)	8	0.0	8	11	2.3	8 to 12	733	41.6	700 to 780
Turbidity (NTU)	25.5	2.1	24 to 28	14	1.0	13 to 15	4.1	0.3	3.9 to 4.5
Total Dissolved Solids (mg/L)	2700	55	2640 to 2750	5860	41	5820 to 5900	29100	158.1	29000 to 29300
Volatile Suspended Solids (mg/L)	8	0.00	8	11	2.3	8 to 12	500	20.0	480 to 520

μ - mean, s - sample variance

Composite Results
Initial Freezing Temperature -25 °C
Thawed Bottom Up at a Thawing Temperature 15 °C

Sample Location	Initial Freezing Temperature -25 °C								
	Top (35 %)			Middle (35 %)			Bottom (30 %)		
	μ	s	range	μ	s	range	μ	s	range
Color (CU)	3030	76.49	2960 to 3110	6310	65.19	6250 to 6380	25100	200.0	24900 to 25300
COD (mg/L)	3140	49.50	3110 to 3200	6380	75.17	6300 to 6450	25300	200.0	25100 to 25500
pH	9.46	0.012	9.46 to 9.47	9.41	0.016	9.39 to 9.42	9.46	0.010	9.45 to 9.47
Total Alkalinity (mg/L CaCO ₃)	656	30.56	630 to 690	1380	30.21	1350 to 1410	5220	85.15	5120 to 5280
Total Suspended Solids (mg/L)	7	2.3	4 to 8	9	2.3	8 to 12	680	30.0	650 to 710
Turbidity (NTU)	15	1.00	14 to 16	8.3	0.55	7.8 to 8.9	3.9	0.35	3.6 to 4.3
Total Dissolved Solids (mg/L)	3140	60.42	3080 to 3200	6400	55.68	6350 to 6460	25300	212.1	25100 to 25500
Volatile Suspended Solids (mg/L)	7	2.3	4 to 8	9	2.3	8 to 12	443	20.7	424 to 465

μ - mean, s - sample variance

Composite Results
Initial Freezing Temperature -25 °C
Thawed Top Down at a Thawing Temperature 4 °C

Sample Location	Initial Freezing Temperature -25 °C								
	Top (35 %)			Middle (35 %)			Bottom (30 %)		
	μ	s	range	μ	s	range	μ	s	range
Color (CU)	9650	65.19	9590 to 9720	10600	158.1	10400 to 10700	14100	200.0	13900 to 14300
COD (mg/L)	9830	80.93	9760 to 9910	10900	100.0	10800 to 11000	14300	158.1	14100 to 14400
pH	9.58	0.007	9.58 to 9.59	9.58	0.007	9.57 to 9.58	9.57	0.01	9.55 to 9.57
Total Alkalinity (mg/L CaCO ₃)	2300	40.62	2260 to 23400	2750	35.36	2720 to 2790	3260	30.82	3230 to 3290
Total Suspended Solids (mg/L)	8	0.00	8	8	0.00	8	348	22.5	325 to 370
Turbidity (NTU)	2.7	0.16	2.5 to 2.8	2.0	0.16	1.8 to 2.1	3.8	0.20	3.6 to 4.0
Total Dissolved Solids (mg/L)	9970	41.8	9920 to 10000	10900	158.1	10700 to 11000	14300	122.5	14200 to 14400
Volatile Suspended Solids (mg/L)	8	0.00	8	8	0.00	8	227	15.0	211 to 241

μ - mean, s - sample variance

APPENDIX H**COMPOSITE RESULTS****ALKALINE EXTRACTION STAGE EFFLUENT**

Composite Results
Initial Freezing Temperature -2 °C
Thawed Bottom Up at a Thawing Temperature 24 °C

Sample Location	Initial Freezing Temperature -2 °C								
	Top (35 %)			Middle (35 %)			Bottom (30 %)		
	μ	s	range	μ	s	range	μ	s	range
Color (CU)	416	30.24	393 to 450	655	31.39	620 to 680	6010	68.19	5930 to 6060
COD(mg/L)	620	14.85	604 to 633	1040	23.45	1030 to 1070	8660	120.6	8530 to 8770
pH	10.57	0.058	10.53 to 10.64	10.84	0.007	10.84 to 10.85	11.36	0.016	11.28 to 11.44
Total Alkalinity (mg/L CaCO ₃)	317	32.97	296 to 355	487	19.16	465 to 500	3780	43.59	3730 to 3810
Total Suspended Solids (mg/L)	<1	0.00	<1	4	0.00	4	473	33.2	432 to 496
Turbidity (NTU)	5.6	0.51	5.2 to 6.2	6.7	1.36	5.1 to 7.6	30	0.70	29 to 30
Total Dissolved Solids (mg/L)	864	24.98	836 to 884	1510	75.83	1460 to 1600	11400	212.1	11200 to 11600
Volatile Suspended Solids (mg/L)	<1	0.00	<1	4	0.00	4	336	50.1	288 to 388

μ - mean, s - sample variance

Composite Results
Initial Freezing Temperature -2 °C
Thawed Bottom Up at a Thawing Temperature 15 °C

Sample Location	Initial Freezing Temperature -2 °C								
	Top (35 %)			Middle (35 %)			Bottom (30 %)		
	μ	s	range	μ	s	range	μ	s	range
Color (CU)	519	22.03	496 to 540	1240	35.70	1210 to 1280	5670	45.83	5620 to 5710
COD(mg/L)	803	37.69	763 to 838	1830	72.11	1750 to 1890	8130	78.10	8080 to 8220
pH	10.52	0.064	10.45 to 10.57	11.01	0.046	10.96 to 11.05	11.34	0.046	11.29 to 11.38
Total Alkalinity (mg/L CaCO ₃)	318	6.08	314 to 325	893	20.82	870 to 910	3950	20.00	3930 to 3970
Total Suspended Solids (mg/L)	4	0.00	4	4	0.00	4	440	21.79	425 to 465
Turbidity (NTU)	5.7	0.52	5.1 to 6.1	4.3	0.21	4.1 to 4.5	27	1.6	26 to 29
Total Dissolved Solids (mg/L)	1050	123.1	936 to 1180	2530	78.1	2480 to 2620	10600	70.7	10500 to 10600
Volatile Suspended Solids (mg/L)	4	0.00	4	4	0.00	4	300	13.6	290 to 316

μ - mean, s - sample variance

Composite Results
Initial Freezing Temperature -2 °C
Thawed Bottom Up at a Thawing Temperature 4 °C

Sample Location	Initial Freezing Temperature -2 °C								
	Top (35 %)			Middle (35 %)			Bottom (30 %)		
	μ	s	range	μ	s	range	μ	s	range
Color (CU)	833	35.48	795 to 865	1480	61.6	1420 to 1540	4590	160.5	4440 to 4760
COD (mg/L)	1260	51.0	1200 to 1300	2180	86.3	2090 to 2260	6630	230.7	6410 to 6870
pH	10.56	0.0158	10.55 to 10.58	10.91	0.065	10.85 to 10.98	11.28	0.035	11.24 to 11.31
Total Alkalinity (mg/L CaCO ₃)	965	15.00	950 to 980	1140	23.45	1120 to 1160	2040	25.50	2010 to 2060
Total Suspended Solids (mg/L)	4	0.00	4	4	0.00	4	409	19.14	388 to 425
Turbidity (NTU)	4.1	0.30	3.8 to 4.4	3.2	0.41	2.8 to 3.6	25	2.0	23 to 27
Total Dissolved Solids (mg/L)	1800	66.7	1730 to 1860	2990	106.1	2870 to 3010	8640	295.7	8360 to 8950
Volatile Suspended Solids (mg/L)	4	0.00	4	4	0.00	4	292	17.6	215 to 245

μ - mean, s - sample variance

Composite Results
Initial Freezing Temperature -2 °C
Thawed Top Down at a Thawing Temperature 24 °C

Sample Location	Initial Freezing Temperature -2 °C								
	Top (35 %)			Middle (35 %)			Bottom (30 %)		
	μ	s	range	μ	s	range	μ	s	range
Color (CU)	1640	104.40	1520 to 1710	1770	80.31	1690 to 1850	4970	137.48	4850 to 5120
COD (mg/L)	1940	131.15	1820 to 2080	2140	127.67	2030 to 2280	7330	85.15	7240 to 7410
pH	10.71	0.025	10.69 to 10.74	10.68	0.032	10.64 to 10.71	10.99	0.031	10.96 to 11.02
Total Alkalinity (mg/L CaCO ₃)	683	22.55	660 to 705	855	15.00	840 to 870	2770	81.85	2680 to 2840
Total Suspended Solids (mg/L)	12	0.00	12	4	0.00	4	364	22.73	340 to 385
Turbidity (NTU)	9.1	0.12	8.9 to 9.2	9.2	0.29	8.8 to 9.3	24	0.7	23 to 24
Total Dissolved Solids (mg/L)	2440	119.37	2310 to 2540	2850	96.18	2750 to 2940	9490	109.77	9400 to 9610
Volatile Suspended Solids (mg/L)	12	0.00	12	4	0.00	4	314	15.5	296 to 325

μ - mean, s - sample variance

Composite Results
Initial Freezing Temperature -2 °C
Thawed Top Down at a Thawing Temperature 15 °C

Sample Location	Initial Freezing Temperature -2 °C								
	Top (35 %)			Middle (35 %)			Bottom (30 %)		
	μ	s	range	μ	s	range	μ	s	range
Color (CU)	1530	55.7	1480 to 1590	1680	35.4	1640 to 1710	5150	171.0	4950 to 5280
COD (mg/L)	2250	64.1	2180 to 2340	2460	55.2	2410 to 2510	7390	136.6	7240 to 7510
pH	10.71	0.020	10.69 to 10.73	10.70	0.0158	10.68 to 10.71	11.02	0.35	10.98 to 11.05
Total Alkalinity (mg/L CaCO ₃)	660	31.2	635 to 695	818	12.6	805 to 830	2910	64.4	2860 to 2980
Total Suspended Solids (mg/L)	8	0.00	8	4	0.00	4	353	17.6	335 to 370
Turbidity (NTU)	7.2	0.32	6.9 to 7.6	7.5	0.60	6.9 to 8.1	23	2.12	21 to 25
Total Dissolved Solids (mg/L)	2760	45.3	2720 to 2810	3080	32.4	3060 to 3120	9720	36.1	9690 to 9760
Volatile Suspended Solids (mg/L)	8	0.00	8	4	0.00	4	302	15.3	285 to 315

μ - mean, s - sample variance

Composite Results
Initial Freezing Temperature -2 °C
Thawed Top Down at a Thawing Temperature 4 °C

Sample Location	Initial Freezing Temperature -2 °C								
	Top (35 %)			Middle (35 %)			Bottom (30 %)		
	μ	s	range	μ	s	range	μ	s	range
Color (CU)	1480	72.1	1420 to 1560	1630	57.0	1580 to 1690	5220	60.4	5160 to 5280
COD (mg/L)	2190	100.00	2090 to 2290	2390	83.4	2320 to 2480	7520	85.4	7440 to 7610
pH	10.70	0.025	10.68 to 10.73	10.69	0.007	10.67 to 10.71	11.04	0.071	10.96 to 11.10
Total Alkalinity (mg/L CaCO ₃)	692	12.6	680 to 705	823	12.6	810 to 835	2840	57.0	2780 to 2890
Total Suspended Solids (mg/L)	8	0.00	8	4	0.00	4	370	28.7	345 to 390
Turbidity (NTU)	7.9	0.22	7.6 to 8.1	6.2	0.31	5.9 to 6.5	24	3.6	21 to 28
Total Dissolved Solids (mg/L)	2980	36.1	2870 to 3120	3240	112.5	3160 to 3360	9770	110.7	9670 to 9890
Volatile Suspended Solids (mg/L)	8	0.00	8	4	0.00	4	308	15.8	295 to 325

μ - mean, s - sample variance

Composite Results
Initial Freezing Temperature -15 °C
Thawed Top Down at a Thawing Temperature 24 °C

Sample Location	Initial Freezing Temperature -2 °C								
	Top (35 %)			Middle (35 %)			Bottom (30 %)		
	μ	s	range	μ	s	range	μ	s	range
Color (CU)	1740	51.48	1680 to 1780	1740	36.06	1690 to 1810	3530	98.49	3420 to 3610
COD (mg/L)	2530	100.25	2420 to 2610	2560	86.31	2480 to 2650	5090	118.53	4950 to 5160
pH	10.71	0.025	10.68 to 10.73	10.73	0.021	10.71 to 10.75	10.87	0.041	10.83 to 10.91
Total Alkalinity (mg/L CaCO ₃)	1030	21.21	1010 to 1050	1240	36.06	1210 to 1280	1860	45.28	1810 to 1900
Total Suspended Solids (mg/L)	<1	0.00	<1	4	0.00	4	281	11.5	268 to 290
Turbidity (NTU)	5.2	0.51	4.6 to 5.6	3.3	0.47	2.9 to 3.8	27	1.7	26 to 29
Total Dissolved Solids (mg/L)	34500	102.96	3340 to 3530	3460	111.36	3360 to 3580	6710	181.93	6510 to 6850
Volatile Suspended Solids (mg/L)	<1	0.00	<1	4	0.00	4	239	11.02	228 to 250

μ - mean, s - sample variance

Composite Results
Initial Freezing Temperature -15 °C
Thawed Top Down at a Thawing Temperature 15 °C

Sample Location	Initial Freezing Temperature -15 °C								
	Top (35 %)			Middle (35 %)			Bottom (30 %)		
	μ	s	range	μ	s	range	μ	s	range
Color (CU)	1670	45.8	1620 to 1710	1770	45.8	1730 to 1820	3570	57.0	3510 to 3620
COD (mg/L)	2450	66.7	2380 to 2510	2600	66.7	2540 to 2670	5170	52.0	5080 to 5240
pH	10.71	0.030	10.68 to 10.73	10.74	0.010	10.73 to 10.75	10.88	0.031	10.85 to 10.91
Total Alkalinity (mg/L CaCO ₃)	1010	20.00	990 to 1030	1210	15.8	1190 to 1220	1850	15.8	1830 to 1860
Total Suspended Solids (mg/L)	<1	0.00	<1	4	0.00	4	267	20.2	245 to 285
Turbidity (NTU)	4.7	0.47	4.2 to 5.1	3.3	0.51	2.7 to 3.7	25	1.6	24 to 27
Total Dissolved Solids (mg/L)	2130	25.5	2100 to 2150	3510	86.3	3430 to 3600	6780	102.7	6670 to 6870
Volatile Suspended Solids (mg/L)	<1	0.00	<1	4	0.00	4	218	20.2	200 to 240

μ - mean, s - sample variance

Composite Results
Initial Freezing Temperature -15 °C
Thawed Top Down at a Thawing Temperature 4 °C

Sample Location	Initial Freezing Temperature -15 °C								
	Top (35 %)			Middle (35 %)			Bottom (30 %)		
	μ	s	range	μ	s	range	μ	s	range
Color (CU)	1630	50.5	1580 to 1680	1780	26.5	1750 to 1800	3620	65.6	3550 to 3680
COD (mg/L)	2420	38.7	2390 to 2470	2590	35.4	2560 to 2630	5240	60.1	5180 to 5300
pH	10.72	0.025	10.69 to 10.74	10.75	0.026	10.72 to 10.77	10.98	0.030	10.95 to 11.01
Total Alkalinity (mg/L CaCO ₃)	1130	25.5	1100 to 1150	1240	40.6	1200 to 1280	2260	55.2	2210 to 2300
Total Suspended Solids (mg/L)	<1	0.00	<1	4	0.00	4	310	15.0	295 to 325
Turbidity (NTU)	4.5	0.33	4.0 to 5.3	3.6	0.40	2.7 to 3.9	22	1.6	20 to 25
Total Dissolved Solids (mg/L)	3260	90.8	3160 to 3340	3530	52.0	3470 to 3560	6870	121.2	6740 to 6980
Volatile Suspended Solids (mg/L)	<1	0.00	<1	4	0.00	4	262	7.5	255 to 270

μ - mean, s - sample variance

Composite Results
Initial Freezing Temperature -15 °C
Thawed Bottom Up at a Thawing Temperature 24 °C

Sample Location	Initial Freezing Temperature -15 °C								
	Top (35 %)			Middle (35 %)			Bottom (30 %)		
	μ	s	range	μ	s	range	μ	s	range
Color (CU)	618	12.53	605 to 630	980	36.06	940 to 1010	4520	25.50	4490 to 4540
COD (mg/L)	10206 20	30.00	990 to 1040	1470	41.83	1420 to 1510	6530	21.21	6510 to 6550
pH	10.63	0.035	10.58 to 10.67	10.83	0.016	10.81 to 10.84	10.88	0.725	10.86 to 10.91
Total Alkalinity (mg/L CaCO ₃)	423	10.42	415 to 435	1033	25.56	1010 to 1050	2710	20.00	2690 to 2730
Total Suspended Solids (mg/L)	4	0.00	4	4	0.00	4	409	11.5	398 to 421
Turbidity (NTU)	4.9	0.76	4.4 to 5.8	3.7	0.23	3.4 to 3.8	23	1.6	21 to 24
Total Dissolved Solids (mg/L)	1320	38.08	1290 to 1360	2080	58.74	2010 to 2120	7660	38.08	7620 to 7690
Volatile Suspended Solids (mg/L)	4	0.00	4	4	0.00	4	292	11.0	281 to 303

μ - mean, s - sample variance

Composite Results
Initial Freezing Temperature -15 °C
Thawed Bottom Up at a Thawing Temperature 15 °C

Sample Location	Initial Freezing Temperature -15 °C								
	Top (35 %)			Middle (35 %)			Bottom (30 %)		
	μ	s	range	μ	s	range	μ	s	range
Color (CU)	647	35.1	610 to 680	1090	36.1	1050 to 1120	4300	21.2	4280 to 4320
COD (mg/L)	943	10.4	935 to 955	1600	30.8	1570 to 1630	6230	30.8	6200 to 6260
pH	10.68	0.042	10.63 to 10.71	10.85	0.041	10.81 to 10.89	10.92	0.026	10.90 to 10.95
Total Alkalinity (mg/L CaCO ₃)	503	15.3	490 to 520	1100	20.00	1080 to 1120	2610	15.8	2600 to 2630
Total Suspended Solids (mg/L)	4	0.00	4	4	0.00	4	287	10.4	275 to 290
Turbidity (NTU)	5.3	0.38	4.9 to 5.6	4.4	0.36	4.1 to 4.8	20	1.6	19 to 22
Total Dissolved Solids (mg/L)	1430	25.5	1400 to 1450	2240	40.00	2200 to 2280	8180	41.8	8130 to 8210
Volatile Suspended Solids (mg/L)	4	0.00	4	4	0.00	4	200	10.0	190 to 210

μ - mean, s - sample variance

Composite Results
Initial Freezing Temperature -15 °C
Thawed Bottom Up at a Thawing Temperature 4 °C

Sample Location	Initial Freezing Temperature -15 °C								
	Top (35 %)			Middle (35 %)			Bottom (30 %)		
	μ	s	range	μ	s	range	μ	s	range
Color (CU)	750	87.2	690 to 850	1280	41.8	1230 to 1310	3960	102.5	3850 to 4120
COD (mg/L)	1110	66.7	1050 to 1180	1860	35.4	1820 to 1890	5630	86.3	5540 to 5710
pH	10.75	0.35	10.71 to 10.78	10.88	0.03	10.85 to 10.91	11.02	0.031	10.99 to 11.05
Total Alkalinity (mg/L CaCO ₃)	533	15.3	520 to 550	1130	30.00	1100 to 1160	2530	26.5	2500 to 2550
Total Suspended Solids (mg/L)	4	0.00	4	5.3	2.3	4 to 8	248	17.6	230 to 265
Turbidity (NTU)	5.6	0.62	4.9 to 6.1	4.5	0.300	4.2 to 4.8	18	2.00	16 to 20
Total Dissolved Solids (mg/L)	1630	80.3	1550 to 1710	2570	36.1	2530 to 2600	7400	45.3	7360 to 7450
Volatile Suspended Solids (mg/L)	4	0.00	4	5.3	2.3	4 to 8	172	20.2	150 to 190

μ - mean, s - sample variance

Composite Results
Initial Freezing Temperature -25 °C
Thawed Bottom Up at a Thawing Temperature 24 °C

Sample Location	Initial Freezing Temperature -25 °C								
	Top (35 %)			Middle (35 %)			Bottom (30 %)		
	μ	s	range	μ	s	range	μ	s	range
Color (CU)	645	34.53	611 to 680	992	82.61	927 to 1080	4020	168.2	3830 to 4150
COD(mg/L)	1000	33.38	975 to 1040	1590	80.31	1510 to 1670	6400	180.3	6200 to 6550
pH	10.55	0.020	10.53 to 10.57	10.68	0.036	10.64 to 10.71	10.99	0.051	10.95 to 11.05
Total Alkalinity (mg/L CaCO ₃)	477	10.61	467 to 488	768	15.28	755 to 785	2640	21.21	2620 to 2660
Total Suspended Solids (mg/L)	8	0.00	8	8	0.00	8	342	22.55	320 to 365
Turbidity (NTU)	3.9	0.20	3.7 to 4.1	4.2	0.16	4.1 to 4.4	26	2.1	24 to 28
Total Dissolved Solids (mg/L)	1410	35.36	1380 to 1450	2270	80.31	2190 to 2350	8320	168.2	8130 to 8450
Volatile Suspended Solids (mg/L)	8	0.00	8	8	0.00	8	242	19.6	221 to 260

μ - mean, s - sample variance

Composite Results
Initial Freezing Temperature -25 °C
Thawed Bottom Up at a Thawing Temperature 15 °C

Sample Location	Initial Freezing Temperature -25 °C								
	Top (35 %)			Middle (35 %)			Bottom (30 %)		
	μ	s	range	μ	s	range	μ	s	range
Color (CU)	663	15.28	650 to 680	1080	25.50	1050 to 1100	4310	45.28	4260 to 4350
COD(mg/L)	1010	15.81	1000 to 1030	1600	30.00	1570 to 1630	6240	29.15	6200 to 6280
pH	10.62	0.0158	10.60 to 10.63	10.72	0.0361	10.69 to 10.75	11.05	0.041	11.01 to 11.09
Total Alkalinity (mg/L CaCO ₃)	529	12.06	516 to 540	772	12.58	760 to 785	3990	20.00	3970 to 4010
Total Suspended Solids (mg/L)	9	2.3	8 to 12	9	2.3	8 to 12	313	10.4	305 to 325
Turbidity (NTU)	4.8	0.30	4.5 to 5.1	5.1	0.38	4.8 to 5.5	21	2.12	19 to 23
Total Dissolved Solids (mg/L)	1490	35.36	1450 to 1520	2230	30.00	2200 to 2260	8160	40.00	8120 to 8200
Volatile Suspended Solids (mg/L)	8	0.00	8	8	0.00	8	230	10.00	220 to 240

μ - mean, s - sample variance

Composite Results
Initial Freezing Temperature -25 °C
Thawed Top Down at a Thawing Temperature 24 °C

Sample Location	Initial Freezing Temperature -25 °C								
	Top (35 %)			Middle (35 %)			Bottom (30 %)		
	μ	s	range	μ	s	range	μ	s	range
Color (CU)	1720	49.50	1660 to 1750	1830	85.44	1750 to 1920	2630	73.25	2550 to 2720
COD (mg/L)	2580	25.50	2560 to 2610	2700	110.68	2580 to 2800	3850	85.15	3750 to 3910
pH	10.71	0.030	10.68 to 10.74	10.79	0.057	10.72 to 10.83	10.91	0.045	10.86 to 10.96
Total Alkalinity (mg/L CaCO ₃)	1180	25.25	1155 to 1210	1230	16.20	1210 to 1240	1590	21.21	1570 to 1610
Total Suspended Solids (mg/L)	<1	0.00	<1	4	0.00	4	286	18.91	265 to 301
Turbidity (NTU)	4.0	0.16	3.9 to 4.2	2.8	0.22	2.5 to 3.1	27	2.12	25 to 29
Total Dissolved Solids (mg/L)	3600	93.00	3490 to 3660	3820	107.00	3700 to 3910	4970	108.63	4830 to 5110
Volatile Suspended Solids (mg/L)	<1	0.00	<1	4	0.00	4	231	15.30	215 to 245

μ - mean, s - sample variance

Composite Results
Initial Freezing Temperature -25 °C
Thawed Bottom Up at a Thawing Temperature 4 °C

Sample Location	Initial Freezing Temperature -25 °C								
	Top (35 %)			Middle (35 %)			Bottom (30 %)		
	μ	s	range	μ	s	range	μ	s	range
Color (CU)	790	30.00	760 to 820	1280	30.8	1250 to 1310	3980	70.00	3910 to 4050
COD (mg/L)	1180	35.4	1150 to 1220	1890	36.1	1850 to 1920	5740	90.8	5640 to 5820
pH	10.66	0.0158	10.65 to 10.68	10.77	0.0212	10.75 to 10.79	11.05	0.031	11.02 to 11.08
Total Alkalinity (mg/L CaCO ₃)	602	18.9	580 to 615	932	22.1	910 to 950	3680	35.4	3650 to 3720
Total Suspended Solids (mg/L)	9.3	2.3	8 to 12	9.3	2.3	8 to 12	283	12.6	270 to 295
Turbidity (NTU)	5.1	0.30	4.8 to 5.4	4.9	0.20	4.7 to 5.1	22	2.6	19 to 24
Total Dissolved Solids (mg/L)	1720	40.00	1680 to 1760	2590	30.00	2560 to 2620	7560	77.8	7500 to 7650
Volatile Suspended Solids (mg/L)	8	0.00	8	8	0.00	8	183	12.6	170 to 195

μ - mean, s - sample variance

Composite Results
Initial Freezing Temperature -25 °C
Thawed Top Down at a Thawing Temperature 15 °C

Sample Location	Initial Freezing Temperature -25 °C								
	Top (35 %)			Middle (35 %)			Bottom (30 %)		
	μ	s	range	μ	s	range	μ	s	range
Color (CU)	1700	45.8	1650 to 1740	1770	40.6	1730 to 1810	2610	35.4	2580 to 2650
COD (mg/L)	2590	25.5	2570 to 2620	2620	30.8	2590 to 2650	3770	58.7	3730 to 3840
pH	10.73	0.020	10.71 to 10.75	10.86	0.010	10.85 to 10.87	11.01	0.025	10.98 to 11.03
Total Alkalinity (mg/L CaCO ₃)	1210	25.5	1190 to 1240	1230	15.8	1220 to 1250	1620	30.8	1590 to 1650
Total Suspended Solids (mg/L)	<1	0.00	<1	4	0.00	4	278	12.6	265 to 290
Turbidity (NTU)	5.3	0.45	4.9 to 5.8	4.9	0.35	4.6 to 5.3	22	3.5	19 to 26
Total Dissolved Solids (mg/L)	3590	45.8	3550 to 3640	3720	55.7	3670 to 3780	4990	45.3	4950 to 5040
Volatile Suspended Solids (mg/L)	<1	0.00	<1	4	0.00	4	193	12.6	180 to 205

μ - mean, s - sample variance

Composite Results
Initial Freezing Temperature -25 °C
Thawed Top Down at a Thawing Temperature 4 °C

Sample Location	Initial Freezing Temperature -25 °C								
	Top (35 %)			Middle (35 %)			Bottom (30 %)		
	μ	s	range	μ	s	range	μ	s	range
Color (CU)	1700	21.1	1680 to 1720	1770	47.4	1730 to 1820	2640	61.2	2590 to 2710
COD (mg/L)	2530	21.2	2510 to 2550	2620	25.5	2590 to 2640	3820	105.8	3740 to 3940
pH	10.74	0.010	10.74 to 10.75	10.83	0.020	10.81 to 10.86	10.98	0.030	10.95 to 11.01
Total Alkalinity (mg/L CaCO ₃)	1230	25.5	1200 to 1250	1240	25.5	1210 to 1260	1590	36.1	1560 to 1630
Total Suspended Solids (mg/L)	<1	0.00	<1	4	0.00	4	262	12.6	250 to 275
Turbidity (NTU)	5.0	0.158	4.8 to 5.4	4.9	0.46	4.6 to 5.4	23	2.3	20 to 24
Total Dissolved Solids (mg/L)	3440	50.5	3390 to 3490	3700	30.00	3670 to 3730	4970	85.4	4890 to 5060
Volatile Suspended Solids (mg/L)	<1	0.00	<1	4	0.00	4	165	13.2	160 to 180

μ - mean, s - sample variance